UNIVERSITY OF OKLAHOMA

GRADUATE COLLEGE

A COMPARISON OF THE EVOKED ACTIVITY FROM OSCILLATING AUDITORY TONES: AMPLITUDE-MODULATED (AM) TONES AND BINAURAL BEATS (BB)

A DISSERTATION

SUBMITTED TO THE GRADUATE FACULTY

in partial fulfillment of the requirements for the

Degree of

DOCTOR OF PHILOSOPHY

By

LINDSEY R. TATE
Norman, Oklahoma
2018

Downloaded from SHAREOK. Persistent Handle URL: https://hdl.handle.net/11244/302099

A COMPARISON OF THE EVOKED ACTIVITY FROM OSCILLATING AUDITORY TONES: AMPLITUDE-MODULATED (AM) TONES AND BINAURAL BEATS (BB)

A DISSERTATION APPROVED FOR THE
DEPARTMENT OF PSYCHOLOGY

BY

Dr. Lauren Ethridge, Chair

Dr. Scott Gronlund

Dr. Hairong Song

Dr. Barbara Carlson

Dr. Ari Berkowitz

© Copyright by LINDSEY R. TATE 2018

All Rights Reserved.

Table of Contents

Acknowledgements vii

Abstract ix

Literature Review 1

Basics of the Human Auditory Pathway 1

Sensory Processing and Encoding 1

Auditory Perception 2

Binaural Connections 3

Stimuli and EEG Correlates Used to Study Auditory Perception 4

Amplitude-Modulated Stimuli and the Auditory Steady State Response (ASSR) 4

Binaural Beats 6

Binaural Beats vs. Amplitude-Modulated Tones 8

EEG for Evaluating Auditory Processing 8

FFT: Power and Phase Analysis 9

Connectivity Analysis 10

Potential Therapeutic Application of Binaural Beats: Increases in Connectivity with Prolonged Use 11

Hypotheses and Goals 14

Methods 15

Study Design 15

Procedure 15

Participants 15

Setting. 17

Data Collection Sessions 17
Data Collection and Analysis 20
Results 26
Power Analysis 26
Phase-Locking Analysis 35
DICS Source Analysis 36
DICS Connectivity Analysis 40
DICS Source and Connectivity Analyses: BB vs. AM Comparisons 54
Source Analysis 54
Connectivity Analysis 54
Discussion 59
Hypotheses 59
Frequency Analysis and ASSR 59
Source Analysis 62
Connectivity Analysis 62
Clinical Importance of Functional Connectivity 62
Connectivity in BB 6 Hz 63
Biological Basis of EEG Connectivity 64
Connectivity in Language Areas 65
Summary of Findings 66
Limitations and Recommendations 67
Next Steps 70
Conclusion 70

References 72

Appendix: FFT Images 80

Appendix: DICS Source Analysis Images 152

Appendix: DICS Connectivity Images 168

Appendix: Amplitude Modulated Versus Binaural Beat Comparison 312

Acknowledgements

I would like to extend my sincerest thanks to my advisor, Dr. Lauren Ethridge, without whose advice and assistance this work would not have been possible. I thank her personally for stepping up to bat for me, helping me to realize both my masters and my Ph.D., and providing priceless support, honesty, and inspiration. She has been the role model every advisor should be, and I am honored to have been part of her lab.

I am grateful to all my Advisory Committee members for their guidance and suggestions which have enriched this work and my career in general. In particular, I would like to thank Dr. Barbara Carlson for her part in inspiring and piloting this project as well as for years of collaboration that enhanced my career with unique experiences. I am grateful to Dr. Ari Berkowitz for the attention and effort spent ensuring my biological knowledge and for his excellent example in how rigorous we should all be with our teaching and community outreach. Thank you to Dr. Hairong Song for showing the deep passion for statistics that begat my own. Thank you to Dr. Scott Gronlund for connecting me to Cognitive Psychology and for a rough but immensely influential crash course through modeling.

Thank you to all the faculty, staff, and students of the Departments of Psychology and Biology, without whom I wouldn't have made it to the beginning of this work. Thank you to the undergraduate and graduate research assistants I have had the pleasure of researching alongside. In particular, I am indebted to those who helped collect this data, including Lisa De Stefano, Nick Woodruff, and Kara Brown.

Finally, I offer my gratitude, love, and devotion to my family, who have made my life, education, and research possible. As a first-generation college graduate, I am grateful for the lineage of hard workers that lifted me up. My parents continue to provide their support in all my

wild dreams, celebrating me each step of the way. Most importantly, I thank Erik, Becky, and Potter for their daily support and love, without which I would be lost. For all you've done to get me here, this work is dedicated to you.

Abstract

This study compares the neural response to binaural beat (BB) and amplitude-modulated tone (AM) auditory stimulation using power, phase-locking, and functional brain connectivity as assessed by electroencephalography (EEG). BB are produced when a different frequency sound is played in each ear, producing a pulsing or beat perception at the difference between the frequencies in each ear. The overarching goal of the study was to inform the understanding of the human auditory system and potential evidence-based therapies using binaural beats.

BB 25 Hz and AM 25 Hz were processed very similarly, including: (1) a prominent phase-locking response at 50 Hz, (2) an increase in power at 50 Hz in the same bilateral auditory cortex electrodes, (3) the same right central cortical dipole identified for the maximum power in 50 Hz, (4) an unexpected decrease in power at 12 Hz, and (5) no differences in connectivity on the same scale as the 6 Hz stimuli differences. BB 6 Hz showed an auditory steady state response (ASSR) at 6 Hz and 12 Hz. AM 6 Hz drove higher increases in connectivity (relative to baseline) in some brain areas. BB 6 Hz drove connectivity increases in frontal, auditory, and occipital cortex-- areas that have been implicated in disorders with decreased connectivity.

Because this study contains information about connectivity driven by BB, the findings from this study can inform future therapies for disorders where brain connectivity is decreased. Specific recommendations for therapies include using low-frequency binaural beats to induce increases in connectivity between any combination of frontal, auditory, and occipital areas. Because the 5-minute conditions did not show the same driving in frequency power that was shown for the 3-second conditions, our results suggest that repeated shorter bursts of stimulation are more effective than relatively long exposure times, which may be the result of habituation.

Keywords: binaural beats, EEG source analysis, Dynamic Imaging of Coherent Sources (DICS)

Literature Review

Auditory systems serve to decipher an impressive amount of information present in variations of the atmosphere we live in. At the most fundamental level, processing sounds provides threat detection, situational awareness, and a three-dimensional sense of our bodies and the environments that they are in. Socially, the majority of people today use spoken language to communicate, which has served a critical role in social organization and culture. Many academics, researchers, and businesses have sought to understand the mechanisms by which animals with auditory systems can sense and use this ever-present information. Binaural beats are one type of auditory stimulus that has come into focus as a unique situation optimal for understanding the structure and function of our auditory nervous system. Furthermore, binaural beats have been suggested as a form of non-invasive therapy for a variety of disorders, primarily under the hypothesis that binaural beats may alter functional connectivity between brain areas.

Basics of the Human Auditory Pathway

In order to evaluate the electrophysiological signals coming from the auditory pathway it is important to first understand the basic structure and function of its constituent parts, and the relevant information is summarized here (Nicholls, Martin, Fuchs, Brown, Diamond, & Weisblat, 2012; Squire, Berg, Bloom, du Lac, Ghosh, & Spitzer, 2013). Because this project uses electroencephalography (EEG), it is also important to consider how EEG features measure sensory encoding, perception, and auditory interpretation throughout the system.

Sensory Processing and Encoding. Vibrations of the air are focused and directed into the ear by the outer ear, which is composed of a protrusion of the skull, cartilage, and skin. The skull protrusion, called the pinna, is angled so that it directs more sound coming from the front of the person than behind them for high frequencies. Air moves in the ear canal, ending with the

tympanic membrane. As the first part of the transduction mechanism, this membrane conducts vibrations to the ear bones, which vibrate the oval window of the cochlea. Sensing sound begins with the cochlea, where sounds are first encoded as neural signals. As fluid in the cochlea vibrates, it activates mechanically-gated inner hair cells on the basilar membrane. The coiled, conical structure of the basilar membrane within the cochlea leads to inner hair cells responding to different frequencies of sound based on their position along the basilar membrane, such that lower frequencies activate hair cells closer to the apex and higher frequencies activate hair cells near the base.

Speaking strictly to ascending connections, neurons signal from the cochlear nuclei in the medulla to the inferior colliculus in the midbrain, then to the medial geniculate nucleus of the thalamus, and finally to the auditory cortex in the temporal lobe (with the primary auditory cortex, A1, on the superior bank of the temporal lobe). However, there are also bilateral connections from the ventral cochlear nuclei to the superior olivary nuclei as well as bilateral connections in the inferior colliculus which are necessary for processes that use input from both ears such as sound localization.

A deficit in hearing can be due to damage to sensory cells from long-term exposure to loud sounds, trauma to the ear, certain diseases such as diabetes, and certain medications; furthermore, aging can cause changes to the outer and middle ear, such as increased tympanic membrane rigidity or calcification of inner ear bones, that lead to hearing loss (NIDCD, 2018). Further impediments to hearing can be any item or substance that blocks or distorts the sound as it travels through the ear canal, such as ear plugs or earwax buildup.

Auditory Perception. Perception of sound occurs when stimuli from the cochlea reach the auditory cortex and is dependent upon the activation of specialized nerve fiber located in the

cochlea. Inner hair cells within the cochlea selectively synapse with afferent auditory nerve fibers, creating approximately 10,000 frequency-labeled lines ending in the cochlear nuclei of the medulla. The tonotopic organization established here continues throughout the auditory pathway and into the cortex. This "place code" works best at stimulation frequencies above 300Hz.

In addition to these frequency-labeled lines, relative firing rates of auditory neurons communicate information about stimulus frequency. For example, the same auditory neuron may respond to different frequencies but maintain the frequency information by firing more times per second for higher frequencies than lower ones. Higher pitches in the audible range (i.e., > 1,000 Hz) cannot be represented one-to-one by the firing rate of a single neuron because an auditory neuron's maximum firing rate is lower than the maximum audible frequency (Purves, Augustine, & Fitzpatrick, 2001). Auditory neurons tend to fire action potentials simultaneously in a manner corresponding to the peak phase of the stimulus waveform, known as phase locking. Therefore, neurons with staggered firing can pool resources to maintain the information about higher frequencies. This "temporal code" works best at stimulation frequencies below 300 Hz. This coding pattern is maintained throughout the ascending pathways all the way to primary auditory cortex.

Binaural Connections. Binaural connections are thought to have evolved primarily for sound localization purposes. Sound localization in mammals is performed using interaural level and time differences. Interaural intensity or level differences are a difference in sound pressure of a sound (related to perceived loudness) when it reaches one ear versus the other due to the stimulus being offset horizontally[1] relative to the listener (Fontaine & Peremans, 2007; Wall, McDaid, Maguire, & Mcginnity, 2012). Neurons in the lateral superior olive (LSO) respond

[1] Or, due to sound-frequency-dependent filtering by the head, offset vertically.

selectively to intensity differences (Park, Grothe, Pollak, Schuller, & Koch, 1996; Tollin, 2003; Fontaine & Peremans, 2007). Interaural time difference or delay (ITD) is the gap in time between when a sound reaches one ear and when it reaches the other ear. ITDs can be measured in microseconds (Skottun, Shackleton, Arnott, & Palmer, 2001). In mammals, the computation of this time difference is performed in the medial superior olive (MSO) of the auditory brain stem (Jercog, Svirskis, Kotak, Sanes, & Rinzel, 2010). There is evidence that mammals possess neurons that respond selectively to ITD (Jercog, Svirskis, Kotak, Sanes, & Rinzel, 2010; van der Heijden, Lorteije, Plauška, Roberts, Golding, Borst, 2013). Each neuron in the MSO in the brainstem has its own "best ITD" that it responds to optimally (van der Heijden, Lorteije, Plauška, Roberts, Golding, Borst, 2013). While the primary auditory cortex (A1) is formed of modular columns that maintain the tonotopic organization from the cochlea, it also maintains clustering by the interaural differences calculated in the olivary nuclei.

Stimuli and EEG Correlates Used to Study Auditory Perception

Amplitude-Modulated Stimuli and the Auditory Steady State Response (ASSR).

Amplitude modulation (AM) is encoded throughout the auditory pathway from the auditory nerve to the cortex (Joris, Schreiner, Rees, 2004). There are two competing hypotheses for the detection of AM: [1] processing by the cochlea (equal to a bandpass filter and a half-wave rectifier) followed by a low-pass filter, or [2] a bank of bandpass filters that are sensitive to different ranges of modulation frequency, like a map (Joris, Schreiner, & Rees, 2004). Modulation frequency[2] is encoded in two ways: through synchronization of neural activity (i.e., currents within a population of neurons flowing in the same direction at the same time),

[2] For purposes of this paper, "modulation frequency" refers to amplitude modulation frequency. However, it should be noted that neurons also respond to stimulus frequency modulation.

especially in peripheral neural structures, and through average firing rate, especially in the central neural structures such as cortex (Joris, Schreiner, & Rees, 2004).

Peripheral neurons are tuned such that they only respond to a small range of modulation frequencies, and this tuning persists in the central structures via average firing rate (Joris, Schreiner, & Rees, 2004). There is a suggested topographic map of modulation frequencies orthogonal to the tonotopic map in the auditory cortex (Joris, Schreiner, & Rees, 2004). However, psychophysiological and event-related potentials (ERP) measures in humans fail to give evidence for the bandpass tuning featured in single-neuron recordings (Joris, Schreiner, & Rees, 2004). Lesion studies in humans have demonstrated the auditory cortex's relevance for detecting AM frequencies below but not above 30 Hz (Grigoreva, Figurina, & Vasilev, 1988). However, a case study in developmental dyslexia showed that the path up to and including primary auditory cortex was not sufficient for the detection of temporal pattern, such as AM, in a patient with a large frontal lobe lesion and a single intact right auditory cortex (Griffiths, Penhune, Peretz, Dean, Patterson, & Green, 2000).

Auditory steady-state response (ASSR) is a neural response to periodical auditory stimulation, such as click trains or amplitude-modulated tones (Legget, Hild, Steinmetz, Simon, & Rojas, 2017). In response to amplitude-modulated stimuli, the frequency of modulation is encoded by neural synchronization at the modulation frequency (Joris, Schreiner, Rees, 2004). ASSR only occurs within a particular range of modulation frequencies (Joris, Schreiner, Rees, 2004); it is strongest at 40 Hz in humans (Legget et al., 2017) but has been found as low as 12 Hz (Herman et al., 2002) and 4 Hz (Farahani et al., 2017). The mechanism behind variations in strength of ASSR is still debated, but there is evidence supporting linear superposition theory--the theory that ASSR generation is a linear mixing of multiple transient auditory evoked

potentials (AEP)-- which accounts for the peak at 40 Hz due to latencies of particular AEP components (Tan, Fu, Yuan, Ding, & Wang, 2017). ASSR has been observed in humans in response to AM stimuli, including AM tones, using EEG and magnetoencephalography (MEG), observable as increased power in the modulation frequency (Rees, Green, & Kay, 1986; Plourde, Stapells, & Picton, 1991; Picton, John, Dimitrijevic, & Purcell, 2003; Legget et al., 2017). Additionally, increased inter-trial phase coherence of the EEG/MEG signal at the modulation frequency has been observed for multiple AM stimuli, including AM tones (Joris, Schreiner, Rees, 2004; Krishnan, Hetrick, Brenner, Shekhar, Steffan, & O'Donnell, 2009; Legget et al., 2017; Griskova-Bulanova, Dapsys, Melynyte, Voicikas, Maciulis, Andruskevicius, & Korostenskaja, 2018). The ASSR has adequate test-retest reliability using both EEG (McFadden, Steinmetz, Carroll, Simon, Wallace, & Rojas, 2014) and MEG (Legget et al., 2017). Abnormal ASSR presentation has been reported in autism, schizophrenia, and bipolar disorder (Legget, Hild, Steinmetz, Simon, & Rojas 2017).

Binaural Beats. Binaural beats (BB) are generated when two tones of slightly different[3] frequencies are played (Gao et al., 2014; Ross, Miyazaki, Thompson, Jamali, & Fujioka, 2014), with one frequency per ear (e.g., a tone of 525 Hz in the left ear, $\boldsymbol{f_1}$, and 531 Hz in the right ear, $\boldsymbol{f_2}$). When the two tones are listened to simultaneously, a pulse or beat is perceived at a frequency equal to the difference in frequencies (i.e., $\boldsymbol{f_1 - f_2}$; the previous example would produce a binaural beat of 6 Hz).

Binaural beats differ from stimuli used for evoking auditory steady state because binaural beats do not exist as a physical stimulus but as a combination of multiple physical stimuli. Although BB are not perceived in each ear individually, the perception of a binaural beat

[3] Between 3 Hz and 30 Hz difference.

between 3 Hz and 30 Hz is that of varying tone amplitude (AM). For frequency differences smaller than 3 Hz, the listener perceives separate auditory events that change location (e.g., a rotating speaker), whereas larger frequency differences (> 30 Hz difference) are perceived as two separate tones (Gao et al., 2014; Ross et al., 2014).

The neural mechanism for the perception of binaural beats is still debated by researchers. As binaural beats are a perceptual phenomenon involving stimulation of both ears, the first possible location of neural encoding would be the olivary nuclei because it is the first location of bilateral connections (Nicholls et al., 2012; Squire et al., 2013). Becher et al. (2014) compared BB and AM stimulation in 10 presurgical epilepsy patients while collecting surface EEG over the head and intracranial EEG in the temporal lobe. Their power analyses primarily uncovered decreases in power at the harmonics of the stimulation beats, although ASSR in response to AM stimulation was also observed (Becher et al., 2014). Ross et al. (2014) used AM and BB stimulation with continuously varying beat rates between 3 Hz and 60 Hz in order to examine binaural hearing mechanisms within and outside of the frequency difference range for binaural beat perception. Much of their analyses focused on very low frequency differences where the differences are thought to be involved in sound localization (Ross et al., 2014). However, they also observed BB-evoked gamma oscillations at every frequency difference, the largest gamma power increase observable with a 40 Hz difference between ears (Ross et al., 2014). The authors suggested that this gamma increase provides a mechanism for the precise timing and synchronization of cortical neuron firing (Ross et al., 2014). Gao et al. (2014) found that different brain areas were activated during varying binaural-beat stimulation, including central and other non-auditory areas, which suggested top-down control. Solcà, Mottaz, and Guggisberg

(2016) found increased alpha-band oscillation synchrony between the left and right auditory cortices, which they suggested indicated binaural integration.

Binaural Beats vs. Amplitude-Modulated Tones. Amplitude-modulated tones are similar to binaural beats in the pulse/beat perception, but the pulse is due directly to physical properties of the stimulus, specifically two frequencies added together, and the ability to detect the pulsing in each ear separately. Unlike binaural beats, the beats from an amplitude-modulated tone can be heard by listening with one ear only. ASSR (frequency following or entrainment) can be a result of amplitude-modulated tone stimulation, sometimes referred to as monaural, physical, or peripheral beats (Ross et al., 2014), but not binaural beat stimulation (Gao et al., 2014; Solcà, Mottaz, & Guggisberg, 2016), indicating that perception of pulses in each case is processed differently by the brain.

Pratt and colleagues (2009, 2010) studied binaural beats compared to amplitude-modulated tones using ERPs and found no source space differences between the conditions (both were left temporally located), although they did find significant differences in beats-evoked oscillation amplitude, with AM driving higher ERP component amplitudes. Becher, Höhne, Axmacher, Chaieb, Elger, and Fell (2014) also found power and phase changes related to AM and BB stimulation in the temporal lobe, including an ASSR to the 40 Hz AM stimulus. To date, there is no additional evidence regarding the neural mechanisms behind how binaural beats are perceived and processed in the human brain.

EEG for Evaluating Auditory Processing. EEG is a common tool for measurement in auditory paradigms due to its high temporal resolution. Key areas for observation vary depending on the question at hand (e.g., research about language may measure from left-lateralized language areas specifically), but EEG is generally used for measuring from cerebral cortex and,

in the case of auditory stimulation, auditory cortices specifically. ERPs are a particular EEG paradigm that involves collecting hundreds of short (e.g., one second) stimulus presentations, then averaging the waveform by sensor or source space. Many ERP studies center around stereotypical components that occur in predictable time ranges and sometimes predictable brain areas. The approach taken in this project, however, is not ERP but time-frequency decomposition, which is later followed up with functional connectivity analysis.

FFT: Power and Phase Analysis. In order to examine neural response to oscillating stimuli, EEG waveforms must be broken down into their component frequencies, representing the underlying network oscillations contributing to the signal at each electrode. Using techniques such as the Fast Fourier Transform (FFT), the collected waveforms from each electrode can be decomposed into component sine waves at specified frequency bands, each with their own amplitude (referred to as "power" after a transformation) and phase values.

Increased power in a particular frequency is thought to indicate the cooperation and coordination of large populations of cells (Başar, Başar-Eroglu, Karakaş, & Schürmann, 2001; Başar, Başar-Eroğlu, Güntekin, & Yener, 2013). Defined frequency bands (named delta [0.5 - 3.5 Hz], theta [4 - 7 Hz], alpha [8 - 13 Hz], beta [15 - 28 Hz], and gamma [30 - 70 Hz]) may be used in combinations as building blocks for sensory-cognitive processes, as each is present throughout the brain and has been associated with multiple cognitive processes (Başar et al., 2001; Başar et al., 2013).

The cellular mechanisms to produce these rhythms are unknown, though various hypotheses exist. For example, Bazanova and Vernon (2014) suggested that rhythmic GABA-ergic input from an inter-neuronal network may be central to producing the spindle-like segments of alpha rhythms produced in high-threshold bursting thalamocortical neurons.

Relatedly, the Pyramidal-Interneuron Gamma (PING) hypothesis proposes a mechanism wherein the gamma cycle is created by groups of neurons firing with brief pauses in between (Krupa, Gielen, & Gutkin, 2014). According to PING, each cycle has four main steps: the cycle is initiated by the activation of pyramidal neurons; this activation results in locally-connected interneurons firing; the interneurons, in turn, provide feedback inhibition to the pyramidal cells, silencing them temporarily; and finally, the cycle starts over as the inhibition wears off and the pyramidal cells are able to fire again (Krupa, Gielen, & Gutkin, 2014).

In addition to changes in amplitude, the phase of the neural response in each frequency band is calculated from the angle of the complex FFT. For each trial period with the same stimulus, it is assumed that the stimulus is at the same phase at the same time point, and phase-locking refers to the coherence in phase of neural response across trials. The inter-trial phase coherence (ITPC; aka inter-trial coherence, ITC; aka phase-locking factor, PLF) ranges between 0, meaning completely non-phase-locked across trials, and 1, meaning perfectly phase-locked across trials. ITPC is measured for a single sensor or source space, so it is not a measure of connectivity between sensors or areas; instead, it is a measure of the stability of the neural response over multiple presentations of the same signal. If the sinusoidal stimulus begins at the same phase each time it is played, then every trial has the same stimulus phase progression, and the stability of neural response over multiple presentations could be encoding stimulus phase.

Connectivity Analysis. Connectivity analysis, as defined for this project, is a set of analyses that seek to characterize the interactions between brain areas using the neural activity measured by EEG or MEG during a mental task. Connectivity is described as “task-dependent information transfer between brain regions” (Haufe, 2012). This group of analyses is one of the

intermediate steps bridging small scale (e.g., single-neuron physiology) and large scale (e.g., neuroimaging) information towards the ultimate goal of unified brain modeling (Haufe, 2012).

Various calculations and models fall under the umbrella term "connectivity analysis." At its simplest, connectivity is indicated by coherence between sensors, but this is a flawed approach. Due to electromagnetic field spread, the same brain activity is registered, to varying degrees, in multiple sensors, with deeper brain activity being registered in more sensors than more superficial brain activity. Therefore, source analysis, wherein algorithms and specific head models are used to estimate the within-brain source of scalp-measured activity, is typically performed before connectivity analysis. Connectivity can be measured functionally (covariation without direction) or effectively (assumption-based models and statistical techniques to indicate directional causality between areas) between sensors or source areas.

EEG connectivity in its simplest definition is increased communication between two indicated brain areas. Given this definition, an increase in connectivity over transient stimulation only indicates which areas are working together. Regarding potential therapies, the goal would be to induce structural connectivity via long-term potentiation (LTP) and repeated stimulation with a stimulus known to increase functional connectivity. Connectivity with the frontal cortex is of particular interest because of its importance in executive function and regulation when connected to other brain areas (e.g., top-down control).

Potential Therapeutic Application of Binaural Beats: Increases in Connectivity with Prolonged Use. It has been suggested that binaural beats affect functional connectivity. Gao et al. (2014) found stimulus-dependent changes in connectivity between frontal and posterior (occipital, temporal) areas, frontal and central (i.e., corresponding to M/EEG central electrodes)

areas, and adjacent (e.g., central and parietal) brain areas during BB stimulation[4], including increases in connectivity between temporal and frontal electrodes. If these effects are lasting or could be trained using biofeedback, binaural beats could serve as an evidence-based therapy or therapeutic aid in disorders with connectivity impairments. A therapy that increased connectivity could improve long-distance connectivity and sensory integration in autism, as well as strengthen small-world network organization, which is affected in several psychiatric disorders. This project enhances our knowledge of binaural beat processing in a healthy young adult brain, which provides insight into mechanisms of related disorders in future studies.

Although binaural-beat-inducing music is commercially marketed as an alternative therapeutic agent, there is a lack of information regarding the neural mechanisms behind the perception or effect of binaural beats. Researchers and clinicians have suggested binaural beats as a potential therapeutic tool, in part because of the potential for binaural beats to increase the functional connectivity between cortices. However, the only study to examine connectivity changes related to binaural beats to date was Gao et al. (2014), and the analysis contained technical mistakes (e.g., a lack of statistical correction for multiple comparisons, calculating coherence in sensor space) as well as experimental flaws (e.g., control was non-modulated pink noise). One particular experimental flaw was the use of beat frequencies that were harmonics of one another (5 Hz, 10 Hz, 20 Hz, etc.) which can confound frequency analysis because the relationship between stimulus frequency and evoked power changes becomes unclear. For example, an increase in the power in 40 Hz after stimulation with both 10 Hz and 20 Hz could be because of either: (1) an increase in the fourth and second harmonics respectively, possibly as an

[4] Decrease in connectivity between right temporal, frontal, and occipital electrodes; between frontal and occipital electrodes; and between central and parietal electrodes. Increase in connectivity between left frontal and right temporal electrodes; and between left frontal and left temporal electrodes.

artifact of measuring large populations of neurons with each sensor, or (2) an increase in gamma due to another process such as precise neural firing.

Current binaural beats delivery methods mimic this style of presentation (e.g., CDs or mp3 files with several minutes of binaural beats, typically overlaid with other sounds to make listening more comfortable). While studies observing long-term changes in functional connectivity are sparse, clinical applications to increase connectivity would likely take the form of repeated exposure to several minutes of binaural beats. For example, Fingelkurts, Fingelkurts, and Kallio-Tamminen (2016) observed long-term changes in functional connectivity, including an increase in the frontal default mode network operational synchrony, after instructing participants in a meditation class which required them to meditate daily for 20 minutes for four consecutive months. For opioid-dependent patients undergoing at least six months of methadone treatment, functional connectivity was corrected to that of healthy controls (Fingelkurts, Fingelkurts, Kivisaari, Autti, Borisov, Puuskari, Jokela, & Kähkönen, 2009). While these studies do not utilize auditory therapies, along with the understanding of long-term potentiation as needing multiple stimulus presentations these studies suggest a therapy consisting of multiple sessions spread over several months.

Given the ultimate structure for a potential therapy with binaural beats, determining the length of stimulation for each session is a critical but perplexing problem. Vernon, Peryer, Louch, and Shaw (2012) failed to find any power changes related to binaural beats during one-minute stimulation periods, prompting Gao et al. (2014) to stimulate with binaural beats for five-minute periods which were later analyzed in one-minute time bins. Because Gao et al. (2014) observed connectivity changes during this period, we opted to maintain the stimulation length while improving upon other elements of the study as described above.

Hypotheses and Goals

The central hypothesis of this study is that BB promotes increases in connectivity not induced by AM beats. In this study, we compare BB and AM stimulation using EEG measures of brain steady state response and connectivity. Specifically, we evaluate the following in young, healthy adults:

I. Replication of the findings in Gao et al. (2014) using frequencies that are not harmonics of each other:
   a. Relative power increases and decreases as a result of BB stimulation specifically, which may occur in the same or different frequency bands relative to the stimulation frequency.
   b. Extent of entrainment or steady state response from BB stimulation.
   c. BB stimulation effects on functional brain connectivity.

II. Comparison of BB and AM stimulation using relative power, phase-locking, and functional connectivity analyses.

III. Assessment of changes in EEG measures over time and evaluation of response to continuing exposure.

By examining auditory illusions (Pratt, Starr, Michalewski, Dimitrijevic, Bleich, & Mittelman, 2009; Ioannou, Pereda, Lindsen, & Bhattacharya, 2015) like binaural beats, we learn about the structure and function of our auditory system. In order to adequately examine the neural response to binaural beats, a comparable oscillating auditory stimulus needs to be used as a control condition in order to account for common pathways; however, the only non-ERP study that used AM as a control stimulus focused on temporal areas and did not utilize source analysis techniques. Furthermore, while clinicians are interested in the potential for binaural beats to

increase connectivity, the only previous study on this topic was experimentally and analytically flawed. Therefore, findings from this research can inform future evidence-based therapies for disorders where brain connectivity is decreased, such as major depressive disorder (Zhang et al., 2011) or autism (Belmonte et al., 2004).

Methods

Study Design

This exploratory within-participants study was conducted in a sound-attenuated room at an EEG laboratory on the research campus of the University of Oklahoma in Norman, OK. After determining eligibility (see below for inclusion/exclusion criteria), participants underwent one 2.5-hour[5] data collection session. All sessions were done in the late morning and afternoon in order to evaluate participants during a similar time in their circadian cycles where their likelihood of falling asleep was minimized[6]. Participants were monitored using 128-channel EEG to estimate the strength of connectivity between auditory cortices bilaterally and connectivity of response frequencies from the auditory cortex to other cortices.

Procedure

Participants. Participants (64% female) were recruited using University email (including OUMM listserve) and by word of mouth. Upon arrival at the laboratory, participants were provided with an IRB-approved consent form, detailing the purpose, risks, and benefits of the study. They were given as much time as they needed to read the consent form, and asked to sign

[5] Maximum, but times varied between participants due to individual factors, such as time spent reading the Informed Consent, time spent on breaks between conditions, and time spent on EEG net application and impedances, which is related to hair length and thickness as well as dead skin and oil on the scalp. A typical session would last 1.5 to 2 hours from participant arrival to participant departure.

[6] The interest of this study was in waking processing. Future studies may examine sleep processing; refer to the Discussion. The nature of the environment as dark and quiet in conjunction with repetitive stimuli and restriction of movement indicate that sleepiness should be eliminated as best as possible.

the form if they wished to participate in the study. The sample size of 15[7] participants for this study was based on effect estimates derived from the study by Gao et al. (2014) which found a large effect of binaural beats on the cortical EEG in young adults. The sample size estimate from power analysis using Gao et al. (2014) was nine participants from their strongest connectivity effects and 21 from their weakest connectivity effects. Power analysis of the power differences observed in our pilot data (collected on laboratory member volunteers while they listened to binaural beats and AM tones with the same equipment and setting) also indicated 15 participants to achieve power of .80.

Subject screenings were done by telephone or in person for key criteria (e.g., inclusions: age 18-35; exclusions: seizure disorder, ADHD, sleep debt), with further screening done at the laboratory. All participants were required to (1) be right-handed, (2) be able to perceive a series of binaural tones at 60 decibels without a hearing aid, (3) read or speak English, (4) have no recent history (<5 years) of mental illnesses or attention deficit disorders, and (5) be free from sleep debt as assessed by the Epworth Sleepiness Scale (score of 10 or less; Johns, 1991; Johns, 1992; Johns, 2000). Potential participants were excluded for (1) current recreational drug use, (2) daily intake of alcohol > 3 drinks per day in a week, (3) head trauma, loss of consciousness or general anesthesia in the past 6 months, (4) any chronic medical condition affecting the nervous system, (5) medications that would complicate the interpretation of the EEG (e.g., anticonvulsants, beta blockers, antidepressants), and (6) pregnancy, assessed via questionnaire. A trained graduate assistant conducted screens prior to the data collection session. If found to be eligible for participation, the participant was invited to come to the laboratory for a 2.5-hour data collection session.

[7] 16 participants consented, but one participant had to be excluded because the participant was unable to complete data collection.

Due to limited resources, we were not able to conduct audiometry testing, perception reporting, self-report of exposure to ear trauma or loud noises, medical checkup for earwax accumulation as well as other relevant factors such as illness, and an index of musical training and talent. However, our participants were excluded based on self-report of hearing loss, hard-of-hearing status, and/or any disorder affecting the nervous system (e.g., vertigo). Furthermore, the majority of participants were OU undergraduate and graduate students and all were young adults, indicating that they were not at risk for certain types of hearing loss such as age-related hearing loss or job-related hearing loss.

Setting. All data collection sessions were conducted during weekdays in a dimly lit, temperature-controlled (20 ˚C), sound-attenuated room. Participants were asked to abstain from any product containing caffeine or alcohol for at least 24 hours before testing. All data collection was done with participants seated with feet on the floor in the same room as the recording and stimulation equipment. Appointment times and equipment remained as consistent as possible between participants.

Data Collection Sessions. Any remaining screening was done at the beginning of the session, and the protocol was explained to the participant. After screening, consent, and introduction, the EEG net was applied to the participant's head.

Scalp sensors were applied at the beginning of each data collection session using a 128-channel EGI (Electrical Geodesics, Eugene, OR) EEG net. Each electrode consisted of a silver-chloride-plated carbon-fiber pellet connected by a 1-meter-long shielded wire to a gold-plated pin. The pellet was surrounded by a sponge and plastic pedestal wall, with the sponge soaked in potassium chloride saline solution. See Figure 2 for the channel configuration.

On average these nets took approximately 15-20 minutes to apply using standard EEG methods. Participants were first asked to remove glasses, jewelry, and hair fasteners. Next, participants were measured for head circumference, which would indicate the EEG net size to use. While the net was soaking in pre-prepared potassium chloride saline solution for 5-minutes, participants were measured to find and mark (with grease pencil) their Cz location. A towel was draped over the participant's shoulders to catch electrode drips. The participant was asked to lean forward slightly and keep their eyes closed, and during this time the experimenter applied the net to the participant's head, using Cz and facial features like the ears and nasion to guide the application. Immediately following, factors influencing participant comfort, such as saline drops on the face or hair over the eyes, were addressed. With the participant comfortable, the experimenter fitted the net to the participant's head using the face straps and their fasteners. Experimenters confirmed proper net application by checking alignment of the net to facial features (e.g., nasion bar at the top of the nose, ears comfortably through the net's ear holes, Cz electrode on top of the Cz grease pencil mark, midline electrodes aligning with the center of the face, Cz lying approximately over the spine if participant sat with a straight back). Next, electrodes were adjusted through the hair and gently rubbed against the scalp to ensure contact between the sponge and the scalp (such that each electrode pedestal was perpendicular to the scalp). Finally, the connector was inserted and locked into the amplifier.

Impedances were checked using the NetStation software setting for impedances. If an electrode was shown on the display as out of the acceptable range (> 20 kΩ), then the experimenter used a plastic eyedropper to add more saline solution to the sponge and moved hair from under the electrode to improve the conductance. In general, experimenters aimed to get every electrode within the acceptable impedance range. Due to varying head shape, hair styles,

and other unknowable factors such as buildup of dead skin on the scalp, some participants offered difficulty for particular sensors; however, each participant had a maximum of three unacceptable electrodes which were subsequently removed from data analysis. Impedances were run just prior to the first condition as well as after each of the second, fourth, and sixth conditions. Biocalibrations[8] followed (5-minutes maximum) and then the auditory stimuli presentation protocol (1 hour 40 minutes).

Next, they donned sound-isolating, etymotics earphones, and the experimenter verbally confirmed that the participant could hear the tones. Etymotic earphones were used to reduce electronic interference that can create signal artifacts[9] in the EEG recording. Participants were instructed to sit still with their eyes faced forward at a focal point on the screen of the stimulus presentation computer. Biocalibrations were collected. Participants were instructed to listen to the tones presented to them during stimulation blocks that were interchanged with blocks of rest, including opportunities to stretch or go to the restroom if desired.

The condition presentation order was randomized between participants. The conditions were: 25 Hz BB 3-sec 6 Hz BB 3-sec, 25 Hz AM 3-sec, 6 Hz AM 3-sec, 25 Hz BB 5-min, 6 Hz BB 5-min, 25 Hz AM 5-min, and 6 Hz AM 5-min.

- The 3-sec conditions were presented as an ERP study with multiple trials and inter-trial intervals (ITI); each of the 100 trials had a stimulus duration of three seconds and a randomized ITI between 1500ms and 2000ms.
- The 5-min conditions were presented as continuous exposure to the stimulus for five minutes.

[8] 1) Eyes open/ahead for one minute, 2) Eyes closed/ahead for one minute, 3) Look up/down for three sets, 4) Three deep breaths, and 5) Grind teeth for ~3-seconds.
[9] Other precautions against signal artifacts were the elimination of fluorescent lights, using an EM meter to find sources of interference, and reducing connections between electrical cords.

Stimulus presentation was equal (i.e., five minutes of exposure) for every condition, but 3-sec conditions included additional rest time in the form of intertrial intervals (approximately 2.5 to 3.5 extra minutes total from the ITI).

Condition presentation order was randomized by participant in order to avoid fatigue and carry-over effects. Participants were monitored for safety and data quality control throughout the data collection by a trained experimenter. While EEG is relatively noninvasive and our participants were healthy young adults, it is always possible when working with human subjects that a participant will need assistance in some way or need to leave the study, necessitating the continual presence of a human experimenter. The most pressing example of threat to data quality was participant sleepiness because (1) the environment and equipment were not arranged for sleep, and (2) processing of auditory stimuli can be affected by sleep (Tan et al., 2017) and this study aimed to study wakeful processing. Therefore, participants were monitored for signs of sleep (e.g., head nodding, closing eyes). Additionally, electrical signal artifacts were minimized prior to data collection, such as by turning off fluorescent lights and minimizing auditory noises; however, the environment and recording were also monitored during collection and troubleshooting (e.g., moving cords from near participants' feet due to an artifact) was performed as necessary.

Data Collection and Analysis

EEG is the method of choice for examining time-sensitive cortical processes in humans because of its high-temporal resolution. In this study, we collected 128 channels of EEG (EGI, Eugene, OR, USA); all were amplified separately, band-pass filtered (LOW BAND: 0.1, HIGH BAND: 65 Hz), 60 Hz notch filtered, and digitized at 1000 Hz. On our EGI nets, the automatic reference electrode is Cz and the ground is an electrode placed on the midline two electrodes

posterior to Cz. Data were re-referenced to common average reference prior to source and connectivity analyses. Data artifact identification and deletion was performed by visual identification and independent components analysis (ICA), where distinctive waveforms and changes in amplitude (e.g., large-amplitude curved deflections accompanied by a distinctive topographic map in its ICA component for blinks) were identified and corrected via component removal or trial rejection.

Relative power analysis for BB (Aim Ia) and AM (Aim II) were assessed using frequency decomposition done with the Fast Fourier Transform (FFT), which is an algorithm that uses the Fourier series to deconstruct any periodic data collected over time (i.e., a wave) into component sinusoidal waves of various frequencies. Each stimulation frequency and corresponding first harmonic are modeled as a sinusoid with its own amplitude and phase angle along with multiple other frequencies from 2 Hz to 60 Hz.

The FFT was conducted on both the 3-sec and 5-min data for all conditions using EEGLAB (Delorme & Makeig, 2004), an open source toolbox for EEG analysis in MATLAB, under its public GNU license. An output of the FFT is frequency power, a transform of the amplitude, in a time resolution inversely proportionate to the frequency resolution. Additionally, using the angle of the complex FFT, the phase of each sinusoid can be calculated and compared across trials, resulting in phase-locking measures (here, intertrial coherence or ITC).

The entire stimulation period was analyzed from 2 Hz to 60 Hz for each the 3-sec and 5-min data, although the 5-min data was first placed into 30-second time bins while the 3-sec data was analyzed in its entirety. FFT was conducted for individual electrodes for a sample of electrodes[10]; FFT was only conducted on these electrodes, which were selected in order to

[10] Left auditory: E45, E58; Left central: E20, E30, E35; Left frontal: E12, E23; Left parietal: E31, E47; Right auditory: E96, E108; Right central: E105, E110, E118; Right frontal: E3, E5; Right parietal: E80, E98

address the a priori hypotheses about activity in particular electrodes as well as to conduct exploratory analysis on adjacent areas. Exploratory electrodes were chosen based on the classification of 128-channel EEG into specific brain areas by Butler and Trainor (2012).

Our primary target frequencies were the stimuli frequencies (i.e., 6 Hz and 25 Hz) and their second harmonics (e.g., 12 Hz and 50 Hz). These frequencies were chosen in order to evaluate ASSR which can be observed at both the frequency of stimulation as well as the first harmonic due to the dynamics of large populations of neurons measured by EEG sensors on the scalp.

Frequency power during stimulation was compared to frequency power during the baseline period[11] using an EEGLAB FFT plotting function set to mask non-significant power changes using permutation statistics ($\alpha = 0.10$ after the correction for multiple comparison using false detection rate). Plots were masked at trend level as the first step in order to more clearly observe patterns in the data, with this visual analysis followed by more rigorous testing via statistical models. Absolute power was calculated over multiple time bins (300 time bins for each FFT run, creating ~11.6 ms bins for the 3-sec conditions and ~100 ms bins for the 5-min conditions), and an RM ANOVA was done comparing all four conditions with main effects for stimulus type (AM vs. BB) and stimulus frequency (6 Hz vs. 25 Hz) as well as an interaction between the two.

Entrainment for BB (Aim Ib) and AM (Aim II) were assessed by determining if the frequency of the beat or modulation was eliciting a relative power response and/or phase-locking response in the same frequency. Measurements of phase-locking are done after transformation of the data from temporal space into frequency space (here through the FFT) using the angle of the

[11] For 3-sec conditions: the one second period immediately prior to the trial. For 5-min conditions: 30 seconds of baseline activity isolated for each subject from their biocalibrations (one minute eyes open) data.

complex FFT result. A phase-locked neural signal shows coherence in phase across trials. Therefore, phase-locking can be measured using inter-trial phase coherence (ITPC; aka inter-trial coherence, ITC, and phase-locking factor, PLF). ITPC ranges from 0 (completely non-phase-locked across trials) to 1 (perfectly phase-locked across trials). ITPC is measured within a single sensor or source space, not across them, so it is not a measure of connectivity but rather a measure of stability of the neural response over multiple presentations of the same signal. Because multiple presentations are required to conduct ITPC, these analyses were only conducted on the 3-sec data, which consisted of 100 repetitions of each stimulus frequency. Similar statistical analyses were conducted for phase-locking as frequency analysis.

Changes in functional brain connectivity during BB (AIM 1c) and AM (Aim II) were assessed using connectivity analyses at (1) auditory cortices (E45/T_7, E108/T_8), (2) frontal (E23 between Fp_1/ F_3 and E3 between Fp_2/F_4) cortex, (2) nearby central (E35, E110) and parietal (E47, E98) areas, and (3) the dipole from source analysis with the maximum power in the frequency of interest for each condition. These sensors were chosen a priori to analysis, and connectivity with other dipoles was not explored. In order to minimize the number of comparisons, dipoles central to frontal and auditory areas were chosen bilaterally. Auditory cortex was chosen due to the nature of the stimulus, and frontal cortex was chosen due to its particular significance in executive function and pathology. Connectivity with the dipole with the maximum power was data-driven and exploratory.

Source analysis, or the triangulation of specified neural activity to particular brain areas via physiological assumptions and model fitting, was conducted with a standard Boundary Element Method (BEM) volume conduction model of the head (i.e., head model) and the Dynamic Imaging of Coherent Sources (DICS) algorithm using FieldTrip, an open source

MATLAB toolbox for EEG and MEG analysis (Oostenveld, Fries, Maris, & Schoffelen, 2011; Donders Institute for Brain, Cognition and Behaviour, Radboud University Nijmegen, the Netherlands; See http://www.ru.nl/neuroimaging/fieldtrip). The head model in a source analysis describes how currents flow through the brain and its surrounding tissue based on the geometry and tissue composition of the head. BEM specifically is derived from the Colin 27 MRI and considers the skin, skull, and brain surfaces (Oostenveld, Stegeman, Praamstra, & van Oosterom, 2003). DICS is one of several source reconstruction algorithms for beamformer dipole analysis available for EEG data for frequency or time-frequency domain data.

In order to examine specific frequencies over time, we required an algorithm that would allow for time-frequency domain EEG data, which substantially limited the available algorithms. DICS is a relatively recent algorithm that improved localization of sources from EEG compared to previous algorithms (Japaridze, Siniatchkin, Muthuraman, Raethjen, Stephani, & Moeller, 2013). DICS was also chosen because of the emphasis of this algorithm on the identification of functionally coherent areas and the characterization of the interactions between areas over time (Gross, Kujala, Hämäläinen, Timmermann, Schnitzler, & Salmelin, 2001). Performing source analysis prior to connectivity analysis reduces the amount of comparisons and provides clearer information about the brain areas involved than only looking at coherence in electrodes. For all connectivity analysis we specifically examined the frequencies of interest (6 Hz, 12 Hz, 25 Hz, and 50 Hz) for each condition.

In addition to artifact removal and bandpass filtering of raw EEG data, several methods were used to differentiate signal from noise according to best practice for the source and connectivity analyses (Oostenveld, 2017). Source and connectivity were calculated as grand averages of both trials and subjects (images of averages presented in Appendices). For source

analyses only, a whole trial (including the one-second-long pre-trial period) common filter was calculated using the DICS algorithm, and the filter was subsequently applied to the source analysis calculations of the pre-trial one-second baseline and the mid-stimulus one-second period. Additionally, we used a noise-correcting feature of DICS that subtracts the noise estimate, which is estimated as the smallest eigenvalue of the cross-spectral density matrix. Finally, all source power and coherence calculations are presented as percent changes from baseline (e.g., difference in power during stimulation and baseline divided by the power during baseline). The recommended statistical masking of DICS source and connectivity images was not available due to computing resources restrictions; when we attempted to provide a substitute with paired t-tests on representative dipoles of maximally activated areas, none of the comparisons met the Bonferroni correction alpha (see Discussion).

Responses to continuing exposure (Aim III) were assessed by analyzing the 5-min conditions with the same techniques used on the 3-sec conditions. The data collected during the 5-min stimulation periods were analyzed altogether as well as in 30-second time bins, which were compared to a baseline 30-second period.

Finally, our sample was restricted to healthy young adults, and excluded potential participants based on age, certain disorders (e.g., epilepsy), certain medications (e.g., anticonvulsants, antidepressants), alcohol consumption, pregnancy, and sleep debt. One possible covariate that was not controlled for experimentally was gender; therefore, gender was explored as a covariate for the statistical models. Although condition presentation was randomized by subject, order of presentation was also investigated as a possible covariate. Furthermore, individual subjects were investigated for individual differences.

Results

Results of the FFT by condition and electrode can be found in Appendix: FFT Images. Summaries of the FFT results are presented in two parts: Power Analysis and Phase-Locking.

Power Analysis

Using the figures output from the FFT in EEGLAB, we searched for patterns in the change in power during stimulation relative to baseline in order to address Aims I and II. Table 1 summarizes the results in the beat/modulation frequencies (6 Hz, 25 Hz) and their second harmonics (12 Hz, 50 Hz) for each condition and electrode of interest. For our exploratory analysis, we were interested in increases or decreases in power across any frequency (2 Hz to 60 Hz) that were consistent across the three seconds of stimulation. Refer to Appendix: FFT Images (Figures 4-75, top graph) for the changes in frequency power (2 Hz - 60 Hz) from baseline across the three seconds of stimulation.

Table 1

Trend-level ($p < .10$) significant changes in power during the middle second of stimulation as compared to baseline during the 3-sec stimulation (3 s) conditions

Stimulus Type	Stimulus Beat/Mod. Frequency	Analysis Freq. of Interest	Electrode Location	Direction
Amplitude Modulation (AM)	6 Hz	6 Hz	E45 (Left auditory)	Increase
			E96 (Right auditory)	Increase
			E31, E47 (Left parietal)	Increase
		12 Hz	E96 (Right auditory)	Increase
			E31 (Left parietal)	Increase
			E30 (Left central)	Increase
		25 Hz	-	-
		50 Hz	-	-
	25 Hz	6 Hz	-	-
		12 Hz	E12, E23 (Left frontal)	Decrease
			E5 (Right frontal)	Decrease
			E20, E30 (Left central)	Decrease
			E105, E118 (Right central)	Decrease
		25 Hz	E23 (Left frontal)	Increase
		50 Hz	E58 (Left auditory)	Increase
			E96 (Right auditory)	Increase
Binaural Beats (BB)	6 Hz	6 Hz	E12 (Left frontal)	Decrease
			E31, E47 (Left parietal)	Decrease
			E20, E30, E35 (Left central)	Decrease
			E105, E110, E118 (Right central)	Decrease
		12 Hz	-	-
		25 Hz	-	-
		50 Hz	-	-
	25 Hz	6 Hz	-	-
		12 Hz	E12, E23 (Left frontal)	Decrease
			E5 (Right frontal)	Decrease
			E30 (Left central)	Decrease
			E105, E118 (Right central)	Decrease
		25 Hz	-	-
		50 Hz	E58 (Left auditory)	Increase
			E96 (Right auditory)	Increase

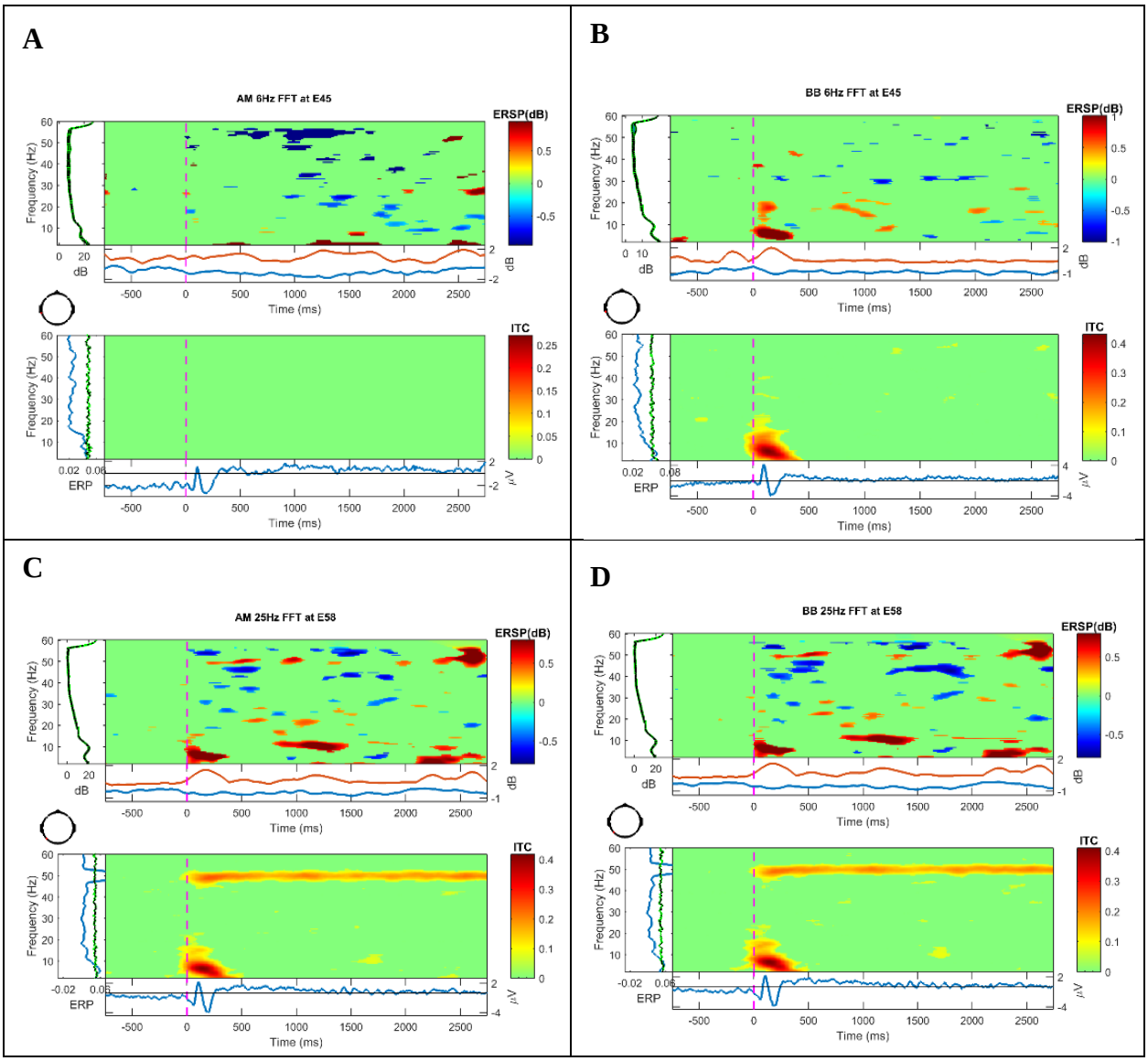

Figure 1. Comparative FFTs. Stimulation period is baseline corrected. Green indicates no significant change from baseline using permutation statistics (α = .10 with false detection rate correction for multiple comparison). X-axis is time, y-axis is frequency. Top graph within each quadrant: Darker blues indicate a decrease in frequency power while darker reds indicate and increase in frequency power from baseline. Bottom graph within each quadrant: Darker reds indicate an increase in phase-locking/inter-trial coherence (ITC) between trials at the specified frequency. A and B: Frequency decomposition done with FFT for E45 (left temporal, auditory cortex) from 2-60 Hz during the one second prior to stimulation and the three seconds during

stimulation with 6 Hz amplitude-modulated tone (A) or 6 Hz binaural beats (B). C and D: Frequency decomposition done with Fast Fourier Transform (FFT) for E58 (left temporal, auditory cortex) from 2-60 Hz during the one second prior to stimulation and the three seconds during stimulation with 25 Hz amplitude-modulated tone (C) or 25 Hz binaural beats (D).

Similarly, the same FFT pattern searching was done for the 5-min conditions for the five minutes (in 30-second bins) of stimulation as compared to thirty seconds of baseline activity isolated for each subject from their biocalibrations (one minute eyes open) data. Visually examining the FFT results for the 5-min conditions provided less information. None of the conditions showed changes in the beat/modulation frequencies (6 Hz, 25 Hz) or their second harmonics (12 Hz, 50 Hz) except that all conditions in most electrodes showed an increase in power centered at about 9-10 Hz (full range of ~6-13 Hz) for most electrodes. Exploratory data analysis uncovered dynamic activity in 55-60 Hz, which primarily showed a decrease in power for AM 25 Hz across electrodes, an increase for BB 25 Hz across electrodes, and a mixture of increases and decreases depending on the electrode for AM 25 Hz and BB 6 Hz. Power in 55-60 Hz during BB 25 Hz appeared to increase over time for bilateral auditory (E45, E58, E108, E96), left parietal (E47), right frontal (E3, E5), and right central (E118, E110). For AM 6 Hz, the decreases in power in 55-60 Hz were located in bilateral auditory (E45, E108) and left parietal (E31) while increases in power were observed in bilateral frontal (E3, E5, E12, E23), bilateral central (E20, E30, E110, E118), and bilateral parietal (E47, E80). For BB 6 Hz, the decreases in power in 55-60 Hz were observed in bilateral frontal electrodes (E5, E12), left auditory (E45), and right parietal (E98).

Statistics. In order to examine the effects of stimulation frequency and duration (3-sec vs. 5-min) on power changes in frequencies of interest, linear mixed effects models (LMEs) were run in MATLAB that accounted for the within-subjects design and possible mean and/or slope differences due to the nested nature of the data within subjects. The same model was run for each area of interest (left and right auditory, frontal, central, and parietal), with the power of each area calculated by averaging the two electrodes used for FFT in that area.

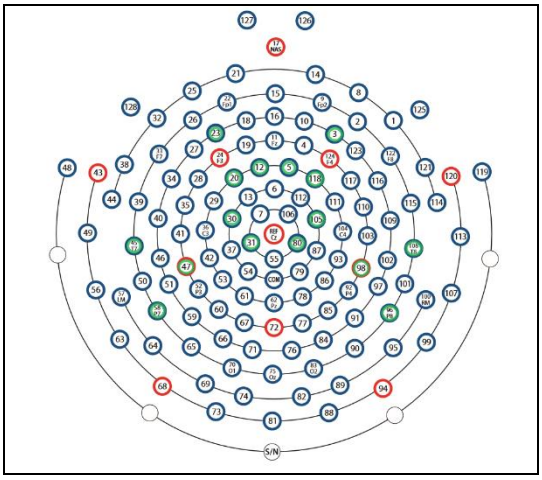

Figure 2. Bird's-eye view of the electrode placements, with the electrodes used in the LMEs indicated by an inner green ring and the participant's face pointing towards the top of the figure.

The mixed linear models used the following linear equations:

$$Y_{ij} = \beta_{oj} + \beta_{1j} * X_{1ij} + \beta_{2j} * X_{2ij} + \beta_{3j} * X_{3ij} + \beta_{4j} * X_{2ij} * X_{3ij} + r_{ij}$$

$$\mu_{oj} = \varepsilon_{00} + \varepsilon_{01} * X_{4j} + \varepsilon_{02} * X_{5j} + \varepsilon_{03} * X_{6j}$$

$$\mu_{1j} = \varepsilon_{10} + \varepsilon_{11} * X_{4j} + \varepsilon_{12} * X_{5j} + \varepsilon_{13} * X_{6j}$$

$$\mu_{2j} = \varepsilon_{20} + \varepsilon_{21} * X_{4j} + \varepsilon_{22} * X_{6j}$$

Where Y_{ij} is power in the frequency of interest, X_{1j} is time in the trial corresponding to the window used in the FFT (ms), X_{2j} is stimulus type (AM or BB), X_{3j} is beat/modulation

frequency in the stimulus (6 Hz or 25 Hz), $X_{4j}$is gender (man or woman), X_{5j} is the order of presentation (ordinal from 1 to 8), and X_{6j} is a nominal subject identifier.

3-sec condition LMEs. All areas except the left auditory cortex had the same pattern regarding power in 12 Hz. Stimulation with a beat/modulation frequency of 6 Hz predicted higher power in 12 Hz than stimulation with a beat/modulation frequency of 25 Hz (β_{3j} = -0.28 ± 0.12, $p < .05$). Additionally, the positive interaction between stimulus type (AM vs. BB) and beat/modulation frequency was significant with a greater effect than the main effect of beat/modulation frequency (β_{4j} = 0.47 ± 0.22, $p < .05$), indicating that binaural beats moderates the effect of beat/modulation frequency such that combining BB with 25 Hz stimulation changes the direction of the effect and makes the power in 12 Hz increase. In the left auditory cortex, the interaction was not significant and the main effect of beat/modulation frequency was reversed such that AM 25 Hz and BB 25 Hz had higher power in 12 Hz than AM 6 Hz and BB 6 Hz (β_{3j} = 0.06, $p < .05$).

The same general pattern emerged for power in 6 Hz as power in 12 Hz where 6 Hz stimulation predicted higher power in left electrodes[12] (β_{3j} = -0.12 ± 0.056, $p < .05$) while stimulating with BB 25 Hz increased (rather than decreased) power in all brain areas (β_{4j} = 0.48 ± 0.17, $p < .05$). Left central cortex showed the same pattern but with an additional main effect for stimulus type such that amplitude-modulated tones had higher power in 6 Hz than binaural beats (β_{2j} = -0.40, $p < .05$). The significant positive interaction effect indicated that combining binaural beats with 25 Hz beat/modulation frequency overcame the main effects to increase power in 6 Hz for BB 25 Hz in the left central cortex. Unlike 12 Hz, power in 6 Hz showed

[12] A positive main effect estimate for stimulation frequency was averaged across left auditory, left central, left frontal, and left parietal electrodes.

lateralization because the main effect of beat/modulation frequency was not significant in right auditory cortex and right central cortex and was reversed in direction for right frontal (β_{3j} = 0.04, $p < .05$) and right parietal (β_{3j} = 0.05, $p < .05$) electrodes.

Regarding ASSR, there is left lateralization in 6 Hz but not 12 Hz. Left auditory cortex in 12 Hz as well as right frontal and right parietal in 6 Hz switch directions in their main effect for beat/modulation frequency such that stimulating with 25 Hz increases (rather than decreases) power in the analysis frequency. Right frontal and right parietal still have a significant interaction effect such that the combination of binaural beats with a beat/modulation frequency of 25 Hz multiplicatively increased power in 12 Hz.

All areas except the right central and left parietal cortices had the same pattern regarding power in 50 Hz. Stimulation with a beat/modulation frequency of 25 Hz predicted higher power in 50 Hz than stimulation with a beat/modulation frequency of 6 Hz (β_{3j} = 0.26 ± 0.11, $p < .05$). Additionally, the interaction between stimulus type (AM vs. BB) and beat/modulation frequency was significant (β_{4j} = -0.35 ± 0.24, $p < .05$), although the effect size in relation to the main effect of stimulus frequency was lateralized. For the left areas (auditory, frontal, central, and parietal) the interaction was stronger than the main effect of stimulus frequency (β_{4j} = -0.48 ± 0.23, $p < .05$), meaning that BB 25 Hz specifically caused decreased power in 50 Hz compared to AM 6 Hz. However, for right areas (auditory, frontal, and parietal) the interaction was also negative but weaker than the main effect of stimulus frequency (β_{4j} = -0.18 ± 0.12, $p < .05$), meaning that AM 25 Hz increased more in power in 50 Hz in comparison to AM 6 Hz than BB 25 Hz increased. The right central area had a negative main effect for beat/modulation frequency such that power in 50 Hz was lower for AM 25 Hz and BB 25 Hz than AM 6 Hz and BB 6 Hz (β_{3j} = -0.02, $p < .05$). The same was true for left parietal (β_{3j} = -0.06, $p < .05$). Also, right central had a

reversed direction for the significant interaction term (β_{4j} = 0.25, p < .05), meaning that that BB 25 Hz increased power in 50 Hz compared to AM 6 Hz.

The models for power in 25 Hz showed the same general pattern across brain areas as the models for power in 6 and 12 Hz. Generally, 6 Hz beat/modulation frequency induced higher power in 25 Hz than 25 Hz beat/modulation frequency (β_{3j} = -0.10 ± 0.048, p < .05), and BB moderated this effect such that BB 25 Hz had the highest power in 25 Hz[13] (β_{4j} = 0.39 ± 0.20, p < .05). For the right frontal area, the main effect of stimulus type was significant such that binaural beats had higher power in 25 Hz than AM tones (β_{2j} = 0.23, p < .05), while the main effect of stimulus frequency showed that 25 Hz conditions had higher power in 25 Hz than 6 Hz conditions (β_{3j} = -0.031, p < .05). The combination of BB and 25 Hz lessened the increase in power (β_{4j} = -0.10, p < .05), but BB 25 Hz still had higher power than AM 6 Hz.

Several grouping or random effects, which allowed for the variation of the fixed effects described above by grouping variables (gender, order of presentation, and subject), were significant[14] across all or most brain areas by frequency of interest. This approach is appropriate for nested data like this study (e.g., all eight conditions coming from one subject may share some variance due to being from the same subject, such as due to variations in resting frequency power). Initial 6 Hz power values at time zero varied by gender, order of presentation, and subject. The effect of time on power in 6 Hz varied by order of presentation and subject. The effect of stimulus type on power in 6 Hz varied by gender and subject. The same effects existed for 12 Hz, 25 Hz, and 50 Hz except there was no variation by gender for the effect of time on

[13] Positive interaction effect estimates for power in 25 Hz averaged over bilateral auditory, left central, left frontal, and bilateral parietal.

[14] Although the variation by these grouping effects was separated from the fixed effects described above, some further investigation of these effects may be warranted because of their significance. See Discussion.

power in 25 Hz and no variation by gender on initial power in 50 Hz values, the effect of time on power in 50 Hz, or the effect of stimulus time on power in 50 Hz.

Overall, the LME model did well describing the relationships between the predictors ($adj\ R^2 = 0.34 \pm 0.074$) for the 3-second conditions. The model accounted for an exceptional amount of variance in power in 50 Hz ($adj\ R^2 = 0.43 \pm 0.065$), with more than 50% of variance explained for bilateral central electrodes.

5-min condition LMEs. In order to address Aim III, the time bins were concatenated and the same LME model run on the 3-second conditions was run separately on the 5-minute conditions by frequency of interest and brain area. Time during stimulation and stimulus type (AM vs. BB) was non-significant in all brain areas and frequencies. The main effect of beat/modulation frequency (6 vs. 25 Hz) and the interaction between stimulus type and stimulus frequency were significant in every frequency of interest for at least one brain area. ASSR was primarily observed in the second harmonics (i.e., power in 12 Hz for the 6 Hz stimuli and power in 50 Hz for the 25 Hz stimuli)[15]. Although bilateral central electrodes showed ASSR for power in 25 Hz (β_{3j} = 0.091 ± 0.019, $p < .05$), the left parietal and right central were actually higher in power in 6 Hz with 25 Hz stimulation (β_{3j} = 0.10 ± 0.038, $p < .05$). In almost all cases[16], the interaction effect between beat/modulation frequency and stimulus type was negative; exceptions were left auditory (β_{4j} = 0.088, $p < .05$) and right parietal (β_{4j} = 0.14, $p < .05$) for power in 12 Hz as well as right frontal for power in 50 Hz (β_{4j} = 0.10, $p < .05$). Overall, the LME model did

[15] For 12 Hz: bilateral auditory, left central, right frontal, and right parietal (β_{3j} = -0.083 ± 0.027, $p < .05$). For 50 Hz: right auditory, right central, left frontal, and left parietal (β_{3j} = 0.080 ± 0.034, $p < .05$).

[16] For 6 Hz: right auditory, right central, right frontal, bilateral parietal (β_{4j} = -0.13 ± 0.11, $p < .05$). For 12 Hz: right central and bilateral frontal (β_{4j} = -0.15 ± 0.035, $p < .05$). For 25 Hz: right central (β_{4j} = -0.073, $p < .05$). For 50 Hz: bilateral auditory, right central, right frontal, and bilateral parietal (β_{4j} = -0.10 ± 0.020, $p < .05$).

a poor job fitting the 5-minute data, accounting for 1% or less of the variance in any particular frequency of interest or brain region ($adj\ R^2 = \ 0.0044\ \pm 0.0021$).

Phase-Locking Analysis

Using the figures output from the FFT in EEGLAB, we searched for patterns in the change in ITC during stimulation relative to baseline in order to address Aim Ib and Aim II. Specifically, we were interested in phase-locking in the frequency of stimulation and its harmonics that was consistent across the three seconds of stimulation. Results from this analysis are summarized in Table 2. Phase-locking was not examined for the 5-min conditions because, as explained in Methods, inter-trial phase coherence (ITC) and other phase-locking measures indicate consistency across trials, and the 5-min conditions did not have multiple trials.

Table 2

Trend-level ($p < .10$) significant changes in inter-trial coherence (ITC) during the middle second of stimulation as compared to baseline during the 3-sec stimulation (3s) conditions

Stimulus Type	Stimulus Beat/Mod. Frequency	Analysis Freq. of Interest	Electrode Location	Direction
Amplitude Modulation (AM)	6 Hz	6 Hz	-	-
		12 Hz	-	-
		25 Hz	-	-
		50 Hz	-	-
	25 Hz	6 Hz	-	-
		12 Hz	-	-
		25 Hz	-	-
		50 Hz	E45, E58 (Left auditory)	Increase
			E108, E96 (Right auditory)	Increase
			E47 (Left parietal)	Increase
			E98 (Right parietal)	Increase
			E110 (Right central)	Increase
Binaural Beats (BB)	6 Hz	6 Hz	-	-
		12 Hz	-	-
		25 Hz	-	-
		50 Hz	-	-
	25 Hz	6 Hz	-	-
		12 Hz	-	-
		25 Hz	-	-
		50 Hz	E45, E58 (Left auditory)	Increase
			E108, E96 (Right auditory)	Increase
			E47 (Left parietal)	Increase
			E98 (Right parietal)	Increase
			E110 (Right central)	Increase

DICS Source Analysis

To address Aim Ic and Aim II, source analysis of the frequency power was conducted using the DICS algorithm and a standard Boundary Element Method (BEM) head model in an attempt to identify the actual brain areas (as opposed to scalp areas seen in sensor space) that

produced activity in the frequencies of interest (6 Hz, 12 Hz, 25 Hz, and 50 Hz). The unmasked[17] images of this source analysis can be found in Appendix: DICS Source Analysis Images, and the results are summarized here.

Because the 3-second condition showed more consistent results in the sensor space analyses and showed a better fit with model predictions for change in power, additional analyses at the source level were conducted for the 3-second conditions only. For the 3-second conditions, source analysis could have been conducted for each of the one-second periods (one second baseline and each second of stimulation). For the purposes of this report, the baseline period and the one second in the middle of the stimulation period were chosen for analysis. The middle one-second time bin was chosen for the following reasons: (1) in order to compare to baseline to observe stimulus-driven activity, equal-length time bins had to be used (Oostenveld, 2017), so it was impossible to compare the entire stimulation period to baseline; (2) the middle second of stimulation was chosen because it was the least likely to contain artifacts such as onset-related increases in power and phase-locking in lower frequencies; and (3) comparing each of the during-stimulus time bins individually would greatly increase the computational resources needed as this process is computationally expensive, calling for large RAM, large amounts of permanent storage memory, and relatively large amounts of processing time.

Two separate summaries are provided here. Table 3 displays the dipole with the largest power during the middle one second of stimulation only. Table 4 reports the dipole with the largest power during the middle one second of stimulation after the baseline source analysis was subtracted. While dipole coordinates are most accurate for use in the connectivity analyses, the coordinate system is not universal. Descriptions of general areas for the dipole are provided.

[17] Baseline relative and noise controlled, but not filtered by statistical significance.

Table 3

Coordinates and locations of source dipoles with the maximum positive activation (by condition and frequency of interest) during the middle second of stimulation

Stimulus Type	Stimulus Beat/Mod. Frequency	Analysis Freq. of Interest	Maximum Dipole Coordinates (MNI)	Description of Dipole Location
Amplitude Modulation (AM)	6 Hz	6 Hz	[6, 40, -30]	Right anterior medial temporal
		12 Hz	[6, 40, -30]	Right anterior medial temporal
		25 Hz	[6, 40, -30]	Right anterior medial temporal
		50 Hz	[6, 40, -30]	Right anterior medial temporal
	25 Hz	6 Hz	[6, 40, -30]	Right anterior medial temporal
		12 Hz	[6, 40, -30]	Right anterior medial temporal
		25 Hz	[6, 40, -30]	Right anterior medial temporal
		50 Hz	[6, 40, -30]	Right anterior medial temporal
Binaural Beats (BB)	6 Hz	6 Hz	[6, 40, -30]	Right anterior medial temporal
		12 Hz	[6, 40, -30]	Right anterior medial temporal
		25 Hz	[6, 40, -30]	Right anterior medial temporal
		50 Hz	[54, -50, -46]	Right temporoccipital
	25 Hz	6 Hz	[6, 40, -30]	Right anterior medial temporal
		12 Hz	[6, 40, -30]	Right anterior medial temporal
		25 Hz	[6, 40, -30]	Right anterior medial temporal
		50 Hz	[6, 40, -30]	Right anterior medial temporal

It is immediately apparent when comparing Tables 3 and 4 that the maximum dipoles are in entirely different locations. Without the baseline activation subtracted, almost all of the

maximum dipoles reported were in the exact same right temporal location. With the baseline subtracted, therefore only reporting stimulus-driven activity, the areas identified were more varied by condition and frequency. This suggests that there is activity across frequencies coming from one source in the brain that is not stimulus-driven and needs to be subtracted.

Table 4

Coordinates and locations of source dipoles with the maximum positive activation (by condition and frequency of interest) during the middle second of stimulation with the activation from the baseline one-second period subtracted

Stimulus Type	Stimulus Beat/Mod. Frequency	Analysis Freq. of Interest	Maximum Dipole Coordinates (MNI)	Description of Dipole Location
Amplitude Modulation (AM)	6 Hz	6 Hz	[58, -10, 50]	Right parietal cortex
		12 Hz	[-30, -46, 74]	Left parietal cortex
		25 Hz	[66, 14, 22]	Deep right central cortex
		50 Hz	[70, -6, 22]	Right temporal cortex
	25 Hz	6 Hz	[10, -74, -58]	Right occipital cortex
		12 Hz	[-70, -34, -10]	Left temporal cortex
		25 Hz	[-22, 62, 30]	Left frontal cortex
		50 Hz	[58, 02, 46]	Right central cortex
Binaural Beats (BB)	6 Hz	6 Hz	[18, -90, -42]	Right cerebellum
		12 Hz	[-10, -102, 6]	Left occipital cortex
		25 Hz	[-34, -70, -14]	Left occipital cortex
		50 Hz	[-38, -50, -58]	Left occipital cortex
	25 Hz	6 Hz	[10, -74, -58]	Right occipital cortex
		12 Hz	[-70, -34, -10]	Left parietal cortex
		25 Hz	[50, -70, -42]	Right occipital cortex
		50 Hz	[58, 2, 46]	Right central cortex

AM 25 Hz and BB 25 Hz analyzed at the second harmonic of the modulation/beat frequency (50 Hz) both show the highest power in right central area at the same dipole (refer to Figure 83 for source analysis of 50 Hz ASSR for AM 25 Hz; refer to Figure 91 for source analysis of 50 Hz ASSR for BB 25 Hz). AM 6 Hz and BB 6 Hz do not maintain this pattern, with highest second harmonic (12 Hz) power in the left parietal and left occipital cortex respectively.

All conditions differed in the location of the maximum dipole for the beat/modulation frequency. Both BB 6 Hz and BB 25 Hz showed the highest power in the beat frequency in the most posterior parts of the right hemisphere, although the source location for BB 6 Hz placed it so ventral as to be in the cerebellum rather than cortex. The localization of activity to the cerebellum during source or connectivity analysis is likely a misplacement of activity from a subcortical location earlier in the auditory pathway because the further away from the scalp activity is generated, the more likely an error is made in source localization.

DICS Connectivity Analysis

DICS connectivity was run by dipole of interest[18], frequency of interest (6 Hz, 12 Hz, 25 Hz, and 50 Hz), and condition (AM 6 Hz, AM 25 Hz, BB 6 Hz, and BB 25 Hz). Each calculation compared the middle one-second period of stimulation (i.e., 1.00-2.00s) to the baseline one-second period prior to stimulation[19]. Unmasked[20] images averaged across participants can be found in Appendix: DICS Connectivity Images, and this section offers a description of those images. Only changes of 30% or more are described in this section. Overall, AM 25 Hz and BB 25 Hz tended to have decreased connectivity compared to baseline, whereas AM 6 Hz and BB 6 Hz tended to have increased connectivity from baseline.

Figures 92-100 display the changes in 6 Hz coherence from baseline due to 6 Hz amplitude-modulated stimulation. For AM 6 Hz analyzed at 6 Hz, there was increased connectivity with the left auditory dipole for left parietal, right temporal, right frontal, and left

[18] Electrodes used as dipoles for connectivity: Right frontal, E3; Left frontal, E23; Right temporal (T8; auditory cortex), E108; Left temporal (T7; auditory cortex), E45; Right central, E110; Left central, E35; Right parietal, E98; Left parietal, E47. Additional dipoles: maximum dipole during middle one-second of stimulation, middle one-second of stimulation relative to baseline one-second.

[19] In order to compare two source analysis calculations, the same length of time must be used for each the stimulation and baseline periods because each period must have the same number of oscillatory cycles (Oostenveld, 2017).

[20] Baseline subtracted and noise controlled, but not filtered by statistical significance.

cerebellar areas. There was increased connectivity with the right auditory dipole for left parietal, bilateral occipital, right temporal, and multiple cerebellar areas. There was increased connectivity with the left frontal dipole for bilateral parietal, right temporal, bilateral frontal, left dorsal occipital, and right ventral occipital areas as well as decreased connectivity between the left frontal dipole and ventral left occipital cortex. There was increased connectivity with the right frontal dipole throughout most of the brain, particularly with bilateral parietal, bilateral frontal, bilateral temporal, right occipital, and left cerebellar areas. There was increased connectivity with the left parietal dipole throughout most of the brain, particularly with left parietal, bilateral temporal, and right frontal areas. There was increased connectivity between the right parietal dipole and left parietal, bilateral temporal, and left cerebellar areas as well as decreased connectivity between the right parietal dipole and left temporofrontal and some cerebellar areas. There was strongly increased connectivity with the left central dipole throughout the brain, particularly with bilateral parietal, right frontal, right temporal, bilateral occipital, and cerebellar areas. Connectivity increased between the right central dipole and bilateral parietal, bilateral temporal, right frontal, and left cerebellar areas. There was increased connectivity between the dipole with the highest power in 6 Hz (located in right parietal cortex) and left parietal, left frontal, left temporal, left occipital, and multiple cerebellar areas. There was decreased connectivity between the dipole with the highest power in 6 Hz (located in right parietal cortex) and right occipital and right frontal cortex.

Figures 101-109 display the changes in 12 Hz coherence from baseline due to 6 Hz amplitude-modulated stimulation. For AM 6 Hz analyzed at 12 Hz, there was increased connectivity with the left auditory dipole throughout the brain, particularly with bilateral parietal, bilateral temporal, right frontal, and cerebellar areas. There was increased connectivity between

the right auditory dipole and bilateral parietal, bilateral temporal, right frontal, bilateral occipital, and cerebellar areas. There was increased connectivity with the left frontal dipole throughout the brain, particularly with bilateral parietal, left occipital, bilateral temporal, and posterior cerebellar areas as well as decreased connectivity between the left frontal dipole and left frontal and right occipital areas. There was increased connectivity between the right frontal dipole and bilateral parietal, left frontal, bilateral occipital, and posterior cerebellar areas as well as decreased connectivity with a dorsal right occipital area. There was increased connectivity between the left parietal dipole and bilateral parietal, bilateral frontotemporal, right temporal, left temporooccipital, right frontotemporal, and left cerebellar areas, but there was decreased connectivity between the left parietal dipole and a left frontotemporal area. There was increased connectivity between the right parietal dipole and bilateral parietal, bilateral temporal, bilateral occipital, and cerebellar areas as well as decreased connectivity between the right parietal dipole and a left frontal area. There was increased connectivity with the left central dipole throughout the brain, particularly with left parietal, right temporal, right temporofrontal, and cerebellar areas as well as decreased connectivity with a right occipital area. Connectivity with the right central dipole increased throughout the brain, particularly in left parietal, bilateral occipital, right frontal, right temporal, and left cerebellar areas. There was increased connectivity between the dipole with the highest power in 12 Hz (located in left parietal cortex) and bilateral parietal, bilateral frontal, bilateral temporal, bilateral occipital, and posterior cerebellar areas. There was decreased connectivity between the dipole with the highest power in 12 Hz (located in left parietal cortex) and anterior right parietal, deep brain, bilateral frontotemporal, and anterior cerebellar areas.

Figures 110-118 display the changes in 25 Hz coherence from baseline due to 6 Hz amplitude-modulated stimulation. For AM 6 Hz analyzed at 25 Hz, there was increased

connectivity between the left auditory dipole and right parietal and bilateral temporal areas. There was increased connectivity between the right auditory dipole and right frontoparietal and right temporal areas as well as decreased connectivity with a left parietal area. There was increased connectivity between the left frontal dipole and bilateral frontal and right occipital areas as well as decreased connectivity between the left frontal dipole and left occipital, left temporal, and cerebellar areas. There was increased connectivity between the right frontal dipole and right parietal, left temporal, right occipital, left cerebellar areas. There was increased connectivity with the left parietal dipole throughout most of the brain, particularly with right parietal and bilateral temporal areas, but there was decreased connectivity between the left parietal dipole and a left temporal area. There was increased connectivity between the right parietal dipole and right parietal, bilateral temporal, and cerebellar areas as well as decreased connectivity between the right parietal dipole and a left temporal area. There was increased connectivity with the left central dipole throughout the right hemisphere, particularly with right parietal and right temporal areas. Connectivity increased between the right central dipole and right parietal and left cerebellar areas, but connectivity decreased between the right central dipole and left parietal, bilateral frontal, and right cerebellar areas. There was increased connectivity between the dipole with the highest power in 25 Hz (located in deep right central cortex) and bilateral parietal, bilateral occipital, and right frontotemporal areas. There was decreased connectivity between the dipole with the highest power in 25 Hz (located in deep right central cortex) and left temporal and left cerebellar areas.

Figures 119-127 display the changes in 50 Hz coherence from baseline due to 6 Hz amplitude-modulated stimulation. For AM 6 Hz analyzed at 50 Hz, there was increased connectivity between left auditory and bilateral frontal, right parietal, bilateral occipital, and

cerebellar areas. There was increased connectivity between right auditory and bilateral frontal, left temporofrontal, and left cerebellar areas. There was increased connectivity between the left frontal dipole and left occipital, left frontal, cerebellar, and deep brain areas as well as decreased connectivity between the left frontal dipole and a right temporofrontal area. There was increased connectivity between the right frontal dipole and one small area in the right frontal as well as decreased connectivity with bilateral frontal and left temporal areas. There was increased connectivity between the left parietal dipole and right parietal, bilateral frontal, bilateral temporal, and left anterior cerebellar areas. There was increased connectivity between the right parietal dipole and bilateral frontal, bilateral occipital, and right temporal areas as well as decreased connectivity between the right parietal dipole and a left parietal area. There was increased connectivity between the left central dipole and a right temporofrontal area as well as decreased connectivity with right temporal, bilateral occipital, and cerebellar areas. Connectivity with the right central dipole decreased throughout most of the brain, particularly with left parietal, left temporal, bilateral frontal, and cerebellar areas, but connectivity increased between the right central dipole and an anterior right parietal area. There was increased connectivity between the dipole with the highest power in 50 Hz (located in right temporal cortex) and left parietal, bilateral frontal, and posterior cerebellar areas.

Figures 128-136 display the changes in 6 Hz coherence from baseline due to 25 Hz amplitude-modulated stimulation. For AM 25 Hz analyzed at 6 Hz, there was decreased connectivity with the left auditory dipole throughout the brain, particularly with a right temporal area. There was decreased connectivity with the right auditory dipole throughout the brain, particularly with bilateral temporal areas. There was decreased connectivity with the left frontal dipole throughout the brain, particularly with bilateral occipital areas. There was decreased

connectivity with the right frontal dipole throughout the brain, particularly with left occipital cortex and with the left cerebellum. There was decreased connectivity with the left parietal dipole throughout the brain, particularly with bilateral temporal and bilateral frontal areas. There was decreased connectivity with the right parietal dipole throughout the brain, particularly with a right temporal area. There was decreased connectivity with the left central dipole throughout the brain, particularly in a left occipital area. Connectivity with the right central dipole increased throughout much of the brain, particularly with left parietal, right frontal, left occipital, right temporal, and cerebellar areas, but connectivity decreased between the right central dipole and a left temporal area. Connectivity with the right central dipole decreased throughout the brain, particularly with bilateral frontal, deep brain, and right cerebellar areas. There was increased connectivity between the dipole with the highest power in 6 Hz (located in right occipital cortex) and bilateral parietal, bilateral frontal, bilateral temporal, and bilateral cerebellar areas.

Figures 137-145 display the changes in 12 Hz coherence from baseline due to 25 Hz amplitude-modulated stimulation. For AM 25 Hz analyzed at 12 Hz, there was decreased connectivity with the left auditory dipole throughout the brain, particularly for bilateral temporal and cerebellar areas. There was decreased connectivity with the right auditory dipole throughout the brain, particularly with right frontal and anterior cerebellar areas. There was decreased connectivity with the left frontal dipole throughout the brain, particularly with bilateral frontal areas. There was decreased connectivity with the right frontal dipole throughout the brain, particularly with bilateral frontal and left temporal areas. There was decreased connectivity with the left parietal dipole throughout the brain, particularly posterior right parietal and bilateral temporal areas. There was decreased connectivity with the right parietal dipole throughout the brain, particularly with right frontal and cerebellar areas. There was decreased connectivity with

the left central dipole throughout the brain, particularly with bilateral frontal, bilateral temporal, and cerebellar areas. Connectivity with the right central dipole decreased throughout the brain, particularly with a right parietal area. There was increased connectivity between the dipole with the highest power in 12 Hz (located in left temporal cortex) and right parietal, bilateral frontal, left temporal, left occipital, and multiple cerebellar areas.

Figures 146-154 display the changes in 25 Hz coherence from baseline due to 25 Hz amplitude-modulated stimulation. For AM 25 Hz analyzed at 25 Hz, there was decreased connectivity with the left auditory dipole throughout the brain, particularly with a right parietal area. There was increased connectivity with the right auditory dipole throughout the brain, particularly with bilateral frontal, bilateral occipital, and cerebellar areas. There was decreased connectivity with the left frontal dipole throughout the brain, particularly with bilateral frontal, right temporal, and right cerebellar areas. There was increased connectivity between the right frontal dipole and left frontal, bilateral occipital, and right posterior cerebellar areas as well as decreased connectivity with the right frontal dipole and a right dorsal occipital area. There was decreased connectivity with the bilateral parietal dipoles throughout the brain. There was decreased connectivity with the left central dipole throughout the brain. Connectivity increased slightly between the right central dipole and bilateral frontal as well as bilateral occipital areas, but connectivity decreased between the right central dipole and right parietal as well as bilateral temporal areas. There was increased connectivity between the dipole with the highest power in 25 Hz (located in left frontal cortex) and right parietal, left occipital, and multiple cerebellar areas.

Figures 155-163 display the changes in 50 Hz coherence from baseline due to 25 Hz amplitude-modulated stimulation. For AM 25 Hz analyzed at 50 Hz, there was decreased

connectivity with the left auditory dipole throughout the brain, particularly with a right parietal area. There was increased connectivity between the right auditory dipole and a right frontal area as well as decreased connectivity with the right auditory dipole throughout the brain, particularly with a left parietal area. There was decreased connectivity with the left frontal dipole throughout the brain, particularly with right temporofrontal and occipital areas. There was increased connectivity between the right frontal dipole and , one right temporofrontal point as well as bilateral occipital and posterior cerebellar areas, but there was decreased connectivity between the right frontal dipole and bilateral frontal areas. There was decreased connectivity with the left parietal dipole throughout the brain. There was no change in connectivity with the right parietal dipole compared to baseline. There was decreased connectivity with the left central dipole throughout the brain, particularly with a right parietal area. Connectivity with the right central dipole decreased throughout most of the brain, but connectivity increased between the right central dipole and right frontotemporal and posterior cerebellar areas. There was increased connectivity between the dipole with the highest power in 50 Hz (located in right central cortex) and bilateral parietal, bilateral occipital, bilateral frontotemporal, left temporal, and left cerebellar areas.

Figures 164-172 display the changes in 6 Hz coherence from baseline due to 6 Hz binaural beat stimulation. For BB 6 Hz analyzed at 6 Hz, there was increased connectivity between the left auditory dipole and cerebellum as well as decreased connectivity with bilateral parietal, left temporal, and left occipital areas. There was increased connectivity between the right auditory dipole and bilateral parietal, bilateral temporal, occipital, and cerebellar areas. There was increased connectivity between the left frontal dipole and bilateral temporal and temporooccipital areas as well as decreased connectivity between the left frontal dipole and

medial occipital and left cerebellar areas. There was increased connectivity between the right frontal dipole and much of the brain, particularly right frontal and left temporal areas, as well as decreased connectivity with a right occipital area. There was increased connectivity between the left parietal dipole and right frontal, bilateral temporal, and cerebellar areas, as well as decreased connectivity between the left parietal dipole and left occipital and left posterior cerebellar areas. There was increased connectivity between the right parietal dipole and left parietal, bilateral temporal, and cerebellar areas as well as decreased connectivity between the right parietal dipole and adjacent right parietal areas. There was increased connectivity between the left central dipole and bilateral temporal and right cerebellar areas as well as decreased connectivity with right parietal, bilateral occipital, and left cerebellar areas. Connectivity increased between the right central dipole and bilateral parietal, left ventral occipital, bilateral temporal, left frontal, and cerebellar areas, whereas connectivity decreased between the right central dipole and a right dorsal occipital area. There was increased connectivity between the dipole with the highest power in 6 Hz (located in right cerebellum) and right frontal, bilateral parietal, right frontotemporal, left temporal, left occipital, and multiple cerebellar areas.

Figures 173-181 display the changes in 12 Hz coherence from baseline due to 6 Hz binaural beat stimulation. For BB 6 Hz analyzed at 12 Hz, there was increased connectivity with the left auditory dipole throughout the brain, particularly with midline frontal, bilateral occipital, and cerebellar areas, as well as decreased connectivity with right parietal, midline parietal, left temporal, and multiple cerebellar areas. There was increased connectivity between the right auditory dipole and frontal, bilateral temporal, and cerebellar areas. There was increased connectivity between the left frontal dipole and bilateral occipital and left cerebellar areas. There was increased connectivity between the right frontal dipole and bilateral frontal, bilateral

occipital, and right cerebellar areas. There was increased connectivity between the left parietal dipole and bilateral frontal, bilateral temporal, and cerebellar areas, while there was decreased connectivity between the left parietal dipole and a dorsal right parietal area. There was increased connectivity between the right parietal dipole and left cerebellum as well as decreased connectivity between the right parietal dipole and bilateral parietal, left temporal, and anterior cerebellar areas. There was increased connectivity between the left central dipole and bilateral frontal, bilateral occipital, right temporal, and cerebellar areas. Connectivity with the right central dipole increased throughout much of the brain, particularly with bilateral frontal, bilateral occipital, right temporal, and cerebellar areas. There was increased connectivity between the dipole with the highest power in 12 Hz (located in left occipital cortex) and left dorsal parietal, right ventral parietal, bilateral frontal, right temporal, right occipital, and posterior cerebellar areas.

Figures 182-190 display the changes in 25 Hz coherence from baseline due to 6 Hz binaural beat stimulation. For BB 6 Hz analyzed at 25 Hz, there was increased connectivity between the left auditory dipole and right parietal and left frontal areas, as well as decreased connectivity with bilateral temporal areas. There was increased connectivity with the right auditory dipole throughout the brain, particularly with bilateral frontal, bilateral parietal, left temporal, and cerebellar areas as well as decreased connectivity with left occipital and right temporofrontal areas. There was increased connectivity with the left frontal dipole throughout the brain, particularly with bilateral frontal and bilateral occipital areas. There was increased connectivity between the right frontal dipole and left frontal and left occipital areas as well as decreased connectivity between the right frontal dipole and a right occipital area. There was increased connectivity between the left parietal dipole and bilateral parietal, left frontal, and right

temporal areas, but decreased connectivity between the left parietal dipole and bilateral temporooccipital and right frontal areas. There was increased connectivity between the right parietal dipole and right frontal and left occipital areas as well as decreased connectivity between bilateral parietal dipoles and bilateral temporal areas. There was increased connectivity between the left central dipole and bilateral frontal and right temporal areas as well as decreased connectivity with a right parietal area. Connectivity with the right central dipole increased throughout much of the brain, particularly with right parietal and left occipital cortex, while connectivity decreased between the right central dipole and left parietal, left temporal, and right frontal areas. There was increased connectivity between the dipole with the highest power in 25 Hz (located in left occipital cortex) and bilateral parietal and left temporooccipital areas.

Figures 191-199 display the changes in 50 Hz coherence from baseline due to 6 Hz binaural beat stimulation. For BB 6 Hz analyzed at 50 Hz, there was decreased connectivity between the left auditory dipole and left parietal and left temporal areas. There was increased connectivity with the right auditory dipole throughout the brain, particularly with midline frontal, bilateral parietal, midline occipital, and anterior cerebellar areas. There was increased connectivity with the left frontal dipole throughout the brain, particularly with a left occipital area, as well as decreased connectivity with a right temporofrontal area. There was increased connectivity between the right frontal dipole and left occipital and bilateral cerebellar areas as well as decreased connectivity between the right frontal dipole and bilateral frontal and left temporal areas. There was increased connectivity between the left parietal dipole and bilateral parietal, right temporal, and right anterior cerebellar areas. There was increased connectivity between the right parietal dipole and bilateral parietal and cerebellar areas as well as decreased connectivity with left occipital and right temporofrontal areas. There was increased connectivity

between the left central dipole and bilateral parietal, right frontal, and cerebellar areas. There was increased connectivity between the dipole with the highest power in 50 Hz (located in left occipital cortex) and several small parietal, frontal, and occipital areas bilaterally.

Figures 200-208 display the changes in 6 Hz coherence from baseline due to 25 Hz binaural beat stimulation. For BB 25 Hz analyzed at 6 Hz, there was decreased connectivity with the left auditory dipole throughout the brain, particularly with a right temporal area. There was decreased connectivity with the right auditory dipole throughout the brain, particularly bilateral temporal areas. There was decreased connectivity with the left frontal dipole throughout the brain, particularly with right occipital and left cerebellar areas. There was decreased connectivity with the right frontal dipole throughout the brain, particularly with left cerebellum. There was decreased connectivity with the left parietal dipole throughout the brain, particularly right frontal and bilateral temporal areas. There was decreased connectivity with the right parietal dipole throughout the brain, particularly with bilateral temporal and right parietal areas. There was decreased connectivity with the left central dipole throughout the brain, particularly with right parietal and bilateral temporal areas. Connectivity with the right central dipole decreased throughout the brain, particularly with bilateral frontal, deep brain, and right cerebellar areas. There was increased connectivity between the dipole with the highest power in 6 Hz (located in right occipital cortex) and bilateral parietal, right frontal, bilateral temporal, and central cerebellar areas.

Figures 209-217 display the changes in 12 Hz coherence from baseline due to 25 Hz binaural beat stimulation. For BB 25 Hz analyzed at 12 Hz, there was decreased connectivity with the left auditory dipole throughout the brain, particularly with right parietal, bilateral temporal, and cerebellar areas. There was decreased connectivity with the right auditory dipole

throughout the brain, particularly bilateral frontal, right occipital, and anterior cerebellar areas. There was decreased connectivity with the left frontal dipole throughout the brain, particularly with bilateral frontal areas. There was decreased connectivity with the right frontal dipole throughout the brain, particularly with bilateral frontal and left temporal areas. There was decreased connectivity with the left parietal dipole throughout the brain, particularly a right temporooccipital area. There was decreased connectivity with the right parietal dipole throughout the brain, particularly with bilateral frontal and cerebellar areas. There was decreased connectivity with the left central dipole throughout the brain, particularly in bilateral temporal areas. Connectivity with the right central dipole decreased throughout the brain, particularly with right parietal and right frontal areas. There was increased connectivity between the dipole with the highest power in 12 Hz (located in left parietal cortex) and dorsal right parietal, ventral left parietal, bilateral frontal, bilateral occipital, and left posterior cerebellar areas.

Figures 218-226 display the changes in 25 Hz coherence from baseline due to 25 Hz binaural beat stimulation. For BB 25 Hz analyzed at 25 Hz, there was decreased connectivity with the left auditory dipole throughout the brain, particularly with bilateral temporal areas. There was increased connectivity between the right auditory dipole and bilateral frontal, left parietal, bilateral occipital, and cerebellar areas (Figure 219; connectivity with the right auditory cortex at the beat frequency). There was decreased connectivity with the left frontal dipole throughout the brain, particularly with left frontal, right temporal, and right cerebellar areas. There was increased connectivity between the right frontal dipole and left frontal, bilateral occipital, and right posterior cerebellar areas as well as decreased connectivity with adjacent right frontal areas and a right temporal area. There was decreased connectivity with the bilateral parietal throughout the brain. There was decreased connectivity with the left central dipole

throughout the brain. Connectivity increased between the right central dipole and left parietal, bilateral frontal, and posterior cerebellar areas, while connectivity decreased between the right central dipole and right parietal and bilateral temporal areas. There was increased connectivity between the dipole with the highest power in 25 Hz (located in right occipital cortex) and left parietal and bilateral frontal areas.

Figures 227-235 display the changes in 50 Hz coherence from baseline due to 25 Hz binaural beat stimulation. For BB 25 Hz analyzed at 50 Hz, there was decreased connectivity with the left auditory dipole throughout the brain, particularly with a left parietal area. There was increased connectivity between the right auditory dipole and a right frontal area, but, in general, decreased connectivity with the right auditory dipole throughout the brain. There was decreased connectivity with the left frontal dipole throughout the brain, particularly with a right temporofrontal area. There was increased connectivity between the right frontal dipole and one right temporofrontal point as well as right frontal, left occipital, and left cerebellar areas; additionally, there was decreased connectivity between the right frontal dipole and bilateral frontal and left dorsal occipital areas. There was decreased connectivity with the left parietal dipole throughout the brain, particularly with right parietal and bilateral temporal areas. There was decreased connectivity with the right parietal dipole throughout the brain, particularly with a left parietal area. There was decreased connectivity with the left central dipole throughout the brain, particularly with a right parietal area. Connectivity with the right central dipole decreased throughout most of the brain but increased in right frontotemporal and posterior left cerebellar areas. There was increased connectivity between the dipole with the highest power in 50 Hz (located in right central cortex) and bilateral posterior parietal, bilateral occipital, bilateral frontotemporal, and posterior cerebellar areas.

DICS Source and Connectivity Analyses: BB vs. AM Comparisons

In order to directly investigate the differences between binaural beat and amplitude-modulated source activity and connectivity with dipoles placed at particular electrode locations, subtractions of AM activity from corresponding (i.e., same beat/modulation frequency and same analysis) BB activity were plotted and unmasked[21] images averaged across participants can be found in Appendix: Amplitude-modulated vs. Binaural Beat Comparison. This section offers a description of those images. Only changes of 20% or more are described in this section.

Source Analysis. Figures 236-243 display the difference between binaural beat and amplitude-modulated stimulation at the same stimulation frequency in the sources identified for the generation of the indicated frequencies (all conditions baseline corrected). For 6 Hz analysis, BB 6 Hz had higher frontal and left temporal power than AM 6 Hz, whereas AM 6 Hz had higher power in right temporofrontal and occipital areas than BB 6 Hz. BB 25 Hz had higher right occipital power than AM 25 Hz while AM 25 Hz had higher frontal power. For 12 Hz analysis, BB 6 Hz had higher power in left parietal and occipital areas than AM 6 Hz. BB 25 Hz had higher power in left temporal areas while AM 25 Hz had higher power in the frontal lobe. For 25 Hz analysis, BB 6 Hz had higher power in frontal and occipital areas than AM 6 Hz, whereas AM 6 Hz had higher power in bilateral temporofrontal areas. BB 25 Hz and AM 25 Hz did not display noticeable differences. For 50 Hz analysis, BB 6 Hz had higher power throughout the posterior half of the brain, particularly in the occipital lobe, than AM 6 Hz. AM 25 Hz had higher power for the anterior half of the brain overall, particularly in the frontal lobe.

Connectivity Analysis. Figures 244-258 display the difference in coherence between 6 Hz binaural beat and 6 Hz amplitude-modulated stimulation (both conditions baseline corrected).

[21] Baseline subtracted and noise controlled, but not filtered by statistical significance.

At 6 Hz, AM 6 Hz had higher connectivity between the right frontal dipole and most of the brain, except where BB 6 Hz had higher connectivity between the right frontal dipole and a left occipital area. At 6 Hz, AM 6 Hz had higher connectivity between the left frontal dipole and bilateral parietal, bilateral frontal, right occipital, and central cerebellar areas, whereas BB 6 Hz had higher connectivity between the left frontal dipole and left temporal, left temporooccipital, and multiple cerebellar areas. At 6 Hz, AM 6 Hz had higher connectivity between the left auditory dipole and medial parietal, left temporooccipital, and right temporal areas, while BB 6 Hz had higher connectivity between the left auditory dipole and left frontal, right parietal, bilateral temporal, bilateral occipital, and multiple cerebellar areas. At 6 Hz, AM 6 Hz had higher connectivity between the right auditory dipole and most parts of the brain, except in left temporofrontal and midline occipital areas where BB 6 Hz had higher connectivity with the right auditory dipole. At 12 Hz, AM 6 Hz had higher connectivity between the right frontal dipole and bilateral parietal, medial occipital, and posterior cerebellar areas, whereas BB 6 Hz had higher connectivity between the right frontal dipole and right frontal, bilateral occipital, and bilateral cerebellar areas. At 12 Hz, AM 6 Hz had higher connectivity between the left frontal dipole and bilateral parietal, right temporal, right frontal, and multiple cerebellar areas, while BB 6 Hz had higher connectivity between the left frontal dipole and left frontal, left temporal, bilateral occipital, and medial cerebellar areas. At 12 Hz, AM 6 Hz had higher connectivity between the left auditory dipole and left parietal and most cerebellar areas, while BB 6 Hz had higher connectivity between the left auditory dipole and bilateral frontal, right temporal, and bilateral occipital areas. At 12 Hz, AM 6 Hz had higher connectivity between the right auditory dipole and left parietal, right temporal, and multiple cerebellar areas, while BB 6 Hz had higher connectivity between the right auditory dipole and left frontal, right parietal, and right occipital

areas. At 25 Hz, AM 6 Hz had higher connectivity between the right frontal dipole and bilateral parietal, right frontal, and left cerebellar areas, whereas BB 6 Hz had higher connectivity between the right frontal dipole and left frontal, left occipital, and right cerebellar areas. At 25 Hz, AM 6 Hz had higher connectivity between the left frontal dipole and bilateral parietal and posterior frontal areas, while BB 6 Hz had higher connectivity between the left frontal dipole and anterior frontal, left parietal, left occipital, bilateral temporal, and right cerebellar areas. At 25 Hz, AM 6 Hz had higher connectivity between the left auditory dipole and right parietal, bilateral temporal, and most cerebellar areas, while BB 6 Hz had higher connectivity between the left auditory dipole and left parietal, bilateral frontal, and bilateral occipital areas. At 25 Hz, AM 6 Hz had higher connectivity between the right auditory dipole and right parietal and right temporal areas, but BB 6 Hz had higher connectivity between the right auditory dipole and most areas of the brain, including bilateral frontal, left parietal, left temporal, bilateral occipital, and the cerebellar areas. At 50 Hz, AM 6 Hz had higher connectivity between the right frontal dipole and right temporal, while BB 6 Hz had higher connectivity between the right frontal dipole and bilateral frontal, left temporal, bilateral occipital, and posterior cerebellar areas. At 50 Hz, AM 6 Hz had higher connectivity between the left frontal dipole and most of the brain, except in bilateral frontal areas and a left occipital area where BB 6 Hz had higher connectivity with the left frontal dipole. At 50 Hz, AM 6 Hz had higher connectivity between the left auditory dipole and right parietal, bilateral temporal, bilateral occipital, and posterior cerebellar areas, while BB 6 Hz had higher connectivity between the left auditory dipole and left parietal, right medial temporal, and anterior cerebellar areas. At 50 Hz, BB 6 Hz had higher connectivity between the right auditory dipole and the majority of the brain, including bilateral parietal, bilateral frontal, bilateral occipital, and multiple cerebellar areas.

Figures 259-275 display the difference in coherence between 25 Hz binaural beat and 25 Hz amplitude-modulated stimulation (both conditions baseline corrected). At both 6 Hz and 12 Hz analysis, AM 25 Hz and BB 25 Hz did not show striking differences in connectivity at any location. At 25 Hz, AM 25 Hz had higher connectivity between the right frontal dipole and parietal and temporal areas, particularly on the left, whereas BB 25 Hz had higher connectivity between the right frontal dipole and the cerebellum. At 25 Hz, AM 25 Hz had higher connectivity between the left frontal dipole and right parietal, right frontal, and right temporal areas, while BB 25 Hz had higher connectivity between the left frontal dipole and left temporal and cerebellar areas. At 25 Hz, AM 25 Hz had higher connectivity between the left auditory dipole and right parietal and right temporal areas, whereas BB 25 Hz had higher connectivity between the left auditory dipole and a left parietal area. At 25 Hz, AM 25 Hz had higher connectivity between the right auditory dipole and bilateral temporal and right frontal areas, whereas BB 25 Hz had higher connectivity between the right auditory dipole and a left parietal area. At 50 Hz, AM 25 Hz had higher connectivity between the right frontal dipole and occipital and cerebellar areas, while BB 25 Hz had higher connectivity between the right frontal dipole and a left frontal area. At 50 Hz, BB 25 Hz had higher connectivity between the left frontal dipole and most brain areas, particularly a right parietal area. At 50 Hz, AM 25 Hz had higher connectivity between the left auditory dipole and bilateral temporal areas, while BB 25 Hz had higher connectivity between the left auditory dipole and bilateral parietal and left temporooccipital areas. At 50 Hz, AM 25 Hz had higher connectivity between the right auditory dipole and right temporal, right frontal, and right cerebellar areas, while BB 25 Hz had higher connectivity between the right auditory dipole and bilateral parietal as well as left temporal areas.

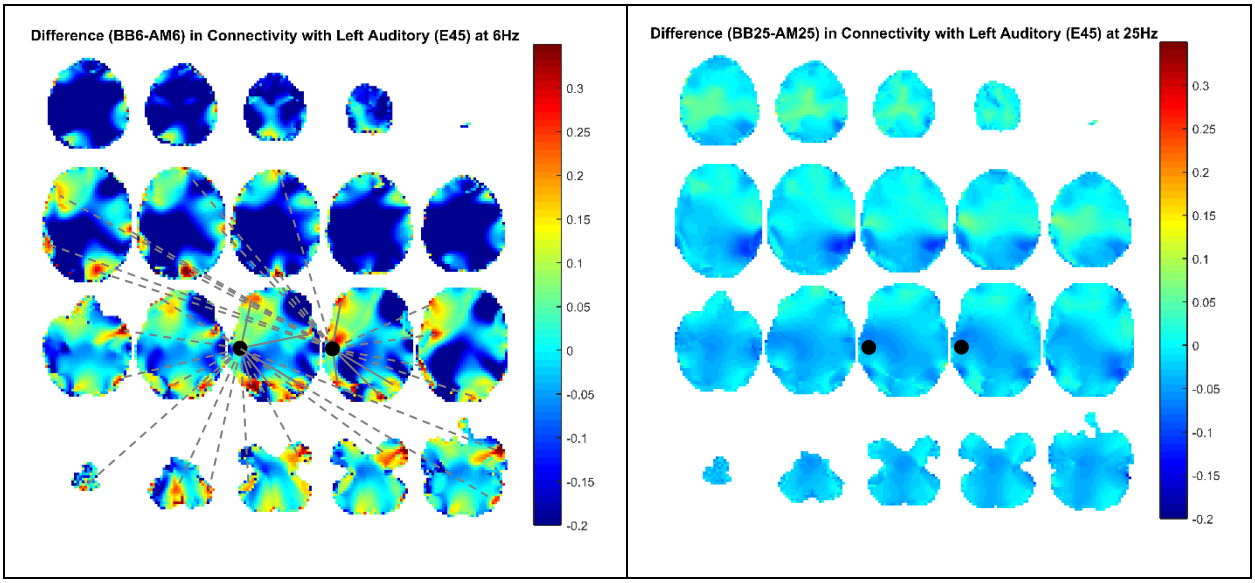

Figure 3. Binaural beat source level connectivity with a dipole at E45 (left temporal, auditory cortex; approximately indicated by the superimposed black dots) during the middle one second of stimulation, with amplitude-modulated connectivity subtracted. Gray lines added to emphasize higher coherence with reference point during BB stimulation; solid gray lines indicate a connection within the same horizontal slice. Connectivity analysis was performed with DICS and a standardized BEM headmodel and was baseline corrected. Darker reds indicate coherence with E45 is higher for BB while darker blues indicate coherence with E45 is higher for AM. Left: BB 6 Hz connectivity minus AM 6 Hz connectivity analyzed at beat/modulation frequency (6 Hz). Right: BB 25 Hz connectivity minus AM 25 Hz connectivity analyzed at beat/modulation frequency (25 Hz).

As shown in the examples provided in Figure 3, The connectivity differences between BB 6 Hz and AM 6 Hz were much larger than the connectivity differences between BB 25 Hz and AM 25 Hz. In general, BB 6 Hz tended to drive connectivity between frontal and occipital areas, auditory and frontal areas, and auditory and occipital areas across all four frequencies of

interest. There was also BB-6 Hz-driven whole-brain connectivity increases with the right auditory dipole at 25 Hz and 50 Hz. At 6 Hz and 12 Hz, there weren't notable differences in AM 25 Hz-driven connectivity and BB 25 Hz-driven connectivity. At 25 and 50 Hz, AM 25 Hz tended to drive more connectivity with right frontal, bilateral temporal, and bilateral occipital areas; however, at 50 Hz, BB 25 Hz had higher connectivity between the left frontal dipole and a right parietal area.

Discussion

Hypotheses

The existing literature set forth several expectations. First, we expected to see a steady state entrainment response[22] to AM stimuli at their modulation frequencies but no such response to BB stimuli at their beat frequencies. Second, we expected to observe an increase in brain coherence or functional connectivity during BB stimulation but not AM stimulation. Finally, we expected to see a difference between long-term stimulation (5-minutes) and short-term stimulation (3-seconds). Reasonable expectations for long-term stimulation included an attenuation effect over time or, alternatively, a sustained or strengthened response over time.

Frequency Analysis and ASSR

To address our first aim, we conducted Fast Fourier Transforms (FFT) in a sample of electrodes. We observed an auditory steady state response (ASSR) to both AM stimulus types as increases in power in the modulation frequency and its second harmonic. BB 25 Hz and AM 25 Hz showed almost identical FFT results, with increased power at 50 Hz in bilateral auditory electrodes as well as a strong phase-locking response at 50 Hz. BB 6 Hz, on the other hand,

[22] In power or phase-locking.

showed a decrease in power at 6 Hz rather than an increase as would be expected for an ASSR. These results were somewhat unexpected as ASSR has been reported in response to AM stimuli but not BB stimuli.

ASSR was verified statistically in the linear fixed effects models predicting power in frequencies of interest. Most areas of interest had significantly higher power in 6 Hz and 12 Hz for stimuli with a 6 Hz beat/modulation, indicating ASSR at both the first and second harmonic for both AM 6 Hz and BB 6 Hz. Interestingly, frequency power ASSR was observed in 50 Hz for 25 Hz beat/modulation stimulation. For most areas of interest, power in 25 Hz was higher for 6 Hz beat/modulation, although a significant interaction between stimulus type and frequency indicated that BB 25 Hz had the highest power in 25 Hz. The interaction effect indicates that, overall, BB 25 Hz had frequency power ASSR at both 25 Hz and 50 Hz, but AM 25 Hz had frequency power ASSR only at 50 Hz. However, a limitation of the LMEs was the inclusion of a 6 Hz harmonic (24 Hz) in the predicted frequency band. Similarly, the phase-locking results for both AM and BB 25 Hz stimulation indicated ASSR at 50 Hz rather than 25 Hz.

Individual Differences. This difference between BB 6 Hz and BB 25 Hz may have to do with the changes in perception of BB-type stimuli (i.e., two tones/click trains/etc. with offset frequencies played one per ear, but not always perceived as a "beat"). For small frequency differences, participants perceive a single tone that moves between the ears (e.g., a rotating speaker). Increasing the frequency difference creates an AM perception known as a "beat" until, following a transition perception described as "roughness," finally the difference is high enough that the participant can perceive both tones separately. The cutoff for the perception of a moving source is considered to be 5-10% of the carrier frequency or an absolute value of 5 Hz, and it is more likely for a 6 Hz frequency difference between the ears to be identified as a "beat" (>80%)

than for a 25 Hz frequency difference to be identified as a "beat" (approximately 70%; Ross et al., 2014). However, this perception does have considerable individual variability, and it may be that our particular sample on average experienced the BB stimuli differently than has been previously reported, such that BB 25 Hz was processed almost identically to AM 25 Hz while BB 6 Hz was processed differently than AM 6 Hz. There is no evidence that the sample size was underpowered or not representative. Instead, the implication of this interpretation would be that individual variability would need to be considered for future studies about binaural beats as well as for therapies developed with binaural beats. For example, given a particular carrier frequency, one individual may perceive a binaural beat for frequency differences from 5 Hz to 20 Hz, while a different individual may only perceive a binaural beat for frequency differences of 9 Hz to 19 Hz. Future studies should verify whether these perceptual differences predict connectivity differences by collecting data regarding an individual's perceptual experience during stimulation. Therapies may need to be restricted to low frequency beats and/or calibrated to each individual's perception of beats in order to induce the desired effects.

In our linear mixed effects models predicting frequency power, several grouping effects were significant across all or most brain areas by frequency of interest. The vast majority of models from every frequency of interest included significant variation by subject of initial values at time zero, the effect of time on frequency power, and the effect of stimulus type on frequency power. Because the fixed effect for stimulus type was generally nonsignificant, clustering may be indicated. Upon investigation of intercept and slope distributions by grouping variables, it became clear that slopes were not all in the same direction. It is possible that unmeasured variables, such as perception and attention, are affecting the neural response as measured by power in frequencies of interest. It is also possible that these slope differences represent real

differences in neural processing of binaural beats even with the same perception, attention, etc. The issue of clustering needs to be further investigated, such as with studies measuring qualities of perception and attention in participants that could be used as covariates in analysis.

Source Analysis

Source analysis indicated which neural locations were responsible for the highest power for all the frequencies of interest. Sources were localized by stimulus type and beat/modulation frequency. AM 6 Hz showed bilateral parietal sources for ASSR, while AM 25 Hz showed right central, assuming all ASSR was at 50 Hz rather than 25 Hz as indicated by the FFT. BB 6 Hz showed highest power occipitally and into the cerebellum or potentially subcortical areas. For BB 6 Hz, the likely source mislocalization (to the cerebellum, an unlikely source for auditory frequency –following activity, but located directly posterior and cortically shallower than the subcortical structures like the olivary nuclei) may indicate that binaural beat-driven activity may occur much earlier in the auditory pathway than the cortex. BB 25 Hz also had occipital activation for 6 Hz and 25 Hz although it diverged to more anterior areas for 12 Hz (left parietal) and 50 Hz (right central). Both AM 25 Hz and BB 25 Hz showed activation in the right central electrodes at the same frequency as their matching 50 Hz phase-locking.

Connectivity Analysis

Clinical Importance of Functional Connectivity. This study was designed to ascertain the neural changes associated with binaural beats, in particular whether binaural beats differ from amplitude-modulated beats in causing increased functional connectivity. BB has been proposed as a potential therapy for increasing neural connectivity (e.g., Gao et al., 2014, suggest BB therapy for schizophrenia), however conclusive evidence of this effect is scant (Gao et al., 2014;

Ioannou, Pereda, Lindsen, & Bhattacharya, 2015; Beauchene et al., 2016). Brain connectivity is altered in patients with major depressive disorder (Zhang, Wang, Wu, Kuang, Huang, He, & Gong, 2011) and autism (Belmonte, Allen, Beckel-Mitchener, Boulanger, Carper, & Webb, 2004). In patients with autism, there is reduced connectivity between the frontal cortex and other areas of the brain, such as the amygdala (Léveillé, Bolduc, Limoges, Chevrier, Mottron, & Godbout, 2013; Hoffmann, Brück, Kreifelts, Ethofer, & Wildgruber, 2015). A disconnect between frontal and temporal cortex has also been demonstrated in schizophrenia (Peled, 2001). Therapies could use binaural beats to improve long-distance connectivity and sensory integration in autism or to strengthen small-world network organization, potentially improving top-down modulation of sensory processing. The few studies that have specifically investigated binaural beats as treatment for disorders have not compared BB to other oscillating auditory stimuli and have not used connectivity measures to investigate potential BB-driven connectivity changes (e.g., Kennel, Taylor, Lyon, & Bourguignon, 2010). Building from these limitations in the literature, our EEG connectivity analysis explored the functional coherence between brain areas in the frequencies of interest relative to the beat/modulation stimuli, with the hypothesis that binaural beats would drive more increases in cortical connectivity than amplitude-modulated stimuli.

Connectivity in BB 6 Hz. Following the source analysis, we investigated whether binaural beats drove increases in coherence between brain areas in the frequencies of interest. Baseline-corrected differences in connectivity between binaural beats and amplitude-modulated tones at the same beat/modulation frequency were found at 6 Hz beat frequency. Our data showed that 6 Hz binaural beats induce coherence between multiple brain areas (namely frontal,

auditory, and occipital areas) above and beyond what would be induced by other oscillating auditory stimuli such as amplitude-modulated tones.

Our source analysis results support the connectivity analysis. BB 6 Hz had higher power than AM 6 Hz in multiple brain areas (6 Hz: frontal, left temporal; 12 Hz: left parietal, occipital; 25 Hz: frontal, occipital; 50 Hz: posterior half of the brain). Additionally, BB 6 Hz drove activity in all frequencies in the cerebellum, potentially indicating binaural beats specific activation in subcortical areas. These multiple levels of processing shown in our source analysis suggests that low-beat-frequency binaural beats are superior to amplitude-modulated stimuli for inducing connectivity changes.

Biological Basis of EEG Connectivity. Because EEG connectivity changes can be measured at a time resolution of seconds, it stands to reason that the biological basis of EEG connectivity analysis is increased signaling between brain areas via synapses that already exist prior to stimulation. Therefore, the goal of a therapy that functions by increasing EEG connectivity would be to induce long-term potentiation and synapse strengthening to seek the goal of greater whole-brain integration. Therapies would most likely take the form of multiple exposures to binaural-beat stimuli to strengthen pre-existing neural connections (i.e., structural connectivity). This therapy could increase long-range EEG coherence in patients with decreased coherence relative to control groups.

Long-range EEG coherence has been found for lower frequencies such as theta and alpha (von Stein & Sarnthein, 2000) while local neural networks tend to exhibit higher frequency activity (e.g., gamma oscillations) that is modulated by low-frequency oscillations (Canolty, Edwards, Soltani, Nagarajan, Kirsch, Berger, Barbaro, & Knight, 2006; Buzsáki & Wang, 2012).

It is hypothesized that low-frequency coherence indicates coordination of multiple brain areas and top-down control.

BB 6 Hz drove more EEG functional connectivity changes and had more differences from the control stimulus than BB 25 Hz. BB 6 Hz drove these changes between frontal and occipital areas, auditory and frontal areas, and auditory and occipital areas across all four frequencies of interest (6, 12, 25, and 50 Hz). It is possible that the 6 Hz beat stimulation is mimicking the long-range, low frequency coherence observed in coordinating distant brain areas. For therapies, it would be ideal to induce the changes associated with BB 6 Hz in this study rather than the changes associated with BB 25 Hz. Further investigation may find that any beat frequency from approximately 5 Hz to 20 Hz, as indicated by previous studies of perception, would produce similar connectivity changes as 6 Hz binaural beats. The neural mechanism of action underlying binaural beats connectivity changes may be an activation of the long-distance, low-frequency pathways that coordinate distinct brain regions and are thought to be involved in processes such as attention.

Connectivity in Language Areas. A left-lateralized, frontotemporal area was consistently connected to frontal and auditory brain areas for BB 6 Hz above and beyond AM 6 Hz. Without MRI data, it is unclear exactly which brain area this activation corresponds to. However, using the MNI coordinates derived from the activated area compared to the MNI coordinates of the Brodmann areas (Papademetris & Scheinost, 2018), our data indicated that the source[23] may be in or just posterior to Broca's area[24], which is classically related to speech production (Elmer & Kühnis, 2016) but has alternatively been implicated in sensory

[23] For connectivity in 6 Hz with right auditory dipole and left frontal dipole. For connectivity in 12 Hz with left auditory dipole and right frontal dipole. For connectivity in 25 Hz with left auditory dipole.
[24] Where Broca's area is defined broadly as activation in Brodmann areas 44 and 45.

representations of words and corresponding articulatory gestures in motor cortex (Flinker, Korzeniewska, Shestyuk, Franaszczuk, Dronkers, Knight, & Crone, 2015). Damage to Broca's area has been demonstrated to affect functional connectivity in the synchronized theta network (Elmer & Kühnis, 2016; Gorišek, Isoski, Belič, Manouilidou, Koritnik, Bon, Meglič, Vrabec, Žibert, Repovš, & Zidar, 2016). Furthermore, interconnectivity between frontal, left occipito-temporal regions, and the cerebellum have been indicated for language production (Ewald, Aristei, Nolte, & Rahman, 2012). Our findings relating language areas to 6 Hz binaural beats stimulation is unexpected and requires further investigation. While amplitude modulation has been identified as an important component of speech (e.g., encasing syllables), binaural beats have not been explored as related to language in general or language production specifically.

Summary of Findings

Our analyses provided a handful of novel insights. AM 25 Hz and BB 25 Hz conditions were very similar, including: (1) a prominent phase-locking response at 50 Hz, (2) an increase in power at 50 Hz in the same bilateral auditory cortex electrodes, (3) the same right central cortical dipole identified for the maximum power in 50 Hz, (4) an unexpected decrease in power at 12 Hz, and (5) no differences in connectivity on the same scale as the 6 Hz stimuli differences. This suggests that BB 25 Hz and AM 25 Hz are processed very similarly in the brain. However, BB 6 Hz and AM 6 Hz exhibited more differences. Unexpectedly, BB 6 Hz did show an ASSR response at 6 Hz and 12 Hz. Also, AM 6 Hz drove higher increases in connectivity (relative to baseline) in some brain areas. However, BB 6 Hz drove connectivity increases in frontal, auditory, and occipital cortex, areas that have been implicated in disorders with decreased connectivity.

Because this study contains information about connectivity driven by binaural beats, the findings from this study can inform future therapies for disorders where brain connectivity is decreased. Specific recommendations for therapies include using low-frequency binaural beats (e.g., 6 Hz) to induce increases in connectivity between any combination of frontal, auditory, and occipital areas. Furthermore, clinicians should calibrate the low-frequency binaural beat stimulus to confirm the participant's perception of binaural beats, given that follow-up studies confirm the role of perception in neural processing. Because the 5-minute conditions did not show the same driving in frequency power that was shown for the 3-second conditions, our results suggest that repeated shorter bursts of stimulation are more effective than relatively long exposure times, which may be the result of habituation. If attention is also indicated as a mediator or moderator, clinicians should instruct patients accordingly.

Limitations and Recommendations

A limitation of this study is one extended to all EEG/MEG source analysis: the inverse problem. Transitioning from electrical activity measured at the scalp to neural areas is a complicated issue with still-developing algorithms and technologies. MEG offers a benefit to source analysis because the position of sensors is measured for each participant prior to analysis and the skull is "transparent" to magnetic fields, whereas EEG uses standardized coordinates for electrodes despite individual differences in head structure and the skull being a poor electrical conductor. The accuracy of EEG source analysis at placing dipoles correctly falls within 3 mm, but accuracy decreases with distance from the sensor of activity origin (e.g., interior brain structures like the basal ganglia are less accurately identified than cortex). This problem may have influenced our source analysis, particularly with subcortical brain areas. It is likely that the

localization of the maximum dipole for BB 6 Hz in the cerebellum is a misidentification of activity earlier in the auditory pathway.

Several updates to the study design could further inform the aims of this project. Source analysis from EEG data is improved with structural MRI data for each participant, so the source areas identified in this study could be further clarified by collecting both EEG and MRI data from participants. This is a particularly salient improvement given our suggested findings that subcortical areas early in the auditory pathway are the locations of some binaural beat-driven activity. EEG alone is not effective for subcortical localization, as the source analysis algorithms are less accurate for deeper activity. The evidence from this study of cerebellar and subcortical activity is sufficient to motivate further investigation with MRI for clearer localization.

The best technique for the most precise localization of binaural beats sources is functional MRI (fMRI), wherein participants would listen to binaural beats while the recruitment of oxygen to specific brain areas was measured with high spatial resolution. This technique does not offer frequency information, so its benefit is specific as a follow-up to the present study and/or in conjunction with MEG/EEG data. For fMRI, the stimulation procedure would need to be adjusted to include a manipulation so that the binaural beats are being saliently attended to (i.e., an additional task that emphasizes the binaural beats over just sensation; e.g., discrimination between beat frequency, indicating a perception of typology). This manipulation, in combination with an AM control group, would be used to increase activity in the brain areas that are specific to actively processing binaural beats, as opposed to all oscillating auditory stimuli.

Furthermore, our baseline interval differing in length from the stimulation interval limited our ability to utilize the entire 3-sec stimulation period. A baseline interval the same length in time as the stimulation interval (e.g., three seconds of baseline followed by three seconds of

stimulation) could have allowed for all of the stimulation period to be source analyzed rather than being binned first. Future work could begin by analyzing the first and last one-second periods relative to the middle period before proceeding to collect another dataset with equal baseline and stimulation periods. Additionally, computing resource restriction limited the use of statistical testing and masking for images in the recommended procedure, which uses information from the trial level to calculate Monte-Carlo estimates of the significance probabilities from the permutation distribution. Although images were produced from experimental and statistical[25] protocols to differentiate signal from noise, we were unable to apply a mask over the images in order to show only deviations statistically divergent from zero. Adding a mask to images would further increase clarity about driven effects. When we attempted to provide null hypothesis significance testing results by conducting dependent t-tests at the subject level, none of the *p*-values fell below the Bonferroni-corrected alpha. We believe that this is due to aggregating the data to such an extent as to have one value per participant for representative single points, leading to less ability to differentiate actual effects.

This protocol was limited by the lack of medical collaboration, such as the lack of audiometry testing and a checkup from a licensed practitioner for potential confounds like illness and earwax buildup. Furthermore, musical training and ability was an unaddressed potential confound which should be addressed in future studies with, at minimum, self-report inventories of experience and, more thoroughly, a brief assessment of musical ability such as identification of pitch or ability to read music.

Although change in EEG connectivity is an intriguing line of research, it is unclear what connectivity changes indicate biologically beyond increased communication between brain areas.

[25] Averaging across participants; units scaled as percent change from baseline; and algorithmic subtraction of noise via eigenvalues during the source or connectivity analysis process.

In this study, connectivity changes were investigated on relatively short time scales which, in addition to being an important first step, is potentially indicative of how the perception of binaural beats is accomplished in the human brain. However, the interest in connectivity changes partially arises from pathology wherein connectivity is impaired. If the connectivity impairment in particular patient populations is permanent and causal of symptoms, then increasing connectivity between brain areas is only interesting clinically if it lasts after treatment. The present study had no measures of lasting effects or correlated behavioral outcomes.

Next Steps. This project was exploratory in nature and indicated multiple avenues for future inquiry. Most immediately, effective connectivity analysis should be conducted to investigate causal relationships between pairs of brain areas. Longer stimulation periods (e.g., 20 minutes) of bursting binaural beats, repeated stimulation sessions (e.g., daily exposure for 1-2 weeks), and lasting effects following treatment would be relevant manipulations moving towards clinical applications in addition to studying clinical populations. Innovations to make treatment more comfortable for patients, such as overlaying beats with music and listening to beats before or during sleep, should be another subject of investigations in the long term. Furthermore, theoretical advancements might be made by emulating these data with modeling simulations, such as a representative network of cortical neurons evoking similar population frequency amplitude and phase-locking patterns. These advancements could increase our understanding of the sensation and perception of binaural beats at the level of small populations of neurons.

Conclusion

This study successfully ascertained that binaural beats differ from amplitude-modulated beats, in part by causing increased neural connectivity between brain areas that exhibit decreased interconnectivity in particular disorders. This project enhanced our knowledge of binaural beat

processing in a healthy young adult brain, which provided insight into mechanisms of binaural beat audition as well as directions for future investigation and inexpensive, noninvasive therapies. The results of this study may be of particular interest to academics and other researchers who study auditory stimuli, including language, as well as clinicians who study or treat psychiatric and neurological disorders.

References

Altmann, C.F., & Gaese, B.H. (2014). Representation of frequency-modulated sounds in the human brain. *Hearing Research, 307*, 74-85.

Başar, E., Başar-Eroglu, C., Karakaş, S., & Schürmann, M. (2001). Gamma, alpha, delta, and theta oscillations govern cognitive processes. *Int'l J of Psychophysiol, 39*, 241-248.

Başar, E., Başar-Eroğlu, C., Güntekin, B., & Yener, G.G. (2013). Brain's alpha, beta, gamma, delta, and theta oscillations in neuropsychiatric diseases: Proposal for biomarker strategies. *Supp to Clin Neurophysiol, 62*, 19-55.

Beauchene, C., Abaid, N., Moran, R., Diana, R.A., & Leonessa, A. (2016). The effect of binaural beats on visuospatial working memory and cortical connectivity. *PLoS ONE 11*(11).

Becher, A., Höhne, M., Axmacher, N., Chaieb, L., Elger, C.E., & Fell, J. (2014). Intracranial electroencephalography power and phase synchronization changes during monaural and binaural beat stimulation. *European J of Neuroscience,* 1-10.

Belmonte, M. K., Allen, G., Beckel-Mitchener, A., Boulanger, L. M., Carper, R. A., & Webb, S. J. (2004). Autism and abnormal development of brain connectivity. *Journal of Neuroscience, 24*(42), 9228-9231.

Butler, B.E., & Trainor, L.J. (2012). Sequencing the cortical processing of pitch-evoking stimuli using EEG analysis and source estimation. *Front. Psychol., 3.*

Buzsáki, G., & Wang, X. (2012). Mechanisms of gamma oscillations. *Annu Rev Neurosci, 2012*(35).

Canolty, R.T., Edwards, E., Dalal, S.S., Soltani, M., Nagarajan, S.S., Kirsch, H.E., Berger, M.S., Barbaro, N.M., & Knight, R.T. (2006). High gamma power is phase-locked to theta oscillations in human neocortex. *Science, 313*(5793).

Delorme, A., & Makeig, S. (2004). EEGLAB: an open source toolbox for analysis of single-trial EEG dynamics, *Journal of Neuroscience Methods, 134*.

Elmer, S., & Kühnis, J. (2016). Functional connectivity in the left dorsal stream facilitates simultaneous language translation: An EEG study. *Front. Hum. Neurosci.*

Ewald, A., Aristei, S., Nolte, G., & Rahman, R.A. (2012). Brain oscillations and functional connectivity during overt language production. *Front Psychol, 3*(166).

Fingelkurts, A.A., Fingelkurts, A.A., & Kallio-Tamminen, T. (2016). Long-term meditation training induced changes in the operational synchrony of default mode network modules during a resting state. *Cognitive Processing, 17*(1).

Fingelkurts, A.A., Fingelkurts, A.A., Kivisaari, R., Autti, T., Borisov, S., Puuskari, V., Jokela, O., & Kähkönen, S. (2009). Methadone restores local and remote EEG functional connectivity in opioid-dependent patients. *The International J of Neuroscience, 119*(9).

Flinker, A., Korzeniewska, A., Shestyuk, A.Y., Franaszczuk, P.J., Dronkers, N.F., Knight, R.T., & Crone, N.E. (2015). Redefining the role of Broca's area in speech. *PNAS, 112*(9).

Fontaine, B., & Peremans, H. (2007). Tuning bat LSO neurons to interaural intensity differences through spike-timing dependent plasticity. *Biol Cybern, 97*. 261-267.

Gao, X., Cao, H., Ming, D., Qi, H., Wang, X., Wang, X., Chen, R., & Zhou, P. (2014). Analysis of EEG activity in response to binaural beats with different frequencies. *Journal of Psychophysiology, 94*, 399-406.

Gorišek, V.R., Isoski, V.Z., Belič, A., Manouilidou, C., Koritnik, B., Bon, J., Meglič, N.P., Vrabec, M., Žibert, J., Repovš, G., & Zidar, J. (2016) Beyond aphasia: Altered EEG connectivity in Broca's patients during working memory task. *Brain and Language, 163.*

Griffiths, T.D., Penhune, V., Peretz, I., Dean, J.L., Patterson, R.D., & Green, G.G. (2000). Frontal processing and auditory perception. *Neuroreport, 11*.

Grigoreva, T.I., Figurina, I.I., & Vasilev, A.G. (1988). Role of the medial geniculate body in the production of conditioned reflexes to amplitude-modulated stimuli in rats. *Zh Vyssh Nervn Deyat, 37.*

Griskova-Bulanova, I., Dapsys, K., Melynyte, S., Voicikas, A., Maciulis, V., Andruskevicius, S., & Korostenskaja, M. (2018). 40 Hz auditory steady-state response in schizophrenia: Sensitivity to stimulation type (clicks versus flutter amplitude-modulated tones). *Neuroscience Letters, 662*, 152-157.

Gross, J., Kujala, J., Hämäläinen, M., Timmermann, L., Schnitzler, A. & Salmelin, R. (2001). Dynamic imaging of coherent sources: Studying neural interactions in the human brain. *PNAS, 98*(2), 694-699.

Hartmann, W.M., & Macaulay, E.J. (2014). Anatomical limits on interaural time differences: An ecological perspective. *Frontiers in Neurosci, 8*(34).

Haufe, S. (2012). *Towards EEG source connectivity analysis* (Doctoral dissertation).

Hoffmann, E., Brück, C., Kreifelts, B., Ethofer, T., & Wildgruber, D. (2015). Social brain network and autism spectrum disorder: Reduced connectivity to the frontal cortex. *Clinical Neurophysiology, 126*(8), e91-e92.

Ioannou, C.I., Pereda, E., Lindsen, J.P., & Bhattacharya, J. (2015). Electrical brain responses to an auditory illusion and the impact of musical expertise. *PLoS ONE, 10*(6).

Japaridze, N., Siniatchkin, M., Muthuraman, M., Raethjen, J., Stephani, U., & Moeller, F. (2013). Dynamic imaging of coherent sources. *Zeitschrift für Epileptologie, 26*(1).

Jercog, P.E., Svirkis, G., Kotak, V.C., Sanes, D.H., & Rinzel, J. (2010). Asymmetric excitatory synaptic dynamics underlie interaural time difference processing in the auditory system. *PLoS Biology, 8*(6).

Johns, M.W. (1991) A new method for measuring daytime sleepiness: the Epworth sleepiness scale. *Sleep, 14.*

Johns, M.W. (1992). Reliability and factor analysis of the Epworth sleepiness scale. *Sleep, 15*, 376-381.

Johns, M.W. (2000). Specificity and sensitivity of the multiple sleep latency test (MSLT), the maintenance of wakefulness test (MWT) and the Epworth sleepiness scale; failure of the MSLT as a gold standard. *Journal of Sleep Research, 9.*

Joris, P.X., Schreiner, C.E., & Rees, A. (2004). Neural processing of amplitude-modulated sounds. *Physiological Reviews, 84*, 541-577.

Kennel, S., Taylor, A.G., Lyon, D., & Bourguignon, C. (2010). Pilot feasibility study of binaural auditory beats for reducing symptoms of inattention in children and adolescents with attention-deficity/hyperactivity disorder. *Journal of Pediatric Nursing, 25*(1), 3-11.

Krishnan, G.P., Hetrick, W.P., Brenner, C.A., Shekhar, A., Steffan, A.N., & O'Donnell, B.F. (2009). Steady state and induced auditory gamma deficits in schizophrenia. *Neuroimage, 47*(4), 1711-9.

Krupa, M.P., Gielen, C.C.A.M., & Gutkin, B. (2014). Adaptation and shunting inhibition leads to pyramidal/interneuron gamma with sparse firing of pyramidal cells. *J of Comp Neuro, 37*, 357-376.

Legget, K.T., Hild, A.K., Steinmetz, S.E., Simon, S.T., & Rojas, D.C. (2017). MEG and EEG demonstrate similar test-retest reliability of the 40 Hz auditory steady-state response. *International Journal of Psychophysiology, 114*, 16-23.

Léveillé, C., Bolduc, C., Limoges, É., Chevrier, É., Mottron, L., & Godbout, R. (2013). Wake EEG coherence before and after sleep in adults with autism: Decreased morning frontal connectivity. *Sleep Medicine, 14*.

McFadden, K.L., Steinmetz, S.E., Carroll, A.M., Simon, S.T., Wallace, A., & Rojas, D.C. (2014). Test-retest reliability of the 40 Hz EEG auditory steady-state response. *PLoS One, 9*.

NIDCD (2018, July 17). Age-Related Hearing Loss. Retrieved from https://www.nidcd.nih.gov/health/age-related-hearing-loss

Nicholls, J.G., Martin, A.R., Fuchs, P.A., Brown, D.A., Diamond, M.E., & Weisblat, D.A. (2012). *From neuron to brain*. Sunderland, MA: Sinauer Associates, Inc.

Oostenveld, R. (2017, August 17). Localizing oscillatory sources using beamformer techniques. Retrieved from http://www.fieldtriptoolbox.org/tutorial/beamformer

Oostenveld, R., Fries, P., Maris, E., Schoffelen, J.M. (2011). FieldTrip: Open source software for advanced analysis of MEG, EEG, and invasive electrophysiological data. *Computational Intelligence and Neuroscience, 2011*.

Oostenveld, R., Stegeman, D.F., Praamstra, P., & van Oosterom, A. (2003). Brain symmetry and topographic analysis of lateralized event-related potentials. *Clin Neurophysiol*, *114*(7).

Papademetris, X., & Scheinost, D. (2018, May 9). *MNI <-> Talairach with Brodmann Areas (1.09)*. Retrieved from http://sprout022.sprout.yale.edu/mni2tal/mni2tal.html

Park, T.J., Grothe, B., Pollak, G.D., Schuller, G., & Koch, U. (1996). Neural delays shape selectivity to interaural intensity differences in the lateral superior olive. *J Neurosci, 16*(20). 6554-6566.

Peled, A. (2001). Functional connectivity and working memory in schizophrenia: An EEG study. *International Journal of Neuroscience, 106*(1/2).

Picton, T.W., John, M.S., Dimitrijevic, A., & Purcell, D. (2003). Human auditory steady-state responses. *Int J Audiol, 42*(4), 177-219.

Plourde, G., Stapells, D.R., & Picton, T.W. (1991). The human auditory steady-state evoked potentials. *Acta Otolaryngol Suppl,* 153-159.

Pratt, H., Starr, A., Michalewski, H.J., Dimitrijevic, A., Bleich, N., & Mittelman, N. (2009). Cortical evoked potential to an auditory illusion: Binaural beats. *Clinical Neurophysiology, 120*, 1514-1524.

Pratt, H., Starr, A., Michalewski, H.J., Dimitrijevic, A., Bleich, N., & Mittelman, N. (2010). A comparison of auditory evoked potentials to acoustic beats and to binaural beats. *Hearing Research, 262*, 34-44.

Purves, D., Augustine, G.J., Fitzpatrick, D. et al., editors. (2001). *Neuroscience*. 2nd edition. Sunderland (MA): Sinauer Associates. Tuning and Timing in the Auditory Nerve. Available from: https://www.ncbi.nlm.nih.gov/books/NBK11105/

Rees, A., Green, G.G., & Kay, R.H. (1986). Steady-state evoked responses to sinusoidally amplitude-modulated sounds recorded in man. *Hear Res, 23*(2), 123-133.

Ross, B., Miyazaki, T., Thompson, J., Jamali, S., & Fujioka, T. (2014). Human cortical responses to slow and fast binaural beats reveal multiple mechanisms of binaural hearing. *J Neurophysiol, 112*, 1871-1884.

Saenz, M., & Langers, D.R.M. (2014). Tonotopic mapping of human auditory cortex. *Hearing Research, 307,* 42-52.

Schwartz, S., Kessler, R., Gaughan, T., & Buckley, A. (2017). Electroencephalogram coherence patterns in autism: An updated review. *Pediatric Neurology, 67.*

Schwarz, D.W.F., & Taylor, P. (2005). Human auditory steady state responses to binaural and monaural beats. *Clinical Neurophysiology, 116,* 658-668.

Skottun, B.C., Shackleton, T.M., Arnott, R.H., & Palmer, A.R. (2001). The ability of inferior colliculus neurons to signal differences in interaural delay. *PNAS, 98*(24).

Squire, L.R., Berg, D., Bloom, F.E., du Lac, S., Ghosh, A., & Spitzer, N.C. (Eds.). (2013). *Fundamental neuroscience*. Boston, MA: Elsevier, Inc.

Tan, X., Fu, Q., Yuan, H., Ding, L., & Wang, T. (2017). Improved transient response estimations predicting 40 Hz auditory steady-state response using deconvolution methods. *Front. Neurosci.*

Tollin, D.J. (2003). The lateral superior olive: A functional role in sound source localization. *Neuroscientist, 9*(2). 127-143.

van der Heijden, M., Lorteije, J.A.M., Plauška, A., Roberts, M.T., Golding, N.L., & Borst, J.G.G. (2013). Directional hearing by linear summation of binaural inputs at the medial superior olive. *Neuron, 78*. 936-948.

Vernon, D., Peryer, G., Louch, J., & Shaw, M. (2012). Tracking EEG changes in response to alpha and beta binaural beats. *International J of Psychophysiology.*

von Stein, A., & Sarnthein, J. (2000). Different frequencies for different scales of cortical integration: From local gamma to long range alpha/theta synchronization. *International Journal of Psychophysiology, 38.*

Wall, J.A., McDaid, L.J., Maguire, L.P., & Mcginnity, T.M. (2012). Spiking neural network model of sound localization using the interaural intensity difference. *IEEE Transactions on Neural Networks and Learning Systems, 23*(4). 574-586.

Zhang, J., Wang, J., Wu, Q., Kuang, W., Huang, X., He, Y., & Gong, Q. (2011). Disrupted brain connectivity networks in drug-naive, first-episode major depressive disorder. *Biological psychiatry, 70*(4), 334-342.

Appendix: FFT Images

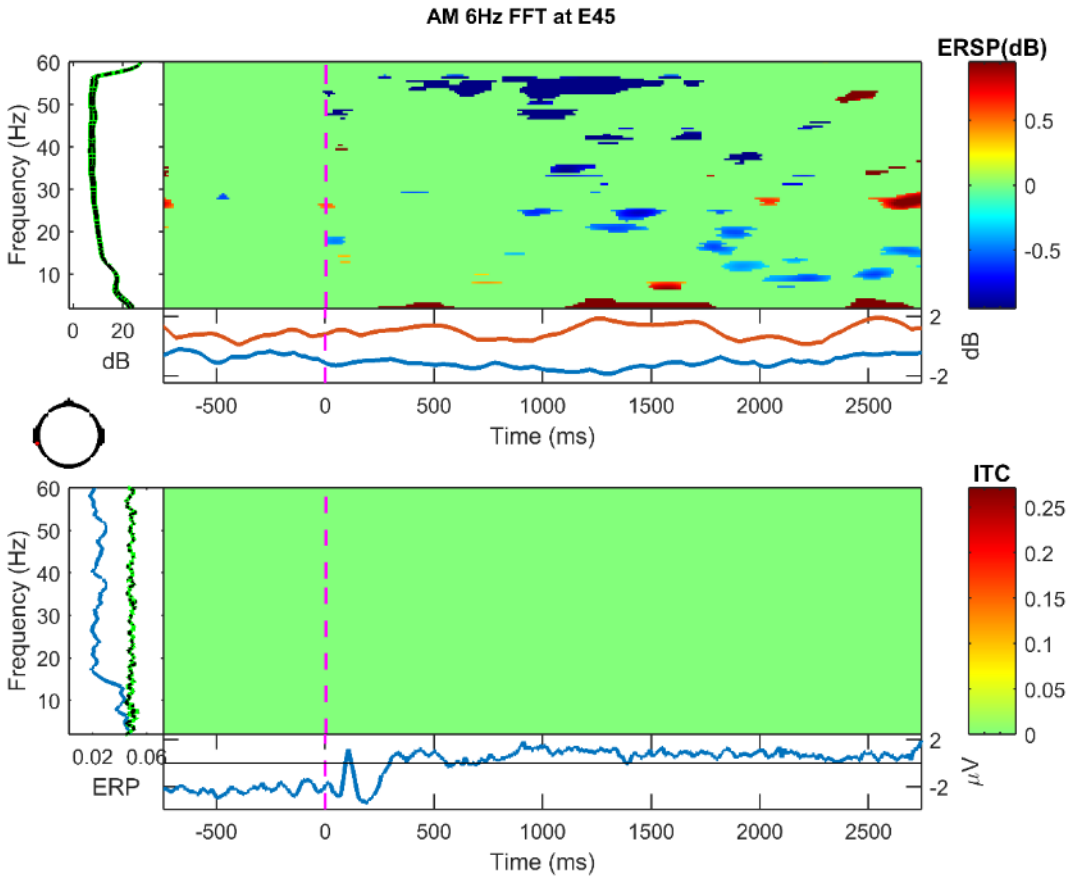

Figure 4. Frequency decomposition done with Fast Fourier Transform (FFT) for E45 (left temporal, auditory cortex) from 2-60 Hz during the one second prior to stimulation and the three seconds during stimulation with 6 Hz amplitude modulated tone. Stimulation period is baseline corrected. Green indicates no significant change from baseline using permutation statistics (α = .10 with false detection rate correction for multiple comparison). X-axis is time, y-axis is frequency. Top: Darker blues indicate a decrease in frequency power while darker reds indicate and increase in frequency power from baseline. Bottom: Darker reds indicate an increase in phase-locking/inter-trial coherence (ITC) between trials at the specified frequency.

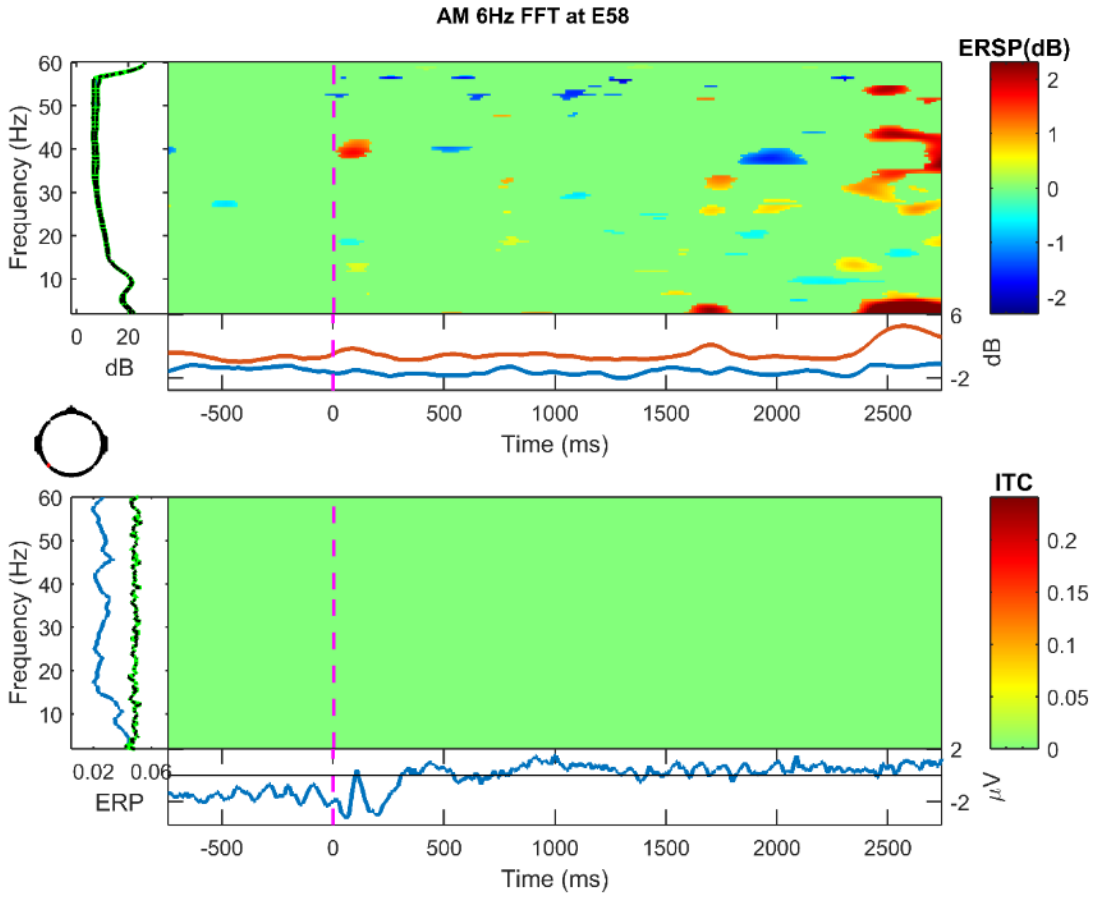

Figure 5. Frequency decomposition done with Fast Fourier Transform (FFT) for E58 (left temporal, auditory cortex) from 2-60 Hz during the one second prior to stimulation and the three seconds during stimulation with 6 Hz amplitude modulated tone. Stimulation period is baseline corrected. Green indicates no significant change from baseline using permutation statistics (α = .10 with false detection rate correction for multiple comparison). X-axis is time, y-axis is frequency. Top: Darker blues indicate a decrease in frequency power while darker reds indicate and increase in frequency power from baseline. Bottom: Darker reds indicate an increase in phase-locking/inter-trial coherence (ITC) between trials at the specified frequency.

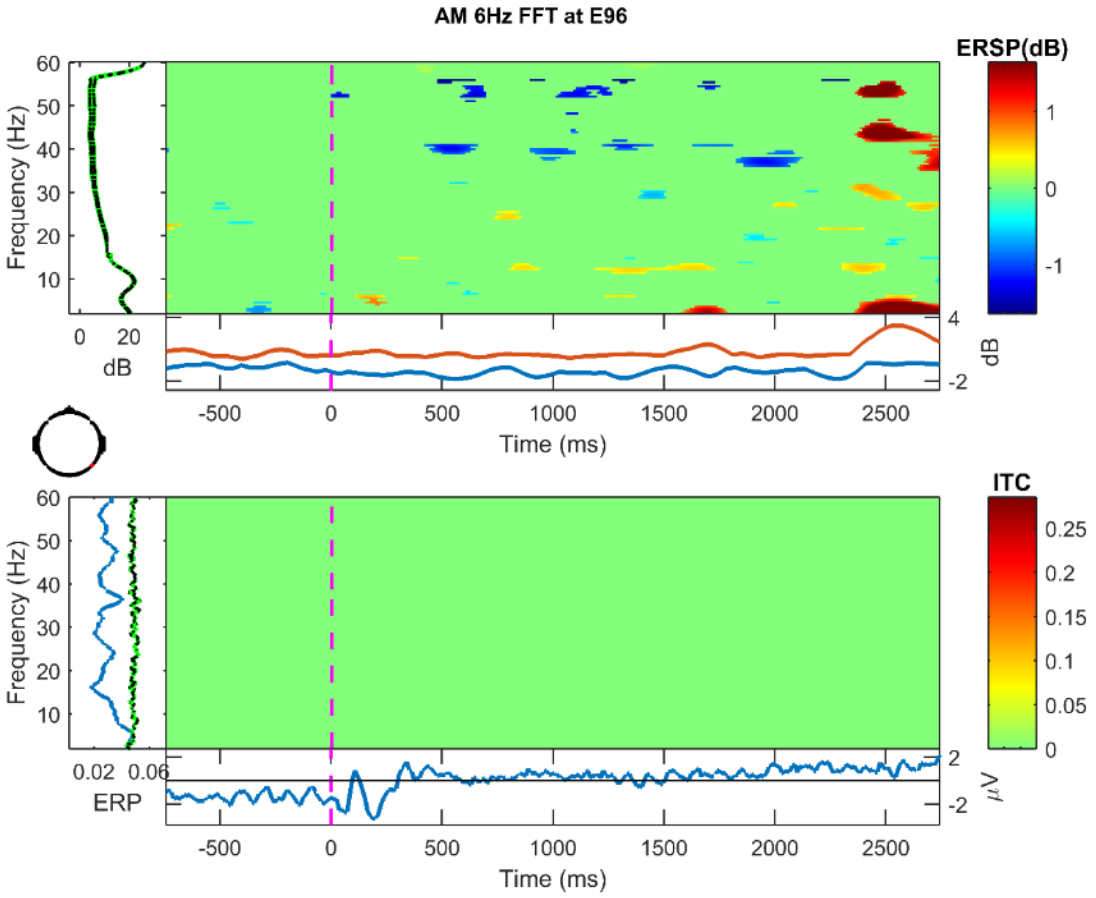

Figure 6. Frequency decomposition done with Fast Fourier Transform (FFT) for E96 (right temporal, auditory cortex) from 2-60 Hz during the one second prior to stimulation and the three seconds during stimulation with 6 Hz amplitude modulated tone. Stimulation period is baseline corrected. Green indicates no significant change from baseline using permutation statistics (α = .10 with false detection rate correction for multiple comparison). X-axis is time, y-axis is frequency. Top: Darker blues indicate a decrease in frequency power while darker reds indicate and increase in frequency power from baseline. Bottom: Darker reds indicate an increase in phase-locking/inter-trial coherence (ITC) between trials at the specified frequency.

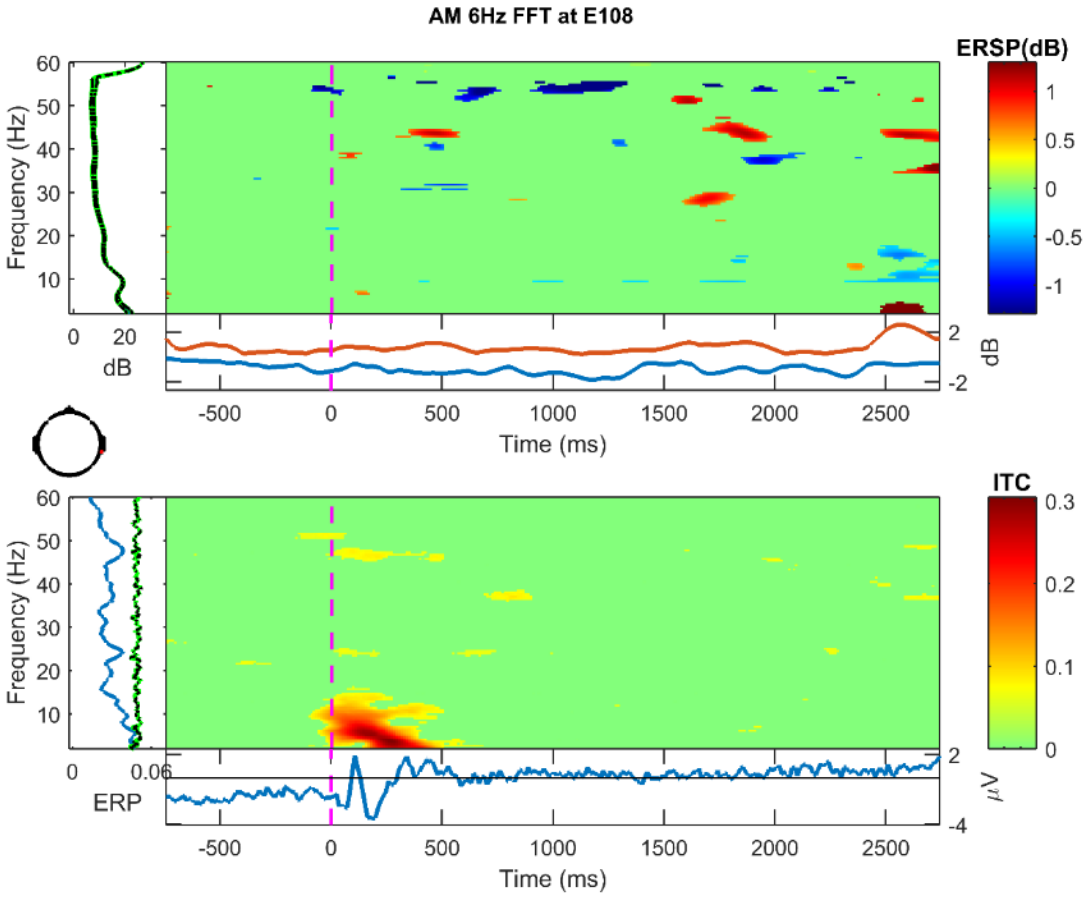

Figure 7. Frequency decomposition done with Fast Fourier Transform (FFT) for E108 (right temporal, auditory cortex) from 2-60 Hz during the one second prior to stimulation and the three seconds during stimulation with 6 Hz amplitude modulated tone. Stimulation period is baseline corrected. Green indicates no significant change from baseline using permutation statistics (α = .10 with false detection rate correction for multiple comparison). X-axis is time, y-axis is frequency. Top: Darker blues indicate a decrease in frequency power while darker reds indicate and increase in frequency power from baseline. Bottom: Darker reds indicate an increase in phase-locking/inter-trial coherence (ITC) between trials at the specified frequency.

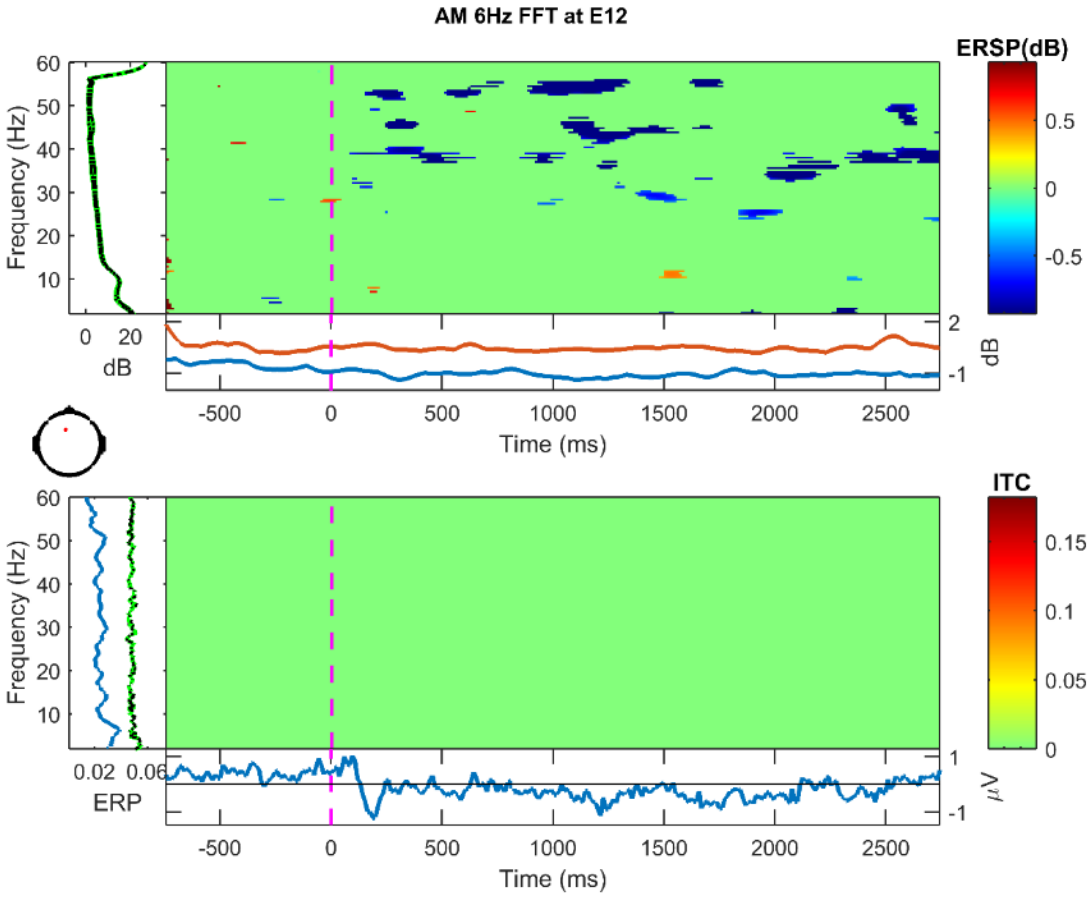

Figure 8. Frequency decomposition done with Fast Fourier Transform (FFT) for E12 (left frontal) from 2-60 Hz during the one second prior to stimulation and the three seconds during stimulation with 6 Hz amplitude modulated tone. Stimulation period is baseline corrected. Green indicates no significant change from baseline using permutation statistics ($\alpha = .10$ with false detection rate correction for multiple comparison). X-axis is time, y-axis is frequency. Top: Darker blues indicate a decrease in frequency power while darker reds indicate and increase in frequency power from baseline. Bottom: Darker reds indicate an increase in phase-locking/inter-trial coherence (ITC) between trials at the specified frequency.

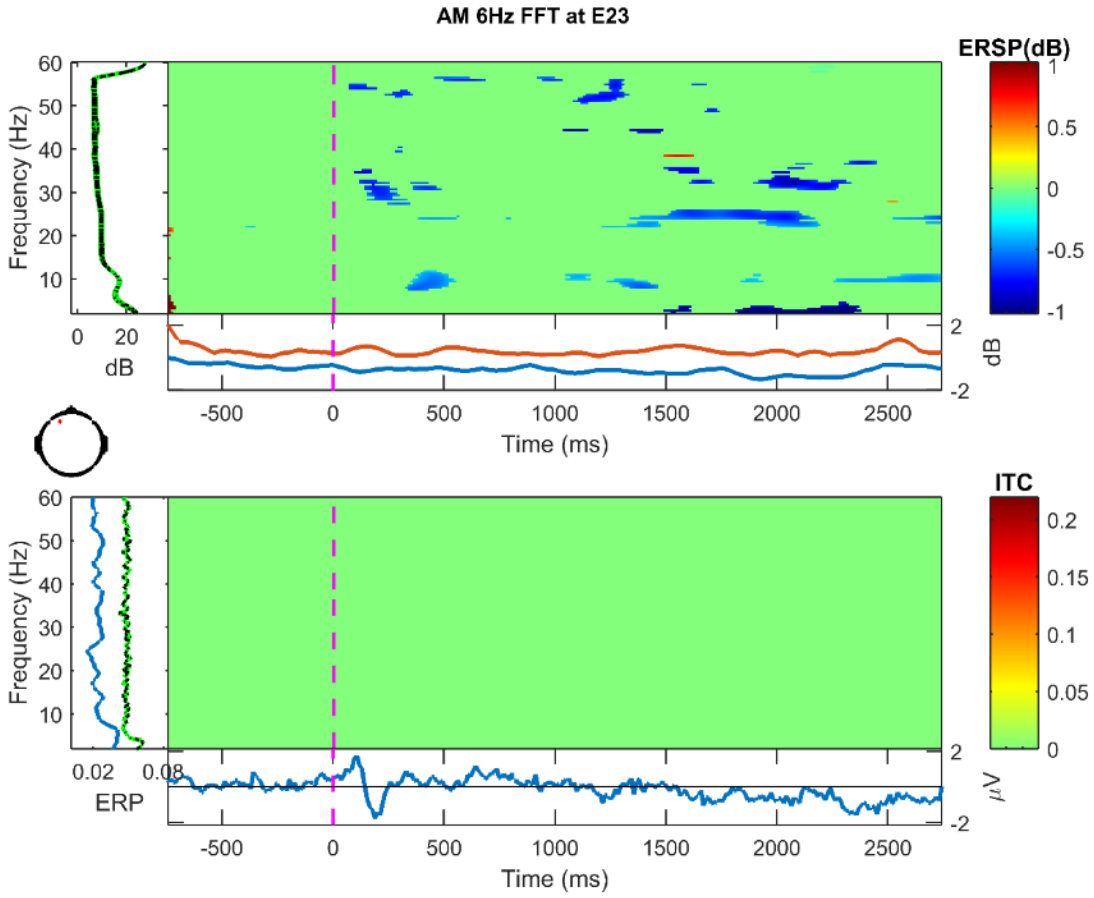

Figure 9. Frequency decomposition done with Fast Fourier Transform (FFT) for E23 (left frontal) from 2-60 Hz during the one second prior to stimulation and the three seconds during stimulation with 6 Hz amplitude modulated tone. Stimulation period is baseline corrected. Green indicates no significant change from baseline using permutation statistics ($\alpha = .10$ with false detection rate correction for multiple comparison). X-axis is time, y-axis is frequency. Top: Darker blues indicate a decrease in frequency power while darker reds indicate and increase in frequency power from baseline. Bottom: Darker reds indicate an increase in phase-locking/inter-trial coherence (ITC) between trials at the specified frequency.

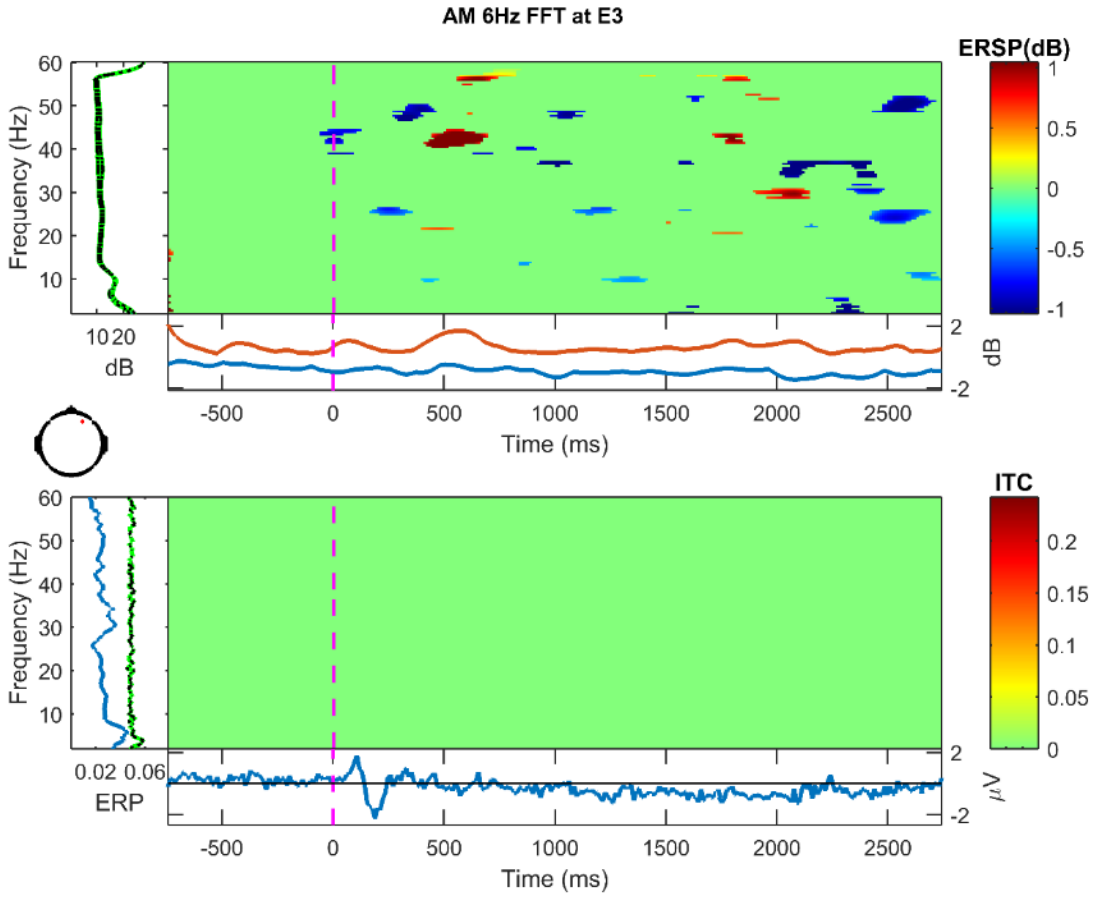

Figure 10. Frequency decomposition done with Fast Fourier Transform (FFT) for E3 (right frontal) from 2-60 Hz during the one second prior to stimulation and the three seconds during stimulation with 6 Hz amplitude modulated tone. Stimulation period is baseline corrected. Green indicates no significant change from baseline using permutation statistics ($\alpha = .10$ with false detection rate correction for multiple comparison). X-axis is time, y-axis is frequency. Top: Darker blues indicate a decrease in frequency power while darker reds indicate and increase in frequency power from baseline. Bottom: Darker reds indicate an increase in phase-locking/inter-trial coherence (ITC) between trials at the specified frequency.

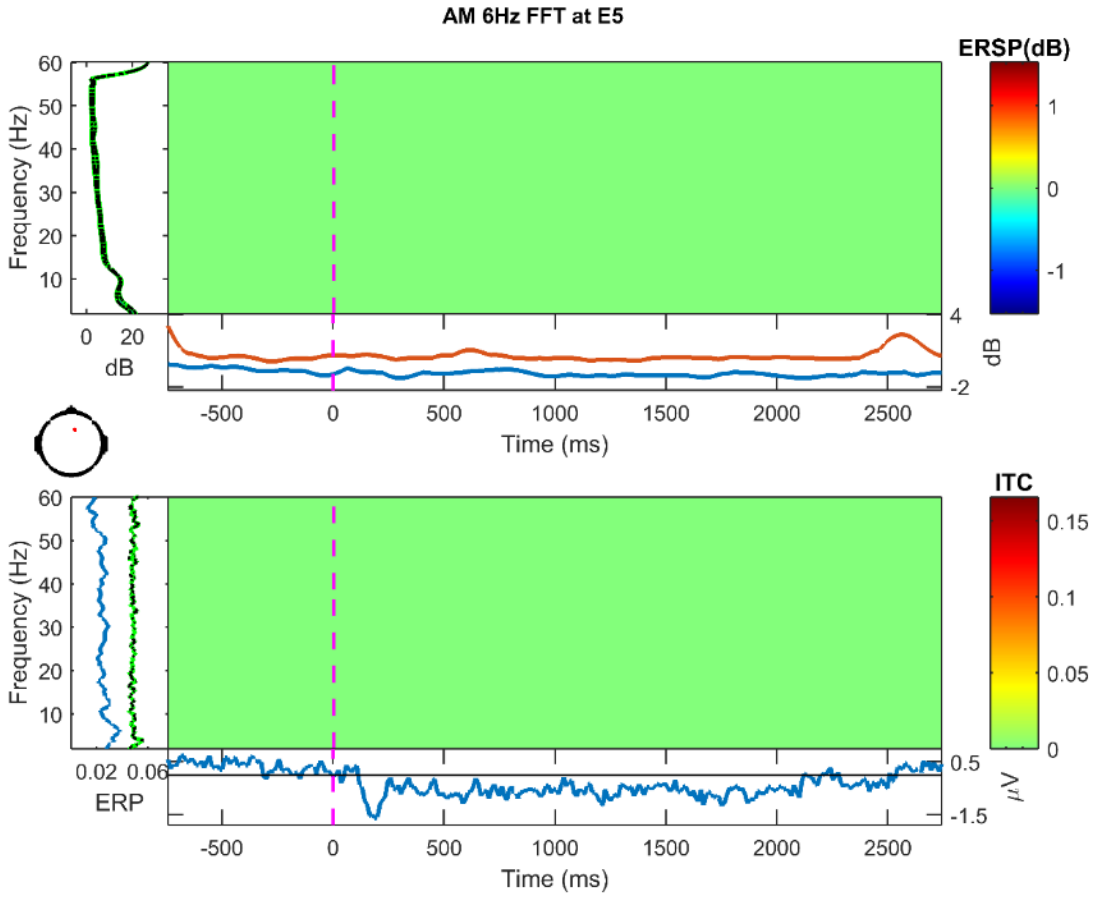

Figure 11. Frequency decomposition done with Fast Fourier Transform (FFT) for E5 (right frontal) from 2-60 Hz during the one second prior to stimulation and the three seconds during stimulation with 6 Hz amplitude modulated tone. Stimulation period is baseline corrected. Green indicates no significant change from baseline using permutation statistics ($\alpha = .10$ with false detection rate correction for multiple comparison). X-axis is time, y-axis is frequency. Top: Darker blues indicate a decrease in frequency power while darker reds indicate and increase in frequency power from baseline. Bottom: Darker reds indicate an increase in phase-locking/inter-trial coherence (ITC) between trials at the specified frequency.

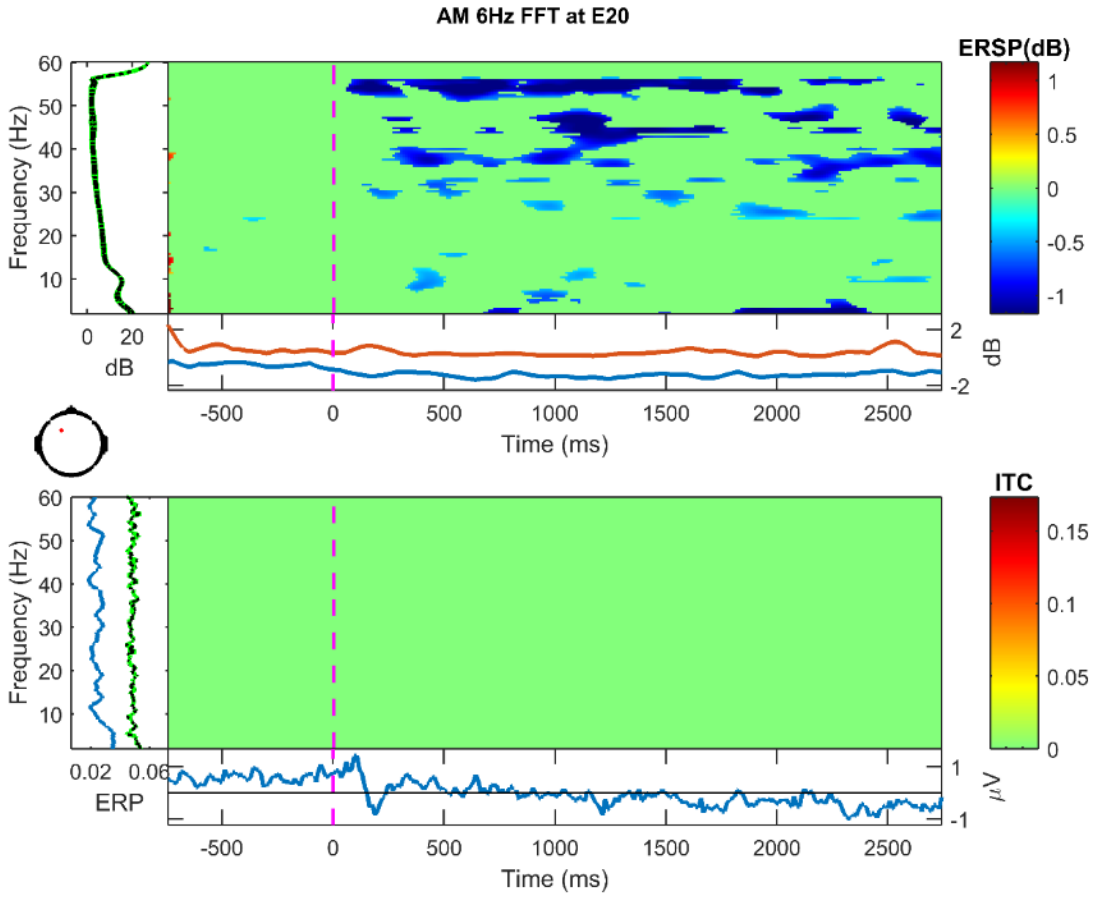

Figure 12. Frequency decomposition done with Fast Fourier Transform (FFT) for E20 (left central) from 2-60 Hz during the one second prior to stimulation and the three seconds during stimulation with 6 Hz amplitude modulated tone. Stimulation period is baseline corrected. Green indicates no significant change from baseline using permutation statistics ($\alpha = .10$ with false detection rate correction for multiple comparison). X-axis is time, y-axis is frequency. Top: Darker blues indicate a decrease in frequency power while darker reds indicate and increase in frequency power from baseline. Bottom: Darker reds indicate an increase in phase-locking/inter-trial coherence (ITC) between trials at the specified frequency.

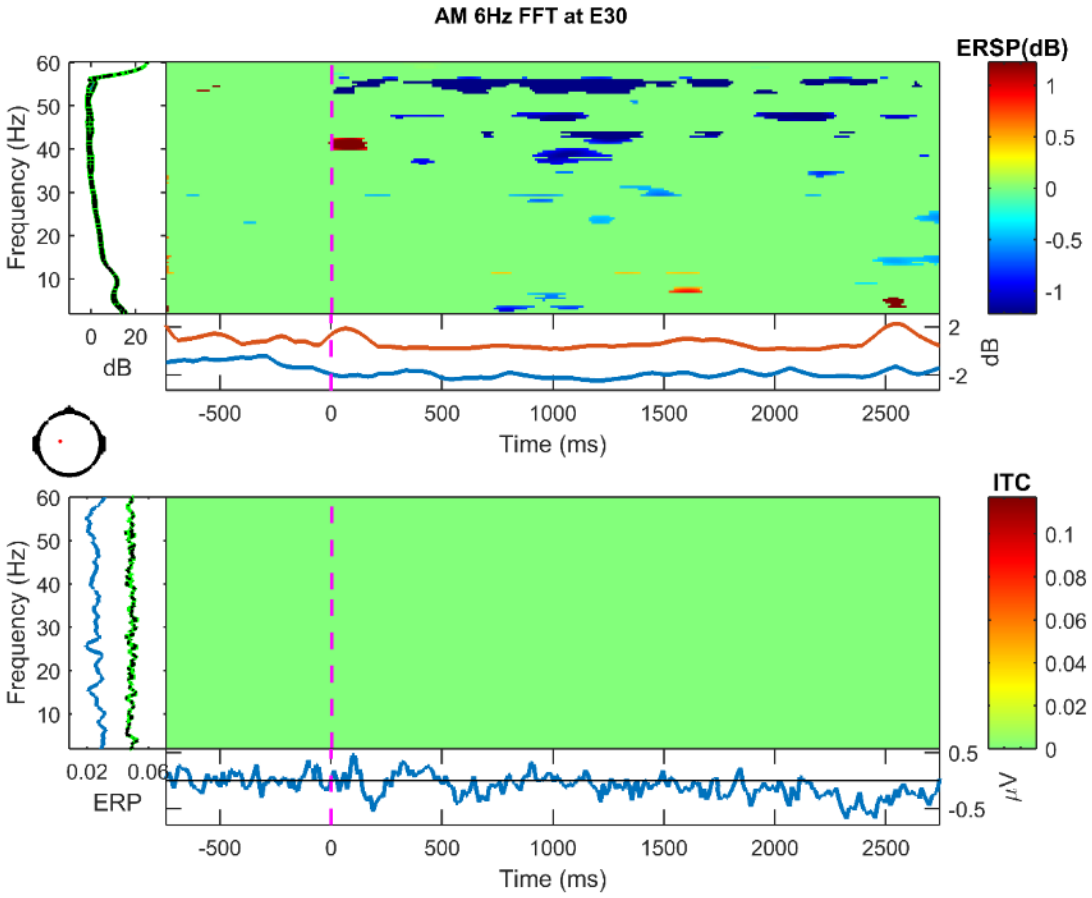

Figure 13. Frequency decomposition done with Fast Fourier Transform (FFT) for E30 (left central) from 2-60 Hz during the one second prior to stimulation and the three seconds during stimulation with 6 Hz amplitude modulated tone. Stimulation period is baseline corrected. Green indicates no significant change from baseline using permutation statistics ($\alpha = .10$ with false detection rate correction for multiple comparison). X-axis is time, y-axis is frequency. Top: Darker blues indicate a decrease in frequency power while darker reds indicate and increase in frequency power from baseline. Bottom: Darker reds indicate an increase in phase-locking/inter-trial coherence (ITC) between trials at the specified frequency.

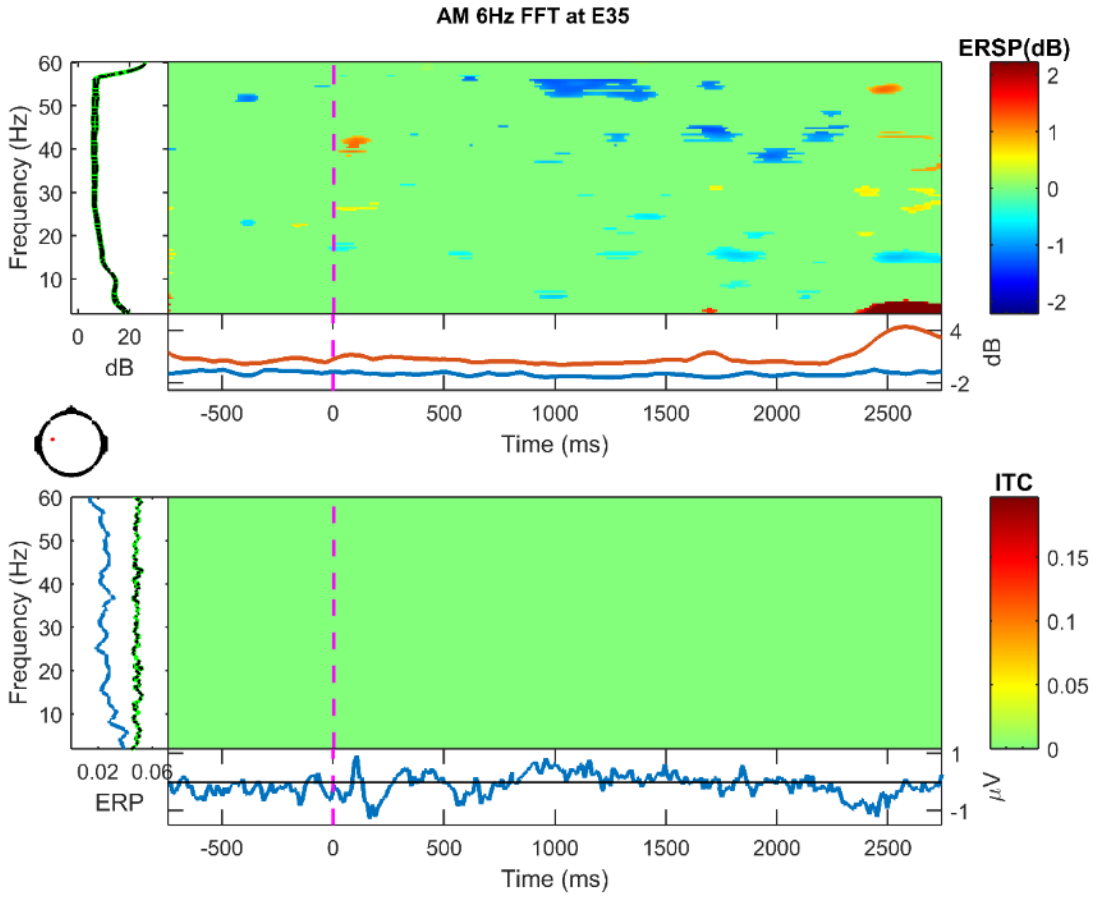

Figure 14. Frequency decomposition done with Fast Fourier Transform (FFT) for E35 (left central) from 2-60 Hz during the one second prior to stimulation and the three seconds during stimulation with 6 Hz amplitude modulated tone. Stimulation period is baseline corrected. Green indicates no significant change from baseline using permutation statistics ($\alpha = .10$ with false detection rate correction for multiple comparison). X-axis is time, y-axis is frequency. Top: Darker blues indicate a decrease in frequency power while darker reds indicate and increase in frequency power from baseline. Bottom: Darker reds indicate an increase in phase-locking/inter-trial coherence (ITC) between trials at the specified frequency.

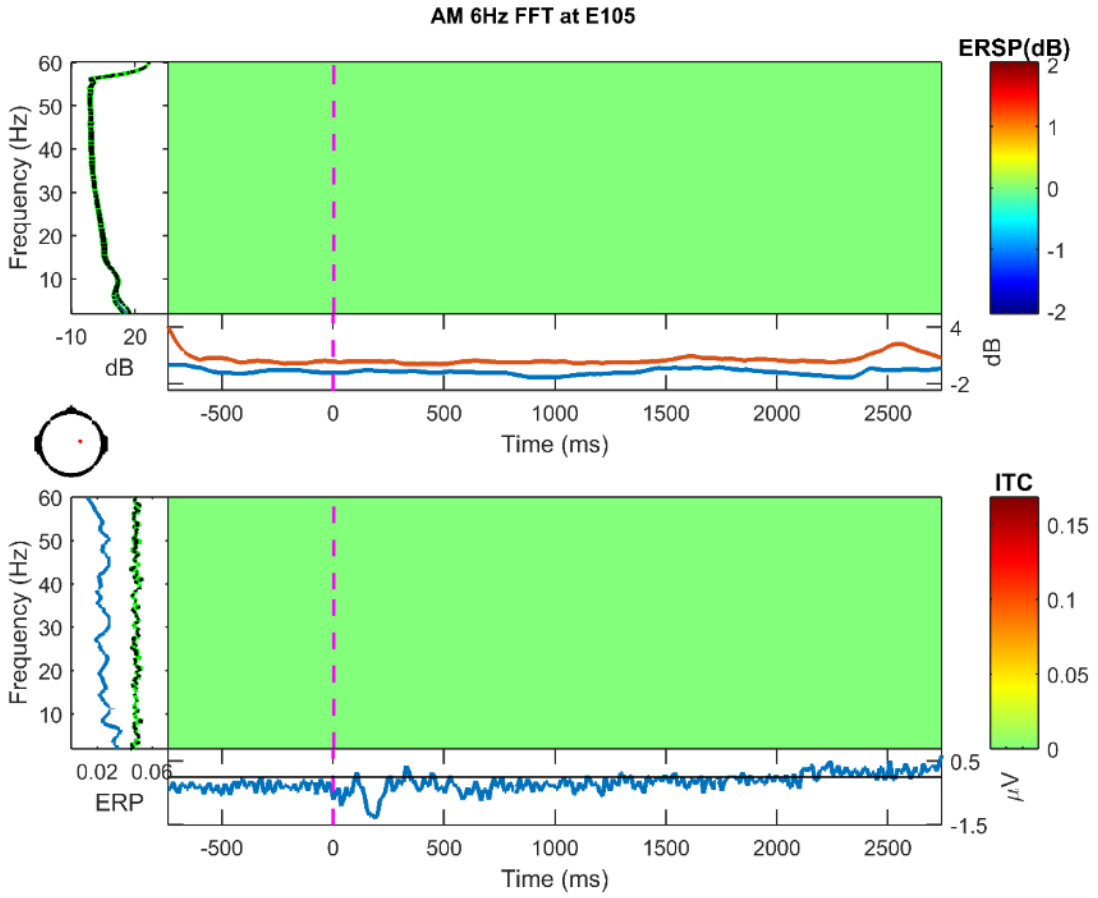

Figure 15. Frequency decomposition done with Fast Fourier Transform (FFT) for E105 (right central) from 2-60 Hz during the one second prior to stimulation and the three seconds during stimulation with 6 Hz amplitude modulated tone. Stimulation period is baseline corrected. Green indicates no significant change from baseline using permutation statistics ($\alpha = .10$ with false detection rate correction for multiple comparison). X-axis is time, y-axis is frequency. Top: Darker blues indicate a decrease in frequency power while darker reds indicate and increase in frequency power from baseline. Bottom: Darker reds indicate an increase in phase-locking/inter-trial coherence (ITC) between trials at the specified frequency.

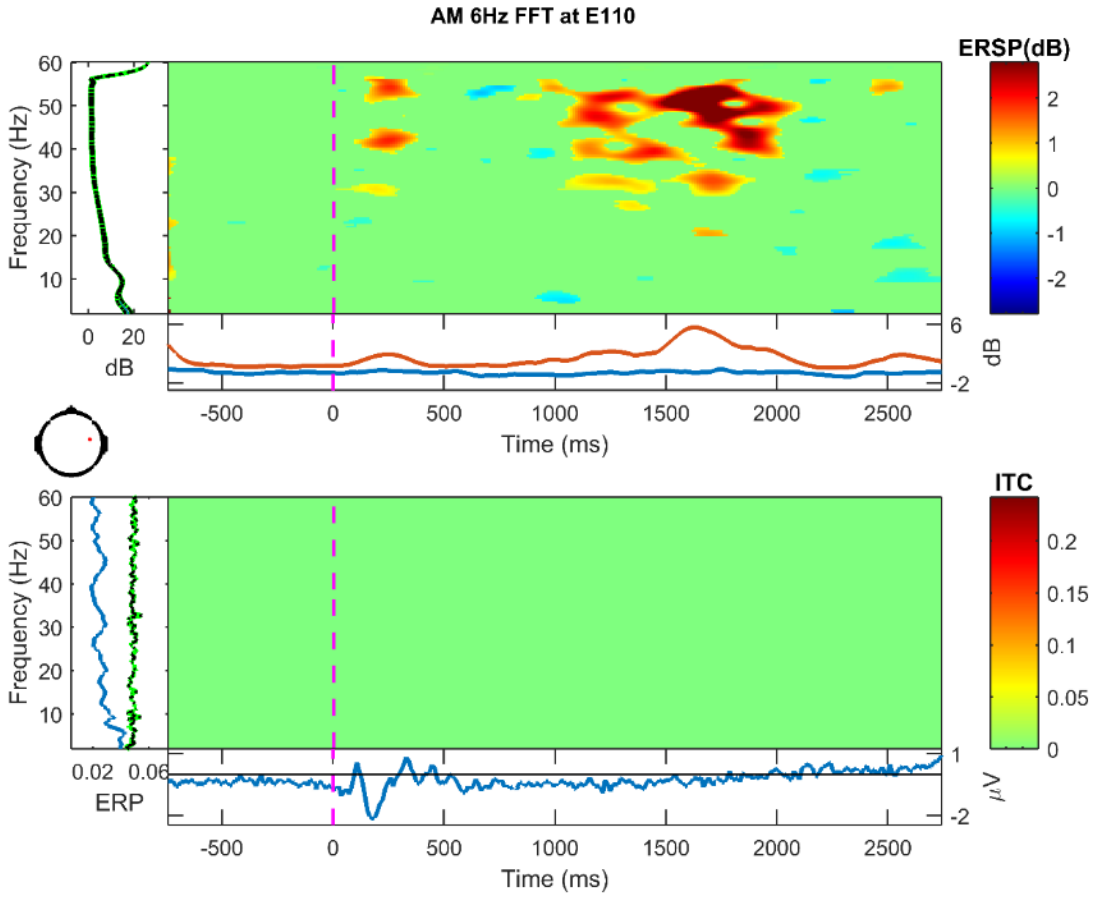

Figure 16. Frequency decomposition done with Fast Fourier Transform (FFT) for E110 (right central) from 2-60 Hz during the one second prior to stimulation and the three seconds during stimulation with 6 Hz amplitude modulated tone. Stimulation period is baseline corrected. Green indicates no significant change from baseline using permutation statistics (α = .10 with false detection rate correction for multiple comparison). X-axis is time, y-axis is frequency. Top: Darker blues indicate a decrease in frequency power while darker reds indicate and increase in frequency power from baseline. Bottom: Darker reds indicate an increase in phase-locking/inter-trial coherence (ITC) between trials at the specified frequency.

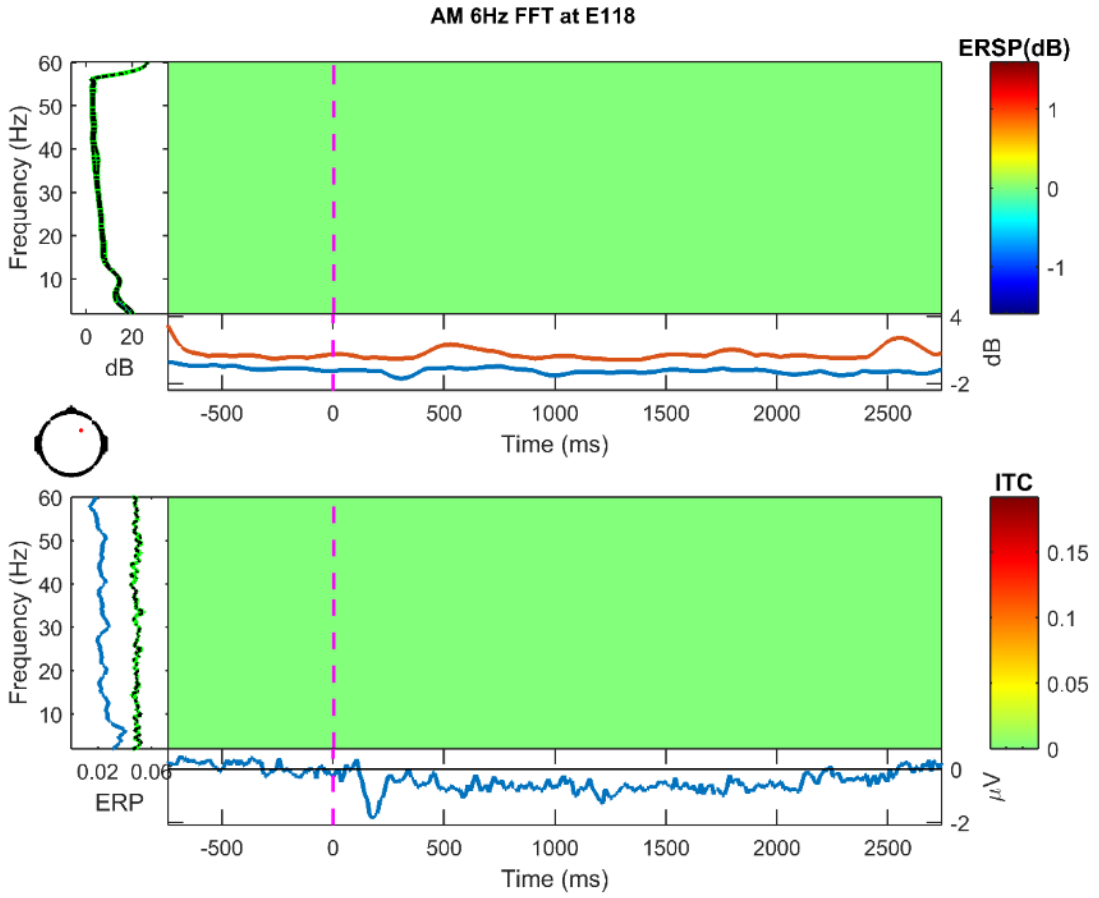

Figure 17. Frequency decomposition done with Fast Fourier Transform (FFT) for E118 (right central) from 2-60 Hz during the one second prior to stimulation and the three seconds during stimulation with 6 Hz amplitude modulated tone. Stimulation period is baseline corrected. Green indicates no significant change from baseline using permutation statistics (α = .10 with false detection rate correction for multiple comparison). X-axis is time, y-axis is frequency. Top: Darker blues indicate a decrease in frequency power while darker reds indicate and increase in frequency power from baseline. Bottom: Darker reds indicate an increase in phase-locking/inter-trial coherence (ITC) between trials at the specified frequency.

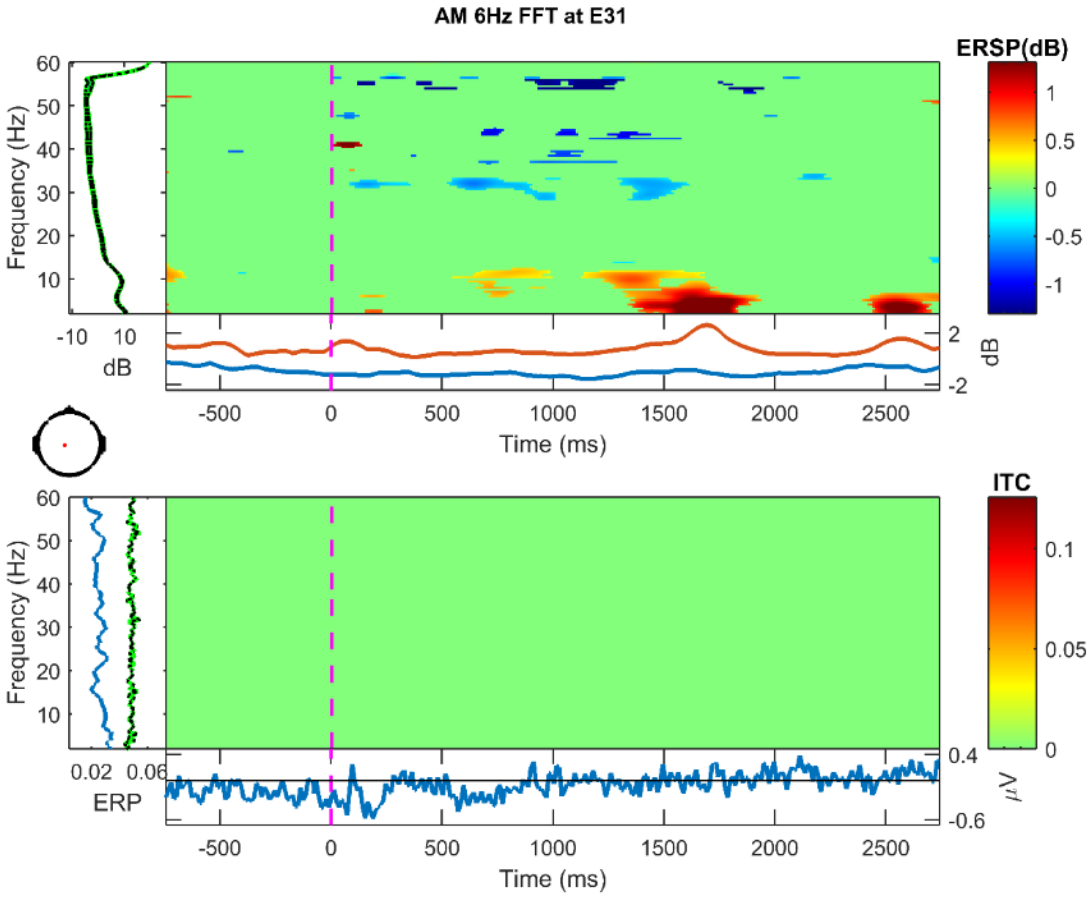

Figure 18. Frequency decomposition done with Fast Fourier Transform (FFT) for E31 (left parietal) from 2-60 Hz during the one second prior to stimulation and the three seconds during stimulation with 6 Hz amplitude modulated tone. Stimulation period is baseline corrected. Green indicates no significant change from baseline using permutation statistics ($\alpha = .10$ with false detection rate correction for multiple comparison). X-axis is time, y-axis is frequency. Top: Darker blues indicate a decrease in frequency power while darker reds indicate and increase in frequency power from baseline. Bottom: Darker reds indicate an increase in phase-locking/inter-trial coherence (ITC) between trials at the specified frequency.

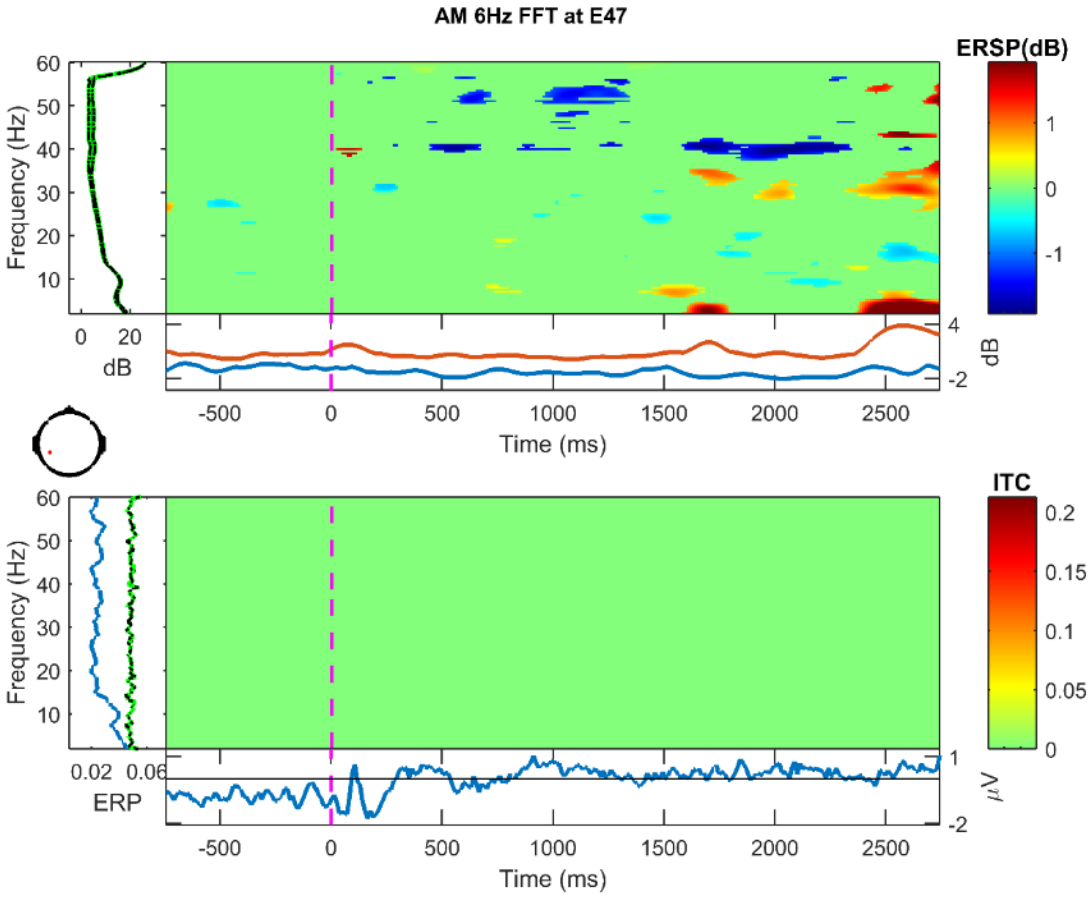

Figure 19. Frequency decomposition done with Fast Fourier Transform (FFT) for E47 (left parietal) from 2-60 Hz during the one second prior to stimulation and the three seconds during stimulation with 6 Hz amplitude modulated tone. Stimulation period is baseline corrected. Green indicates no significant change from baseline using permutation statistics ($\alpha = .10$ with false detection rate correction for multiple comparison). X-axis is time, y-axis is frequency. Top: Darker blues indicate a decrease in frequency power while darker reds indicate and increase in frequency power from baseline. Bottom: Darker reds indicate an increase in phase-locking/inter-trial coherence (ITC) between trials at the specified frequency.

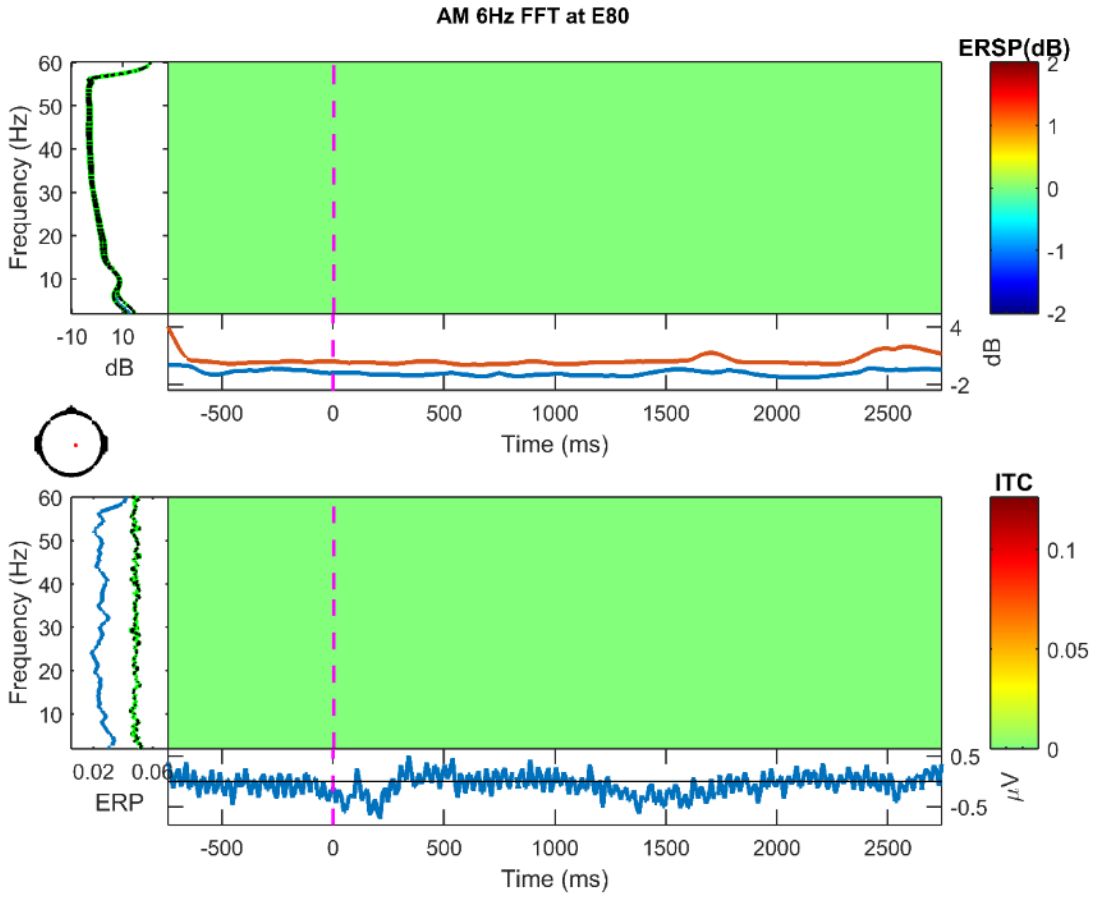

Figure 20. Frequency decomposition done with Fast Fourier Transform (FFT) for E80 (right parietal) from 2-60 Hz during the one second prior to stimulation and the three seconds during stimulation with 6 Hz amplitude modulated tone. Stimulation period is baseline corrected. Green indicates no significant change from baseline using permutation statistics ($\alpha = .10$ with false detection rate correction for multiple comparison). X-axis is time, y-axis is frequency. Top: Darker blues indicate a decrease in frequency power while darker reds indicate and increase in frequency power from baseline. Bottom: Darker reds indicate an increase in phase-locking/inter-trial coherence (ITC) between trials at the specified frequency.

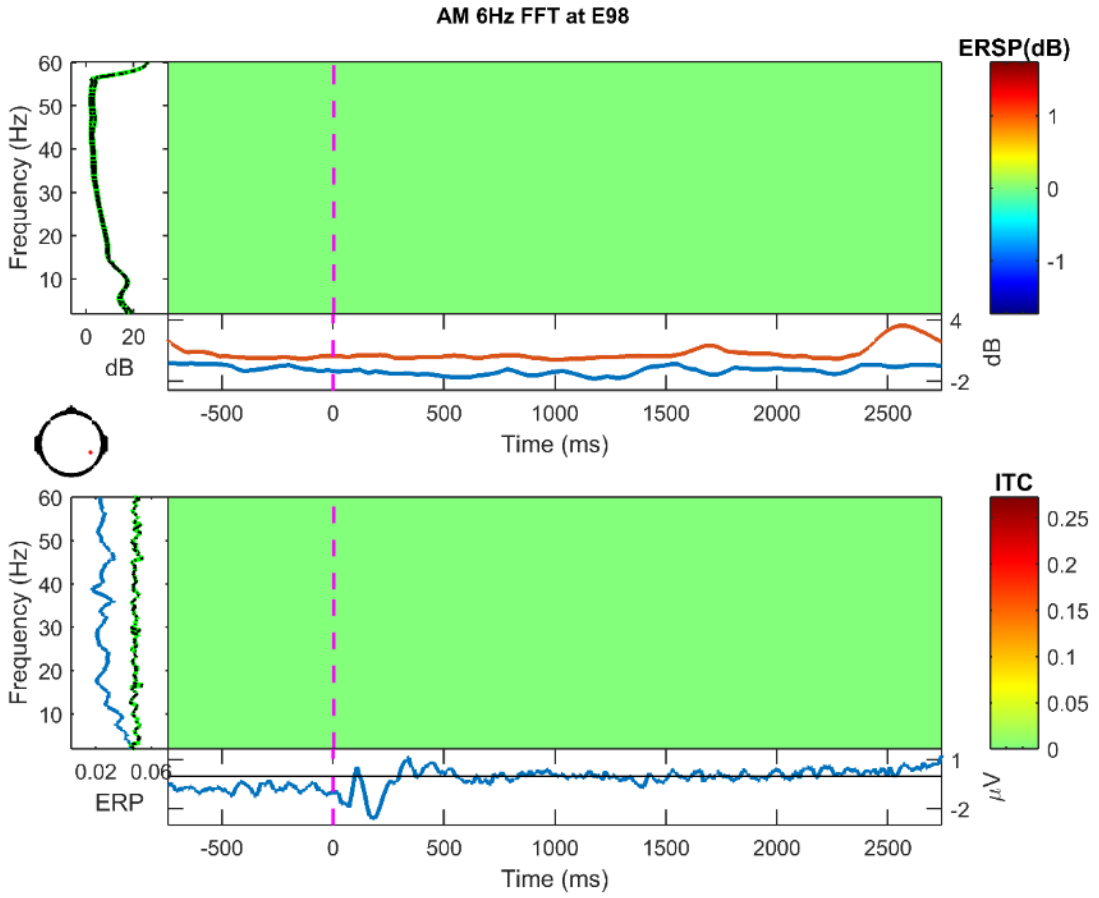

Figure 21. Frequency decomposition done with Fast Fourier Transform (FFT) for E98 (right parietal) from 2-60 Hz during the one second prior to stimulation and the three seconds during stimulation with 6 Hz amplitude modulated tone. Stimulation period is baseline corrected. Green indicates no significant change from baseline using permutation statistics ($\alpha = .10$ with false detection rate correction for multiple comparison). X-axis is time, y-axis is frequency. Top: Darker blues indicate a decrease in frequency power while darker reds indicate and increase in frequency power from baseline. Bottom: Darker reds indicate an increase in phase-locking/inter-trial coherence (ITC) between trials at the specified frequency.

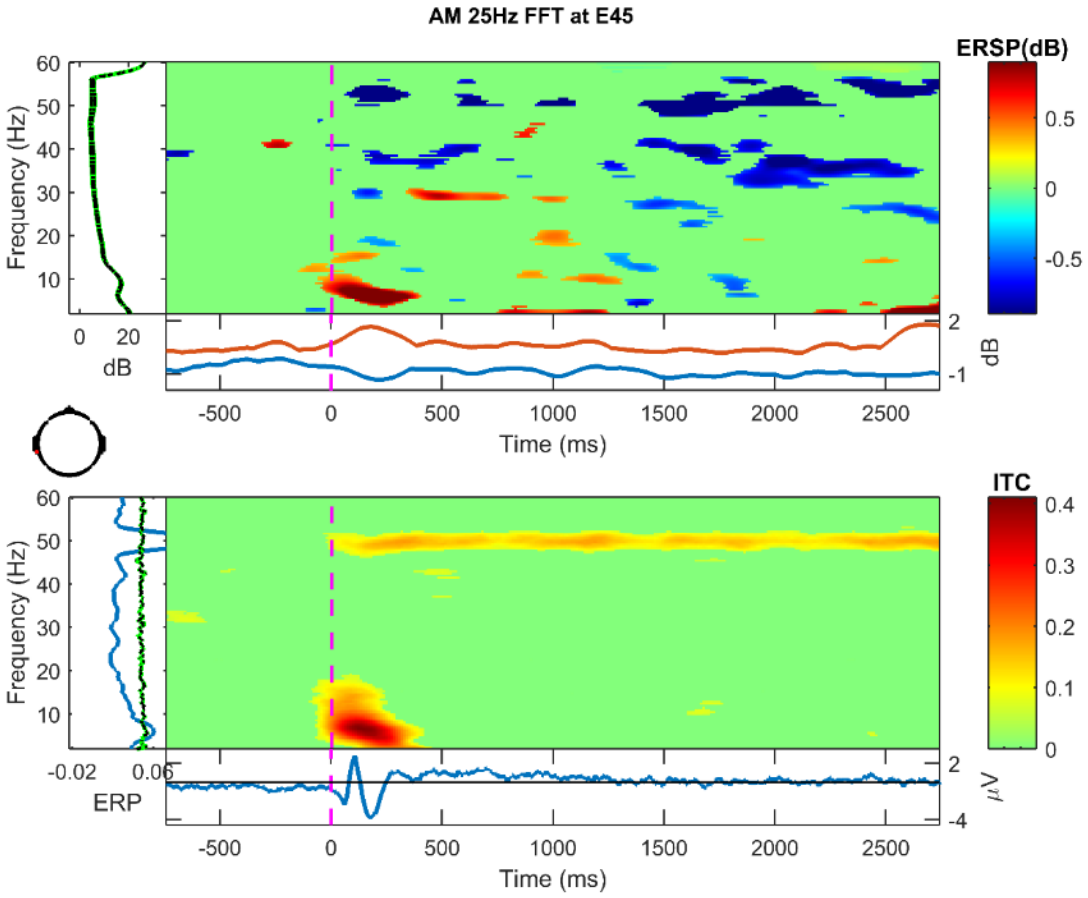

Figure 22. Frequency decomposition done with Fast Fourier Transform (FFT) for E45 (left temporal, auditory cortex) from 2-60 Hz during the one second prior to stimulation and the three seconds during stimulation with 25 Hz amplitude modulated tone. Stimulation period is baseline corrected. Green indicates no significant change from baseline using permutation statistics (α = .10 with false detection rate correction for multiple comparison). X-axis is time, y-axis is frequency. Top: Darker blues indicate a decrease in frequency power while darker reds indicate and increase in frequency power from baseline. Bottom: Darker reds indicate an increase in phase-locking/inter-trial coherence (ITC) between trials at the specified frequency.

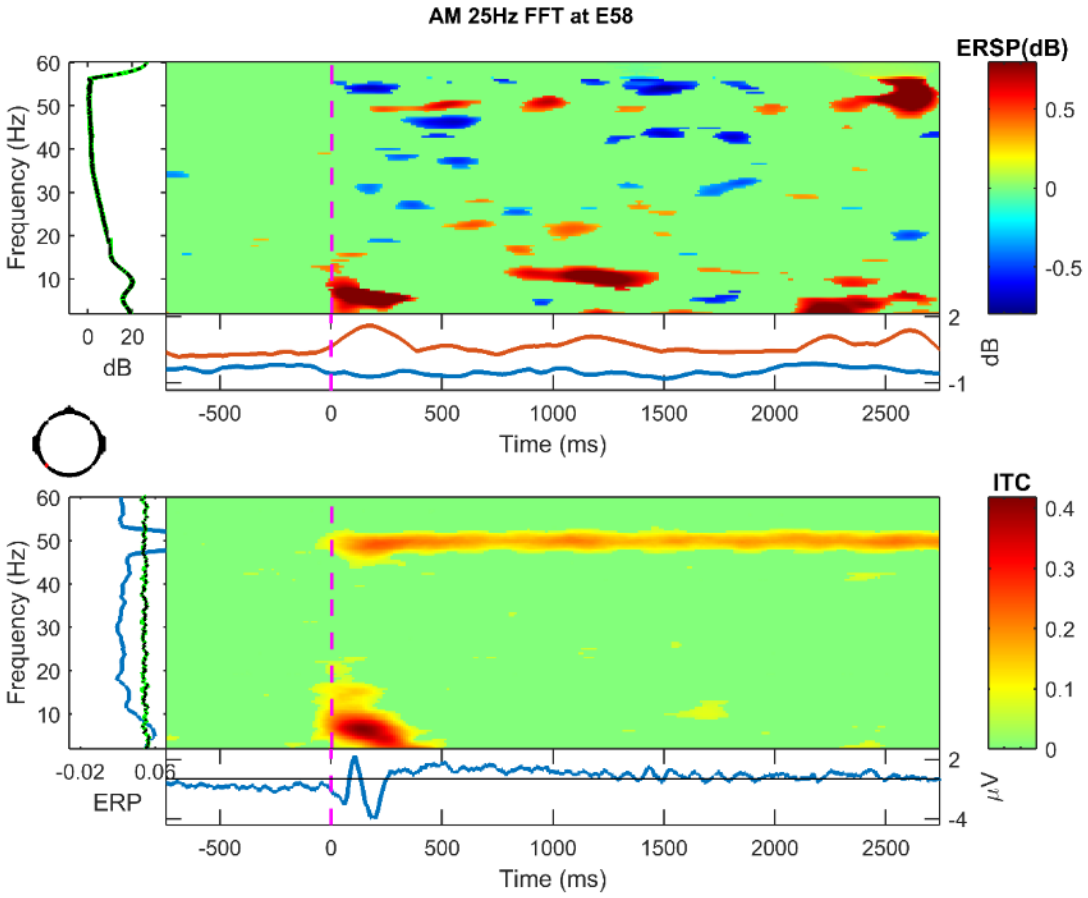

Figure 23. Frequency decomposition done with Fast Fourier Transform (FFT) for E58 (left temporal, auditory cortex) from 2-60 Hz during the one second prior to stimulation and the three seconds during stimulation with 25 Hz amplitude modulated tone. Stimulation period is baseline corrected. Green indicates no significant change from baseline using permutation statistics (α = .10 with false detection rate correction for multiple comparison). X-axis is time, y-axis is frequency. Top: Darker blues indicate a decrease in frequency power while darker reds indicate and increase in frequency power from baseline. Bottom: Darker reds indicate an increase in phase-locking/inter-trial coherence (ITC) between trials at the specified frequency.

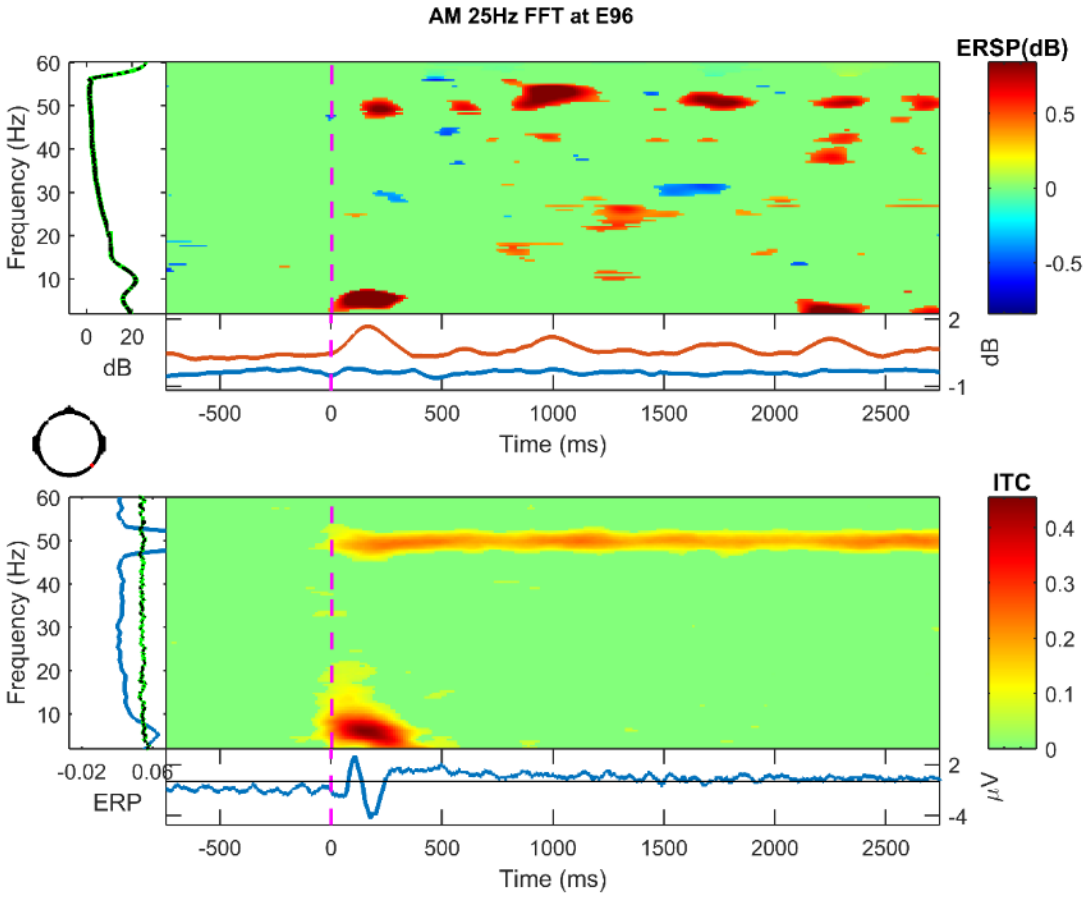

Figure 24. Frequency decomposition done with Fast Fourier Transform (FFT) for E96 (right temporal, auditory cortex) from 2-60 Hz during the one second prior to stimulation and the three seconds during stimulation with 25 Hz amplitude modulated tone. Stimulation period is baseline corrected. Green indicates no significant change from baseline using permutation statistics (α = .10 with false detection rate correction for multiple comparison). X-axis is time, y-axis is frequency. Top: Darker blues indicate a decrease in frequency power while darker reds indicate and increase in frequency power from baseline. Bottom: Darker reds indicate an increase in phase-locking/inter-trial coherence (ITC) between trials at the specified frequency.

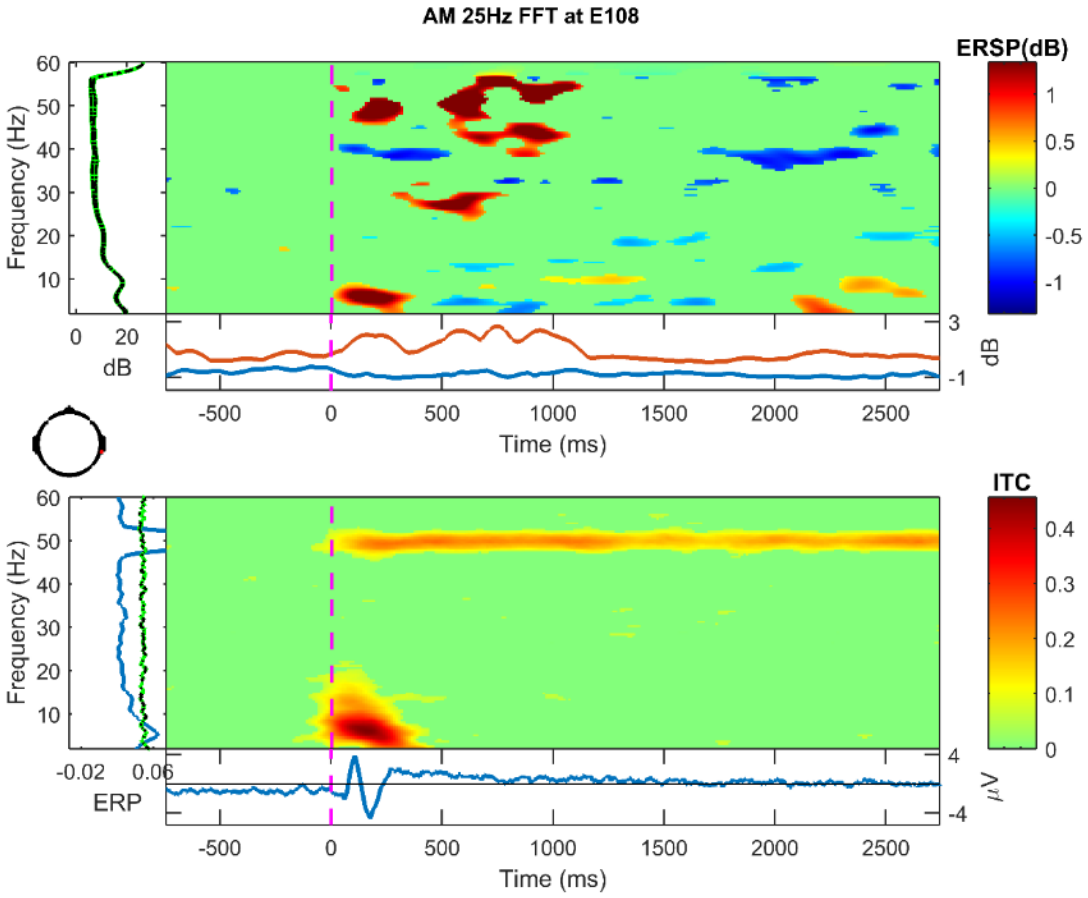

Figure 25. Frequency decomposition done with Fast Fourier Transform (FFT) for E108 (right temporal, auditory cortex) from 2-60 Hz during the one second prior to stimulation and the three seconds during stimulation with 25 Hz amplitude modulated tone. Stimulation period is baseline corrected. Green indicates no significant change from baseline using permutation statistics (α = .10 with false detection rate correction for multiple comparison). X-axis is time, y-axis is frequency. Top: Darker blues indicate a decrease in frequency power while darker reds indicate and increase in frequency power from baseline. Bottom: Darker reds indicate an increase in phase-locking/inter-trial coherence (ITC) between trials at the specified frequency.

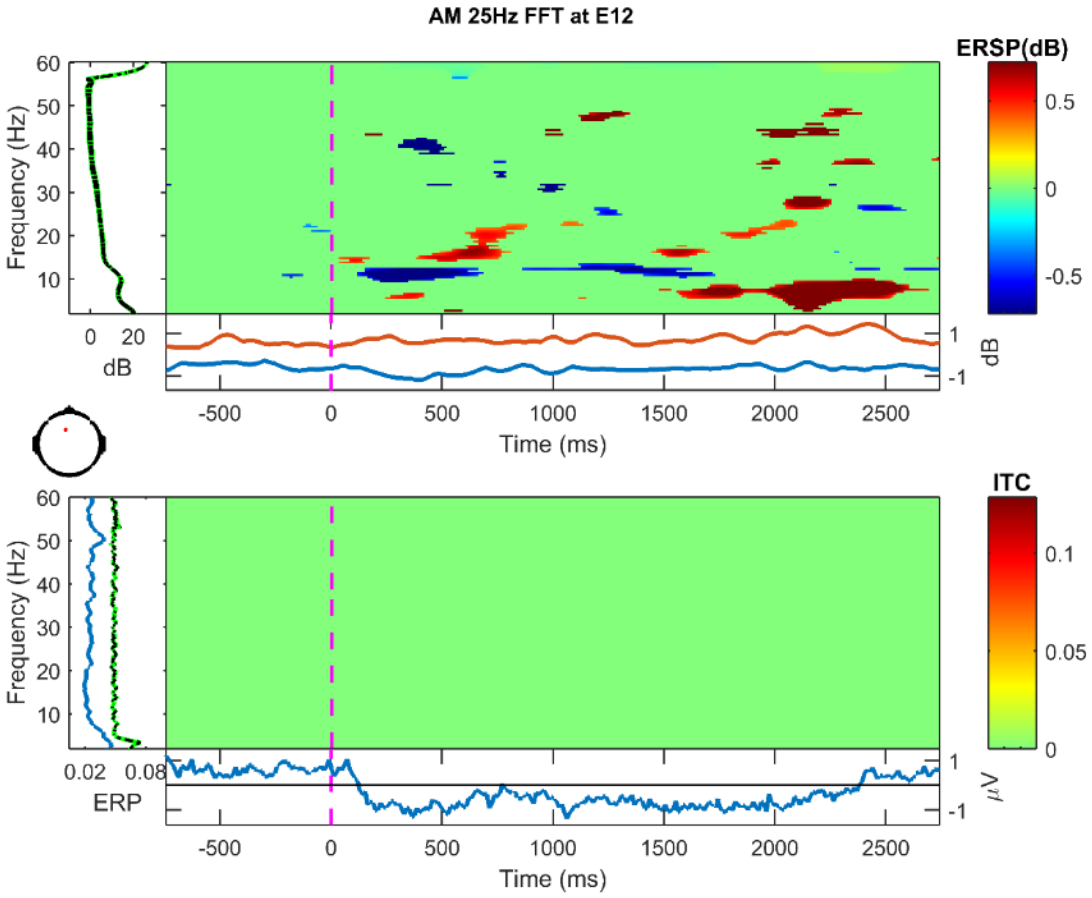

Figure 26. Frequency decomposition done with Fast Fourier Transform (FFT) for E12 (left frontal) from 2-60 Hz during the one second prior to stimulation and the three seconds during stimulation with 25 Hz amplitude modulated tone. Stimulation period is baseline corrected. Green indicates no significant change from baseline using permutation statistics ($\alpha = .10$ with false detection rate correction for multiple comparison). X-axis is time, y-axis is frequency. Top: Darker blues indicate a decrease in frequency power while darker reds indicate and increase in frequency power from baseline. Bottom: Darker reds indicate an increase in phase-locking/inter-trial coherence (ITC) between trials at the specified frequency.

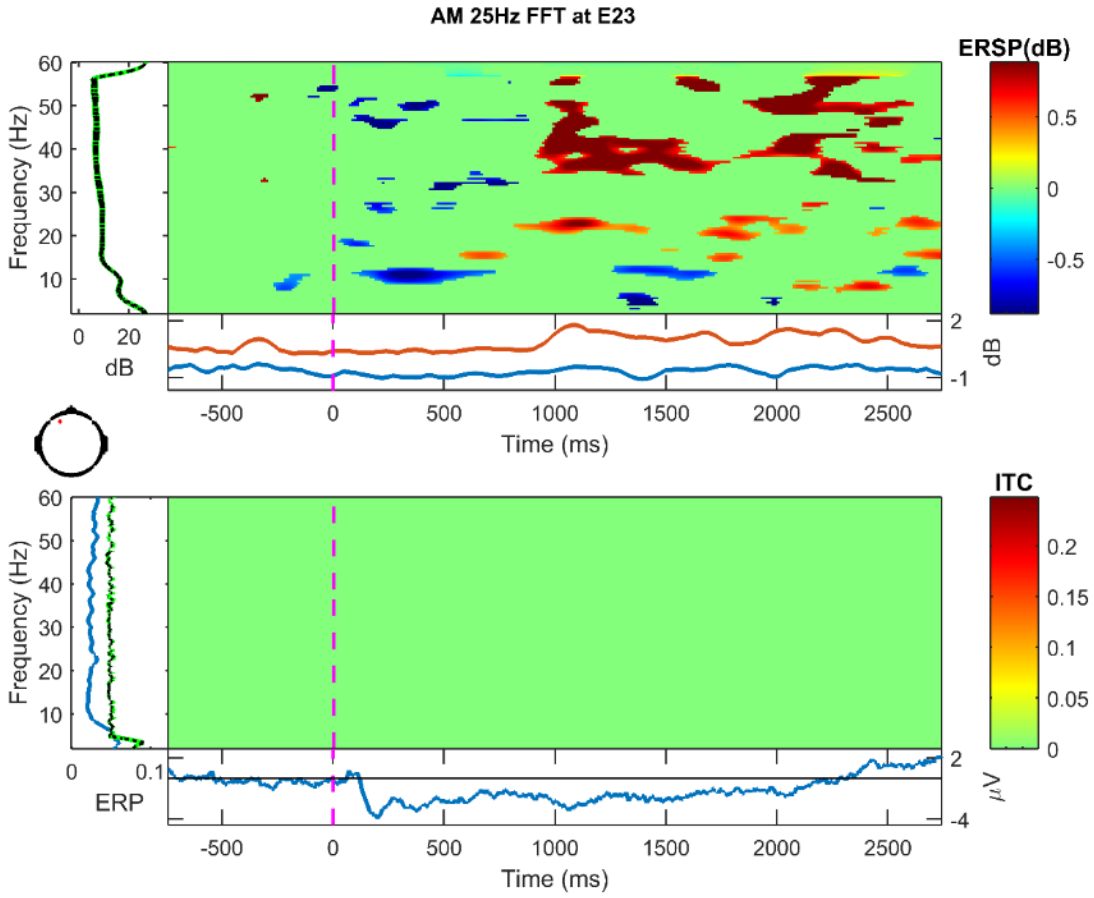

Figure 27. Frequency decomposition done with Fast Fourier Transform (FFT) for E23 (left frontal) from 2-60 Hz during the one second prior to stimulation and the three seconds during stimulation with 25 Hz amplitude modulated tone. Stimulation period is baseline corrected. Green indicates no significant change from baseline using permutation statistics ($\alpha = .10$ with false detection rate correction for multiple comparison). X-axis is time, y-axis is frequency. Top: Darker blues indicate a decrease in frequency power while darker reds indicate and increase in frequency power from baseline. Bottom: Darker reds indicate an increase in phase-locking/inter-trial coherence (ITC) between trials at the specified frequency.

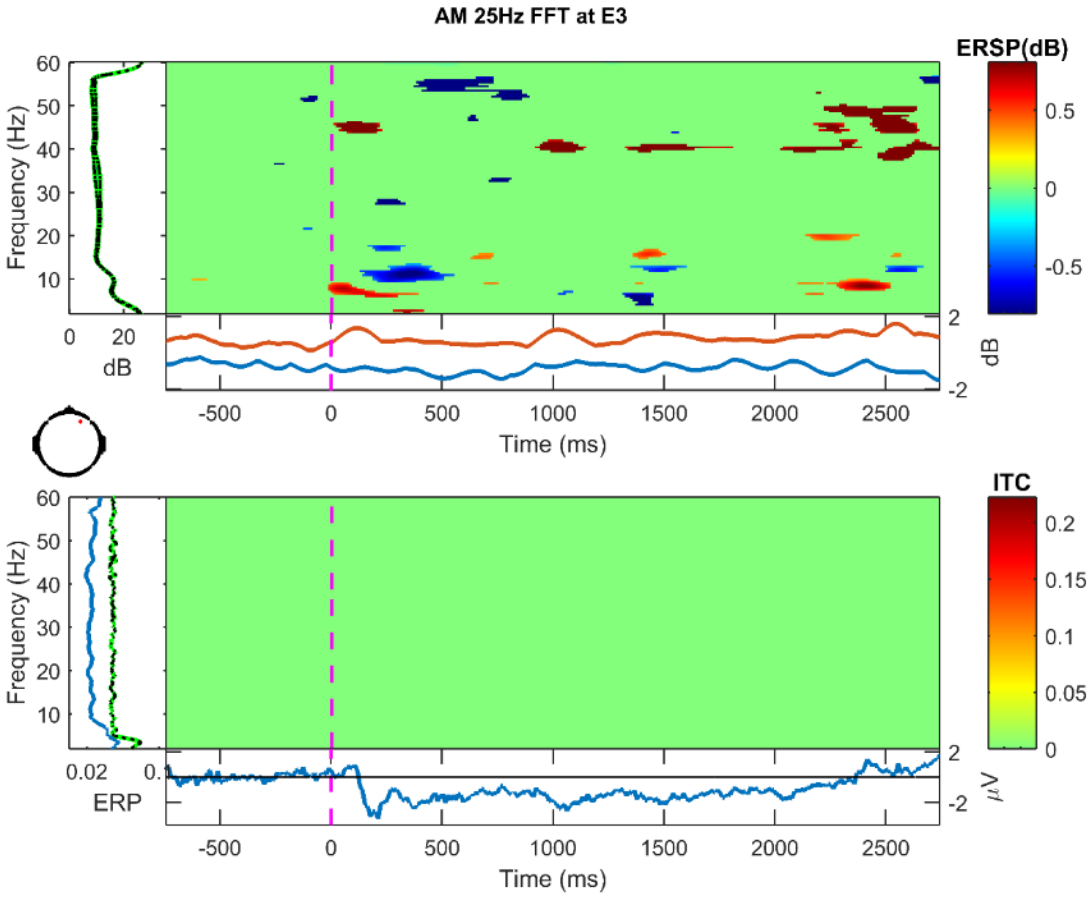

Figure 28. Frequency decomposition done with Fast Fourier Transform (FFT) for E3 (right frontal) from 2-60 Hz during the one second prior to stimulation and the three seconds during stimulation with 25 Hz amplitude modulated tone. Stimulation period is baseline corrected. Green indicates no significant change from baseline using permutation statistics ($\alpha = .10$ with false detection rate correction for multiple comparison). X-axis is time, y-axis is frequency. Top: Darker blues indicate a decrease in frequency power while darker reds indicate and increase in frequency power from baseline. Bottom: Darker reds indicate an increase in phase-locking/inter-trial coherence (ITC) between trials at the specified frequency.

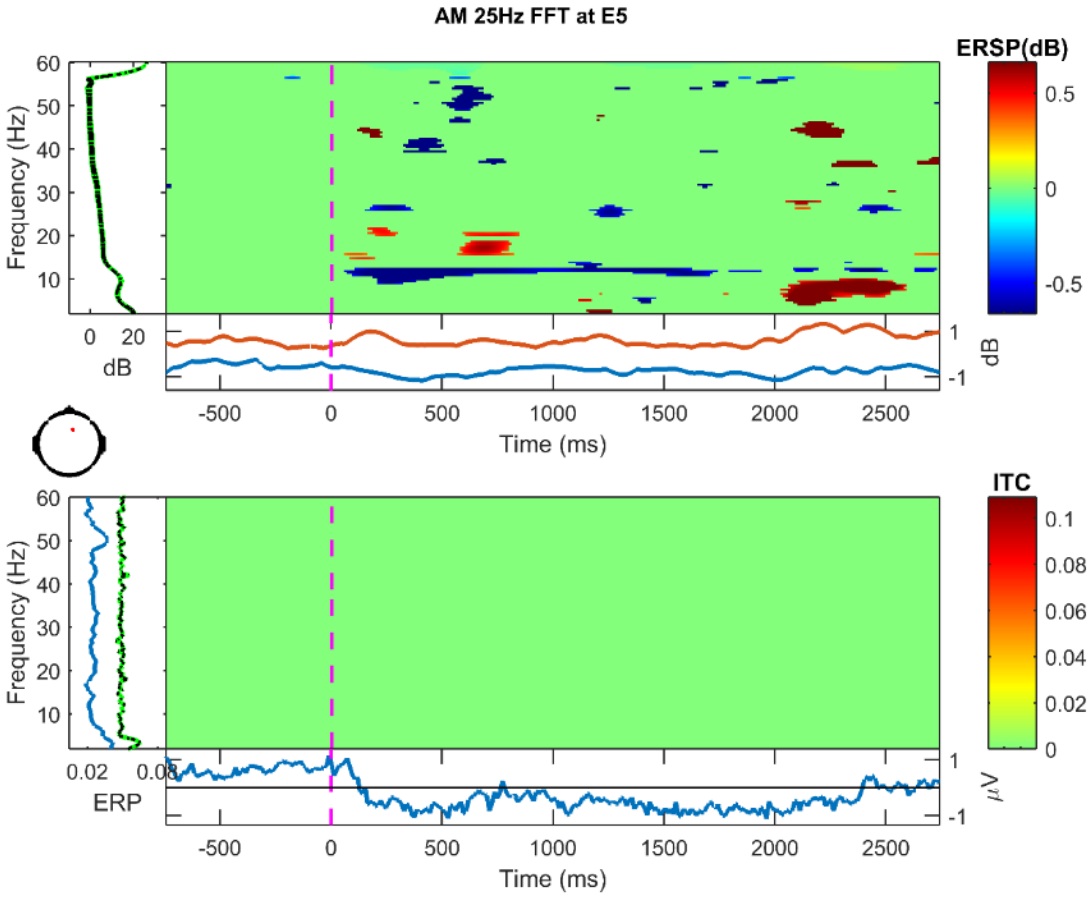

Figure 29. Frequency decomposition done with Fast Fourier Transform (FFT) for E5 (right frontal) from 2-60 Hz during the one second prior to stimulation and the three seconds during stimulation with 25 Hz amplitude modulated tone. Stimulation period is baseline corrected. Green indicates no significant change from baseline using permutation statistics ($\alpha = .10$ with false detection rate correction for multiple comparison). X-axis is time, y-axis is frequency. Top: Darker blues indicate a decrease in frequency power while darker reds indicate and increase in frequency power from baseline. Bottom: Darker reds indicate an increase in phase-locking/inter-trial coherence (ITC) between trials at the specified frequency.

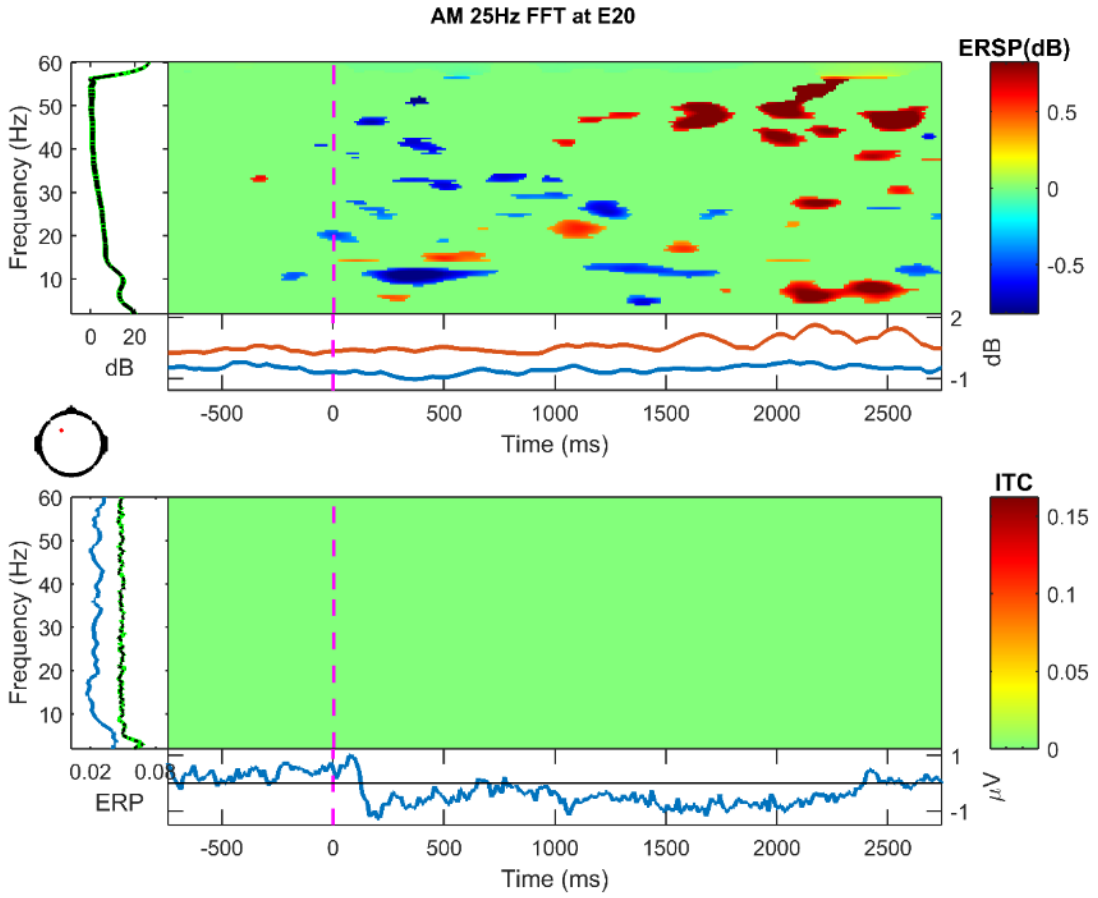

Figure 30. Frequency decomposition done with Fast Fourier Transform (FFT) for E20 (left central) from 2-60 Hz during the one second prior to stimulation and the three seconds during stimulation with 25 Hz amplitude modulated tone. Stimulation period is baseline corrected. Green indicates no significant change from baseline using permutation statistics (α = .10 with false detection rate correction for multiple comparison). X-axis is time, y-axis is frequency. Top: Darker blues indicate a decrease in frequency power while darker reds indicate and increase in frequency power from baseline. Bottom: Darker reds indicate an increase in phase-locking/inter-trial coherence (ITC) between trials at the specified frequency.

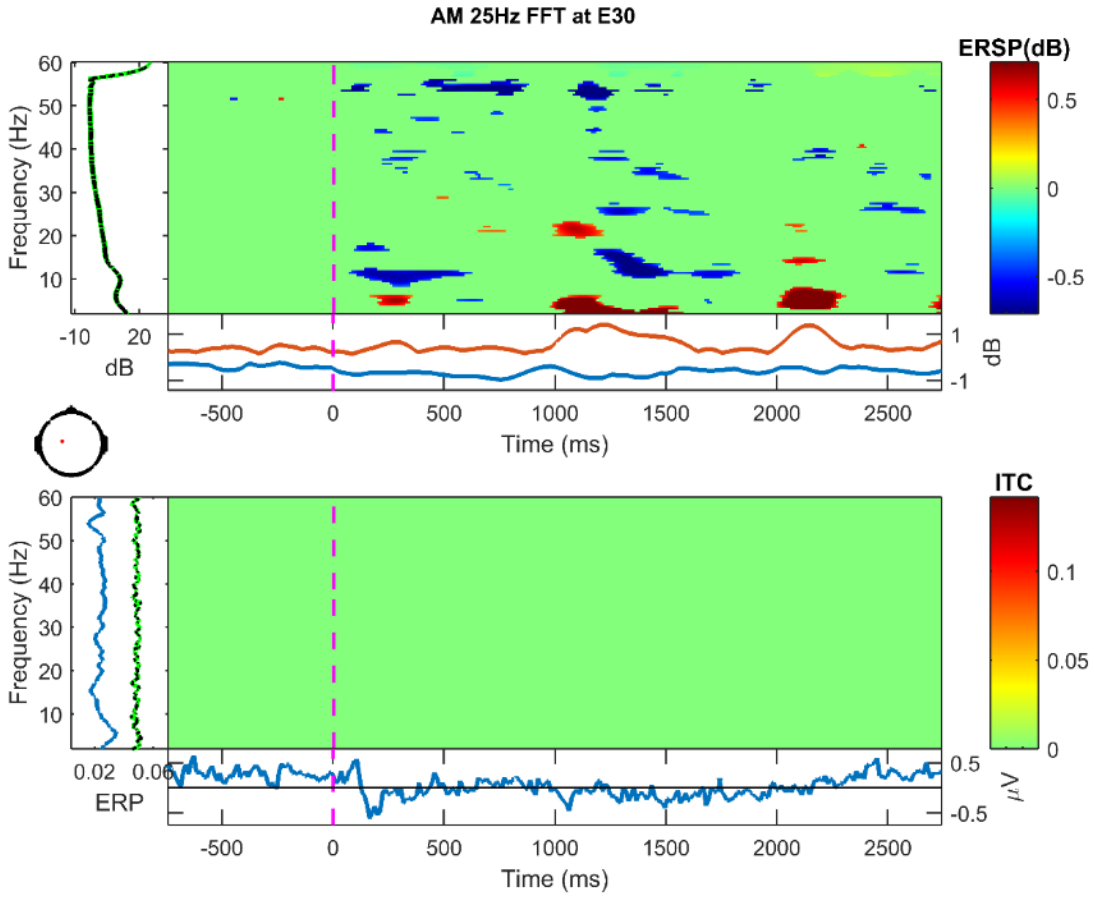

Figure 31. Frequency decomposition done with Fast Fourier Transform (FFT) for E30 (left central) from 2-60 Hz during the one second prior to stimulation and the three seconds during stimulation with 25 Hz amplitude modulated tone. Stimulation period is baseline corrected. Green indicates no significant change from baseline using permutation statistics (α = .10 with false detection rate correction for multiple comparison). X-axis is time, y-axis is frequency. Top: Darker blues indicate a decrease in frequency power while darker reds indicate and increase in frequency power from baseline. Bottom: Darker reds indicate an increase in phase-locking/inter-trial coherence (ITC) between trials at the specified frequency.

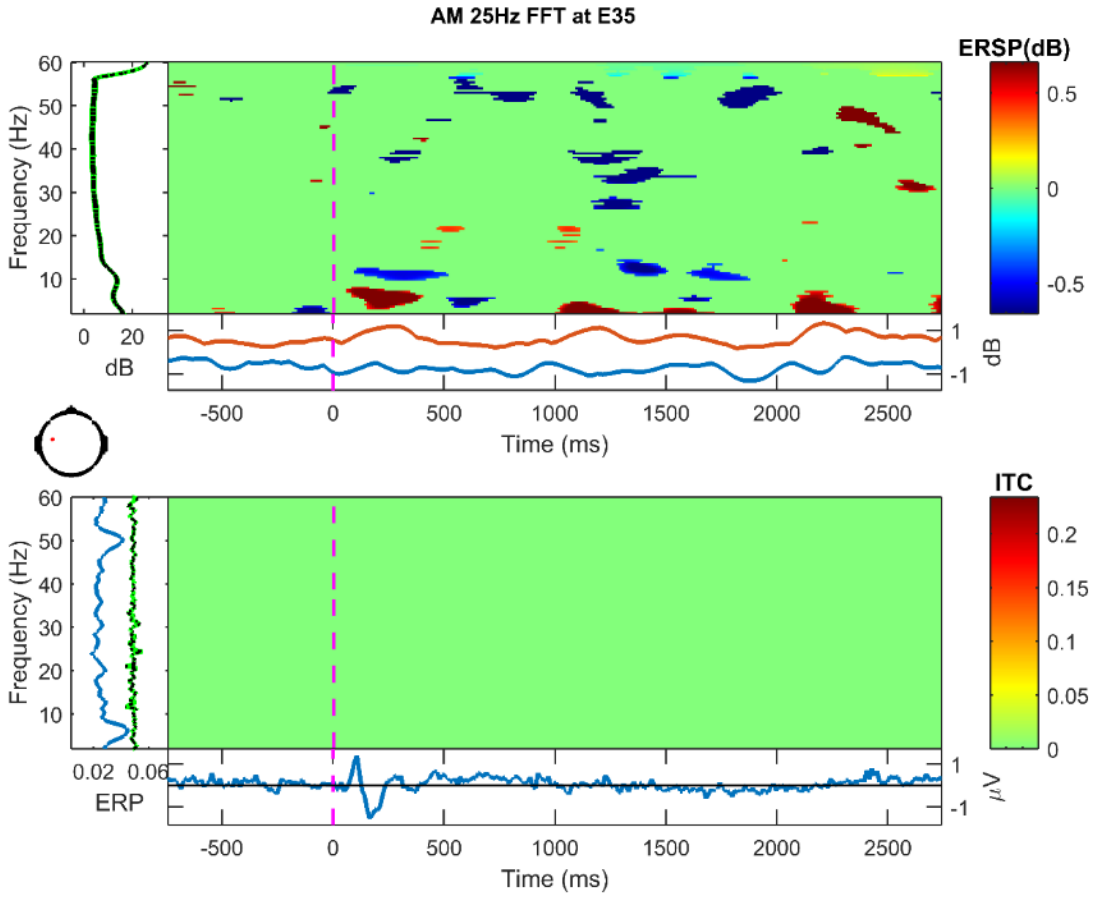

Figure 32. Frequency decomposition done with Fast Fourier Transform (FFT) for E35 (left central) from 2-60 Hz during the one second prior to stimulation and the three seconds during stimulation with 25 Hz amplitude modulated tone. Stimulation period is baseline corrected. Green indicates no significant change from baseline using permutation statistics (α = .10 with false detection rate correction for multiple comparison). X-axis is time, y-axis is frequency. Top: Darker blues indicate a decrease in frequency power while darker reds indicate and increase in frequency power from baseline. Bottom: Darker reds indicate an increase in phase-locking/inter-trial coherence (ITC) between trials at the specified frequency.

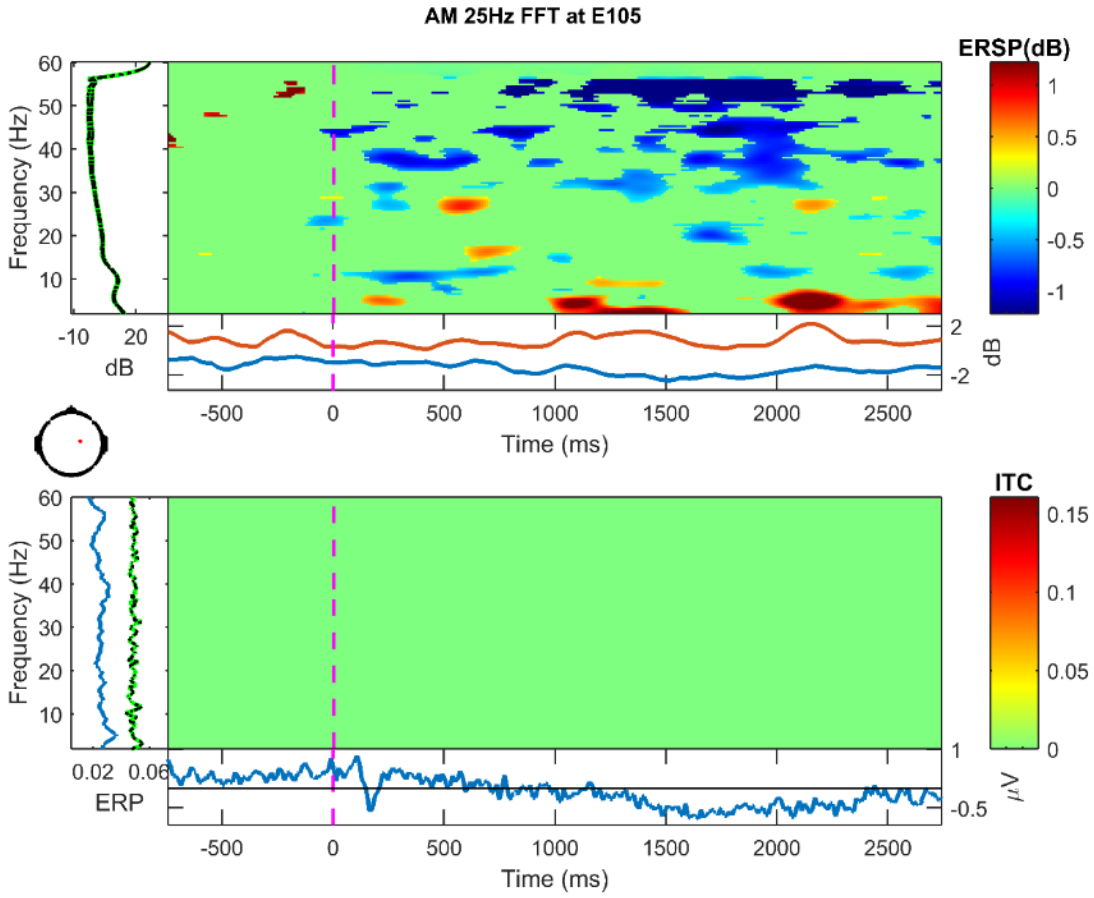

Figure 33. Frequency decomposition done with Fast Fourier Transform (FFT) for E105 (right central) from 2-60 Hz during the one second prior to stimulation and the three seconds during stimulation with 25 Hz amplitude modulated tone. Stimulation period is baseline corrected. Green indicates no significant change from baseline using permutation statistics (α = .10 with false detection rate correction for multiple comparison). X-axis is time, y-axis is frequency. Top: Darker blues indicate a decrease in frequency power while darker reds indicate and increase in frequency power from baseline. Bottom: Darker reds indicate an increase in phase-locking/inter-trial coherence (ITC) between trials at the specified frequency.

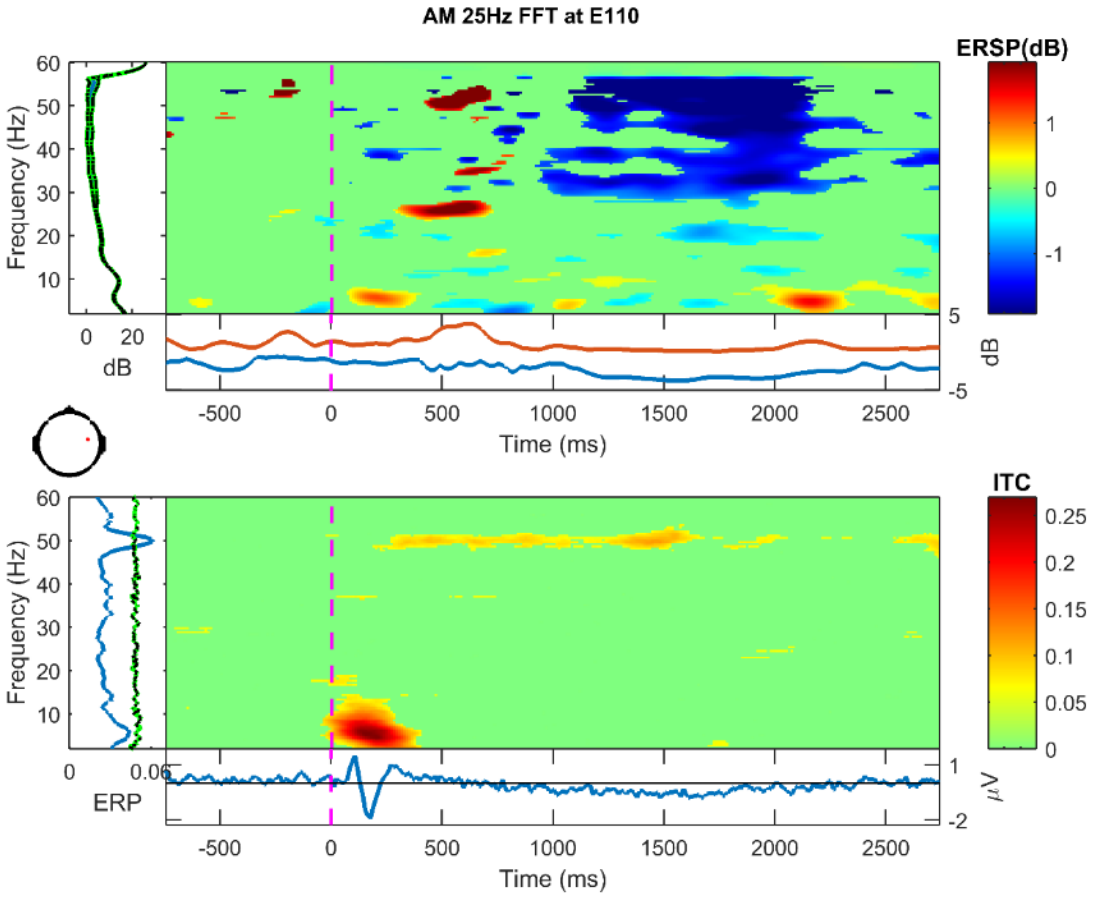

Figure 34. Frequency decomposition done with Fast Fourier Transform (FFT) for E110 (right central) from 2-60 Hz during the one second prior to stimulation and the three seconds during stimulation with 25 Hz amplitude modulated tone. Stimulation period is baseline corrected. Green indicates no significant change from baseline using permutation statistics (α = .10 with false detection rate correction for multiple comparison). X-axis is time, y-axis is frequency. Top: Darker blues indicate a decrease in frequency power while darker reds indicate and increase in frequency power from baseline. Bottom: Darker reds indicate an increase in phase-locking/inter-trial coherence (ITC) between trials at the specified frequency.

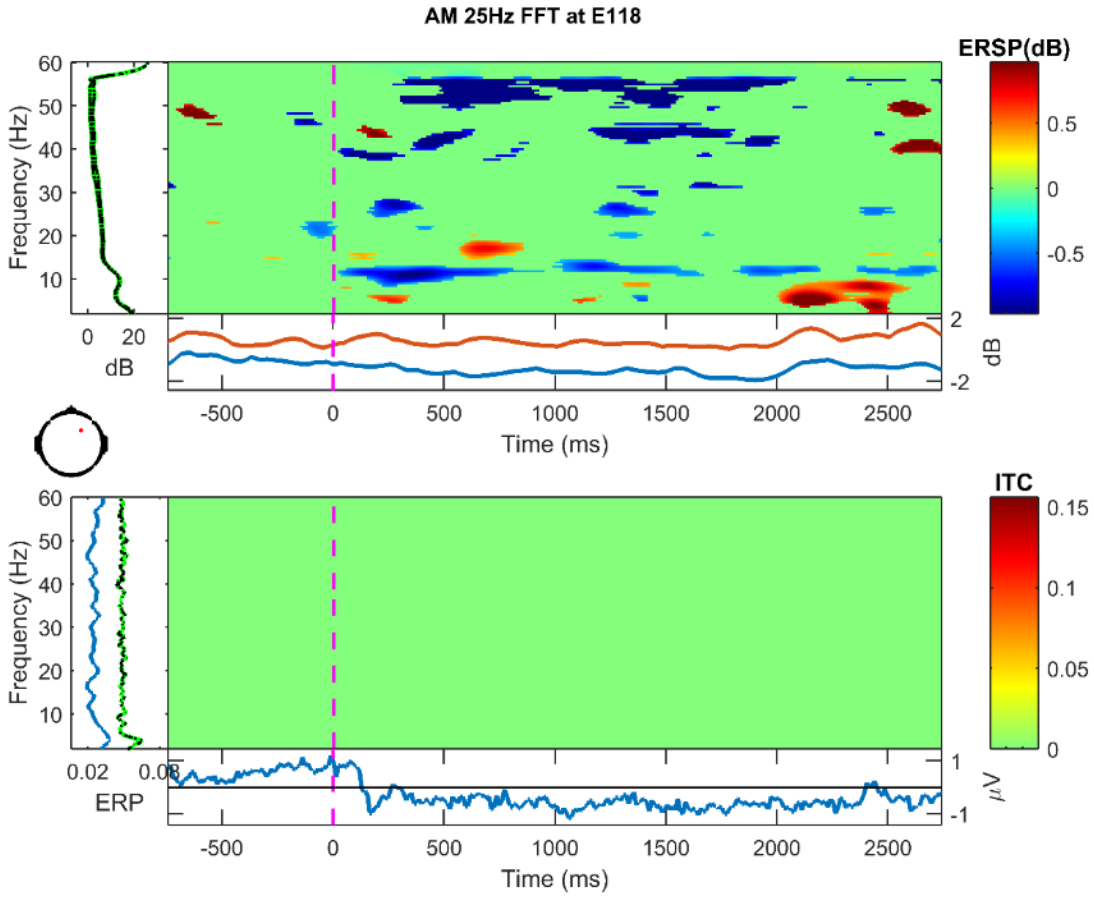

Figure 35. Frequency decomposition done with Fast Fourier Transform (FFT) for E118 (right central) from 2-60 Hz during the one second prior to stimulation and the three seconds during stimulation with 25 Hz amplitude modulated tone. Stimulation period is baseline corrected. Green indicates no significant change from baseline using permutation statistics (α = .10 with false detection rate correction for multiple comparison). X-axis is time, y-axis is frequency. Top: Darker blues indicate a decrease in frequency power while darker reds indicate and increase in frequency power from baseline. Bottom: Darker reds indicate an increase in phase-locking/inter-trial coherence (ITC) between trials at the specified frequency.

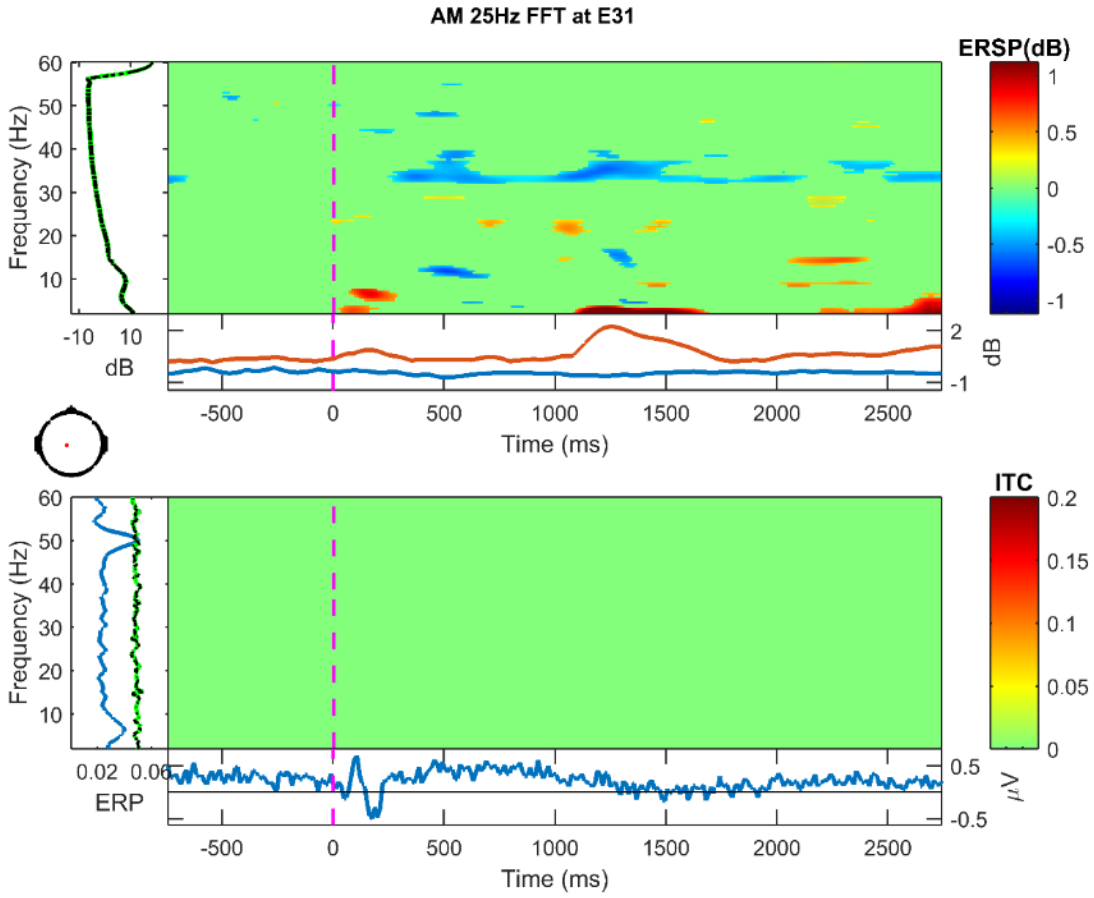

Figure 36. Frequency decomposition done with Fast Fourier Transform (FFT) for E31 (left parietal) from 2-60 Hz during the one second prior to stimulation and the three seconds during stimulation with 25 Hz amplitude modulated tone. Stimulation period is baseline corrected. Green indicates no significant change from baseline using permutation statistics (α = .10 with false detection rate correction for multiple comparison). X-axis is time, y-axis is frequency. Top: Darker blues indicate a decrease in frequency power while darker reds indicate and increase in frequency power from baseline. Bottom: Darker reds indicate an increase in phase-locking/inter-trial coherence (ITC) between trials at the specified frequency.

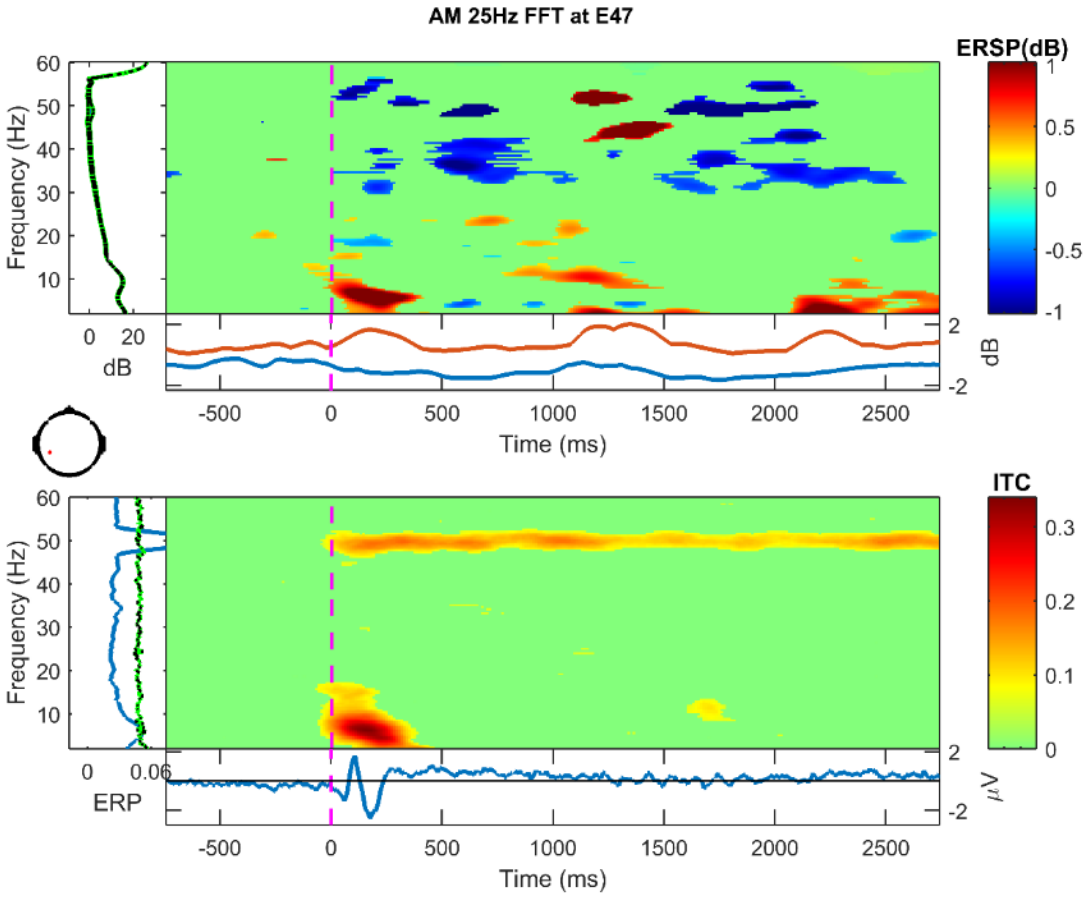

Figure 37. Frequency decomposition done with Fast Fourier Transform (FFT) for E47 (left parietal) from 2-60 Hz during the one second prior to stimulation and the three seconds during stimulation with 25 Hz amplitude modulated tone. Stimulation period is baseline corrected. Green indicates no significant change from baseline using permutation statistics (α = .10 with false detection rate correction for multiple comparison). X-axis is time, y-axis is frequency. Top: Darker blues indicate a decrease in frequency power while darker reds indicate and increase in frequency power from baseline. Bottom: Darker reds indicate an increase in phase-locking/inter-trial coherence (ITC) between trials at the specified frequency.

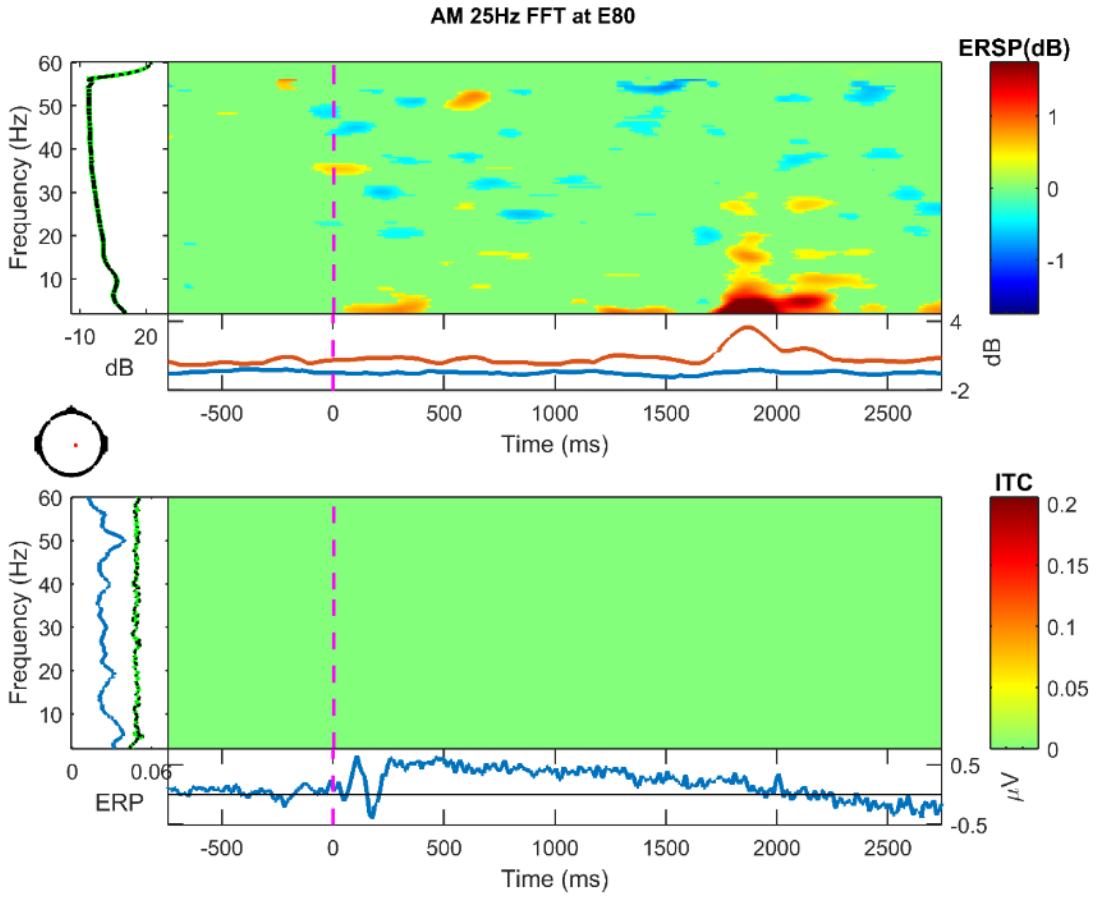

Figure 38. Frequency decomposition done with Fast Fourier Transform (FFT) for E80 (right parietal) from 2-60 Hz during the one second prior to stimulation and the three seconds during stimulation with 25 Hz amplitude modulated tone. Stimulation period is baseline corrected. Green indicates no significant change from baseline using permutation statistics (α = .10 with false detection rate correction for multiple comparison). X-axis is time, y-axis is frequency. Top: Darker blues indicate a decrease in frequency power while darker reds indicate and increase in frequency power from baseline. Bottom: Darker reds indicate an increase in phase-locking/inter-trial coherence (ITC) between trials at the specified frequency.

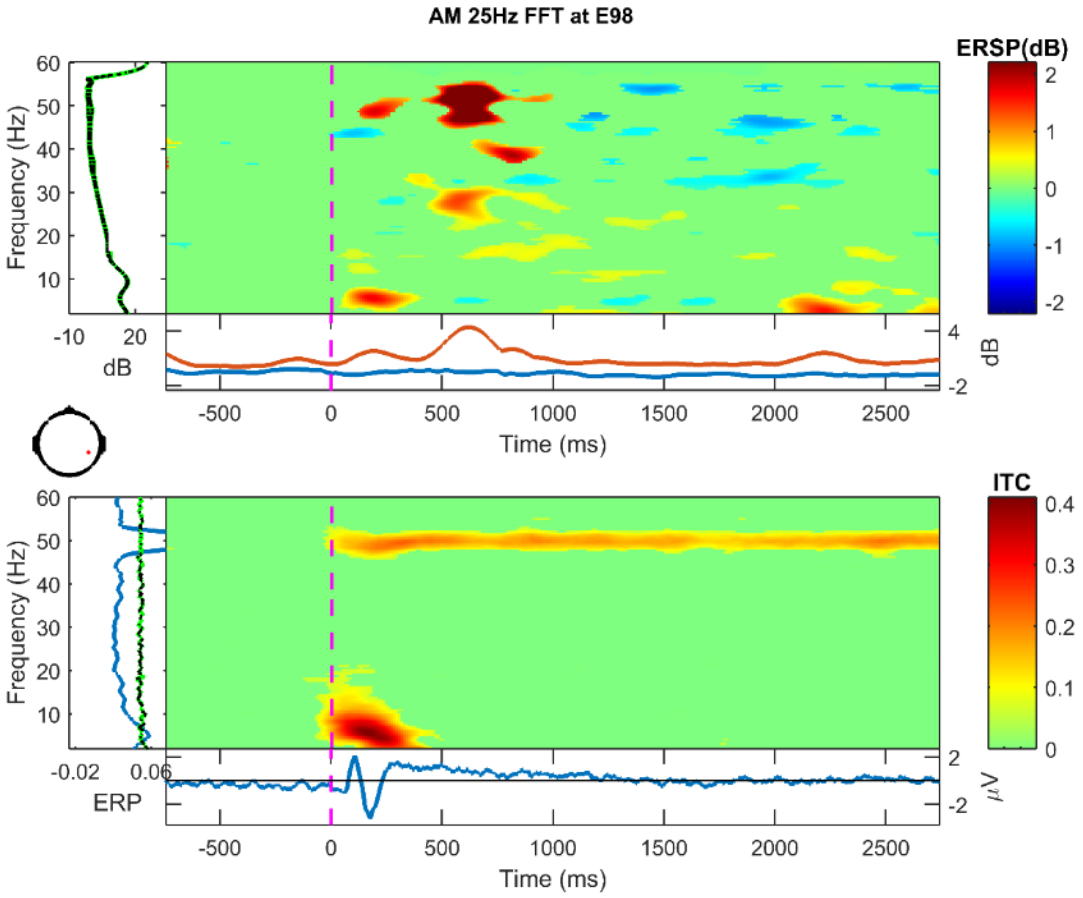

Figure 39. Frequency decomposition done with Fast Fourier Transform (FFT) for E98 (right parietal) from 2-60 Hz during the one second prior to stimulation and the three seconds during stimulation with 25 Hz amplitude modulated tone. Stimulation period is baseline corrected. Green indicates no significant change from baseline using permutation statistics (α = .10 with false detection rate correction for multiple comparison). X-axis is time, y-axis is frequency. Top: Darker blues indicate a decrease in frequency power while darker reds indicate and increase in frequency power from baseline. Bottom: Darker reds indicate an increase in phase-locking/inter-trial coherence (ITC) between trials at the specified frequency.

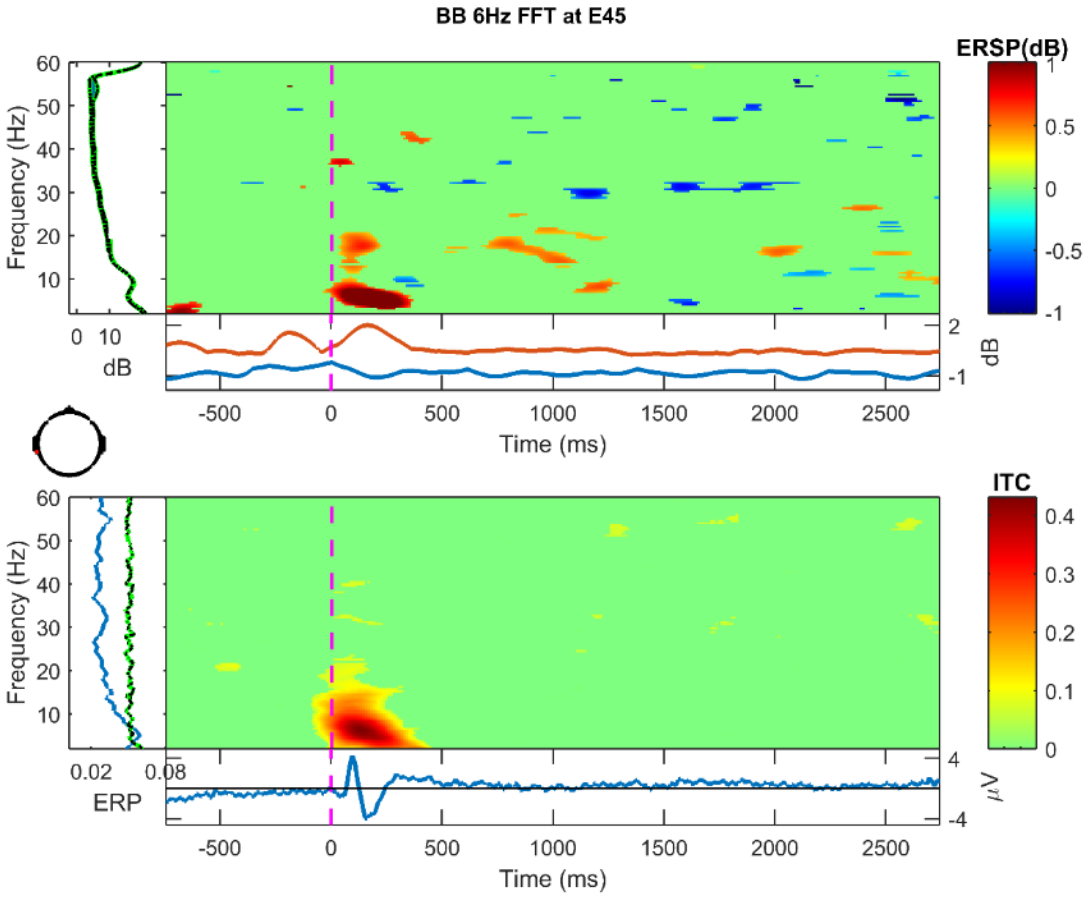

Figure 40. Frequency decomposition done with Fast Fourier Transform (FFT) for E45 (left temporal, auditory cortex) from 2-60 Hz during the one second prior to stimulation and the three seconds during stimulation with 6 Hz binaural beat tone. Stimulation period is baseline corrected. Green indicates no significant change from baseline using permutation statistics (α = .10 with false detection rate correction for multiple comparison). X-axis is time, y-axis is frequency. Top: Darker blues indicate a decrease in frequency power while darker reds indicate and increase in frequency power from baseline. Bottom: Darker reds indicate an increase in phase-locking/inter-trial coherence (ITC) between trials at the specified frequency.

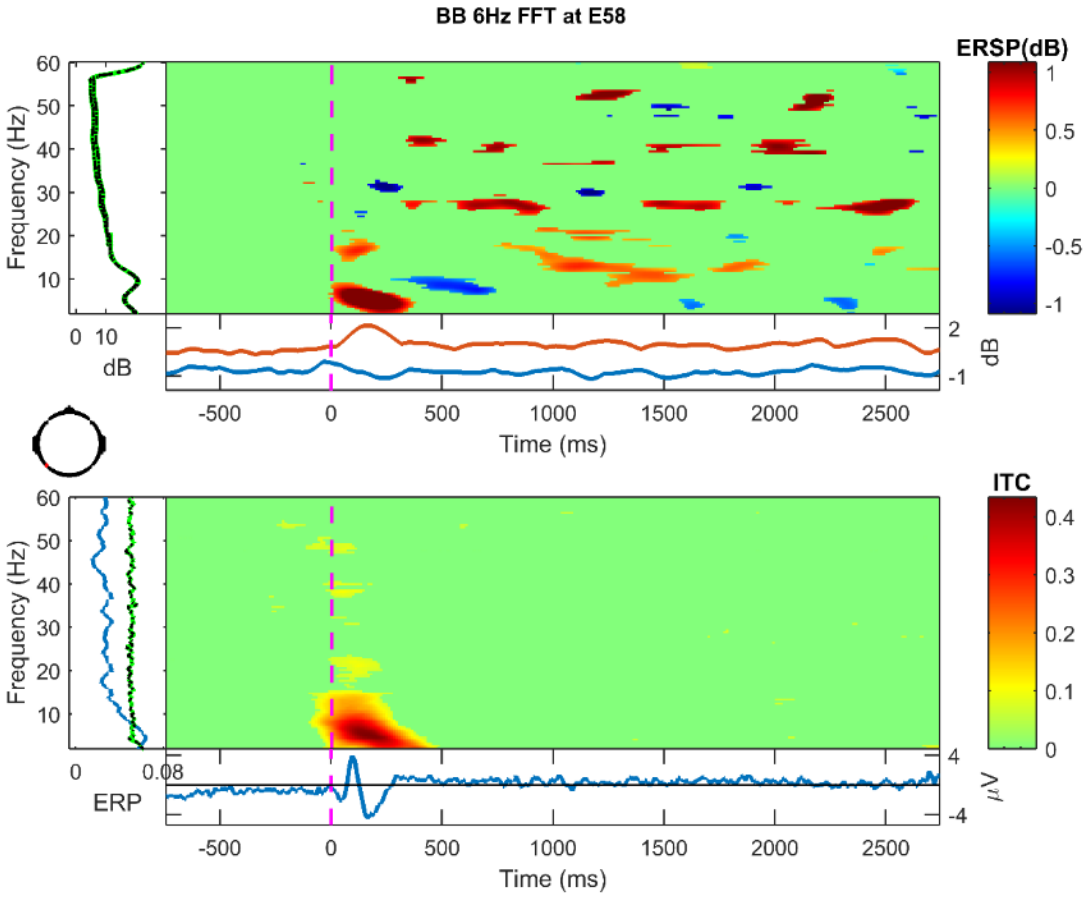

Figure 41. Frequency decomposition done with Fast Fourier Transform (FFT) for E58 (left temporal, auditory cortex) from 2-60 Hz during the one second prior to stimulation and the three seconds during stimulation with 6 Hz binaural beat tone. Stimulation period is baseline corrected. Green indicates no significant change from baseline using permutation statistics (α = .10 with false detection rate correction for multiple comparison). X-axis is time, y-axis is frequency. Top: Darker blues indicate a decrease in frequency power while darker reds indicate and increase in frequency power from baseline. Bottom: Darker reds indicate an increase in phase-locking/inter-trial coherence (ITC) between trials at the specified frequency.

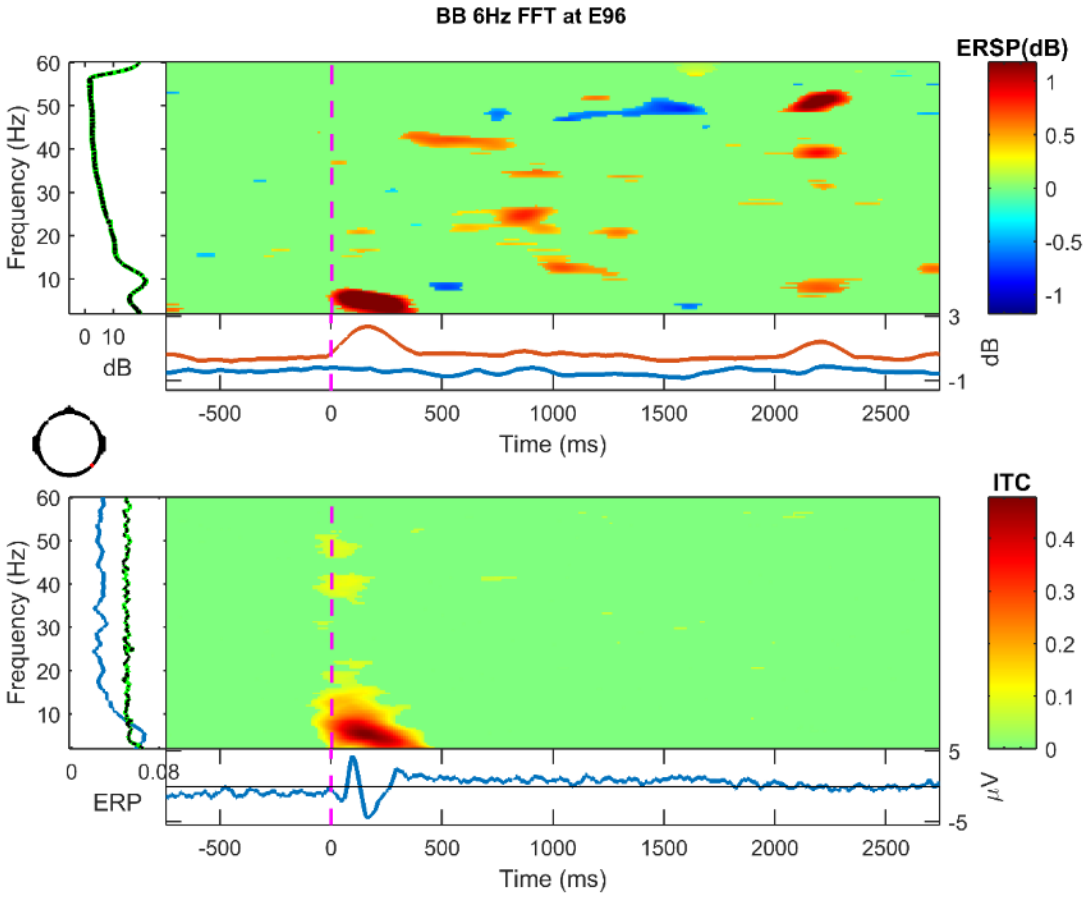

Figure 42. Frequency decomposition done with Fast Fourier Transform (FFT) for E96 (right temporal, auditory cortex) from 2-60 Hz during the one second prior to stimulation and the three seconds during stimulation with 6 Hz binaural beat tone. Stimulation period is baseline corrected. Green indicates no significant change from baseline using permutation statistics (α = .10 with false detection rate correction for multiple comparison). X-axis is time, y-axis is frequency. Top: Darker blues indicate a decrease in frequency power while darker reds indicate and increase in frequency power from baseline. Bottom: Darker reds indicate an increase in phase-locking/inter-trial coherence (ITC) between trials at the specified frequency.

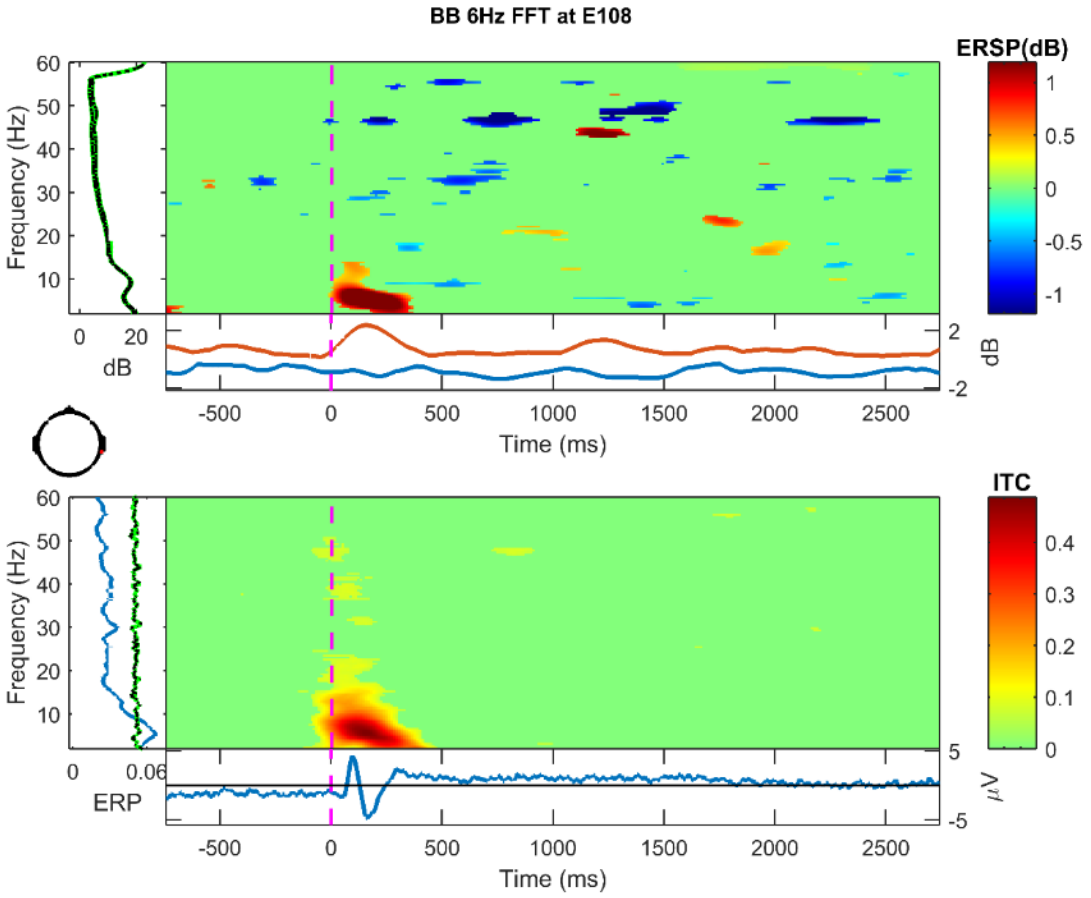

Figure 43. Frequency decomposition done with Fast Fourier Transform (FFT) for E108 (right temporal, auditory cortex) from 2-60 Hz during the one second prior to stimulation and the three seconds during stimulation with 6 Hz binaural beat tone. Stimulation period is baseline corrected. Green indicates no significant change from baseline using permutation statistics (α = .10 with false detection rate correction for multiple comparison). X-axis is time, y-axis is frequency. Top: Darker blues indicate a decrease in frequency power while darker reds indicate and increase in frequency power from baseline. Bottom: Darker reds indicate an increase in phase-locking/inter-trial coherence (ITC) between trials at the specified frequency.

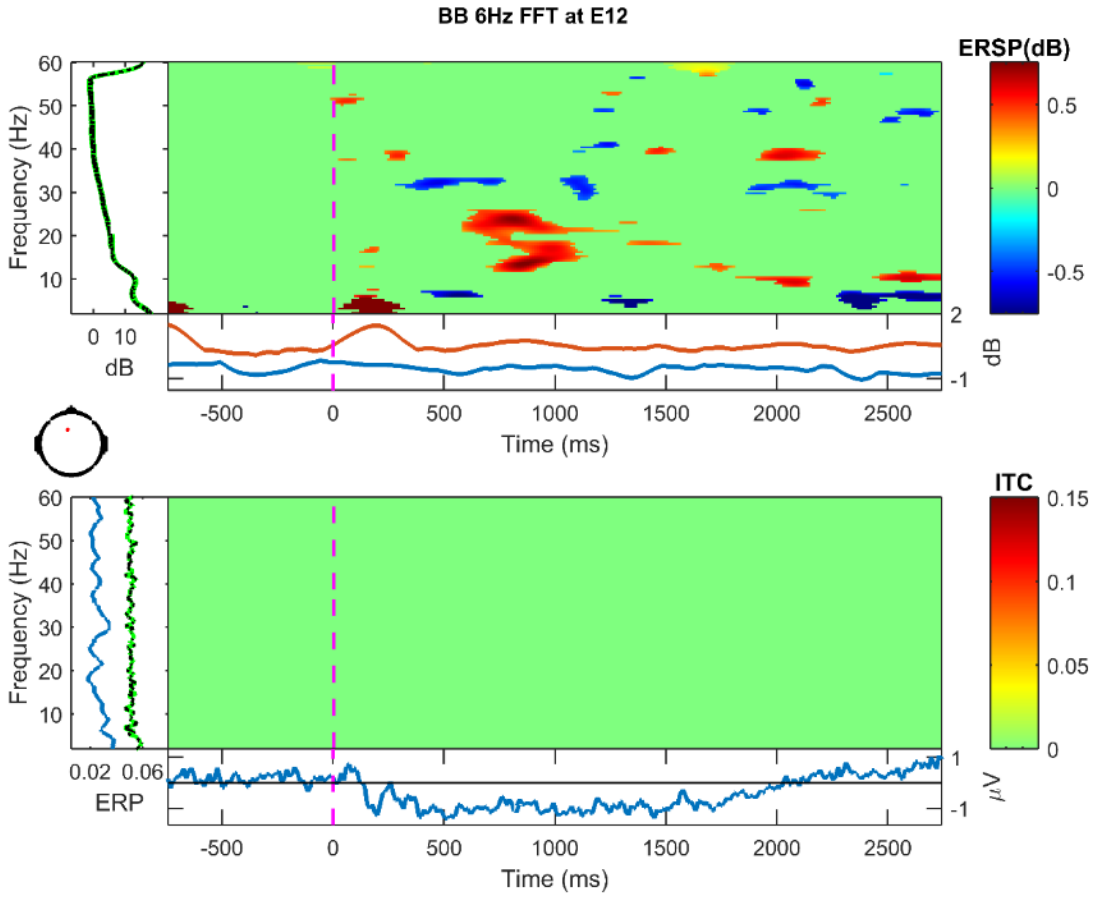

Figure 44. Frequency decomposition done with Fast Fourier Transform (FFT) for E12 (left frontal) from 2-60 Hz during the one second prior to stimulation and the three seconds during stimulation with 6 Hz binaural beat tone. Stimulation period is baseline corrected. Green indicates no significant change from baseline using permutation statistics (α = .10 with false detection rate correction for multiple comparison). X-axis is time, y-axis is frequency. Top: Darker blues indicate a decrease in frequency power while darker reds indicate and increase in frequency power from baseline. Bottom: Darker reds indicate an increase in phase-locking/inter-trial coherence (ITC) between trials at the specified frequency.

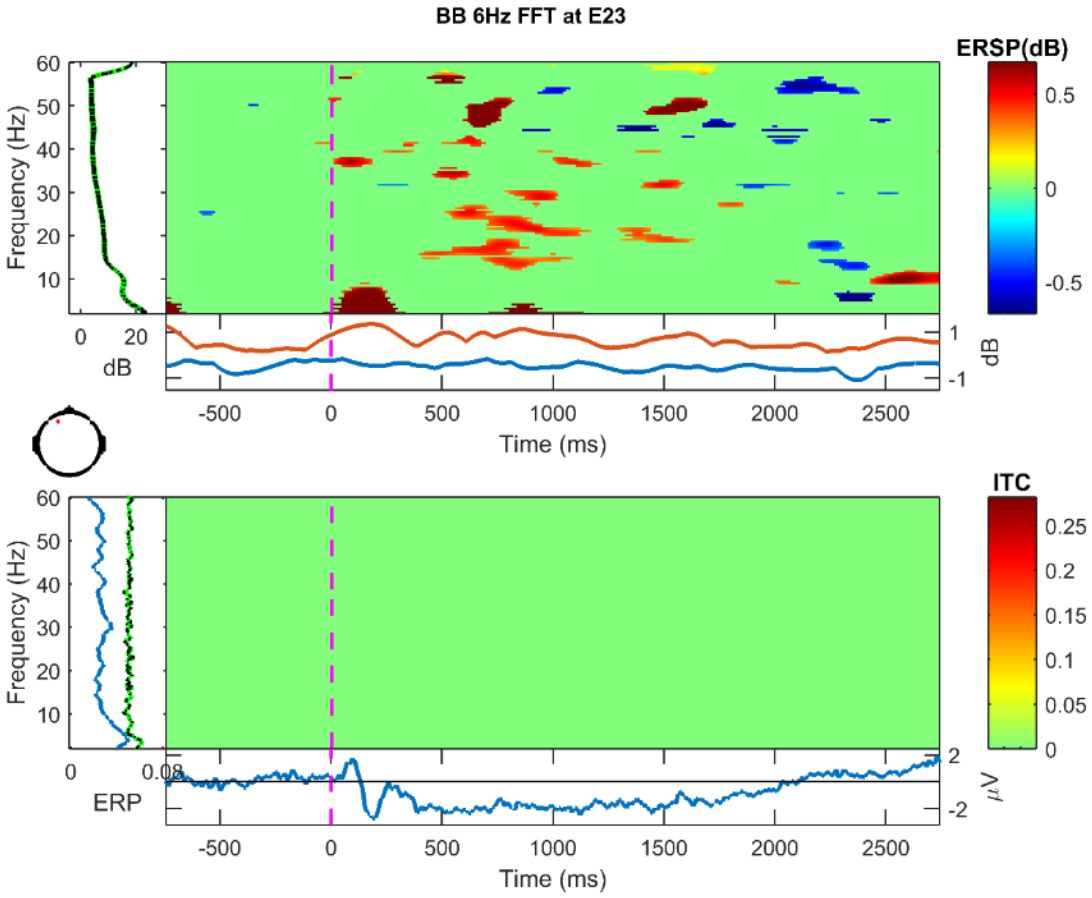

Figure 45. Frequency decomposition done with Fast Fourier Transform (FFT) for E23 (left frontal) from 2-60 Hz during the one second prior to stimulation and the three seconds during stimulation with 6 Hz binaural beat tone. Stimulation period is baseline corrected. Green indicates no significant change from baseline using permutation statistics (α = .10 with false detection rate correction for multiple comparison). X-axis is time, y-axis is frequency. Top: Darker blues indicate a decrease in frequency power while darker reds indicate and increase in frequency power from baseline. Bottom: Darker reds indicate an increase in phase-locking/inter-trial coherence (ITC) between trials at the specified frequency.

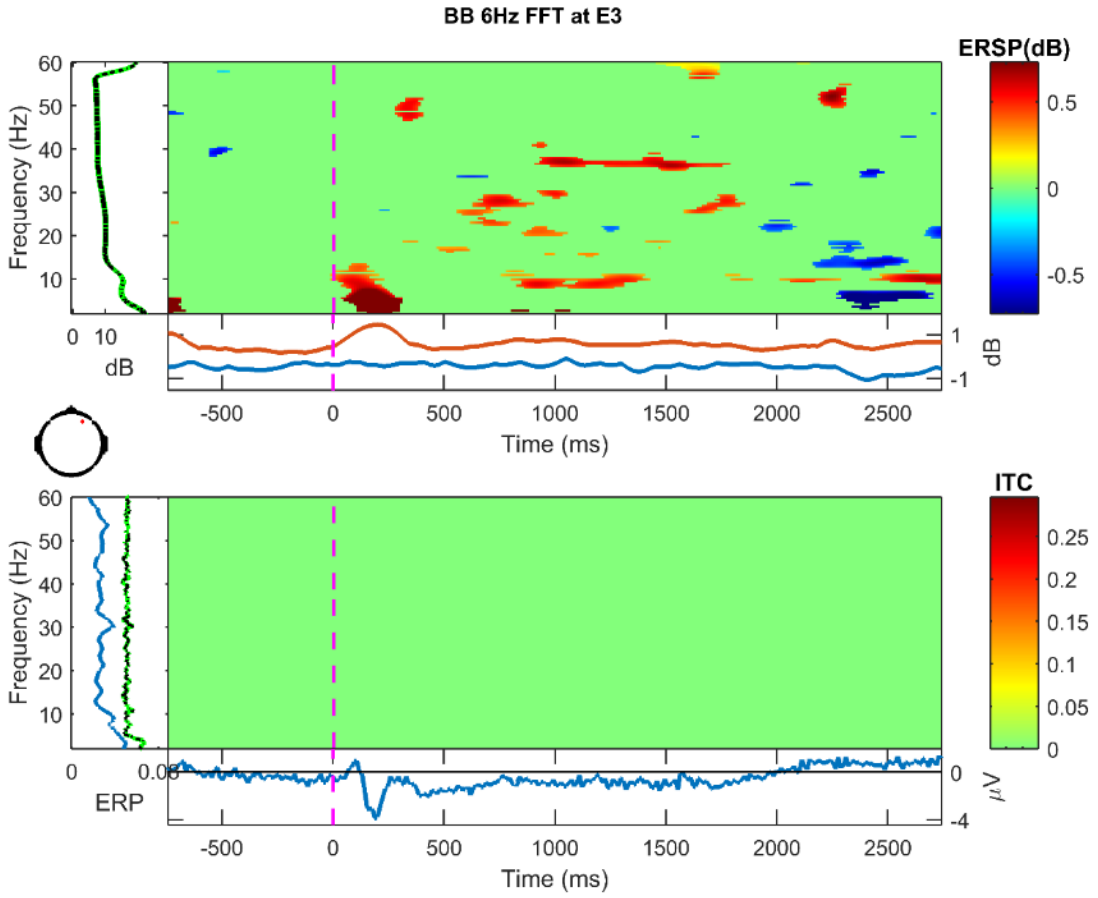

Figure 46. Frequency decomposition done with Fast Fourier Transform (FFT) for E3 (right frontal) from 2-60 Hz during the one second prior to stimulation and the three seconds during stimulation with 6 Hz binaural beat tone. Stimulation period is baseline corrected. Green indicates no significant change from baseline using permutation statistics (α = .10 with false detection rate correction for multiple comparison). X-axis is time, y-axis is frequency. Top: Darker blues indicate a decrease in frequency power while darker reds indicate and increase in frequency power from baseline. Bottom: Darker reds indicate an increase in phase-locking/inter-trial coherence (ITC) between trials at the specified frequency.

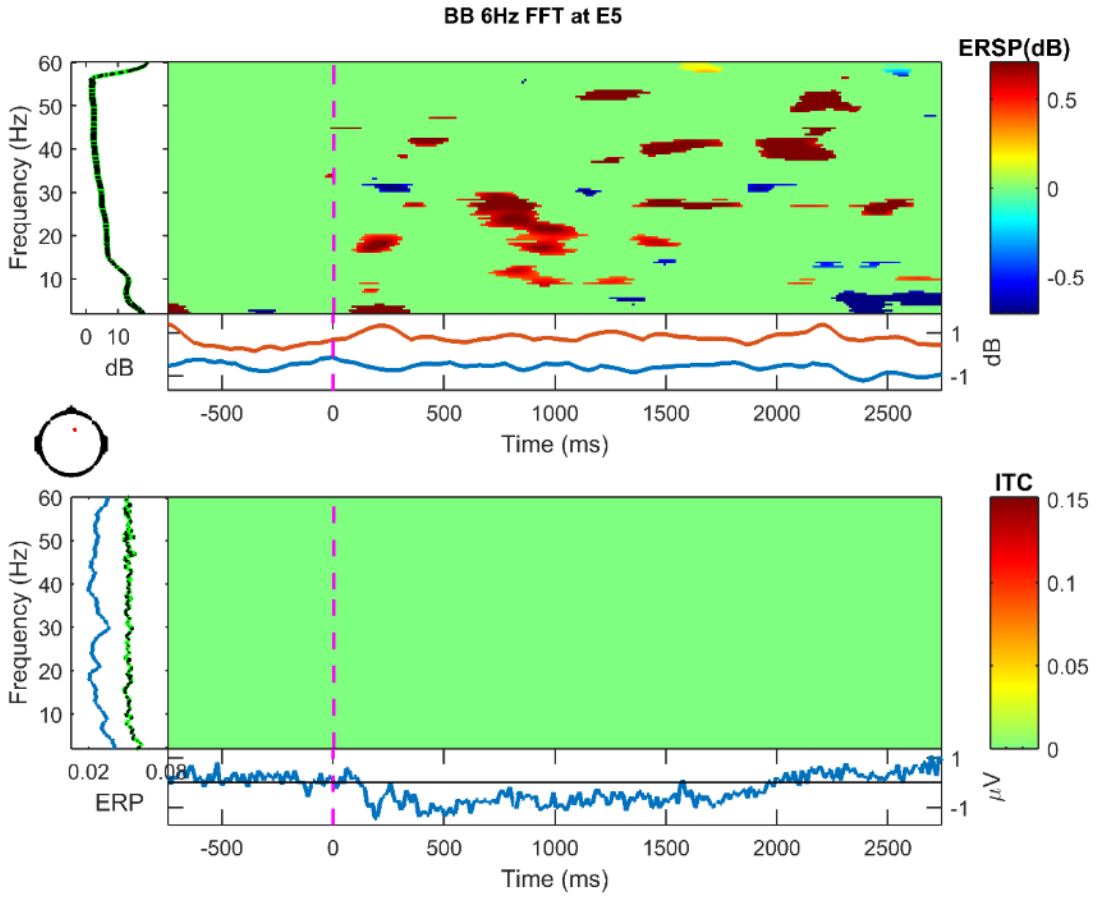

Figure 47. Frequency decomposition done with Fast Fourier Transform (FFT) for E5 (right frontal) from 2-60 Hz during the one second prior to stimulation and the three seconds during stimulation with 6 Hz binaural beat tone. Stimulation period is baseline corrected. Green indicates no significant change from baseline using permutation statistics (α = .10 with false detection rate correction for multiple comparison). X-axis is time, y-axis is frequency. Top: Darker blues indicate a decrease in frequency power while darker reds indicate and increase in frequency power from baseline. Bottom: Darker reds indicate an increase in phase-locking/inter-trial coherence (ITC) between trials at the specified frequency.

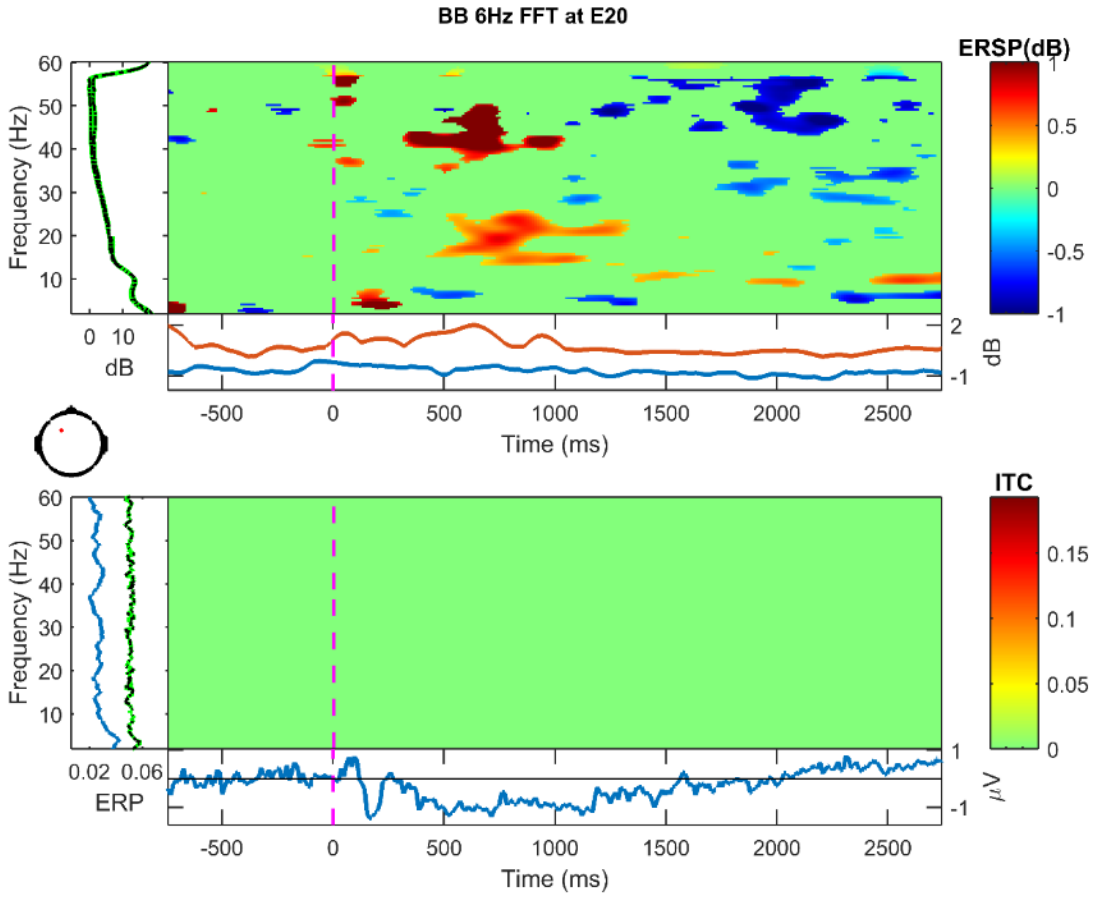

Figure 48. Frequency decomposition done with Fast Fourier Transform (FFT) for E20 (left central) from 2-60 Hz during the one second prior to stimulation and the three seconds during stimulation with 6 Hz binaural beat tone. Stimulation period is baseline corrected. Green indicates no significant change from baseline using permutation statistics (α = .10 with false detection rate correction for multiple comparison). X-axis is time, y-axis is frequency. Top: Darker blues indicate a decrease in frequency power while darker reds indicate and increase in frequency power from baseline. Bottom: Darker reds indicate an increase in phase-locking/inter-trial coherence (ITC) between trials at the specified frequency.

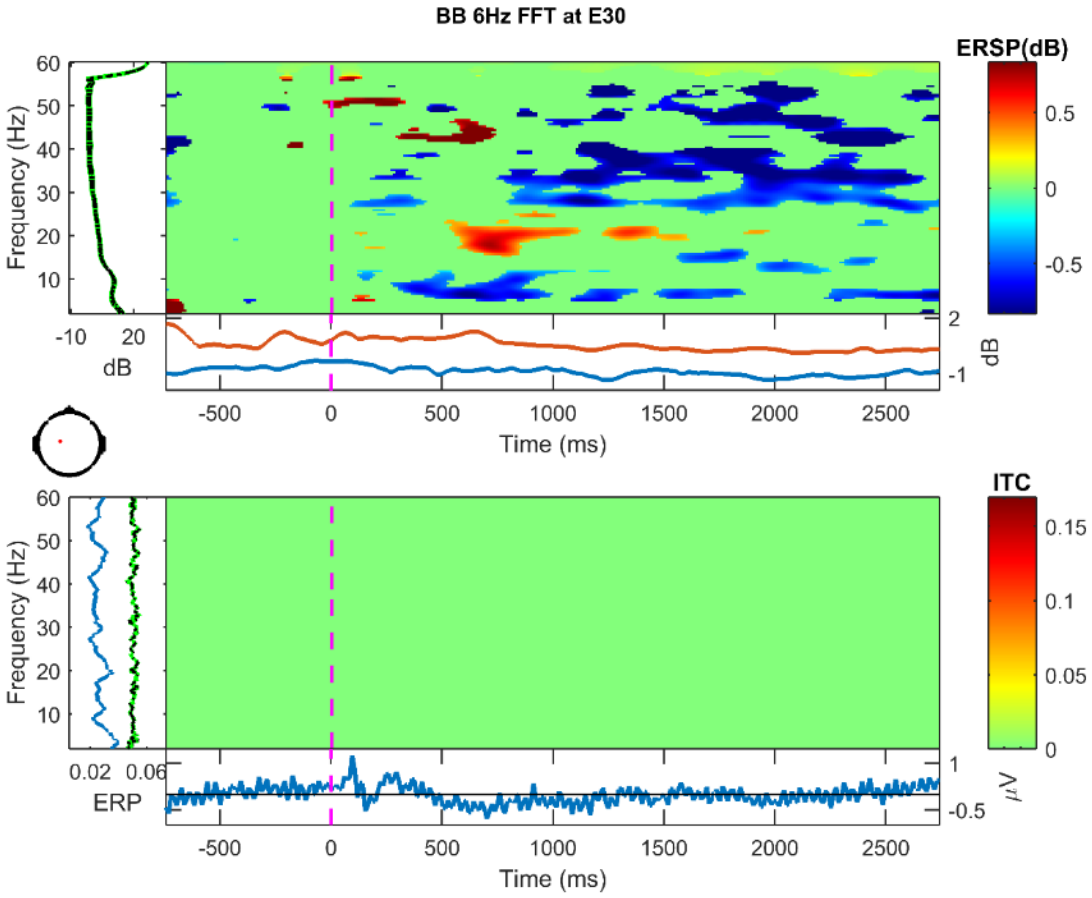

Figure 49. Frequency decomposition done with Fast Fourier Transform (FFT) for E30 (left central) from 2-60 Hz during the one second prior to stimulation and the three seconds during stimulation with 6 Hz binaural beat tone. Stimulation period is baseline corrected. Green indicates no significant change from baseline using permutation statistics ($\alpha = .10$ with false detection rate correction for multiple comparison). X-axis is time, y-axis is frequency. Top: Darker blues indicate a decrease in frequency power while darker reds indicate and increase in frequency power from baseline. Bottom: Darker reds indicate an increase in phase-locking/inter-trial coherence (ITC) between trials at the specified frequency.

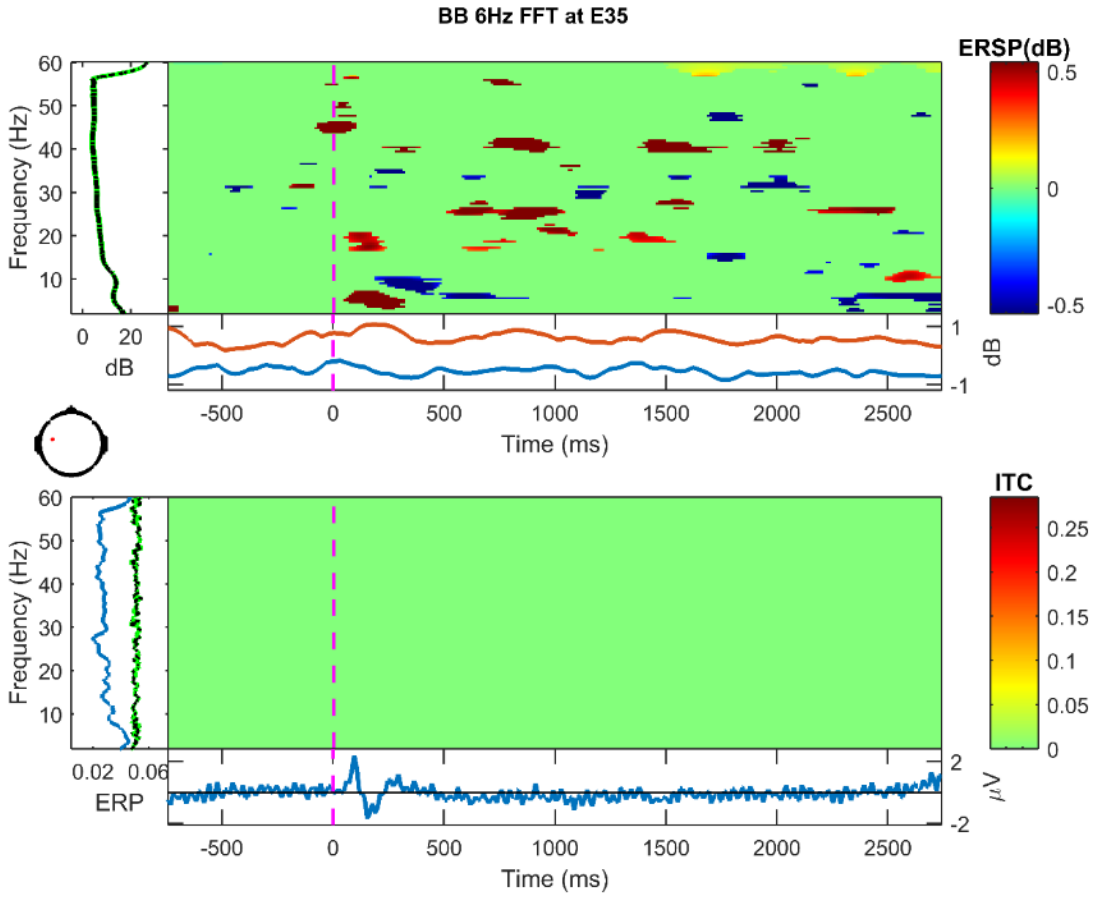

Figure 50. Frequency decomposition done with Fast Fourier Transform (FFT) for E35 (left central) from 2-60 Hz during the one second prior to stimulation and the three seconds during stimulation with 6 Hz binaural beat tone. Stimulation period is baseline corrected. Green indicates no significant change from baseline using permutation statistics ($\alpha = .10$ with false detection rate correction for multiple comparison). X-axis is time, y-axis is frequency. Top: Darker blues indicate a decrease in frequency power while darker reds indicate and increase in frequency power from baseline. Bottom: Darker reds indicate an increase in phase-locking/inter-trial coherence (ITC) between trials at the specified frequency.

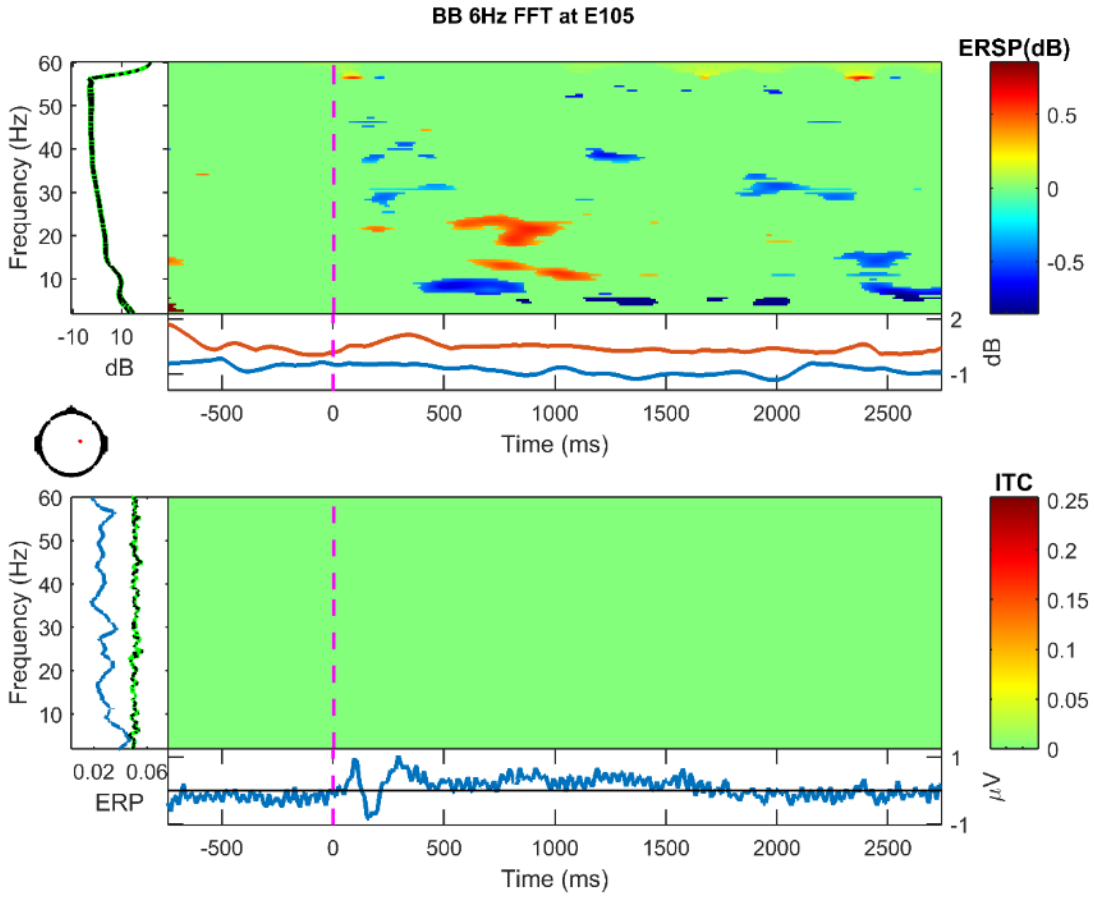

Figure 51. Frequency decomposition done with Fast Fourier Transform (FFT) for E105 (right central) from 2-60 Hz during the one second prior to stimulation and the three seconds during stimulation with 6 Hz binaural beat tone. Stimulation period is baseline corrected. Green indicates no significant change from baseline using permutation statistics (α = .10 with false detection rate correction for multiple comparison). X-axis is time, y-axis is frequency. Top: Darker blues indicate a decrease in frequency power while darker reds indicate and increase in frequency power from baseline. Bottom: Darker reds indicate an increase in phase-locking/inter-trial coherence (ITC) between trials at the specified frequency.

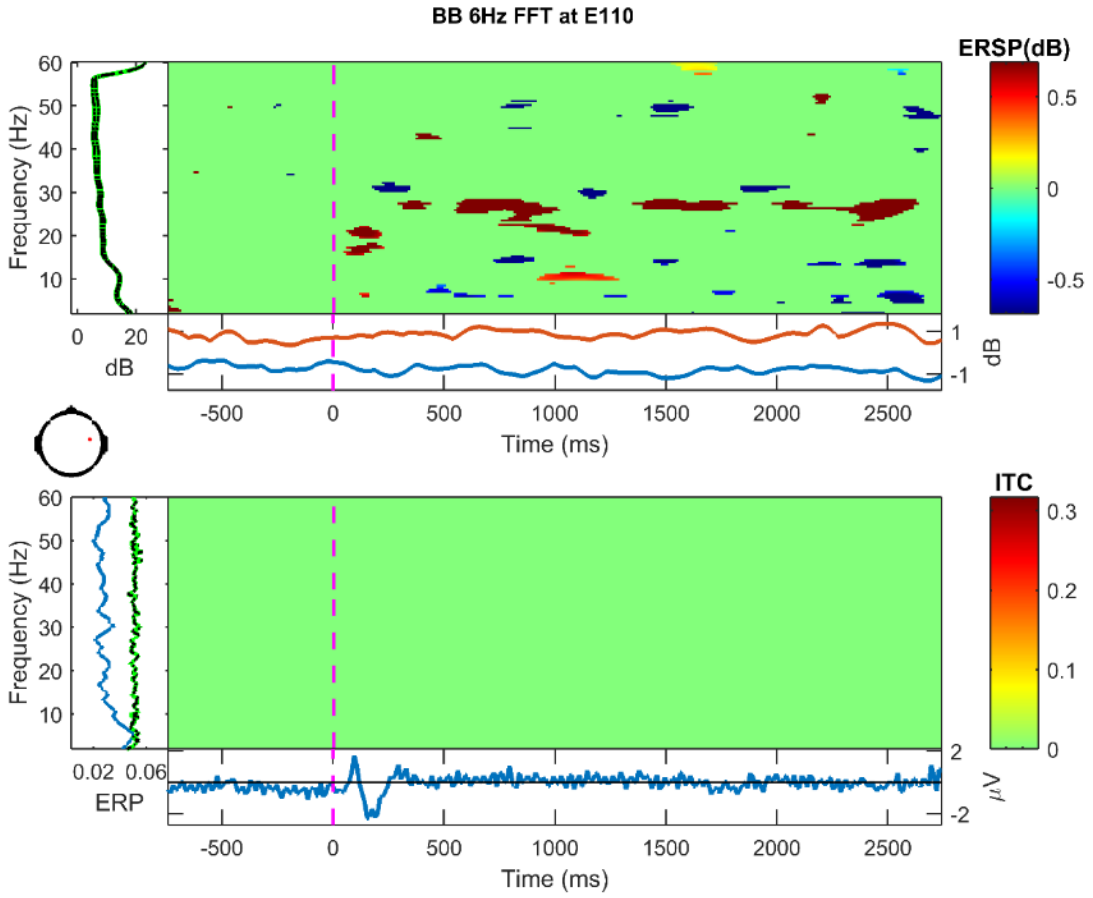

Figure 52. Frequency decomposition done with Fast Fourier Transform (FFT) for E110 (right central) from 2-60 Hz during the one second prior to stimulation and the three seconds during stimulation with 6 Hz binaural beat tone. Stimulation period is baseline corrected. Green indicates no significant change from baseline using permutation statistics ($\alpha = .10$ with false detection rate correction for multiple comparison). X-axis is time, y-axis is frequency. Top: Darker blues indicate a decrease in frequency power while darker reds indicate and increase in frequency power from baseline. Bottom: Darker reds indicate an increase in phase-locking/inter-trial coherence (ITC) between trials at the specified frequency.

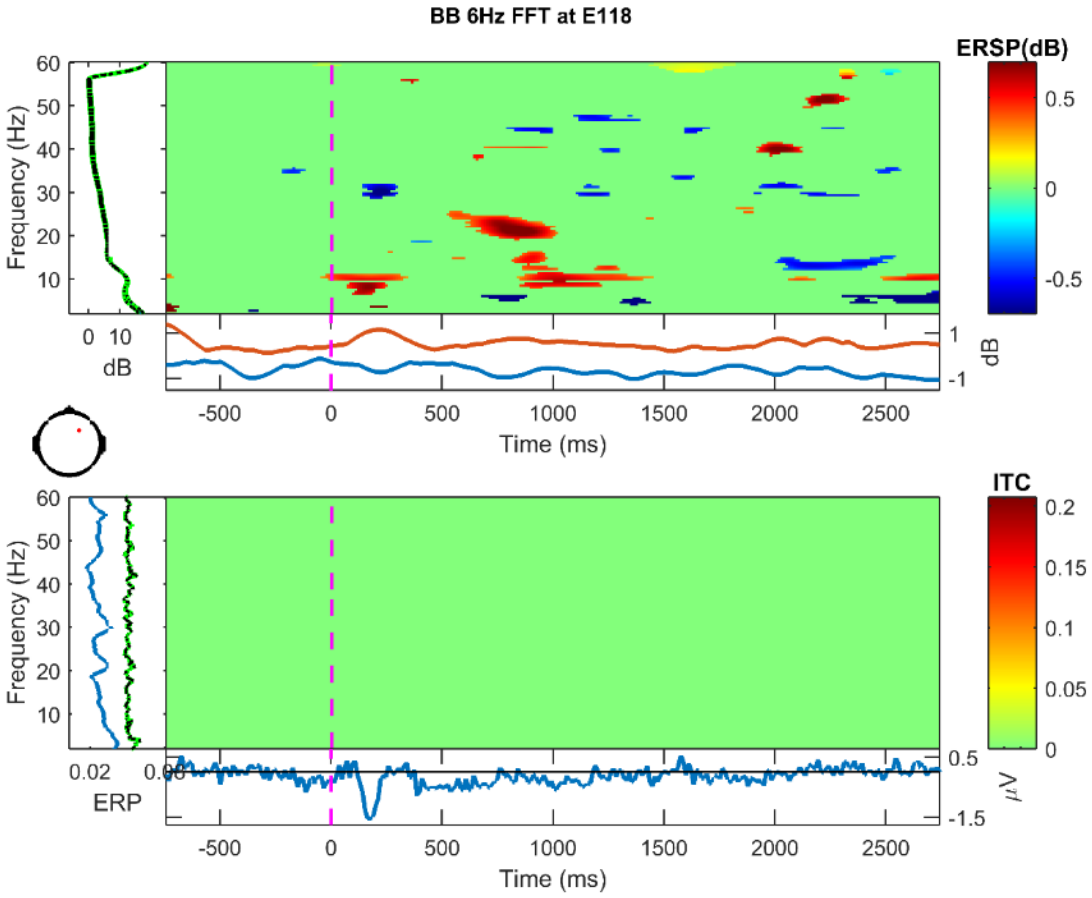

Figure 53. Frequency decomposition done with Fast Fourier Transform (FFT) for E118 (right central) from 2-60 Hz during the one second prior to stimulation and the three seconds during stimulation with 6 Hz binaural beat tone. Stimulation period is baseline corrected. Green indicates no significant change from baseline using permutation statistics ($\alpha = .10$ with false detection rate correction for multiple comparison). X-axis is time, y-axis is frequency. Top: Darker blues indicate a decrease in frequency power while darker reds indicate and increase in frequency power from baseline. Bottom: Darker reds indicate an increase in phase-locking/inter-trial coherence (ITC) between trials at the specified frequency.

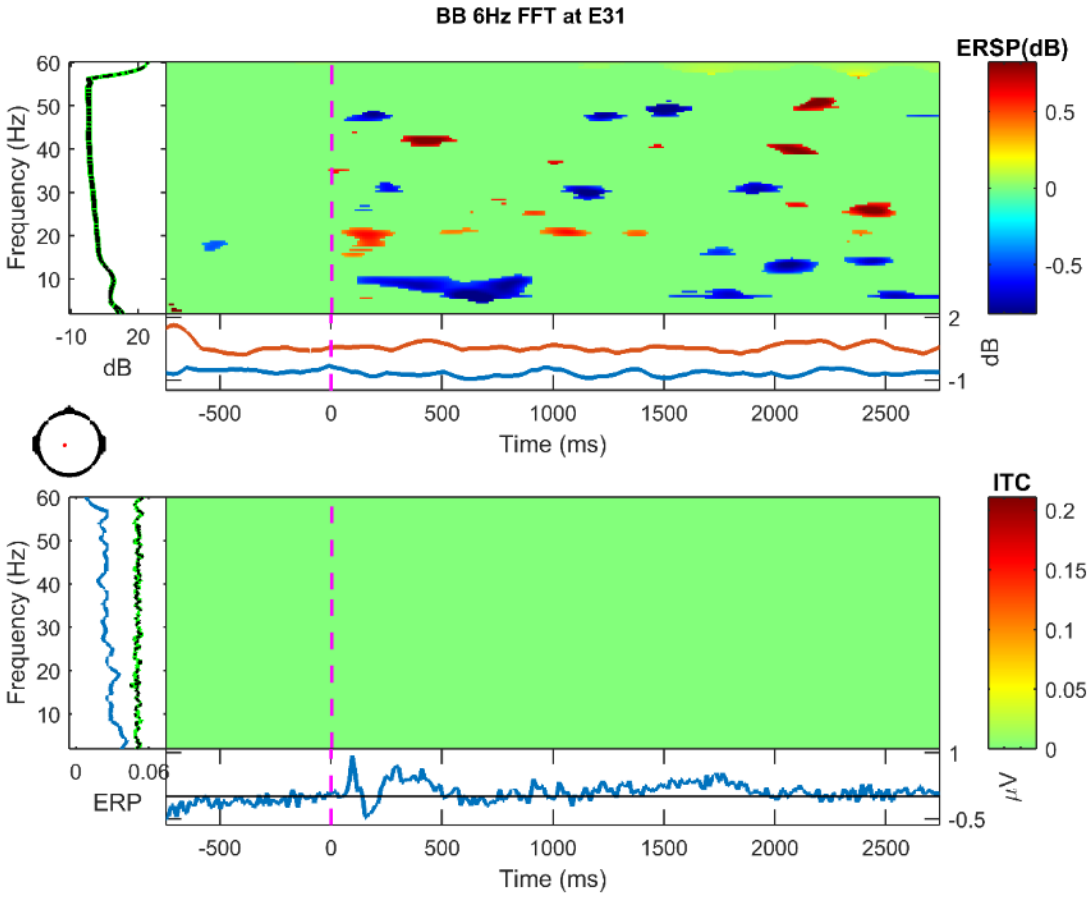

Figure 54. Frequency decomposition done with Fast Fourier Transform (FFT) for E31 (left parietal) from 2-60 Hz during the one second prior to stimulation and the three seconds during stimulation with 6 Hz binaural beat tone. Stimulation period is baseline corrected. Green indicates no significant change from baseline using permutation statistics ($\alpha = .10$ with false detection rate correction for multiple comparison). X-axis is time, y-axis is frequency. Top: Darker blues indicate a decrease in frequency power while darker reds indicate and increase in frequency power from baseline. Bottom: Darker reds indicate an increase in phase-locking/inter-trial coherence (ITC) between trials at the specified frequency.

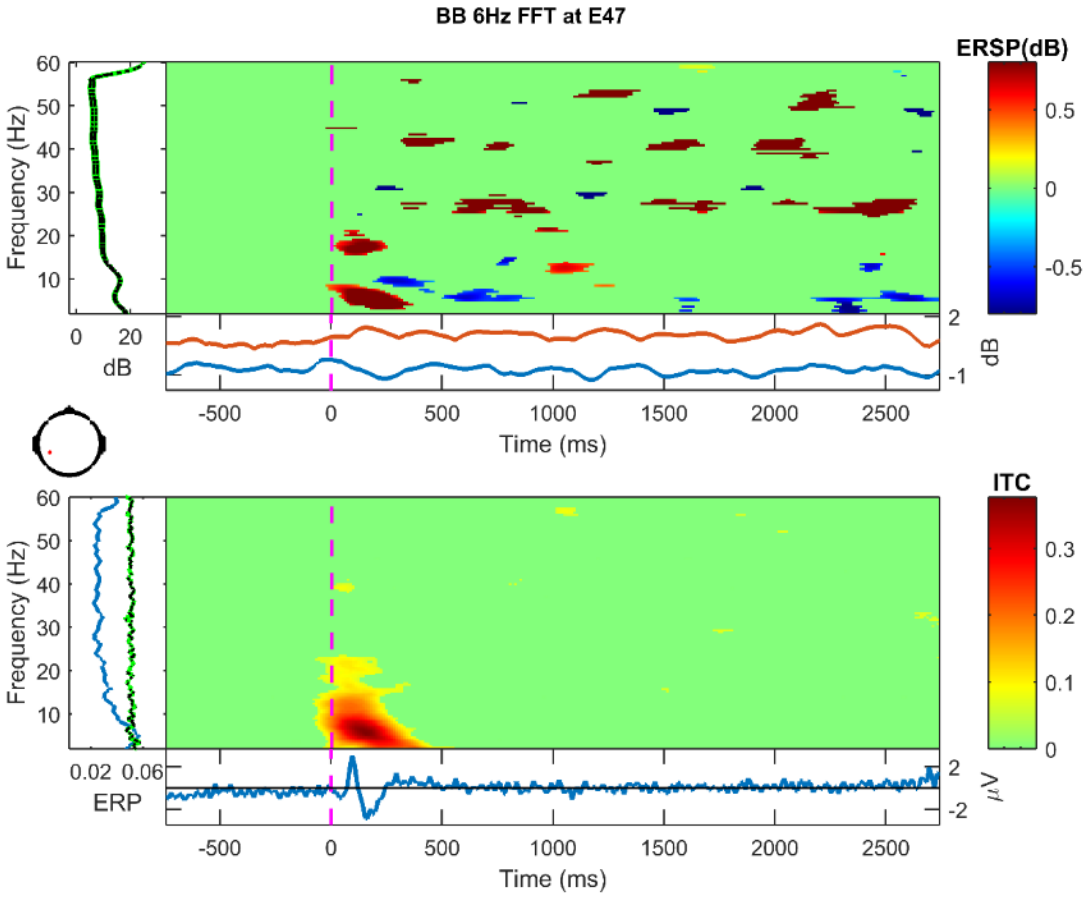

Figure 55. Frequency decomposition done with Fast Fourier Transform (FFT) for E47 (left parietal) from 2-60 Hz during the one second prior to stimulation and the three seconds during stimulation with 6 Hz binaural beat tone. Stimulation period is baseline corrected. Green indicates no significant change from baseline using permutation statistics ($\alpha = .10$ with false detection rate correction for multiple comparison). X-axis is time, y-axis is frequency. Top: Darker blues indicate a decrease in frequency power while darker reds indicate and increase in frequency power from baseline. Bottom: Darker reds indicate an increase in phase-locking/inter-trial coherence (ITC) between trials at the specified frequency.

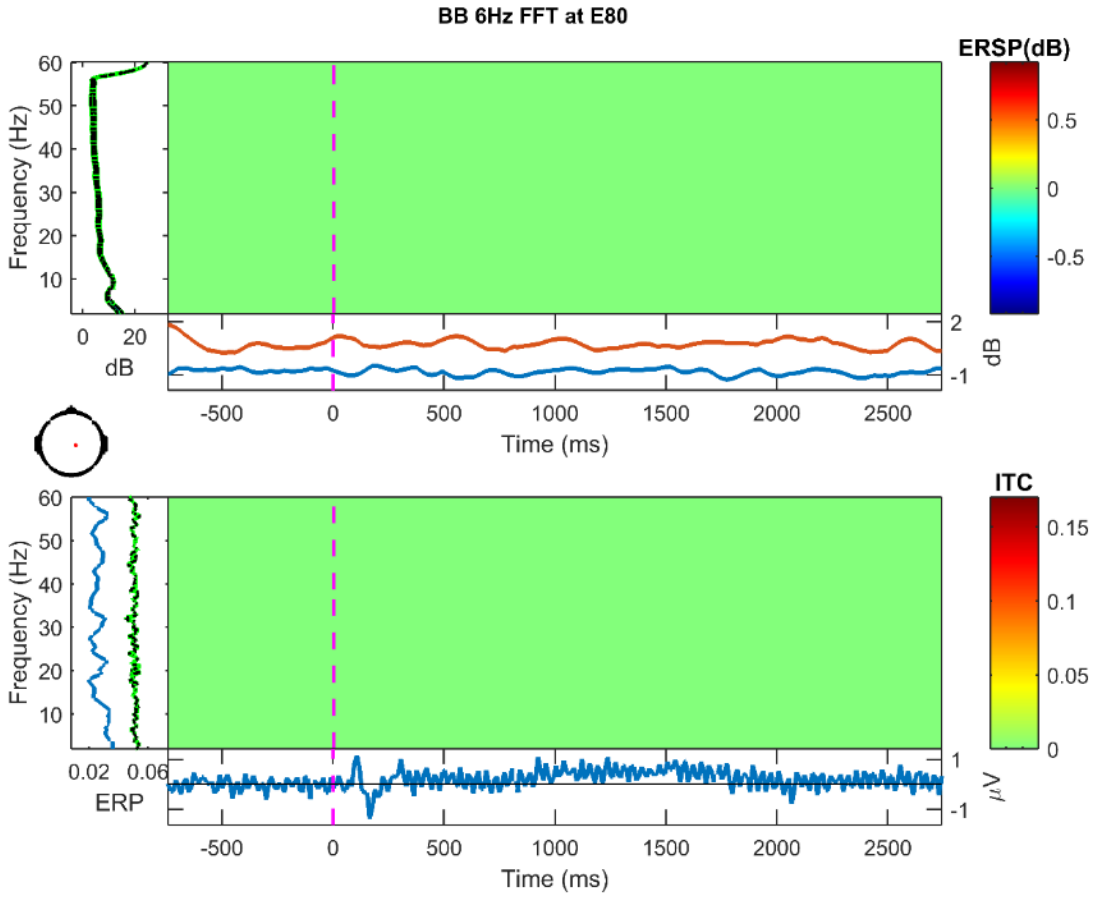

Figure 56. Frequency decomposition done with Fast Fourier Transform (FFT) for E80 (right parietal) from 2-60 Hz during the one second prior to stimulation and the three seconds during stimulation with 6 Hz binaural beat tone. Stimulation period is baseline corrected. Green indicates no significant change from baseline using permutation statistics (α = .10 with false detection rate correction for multiple comparison). X-axis is time, y-axis is frequency. Top: Darker blues indicate a decrease in frequency power while darker reds indicate and increase in frequency power from baseline. Bottom: Darker reds indicate an increase in phase-locking/inter-trial coherence (ITC) between trials at the specified frequency.

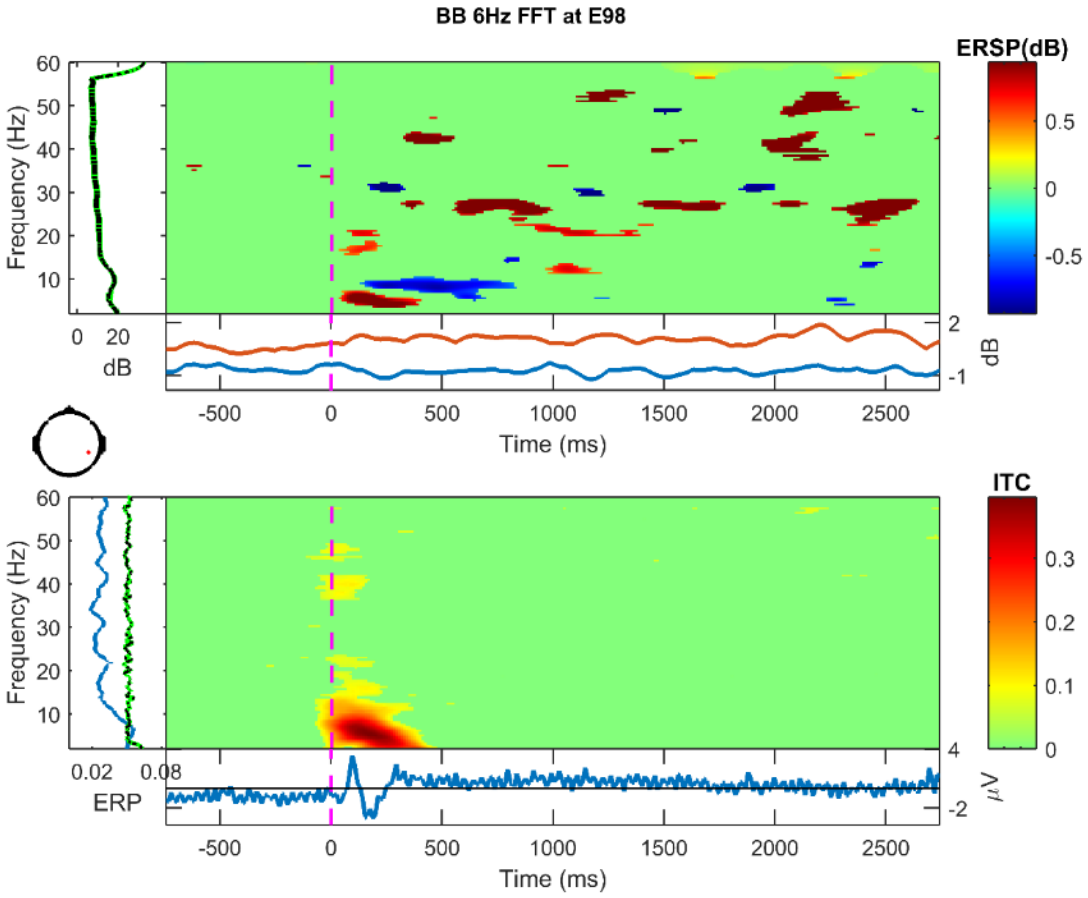

Figure 57. Frequency decomposition done with Fast Fourier Transform (FFT) for E98 (right parietal) from 2-60 Hz during the one second prior to stimulation and the three seconds during stimulation with 6 Hz binaural beat tone. Stimulation period is baseline corrected. Green indicates no significant change from baseline using permutation statistics (α = .10 with false detection rate correction for multiple comparison). X-axis is time, y-axis is frequency. Top: Darker blues indicate a decrease in frequency power while darker reds indicate and increase in frequency power from baseline. Bottom: Darker reds indicate an increase in phase-locking/inter-trial coherence (ITC) between trials at the specified frequency.

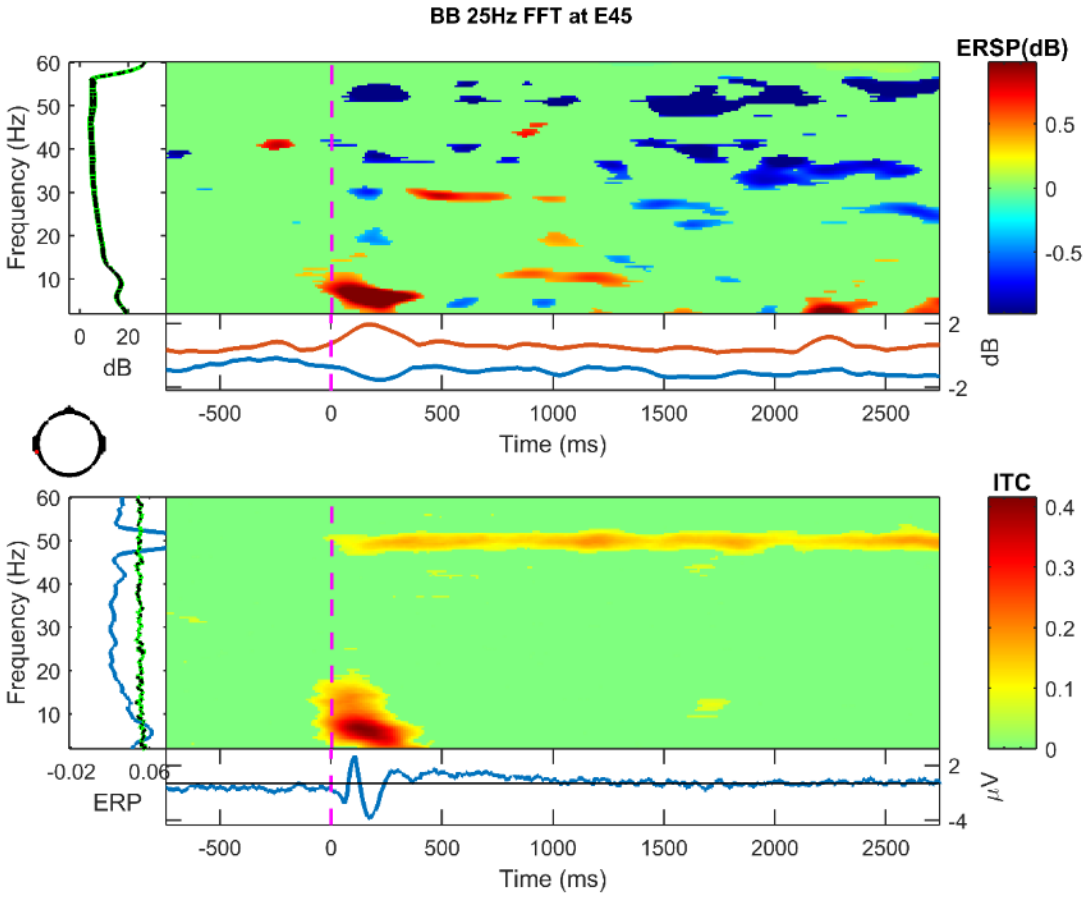

Figure 58. Frequency decomposition done with Fast Fourier Transform (FFT) for E45 (left temporal, auditory cortex) from 2-60 Hz during the one second prior to stimulation and the three seconds during stimulation with 25 Hz binaural beat tone. Stimulation period is baseline corrected. Green indicates no significant change from baseline using permutation statistics (α = .10 with false detection rate correction for multiple comparison). X-axis is time, y-axis is frequency. Top: Darker blues indicate a decrease in frequency power while darker reds indicate and increase in frequency power from baseline. Bottom: Darker reds indicate an increase in phase-locking/inter-trial coherence (ITC) between trials at the specified frequency.

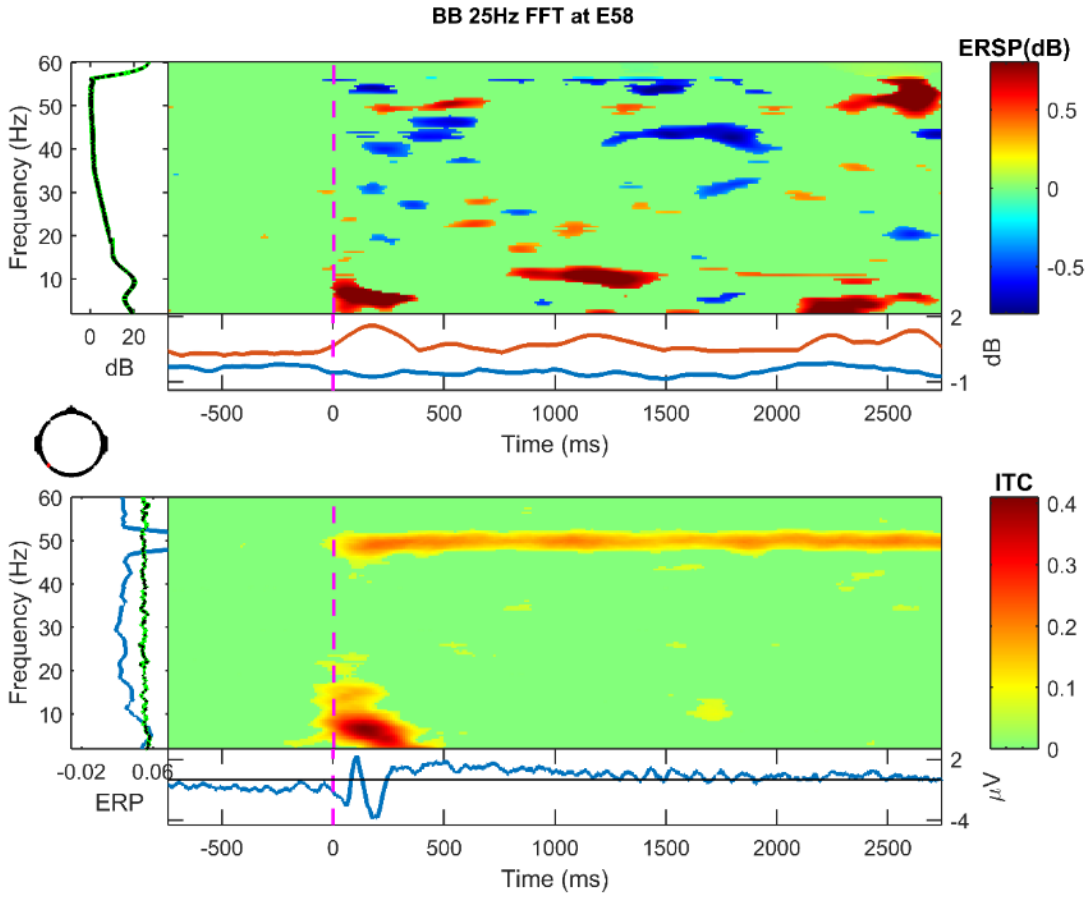

Figure 59. Frequency decomposition done with Fast Fourier Transform (FFT) for E58 (left temporal, auditory cortex) from 2-60 Hz during the one second prior to stimulation and the three seconds during stimulation with 25 Hz binaural beat tone. Stimulation period is baseline corrected. Green indicates no significant change from baseline using permutation statistics (α = .10 with false detection rate correction for multiple comparison). X-axis is time, y-axis is frequency. Top: Darker blues indicate a decrease in frequency power while darker reds indicate and increase in frequency power from baseline. Bottom: Darker reds indicate an increase in phase-locking/inter-trial coherence (ITC) between trials at the specified frequency.

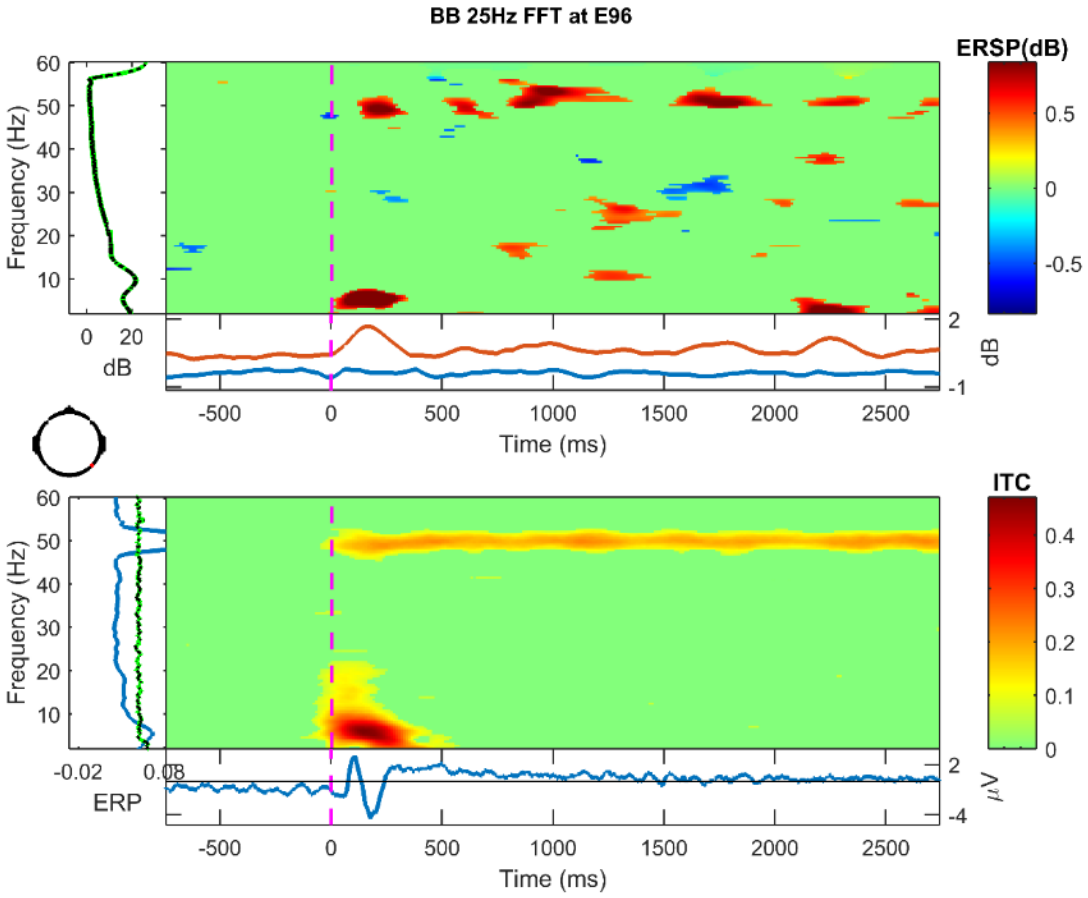

Figure 60. Frequency decomposition done with Fast Fourier Transform (FFT) for E96 (right temporal, auditory cortex) from 2-60 Hz during the one second prior to stimulation and the three seconds during stimulation with 25 Hz binaural beat tone. Stimulation period is baseline corrected. Green indicates no significant change from baseline using permutation statistics (α = .10 with false detection rate correction for multiple comparison). X-axis is time, y-axis is frequency. Top: Darker blues indicate a decrease in frequency power while darker reds indicate and increase in frequency power from baseline. Bottom: Darker reds indicate an increase in phase-locking/inter-trial coherence (ITC) between trials at the specified frequency.

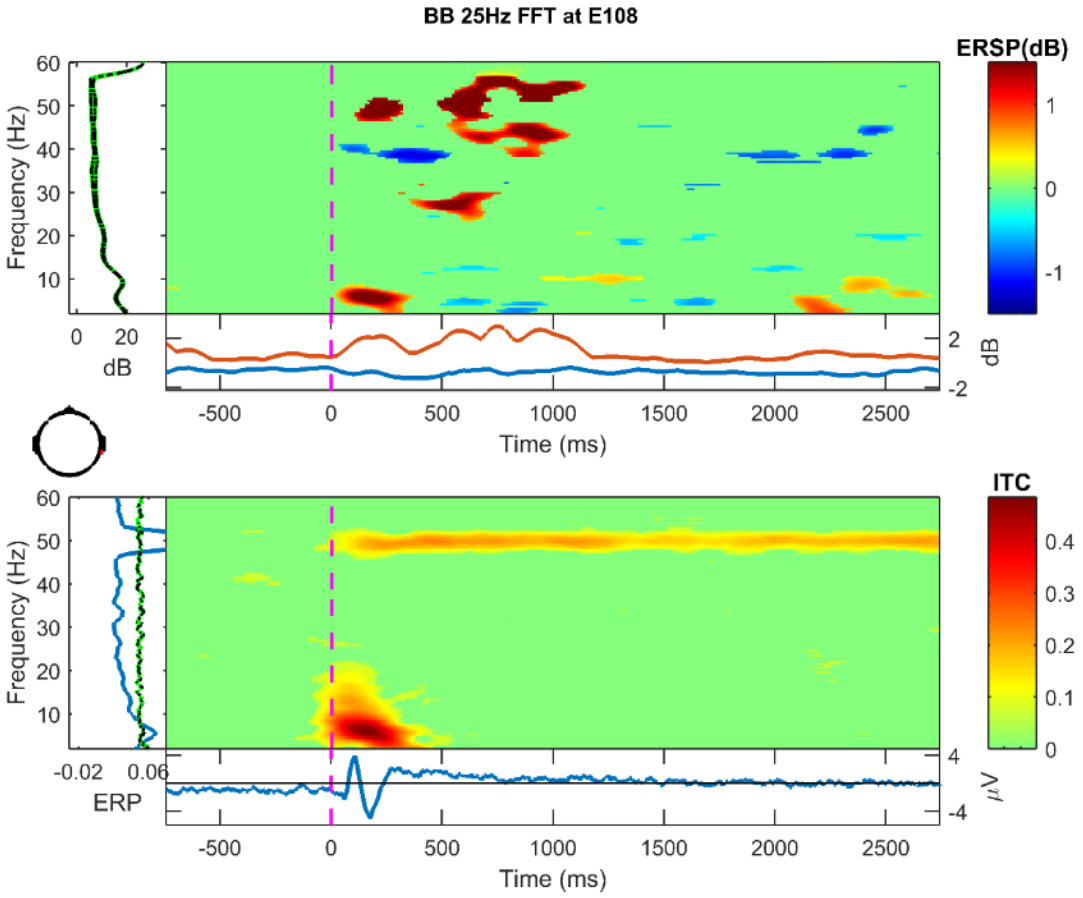

Figure 61. Frequency decomposition done with Fast Fourier Transform (FFT) for E108 (right temporal, auditory cortex) from 2-60 Hz during the one second prior to stimulation and the three seconds during stimulation with 25 Hz binaural beat tone. Stimulation period is baseline corrected. Green indicates no significant change from baseline using permutation statistics (α = .10 with false detection rate correction for multiple comparison). X-axis is time, y-axis is frequency. Top: Darker blues indicate a decrease in frequency power while darker reds indicate and increase in frequency power from baseline. Bottom: Darker reds indicate an increase in phase-locking/inter-trial coherence (ITC) between trials at the specified frequency.

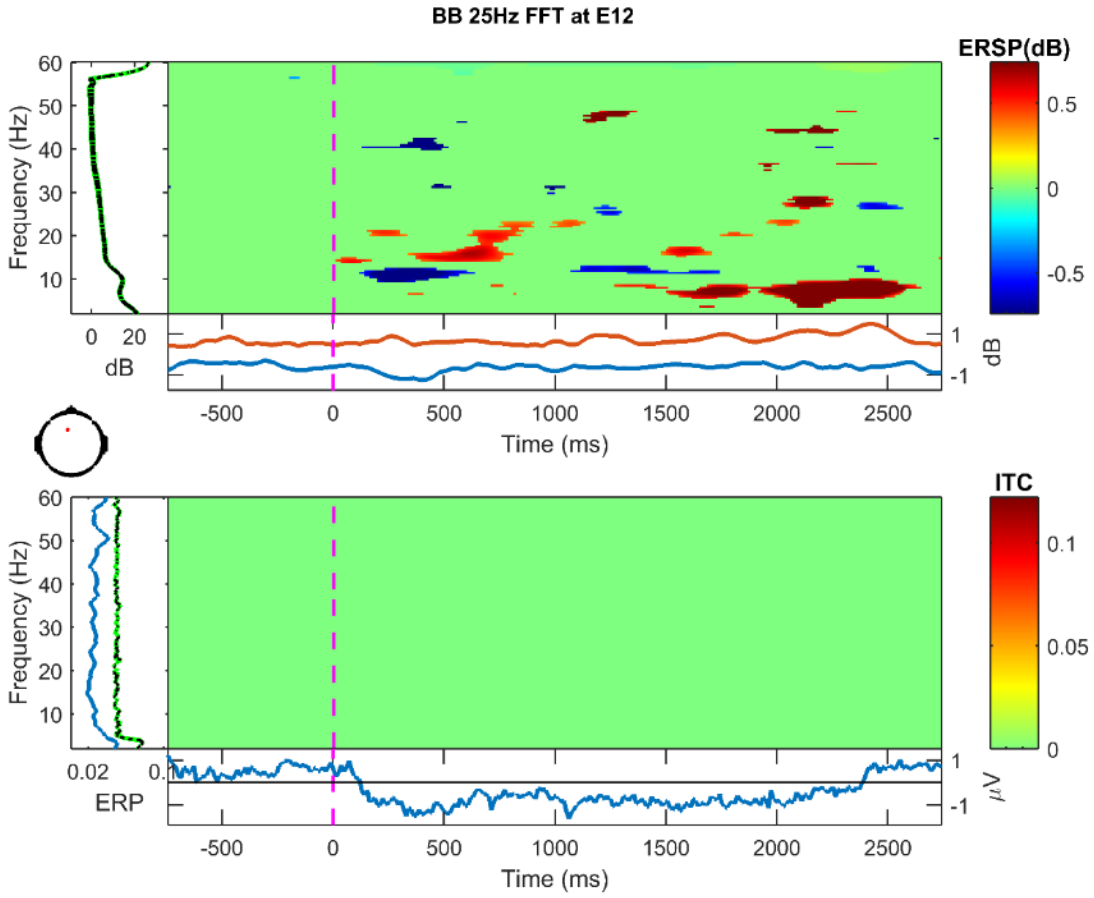

Figure 62. Frequency decomposition done with Fast Fourier Transform (FFT) for E12 (left frontal) from 2-60 Hz during the one second prior to stimulation and the three seconds during stimulation with 25 Hz binaural beat tone. Stimulation period is baseline corrected. Green indicates no significant change from baseline using permutation statistics (α = .10 with false detection rate correction for multiple comparison). X-axis is time, y-axis is frequency. Top: Darker blues indicate a decrease in frequency power while darker reds indicate and increase in frequency power from baseline. Bottom: Darker reds indicate an increase in phase-locking/inter-trial coherence (ITC) between trials at the specified frequency.

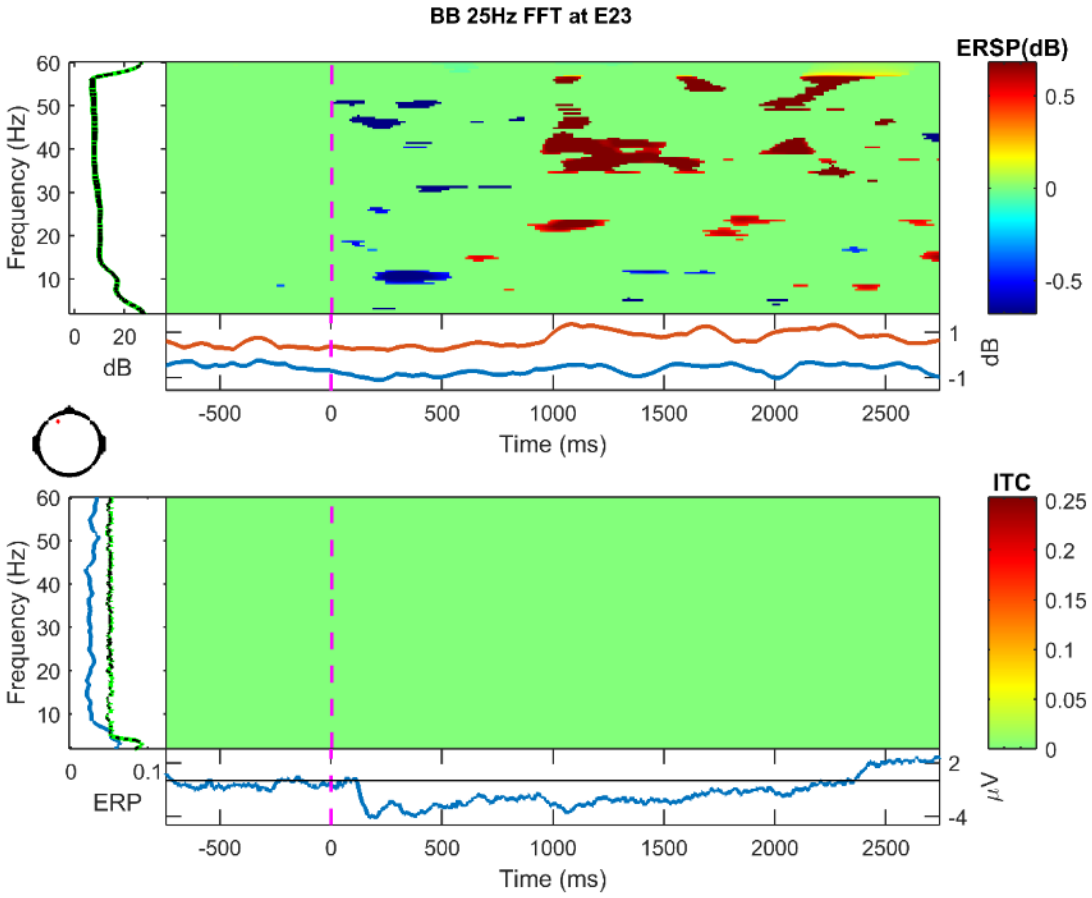

Figure 63. Frequency decomposition done with Fast Fourier Transform (FFT) for E23 (left frontal) from 2-60 Hz during the one second prior to stimulation and the three seconds during stimulation with 25 Hz binaural beat tone. Stimulation period is baseline corrected. Green indicates no significant change from baseline using permutation statistics (α = .10 with false detection rate correction for multiple comparison). X-axis is time, y-axis is frequency. Top: Darker blues indicate a decrease in frequency power while darker reds indicate and increase in frequency power from baseline. Bottom: Darker reds indicate an increase in phase-locking/inter-trial coherence (ITC) between trials at the specified frequency.

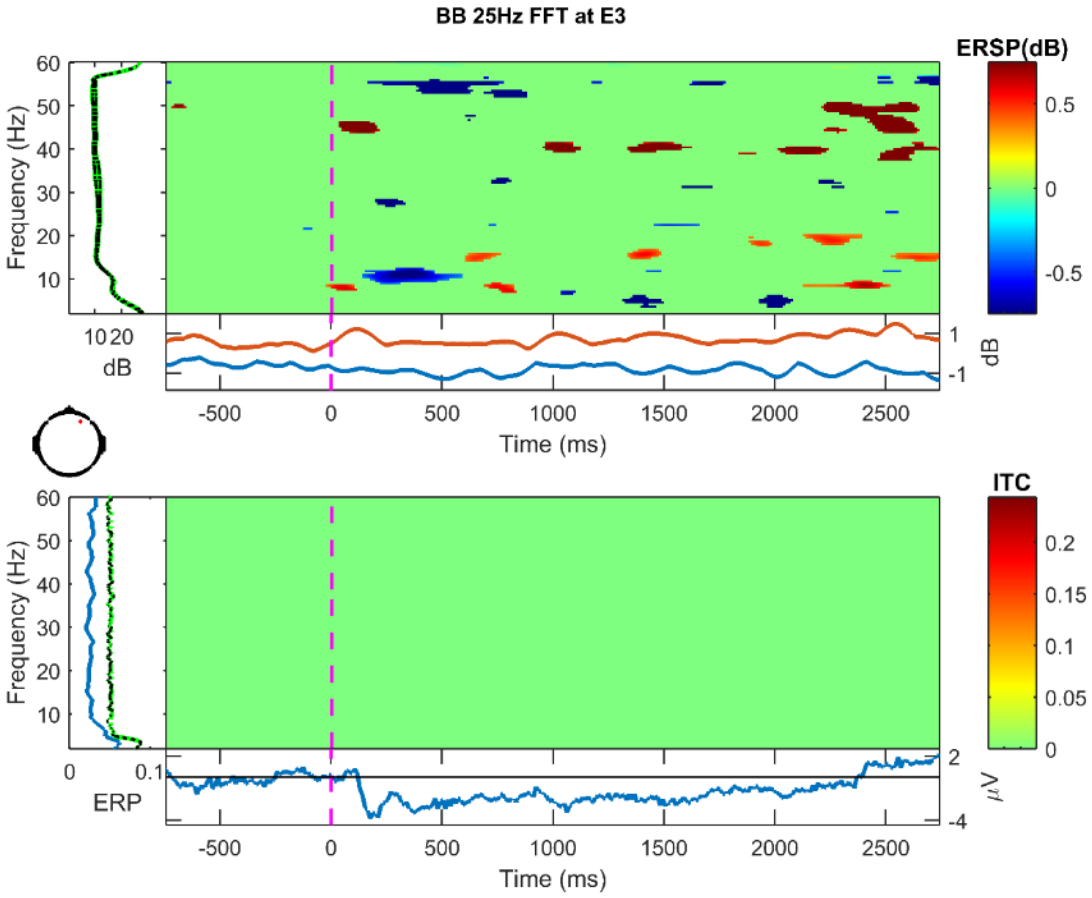

Figure 64. Frequency decomposition done with Fast Fourier Transform (FFT) for E3 (right frontal) from 2-60 Hz during the one second prior to stimulation and the three seconds during stimulation with 25 Hz binaural beat tone. Stimulation period is baseline corrected. Green indicates no significant change from baseline using permutation statistics (α = .10 with false detection rate correction for multiple comparison). X-axis is time, y-axis is frequency. Top: Darker blues indicate a decrease in frequency power while darker reds indicate and increase in frequency power from baseline. Bottom: Darker reds indicate an increase in phase-locking/inter-trial coherence (ITC) between trials at the specified frequency.

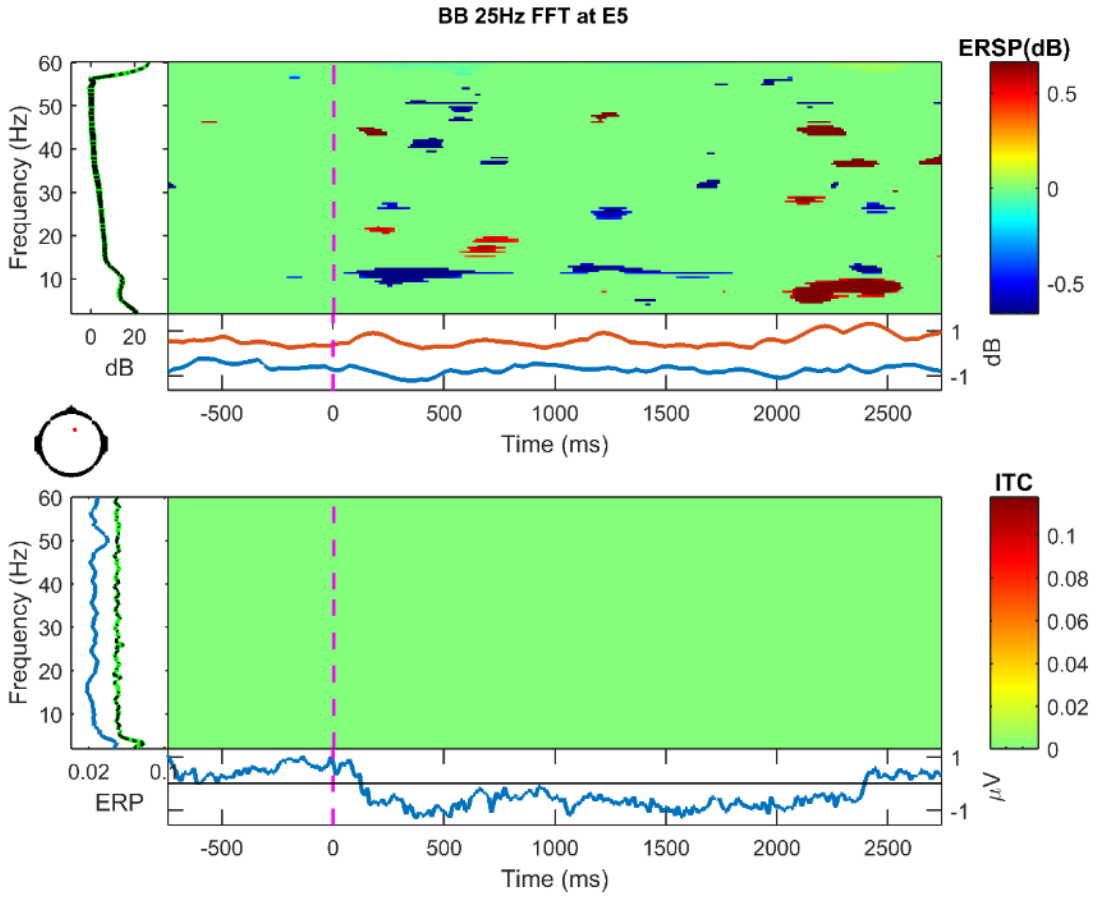

Figure 65. Frequency decomposition done with Fast Fourier Transform (FFT) for E5 (right frontal) from 2-60 Hz during the one second prior to stimulation and the three seconds during stimulation with 25 Hz binaural beat tone. Stimulation period is baseline corrected. Green indicates no significant change from baseline using permutation statistics (α = .10 with false detection rate correction for multiple comparison). X-axis is time, y-axis is frequency. Top: Darker blues indicate a decrease in frequency power while darker reds indicate and increase in frequency power from baseline. Bottom: Darker reds indicate an increase in phase-locking/inter-trial coherence (ITC) between trials at the specified frequency.

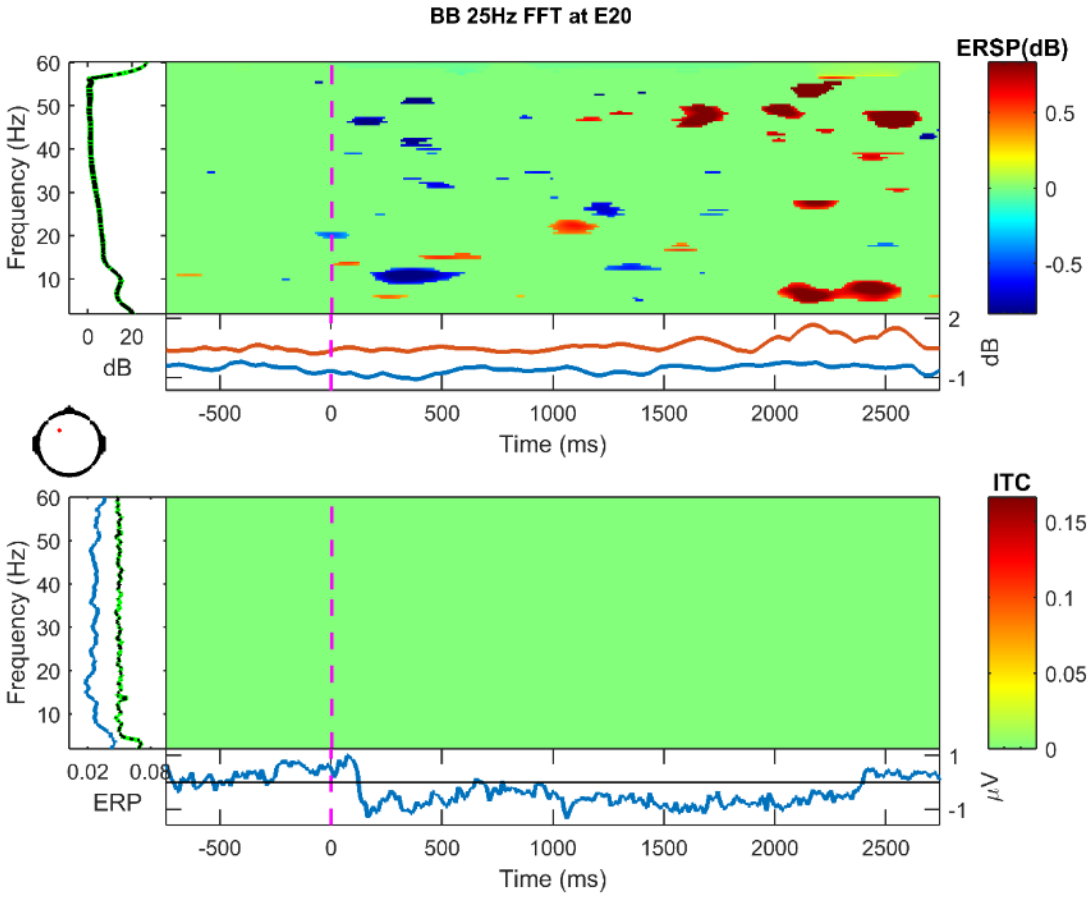

Figure 66. Frequency decomposition done with Fast Fourier Transform (FFT) for E20 (left central) from 2-60 Hz during the one second prior to stimulation and the three seconds during stimulation with 25 Hz binaural beat tone. Stimulation period is baseline corrected. Green indicates no significant change from baseline using permutation statistics (α = .10 with false detection rate correction for multiple comparison). X-axis is time, y-axis is frequency. Top: Darker blues indicate a decrease in frequency power while darker reds indicate and increase in frequency power from baseline. Bottom: Darker reds indicate an increase in phase-locking/inter-trial coherence (ITC) between trials at the specified frequency.

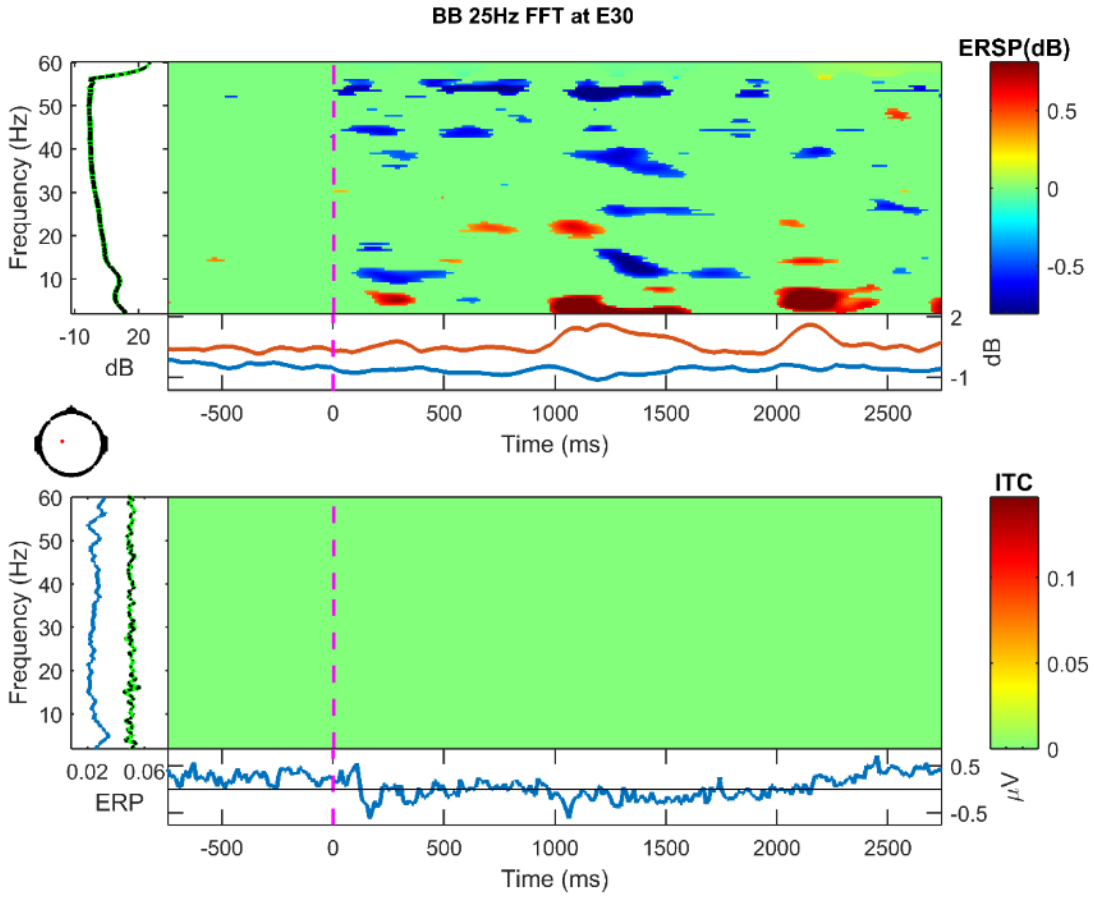

Figure 67. Frequency decomposition done with Fast Fourier Transform (FFT) for E30 (left central) from 2-60 Hz during the one second prior to stimulation and the three seconds during stimulation with 25 Hz binaural beat tone. Stimulation period is baseline corrected. Green indicates no significant change from baseline using permutation statistics ($\alpha = .10$ with false detection rate correction for multiple comparison). X-axis is time, y-axis is frequency. Top: Darker blues indicate a decrease in frequency power while darker reds indicate and increase in frequency power from baseline. Bottom: Darker reds indicate an increase in phase-locking/inter-trial coherence (ITC) between trials at the specified frequency.

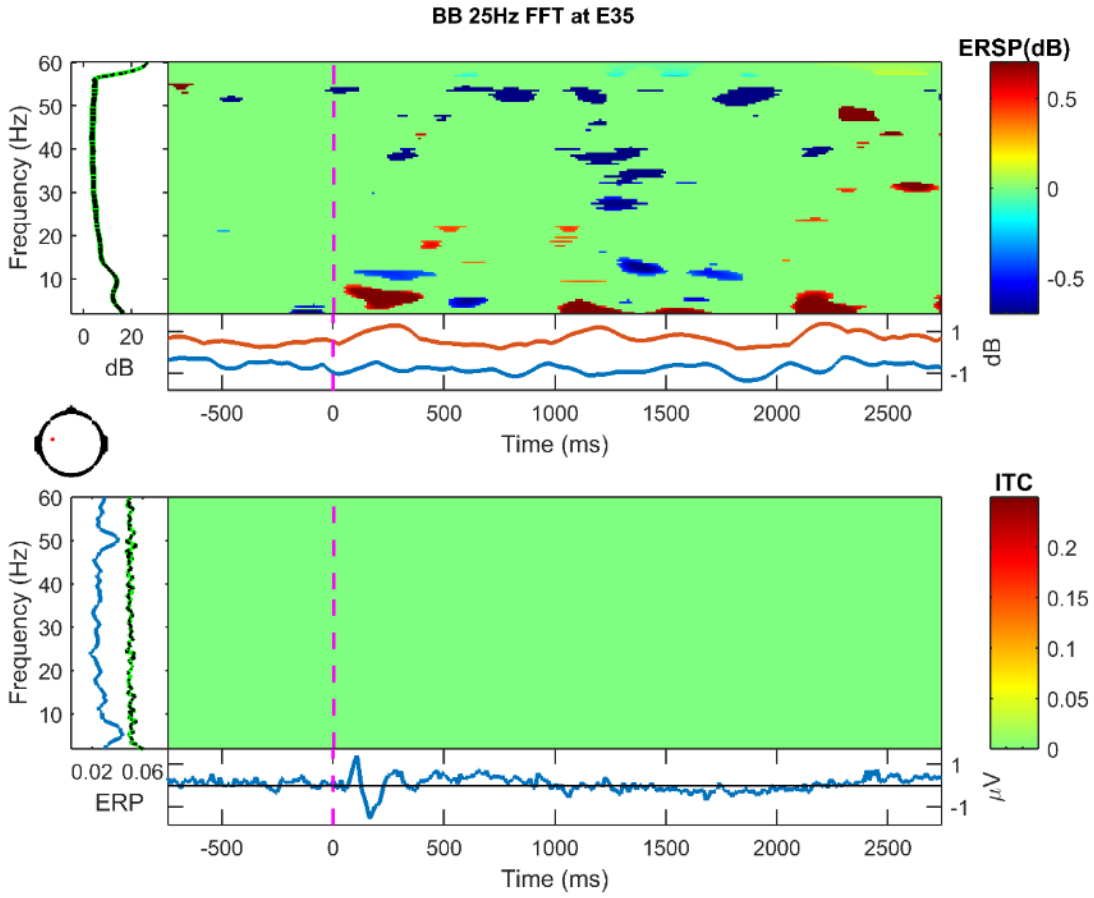

Figure 68. Frequency decomposition done with Fast Fourier Transform (FFT) for E35 (left central) from 2-60 Hz during the one second prior to stimulation and the three seconds during stimulation with 25 Hz binaural beat tone. Stimulation period is baseline corrected. Green indicates no significant change from baseline using permutation statistics ($\alpha = .10$ with false detection rate correction for multiple comparison). X-axis is time, y-axis is frequency. Top: Darker blues indicate a decrease in frequency power while darker reds indicate and increase in frequency power from baseline. Bottom: Darker reds indicate an increase in phase-locking/inter-trial coherence (ITC) between trials at the specified frequency.

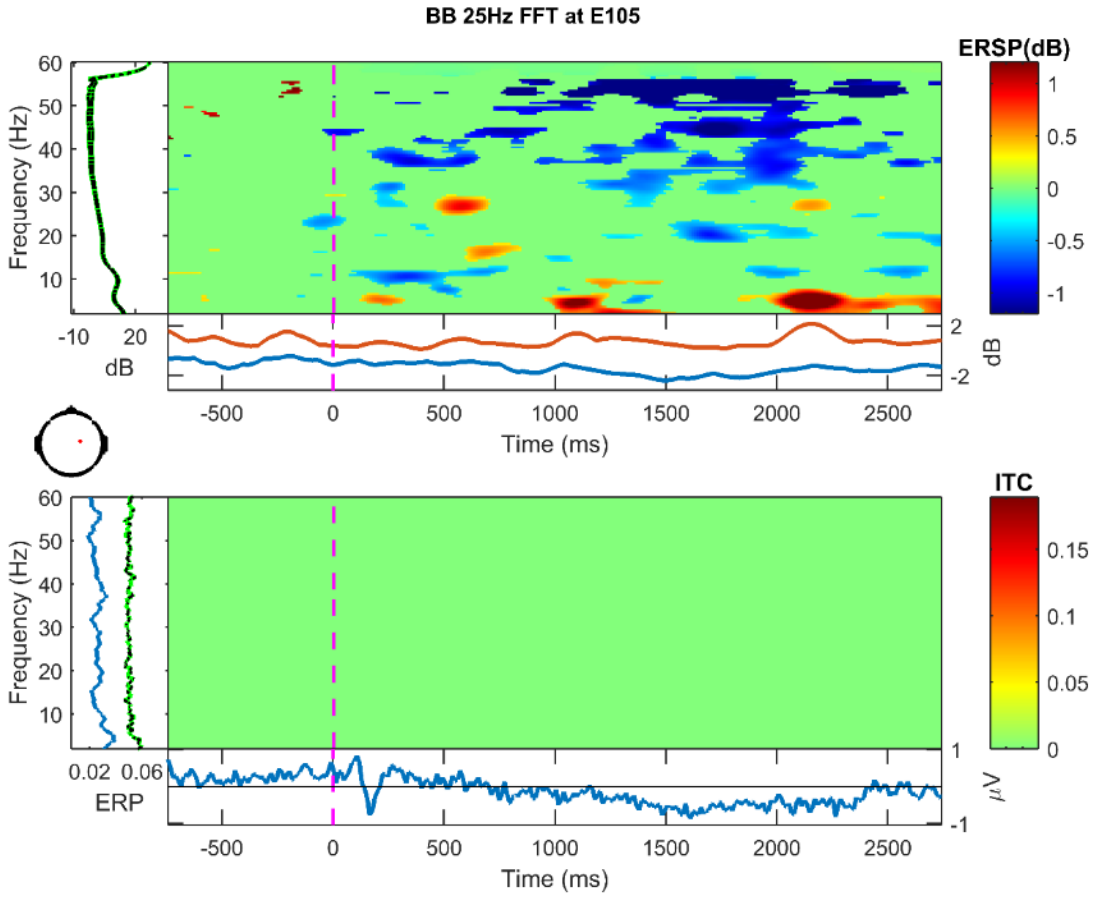

Figure 69. Frequency decomposition done with Fast Fourier Transform (FFT) for E105 (right central) from 2-60 Hz during the one second prior to stimulation and the three seconds during stimulation with 25 Hz binaural beat tone. Stimulation period is baseline corrected. Green indicates no significant change from baseline using permutation statistics (α = .10 with false detection rate correction for multiple comparison). X-axis is time, y-axis is frequency. Top: Darker blues indicate a decrease in frequency power while darker reds indicate and increase in frequency power from baseline. Bottom: Darker reds indicate an increase in phase-locking/inter-trial coherence (ITC) between trials at the specified frequency.

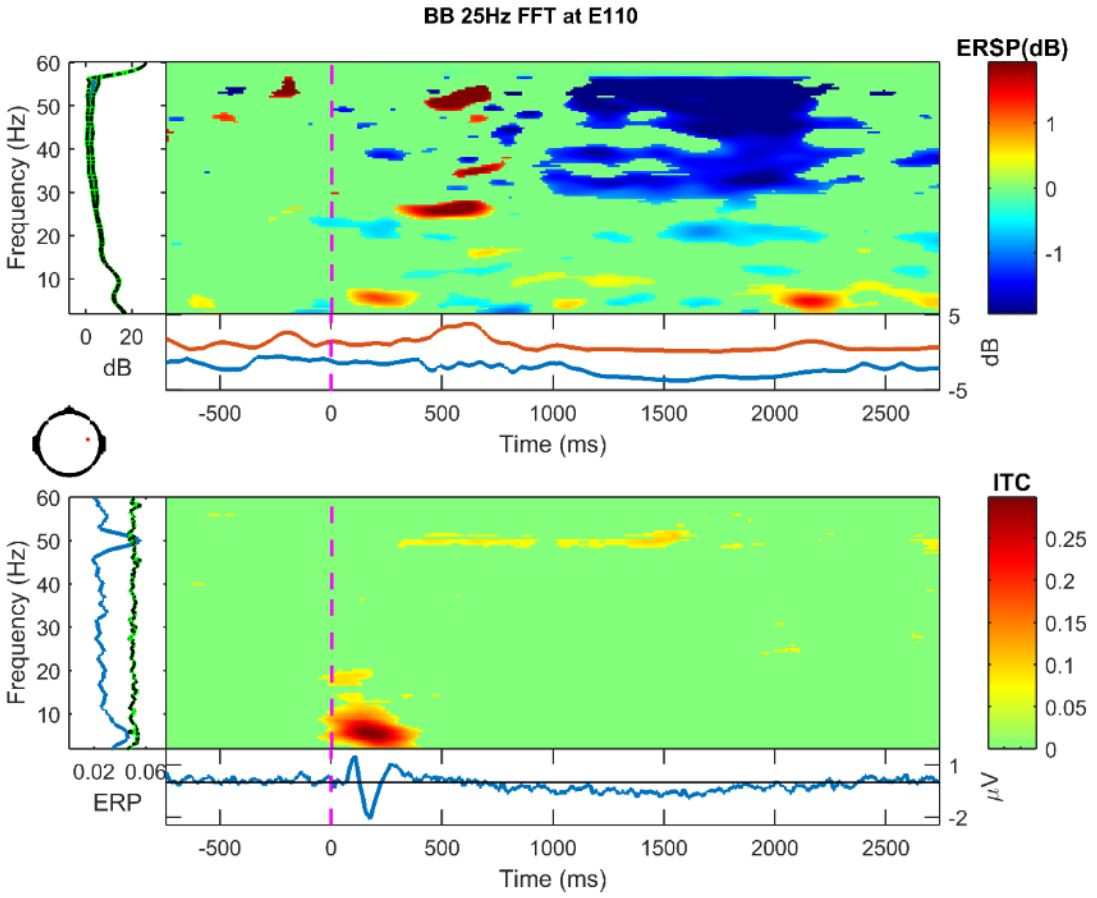

Figure 70. Frequency decomposition done with Fast Fourier Transform (FFT) for E110 (right central) from 2-60 Hz during the one second prior to stimulation and the three seconds during stimulation with 25 Hz binaural beat tone. Stimulation period is baseline corrected. Green indicates no significant change from baseline using permutation statistics (α = .10 with false detection rate correction for multiple comparison). X-axis is time, y-axis is frequency. Top: Darker blues indicate a decrease in frequency power while darker reds indicate and increase in frequency power from baseline. Bottom: Darker reds indicate an increase in phase-locking/inter-trial coherence (ITC) between trials at the specified frequency.

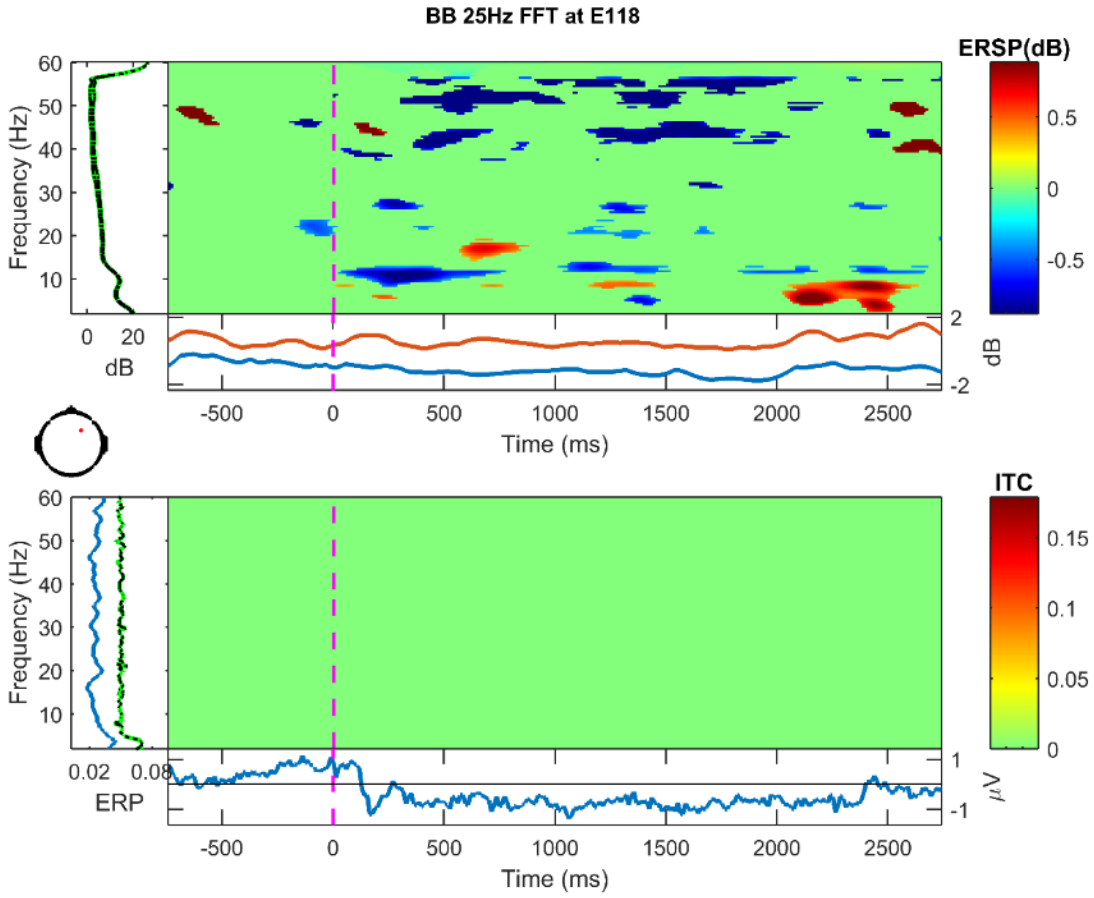

Figure 71. Frequency decomposition done with Fast Fourier Transform (FFT) for E118 (right central) from 2-60 Hz during the one second prior to stimulation and the three seconds during stimulation with 25 Hz binaural beat tone. Stimulation period is baseline corrected. Green indicates no significant change from baseline using permutation statistics (α = .10 with false detection rate correction for multiple comparison). X-axis is time, y-axis is frequency. Top: Darker blues indicate a decrease in frequency power while darker reds indicate and increase in frequency power from baseline. Bottom: Darker reds indicate an increase in phase-locking/inter-trial coherence (ITC) between trials at the specified frequency.

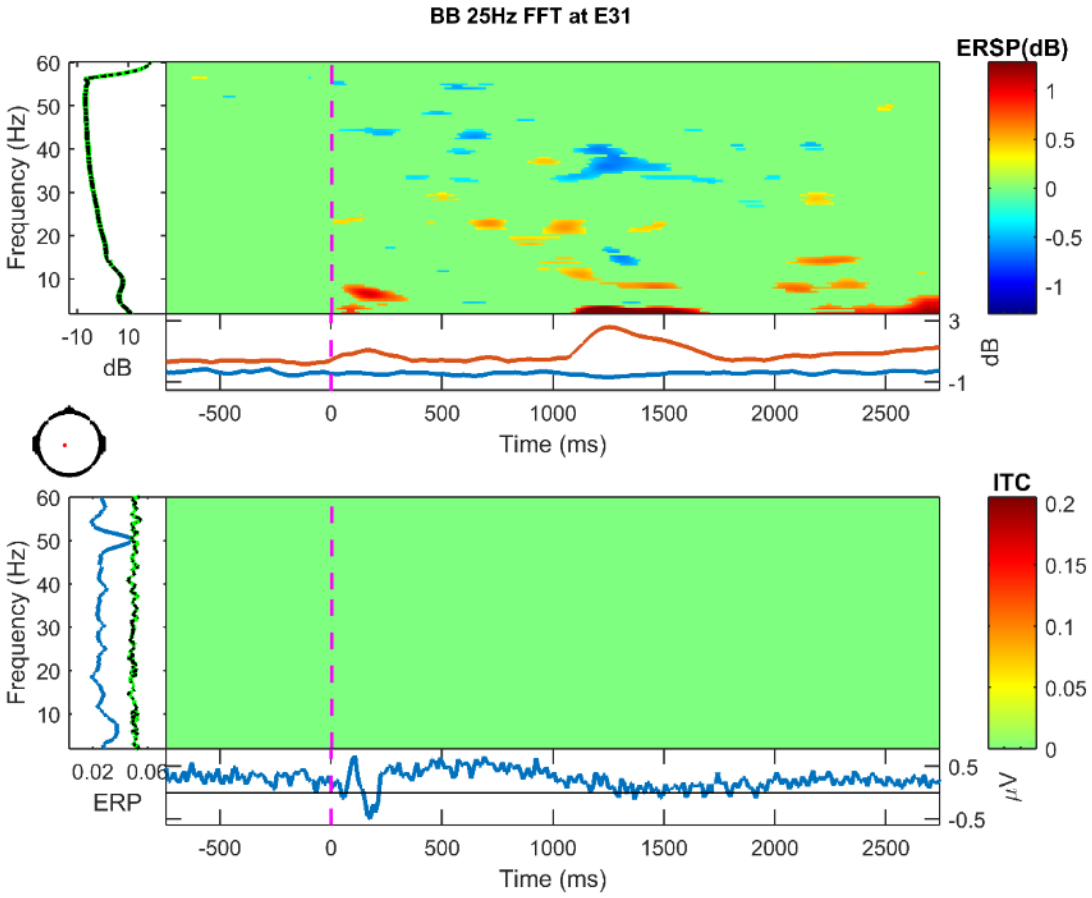

Figure 72. Frequency decomposition done with Fast Fourier Transform (FFT) for E31 (left parietal) from 2-60 Hz during the one second prior to stimulation and the three seconds during stimulation with 25 Hz binaural beat tone. Stimulation period is baseline corrected. Green indicates no significant change from baseline using permutation statistics ($\alpha = .10$ with false detection rate correction for multiple comparison). X-axis is time, y-axis is frequency. Top: Darker blues indicate a decrease in frequency power while darker reds indicate and increase in frequency power from baseline. Bottom: Darker reds indicate an increase in phase-locking/inter-trial coherence (ITC) between trials at the specified frequency.

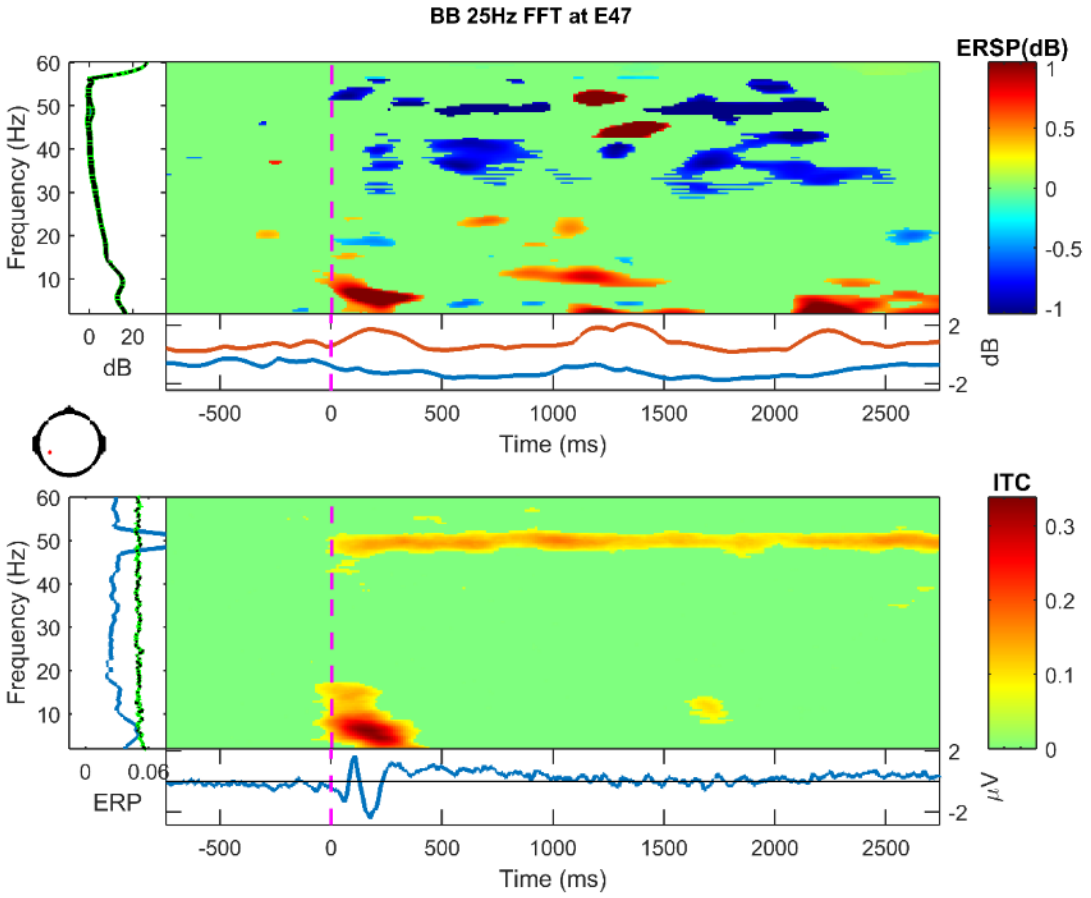

Figure 73. Frequency decomposition done with Fast Fourier Transform (FFT) for E47 (left parietal) from 2-60 Hz during the one second prior to stimulation and the three seconds during stimulation with 25 Hz binaural beat tone. Stimulation period is baseline corrected. Green indicates no significant change from baseline using permutation statistics (α = .10 with false detection rate correction for multiple comparison). X-axis is time, y-axis is frequency. Top: Darker blues indicate a decrease in frequency power while darker reds indicate and increase in frequency power from baseline. Bottom: Darker reds indicate an increase in phase-locking/inter-trial coherence (ITC) between trials at the specified frequency.

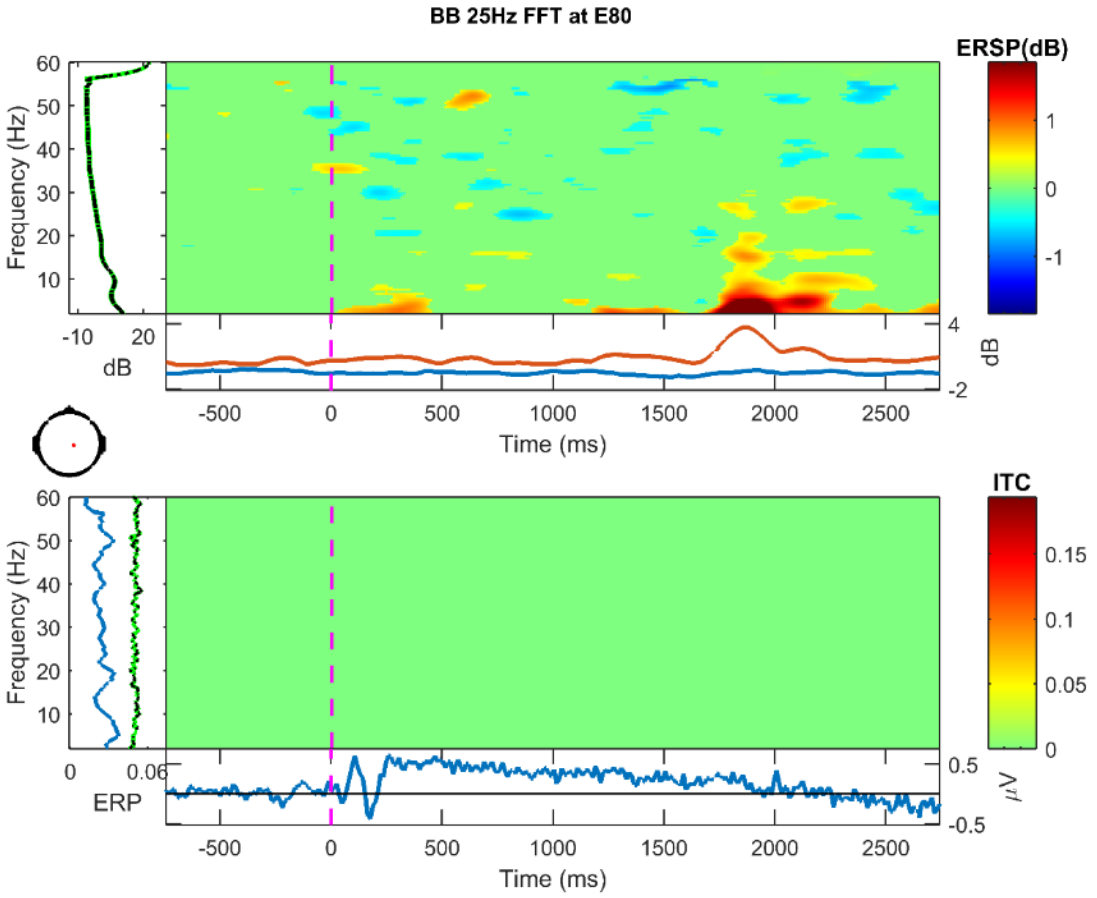

Figure 74. Frequency decomposition done with Fast Fourier Transform (FFT) for E80 (right parietal) from 2-60 Hz during the one second prior to stimulation and the three seconds during stimulation with 25 Hz binaural beat tone. Stimulation period is baseline corrected. Green indicates no significant change from baseline using permutation statistics (α = .10 with false detection rate correction for multiple comparison). X-axis is time, y-axis is frequency. Top: Darker blues indicate a decrease in frequency power while darker reds indicate and increase in frequency power from baseline. Bottom: Darker reds indicate an increase in phase-locking/inter-trial coherence (ITC) between trials at the specified frequency.

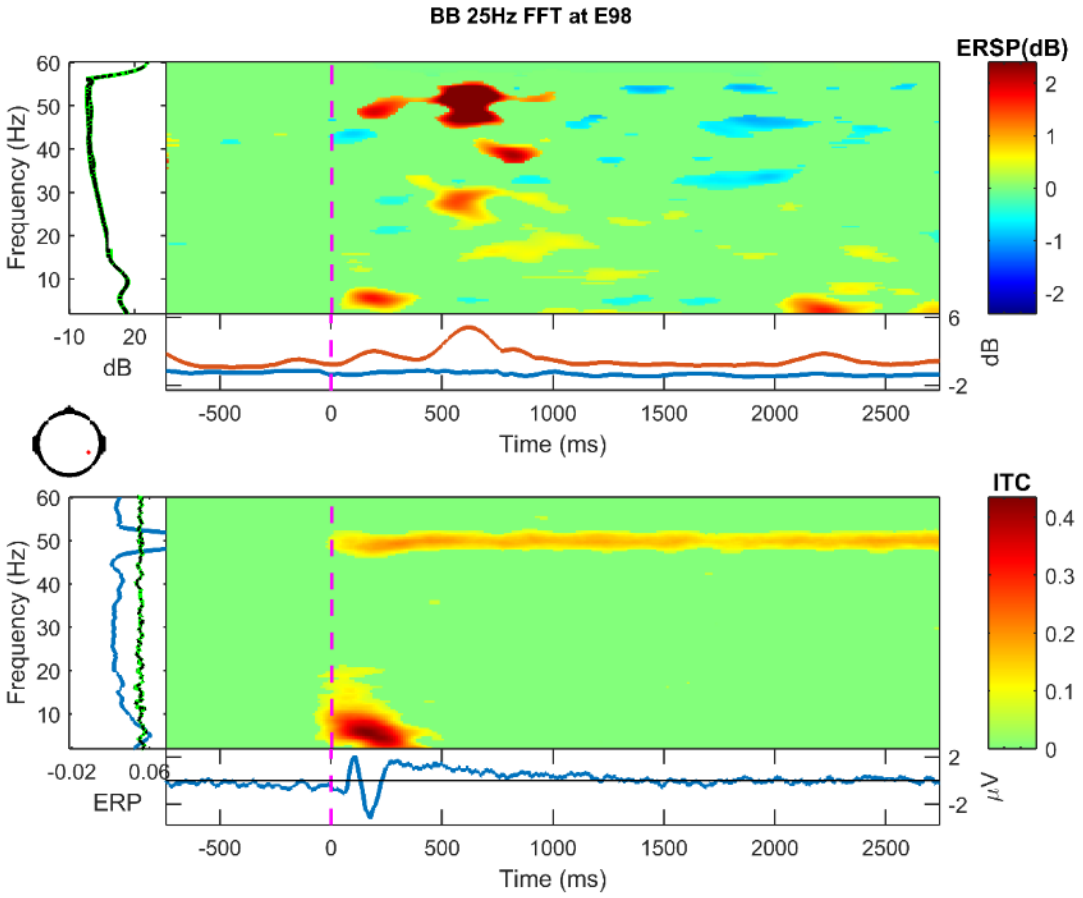

Figure 75. Frequency decomposition done with Fast Fourier Transform (FFT) for E98 (right parietal) from 2-60 Hz during the one second prior to stimulation and the three seconds during stimulation with 25 Hz binaural beat tone. Stimulation period is baseline corrected. Green indicates no significant change from baseline using permutation statistics (α = .10 with false detection rate correction for multiple comparison). X-axis is time, y-axis is frequency. Top: Darker blues indicate a decrease in frequency power while darker reds indicate and increase in frequency power from baseline. Bottom: Darker reds indicate an increase in phase-locking/inter-trial coherence (ITC) between trials at the specified frequency.

Appendix: DICS Source Analysis Images

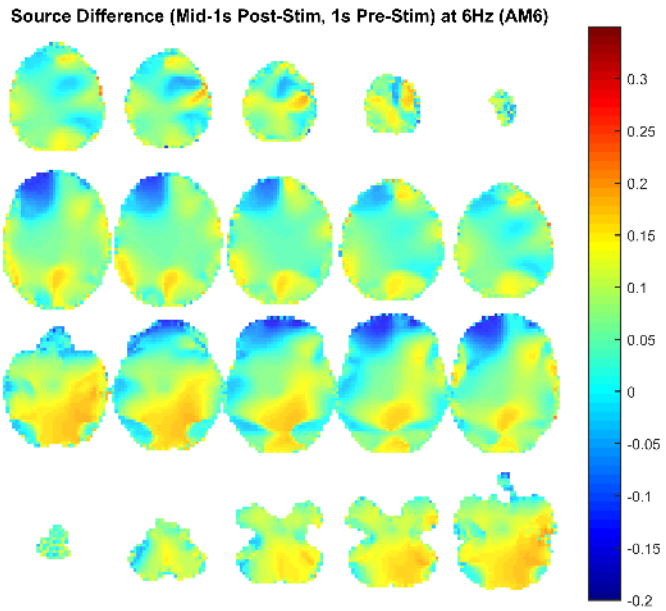

Figure 76. Average source analysis of frequency power in 6 Hz during the middle one-second of stimulation with the 6 Hz amplitude modulated tone computed with Dynamic Imaging of Coherent Sources (DICS) algorithm and standardized Boundary Element Method (BEM) head model derived from Colin 27 MRI. Stimulation period is noise-corrected via a whole-trial filter and the subtraction of the one-second pre-stimulation baseline period. Unit is the percent change in power from baseline (i.e., difference between power during stimulation and power during baseline divided by power during baseline). Darker reds indicate increases in power in the indicated area while darker blues indicate decreases in power from baseline in that area.

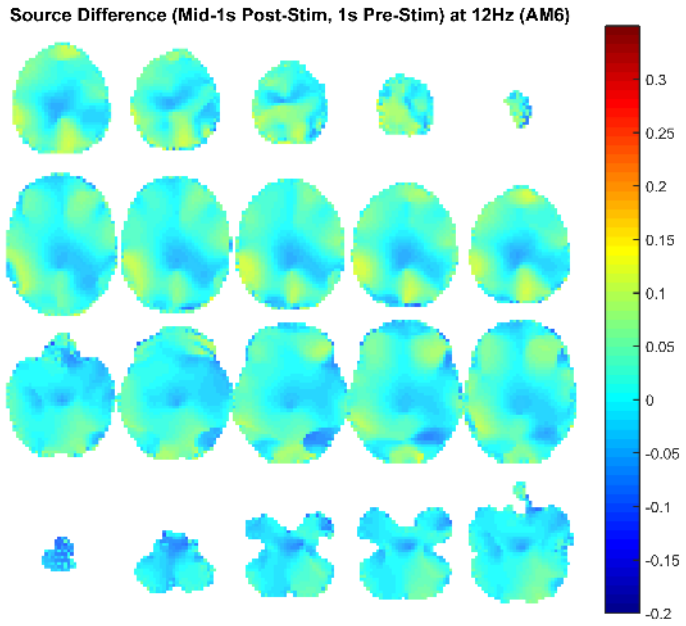

Figure 77. Average source analysis of frequency power in 12 Hz during the middle one-second of stimulation with the 6 Hz amplitude modulated tone computed with Dynamic Imaging of Coherent Sources (DICS) algorithm and standardized Boundary Element Method (BEM) head model derived from Colin 27 MRI. Stimulation period is noise-corrected via a whole-trial filter and the subtraction of the one-second pre-stimulation baseline period. Unit is the percent change in power from baseline (i.e., difference between power during stimulation and power during baseline divided by power during baseline). Darker reds indicate increases in power in the indicated area while darker blues indicate decreases in power from baseline in that area.

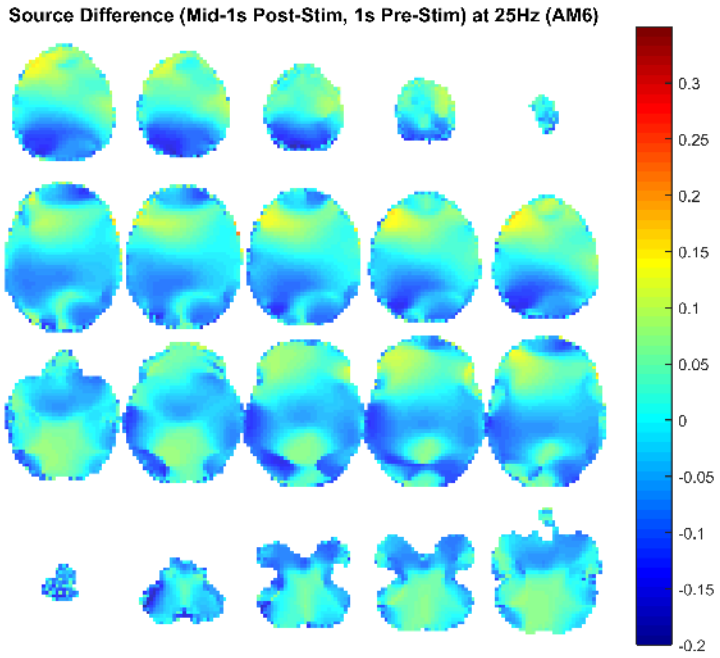

Figure 78. Average source analysis of frequency power in 25 Hz during the middle one-second of stimulation with the 6 Hz amplitude modulated tone computed with Dynamic Imaging of Coherent Sources (DICS) algorithm and standardized Boundary Element Method (BEM) head model derived from Colin 27 MRI. Stimulation period is noise-corrected via a whole-trial filter and the subtraction of the one-second pre-stimulation baseline period. Unit is the percent change in power from baseline (i.e., difference between power during stimulation and power during baseline divided by power during baseline). Darker reds indicate increases in power in the indicated area while darker blues indicate decreases in power from baseline in that area.

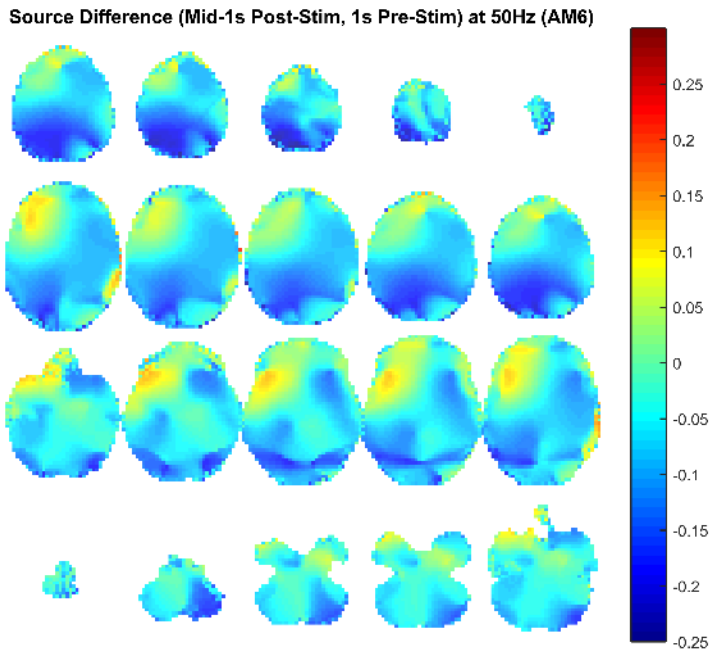

Figure 79. Average source analysis of frequency power in 50 Hz during the middle one-second of stimulation with the 6 Hz amplitude modulated tone computed with Dynamic Imaging of Coherent Sources (DICS) algorithm and standardized Boundary Element Method (BEM) head model derived from Colin 27 MRI. Stimulation period is noise-corrected via a whole-trial filter and the subtraction of the one-second pre-stimulation baseline period. Unit is the percent change in power from baseline (i.e., difference between power during stimulation and power during baseline divided by power during baseline). Darker reds indicate increases in power in the indicated area while darker blues indicate decreases in power from baseline in that area.

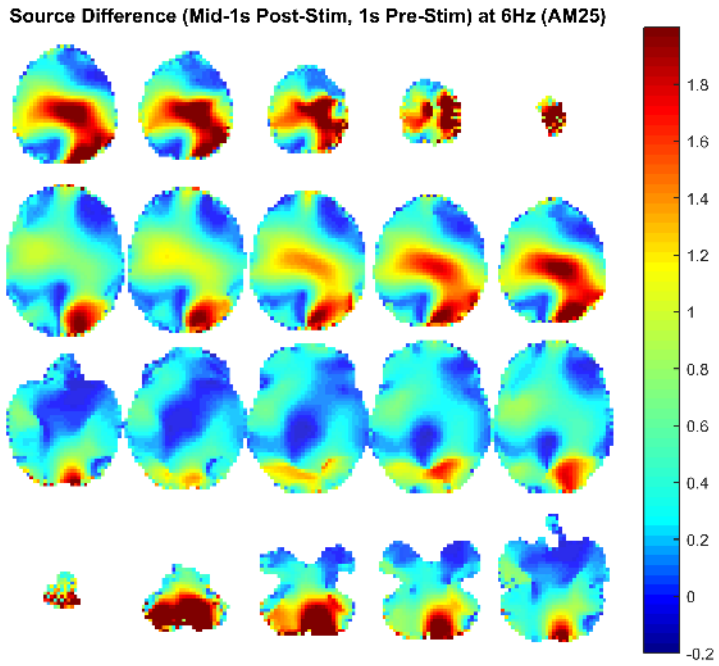

Figure 80. Average source analysis of frequency power in 6 Hz during the middle one-second of stimulation with the 25 Hz amplitude modulated tone computed with Dynamic Imaging of Coherent Sources (DICS) algorithm and standardized Boundary Element Method (BEM) head model derived from Colin 27 MRI. Stimulation period is noise-corrected via a whole-trial filter and the subtraction of the one-second pre-stimulation baseline period. Unit is the percent change in power from baseline (i.e., difference between power during stimulation and power during baseline divided by power during baseline). Darker reds indicate increases in power in the indicated area while darker blues indicate decreases in power from baseline in that area.

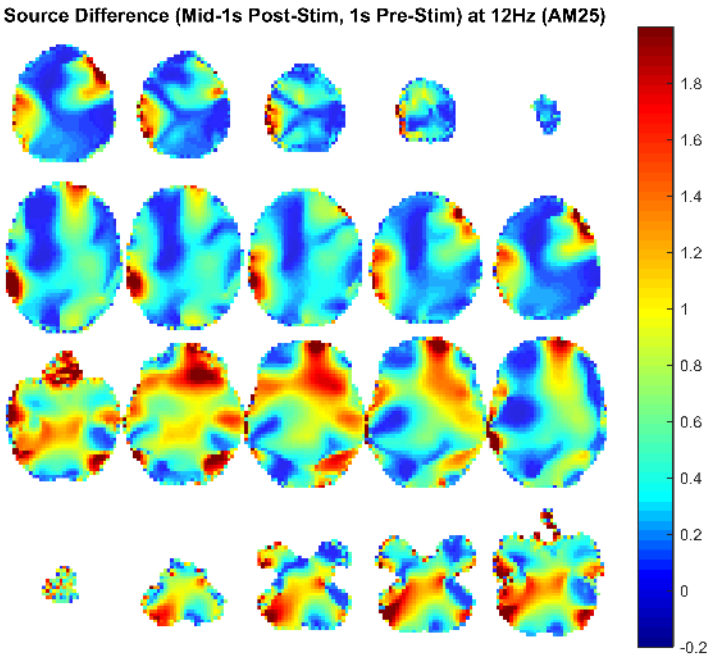

Figure 81. Average source analysis of frequency power in 12 Hz during the middle one-second of stimulation with the 25 Hz amplitude modulated tone computed with Dynamic Imaging of Coherent Sources (DICS) algorithm and standardized Boundary Element Method (BEM) head model derived from Colin 27 MRI. Stimulation period is noise-corrected via a whole-trial filter and the subtraction of the one-second pre-stimulation baseline period. Unit is the percent change in power from baseline (i.e., difference between power during stimulation and power during baseline divided by power during baseline). Darker reds indicate increases in power in the indicated area while darker blues indicate decreases in power from baseline in that area.

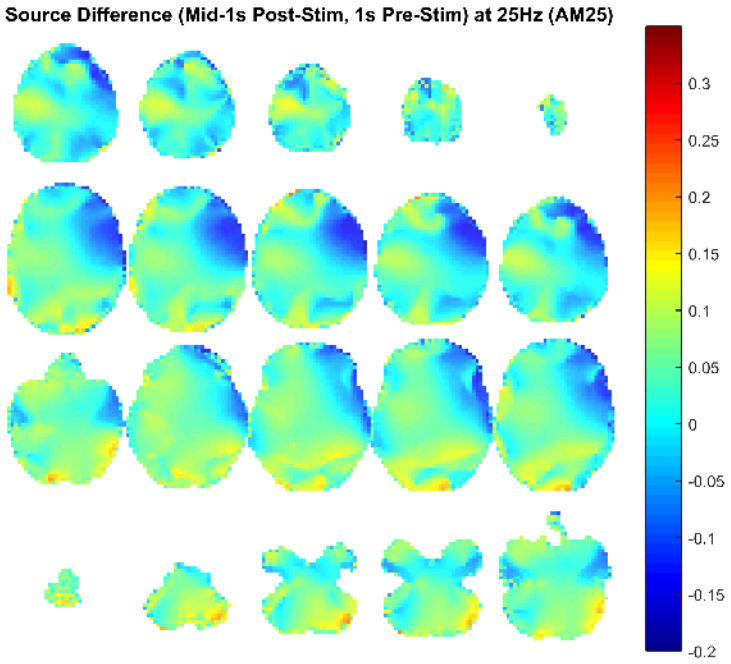

Figure 82. Average source analysis of frequency power in 25 Hz during the middle one-second of stimulation with the 25 Hz amplitude modulated tone computed with Dynamic Imaging of Coherent Sources (DICS) algorithm and standardized Boundary Element Method (BEM) head model derived from Colin 27 MRI. Stimulation period is noise-corrected via a whole-trial filter and the subtraction of the one-second pre-stimulation baseline period. Unit is the percent change in power from baseline (i.e., difference between power during stimulation and power during baseline divided by power during baseline). Darker reds indicate increases in power in the indicated area while darker blues indicate decreases in power from baseline in that area.

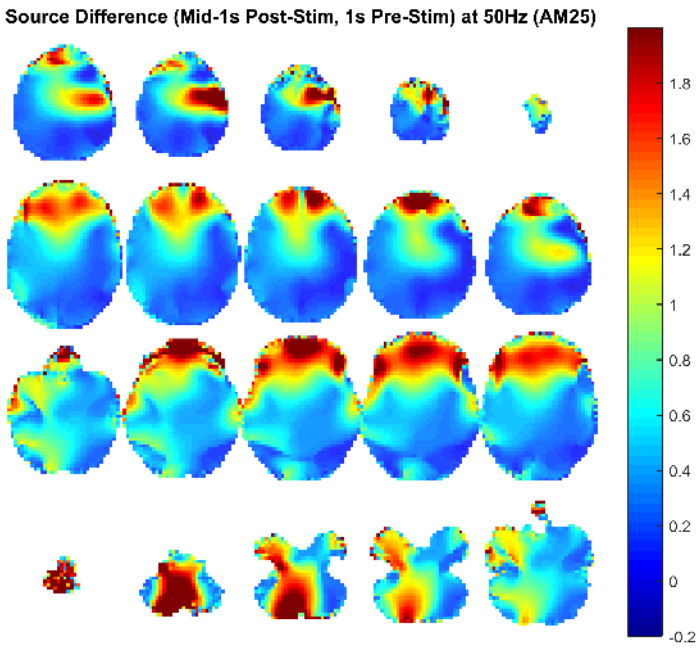

Figure 83. Average source analysis of frequency power in 50 Hz during the middle one-second of stimulation with the 25 Hz amplitude modulated tone computed with Dynamic Imaging of Coherent Sources (DICS) algorithm and standardized Boundary Element Method (BEM) head model derived from Colin 27 MRI. Stimulation period is noise-corrected via a whole-trial filter and the subtraction of the one-second pre-stimulation baseline period. Unit is the percent change in power from baseline (i.e., difference between power during stimulation and power during baseline divided by power during baseline). Darker reds indicate increases in power in the indicated area while darker blues indicate decreases in power from baseline in that area.

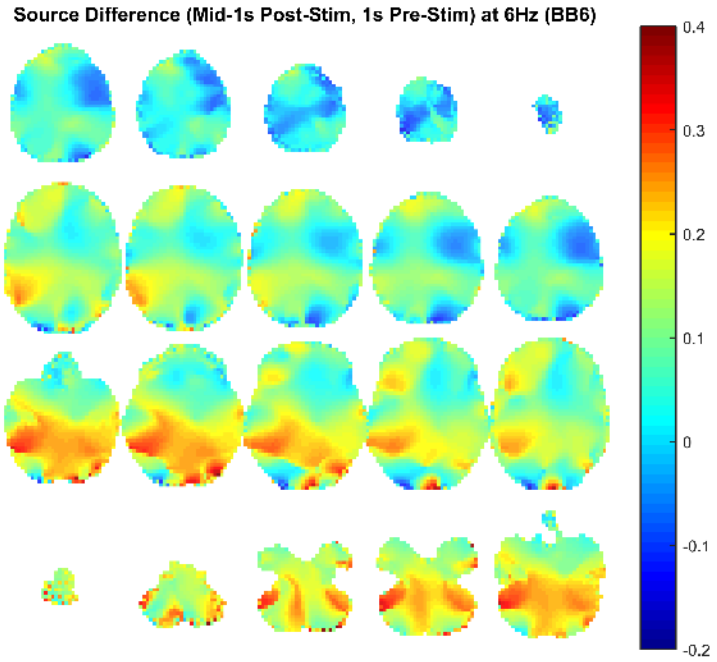

Figure 84. Average source analysis of frequency power in 6 Hz during the middle one-second of stimulation with the 6 Hz binaural beat tone computed with Dynamic Imaging of Coherent Sources (DICS) algorithm and standardized Boundary Element Method (BEM) head model derived from Colin 27 MRI. Stimulation period is noise-corrected via a whole-trial filter and the subtraction of the one-second pre-stimulation baseline period. Unit is the percent change in power from baseline (i.e., difference between power during stimulation and power during baseline divided by power during baseline). Darker reds indicate increases in power in the indicated area while darker blues indicate decreases in power from baseline in that area.

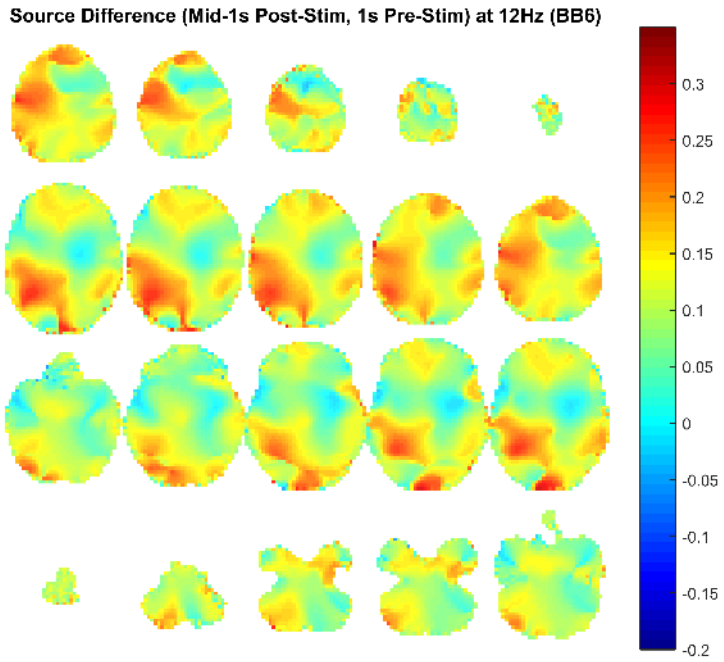

Figure 85. Average source analysis of frequency power in 12 Hz during the middle one-second of stimulation with the 6 Hz binaural beat tone computed with Dynamic Imaging of Coherent Sources (DICS) algorithm and standardized Boundary Element Method (BEM) head model derived from Colin 27 MRI. Stimulation period is noise-corrected via a whole-trial filter and the subtraction of the one-second pre-stimulation baseline period. Unit is the percent change in power from baseline (i.e., difference between power during stimulation and power during baseline divided by power during baseline). Darker reds indicate increases in power in the indicated area while darker blues indicate decreases in power from baseline in that area.

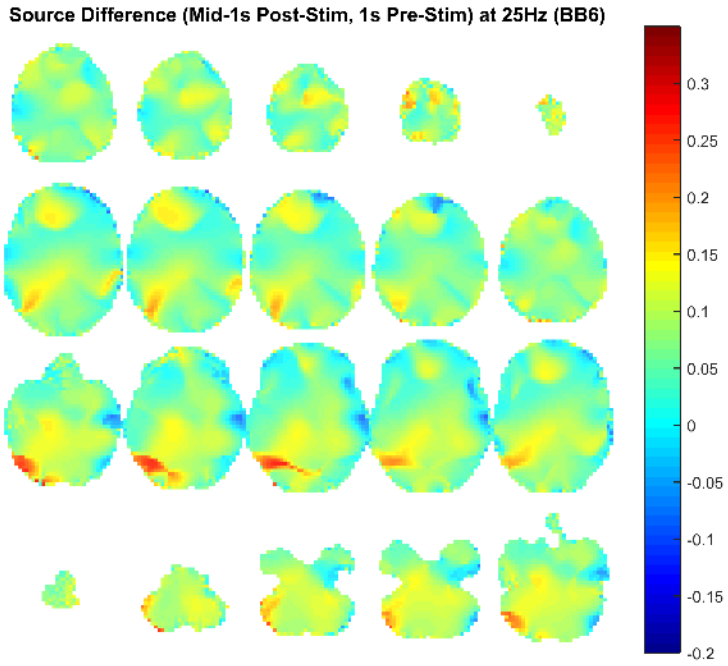

Figure 86. Average source analysis of frequency power in 25 Hz during the middle one-second of stimulation with the 6 Hz binaural beat tone computed with Dynamic Imaging of Coherent Sources (DICS) algorithm and standardized Boundary Element Method (BEM) head model derived from Colin 27 MRI. Stimulation period is noise-corrected via a whole-trial filter and the subtraction of the one-second pre-stimulation baseline period. Unit is the percent change in power from baseline (i.e., difference between power during stimulation and power during baseline divided by power during baseline). Darker reds indicate increases in power in the indicated area while darker blues indicate decreases in power from baseline in that area.

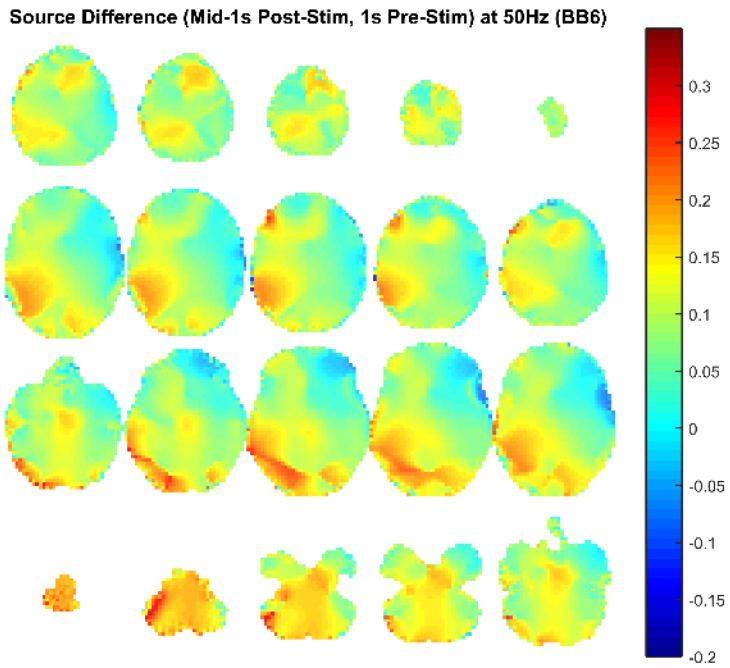

Figure 87. Average source analysis of frequency power in 50 Hz during the middle one-second of stimulation with the 6 Hz binaural beat tone computed with Dynamic Imaging of Coherent Sources (DICS) algorithm and standardized Boundary Element Method (BEM) head model derived from Colin 27 MRI. Stimulation period is noise-corrected via a whole-trial filter and the subtraction of the one-second pre-stimulation baseline period. Unit is the percent change in power from baseline (i.e., difference between power during stimulation and power during baseline divided by power during baseline). Darker reds indicate increases in power in the indicated area while darker blues indicate decreases in power from baseline in that area.

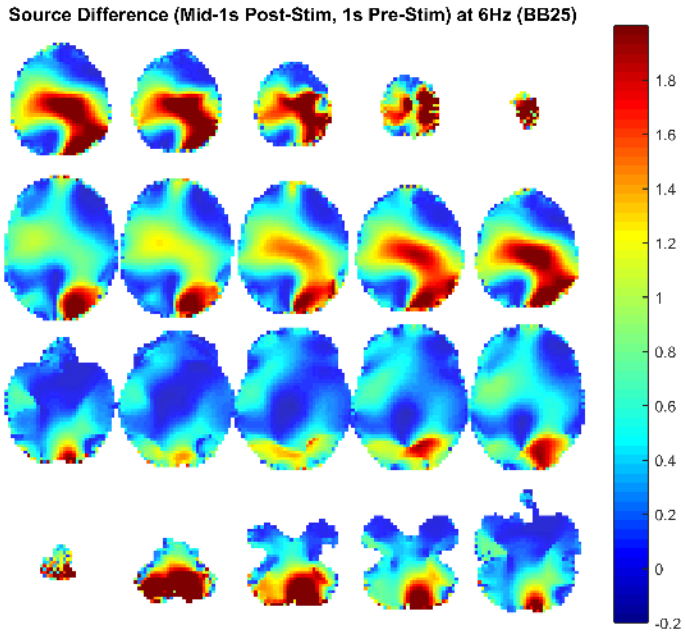

Figure 88. Average source analysis of frequency power in 6 Hz during the middle one-second of stimulation with the 25 Hz binaural beat tone computed with Dynamic Imaging of Coherent Sources (DICS) algorithm and standardized Boundary Element Method (BEM) head model derived from Colin 27 MRI. Stimulation period is noise-corrected via a whole-trial filter and the subtraction of the one-second pre-stimulation baseline period. Unit is the percent change in power from baseline (i.e., difference between power during stimulation and power during baseline divided by power during baseline). Darker reds indicate increases in power in the indicated area while darker blues indicate decreases in power from baseline in that area.

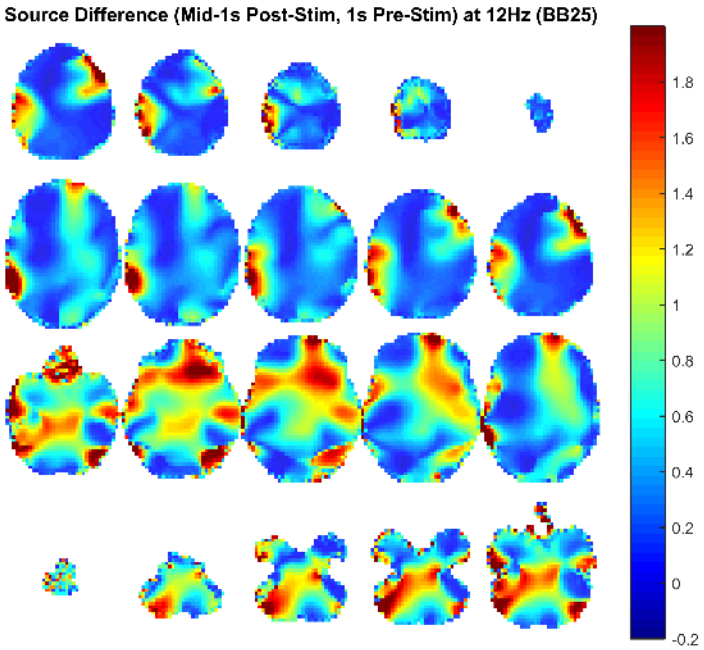

Figure 89. Average source analysis of frequency power in 12 Hz during the middle one-second of stimulation with the 25 Hz binaural beat tone computed with Dynamic Imaging of Coherent Sources (DICS) algorithm and standardized Boundary Element Method (BEM) head model derived from Colin 27 MRI. Stimulation period is noise-corrected via a whole-trial filter and the subtraction of the one-second pre-stimulation baseline period. Unit is the percent change in power from baseline (i.e., difference between power during stimulation and power during baseline divided by power during baseline). Darker reds indicate increases in power in the indicated area while darker blues indicate decreases in power from baseline in that area.

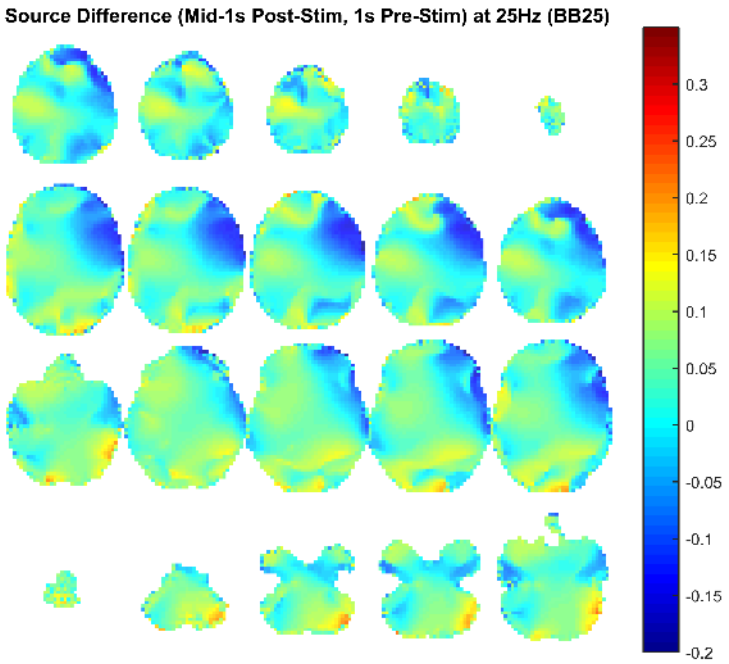

Figure 90. Average source analysis of frequency power in 25 Hz during the middle one-second of stimulation with the 25 Hz binaural beat tone computed with Dynamic Imaging of Coherent Sources (DICS) algorithm and standardized Boundary Element Method (BEM) head model derived from Colin 27 MRI. Stimulation period is noise-corrected via a whole-trial filter and the subtraction of the one-second pre-stimulation baseline period. Unit is the percent change in power from baseline (i.e., difference between power during stimulation and power during baseline divided by power during baseline). Darker reds indicate increases in power in the indicated area while darker blues indicate decreases in power from baseline in that area.

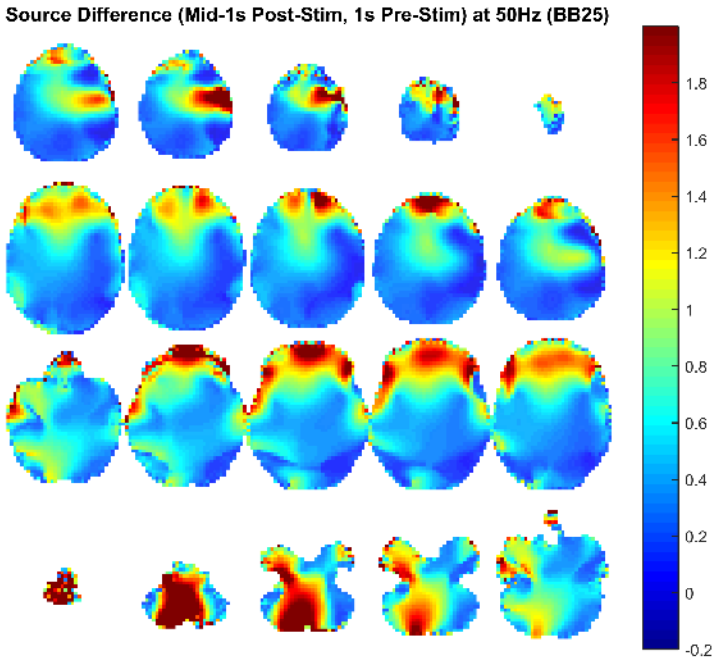

Figure 91. Average source analysis of frequency power in 50 Hz during the middle one-second of stimulation with the 25 Hz binaural beat tone computed with Dynamic Imaging of Coherent Sources (DICS) algorithm and standardized Boundary Element Method (BEM) head model derived from Colin 27 MRI. Stimulation period is noise-corrected via a whole-trial filter and the subtraction of the one-second pre-stimulation baseline period. Unit is the percent change in power from baseline (i.e., difference between power during stimulation and power during baseline divided by power during baseline). Darker reds indicate increases in power in the indicated area while darker blues indicate decreases in power from baseline in that area.

Appendix: DICS Connectivity Images

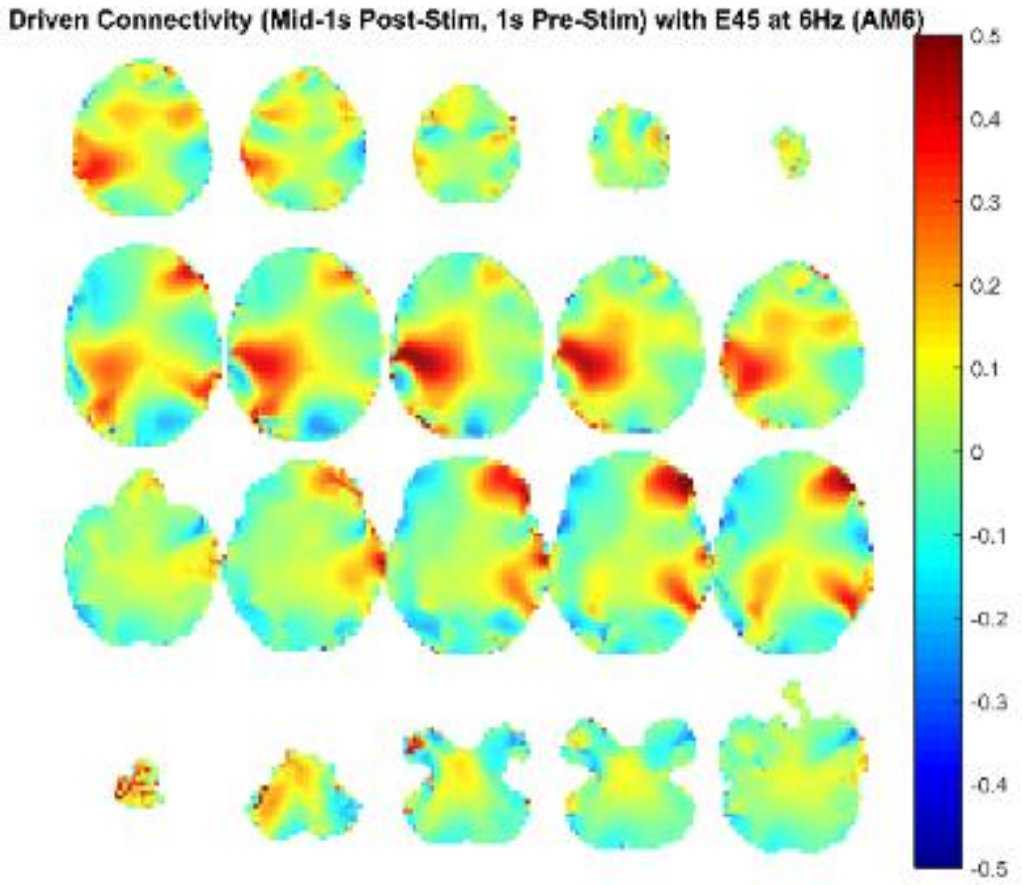

Figure 92. Source level connectivity with a dipole at E45 (left temporal, auditory cortex) in 6 Hz during the middle one-second of 6 Hz amplitude modulated tone stimulation (total stimulation was 3 seconds), performed with DICS and a standardized BEM headmodel. Unit is the percent change in coherence from baseline (i.e., difference between coherence during stimulation and coherence during baseline divided by coherence during baseline). Darker reds indicate increases in coherence with E45 while darker blues indicate decreases in coherence.

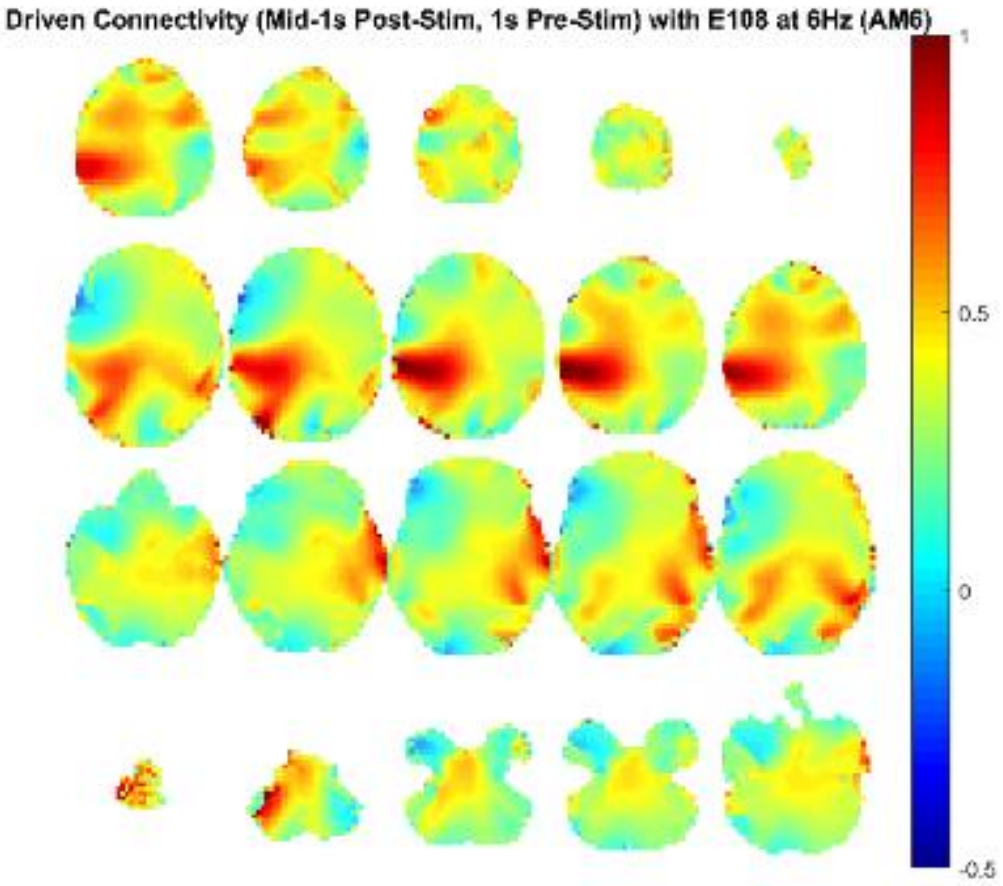

Figure 93. Source level connectivity with a dipole at E108 (right temporal, auditory cortex) in 6 Hz during the middle one-second of 6 Hz amplitude modulated tone stimulation (total stimulation was 3 seconds), performed with DICS and a standardized BEM headmodel. Unit is the percent change in coherence from baseline (i.e., difference between coherence during stimulation and coherence during baseline divided by coherence during baseline). Darker reds indicate increases in coherence with E45 while darker blues indicate decreases in coherence.

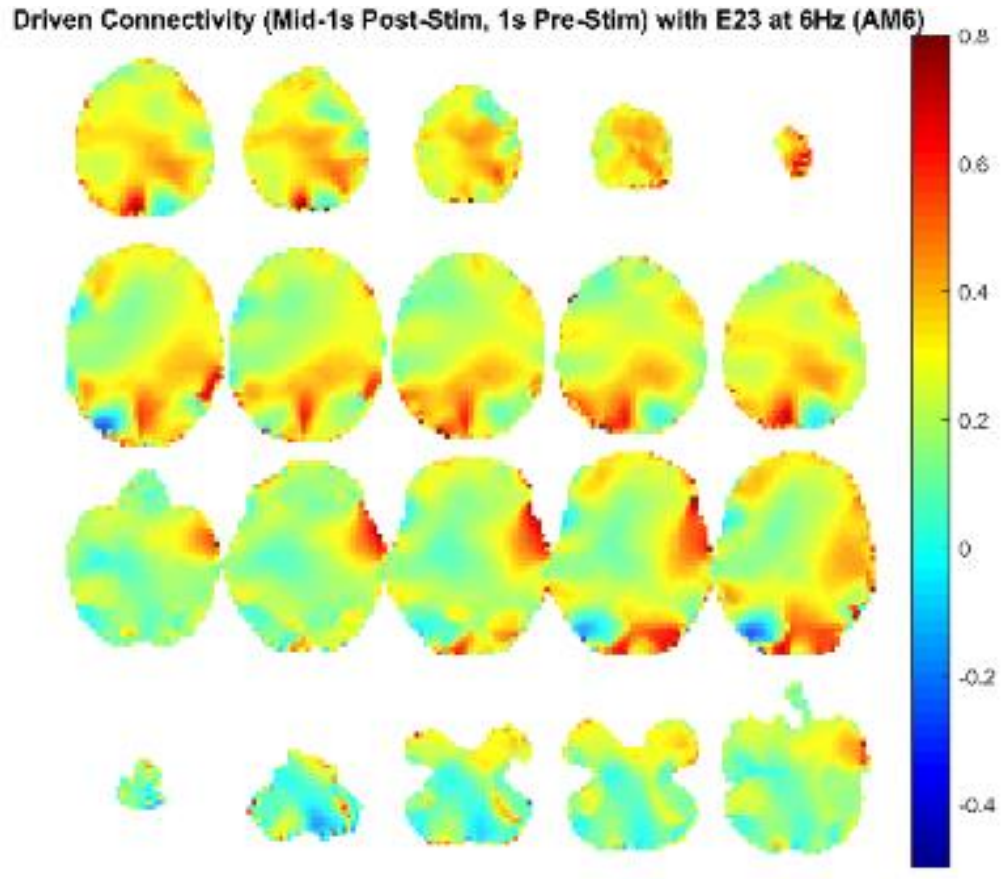

Figure 94. Source level connectivity with a dipole at E23 (left frontal) in 6 Hz during the middle one-second of 6 Hz amplitude modulated tone stimulation (total stimulation was 3 seconds), performed with DICS and a standardized BEM headmodel. Unit is the percent change in coherence from baseline (i.e., difference between coherence during stimulation and coherence during baseline divided by coherence during baseline). Darker reds indicate increases in coherence with E45 while darker blues indicate decreases in coherence.

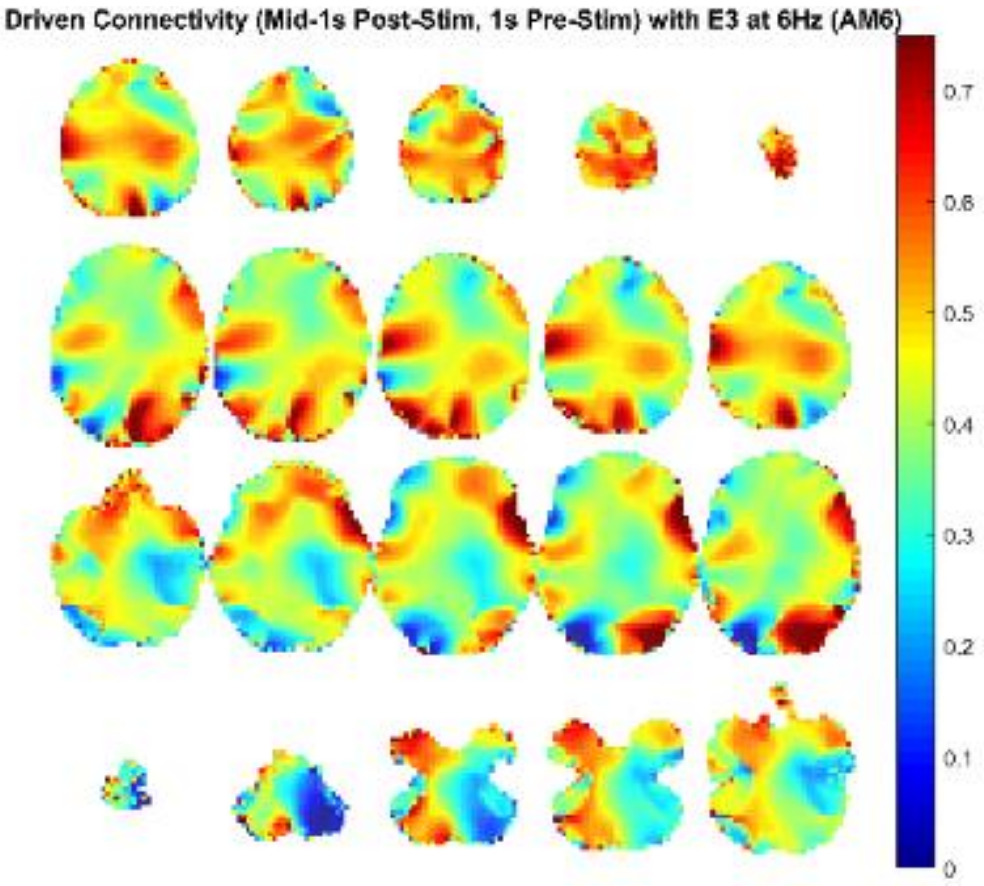

Figure 95. Source level connectivity with a dipole at E3 (right frontal) in 6 Hz during the middle one-second of 6 Hz amplitude modulated tone stimulation (total stimulation was 3 seconds), performed with DICS and a standardized BEM headmodel. Unit is the percent change in coherence from baseline (i.e., difference between coherence during stimulation and coherence during baseline divided by coherence during baseline). Darker reds indicate increases in coherence with E45 while darker blues indicate decreases in coherence.

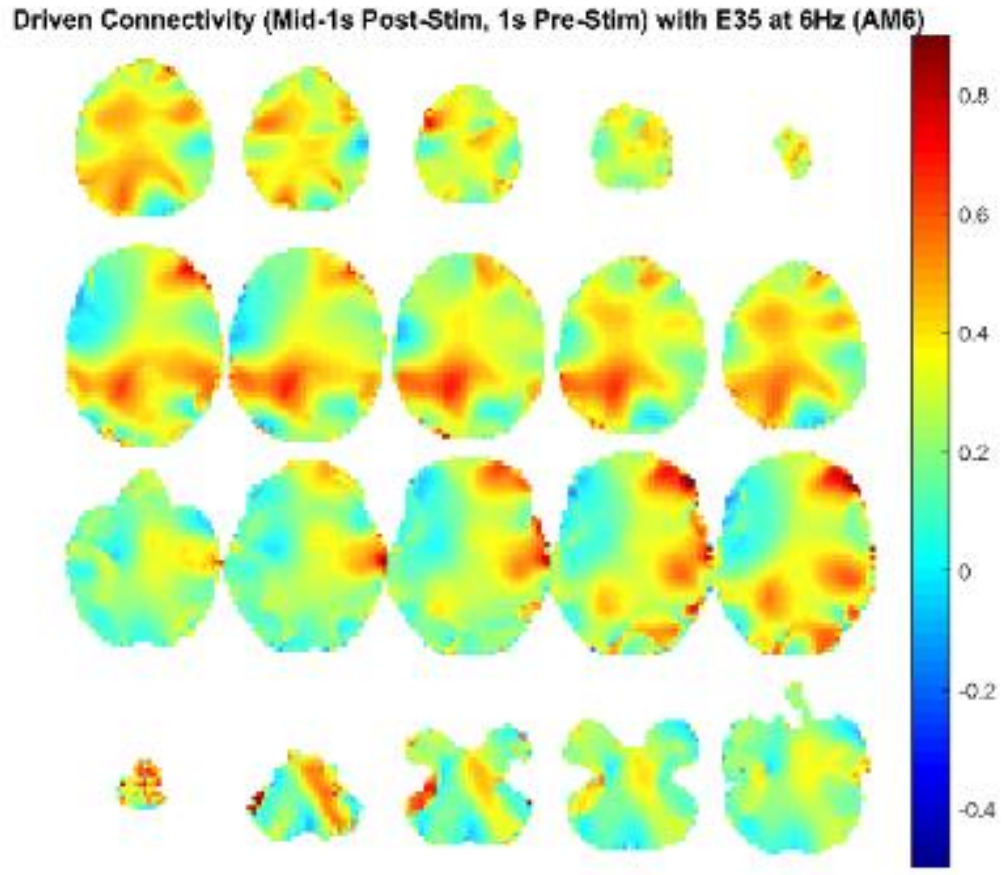

Figure 96. Source level connectivity with a dipole at E35 (left central) in 6 Hz during the middle one-second of 6 Hz amplitude modulated tone stimulation (total stimulation was 3 seconds), performed with DICS and a standardized BEM headmodel. Unit is the percent change in coherence from baseline (i.e., difference between coherence during stimulation and coherence during baseline divided by coherence during baseline). Darker reds indicate increases in coherence with E45 while darker blues indicate decreases in coherence.

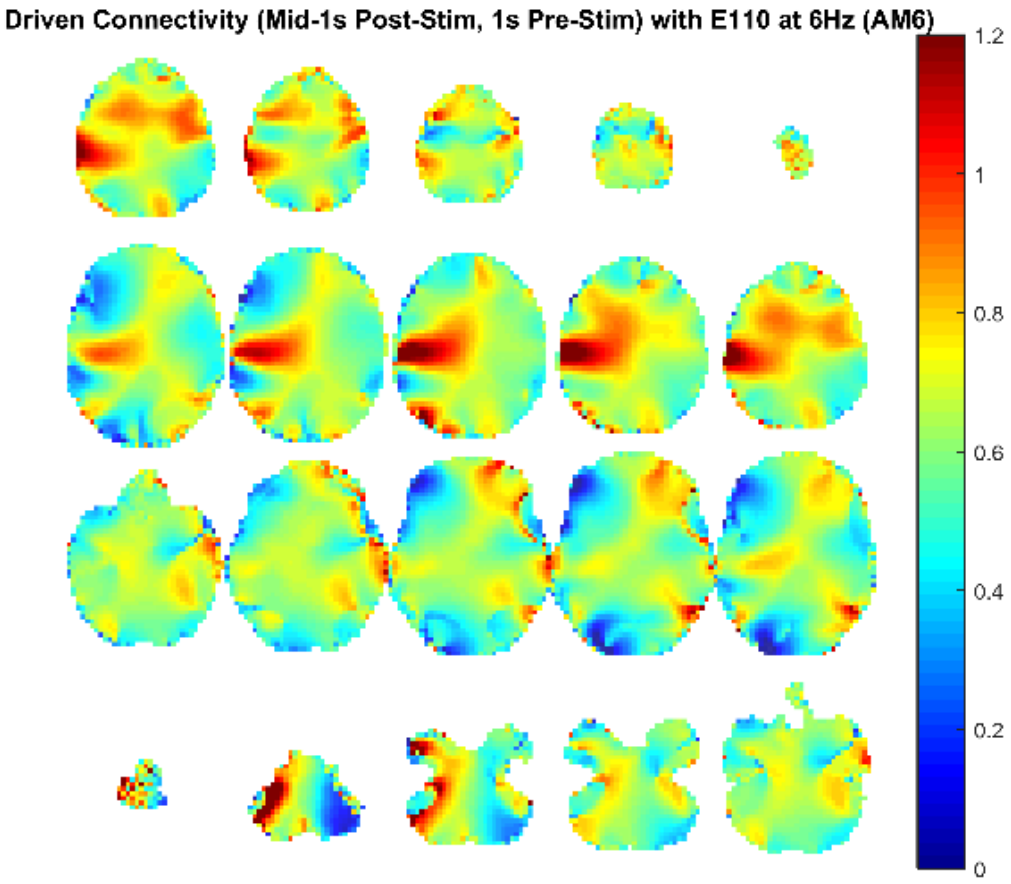

Figure 97. Source level connectivity with a dipole at E110 (right central) in 6 Hz during the middle one-second of 6 Hz amplitude modulated tone stimulation (total stimulation was 3 seconds), performed with DICS and a standardized BEM headmodel. Unit is the percent change in coherence from baseline (i.e., difference between coherence during stimulation and coherence during baseline divided by coherence during baseline). Darker reds indicate increases in coherence with E45 while darker blues indicate decreases in coherence.

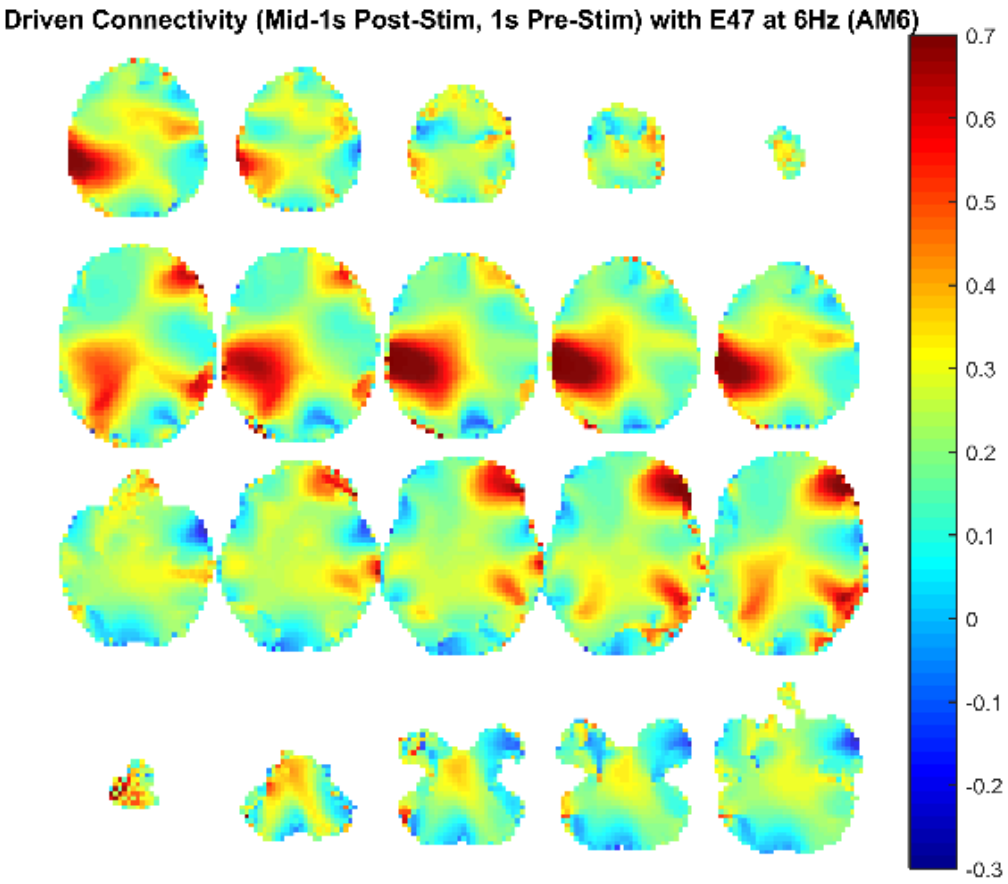

Figure 98. Source level connectivity with a dipole at E47 (left parietal) in 6 Hz during the middle one-second of 6 Hz amplitude modulated tone stimulation (total stimulation was 3 seconds), performed with DICS and a standardized BEM. Unit is the percent change in coherence from baseline (i.e., difference between coherence during stimulation and coherence during baseline divided by coherence during baseline). Darker reds indicate increases in coherence with E45 while darker blues indicate decreases in coherence.

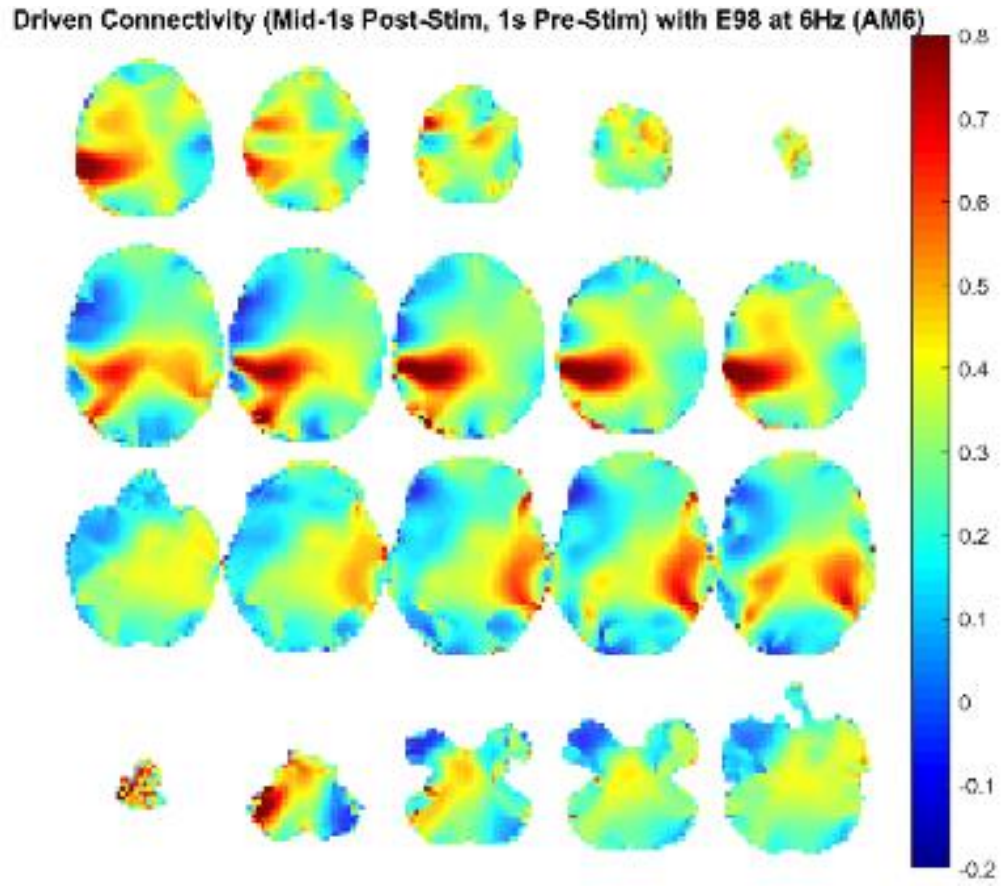

Figure 99. Source level connectivity with a dipole at E98 (right parietal) in 6 Hz during the middle one-second of 6 Hz amplitude modulated tone stimulation (total stimulation was 3 seconds), performed with DICS and a standardized BEM headmodel. Unit is the percent change in coherence from baseline (i.e., difference between coherence during stimulation and coherence during baseline divided by coherence during baseline). Darker reds indicate increases in coherence with E45 while darker blues indicate decreases in coherence.

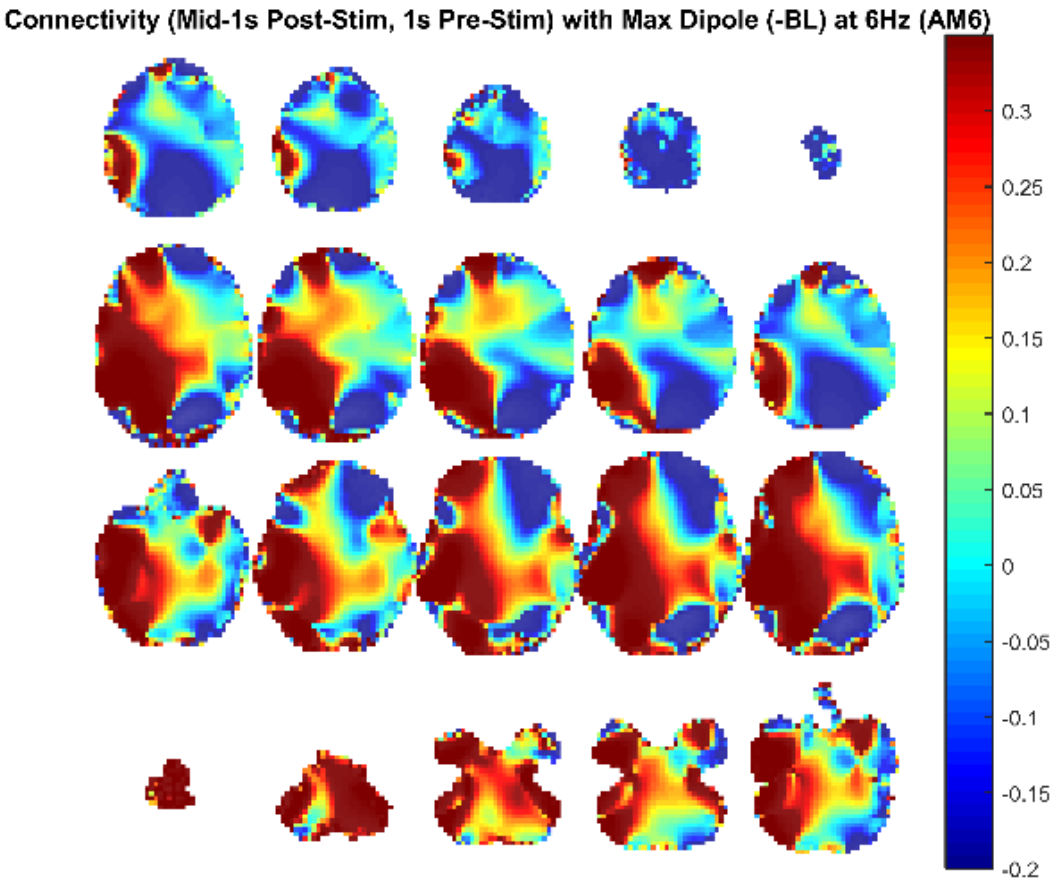

Figure 100. Source level connectivity with a dipole at dip2 (maximum power dipole for the middle one-second period corrected for the baseline one-second period) in 6 Hz during the middle one-second of 6 Hz amplitude modulated tone stimulation (total stimulation was 3 seconds), performed with DICS and a standardized BEM headmodel. Unit is the percent change in coherence from baseline (i.e., difference between coherence during stimulation and coherence during baseline divided by coherence during baseline). Darker reds indicate increases in coherence with E45 while darker blues indicate decreases in coherence.

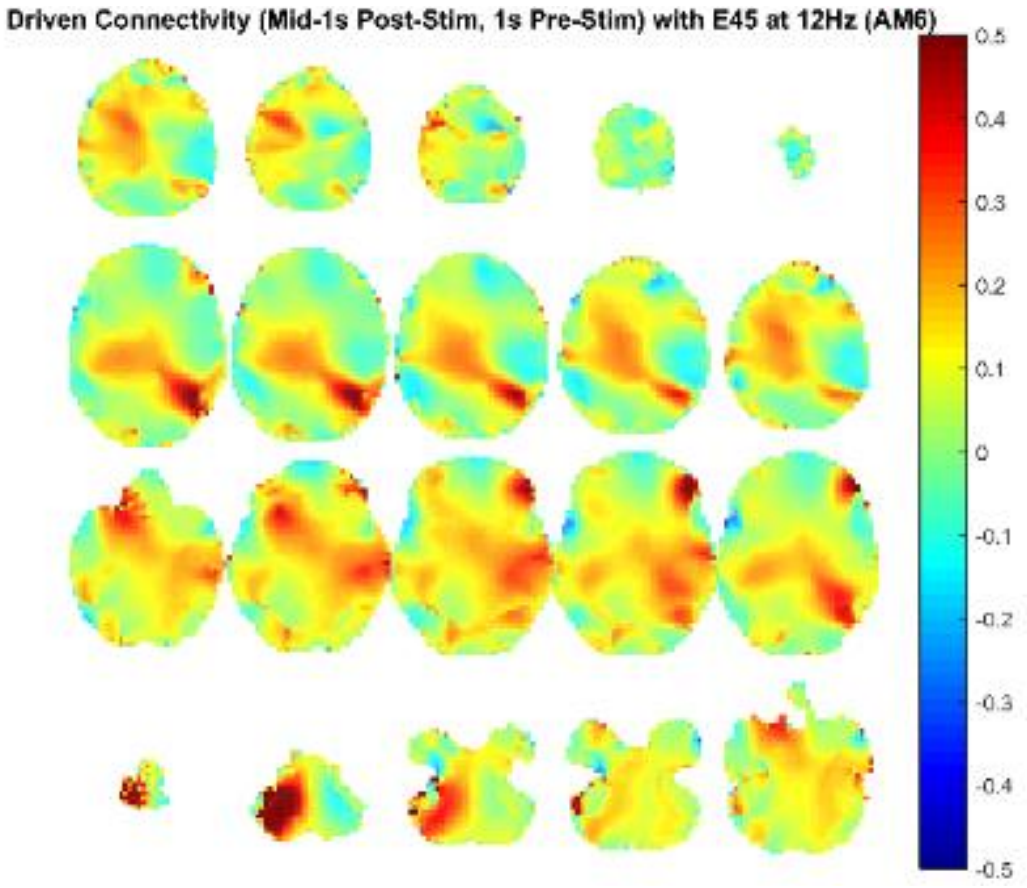

Figure 101. Source level connectivity with a dipole at E45 (left temporal, auditory cortex) in 12 Hz during the middle one-second of 6 Hz amplitude modulated tone stimulation (total stimulation was 3 seconds), performed with DICS and a standardized BEM headmodel. Unit is the percent change in coherence from baseline (i.e., difference between coherence during stimulation and coherence during baseline divided by coherence during baseline). Darker reds indicate increases in coherence with E45 while darker blues indicate decreases in coherence.

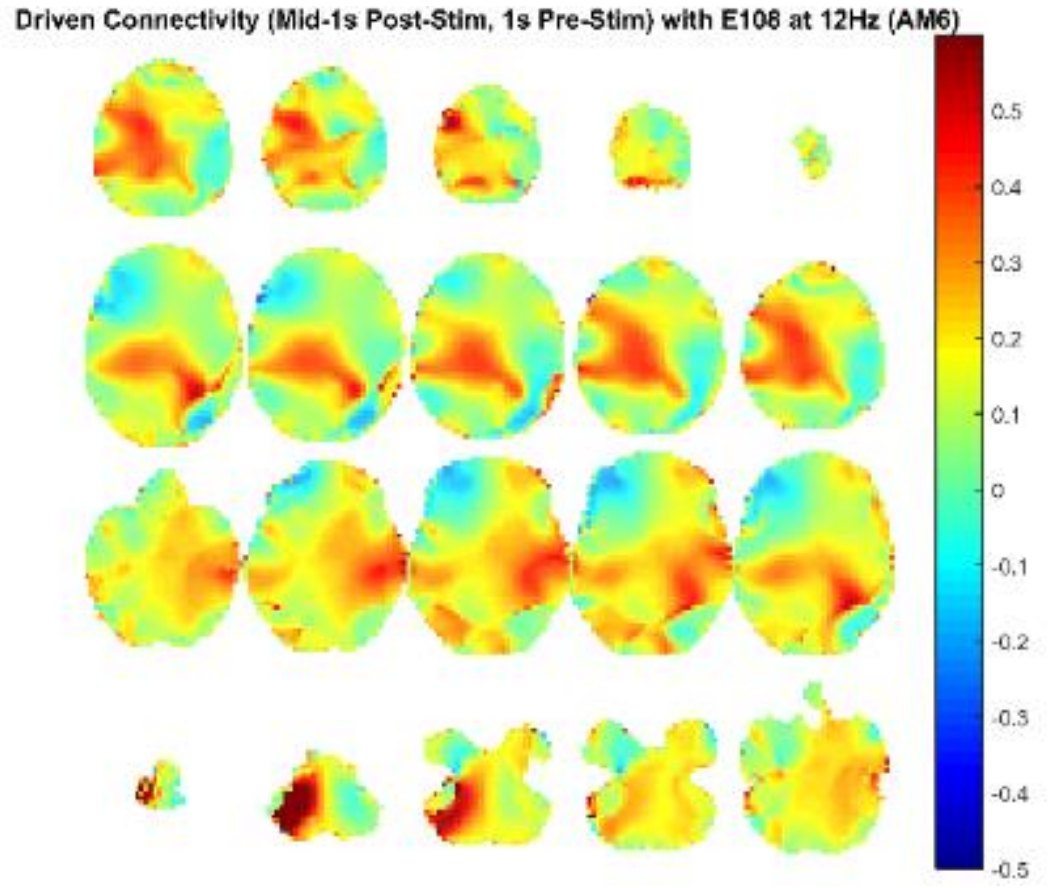

Figure 102. Source level connectivity with a dipole at E108 (right temporal, auditory cortex) in 12 Hz during the middle one-second of 6 Hz amplitude modulated tone stimulation (total stimulation was 3 seconds), performed with DICS and a standardized BEM headmodel. Unit is the percent change in coherence from baseline (i.e., difference between coherence during stimulation and coherence during baseline divided by coherence during baseline). Darker reds indicate increases in coherence with E45 while darker blues indicate decreases in coherence.

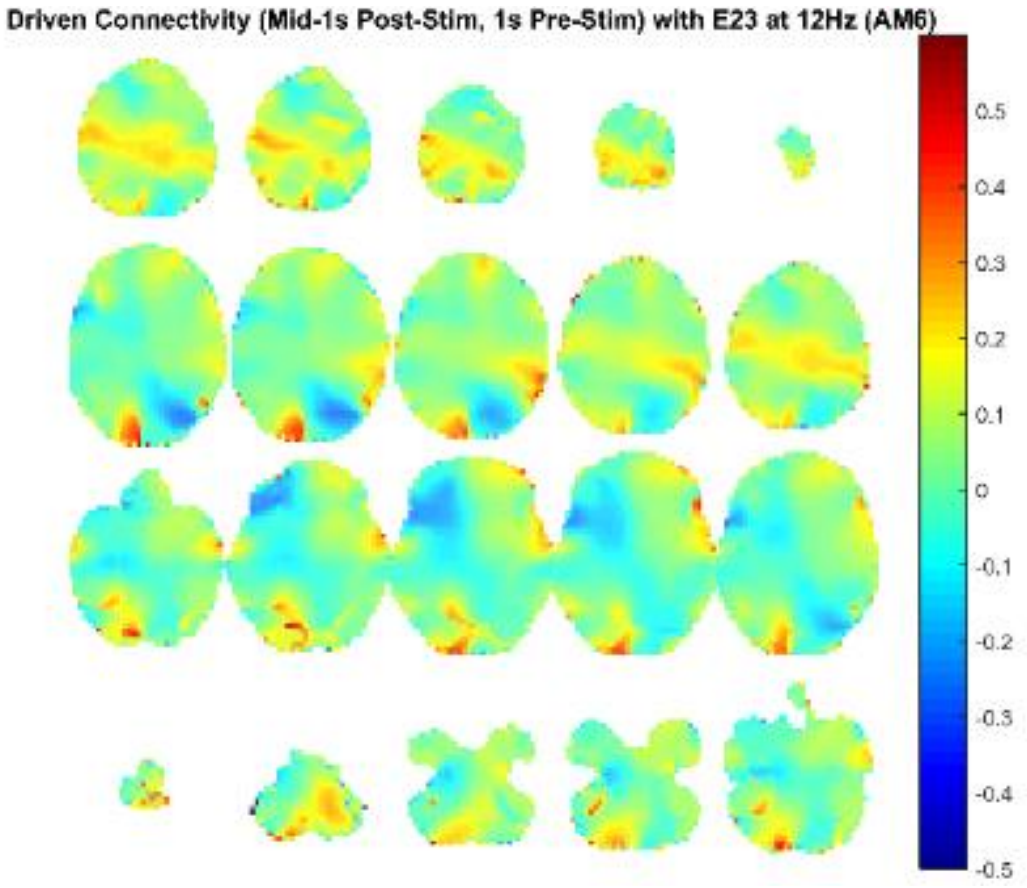

Figure 103. Source level connectivity with a dipole at E23 (left frontal) in 12 Hz during the middle one-second of 6 Hz amplitude modulated tone stimulation (total stimulation was 3 seconds), performed with DICS and a standardized BEM headmodel. Unit is the percent change in coherence from baseline (i.e., difference between coherence during stimulation and coherence during baseline divided by coherence during baseline). Darker reds indicate increases in coherence with E45 while darker blues indicate decreases in coherence.

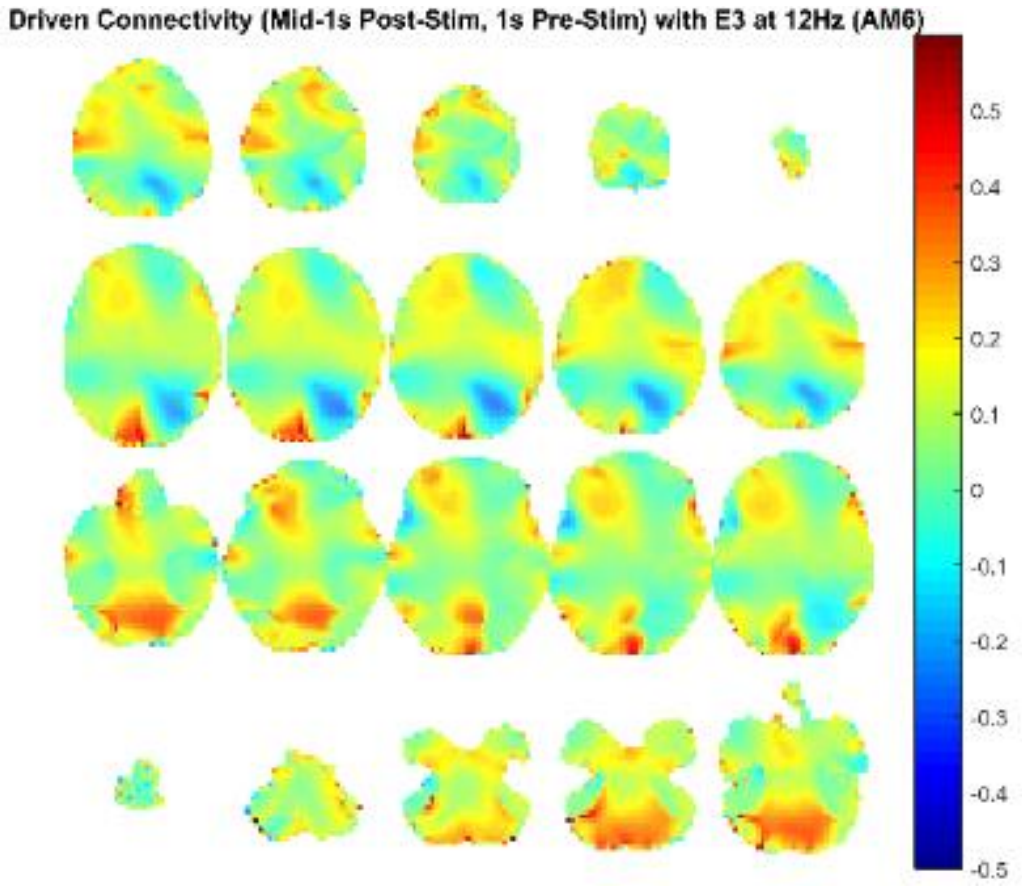

Figure 104. Source level connectivity with a dipole at E3 (right frontal) in 12 Hz during the middle one-second of 6 Hz amplitude modulated tone stimulation (total stimulation was 3 seconds), performed with DICS and a standardized BEM headmodel. Unit is the percent change in coherence from baseline (i.e., difference between coherence during stimulation and coherence during baseline divided by coherence during baseline). Darker reds indicate increases in coherence with E45 while darker blues indicate decreases in coherence.

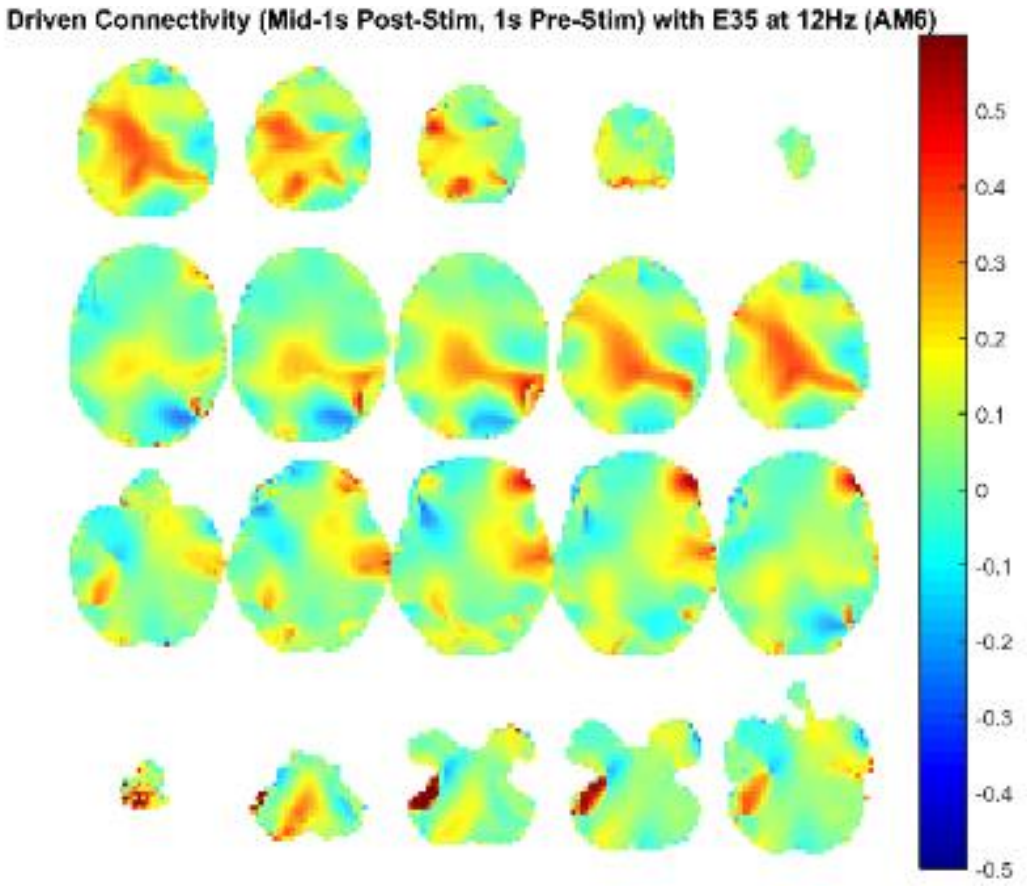

Figure 105. Source level connectivity with a dipole at E35 (left central) in 12 Hz during the middle one-second of 6 Hz amplitude modulated tone stimulation (total stimulation was 3 seconds), performed with DICS and a standardized BEM headmodel. Unit is the percent change in coherence from baseline (i.e., difference between coherence during stimulation and coherence during baseline divided by coherence during baseline). Darker reds indicate increases in coherence with E45 while darker blues indicate decreases in coherence.

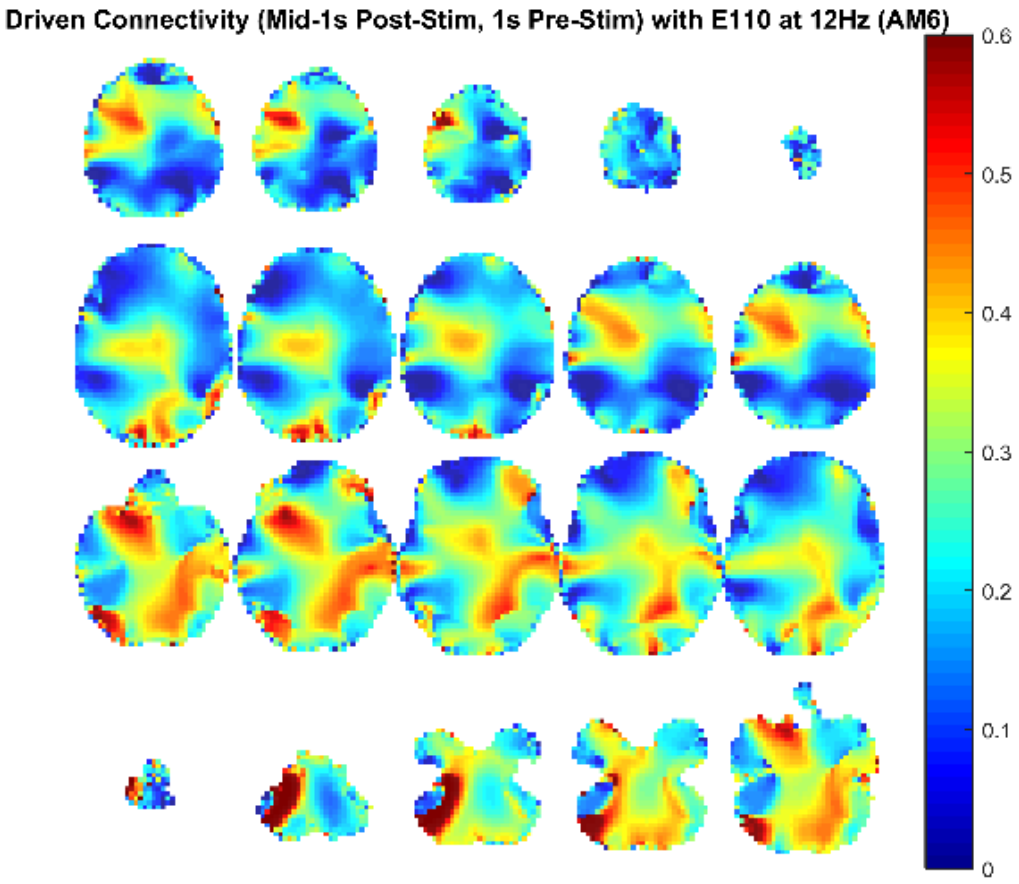

Figure 106. Source level connectivity with a dipole at E110 (right central) in 12 Hz during the middle one-second of 6 Hz amplitude modulated tone stimulation (total stimulation was 3 seconds), performed with DICS and a standardized BEM headmodel. Unit is the percent change in coherence from baseline (i.e., difference between coherence during stimulation and coherence during baseline divided by coherence during baseline). Darker reds indicate increases in coherence with E45 while darker blues indicate decreases in coherence.

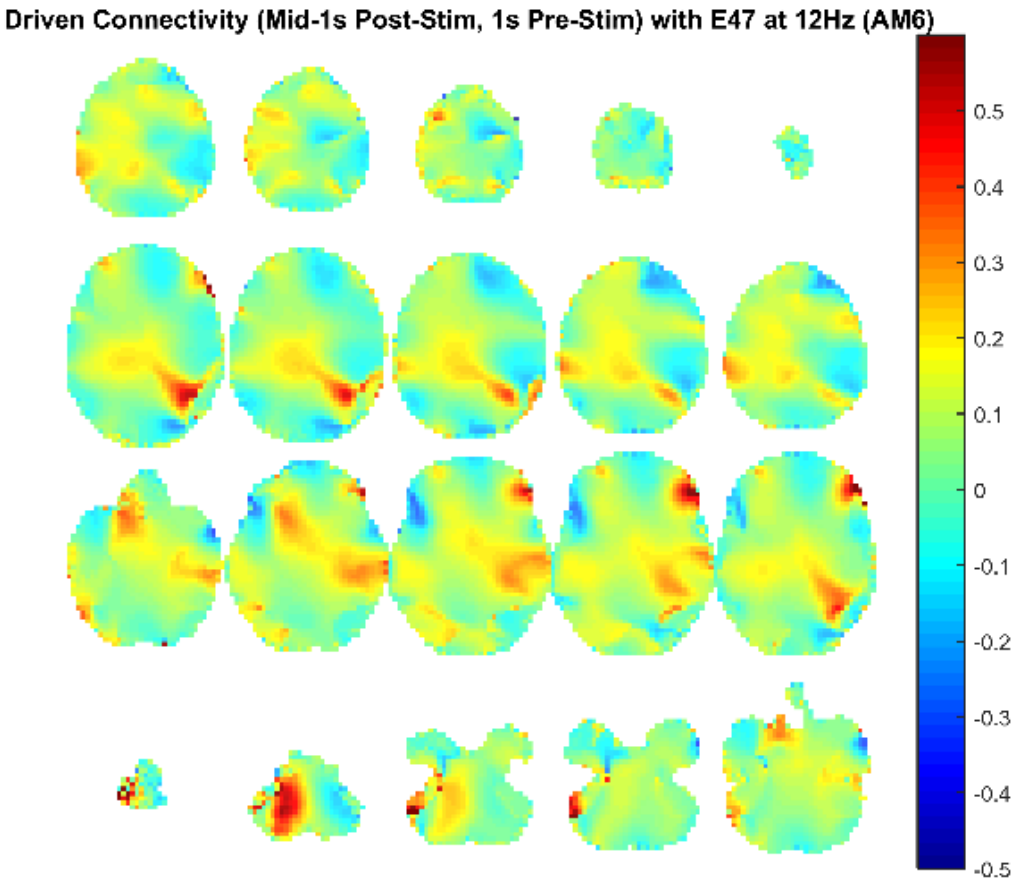

Figure 107. Source level connectivity with a dipole at E47 (left parietal) in 12 Hz during the middle one-second of 6 Hz amplitude modulated tone stimulation (total stimulation was 3 seconds), performed with DICS and a standardized BEM headmodel. Unit is the percent change in coherence from baseline (i.e., difference between coherence during stimulation and coherence during baseline divided by coherence during baseline). Darker reds indicate increases in coherence with E45 while darker blues indicate decreases in coherence.

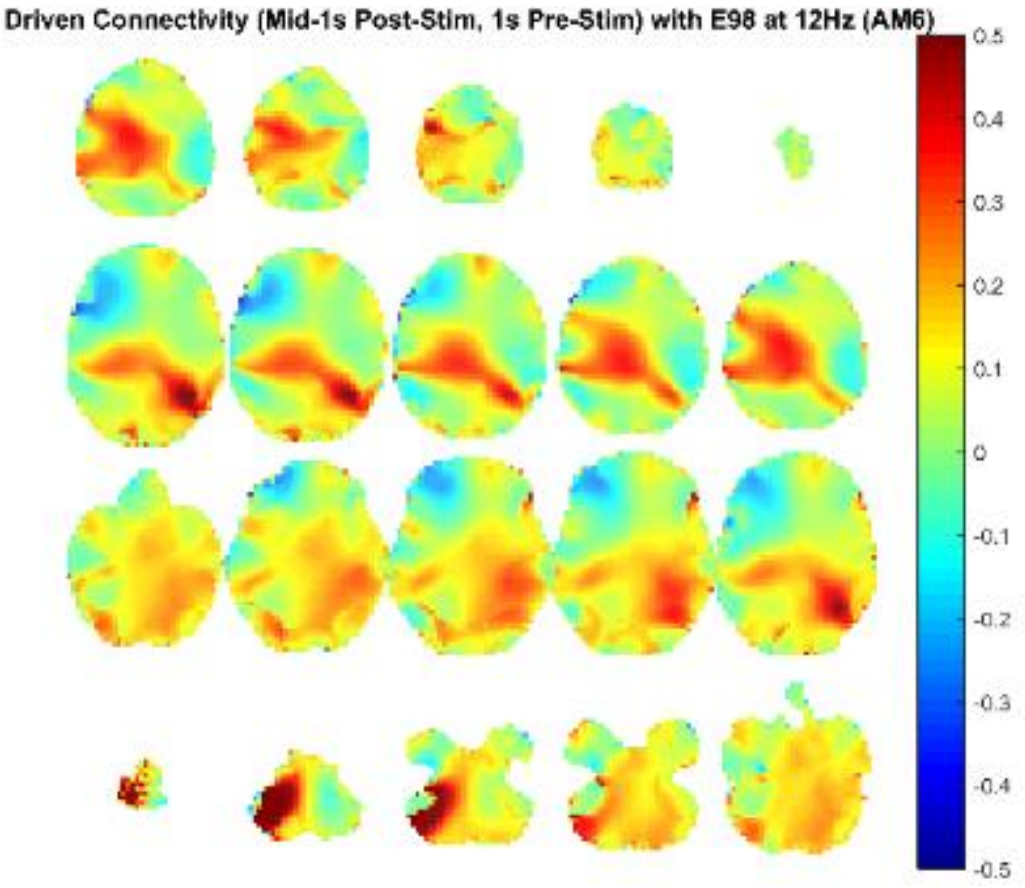

Figure 108. Source level connectivity with a dipole at E98 (right parietal) in 12 Hz during the middle one-second of 6 Hz amplitude modulated tone stimulation (total stimulation was 3 seconds), performed with DICS and a standardized BEM headmodel. Unit is the percent change in coherence from baseline (i.e., difference between coherence during stimulation and coherence during baseline divided by coherence during baseline). Darker reds indicate increases in coherence with E45 while darker blues indicate decreases in coherence.

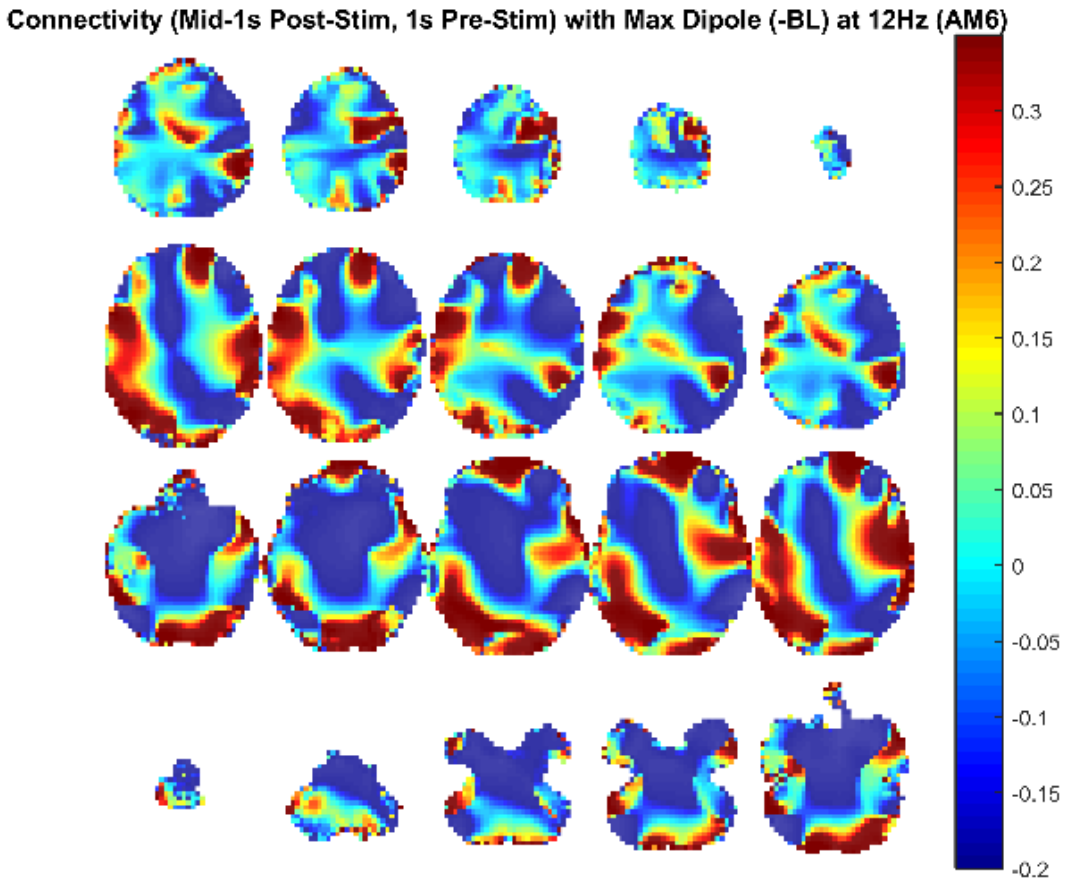

Figure 109. Source level connectivity with a dipole at dip2 (maximum power dipole for the middle one-second period corrected for the baseline one-second period) in 12 Hz during the middle one-second of 6 Hz amplitude modulated tone stimulation (total stimulation was 3 seconds), performed with DICS and a standardized BEM headmodel. Unit is the percent change in coherence from baseline (i.e., difference between coherence during stimulation and coherence during baseline divided by coherence during baseline). Darker reds indicate increases in coherence with E45 while darker blues indicate decreases in coherence.

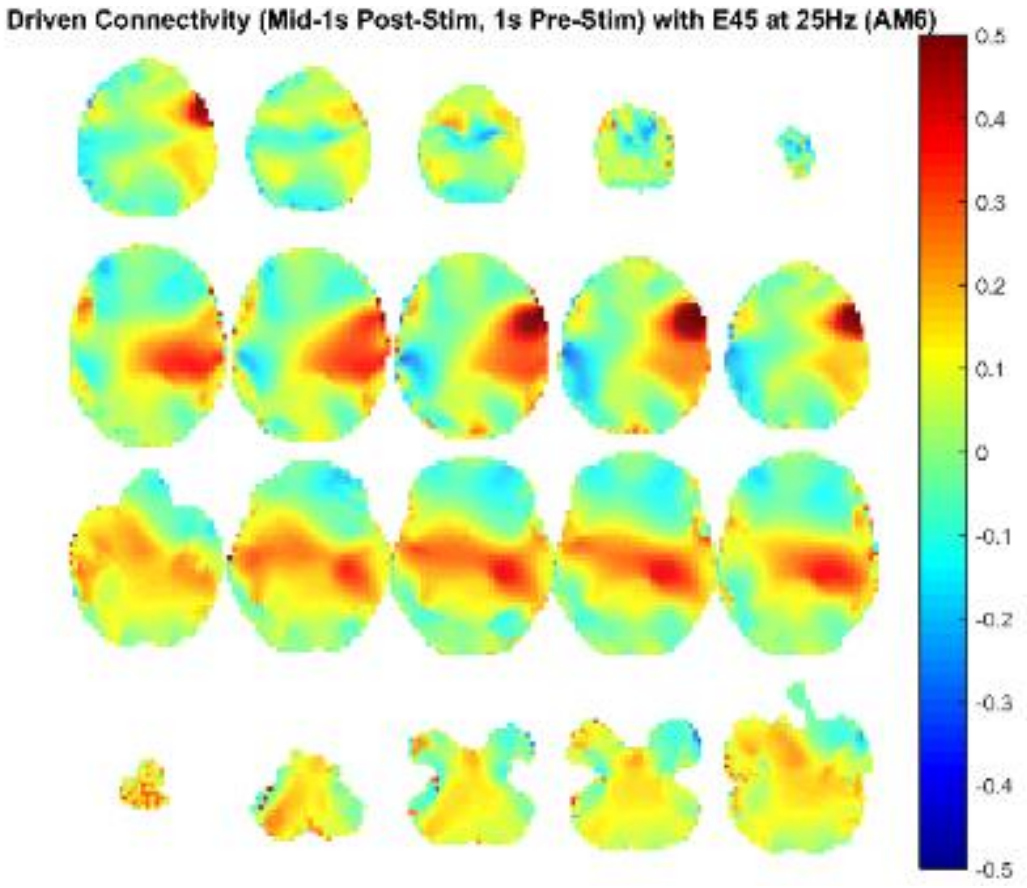

Figure 110. Source level connectivity with a dipole at E45 (left temporal, auditory cortex) in 25 Hz during the middle one-second of 6 Hz amplitude modulated tone stimulation (total stimulation was 3 seconds), performed with DICS and a standardized BEM headmodel. Unit is the percent change in coherence from baseline (i.e., difference between coherence during stimulation and coherence during baseline divided by coherence during baseline). Darker reds indicate increases in coherence with E45 while darker blues indicate decreases in coherence.

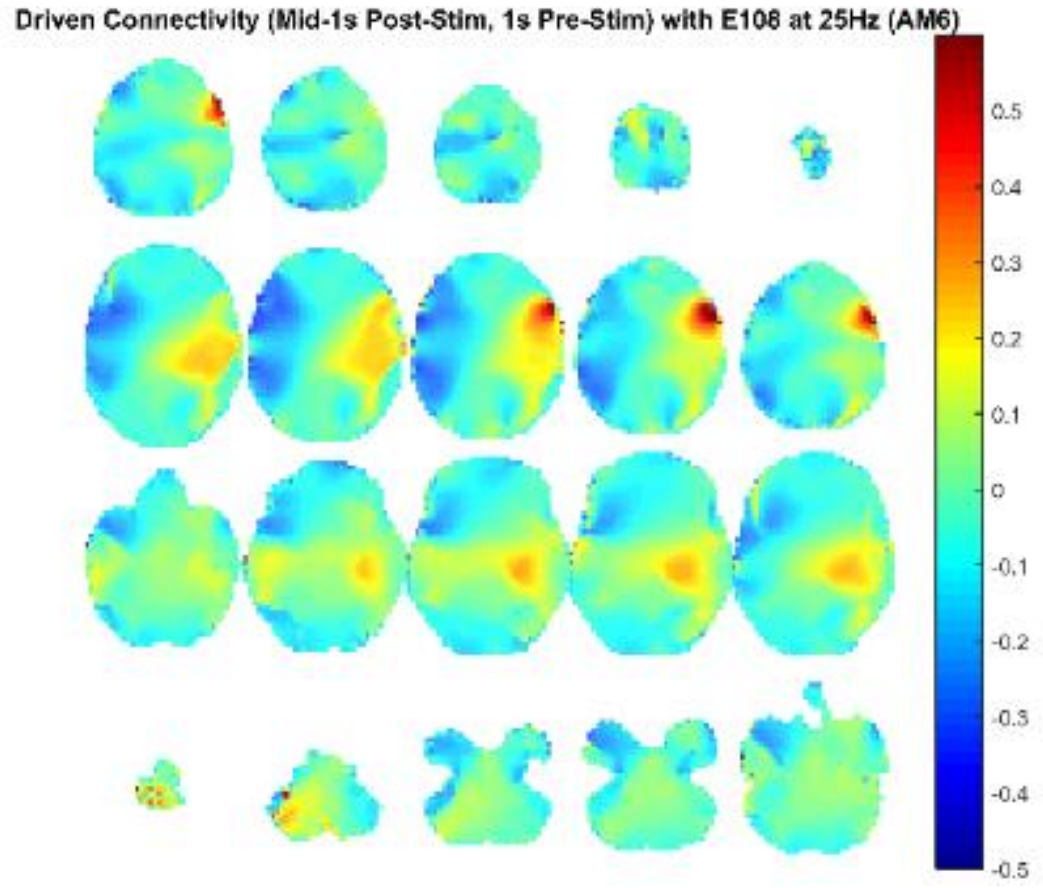

Figure 111. Source level connectivity with a dipole at E108 (right temporal, auditory cortex) in 25 Hz during the middle one-second of 6 Hz amplitude modulated tone stimulation (total stimulation was 3 seconds), performed with DICS and a standardized BEM headmodel. Unit is the percent change in coherence from baseline (i.e., difference between coherence during stimulation and coherence during baseline divided by coherence during baseline). Darker reds indicate increases in coherence with E45 while darker blues indicate decreases in coherence.

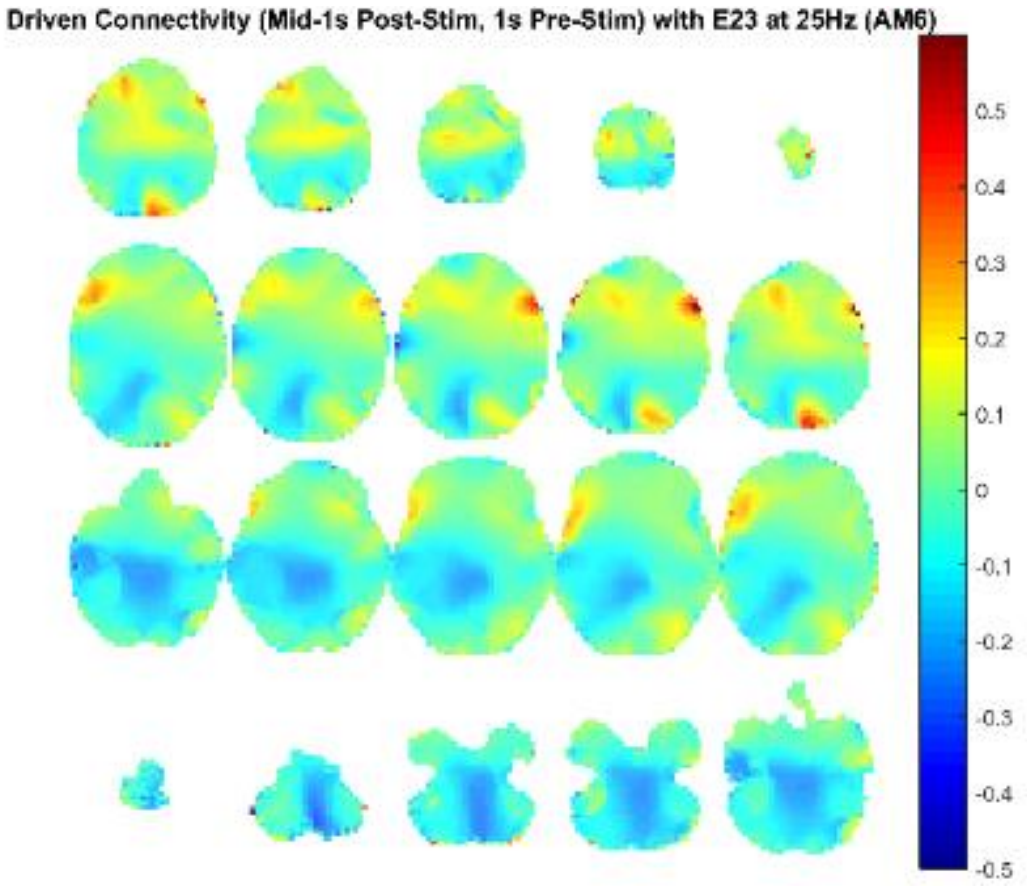

Figure 112. Source level connectivity with a dipole at E23 (left frontal) in 25 Hz during the middle one-second of 6 Hz amplitude modulated tone stimulation (total stimulation was 3 seconds), performed with DICS and a standardized BEM headmodel. Unit is the percent change in coherence from baseline (i.e., difference between coherence during stimulation and coherence during baseline divided by coherence during baseline). Darker reds indicate increases in coherence with E45 while darker blues indicate decreases in coherence.

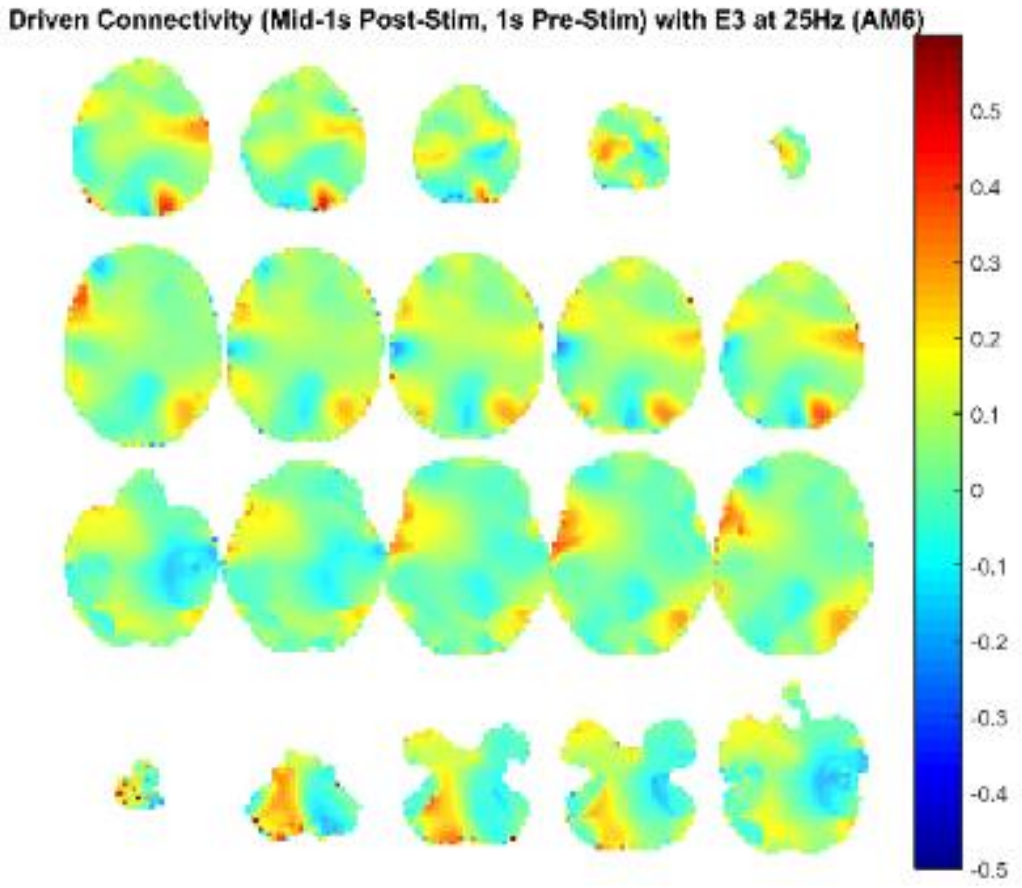

Figure 113. Source level connectivity with a dipole at E3 (right frontal) in 25 Hz during the middle one-second of 6 Hz amplitude modulated tone stimulation (total stimulation was 3 seconds), performed with DICS and a standardized BEM headmodel. Unit is the percent change in coherence from baseline (i.e., difference between coherence during stimulation and coherence during baseline divided by coherence during baseline). Darker reds indicate increases in coherence with E45 while darker blues indicate decreases in coherence.

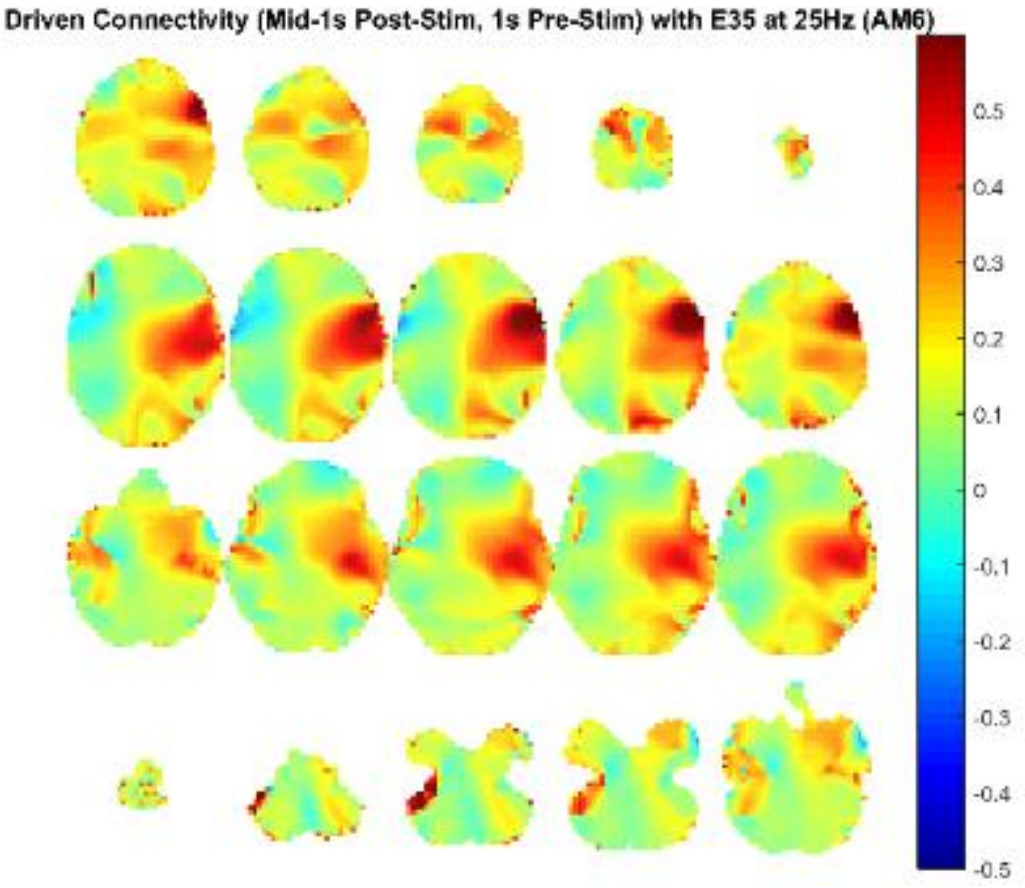

Figure 114. Source level connectivity with a dipole at E35 (left central) in 25 Hz during the middle one-second of 6 Hz amplitude modulated tone stimulation (total stimulation was 3 seconds), performed with DICS and a standardized BEM headmodel. Unit is the percent change in coherence from baseline (i.e., difference between coherence during stimulation and coherence during baseline divided by coherence during baseline). Darker reds indicate increases in coherence with E45 while darker blues indicate decreases in coherence.

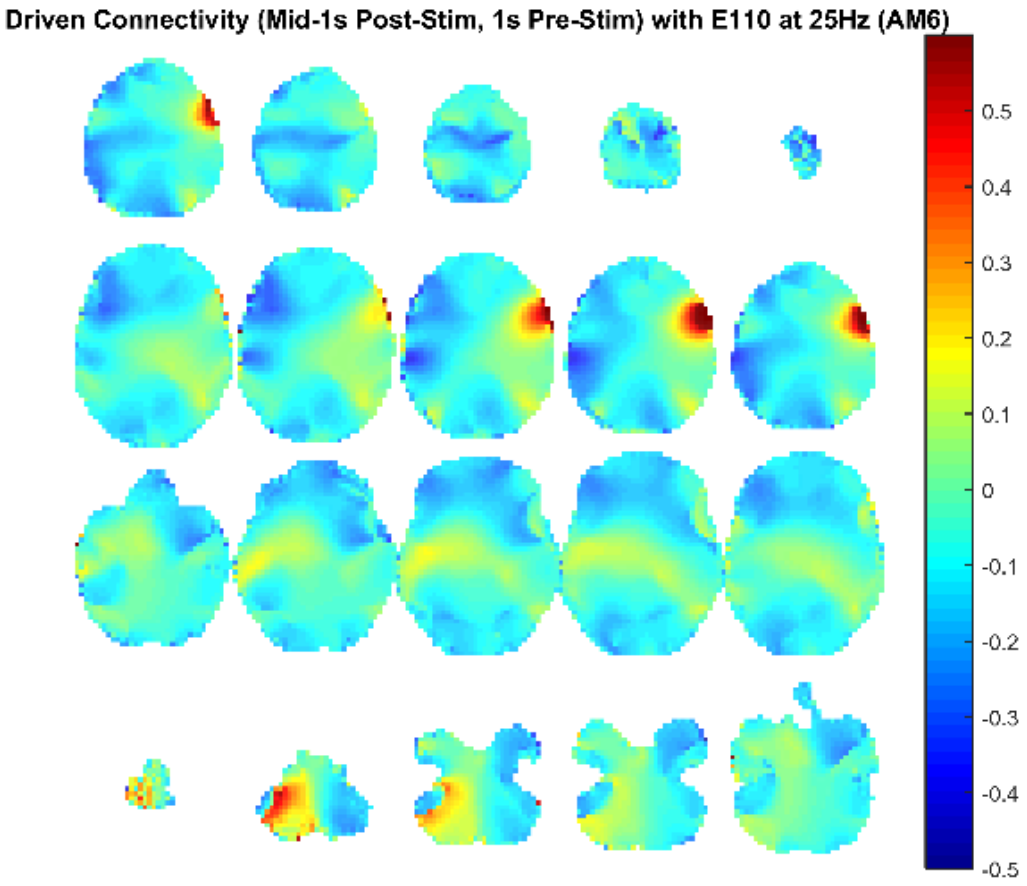

Figure 115. Source level connectivity with a dipole at E110 (right central) in 25 Hz during the middle one-second of 6 Hz amplitude modulated tone stimulation (total stimulation was 3 seconds), performed with DICS and a standardized BEM headmodel. Unit is the percent change in coherence from baseline (i.e., difference between coherence during stimulation and coherence during baseline divided by coherence during baseline). Darker reds indicate increases in coherence with E45 while darker blues indicate decreases in coherence.

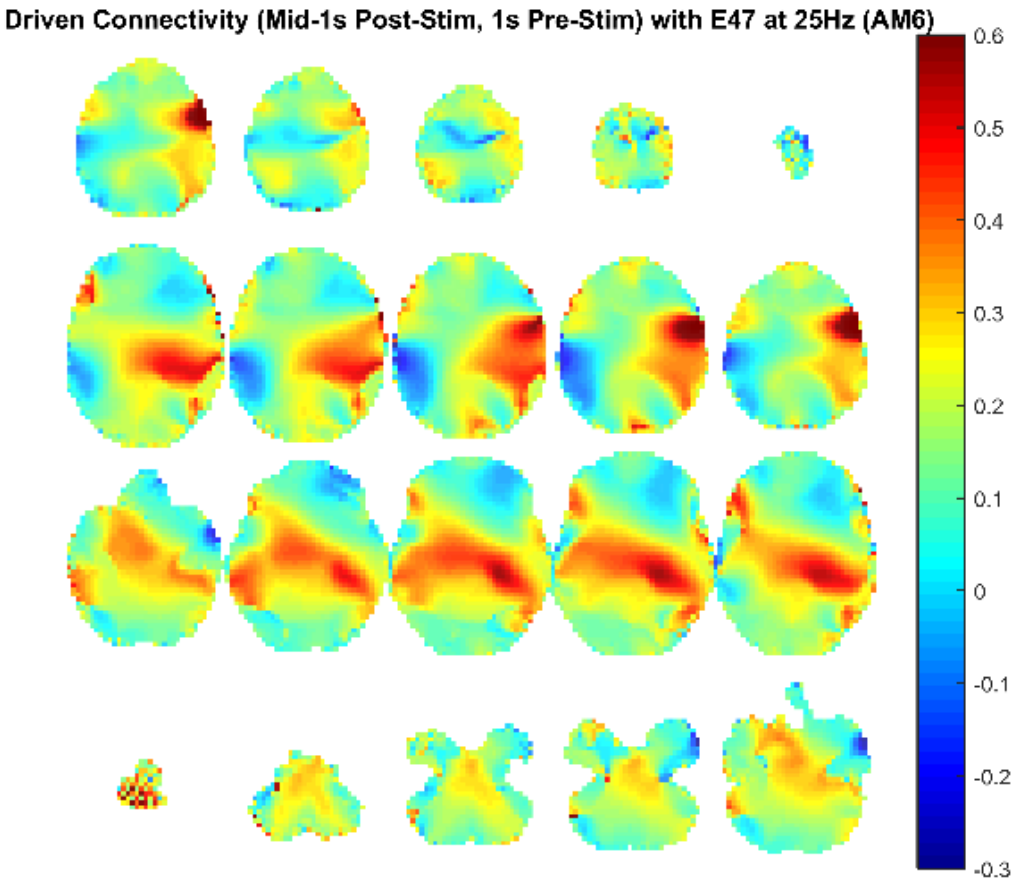

Figure 116. Source level connectivity with a dipole at E47 (left parietal) in 25 Hz during the middle one-second of 6 Hz amplitude modulated tone stimulation (total stimulation was 3 seconds), performed with DICS and a standardized BEM headmodel. Unit is the percent change in coherence from baseline (i.e., difference between coherence during stimulation and coherence during baseline divided by coherence during baseline). Darker reds indicate increases in coherence with E45 while darker blues indicate decreases in coherence.

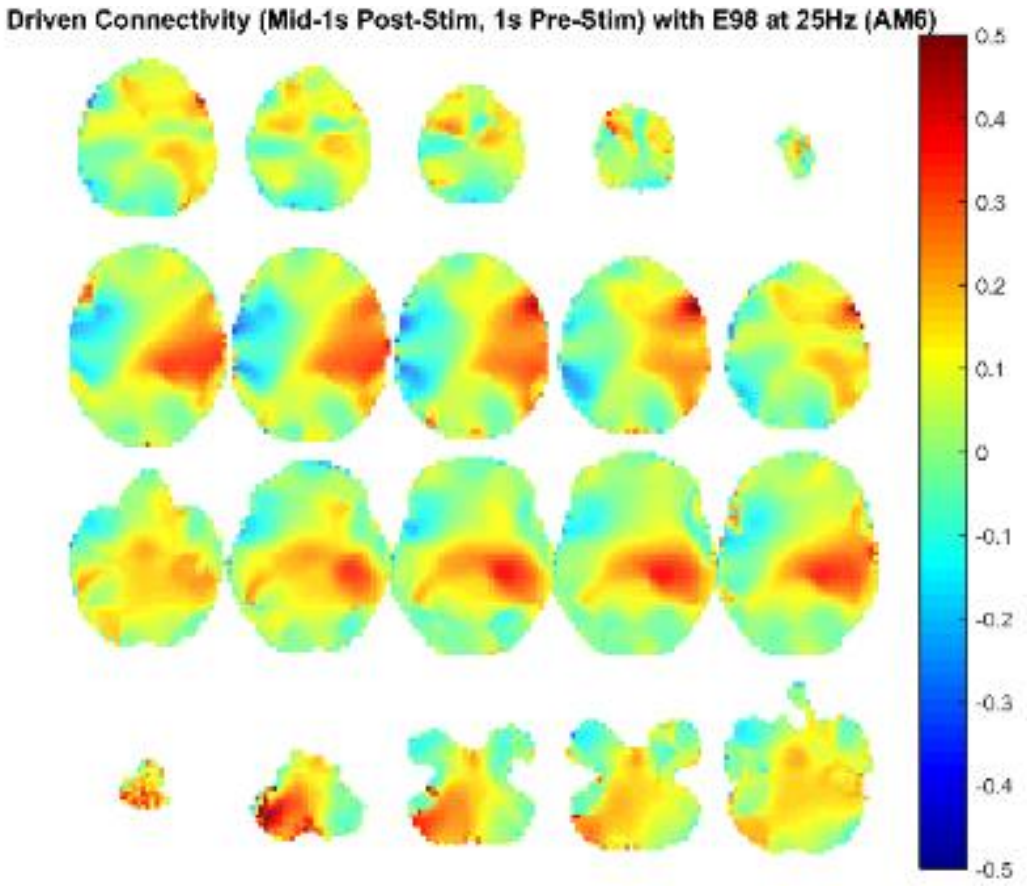

Figure 117. Source level connectivity with a dipole at E98 (right parietal) in 25 Hz during the middle one-second of 6 Hz amplitude modulated tone stimulation (total stimulation was 3 seconds), performed with DICS and a standardized BEM headmodel. Unit is the percent change in coherence from baseline (i.e., difference between coherence during stimulation and coherence during baseline divided by coherence during baseline). Darker reds indicate increases in coherence with E45 while darker blues indicate decreases in coherence.

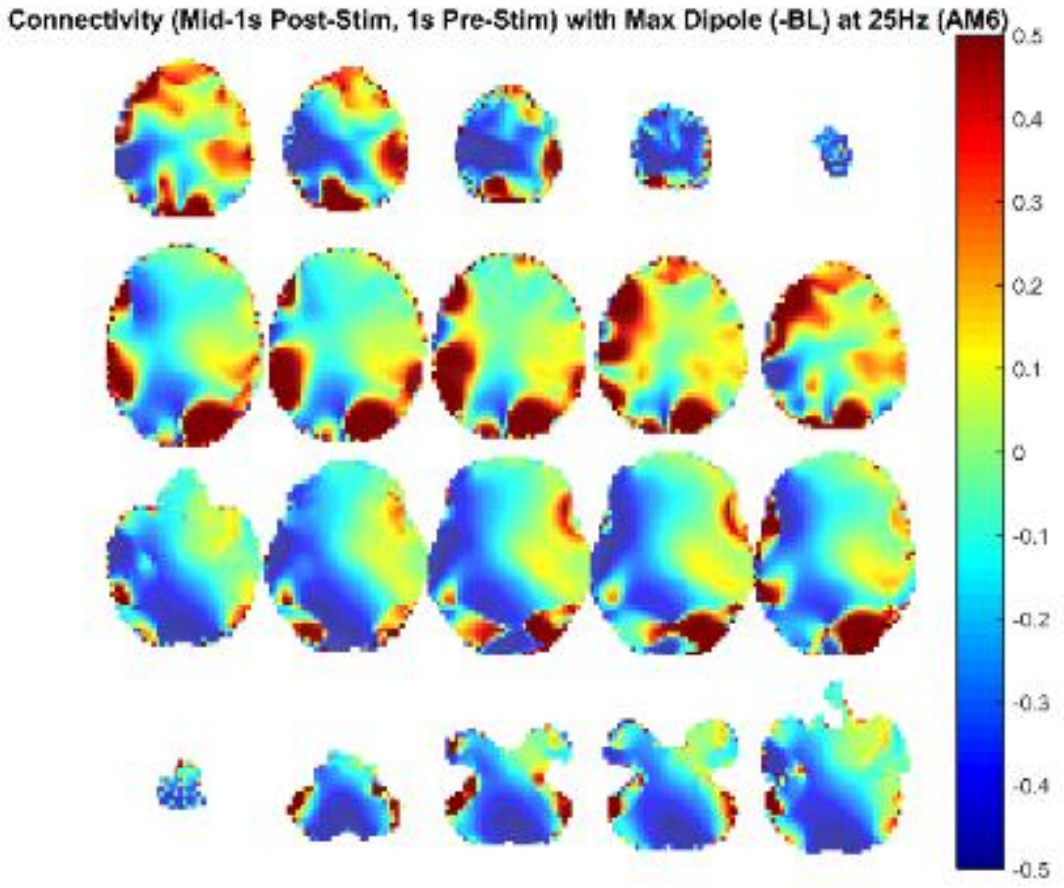

Figure 118. Source level connectivity with a dipole at dip2 (maximum power dipole for the middle one-second period corrected for the baseline one-second period) in 25 Hz during the middle one-second of 6 Hz amplitude modulated tone stimulation (total stimulation was 3 seconds), performed with DICS and a standardized BEM headmodel. Unit is the percent change in coherence from baseline (i.e., difference between coherence during stimulation and coherence during baseline divided by coherence during baseline). Darker reds indicate increases in coherence with E45 while darker blues indicate decreases in coherence.

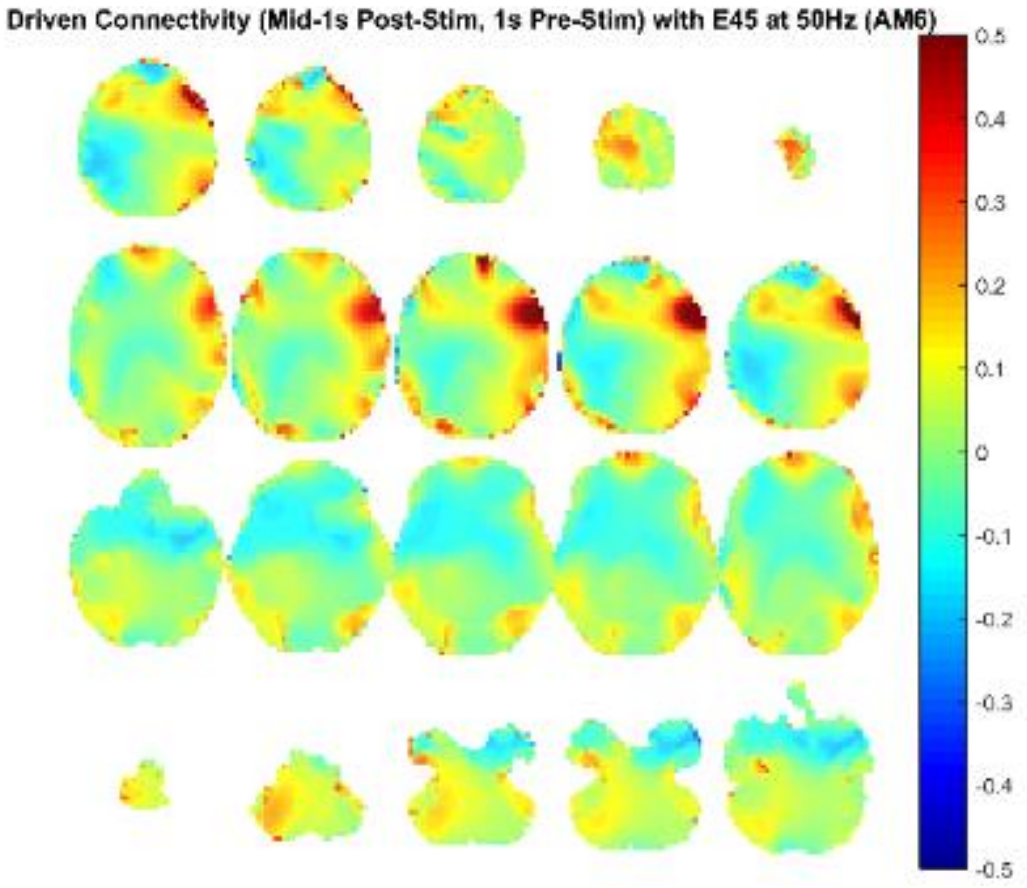

Figure 119. Source level connectivity with a dipole at E45 (left temporal, auditory cortex) in 50 Hz during the middle one-second of 6 Hz amplitude modulated tone stimulation (total stimulation was 3 seconds), performed with DICS and a standardized BEM headmodel. Unit is the percent change in coherence from baseline (i.e., difference between coherence during stimulation and coherence during baseline divided by coherence during baseline). Darker reds indicate increases in coherence with E45 while darker blues indicate decreases in coherence.

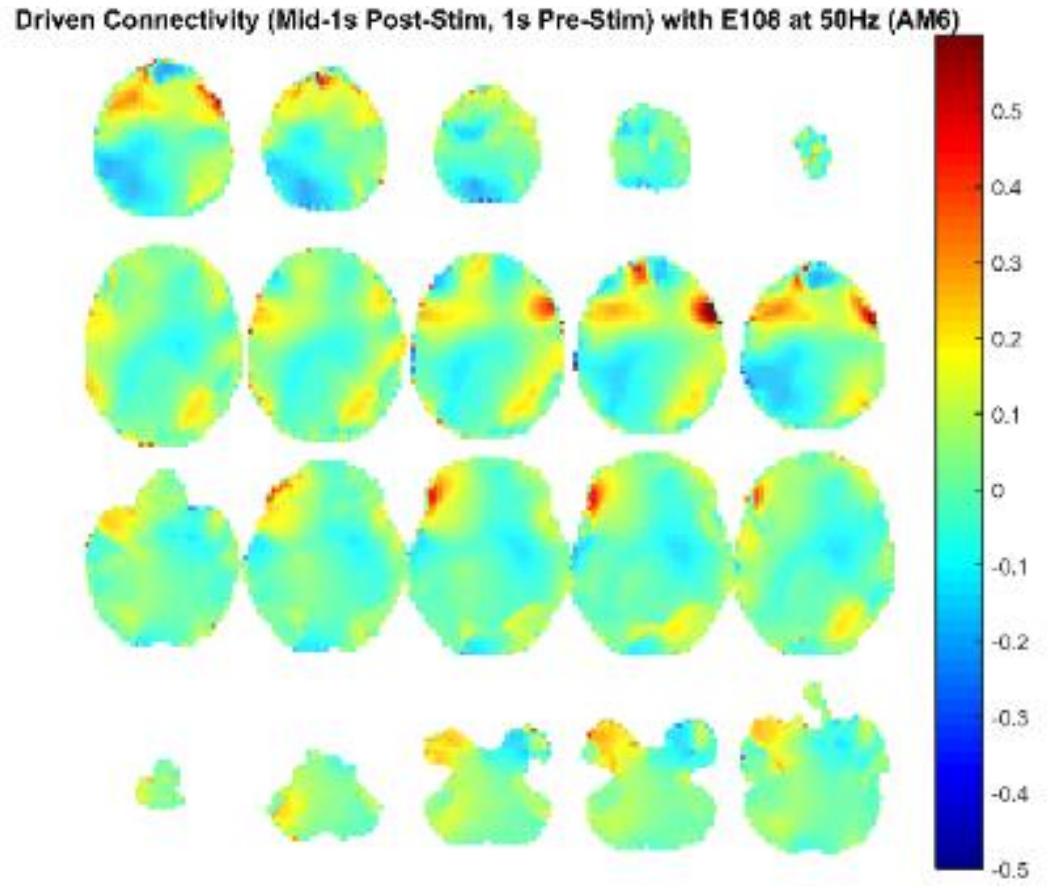

Figure 120. Source level connectivity with a dipole at E108 (right temporal, auditory cortex) in 50 Hz during the middle one-second of 6 Hz amplitude modulated tone stimulation (total stimulation was 3 seconds), performed with DICS and a standardized BEM headmodel. Unit is the percent change in coherence from baseline (i.e., difference between coherence during stimulation and coherence during baseline divided by coherence during baseline). Darker reds indicate increases in coherence with E45 while darker blues indicate decreases in coherence.

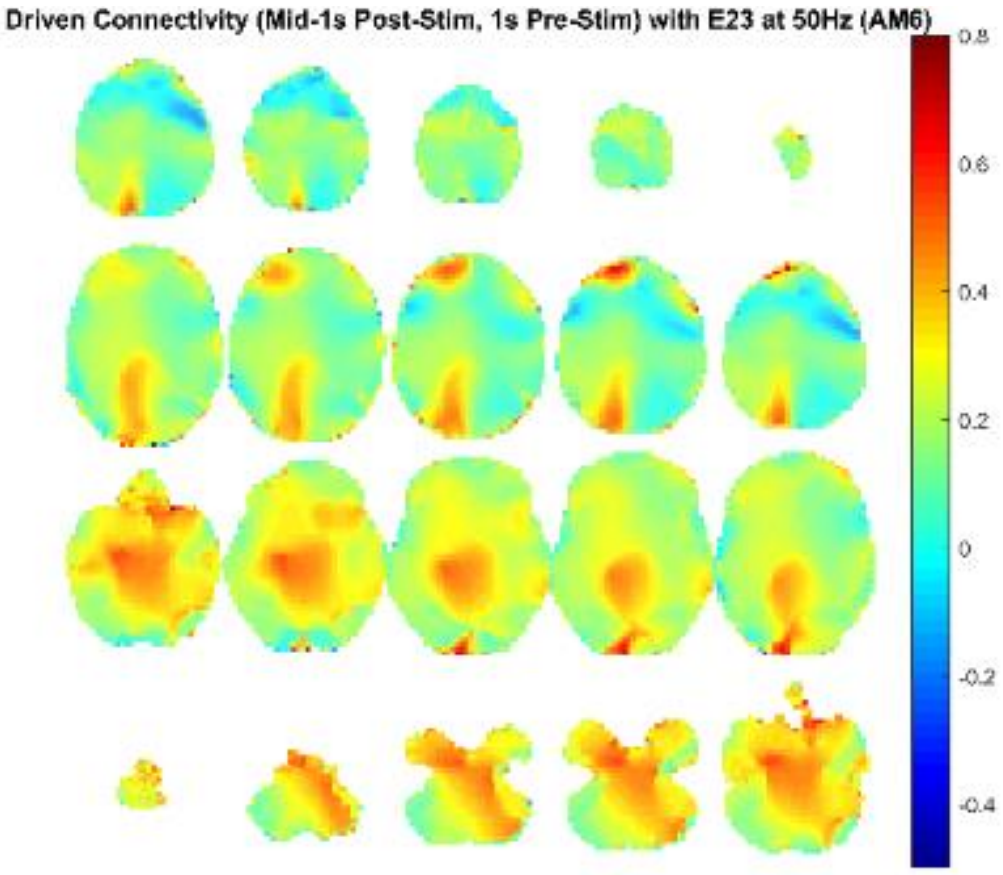

Figure 121. Source level connectivity with a dipole at E23 (left frontal) in 50 Hz during the middle one-second of 6 Hz amplitude modulated tone stimulation (total stimulation was 3 seconds), performed with DICS and a standardized BEM headmodel. Unit is the percent change in coherence from baseline (i.e., difference between coherence during stimulation and coherence during baseline divided by coherence during baseline). Darker reds indicate increases in coherence with E45 while darker blues indicate decreases in coherence.

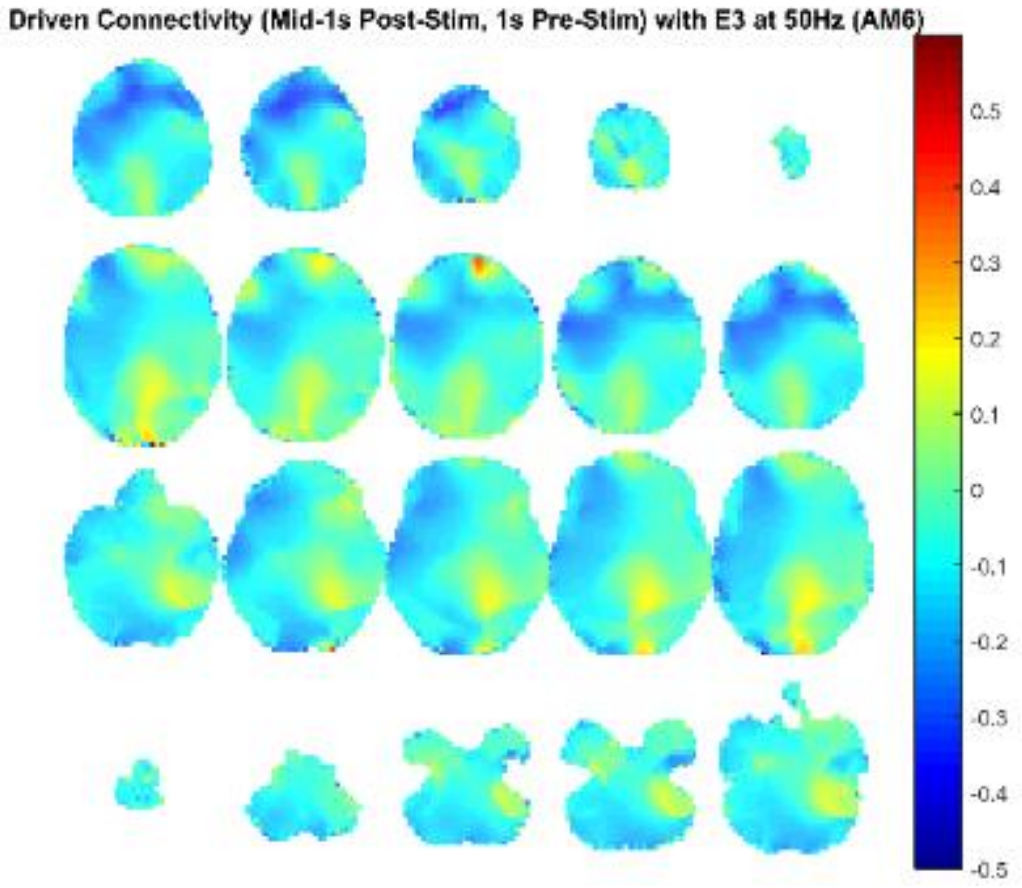

Figure 122. Source level connectivity with a dipole at E3 (right frontal) in 50 Hz during the middle one-second of 6 Hz amplitude modulated tone stimulation (total stimulation was 3 seconds), performed with DICS and a standardized BEM headmodel. Unit is the percent change in coherence from baseline (i.e., difference between coherence during stimulation and coherence during baseline divided by coherence during baseline). Darker reds indicate increases in coherence with E45 while darker blues indicate decreases in coherence.

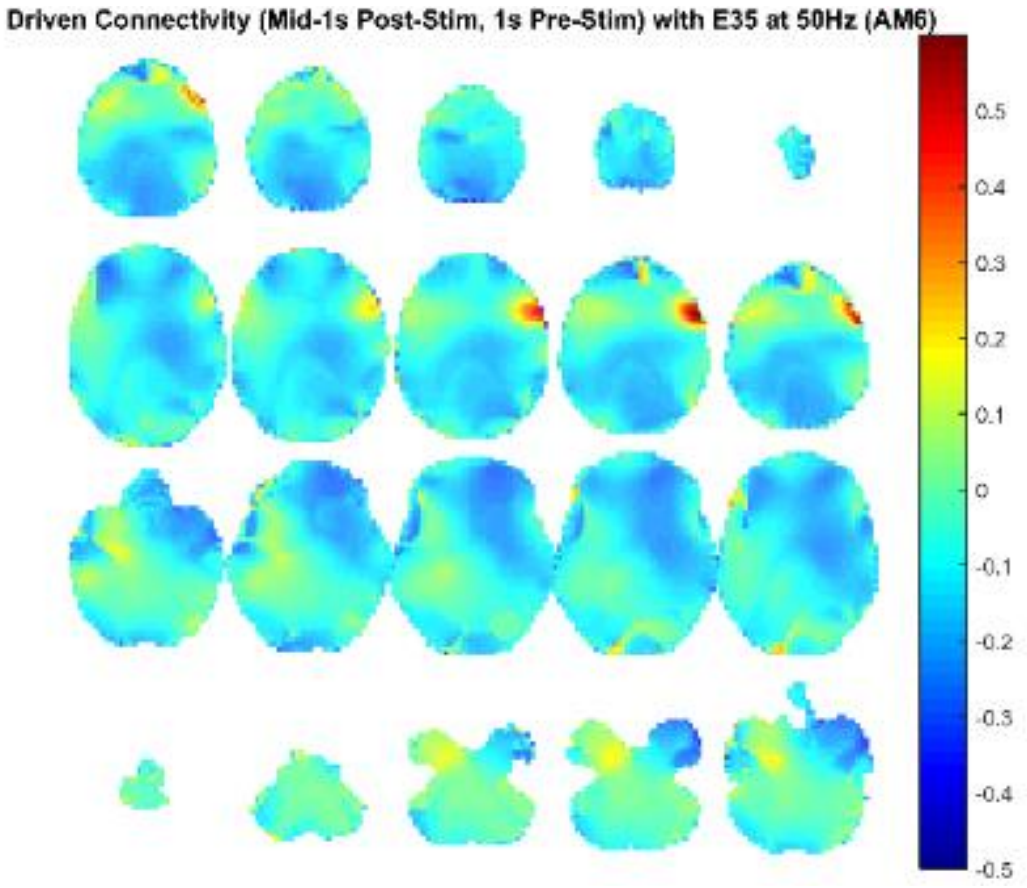

Figure 123. Source level connectivity with a dipole at E35 (left central) in 50 Hz during the middle one-second of 6 Hz amplitude modulated tone stimulation (total stimulation was 3 seconds), performed with DICS and a standardized BEM headmodel. Unit is the percent change in coherence from baseline (i.e., difference between coherence during stimulation and coherence during baseline divided by coherence during baseline). Darker reds indicate increases in coherence with E45 while darker blues indicate decreases in coherence.

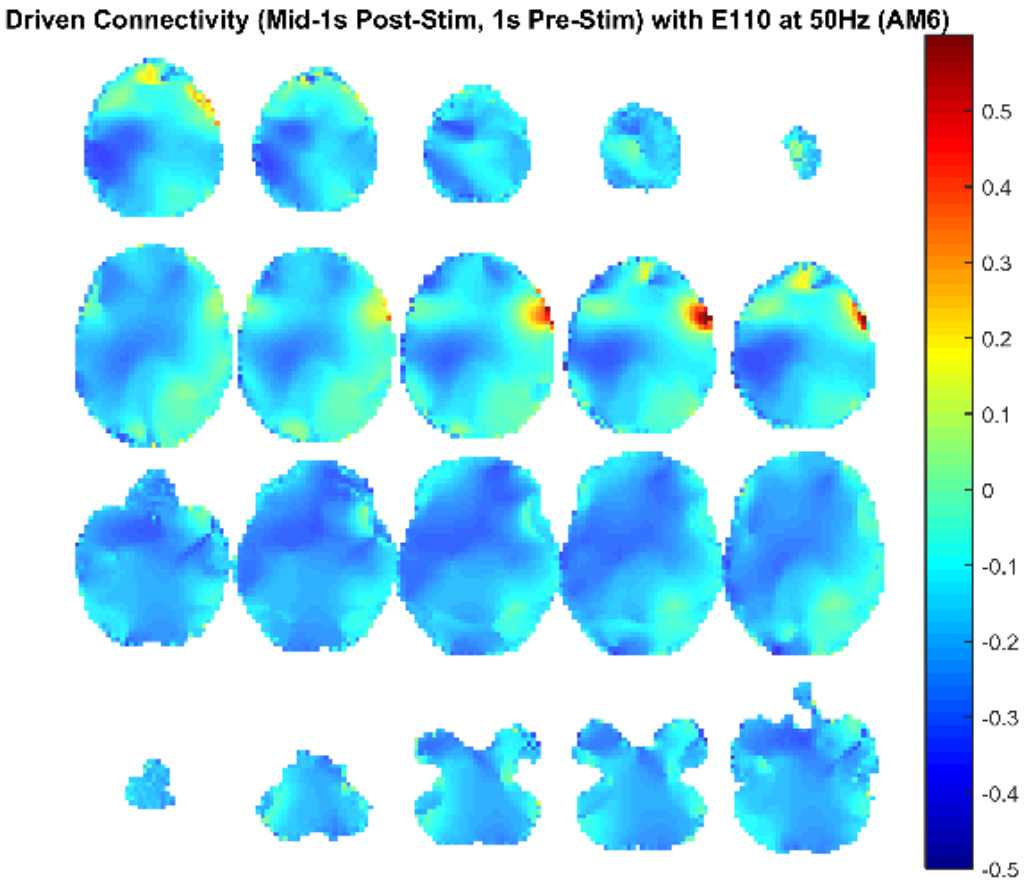

Figure 124. Source level connectivity with a dipole at E110 (right central) in 50 Hz during the middle one-second of 6 Hz amplitude modulated tone stimulation (total stimulation was 3 seconds), performed with DICS and a standardized BEM headmodel. Unit is the percent change in coherence from baseline (i.e., difference between coherence during stimulation and coherence during baseline divided by coherence during baseline). Darker reds indicate increases in coherence with E45 while darker blues indicate decreases in coherence.

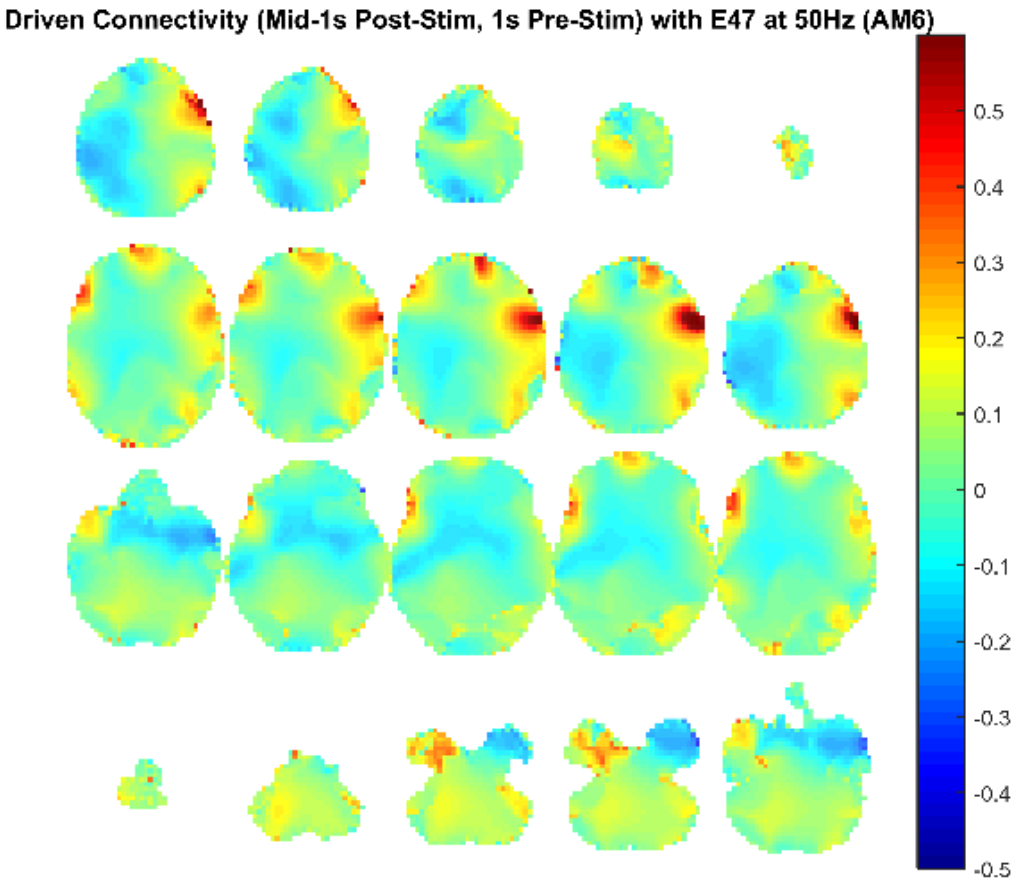

Figure 125. Source level connectivity with a dipole at E47 (left parietal) in 50 Hz during the middle one-second of 6 Hz amplitude modulated tone stimulation (total stimulation was 3 seconds), performed with DICS and a standardized BEM headmodel. Unit is the percent change in coherence from baseline (i.e., difference between coherence during stimulation and coherence during baseline divided by coherence during baseline). Darker reds indicate increases in coherence with E45 while darker blues indicate decreases in coherence.

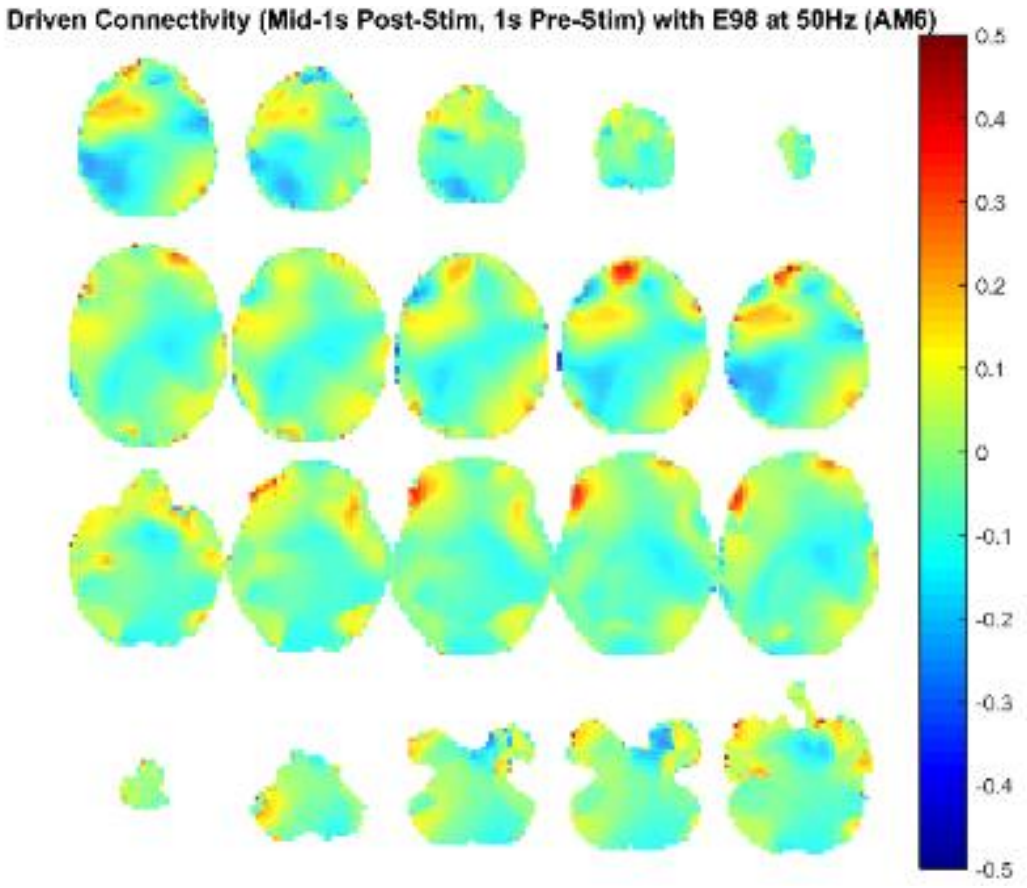

Figure 126. Source level connectivity with a dipole at E98 (right parietal) in 50 Hz during the middle one-second of 6 Hz amplitude modulated tone stimulation (total stimulation was 3 seconds), performed with DICS and a standardized BEM headmodel. Unit is the percent change in coherence from baseline (i.e., difference between coherence during stimulation and coherence during baseline divided by coherence during baseline). Darker reds indicate increases in coherence with E45 while darker blues indicate decreases in coherence.

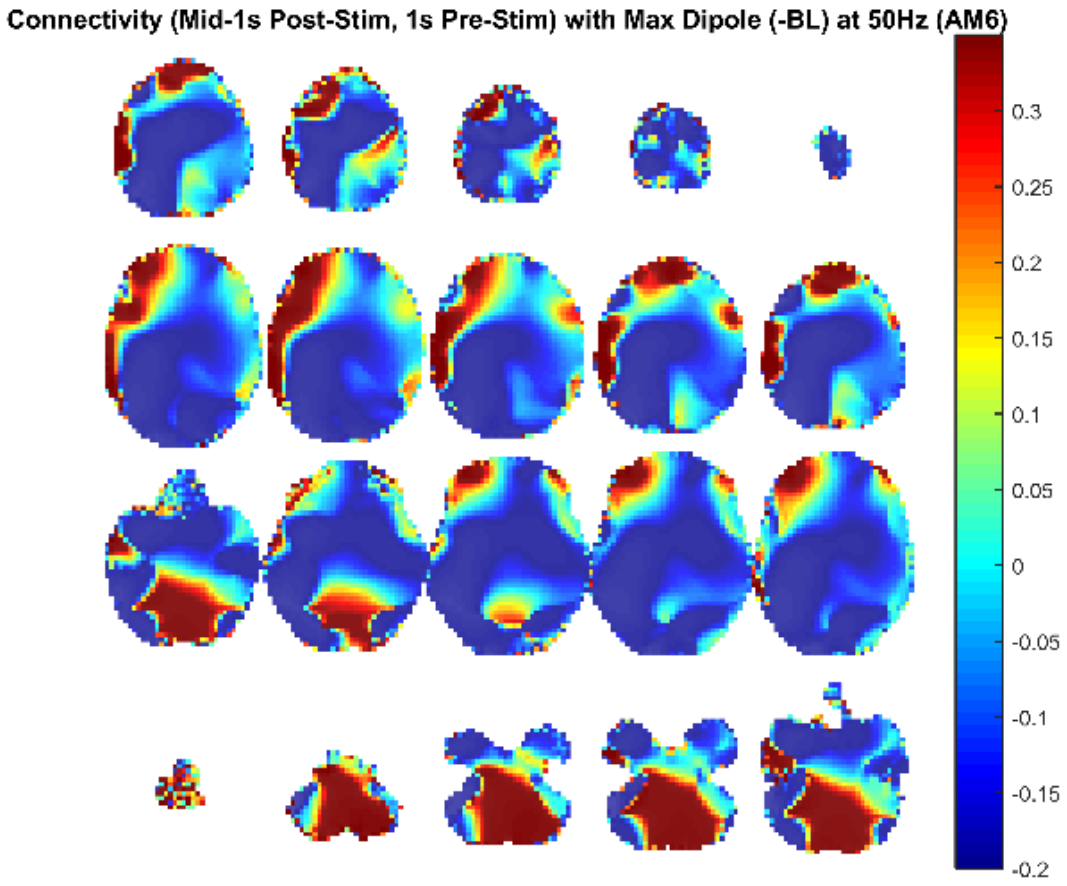

Figure 127. Source level connectivity with a dipole at dip2 (maximum power dipole for the middle one-second period corrected for the baseline one-second period) in 50 Hz during the middle one-second of 6 Hz amplitude modulated tone stimulation (total stimulation was 3 seconds), performed with DICS and a standardized BEM headmodel. Unit is the percent change in coherence from baseline (i.e., difference between coherence during stimulation and coherence during baseline divided by coherence during baseline). Darker reds indicate increases in coherence with E45 while darker blues indicate decreases in coherence.

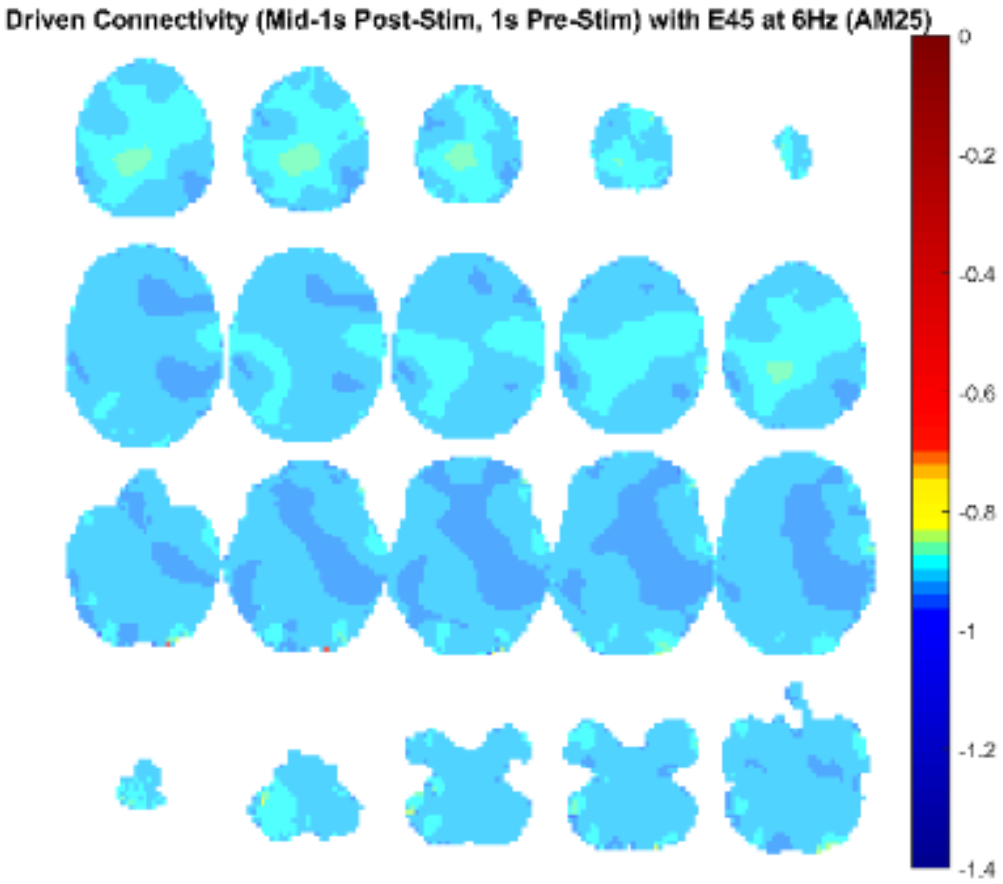

Figure 128. Source level connectivity with a dipole at E45 (left temporal, auditory cortex) in 6 Hz during the middle one-second of 25 Hz amplitude modulated tone stimulation (total stimulation was 3 seconds), performed with DICS and a standardized BEM headmodel. Unit is the percent change in coherence from baseline (i.e., difference between coherence during stimulation and coherence during baseline divided by coherence during baseline). Darker reds indicate increases in coherence with E45 while darker blues indicate decreases in coherence.

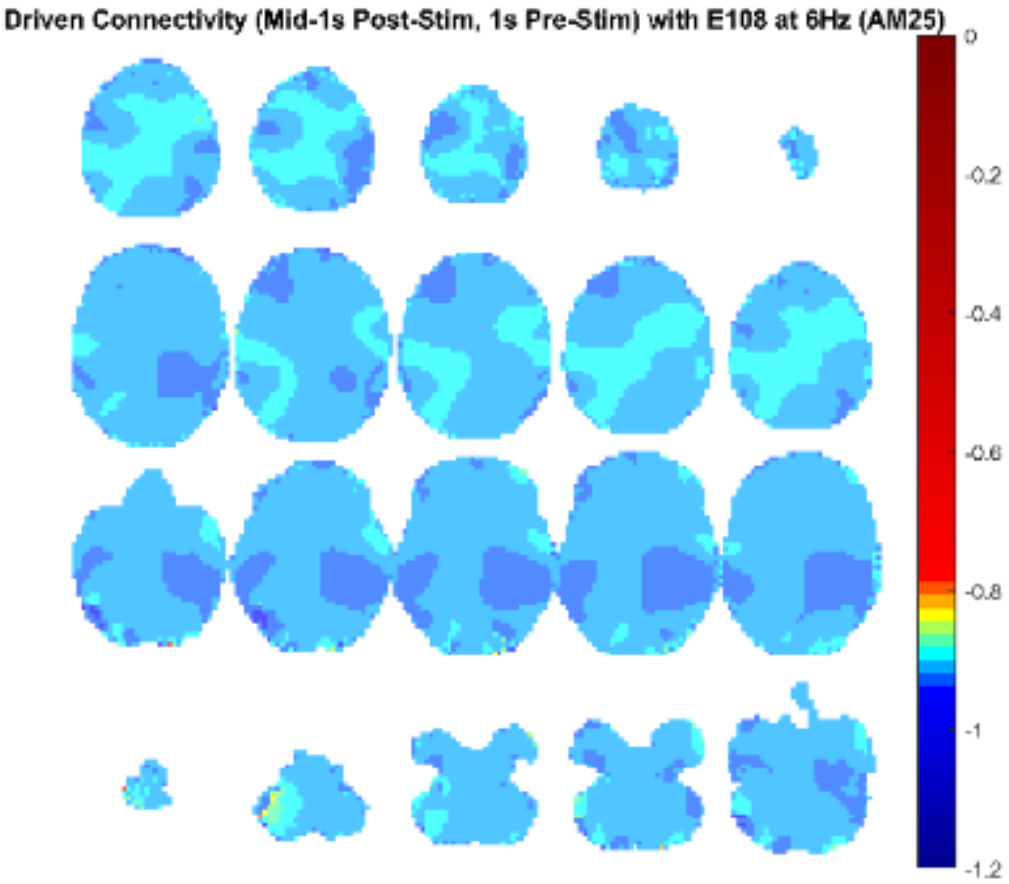

Figure 129. Source level connectivity with a dipole at E108 (right temporal, auditory cortex) in 6 Hz during the middle one-second of 25 Hz amplitude modulated tone stimulation (total stimulation was 3 seconds), performed with DICS and a standardized BEM headmodel. Unit is the percent change in coherence from baseline (i.e., difference between coherence during stimulation and coherence during baseline divided by coherence during baseline). Darker reds indicate increases in coherence with E45 while darker blues indicate decreases in coherence.

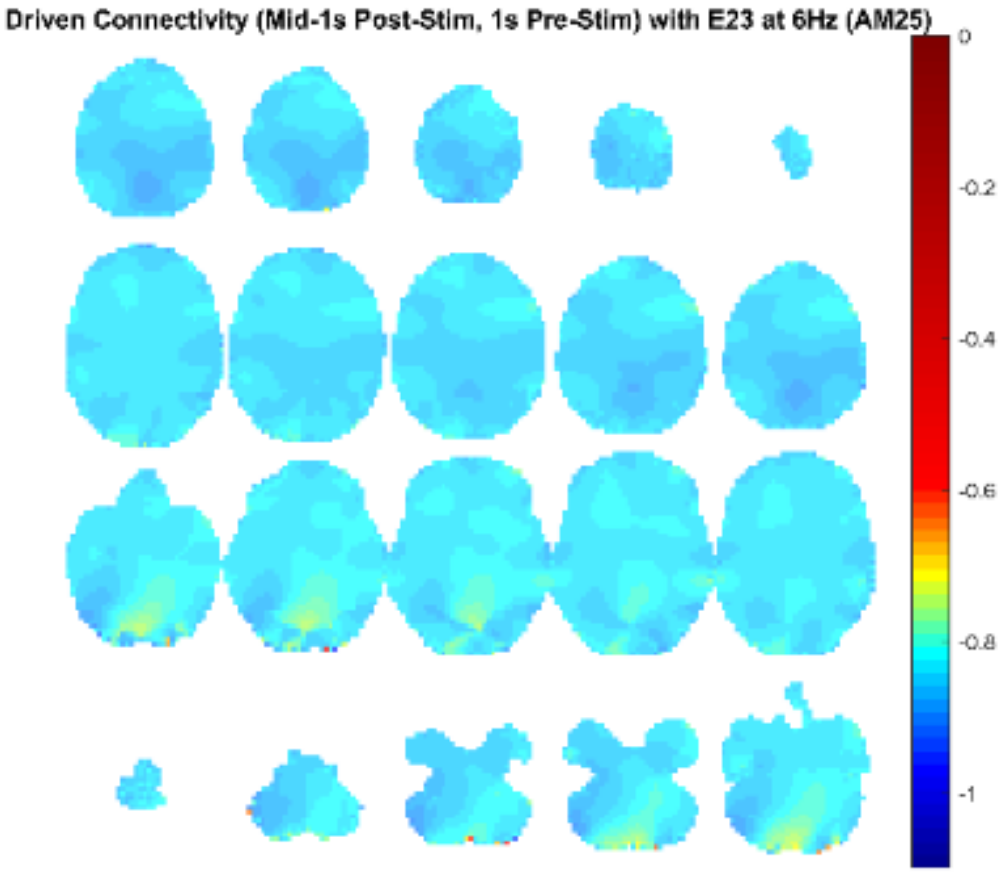

Figure 130. Source level connectivity with a dipole at E23 (left frontal) in 6 Hz during the middle one-second of 25 Hz amplitude modulated tone stimulation (total stimulation was 3 seconds), performed with DICS and a standardized BEM headmodel. Unit is the percent change in coherence from baseline (i.e., difference between coherence during stimulation and coherence during baseline divided by coherence during baseline). Darker reds indicate increases in coherence with E45 while darker blues indicate decreases in coherence.

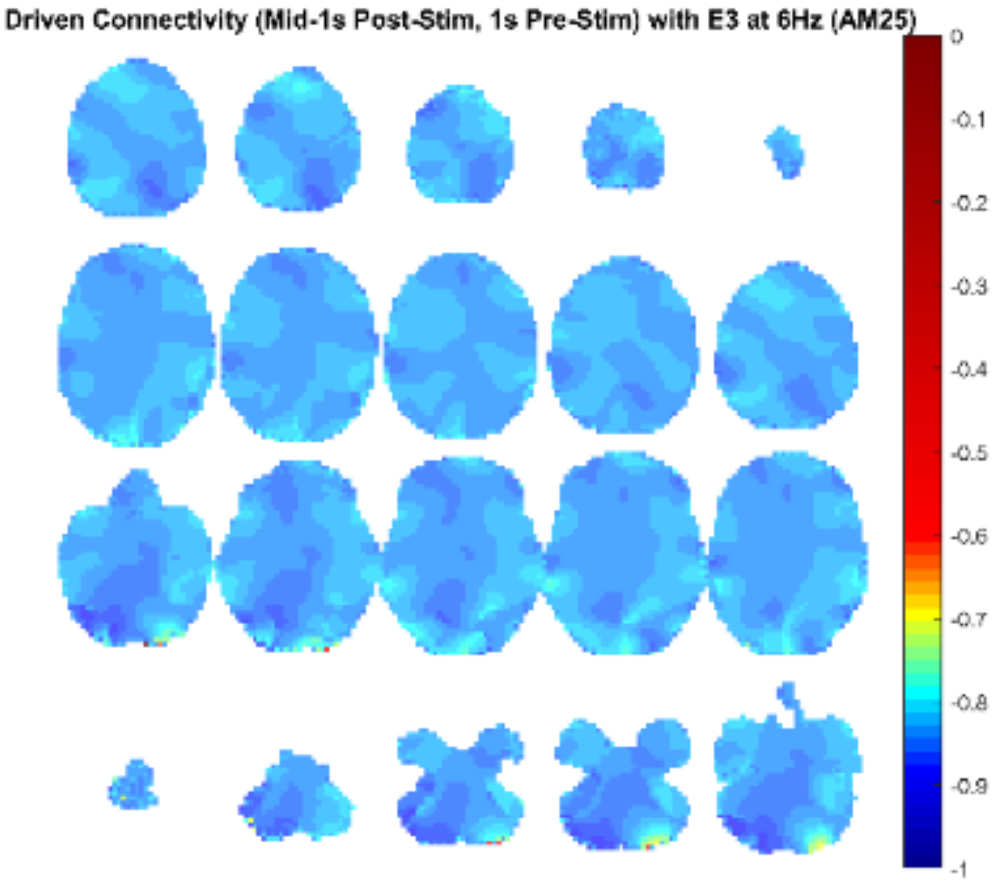

Figure 131. Source level connectivity with a dipole at E3 (right frontal) in 6 Hz during the middle one-second of 25 Hz amplitude modulated tone stimulation (total stimulation was 3 seconds), performed with DICS and a standardized BEM headmodel. Unit is the percent change in coherence from baseline (i.e., difference between coherence during stimulation and coherence during baseline divided by coherence during baseline). Darker reds indicate increases in coherence with E45 while darker blues indicate decreases in coherence.

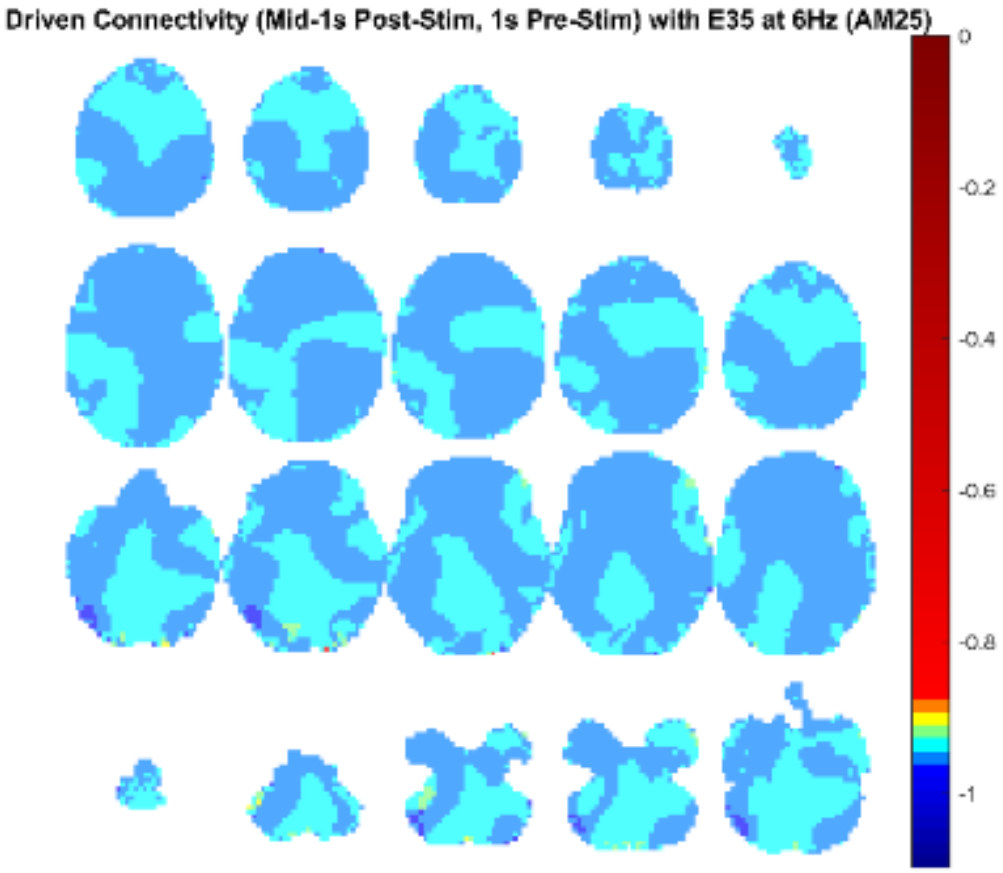

Figure 132. Source level connectivity with a dipole at E35 (left central) in 6 Hz during the middle one-second of 25 Hz amplitude modulated tone stimulation (total stimulation was 3 seconds), performed with DICS and a standardized BEM headmodel. Unit is the percent change in coherence from baseline (i.e., difference between coherence during stimulation and coherence during baseline divided by coherence during baseline). Darker reds indicate increases in coherence with E45 while darker blues indicate decreases in coherence.

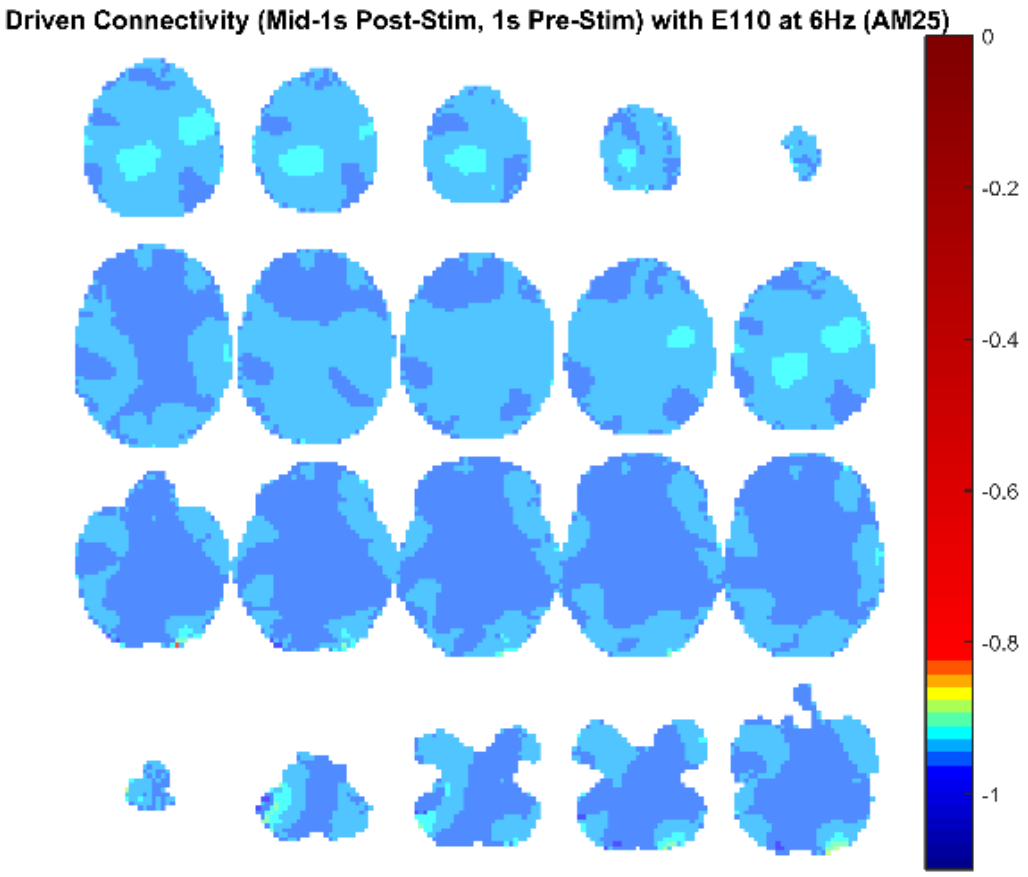

Figure 133. Source level connectivity with a dipole at E110 (right central) in 6 Hz during the middle one-second of 25 Hz amplitude modulated tone stimulation (total stimulation was 3 seconds), performed with DICS and a standardized BEM headmodel. Unit is the percent change in coherence from baseline (i.e., difference between coherence during stimulation and coherence during baseline divided by coherence during baseline). Darker reds indicate increases in coherence with E45 while darker blues indicate decreases in coherence.

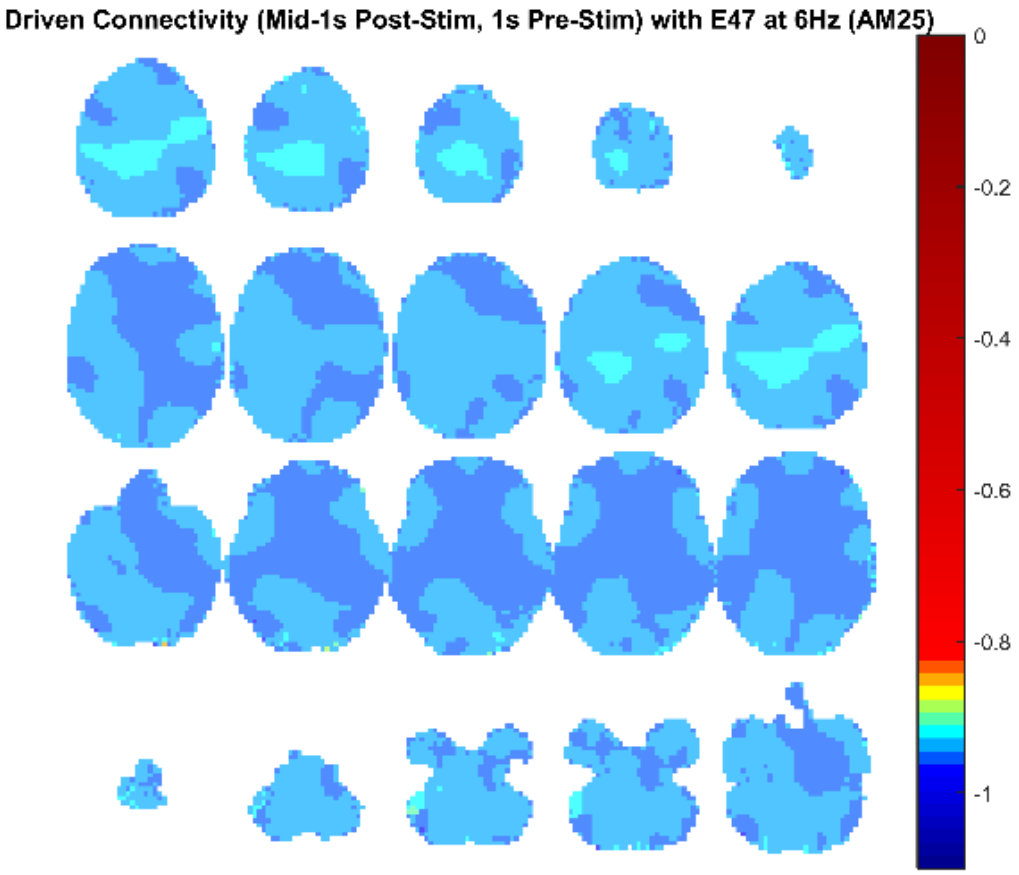

Figure 134. Source level connectivity with a dipole at E47 (left parietal) in 6 Hz during the middle one-second of 25 Hz amplitude modulated tone stimulation (total stimulation was 3 seconds), performed with DICS and a standardized BEM headmodel. Unit is the percent change in coherence from baseline (i.e., difference between coherence during stimulation and coherence during baseline divided by coherence during baseline). Darker reds indicate increases in coherence with E45 while darker blues indicate decreases in coherence.

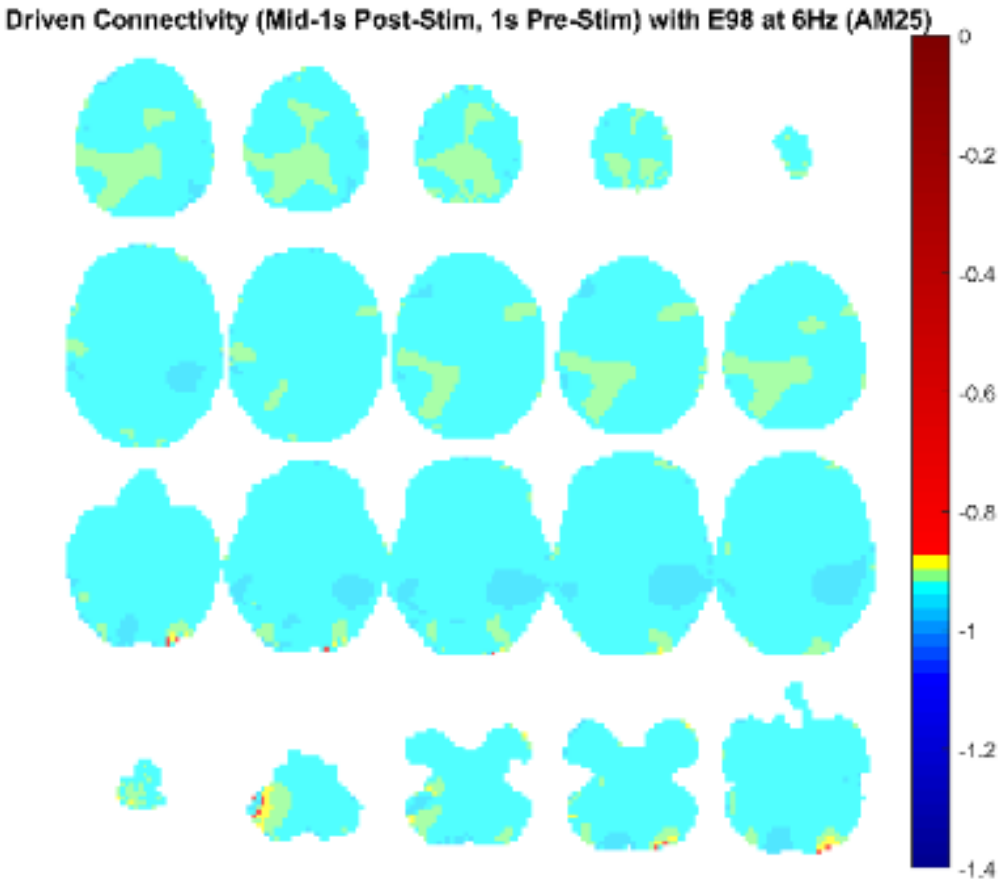

Figure 135. Source level connectivity with a dipole at E98 (right parietal) in 6 Hz during the middle one-second of 25 Hz amplitude modulated tone stimulation (total stimulation was 3 seconds), performed with DICS and a standardized BEM headmodel. Unit is the percent change in coherence from baseline (i.e., difference between coherence during stimulation and coherence during baseline divided by coherence during baseline). Darker reds indicate increases in coherence with E45 while darker blues indicate decreases in coherence.

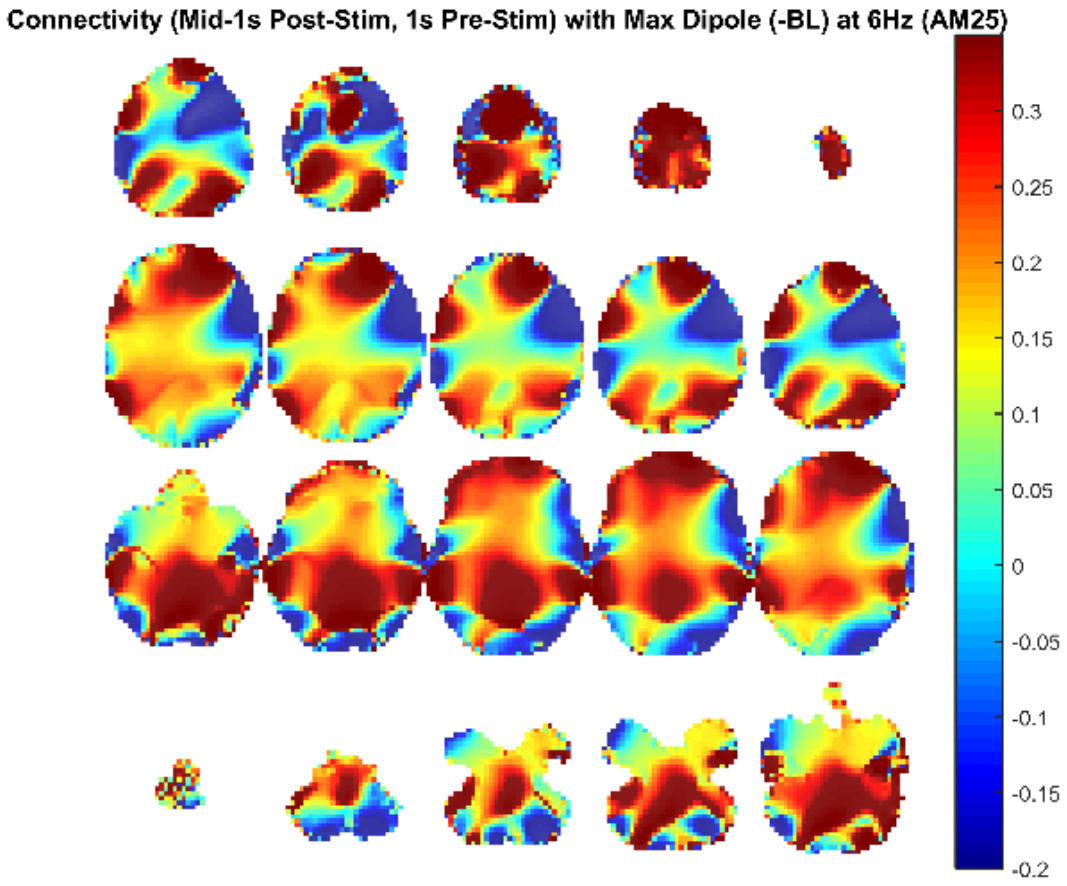

Figure 136. Source level connectivity with a dipole at dip2 (maximum power dipole for the middle one-second period corrected for the baseline one-second period) in 6 Hz during the middle one-second of 25 Hz amplitude modulated tone stimulation (total stimulation was 3 seconds), performed with DICS and a standardized BEM headmodel. Unit is the percent change in coherence from baseline (i.e., difference between coherence during stimulation and coherence during baseline divided by coherence during baseline). Darker reds indicate increases in coherence with E45 while darker blues indicate decreases in coherence.

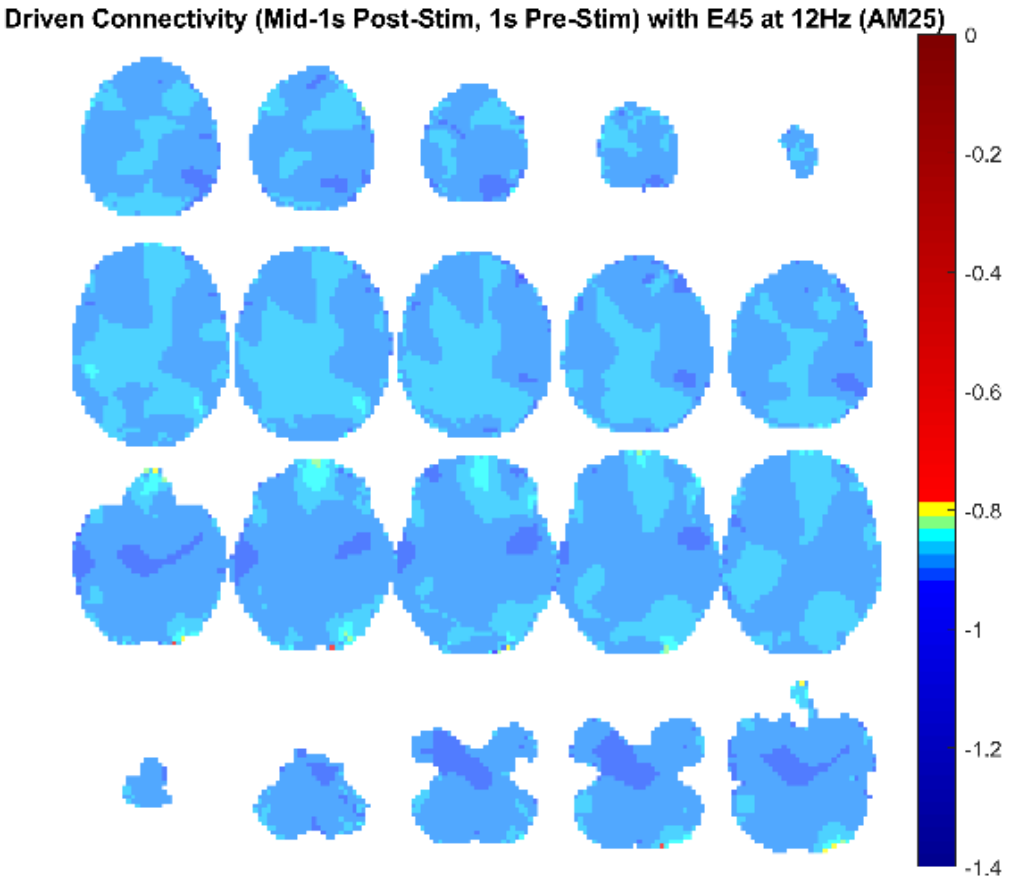

Figure 137. Source level connectivity with a dipole at E45 (left temporal, auditory cortex) in 12 Hz during the middle one-second of 25 Hz amplitude modulated tone stimulation (total stimulation was 3 seconds), performed with DICS and a standardized BEM headmodel. Unit is the percent change in coherence from baseline (i.e., difference between coherence during stimulation and coherence during baseline divided by coherence during baseline). Darker reds indicate increases in coherence with E45 while darker blues indicate decreases in coherence.

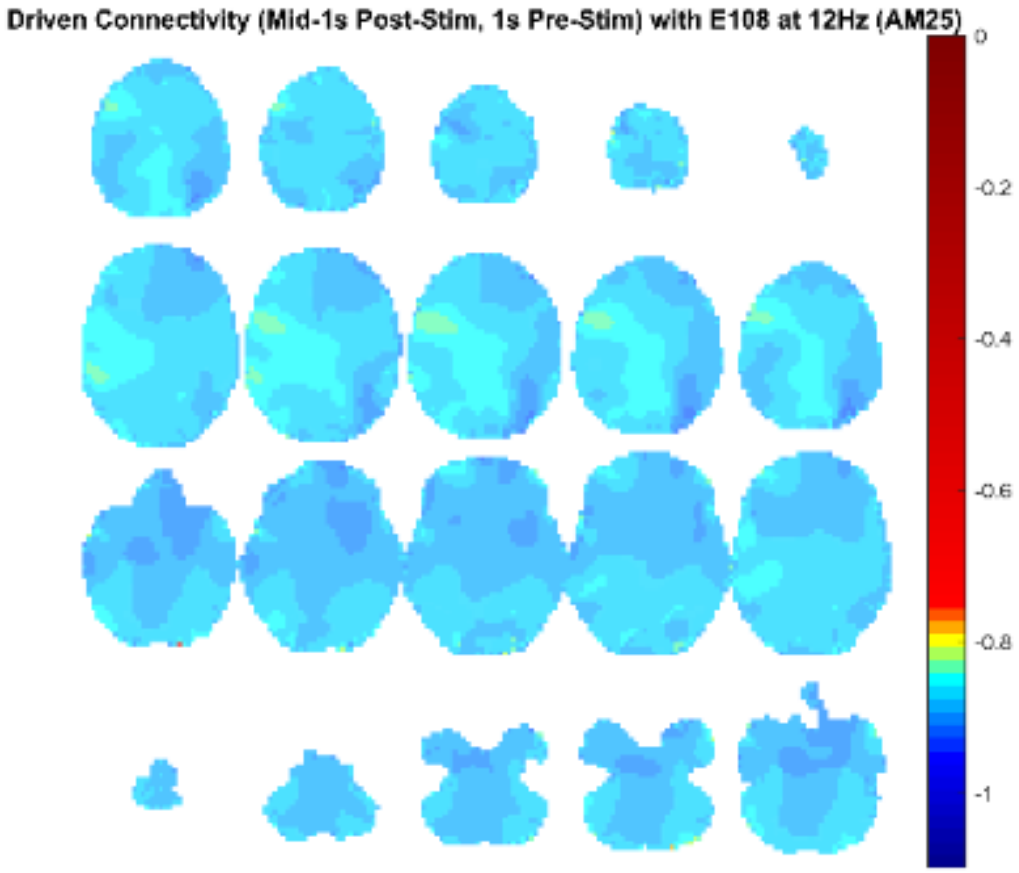

Figure 138. Source level connectivity with a dipole at E108 (right temporal, auditory cortex) in 12 Hz during the middle one-second of 25 Hz amplitude modulated tone stimulation (total stimulation was 3 seconds), performed with DICS and a standardized BEM headmodel. Unit is the percent change in coherence from baseline (i.e., difference between coherence during stimulation and coherence during baseline divided by coherence during baseline). Darker reds indicate increases in coherence with E45 while darker blues indicate decreases in coherence.

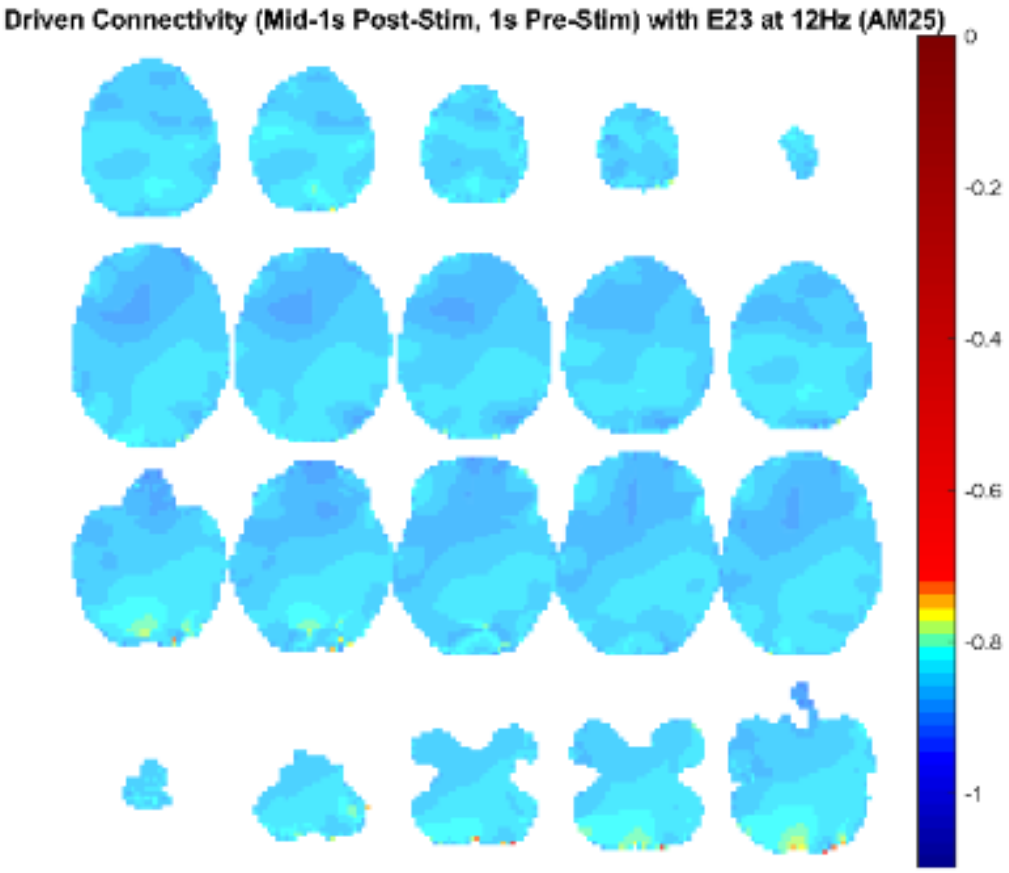

Figure 139. Source level connectivity with a dipole at E23 (left frontal) in 12 Hz during the middle one-second of 25 Hz amplitude modulated tone stimulation (total stimulation was 3 seconds), performed with DICS and a standardized BEM headmodel. Unit is the percent change in coherence from baseline (i.e., difference between coherence during stimulation and coherence during baseline divided by coherence during baseline). Darker reds indicate increases in coherence with E45 while darker blues indicate decreases in coherence.

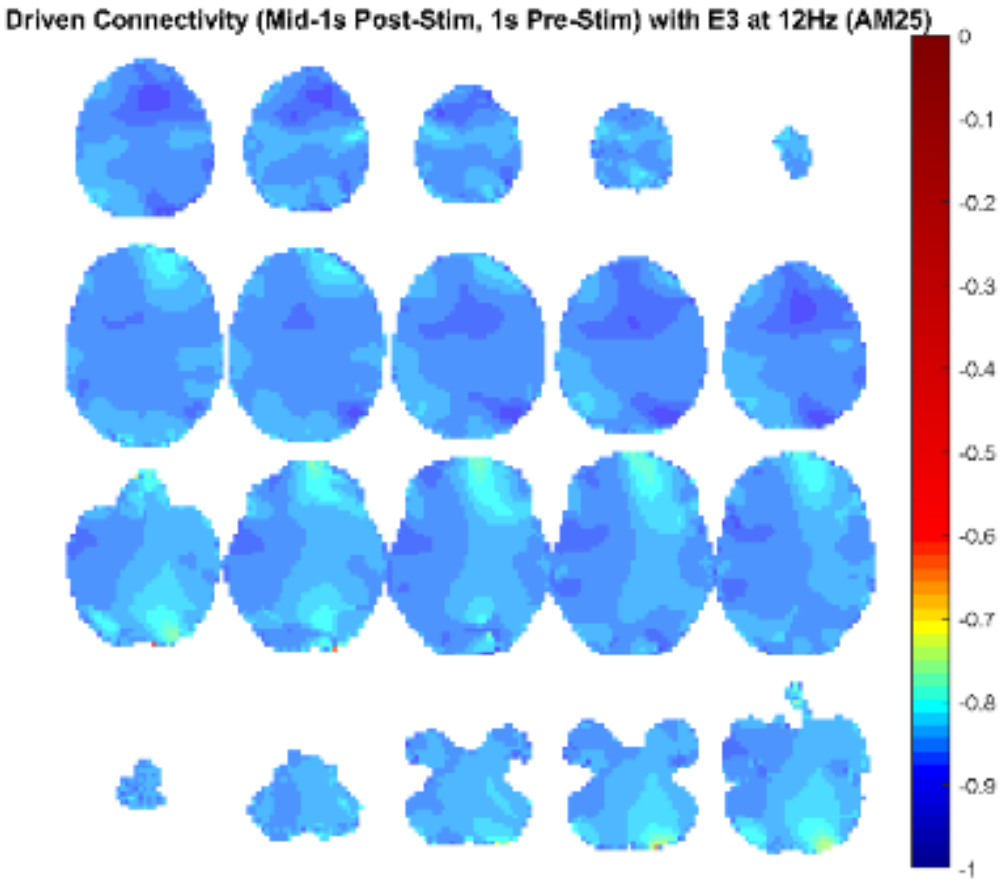

Figure 140. Source level connectivity with a dipole at E3 (right frontal) in 12 Hz during the middle one-second of 25 Hz amplitude modulated tone stimulation (total stimulation was 3 seconds), performed with DICS and a standardized BEM headmodel. Unit is the percent change in coherence from baseline (i.e., difference between coherence during stimulation and coherence during baseline divided by coherence during baseline). Darker reds indicate increases in coherence with E45 while darker blues indicate decreases in coherence.

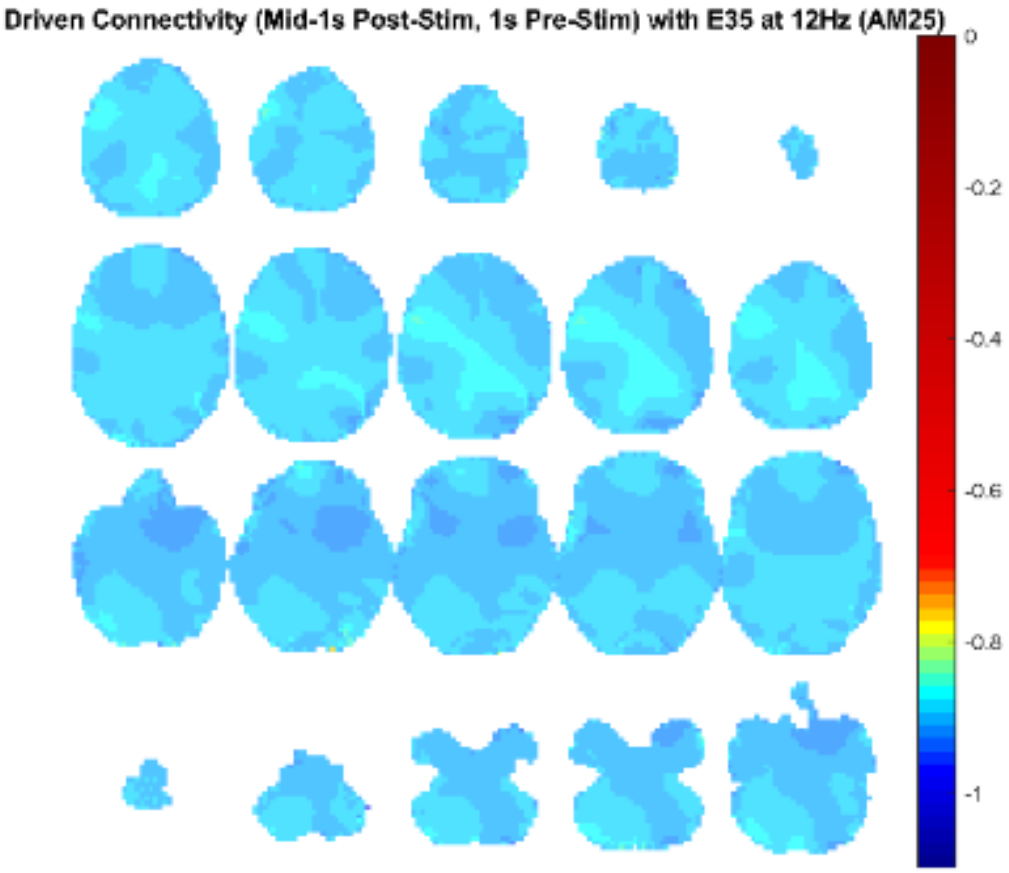

Figure 141. Source level connectivity with a dipole at E35 (left central) in 12 Hz during the middle one-second of 25 Hz amplitude modulated tone stimulation (total stimulation was 3 seconds), performed with DICS and a standardized BEM headmodel. Unit is the percent change in coherence from baseline (i.e., difference between coherence during stimulation and coherence during baseline divided by coherence during baseline). Darker reds indicate increases in coherence with E45 while darker blues indicate decreases in coherence.

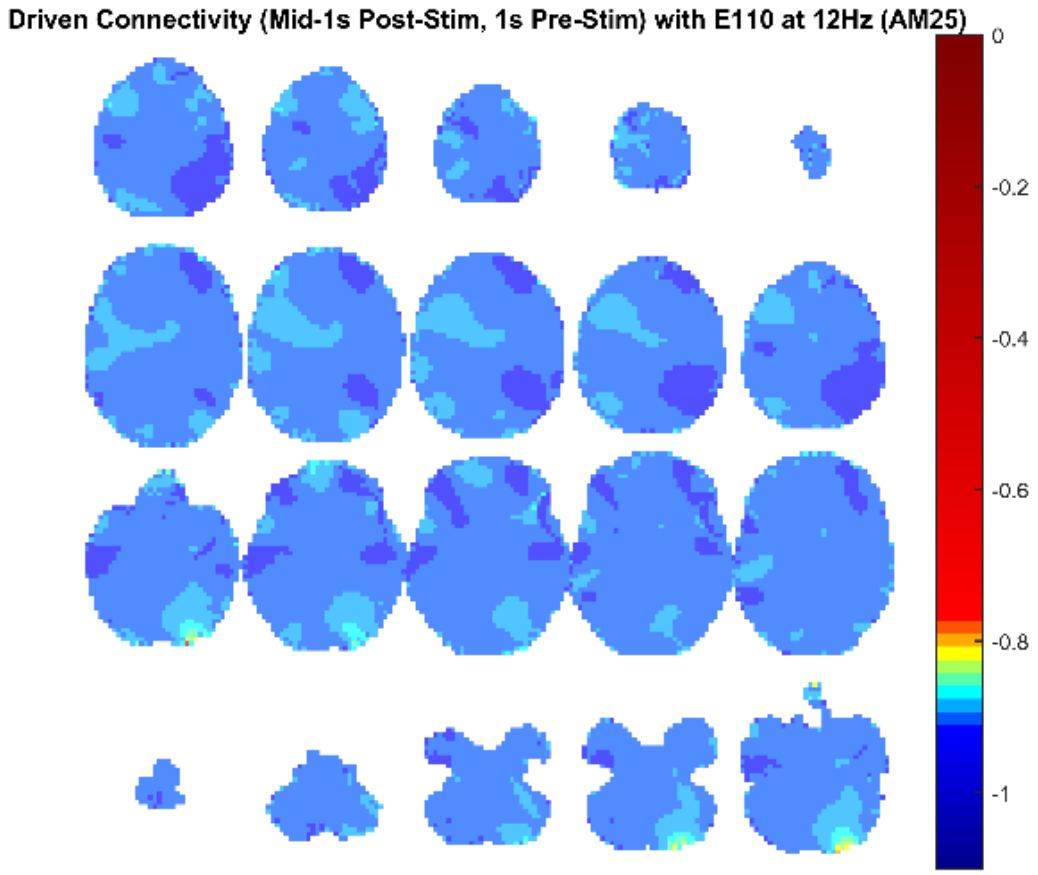

Figure 142. Source level connectivity with a dipole at E110 (right central) in 12 Hz during the middle one-second of 25 Hz amplitude modulated tone stimulation (total stimulation was 3 seconds), performed with DICS and a standardized BEM headmodel. Unit is the percent change in coherence from baseline (i.e., difference between coherence during stimulation and coherence during baseline divided by coherence during baseline). Darker reds indicate increases in coherence with E45 while darker blues indicate decreases in coherence.

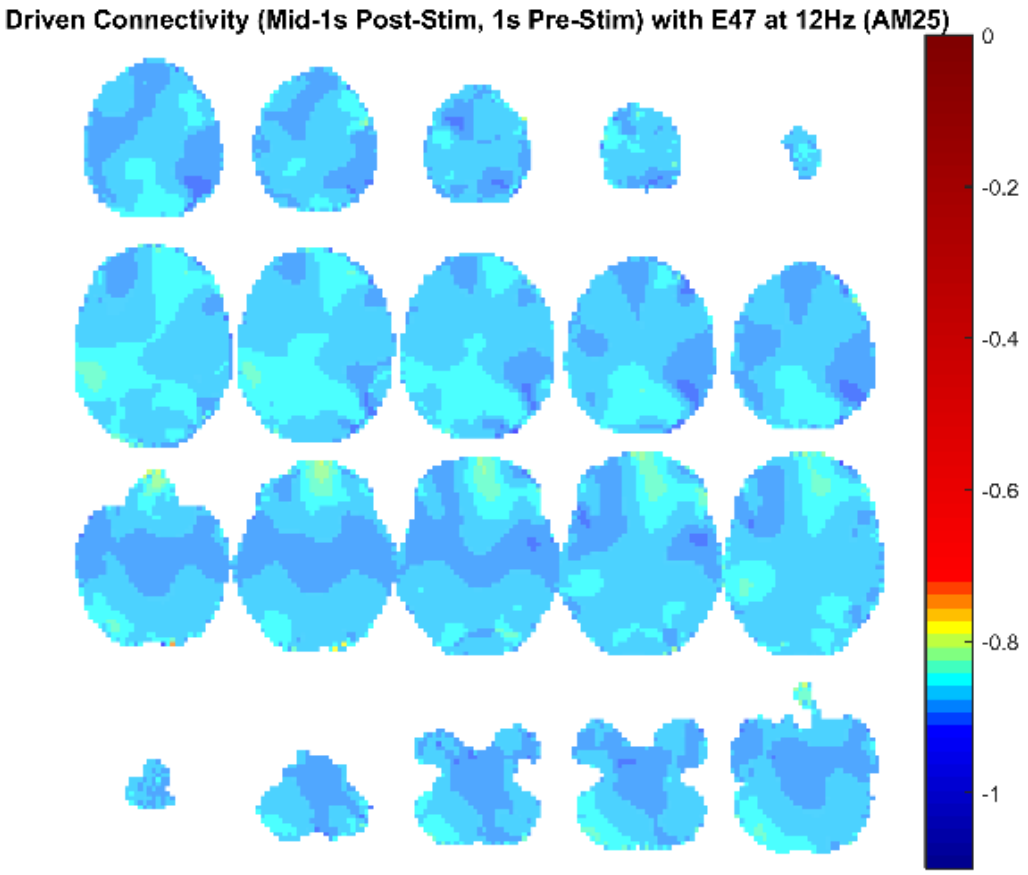

Figure 143. Source level connectivity with a dipole at E47 (left parietal) in 12 Hz during the middle one-second of 25 Hz amplitude modulated tone stimulation (total stimulation was 3 seconds), performed with DICS and a standardized BEM headmodel. Unit is the percent change in coherence from baseline (i.e., difference between coherence during stimulation and coherence during baseline divided by coherence during baseline). Darker reds indicate increases in coherence with E45 while darker blues indicate decreases in coherence.

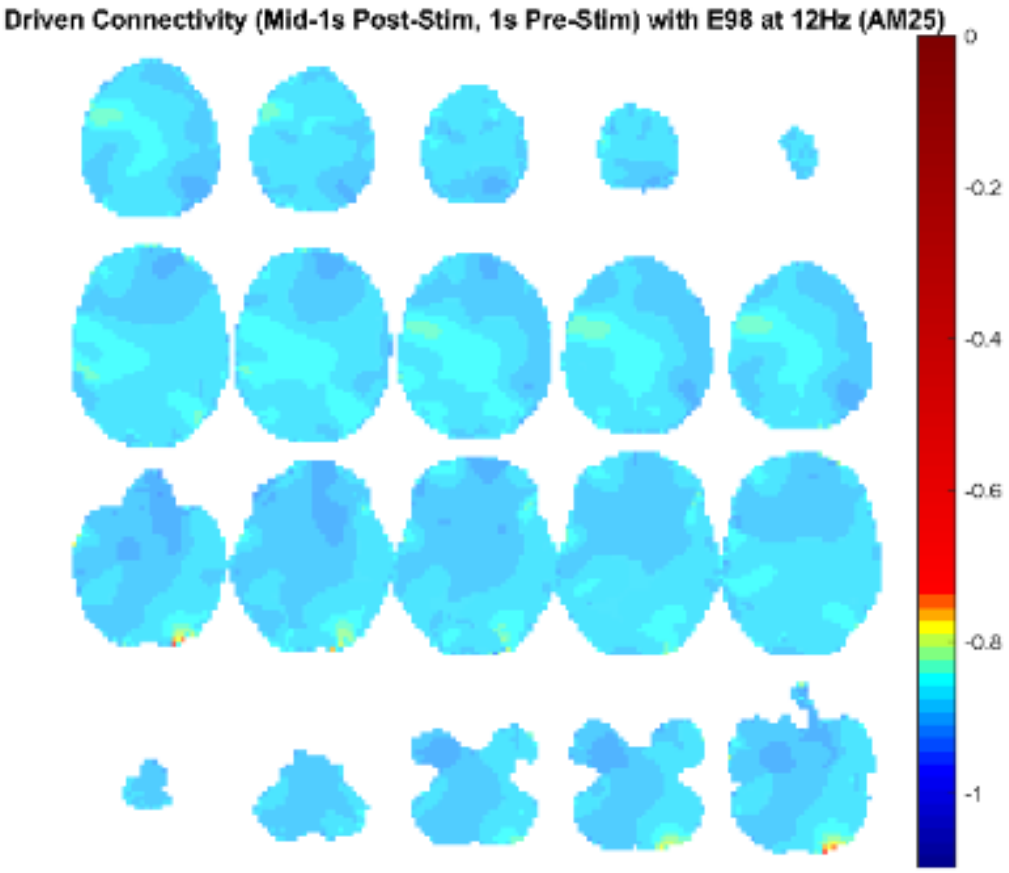

Figure 144. Source level connectivity with a dipole at E98 (right parietal) in 12 Hz during the middle one-second of 25 Hz amplitude modulated tone stimulation (total stimulation was 3 seconds), performed with DICS and a standardized BEM headmodel. Unit is the percent change in coherence from baseline (i.e., difference between coherence during stimulation and coherence during baseline divided by coherence during baseline). Darker reds indicate increases in coherence with E45 while darker blues indicate decreases in coherence.

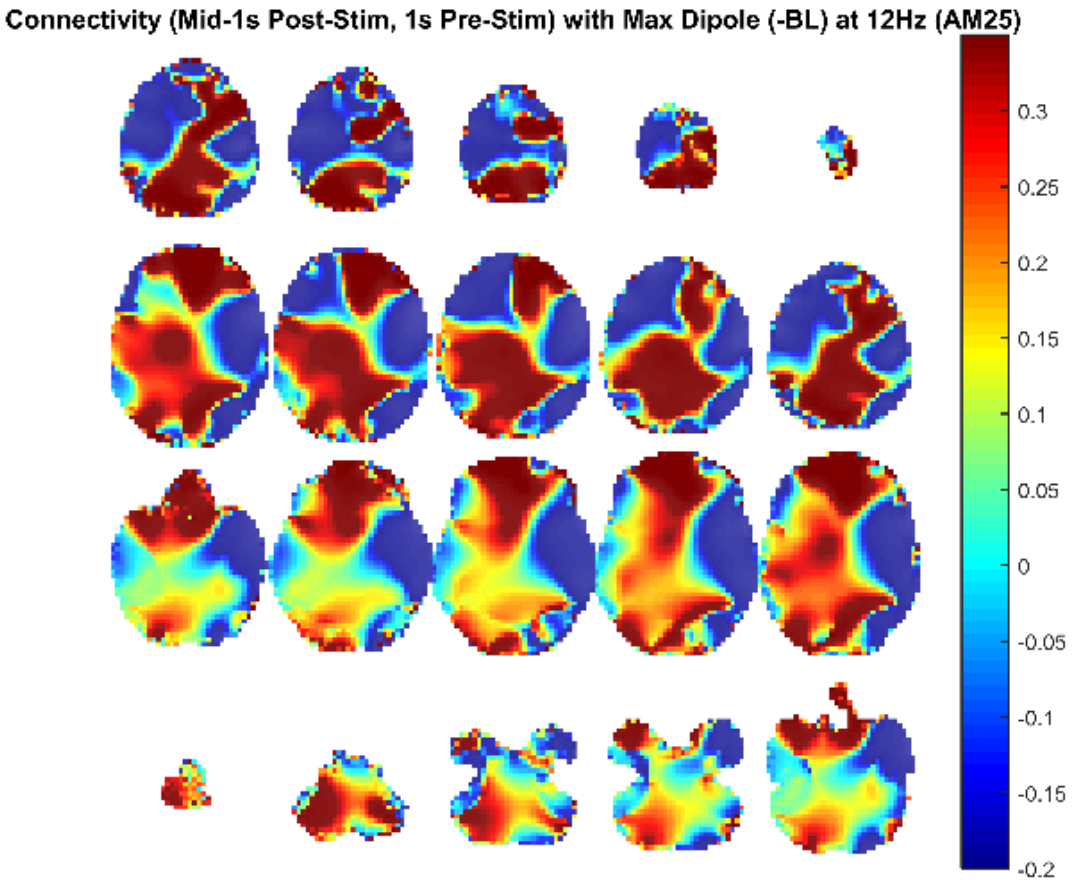

Figure 145. Source level connectivity with a dipole at dip2 (maximum power dipole for the middle one-second period corrected for the baseline one-second period) in 12 Hz during the middle one-second of 25 Hz amplitude modulated tone stimulation (total stimulation was 3 seconds), performed with DICS and a standardized BEM headmodel. Unit is the percent change in coherence from baseline (i.e., difference between coherence during stimulation and coherence during baseline divided by coherence during baseline). Darker reds indicate increases in coherence with E45 while darker blues indicate decreases in coherence.

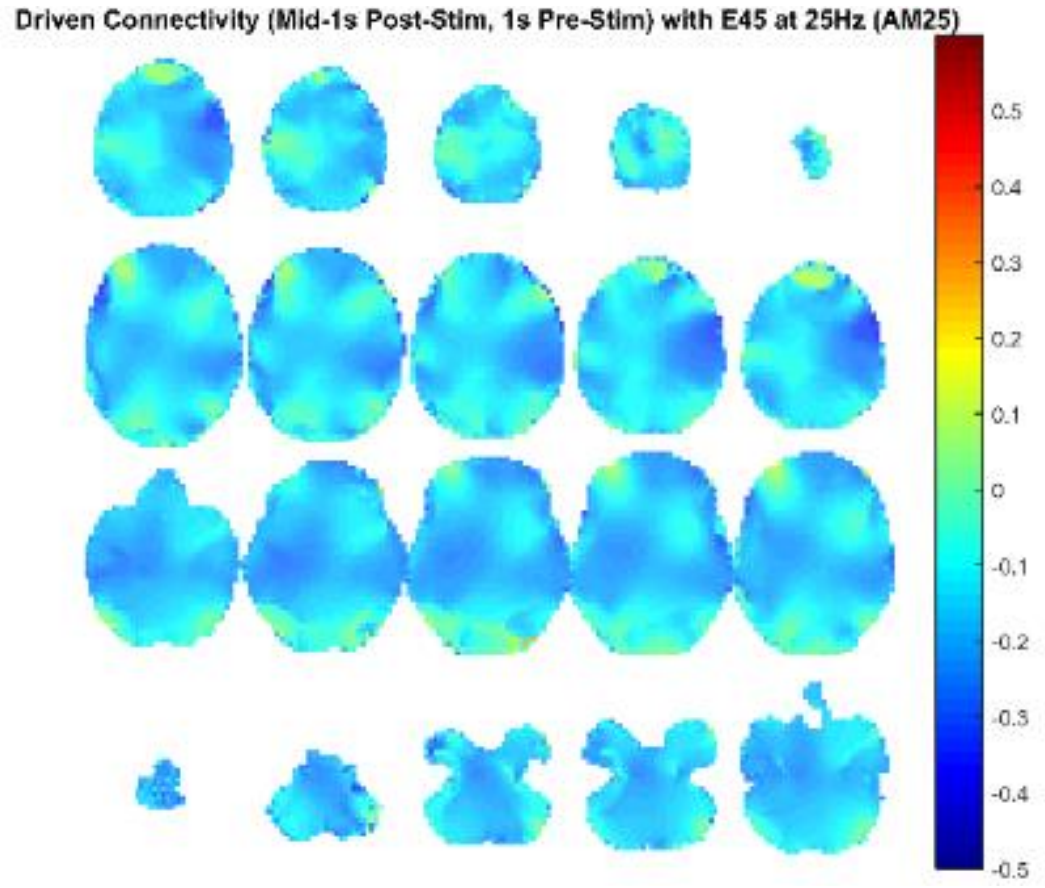

Figure 146. Source level connectivity with a dipole at E45 (left temporal, auditory cortex) in 25 Hz during the middle one-second of 25 Hz amplitude modulated tone stimulation (total stimulation was 3 seconds), performed with DICS and a standardized BEM headmodel. Unit is the percent change in coherence from baseline (i.e., difference between coherence during stimulation and coherence during baseline divided by coherence during baseline). Darker reds indicate increases in coherence with E45 while darker blues indicate decreases in coherence.

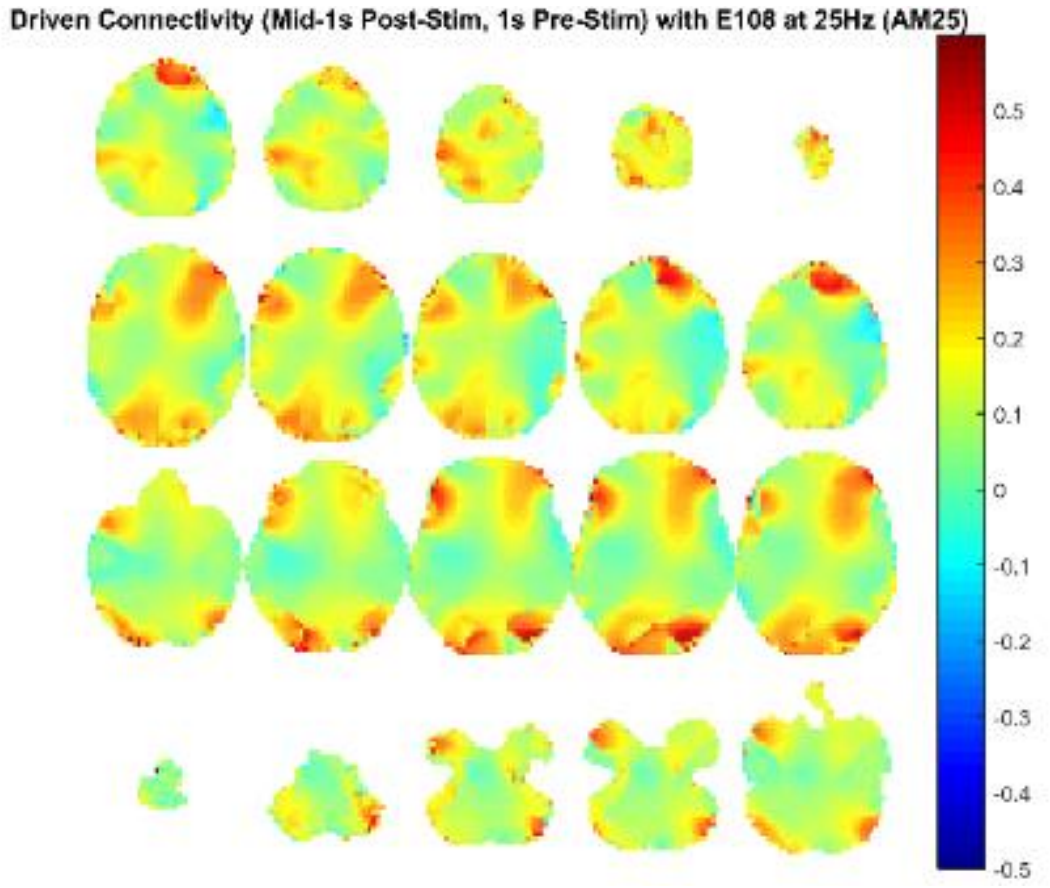

Figure 147. Source level connectivity with a dipole at E108 (right temporal, auditory cortex) in 25 Hz during the middle one-second of 25 Hz amplitude modulated tone stimulation (total stimulation was 3 seconds), performed with DICS and a standardized BEM headmodel. Unit is the percent change in coherence from baseline (i.e., difference between coherence during stimulation and coherence during baseline divided by coherence during baseline). Darker reds indicate increases in coherence with E45 while darker blues indicate decreases in coherence.

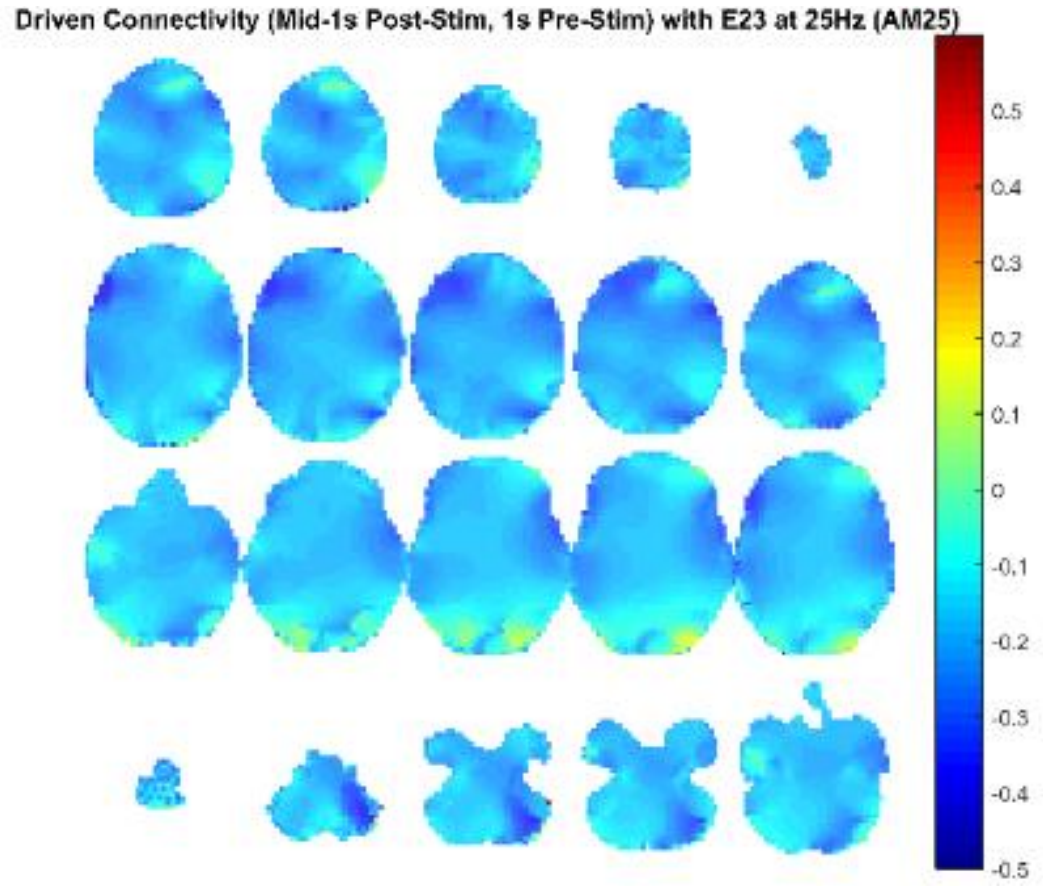

Figure 148. Source level connectivity with a dipole at E23 (left frontal) in 25 Hz during the middle one-second of 25 Hz amplitude modulated tone stimulation (total stimulation was 3 seconds), performed with DICS and a standardized BEM headmodel. Unit is the percent change in coherence from baseline (i.e., difference between coherence during stimulation and coherence during baseline divided by coherence during baseline). Darker reds indicate increases in coherence with E45 while darker blues indicate decreases in coherence.

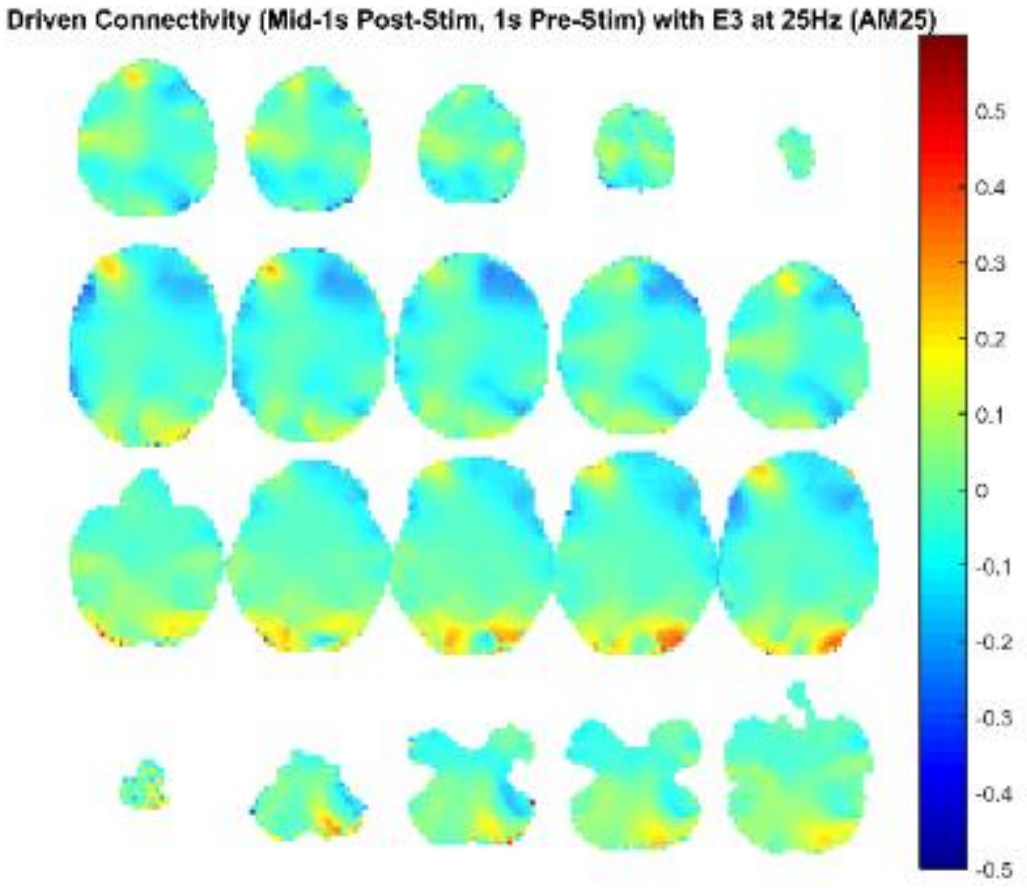

Figure 149. Source level connectivity with a dipole at E3 (right frontal) in 25 Hz during the middle one-second of 25 Hz amplitude modulated tone stimulation (total stimulation was 3 seconds), performed with DICS and a standardized BEM headmodel. Unit is the percent change in coherence from baseline (i.e., difference between coherence during stimulation and coherence during baseline divided by coherence during baseline). Darker reds indicate increases in coherence with E45 while darker blues indicate decreases in coherence.

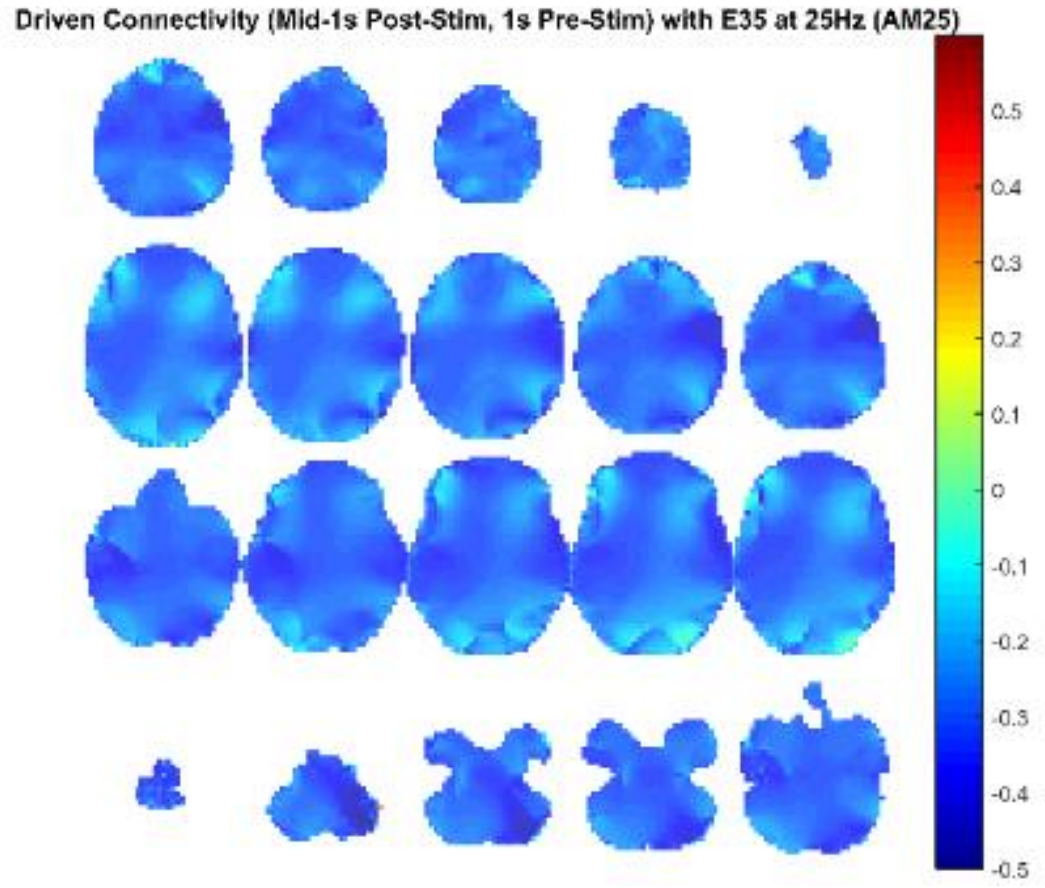

Figure 150. Source level connectivity with a dipole at E35 (left central) in 25 Hz during the middle one-second of 25 Hz amplitude modulated tone stimulation (total stimulation was 3 seconds), performed with DICS and a standardized BEM headmodel. Unit is the percent change in coherence from baseline (i.e., difference between coherence during stimulation and coherence during baseline divided by coherence during baseline). Darker reds indicate increases in coherence with E45 while darker blues indicate decreases in coherence.

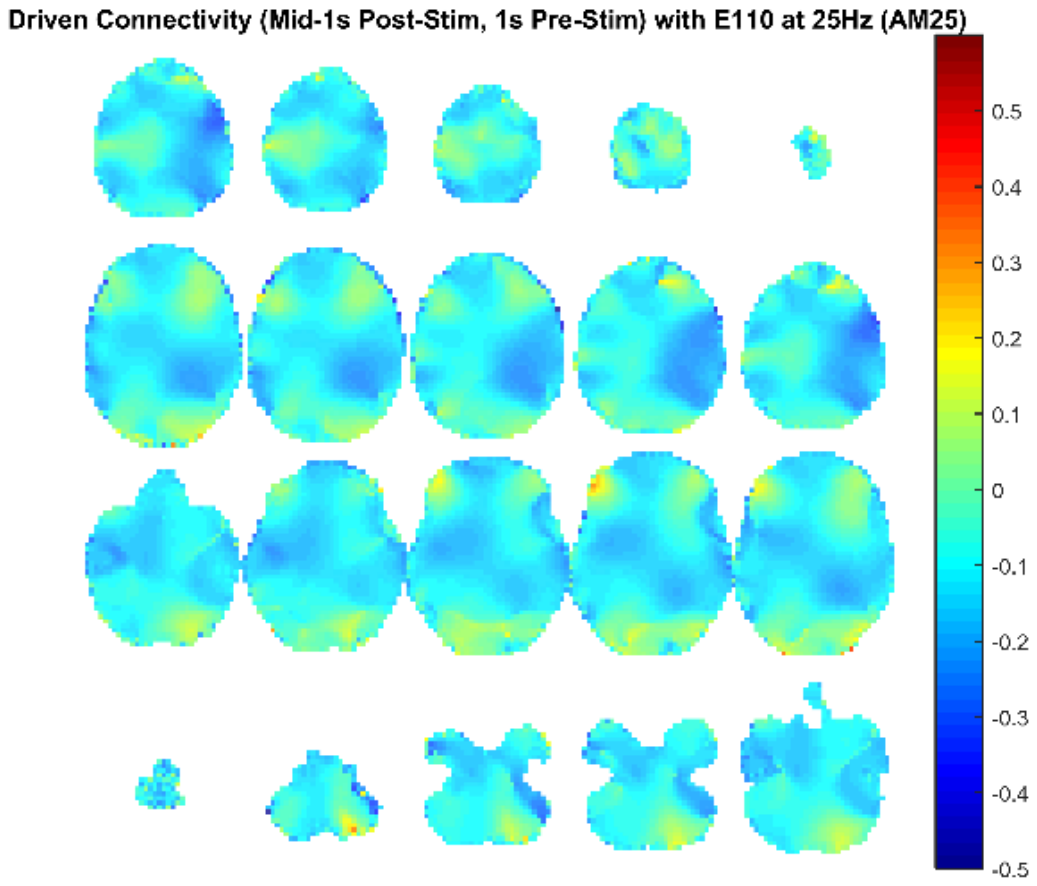

Figure 151. Source level connectivity with a dipole at E110 (right central) in 25 Hz during the middle one-second of 25 Hz amplitude modulated tone stimulation (total stimulation was 3 seconds), performed with DICS and a standardized BEM headmodel. Unit is the percent change in coherence from baseline (i.e., difference between coherence during stimulation and coherence during baseline divided by coherence during baseline). Darker reds indicate increases in coherence with E45 while darker blues indicate decreases in coherence.

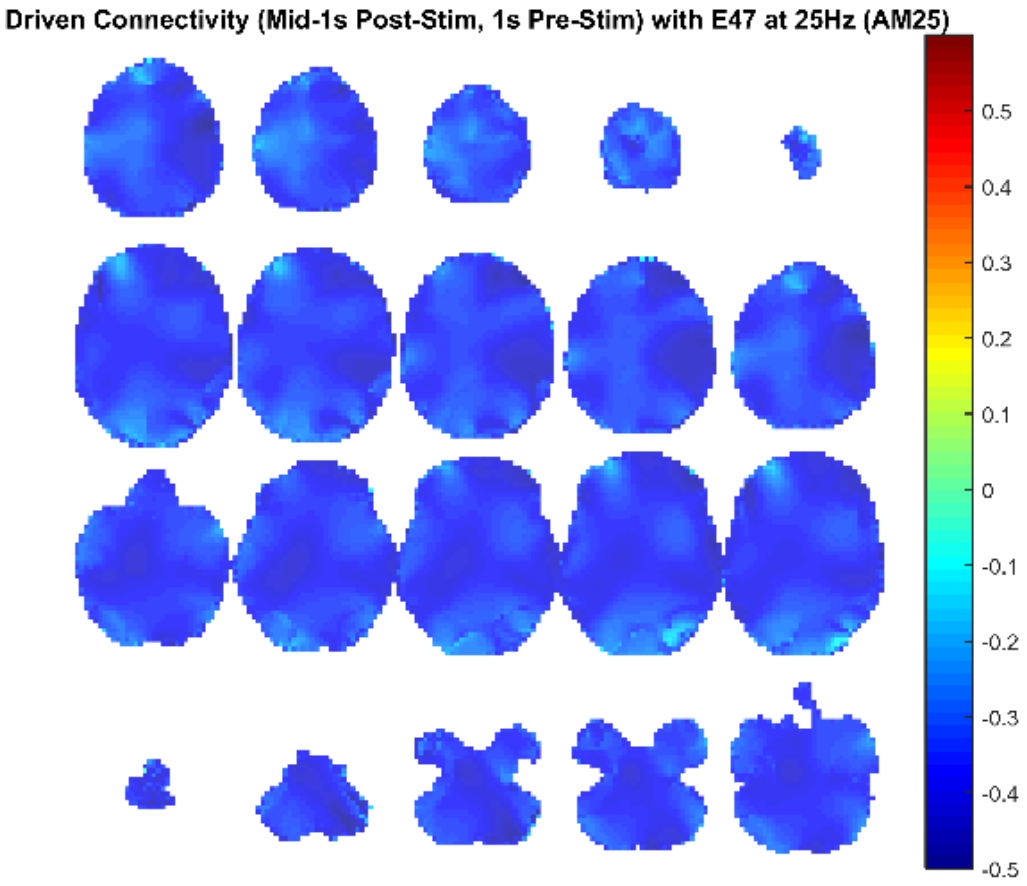

Figure 152. Source level connectivity with a dipole at E47 (left parietal) in 25 Hz during the middle one-second of 25 Hz amplitude modulated tone stimulation (total stimulation was 3 seconds), performed with DICS and a standardized BEM headmodel. Unit is the percent change in coherence from baseline (i.e., difference between coherence during stimulation and coherence during baseline divided by coherence during baseline). Darker reds indicate increases in coherence with E45 while darker blues indicate decreases in coherence.

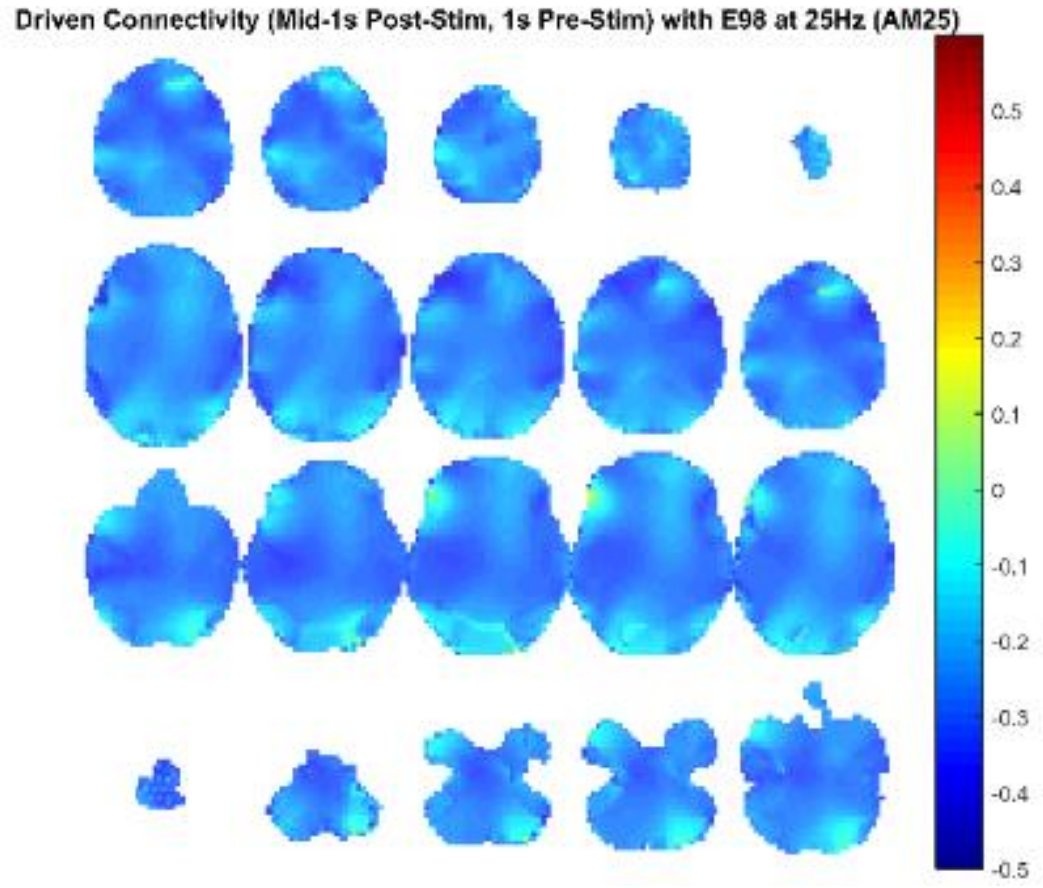

Figure 153. Source level connectivity with a dipole at E98 (right parietal) in 25 Hz during the middle one-second of 25 Hz amplitude modulated tone stimulation (total stimulation was 3 seconds), performed with DICS and a standardized BEM headmodel. Unit is the percent change in coherence from baseline (i.e., difference between coherence during stimulation and coherence during baseline divided by coherence during baseline). Darker reds indicate increases in coherence with E45 while darker blues indicate decreases in coherence.

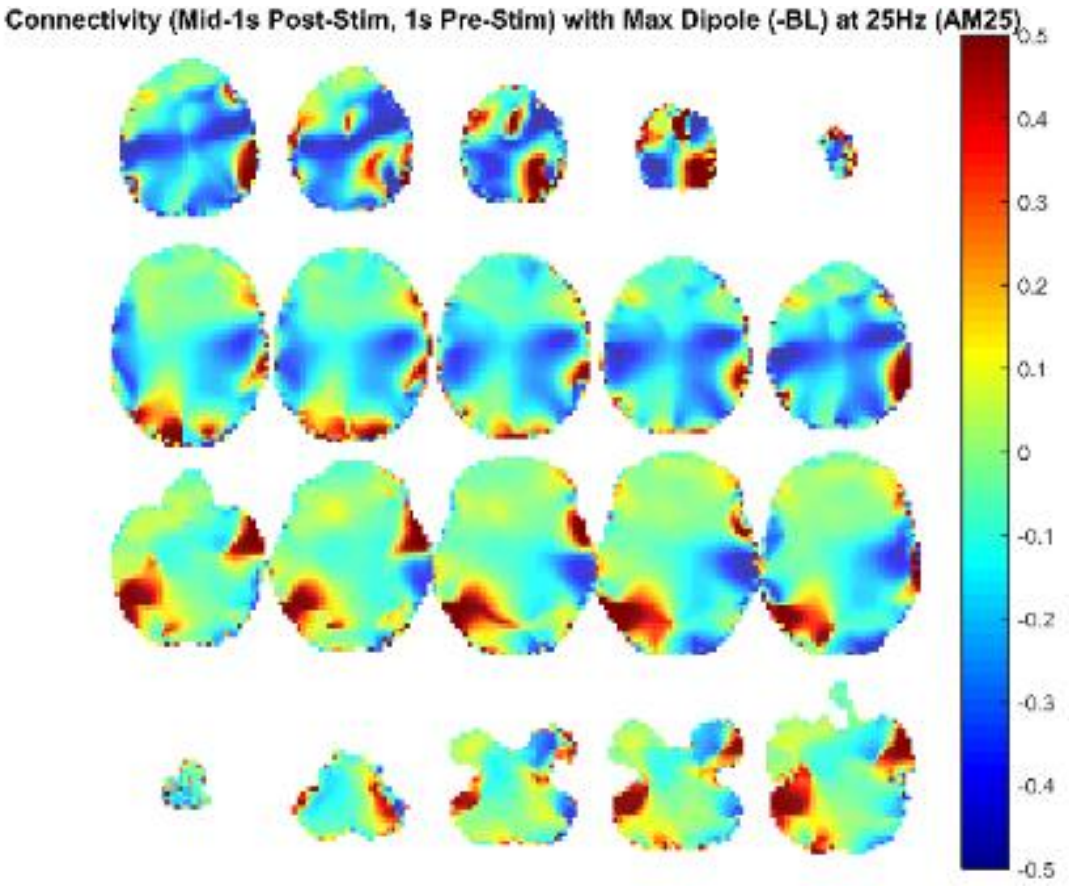

Figure 154. Source level connectivity with a dipole at dip2 (maximum power dipole for the middle one-second period corrected for the baseline one-second period) in 25 Hz during the middle one-second of 25 Hz amplitude modulated tone stimulation (total stimulation was 3 seconds), performed with DICS and a standardized BEM headmodel. Unit is the percent change in coherence from baseline (i.e., difference between coherence during stimulation and coherence during baseline divided by coherence during baseline). Darker reds indicate increases in coherence with E45 while darker blues indicate decreases in coherence.

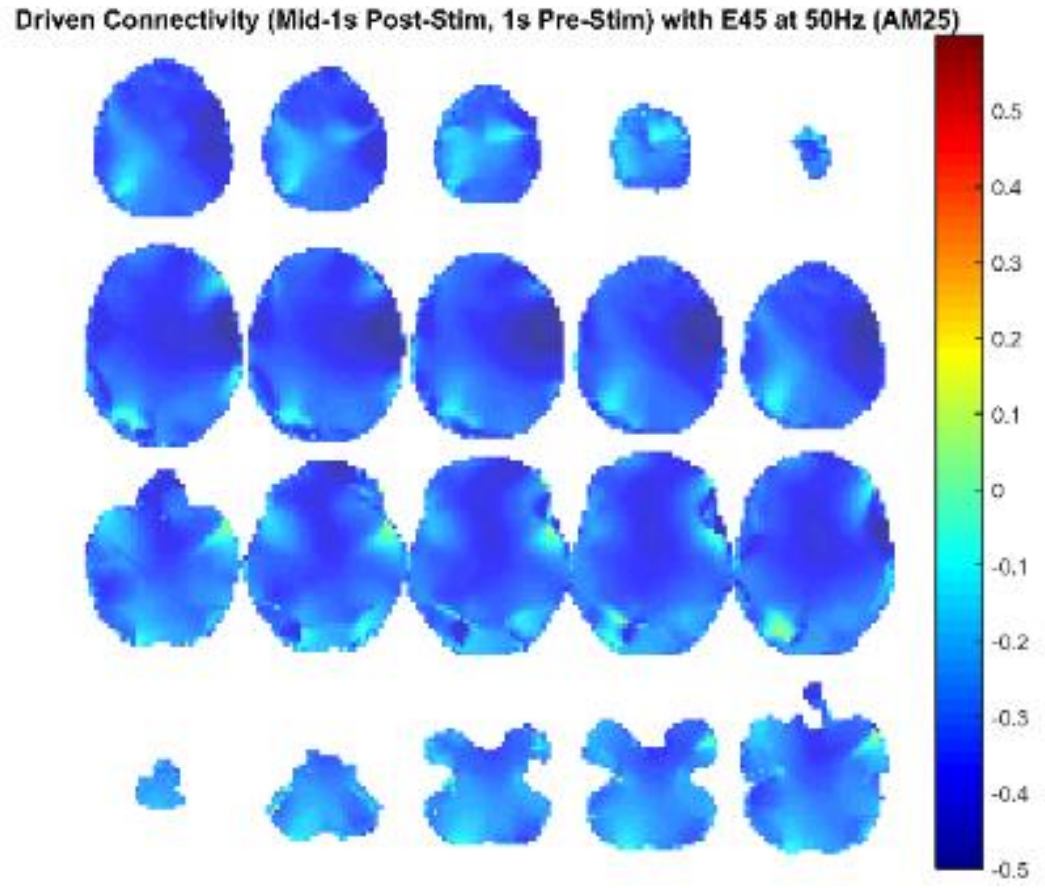

Figure 155. Source level connectivity with a dipole at E45 (left temporal, auditory cortex) in 50 Hz during the middle one-second of 25 Hz amplitude modulated tone stimulation (total stimulation was 3 seconds), performed with DICS and a standardized BEM headmodel. Unit is the percent change in coherence from baseline (i.e., difference between coherence during stimulation and coherence during baseline divided by coherence during baseline). Darker reds indicate increases in coherence with E45 while darker blues indicate decreases in coherence.

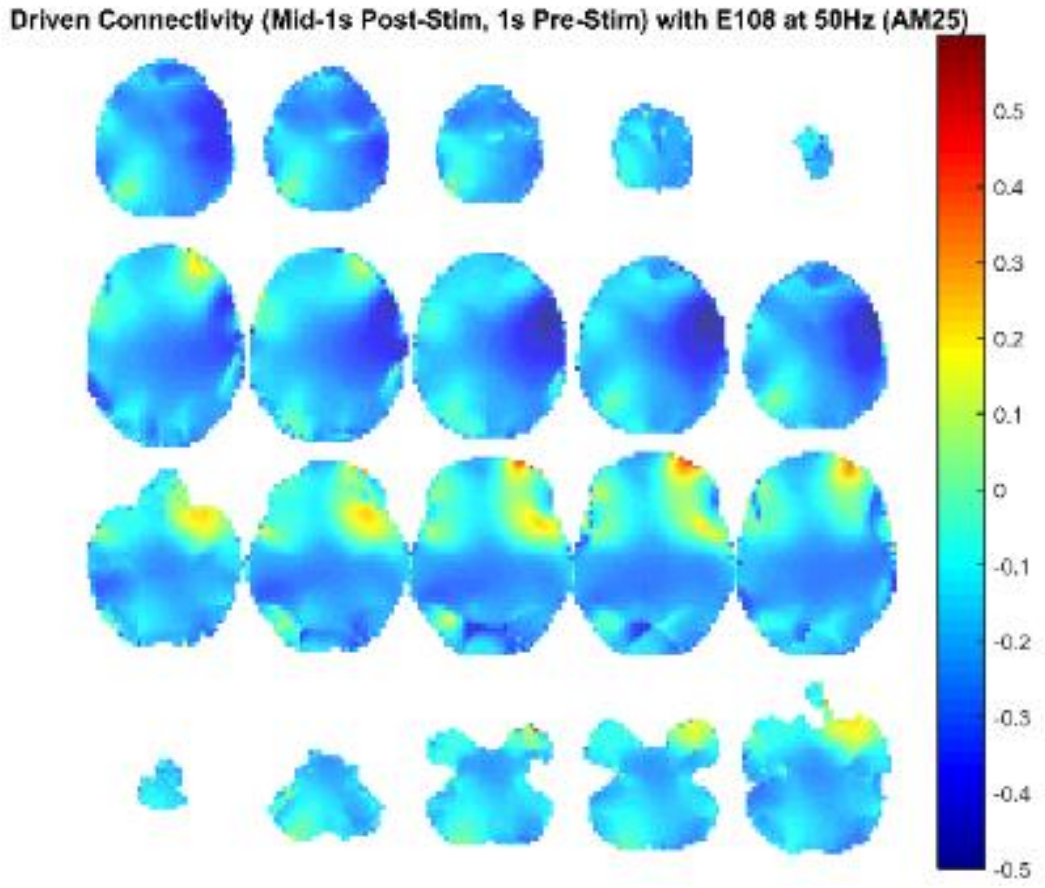

Figure 156. Source level connectivity with a dipole at E108 (right temporal, auditory cortex) in 50 Hz during the middle one-second of 25 Hz amplitude modulated tone stimulation (total stimulation was 3 seconds), performed with DICS and a standardized BEM headmodel. Unit is the percent change in coherence from baseline (i.e., difference between coherence during stimulation and coherence during baseline divided by coherence during baseline). Darker reds indicate increases in coherence with E45 while darker blues indicate decreases in coherence.

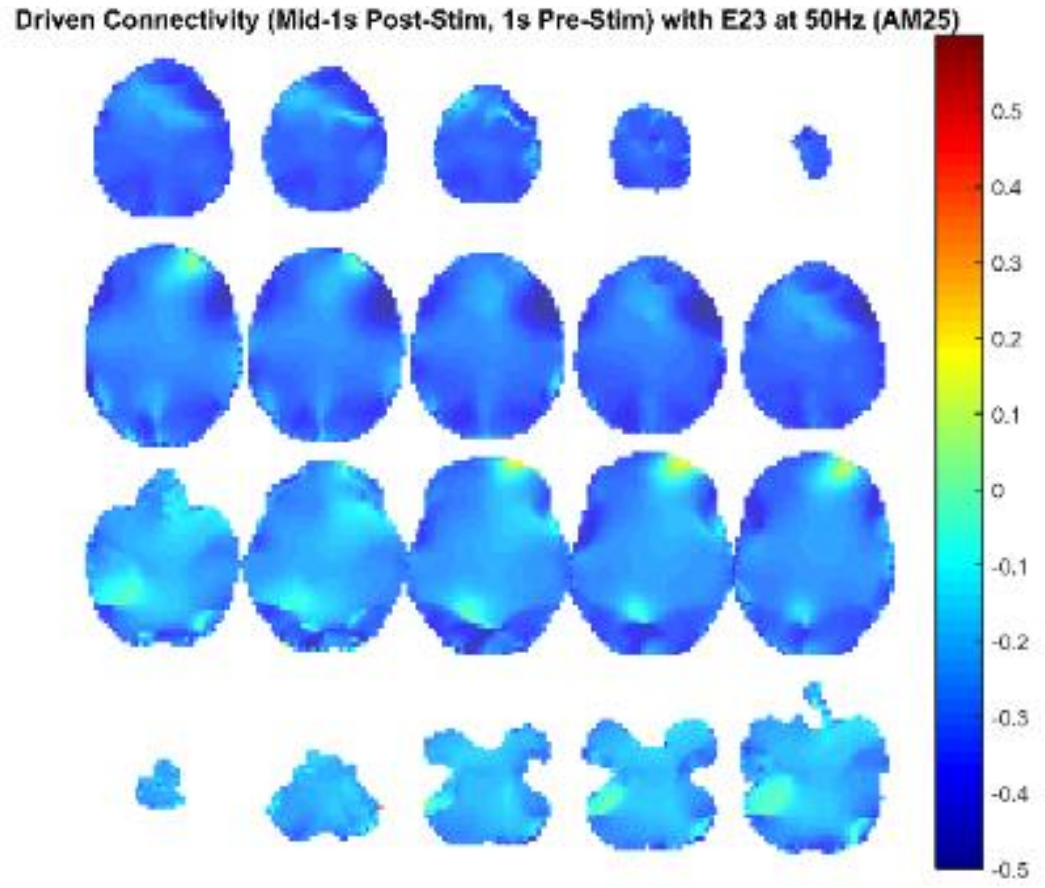

Figure 157. Source level connectivity with a dipole at E23 (left frontal) in 50 Hz during the middle one-second of 25 Hz amplitude modulated tone stimulation (total stimulation was 3 seconds), performed with DICS and a standardized BEM headmodel. Unit is the percent change in coherence from baseline (i.e., difference between coherence during stimulation and coherence during baseline divided by coherence during baseline). Darker reds indicate increases in coherence with E45 while darker blues indicate decreases in coherence.

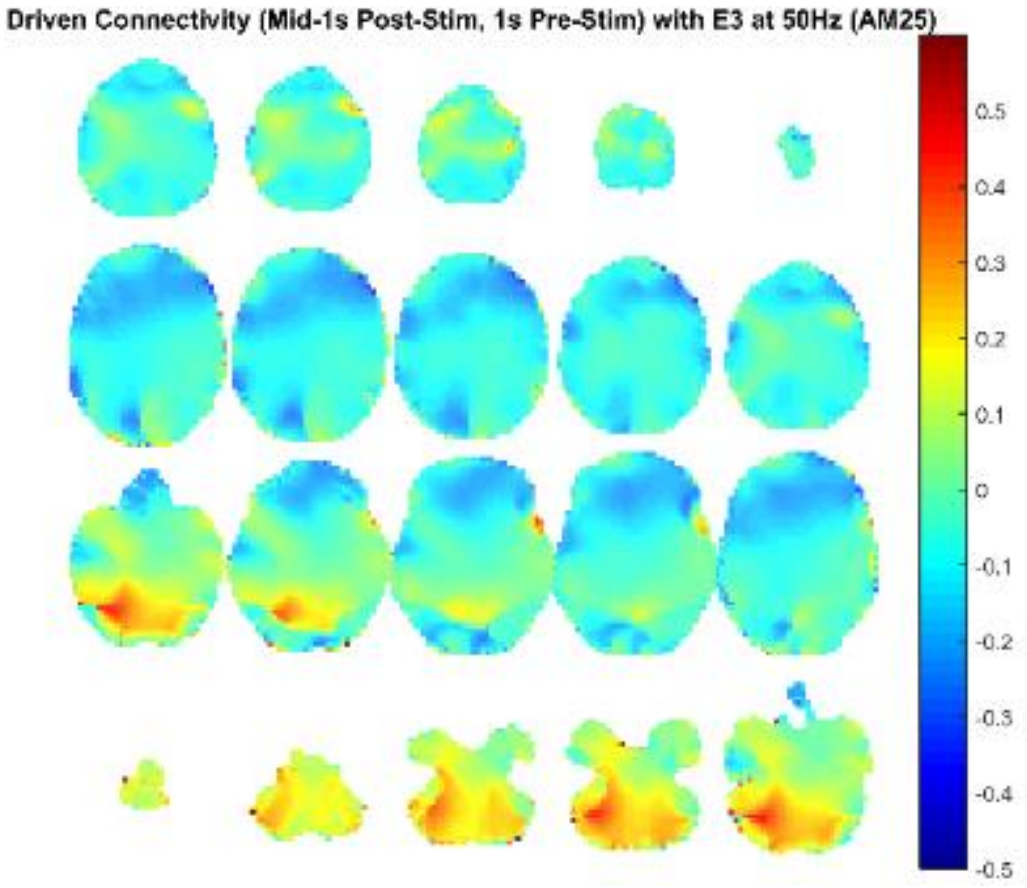

Figure 158. Source level connectivity with a dipole at E3 (right frontal) in 50 Hz during the middle one-second of 25 Hz amplitude modulated tone stimulation (total stimulation was 3 seconds), performed with DICS and a standardized BEM headmodel. Unit is the percent change in coherence from baseline (i.e., difference between coherence during stimulation and coherence during baseline divided by coherence during baseline). Darker reds indicate increases in coherence with E45 while darker blues indicate decreases in coherence.

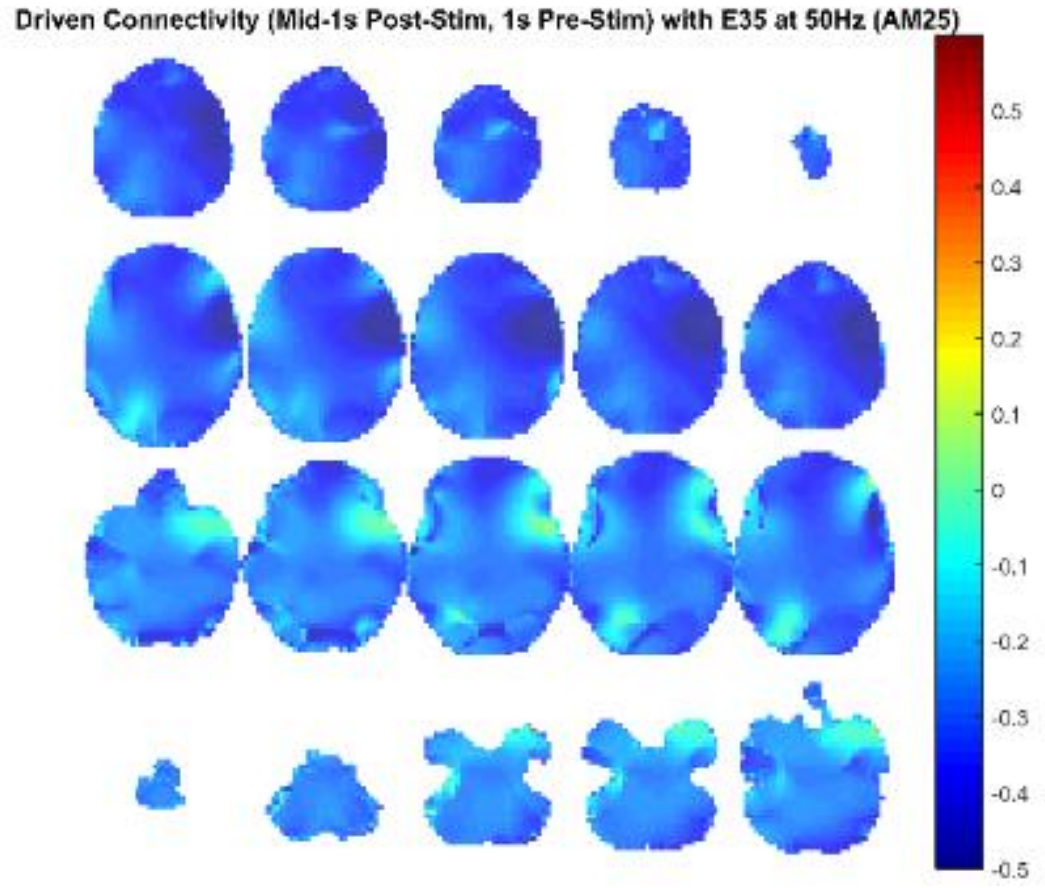

Figure 159. Source level connectivity with a dipole at E35 (left central) in 50 Hz during the middle one-second of 25 Hz amplitude modulated tone stimulation (total stimulation was 3 seconds), performed with DICS and a standardized BEM headmodel. Unit is the percent change in coherence from baseline (i.e., difference between coherence during stimulation and coherence during baseline divided by coherence during baseline). Darker reds indicate increases in coherence with E45 while darker blues indicate decreases in coherence.

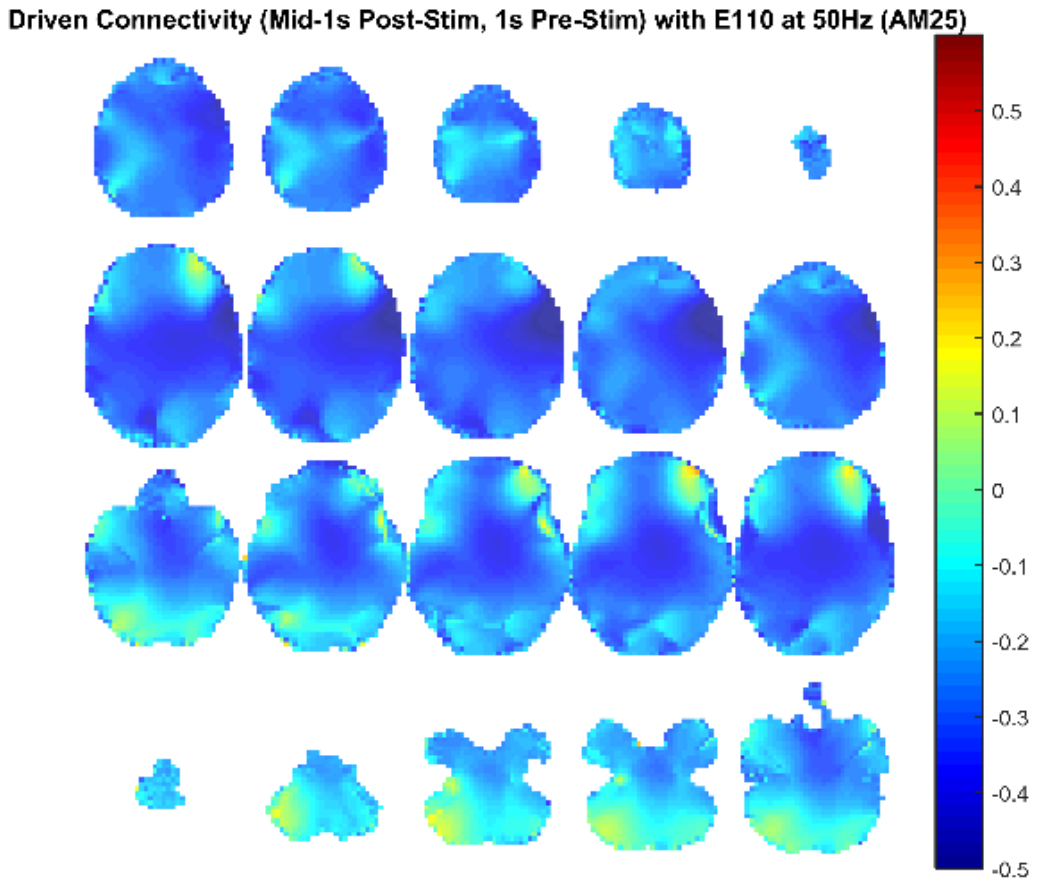

Figure 160. Source level connectivity with a dipole at E110 (right central) in 50 Hz during the middle one-second of 25 Hz amplitude modulated tone stimulation (total stimulation was 3 seconds), performed with DICS and a standardized BEM headmodel. Unit is the percent change in coherence from baseline (i.e., difference between coherence during stimulation and coherence during baseline divided by coherence during baseline). Darker reds indicate increases in coherence with E45 while darker blues indicate decreases in coherence.

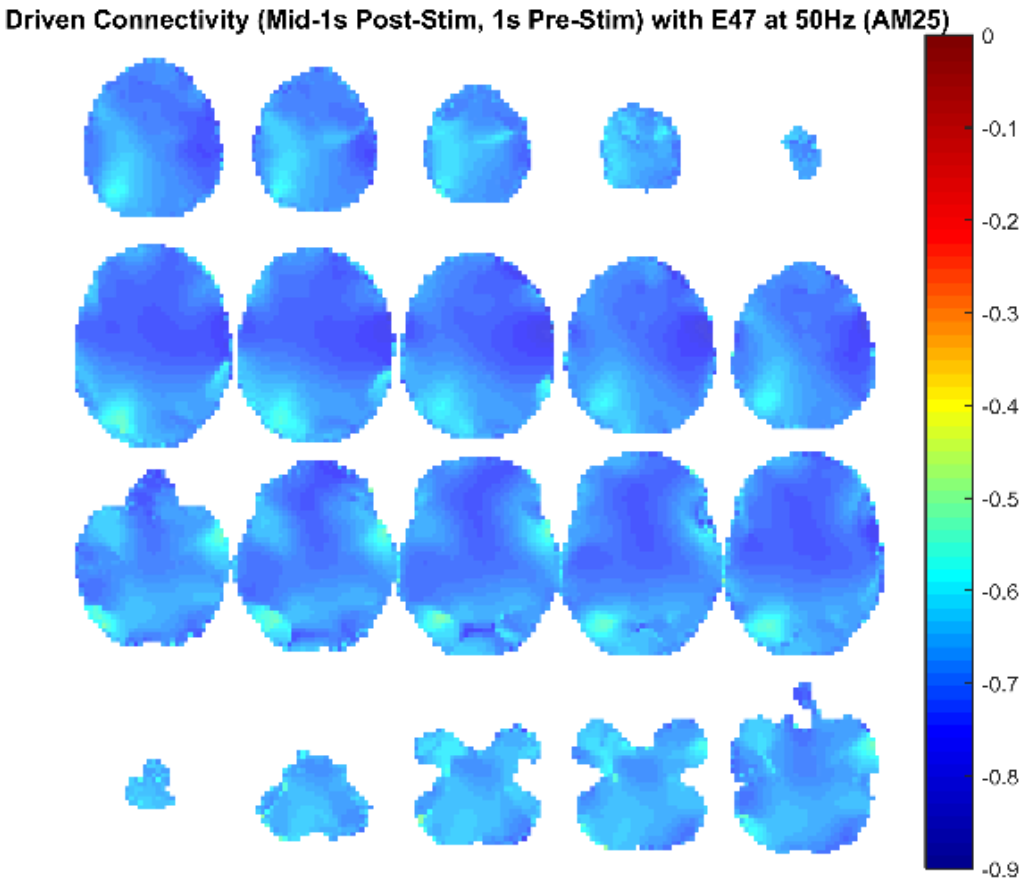

Figure 161. Source level connectivity with a dipole at E47 (left parietal) in 50 Hz during the middle one-second of 25 Hz amplitude modulated tone stimulation (total stimulation was 3 seconds), performed with DICS and a standardized BEM headmodel. Unit is the percent change in coherence from baseline (i.e., difference between coherence during stimulation and coherence during baseline divided by coherence during baseline). Darker reds indicate increases in coherence with E45 while darker blues indicate decreases in coherence.

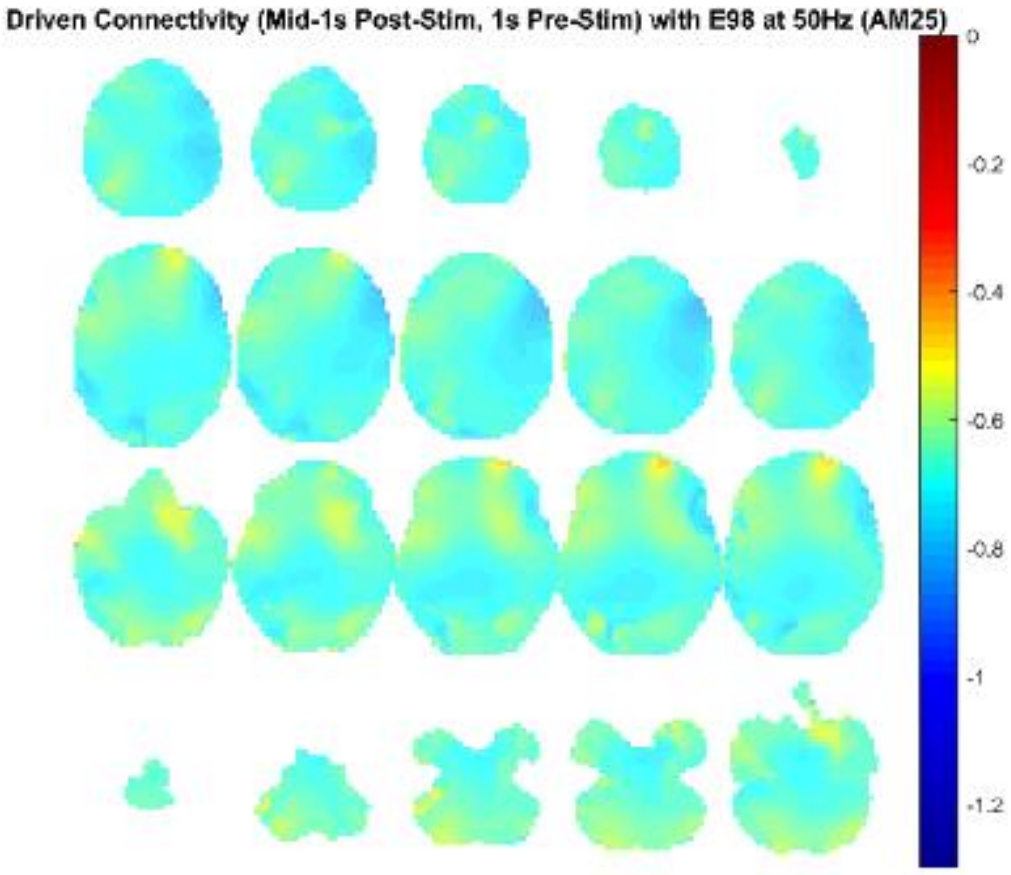

Figure 162. Source level connectivity with a dipole at E98 (right parietal) in 50 Hz during the middle one-second of 25 Hz amplitude modulated tone stimulation (total stimulation was 3 seconds), performed with DICS and a standardized BEM headmodel. Unit is the percent change in coherence from baseline (i.e., difference between coherence during stimulation and coherence during baseline divided by coherence during baseline). Darker reds indicate increases in coherence with E45 while darker blues indicate decreases in coherence.

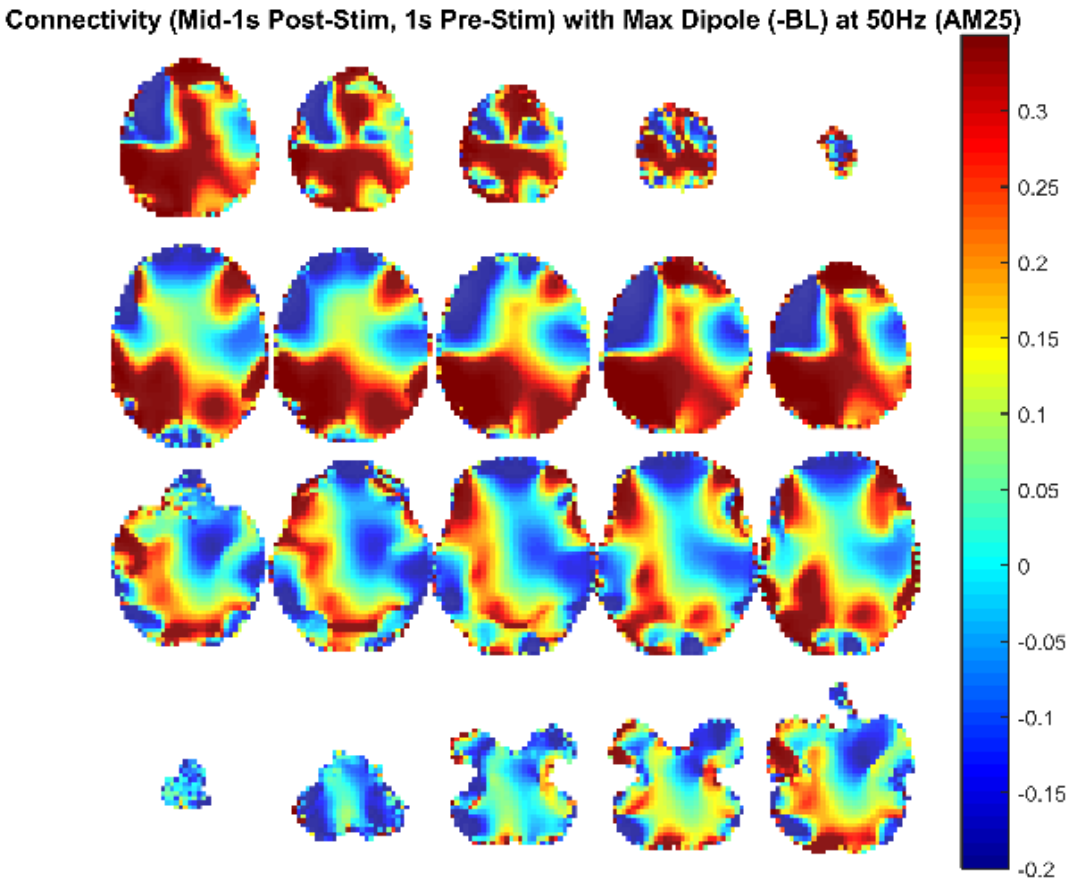

Figure 163. Source level connectivity with a dipole at dip2 (maximum power dipole for the middle one-second period corrected for the baseline one-second period) in 50 Hz during the middle one-second of 25 Hz amplitude modulated tone stimulation (total stimulation was 3 seconds), performed with DICS and a standardized BEM headmodel. Unit is the percent change in coherence from baseline (i.e., difference between coherence during stimulation and coherence during baseline divided by coherence during baseline). Darker reds indicate increases in coherence with E45 while darker blues indicate decreases in coherence.

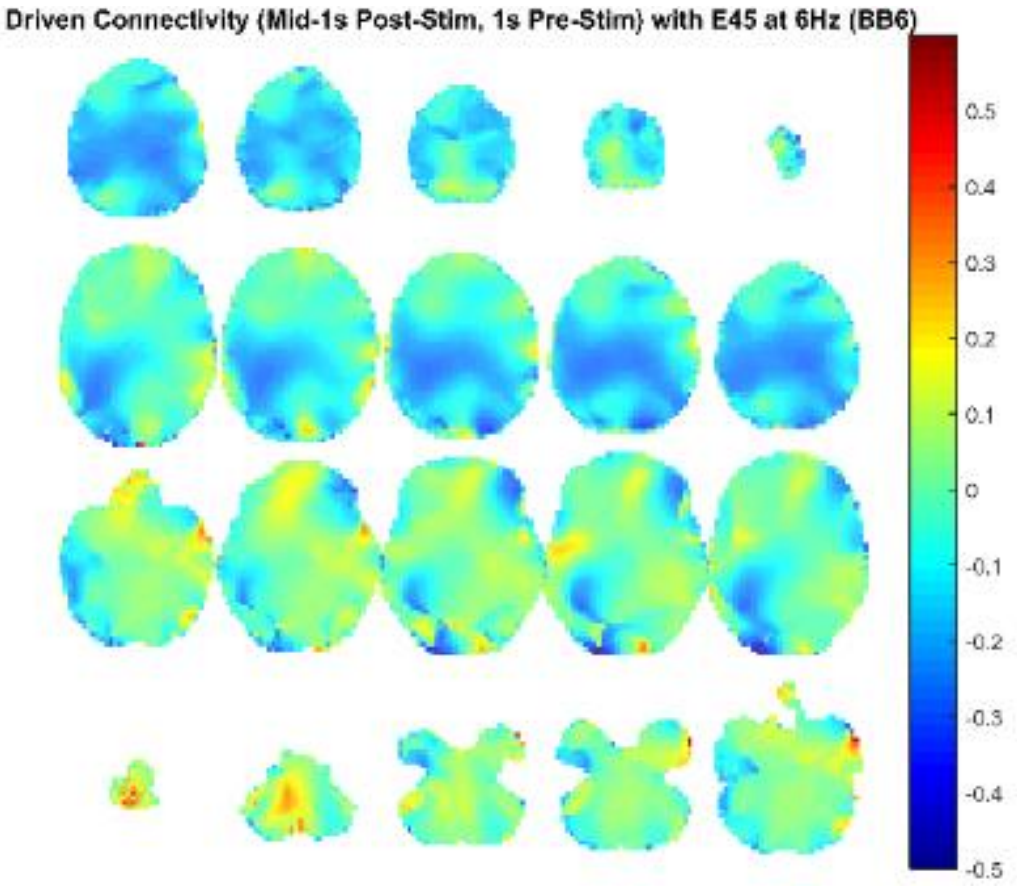

Figure 164. Source level connectivity with a dipole at E45 (left temporal, auditory cortex) in 6 Hz during the middle one-second of 6 Hz binaural beat tone stimulation (total stimulation was 3 seconds), performed with DICS and a standardized BEM headmodel. Unit is the percent change in coherence from baseline (i.e., difference between coherence during stimulation and coherence during baseline divided by coherence during baseline). Darker reds indicate increases in coherence with E45 while darker blues indicate decreases in coherence.

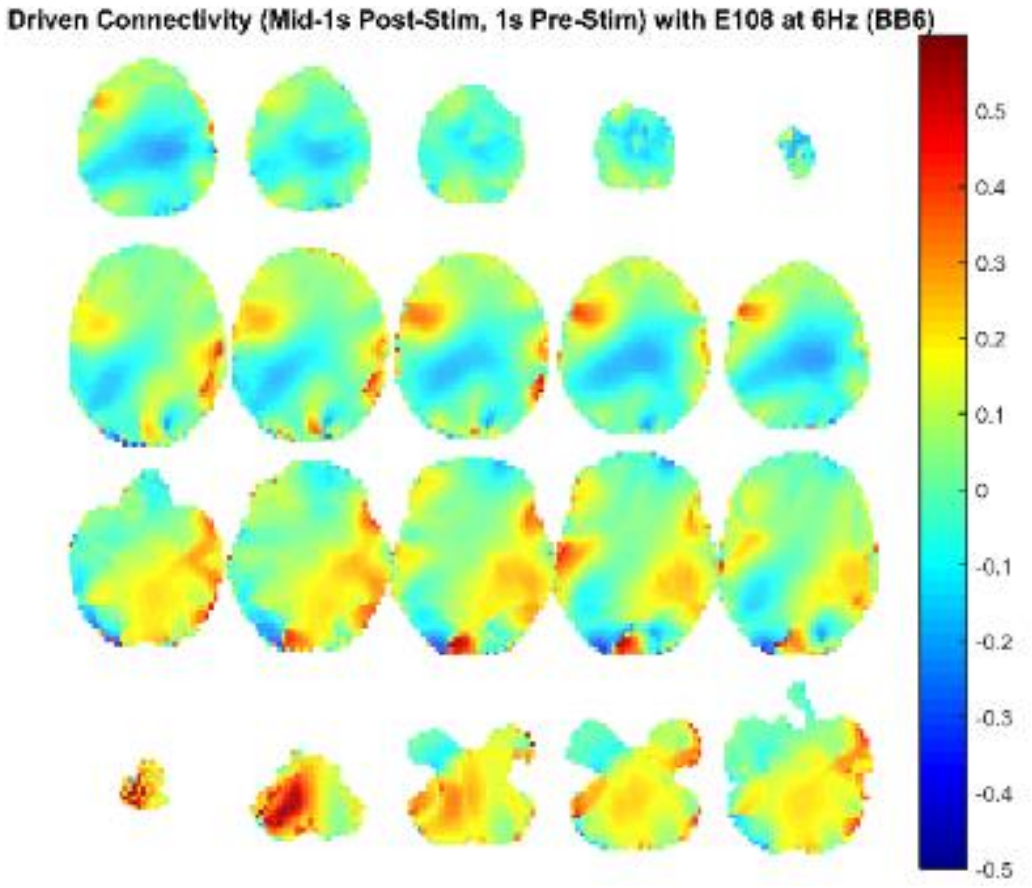

Figure 165. Source level connectivity with a dipole at E108 (right temporal, auditory cortex) in 6 Hz during the middle one-second of 6 Hz binaural beat tone stimulation (total stimulation was 3 seconds), performed with DICS and a standardized BEM headmodel. Unit is the percent change in coherence from baseline (i.e., difference between coherence during stimulation and coherence during baseline divided by coherence during baseline). Darker reds indicate increases in coherence with E45 while darker blues indicate decreases in coherence.

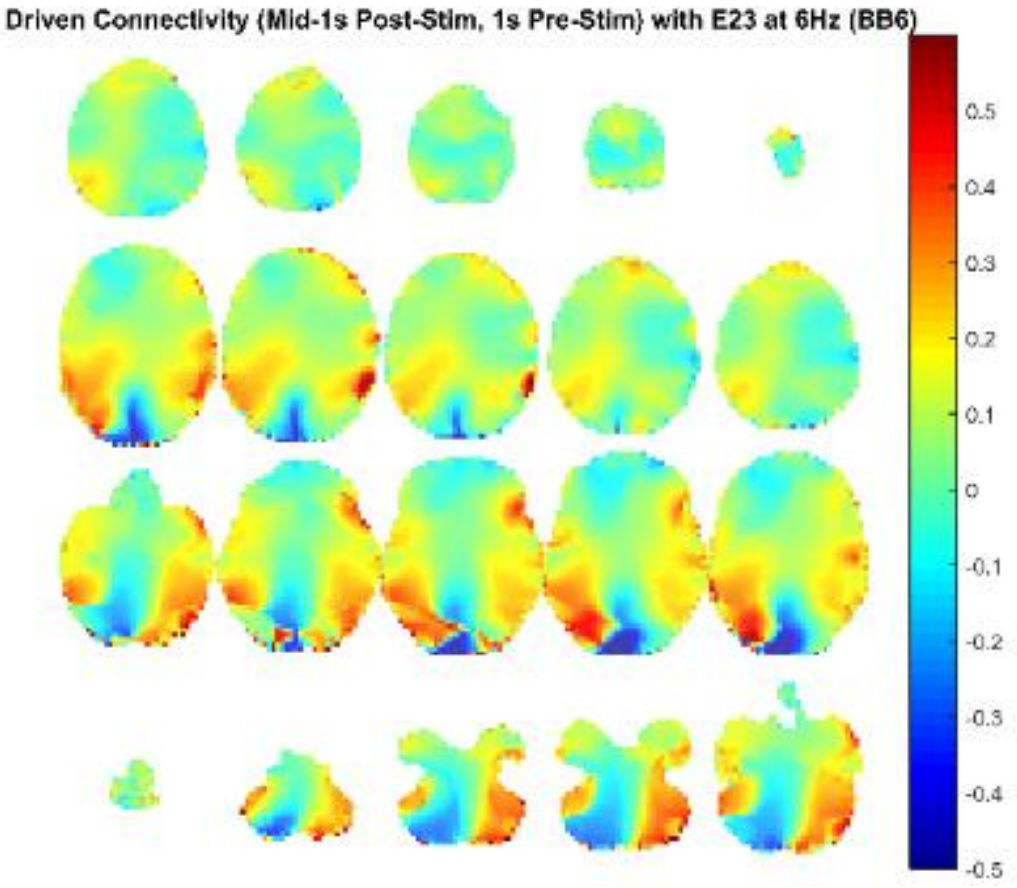

Figure 166. Source level connectivity with a dipole at E23 (left frontal) in 6 Hz during the middle one-second of 6 Hz binaural beat tone stimulation (total stimulation was 3 seconds), performed with DICS and a standardized BEM headmodel. Unit is the percent change in coherence from baseline (i.e., difference between coherence during stimulation and coherence during baseline divided by coherence during baseline). Darker reds indicate increases in coherence with E45 while darker blues indicate decreases in coherence.

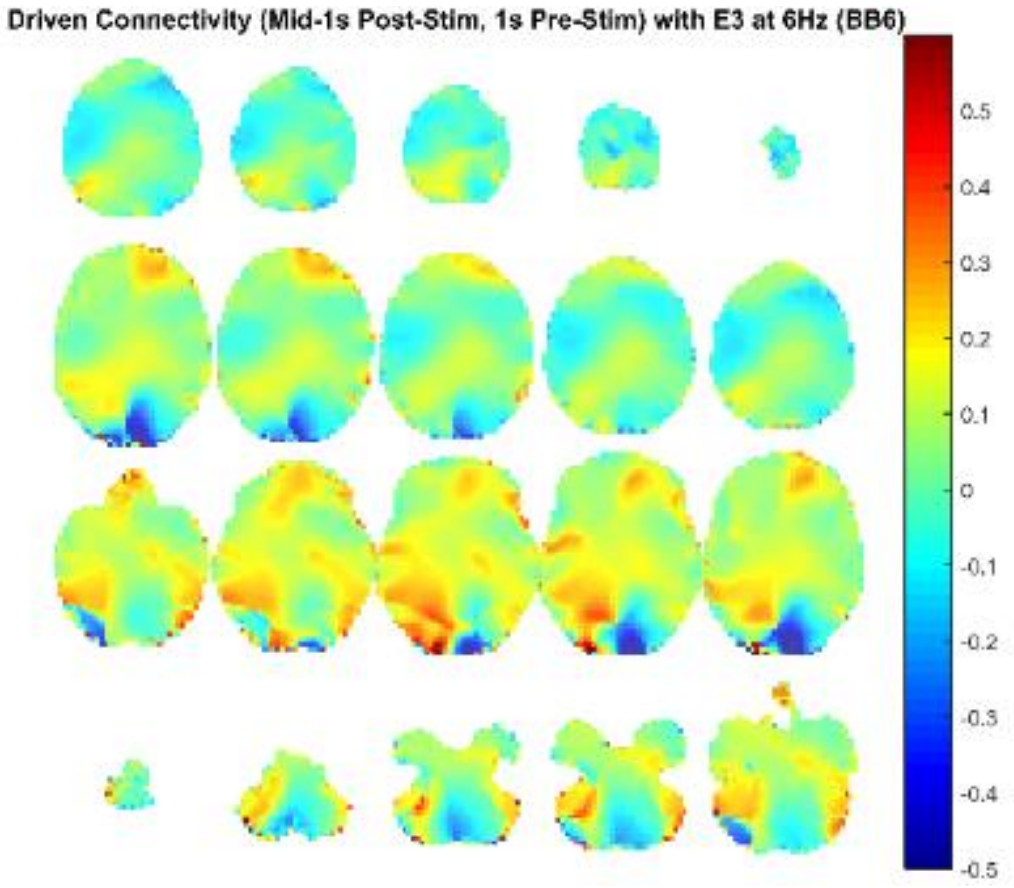

Figure 167. Source level connectivity with a dipole at E3 (right frontal) in 6 Hz during the middle one-second of 6 Hz binaural beat tone stimulation (total stimulation was 3 seconds), performed with DICS and a standardized BEM headmodel. Unit is the percent change in coherence from baseline (i.e., difference between coherence during stimulation and coherence during baseline divided by coherence during baseline). Darker reds indicate increases in coherence with E45 while darker blues indicate decreases in coherence.

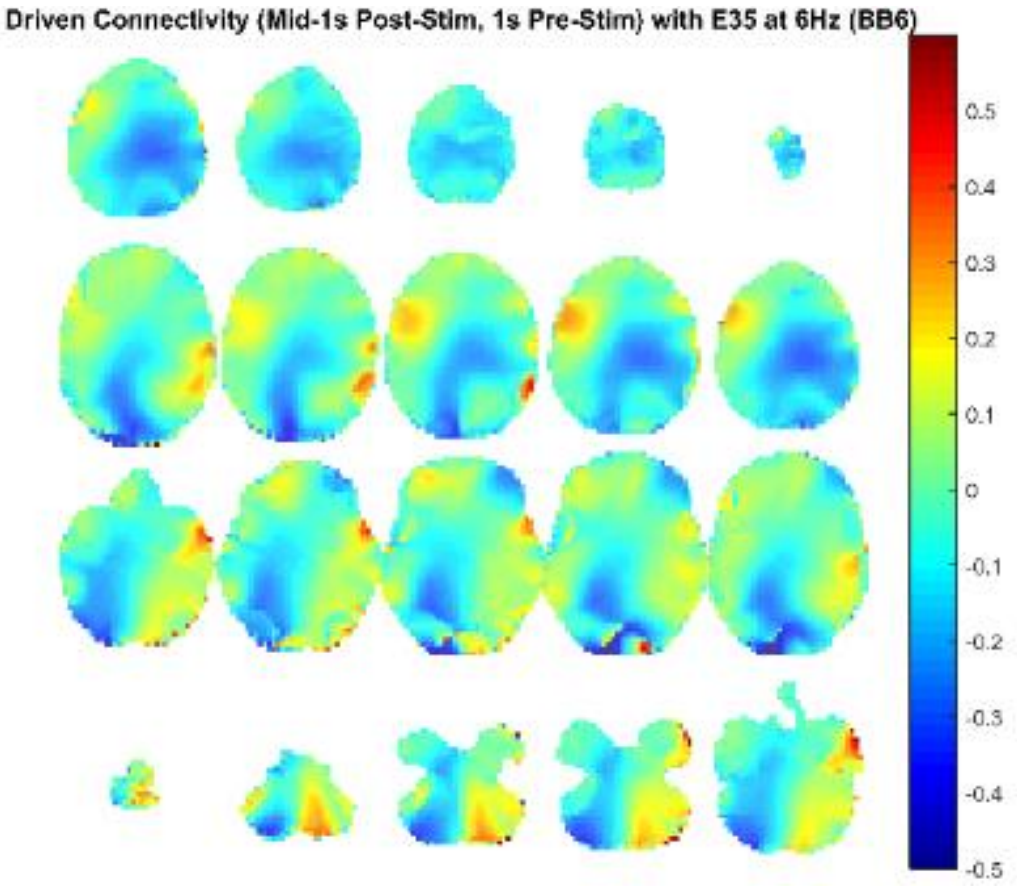

Figure 168. Source level connectivity with a dipole at E35 (left central) in 6 Hz during the middle one-second of 6 Hz binaural beat tone stimulation (total stimulation was 3 seconds), performed with DICS and a standardized BEM headmodel. Unit is the percent change in coherence from baseline (i.e., difference between coherence during stimulation and coherence during baseline divided by coherence during baseline). Darker reds indicate increases in coherence with E45 while darker blues indicate decreases in coherence.

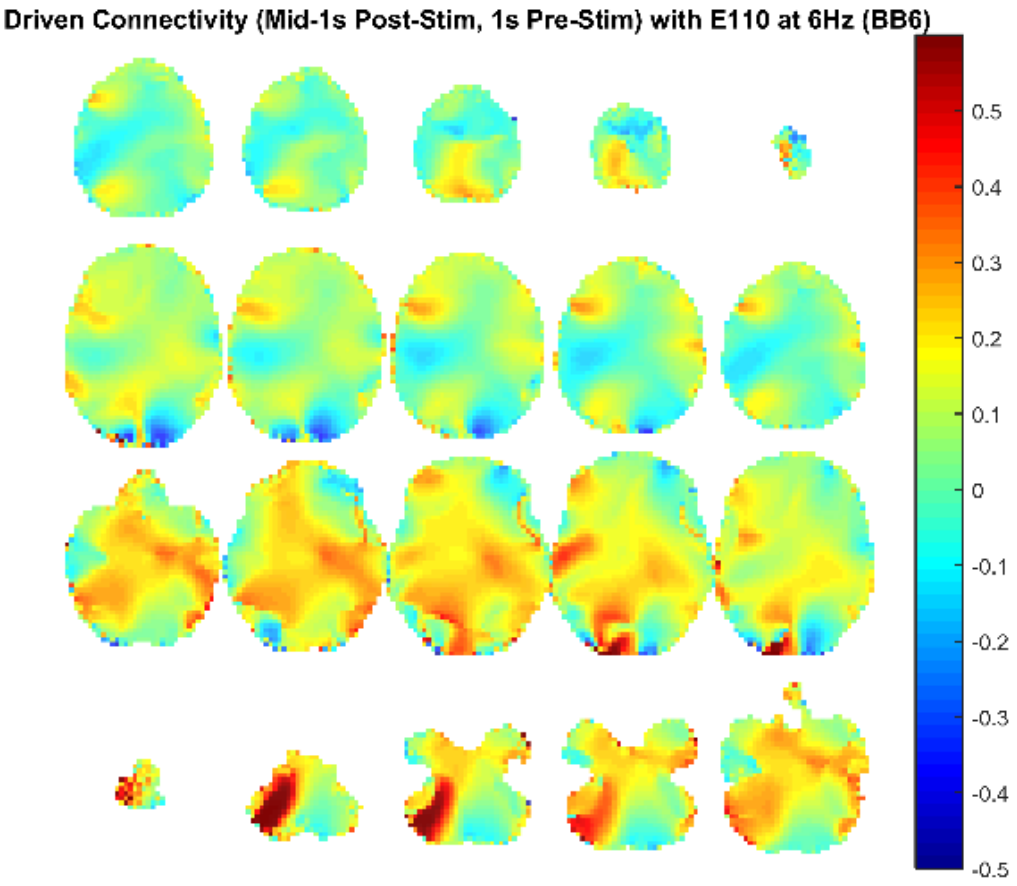

Figure 169. Source level connectivity with a dipole at E110 (right central) in 6 Hz during the middle one-second of 6 Hz binaural beat tone stimulation (total stimulation was 3 seconds), performed with DICS and a standardized BEM headmodel. Unit is the percent change in coherence from baseline (i.e., difference between coherence during stimulation and coherence during baseline divided by coherence during baseline). Darker reds indicate increases in coherence with E45 while darker blues indicate decreases in coherence.

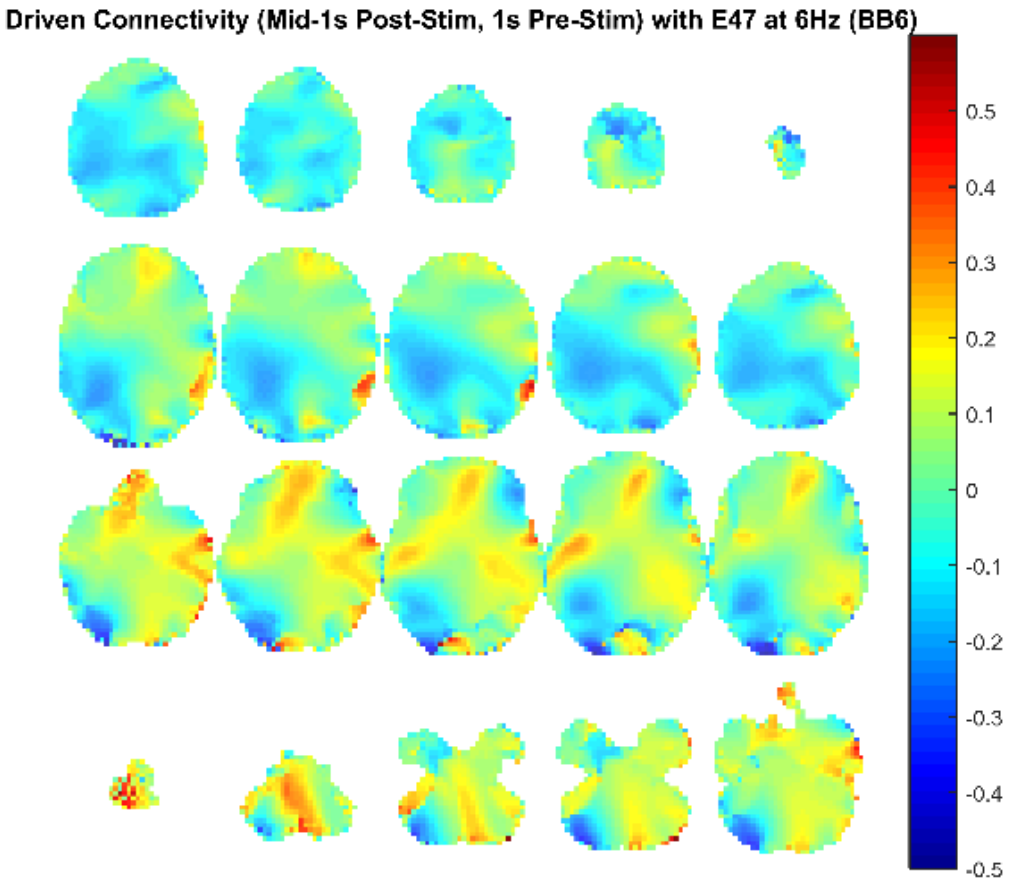

Figure 170. Source level connectivity with a dipole at E47 (left parietal) in 6 Hz during the middle one-second of 6 Hz binaural beat tone stimulation (total stimulation was 3 seconds), performed with DICS and a standardized BEM headmodel. Unit is the percent change in coherence from baseline (i.e., difference between coherence during stimulation and coherence during baseline divided by coherence during baseline). Darker reds indicate increases in coherence with E45 while darker blues indicate decreases in coherence.

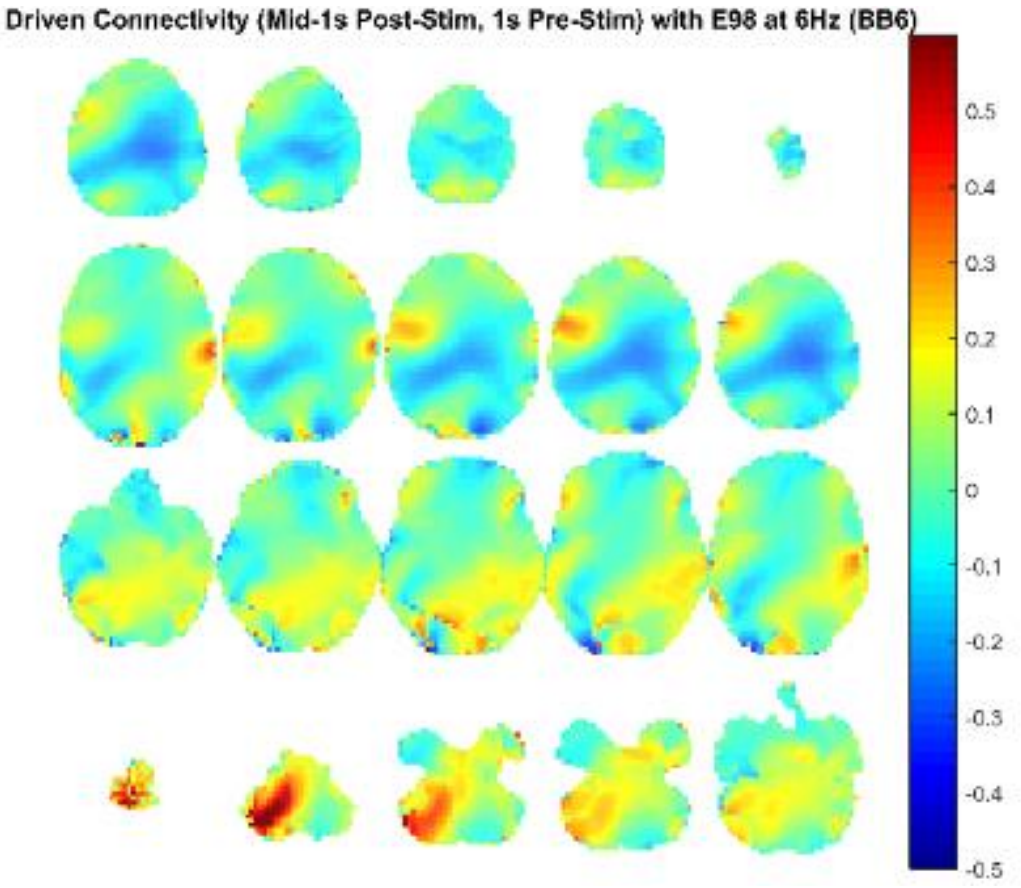

Figure 171. Source level connectivity with a dipole at E98 (right parietal) in 6 Hz during the middle one-second of 6 Hz binaural beat tone stimulation (total stimulation was 3 seconds), performed with DICS and a standardized BEM headmodel. Unit is the percent change in coherence from baseline (i.e., difference between coherence during stimulation and coherence during baseline divided by coherence during baseline). Darker reds indicate increases in coherence with E45 while darker blues indicate decreases in coherence.

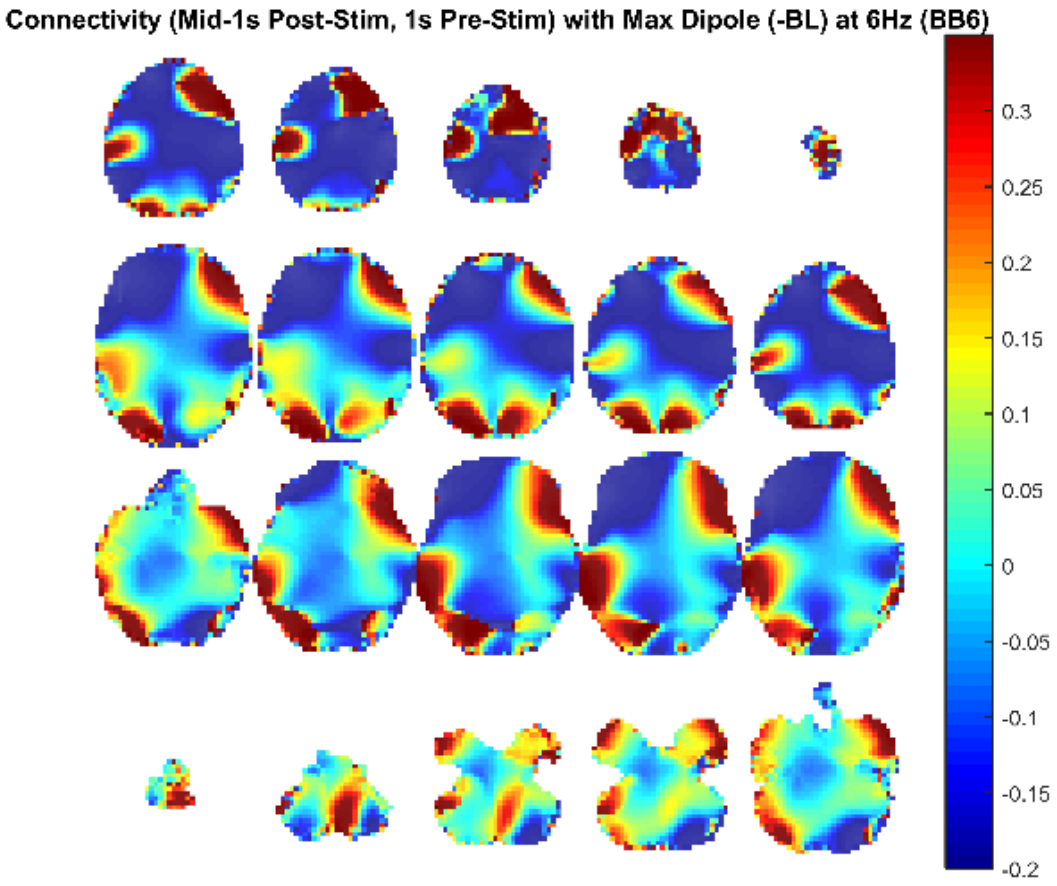

Figure 172. Source level connectivity with a dipole at dip2 (maximum power dipole for the middle one-second period corrected for the baseline one-second period) in 6 Hz during the middle one-second of 6 Hz binaural beat tone stimulation (total stimulation was 3 seconds), performed with DICS and a standardized BEM headmodel. Unit is the percent change in coherence from baseline (i.e., difference between coherence during stimulation and coherence during baseline divided by coherence during baseline). Darker reds indicate increases in coherence with E45 while darker blues indicate decreases in coherence.

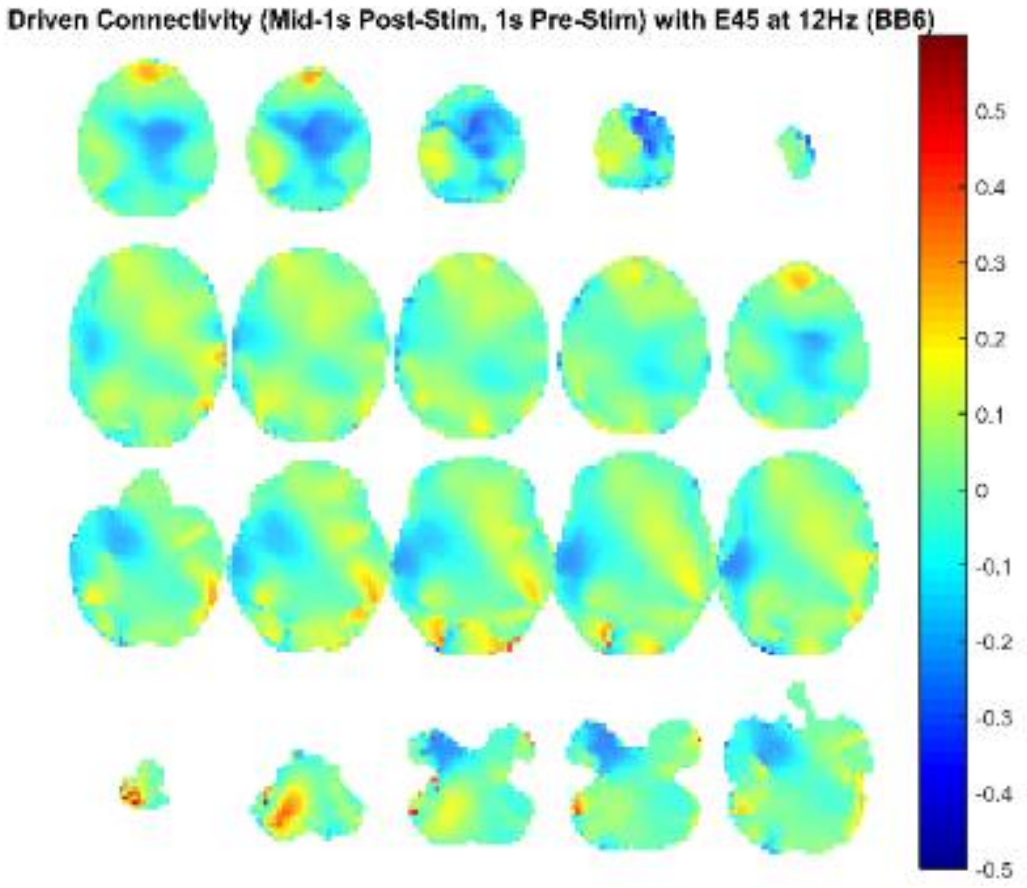

Figure 173. Source level connectivity with a dipole at E45 (left temporal, auditory cortex) in 12 Hz during the middle one-second of 6 Hz binaural beat tone stimulation (total stimulation was 3 seconds), performed with DICS and a standardized BEM headmodel. Unit is the percent change in coherence from baseline (i.e., difference between coherence during stimulation and coherence during baseline divided by coherence during baseline). Darker reds indicate increases in coherence with E45 while darker blues indicate decreases in coherence.

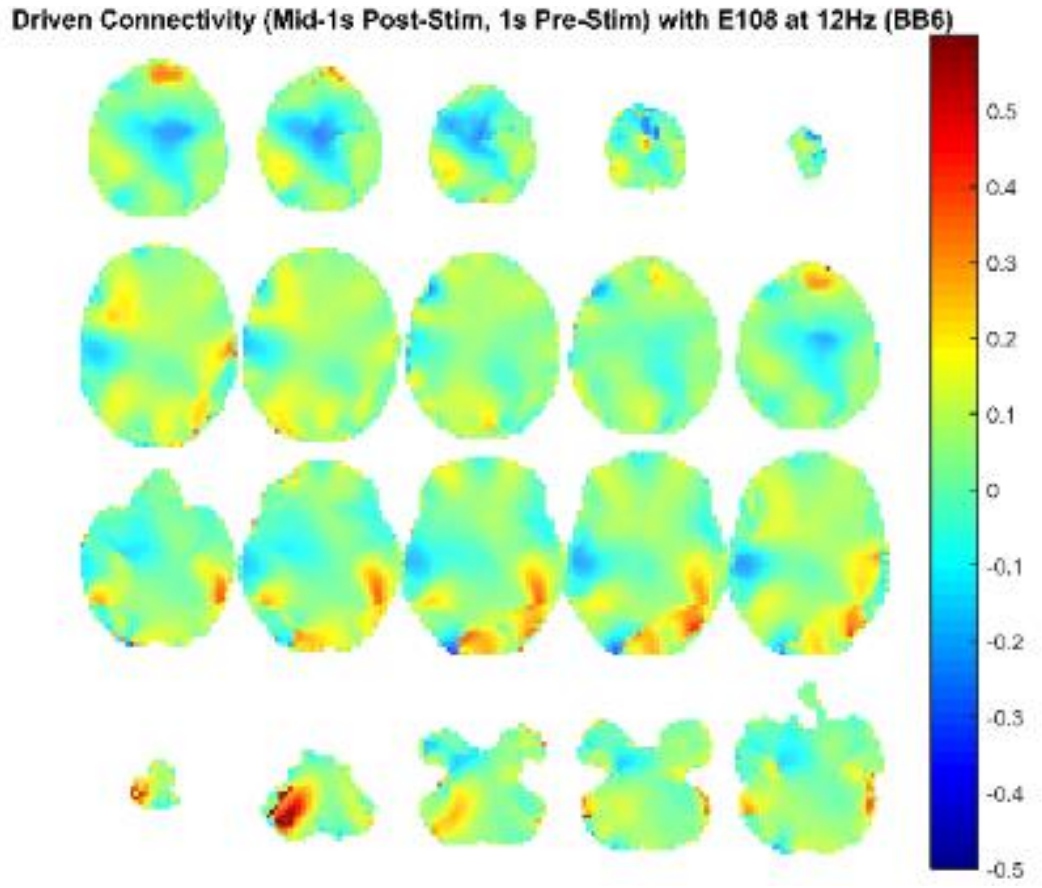

Figure 174. Source level connectivity with a dipole at E108 (right temporal, auditory cortex) in 12 Hz during the middle one-second of 6 Hz binaural beat tone stimulation (total stimulation was 3 seconds), performed with DICS and a standardized BEM headmodel. Unit is the percent change in coherence from baseline (i.e., difference between coherence during stimulation and coherence during baseline divided by coherence during baseline). Darker reds indicate increases in coherence with E45 while darker blues indicate decreases in coherence.

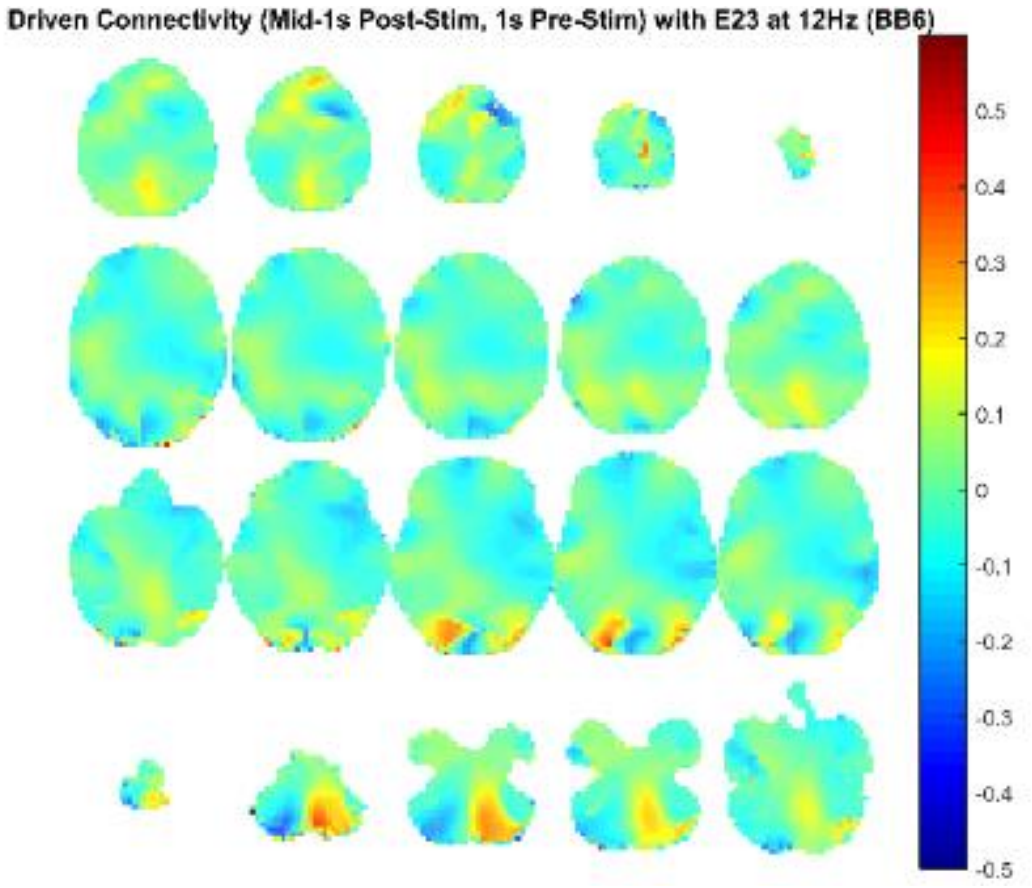

Figure 175. Source level connectivity with a dipole at E23 (left frontal) in 12 Hz during the middle one-second of 6 Hz binaural beat tone stimulation (total stimulation was 3 seconds), performed with DICS and a standardized BEM headmodel. Unit is the percent change in coherence from baseline (i.e., difference between coherence during stimulation and coherence during baseline divided by coherence during baseline). Darker reds indicate increases in coherence with E45 while darker blues indicate decreases in coherence.

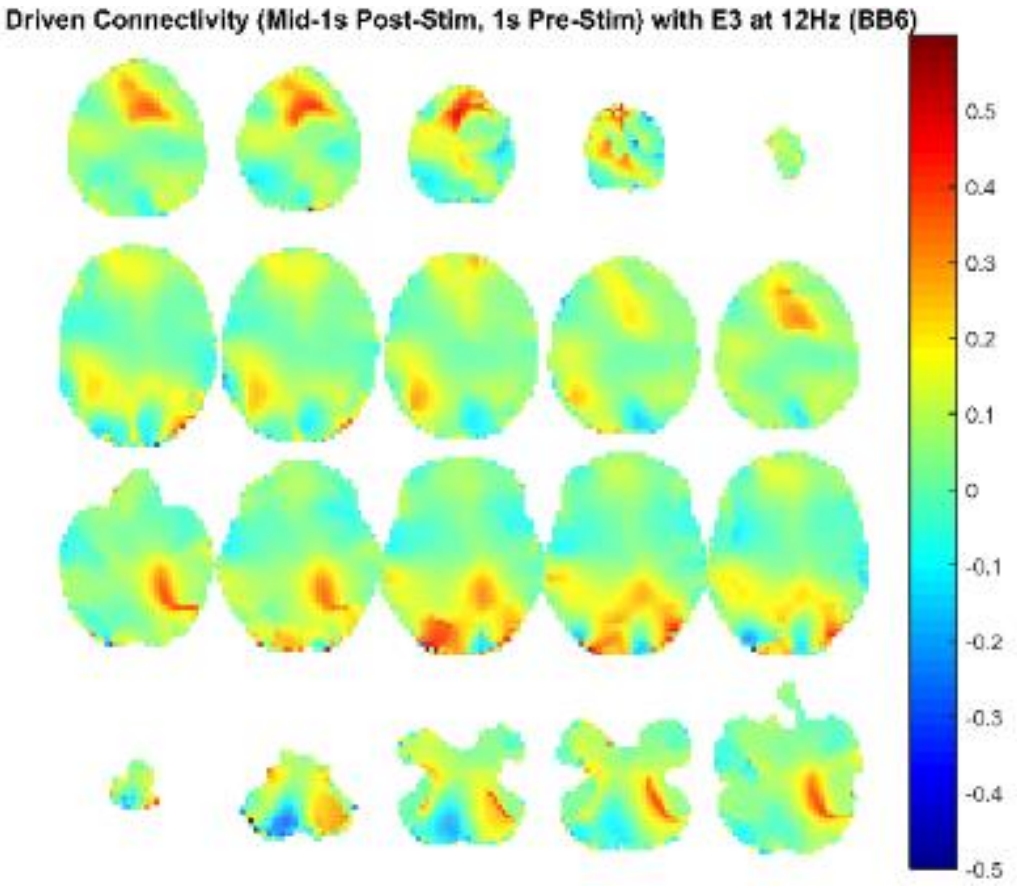

Figure 176. Source level connectivity with a dipole at E3 (right frontal) in 12 Hz during the middle one-second of 6 Hz binaural beat tone stimulation (total stimulation was 3 seconds), performed with DICS and a standardized BEM headmodel. Unit is the percent change in coherence from baseline (i.e., difference between coherence during stimulation and coherence during baseline divided by coherence during baseline). Darker reds indicate increases in coherence with E45 while darker blues indicate decreases in coherence.

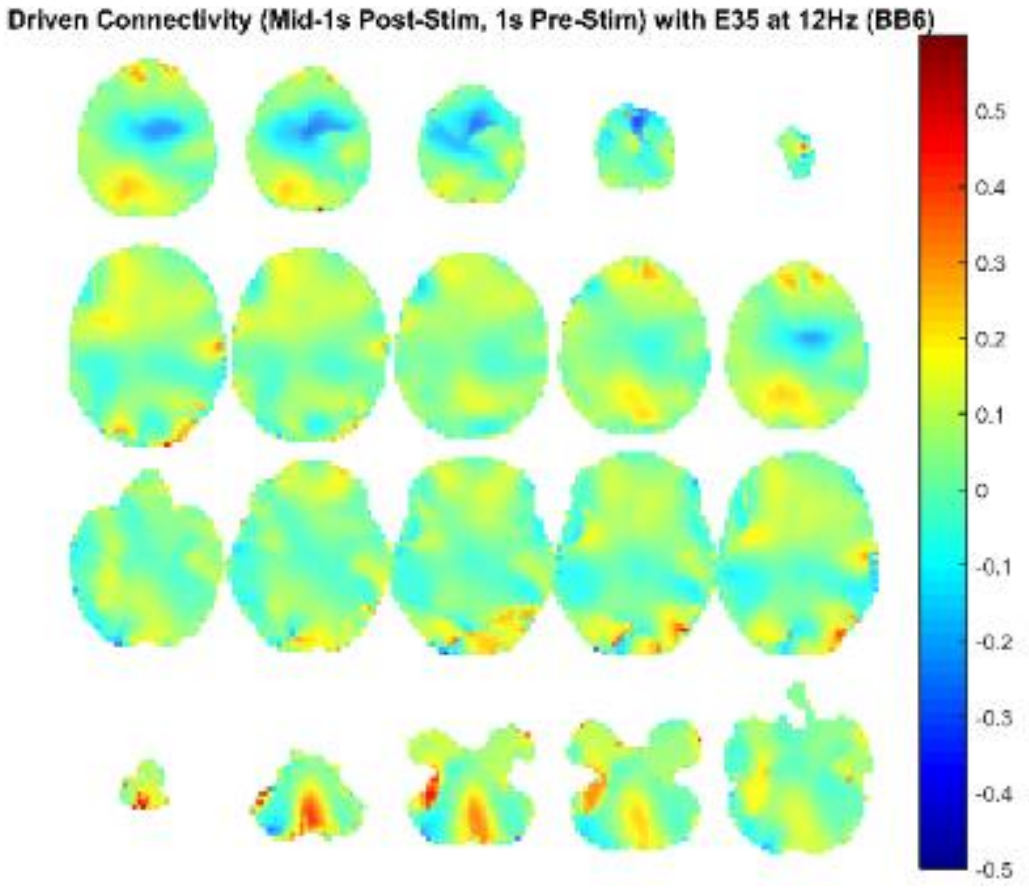

Figure 177. Source level connectivity with a dipole at E35 (left central) in 12 Hz during the middle one-second of 6 Hz binaural beat tone stimulation (total stimulation was 3 seconds), performed with DICS and a standardized BEM headmodel. Unit is the percent change in coherence from baseline (i.e., difference between coherence during stimulation and coherence during baseline divided by coherence during baseline). Darker reds indicate increases in coherence with E45 while darker blues indicate decreases in coherence.

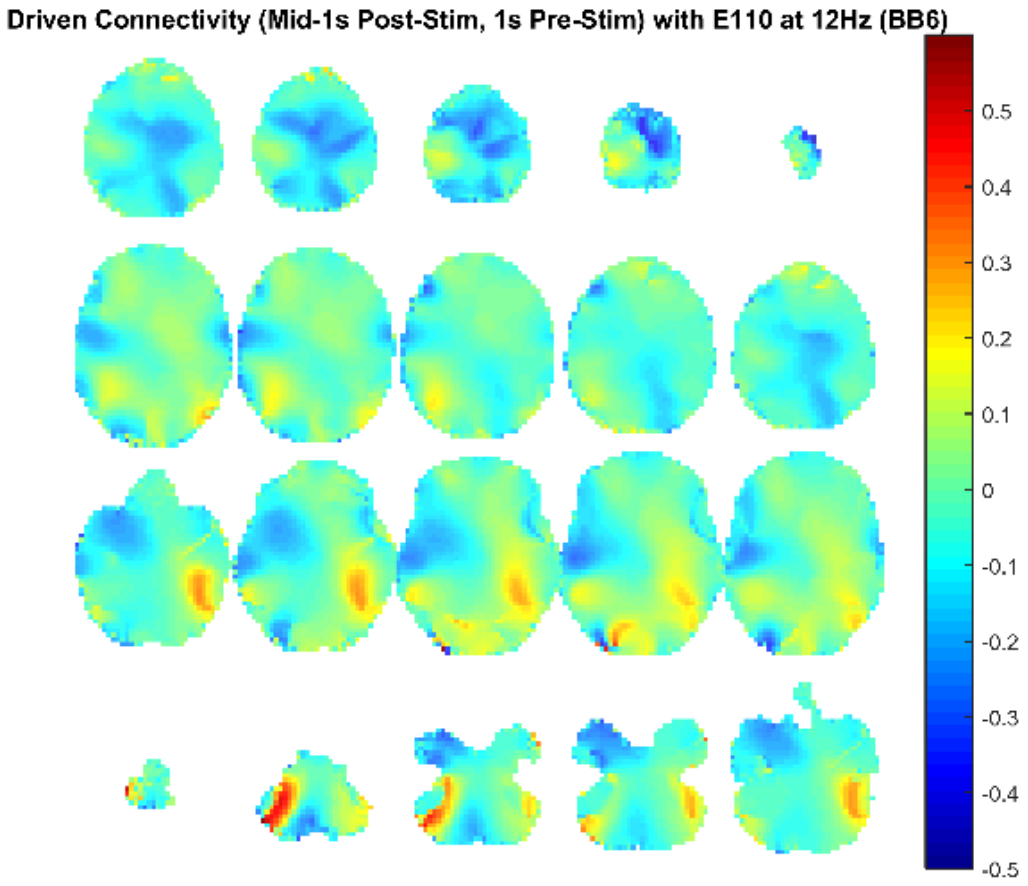

Figure 178. Source level connectivity with a dipole at E110 (right central) in 12 Hz during the middle one-second of 6 Hz binaural beat tone stimulation (total stimulation was 3 seconds), performed with DICS and a standardized BEM headmodel. Unit is the percent change in coherence from baseline (i.e., difference between coherence during stimulation and coherence during baseline divided by coherence during baseline). Darker reds indicate increases in coherence with E45 while darker blues indicate decreases in coherence.

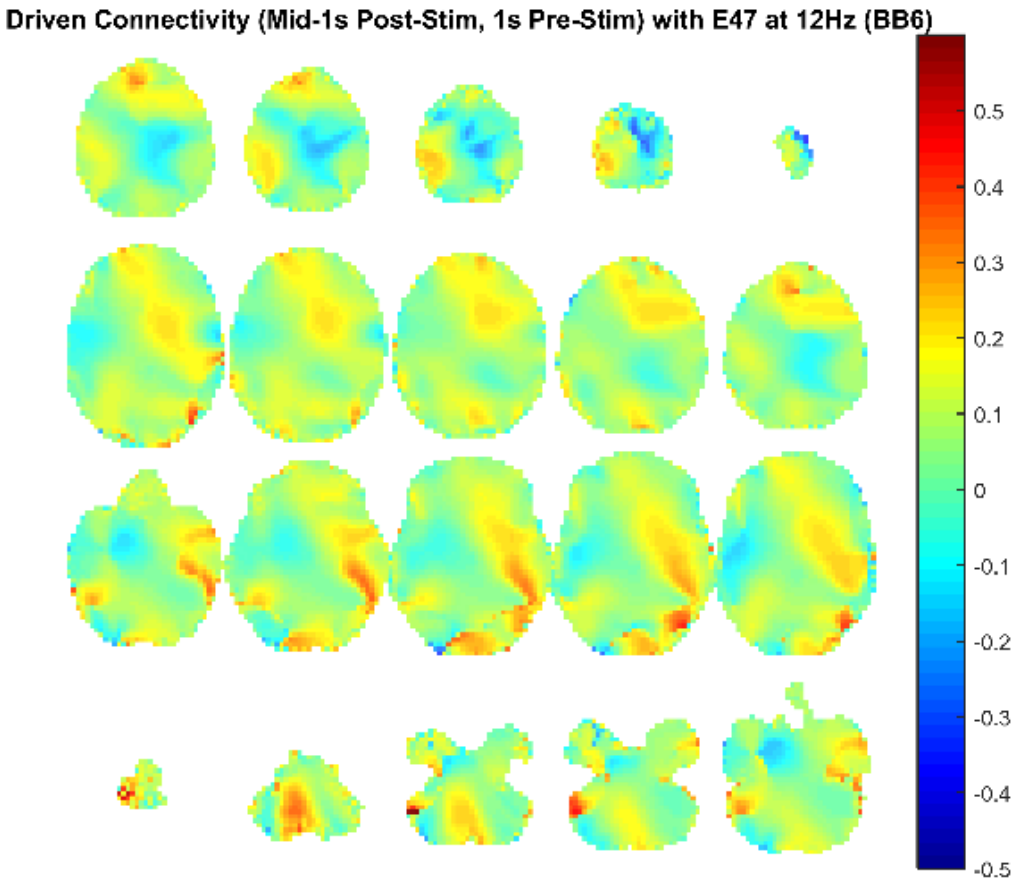

Figure 179. Source level connectivity with a dipole at E47 (left parietal) in 12 Hz during the middle one-second of 6 Hz binaural beat tone stimulation (total stimulation was 3 seconds), performed with DICS and a standardized BEM headmodel. Unit is the percent change in coherence from baseline (i.e., difference between coherence during stimulation and coherence during baseline divided by coherence during baseline). Darker reds indicate increases in coherence with E45 while darker blues indicate decreases in coherence.

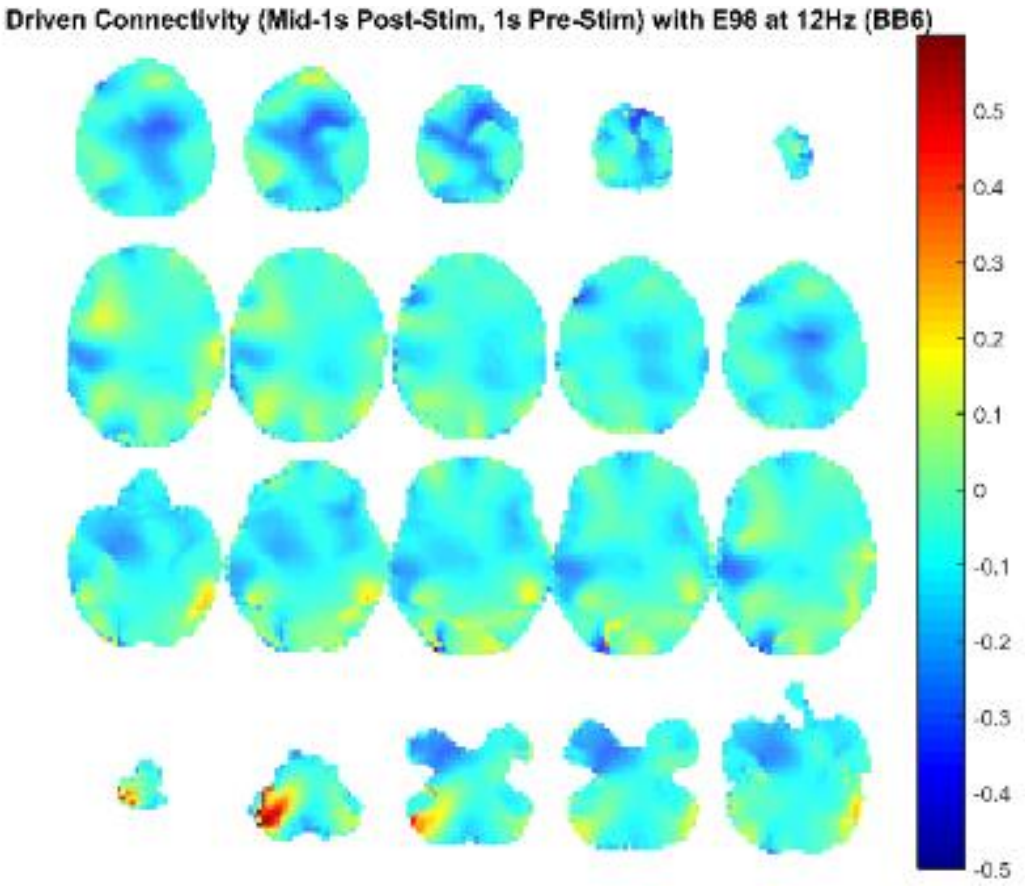

Figure 180. Source level connectivity with a dipole at E98 (right parietal) in 12 Hz during the middle one-second of 6 Hz binaural beat tone stimulation (total stimulation was 3 seconds), performed with DICS and a standardized BEM headmodel. Unit is the percent change in coherence from baseline (i.e., difference between coherence during stimulation and coherence during baseline divided by coherence during baseline). Darker reds indicate increases in coherence with E45 while darker blues indicate decreases in coherence.

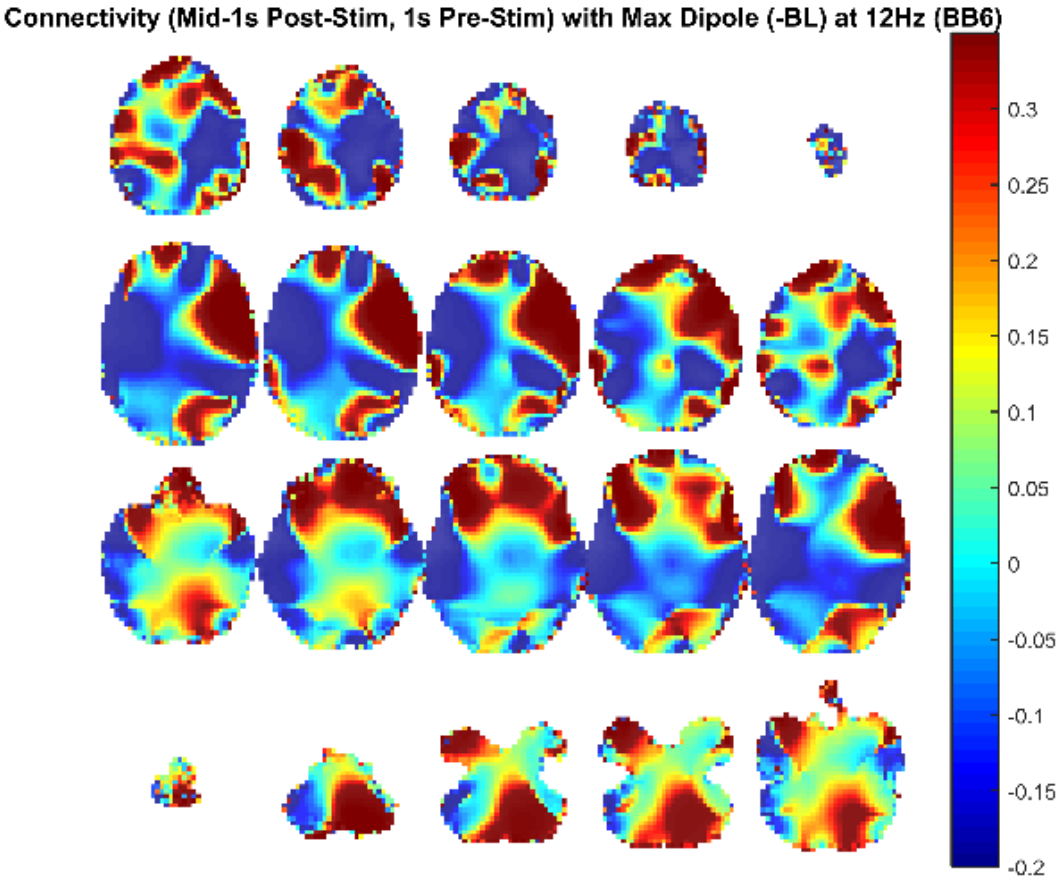

Figure 181. Source level connectivity with a dipole at dip2 (maximum power dipole for the middle one-second period corrected for the baseline one-second period) in 12 Hz during the middle one-second of 6 Hz binaural beat tone stimulation (total stimulation was 3 seconds), performed with DICS and a standardized BEM headmodel. Unit is the percent change in coherence from baseline (i.e., difference between coherence during stimulation and coherence during baseline divided by coherence during baseline). Darker reds indicate increases in coherence with E45 while darker blues indicate decreases in coherence.

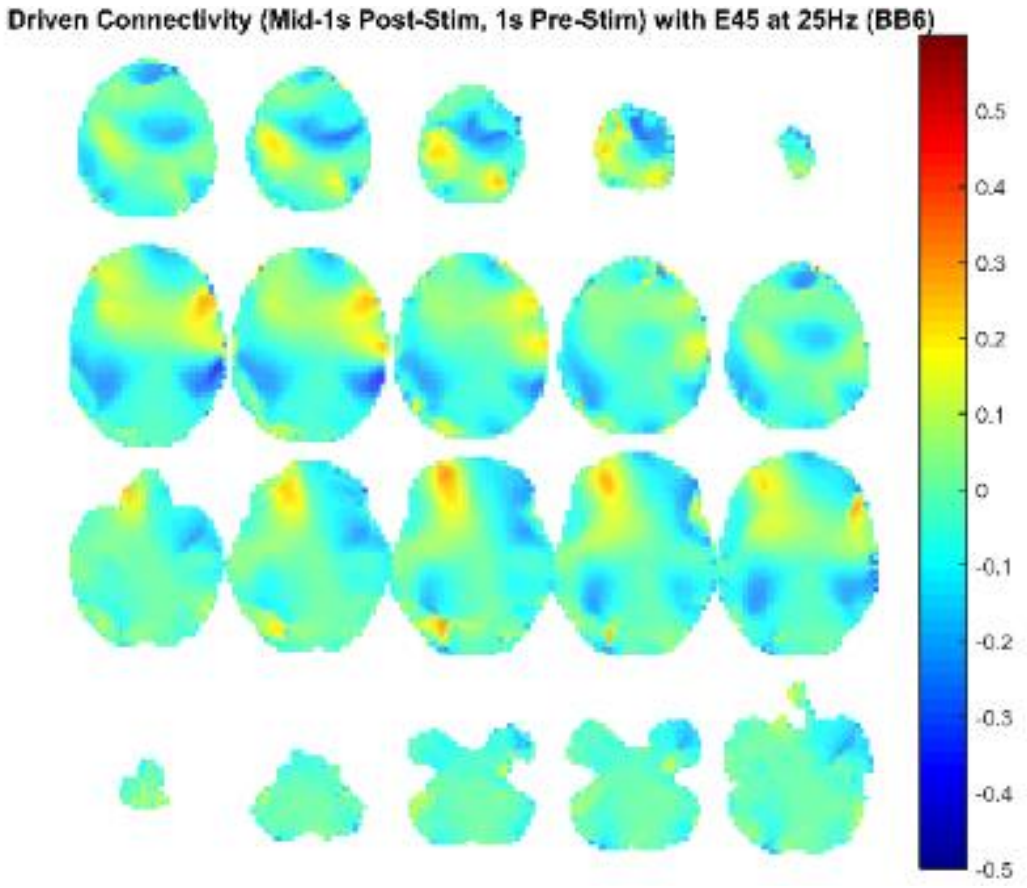

Figure 182. Source level connectivity with a dipole at E45 (left temporal, auditory cortex) in 25 Hz during the middle one-second of 6 Hz binaural beat tone stimulation (total stimulation was 3 seconds), performed with DICS and a standardized BEM headmodel. Unit is the percent change in coherence from baseline (i.e., difference between coherence during stimulation and coherence during baseline divided by coherence during baseline). Darker reds indicate increases in coherence with E45 while darker blues indicate decreases in coherence.

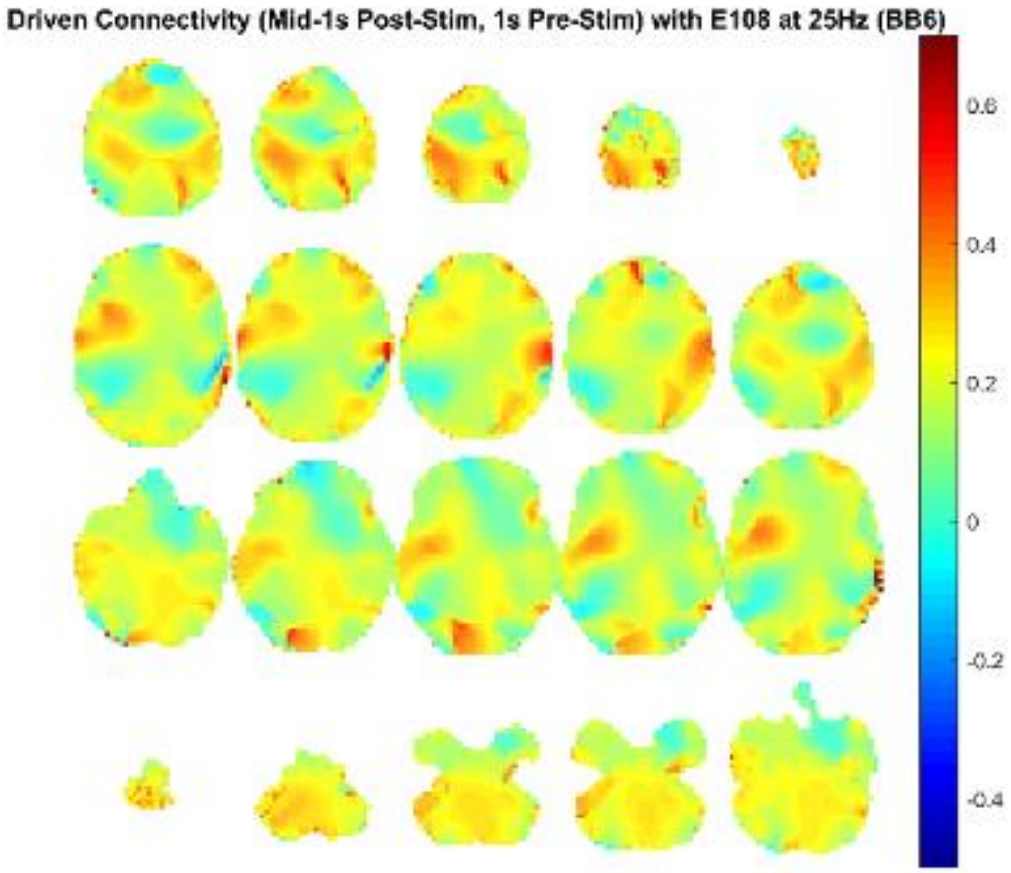

Figure 183. Source level connectivity with a dipole at E108 (right temporal, auditory cortex) in 25 Hz during the middle one-second of 6 Hz binaural beat tone stimulation (total stimulation was 3 seconds), performed with DICS and a standardized BEM headmodel. Unit is the percent change in coherence from baseline (i.e., difference between coherence during stimulation and coherence during baseline divided by coherence during baseline). Darker reds indicate increases in coherence with E45 while darker blues indicate decreases in coherence.

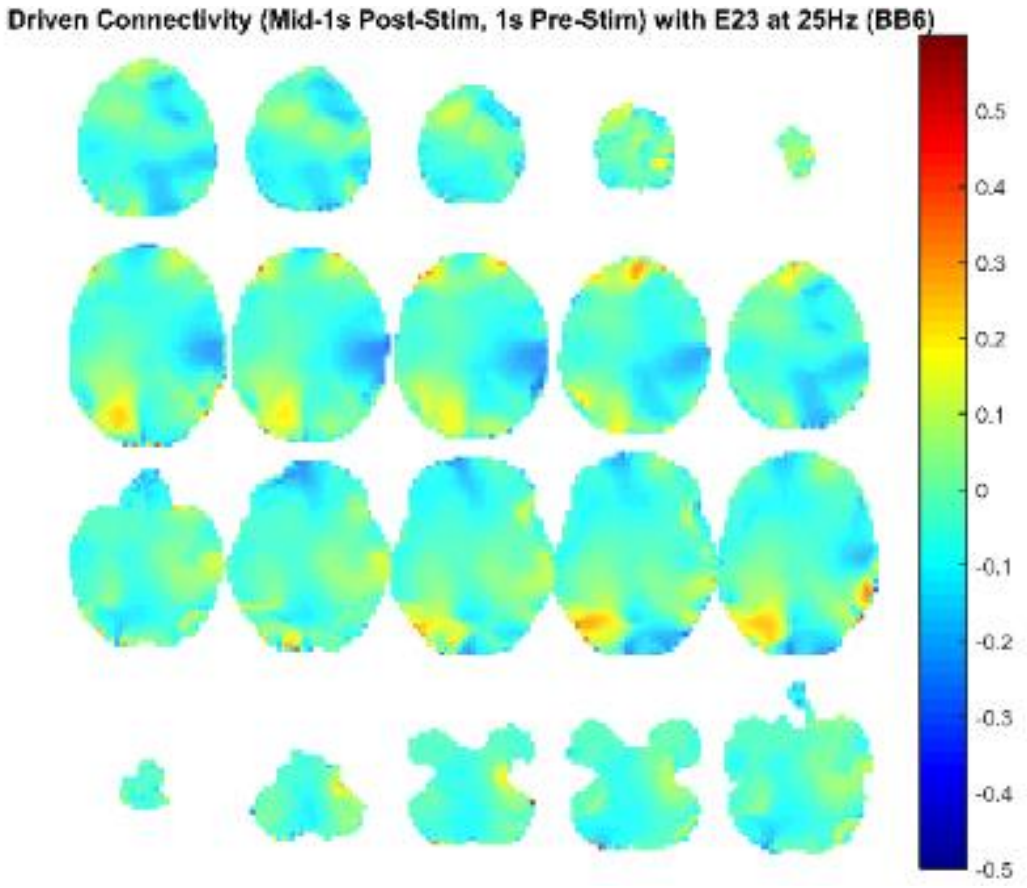

Figure 184. Source level connectivity with a dipole at E23 (left frontal) in 25 Hz during the middle one-second of 6 Hz binaural beat tone stimulation (total stimulation was 3 seconds), performed with DICS and a standardized BEM headmodel. Unit is the percent change in coherence from baseline (i.e., difference between coherence during stimulation and coherence during baseline divided by coherence during baseline). Darker reds indicate increases in coherence with E45 while darker blues indicate decreases in coherence.

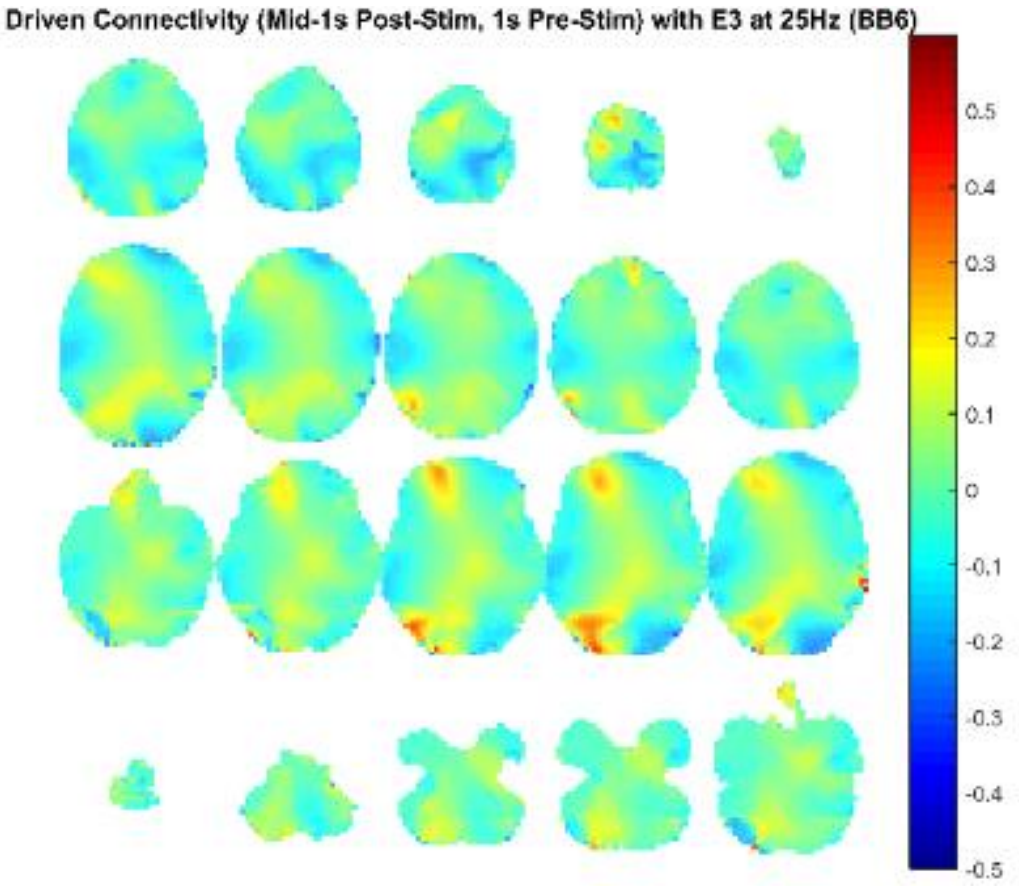

Figure 185. Source level connectivity with a dipole at E3 (right frontal) in 25 Hz during the middle one-second of 6 Hz binaural beat tone stimulation (total stimulation was 3 seconds), performed with DICS and a standardized BEM headmodel. Unit is the percent change in coherence from baseline (i.e., difference between coherence during stimulation and coherence during baseline divided by coherence during baseline). Darker reds indicate increases in coherence with E45 while darker blues indicate decreases in coherence.

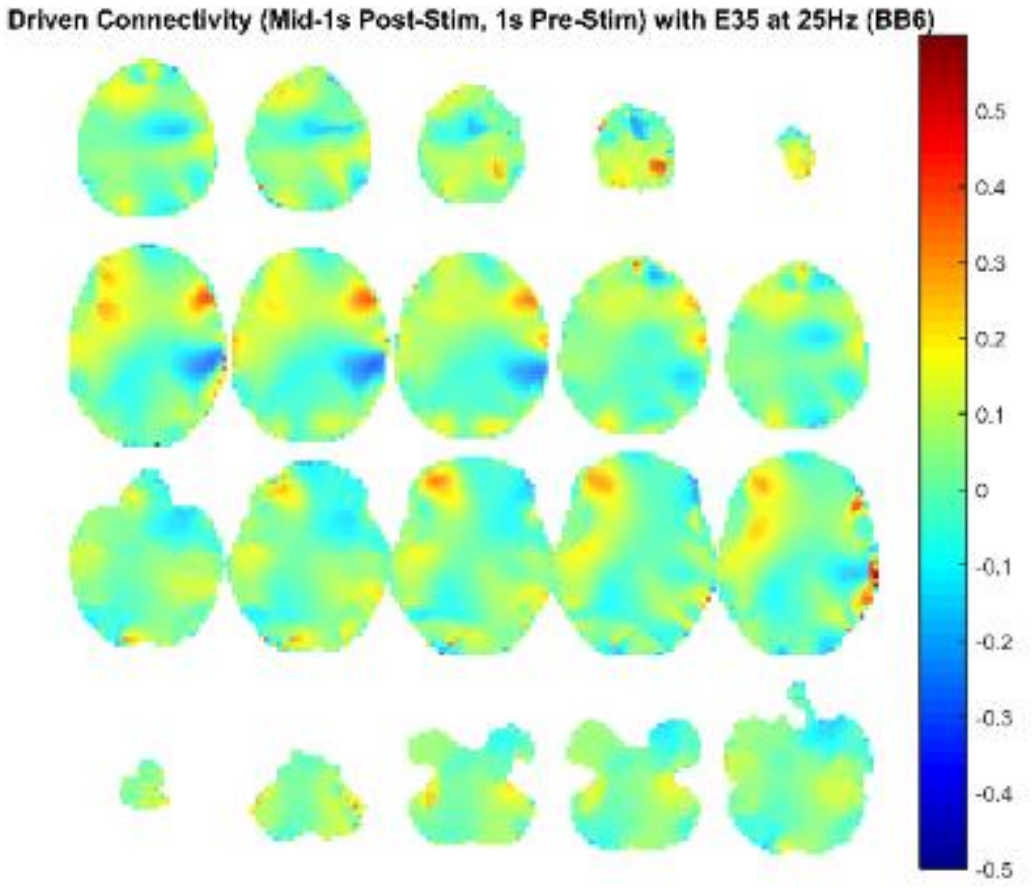

Figure 186. Source level connectivity with a dipole at E35 (left central) in 25 Hz during the middle one-second of 6 Hz binaural beat tone stimulation (total stimulation was 3 seconds), performed with DICS and a standardized BEM headmodel. Unit is the percent change in coherence from baseline (i.e., difference between coherence during stimulation and coherence during baseline divided by coherence during baseline). Darker reds indicate increases in coherence with E45 while darker blues indicate decreases in coherence.

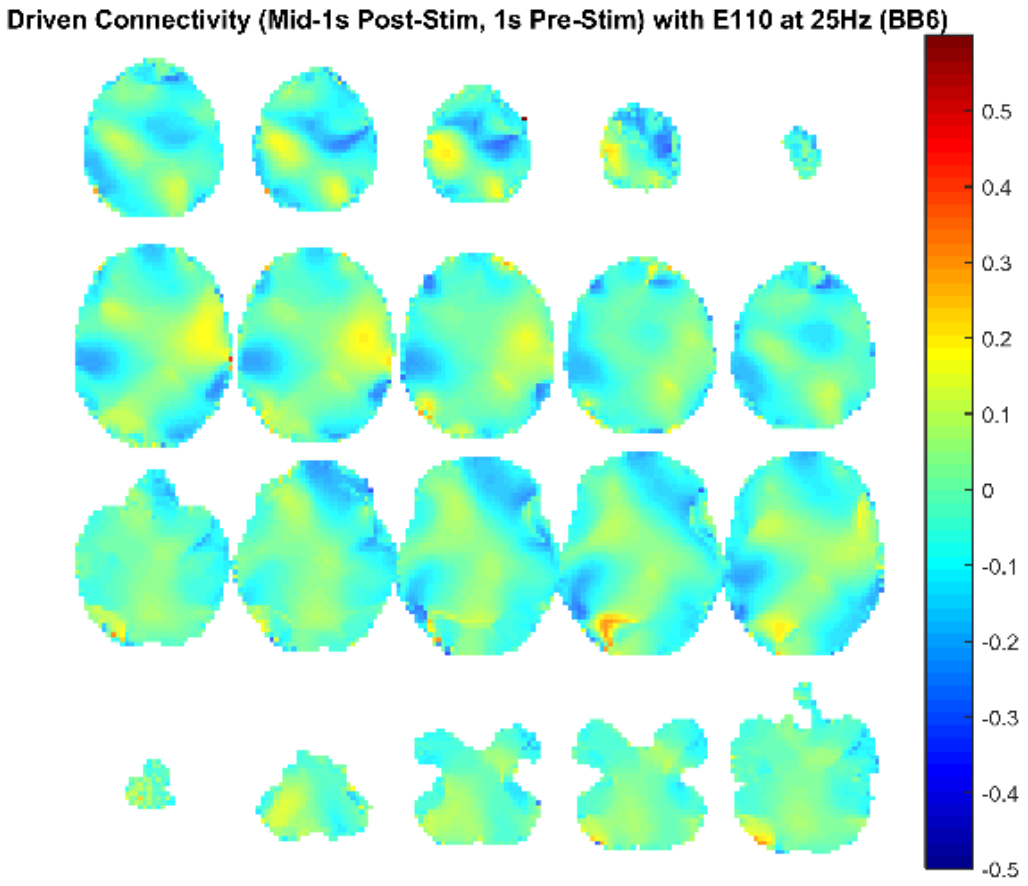

Figure 187. Source level connectivity with a dipole at E110 (right central) in 25 Hz during the middle one-second of 6 Hz binaural beat tone stimulation (total stimulation was 3 seconds), performed with DICS and a standardized BEM headmodel. Unit is the percent change in coherence from baseline (i.e., difference between coherence during stimulation and coherence during baseline divided by coherence during baseline). Darker reds indicate increases in coherence with E45 while darker blues indicate decreases in coherence.

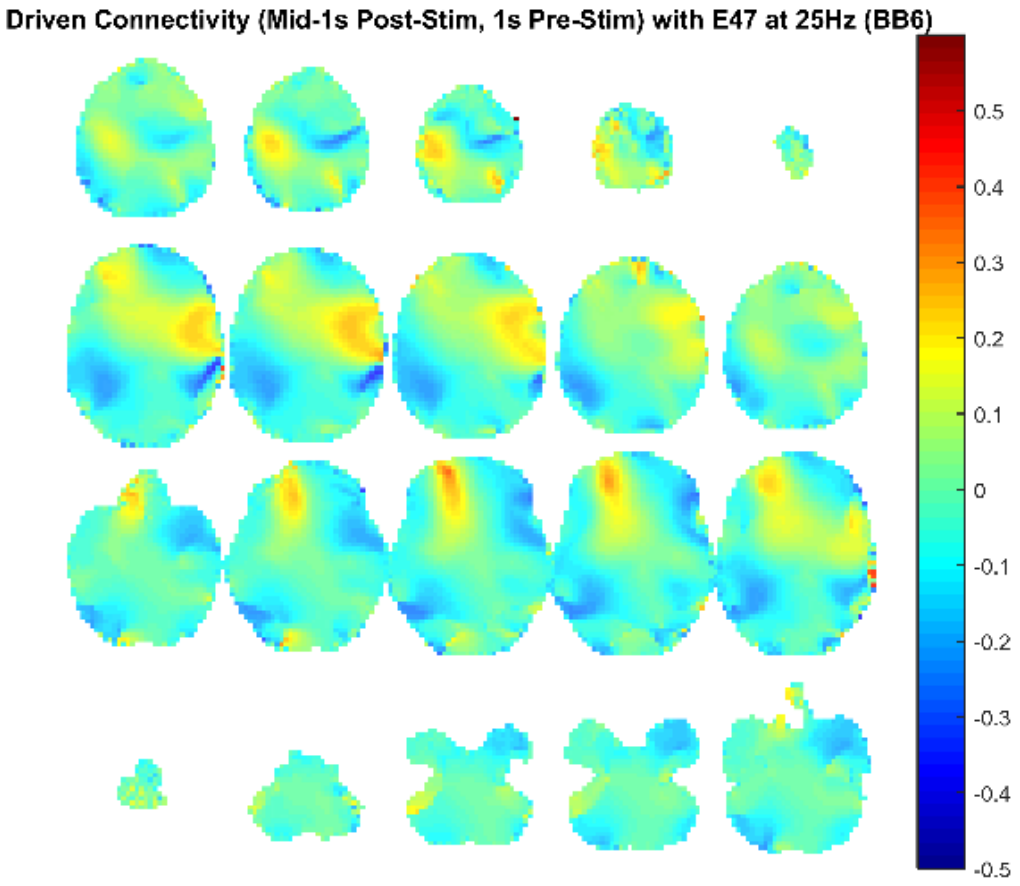

Figure 188. Source level connectivity with a dipole at E47 (left parietal) in 25 Hz during the middle one-second of 6 Hz binaural beat tone stimulation (total stimulation was 3 seconds), performed with DICS and a standardized BEM headmodel. Unit is the percent change in coherence from baseline (i.e., difference between coherence during stimulation and coherence during baseline divided by coherence during baseline). Darker reds indicate increases in coherence with E45 while darker blues indicate decreases in coherence.

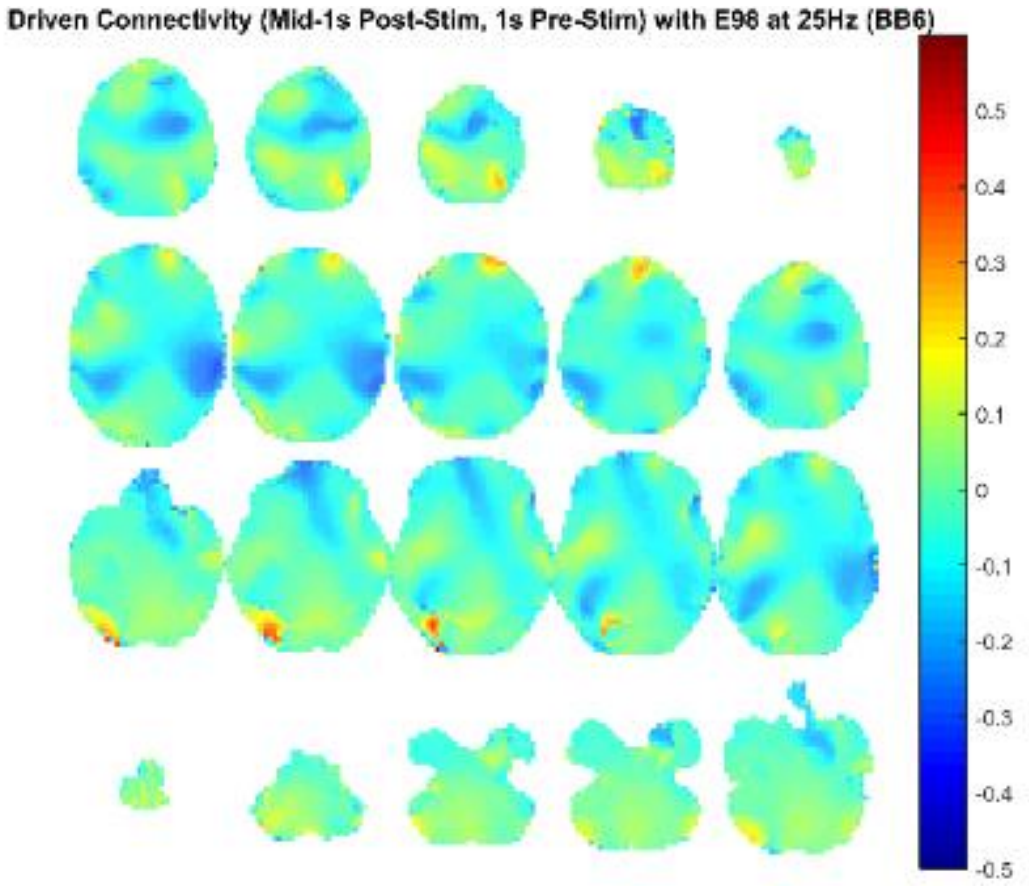

Figure 189. Source level connectivity with a dipole at E98 (right parietal) in 25 Hz during the middle one-second of 6 Hz binaural beat tone stimulation (total stimulation was 3 seconds), performed with DICS and a standardized BEM headmodel. Unit is the percent change in coherence from baseline (i.e., difference between coherence during stimulation and coherence during baseline divided by coherence during baseline). Darker reds indicate increases in coherence with E45 while darker blues indicate decreases in coherence.

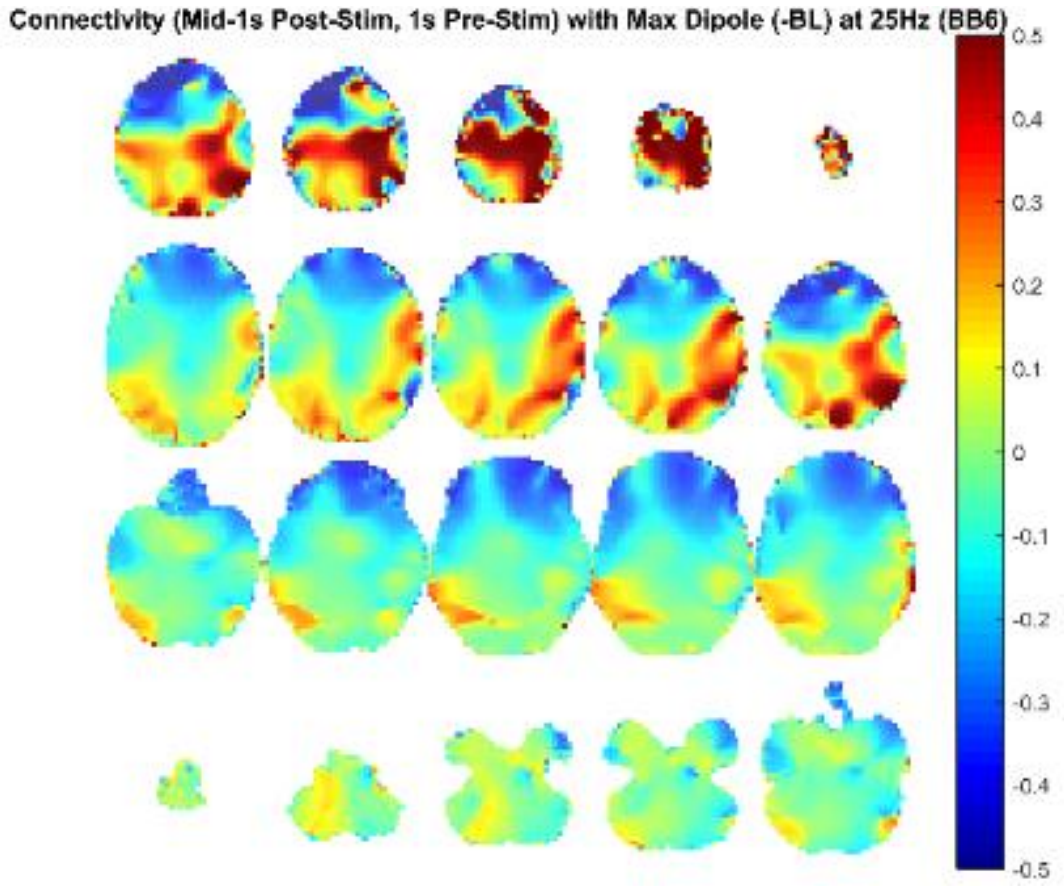

Figure 190. Source level connectivity with a dipole at dip2 (maximum power dipole for the middle one-second period corrected for the baseline one-second period) in 25 Hz during the middle one-second of 6 Hz binaural beat tone stimulation (total stimulation was 3 seconds), performed with DICS and a standardized BEM headmodel. Unit is the percent change in coherence from baseline (i.e., difference between coherence during stimulation and coherence during baseline divided by coherence during baseline). Darker reds indicate increases in coherence with E45 while darker blues indicate decreases in coherence.

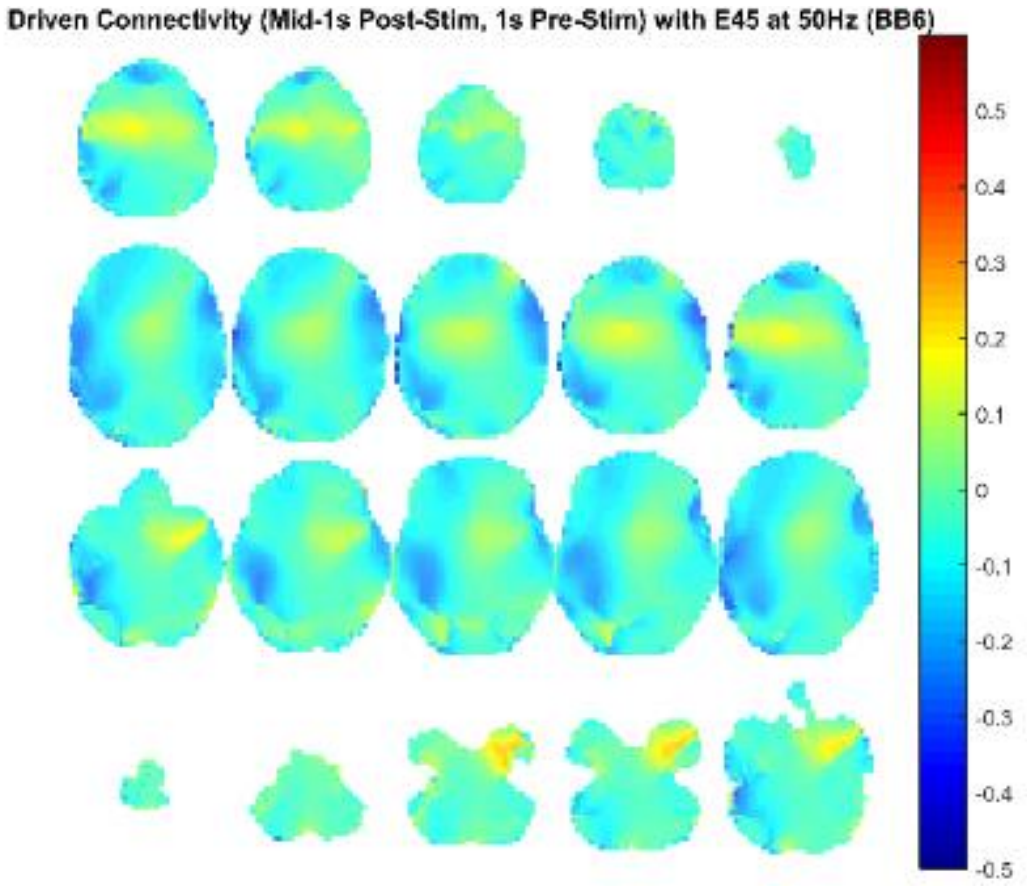

Figure 191. Source level connectivity with a dipole at E45 (left temporal, auditory cortex) in 50 Hz during the middle one-second of 6 Hz binaural beat tone stimulation (total stimulation was 3 seconds), performed with DICS and a standardized BEM headmodel. Unit is the percent change in coherence from baseline (i.e., difference between coherence during stimulation and coherence during baseline divided by coherence during baseline). Darker reds indicate increases in coherence with E45 while darker blues indicate decreases in coherence.

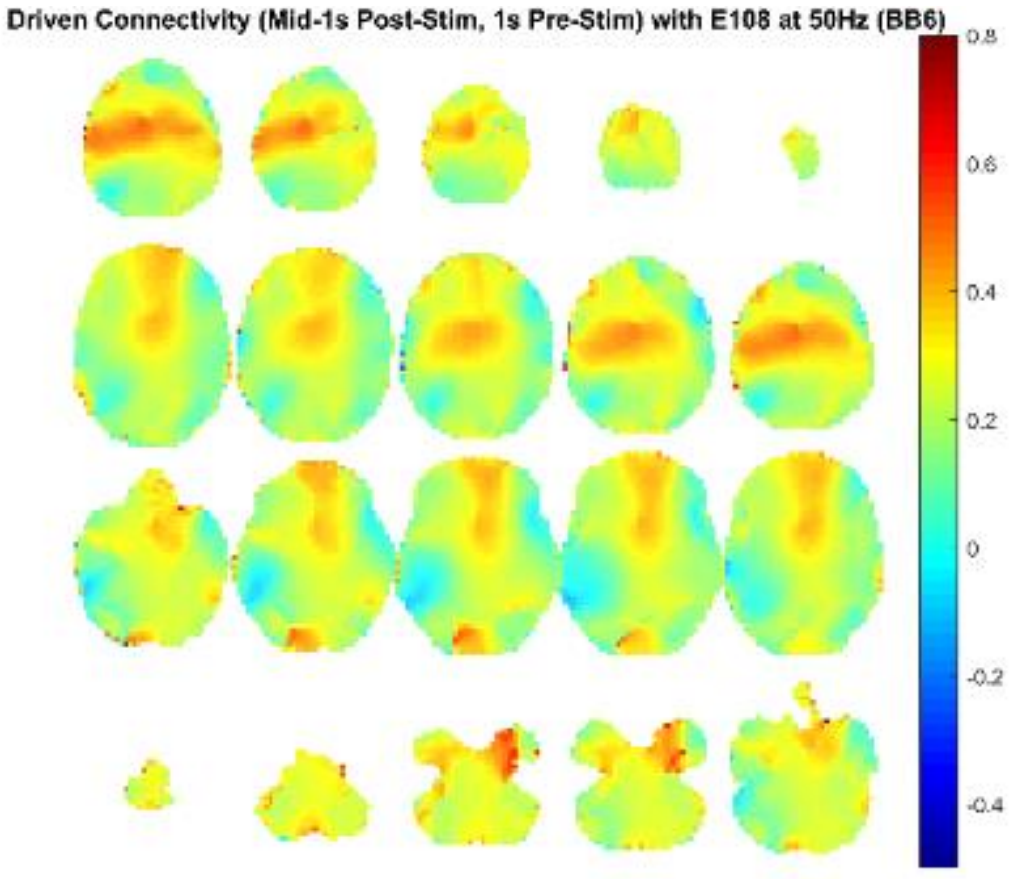

Figure 192. Source level connectivity with a dipole at E108 (right temporal, auditory cortex) in 50 Hz during the middle one-second of 6 Hz binaural beat tone stimulation (total stimulation was 3 seconds), performed with DICS and a standardized BEM headmodel. Unit is the percent change in coherence from baseline (i.e., difference between coherence during stimulation and coherence during baseline divided by coherence during baseline). Darker reds indicate increases in coherence with E45 while darker blues indicate decreases in coherence.

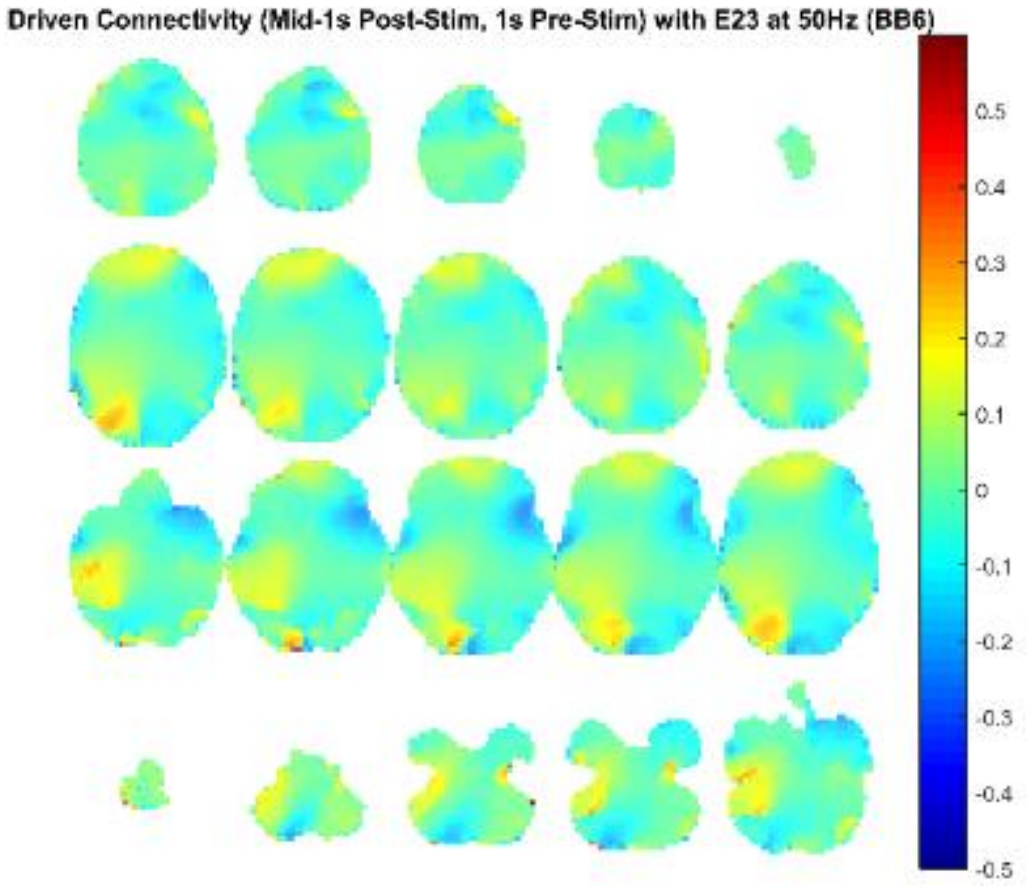

Figure 193. Source level connectivity with a dipole at E23 (left frontal) in 50 Hz during the middle one-second of 6 Hz binaural beat tone stimulation (total stimulation was 3 seconds), performed with DICS and a standardized BEM headmodel. Unit is the percent change in coherence from baseline (i.e., difference between coherence during stimulation and coherence during baseline divided by coherence during baseline). Darker reds indicate increases in coherence with E45 while darker blues indicate decreases in coherence.

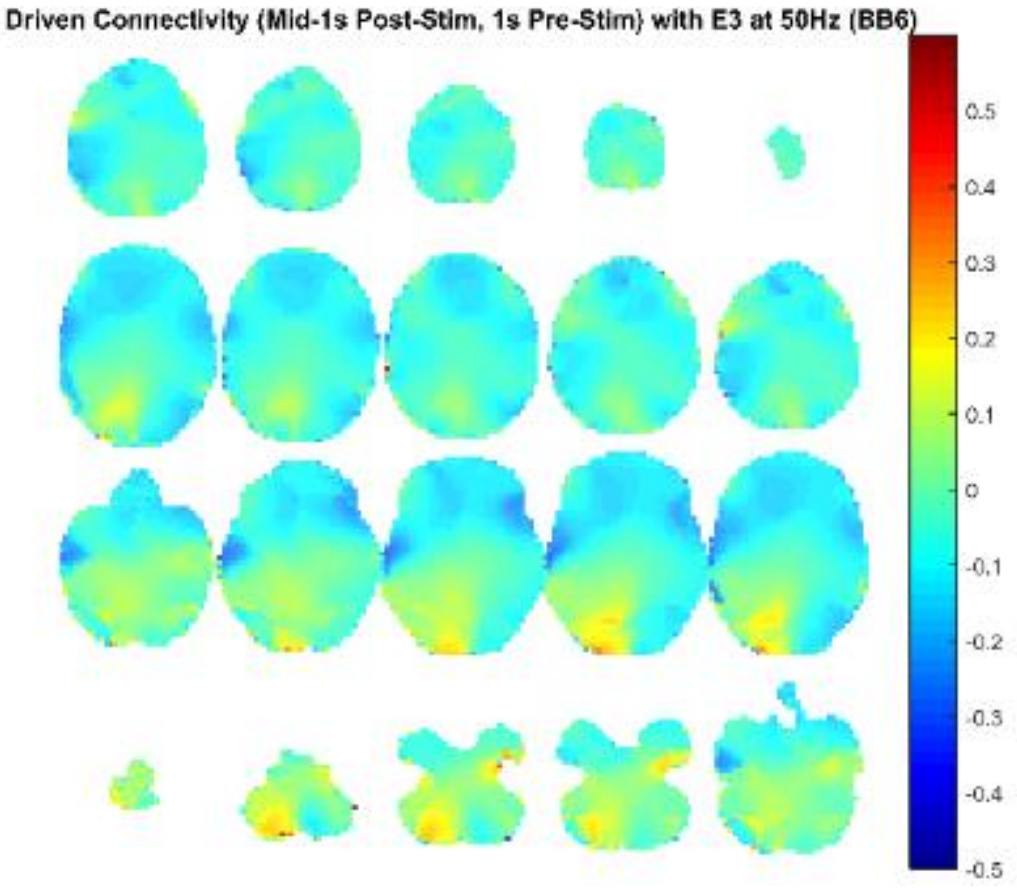

Figure 194. Source level connectivity with a dipole at E3 (right frontal) in 50 Hz during the middle one-second of 6 Hz binaural beat tone stimulation (total stimulation was 3 seconds), performed with DICS and a standardized BEM headmodel. Unit is the percent change in coherence from baseline (i.e., difference between coherence during stimulation and coherence during baseline divided by coherence during baseline). Darker reds indicate increases in coherence with E45 while darker blues indicate decreases in coherence.

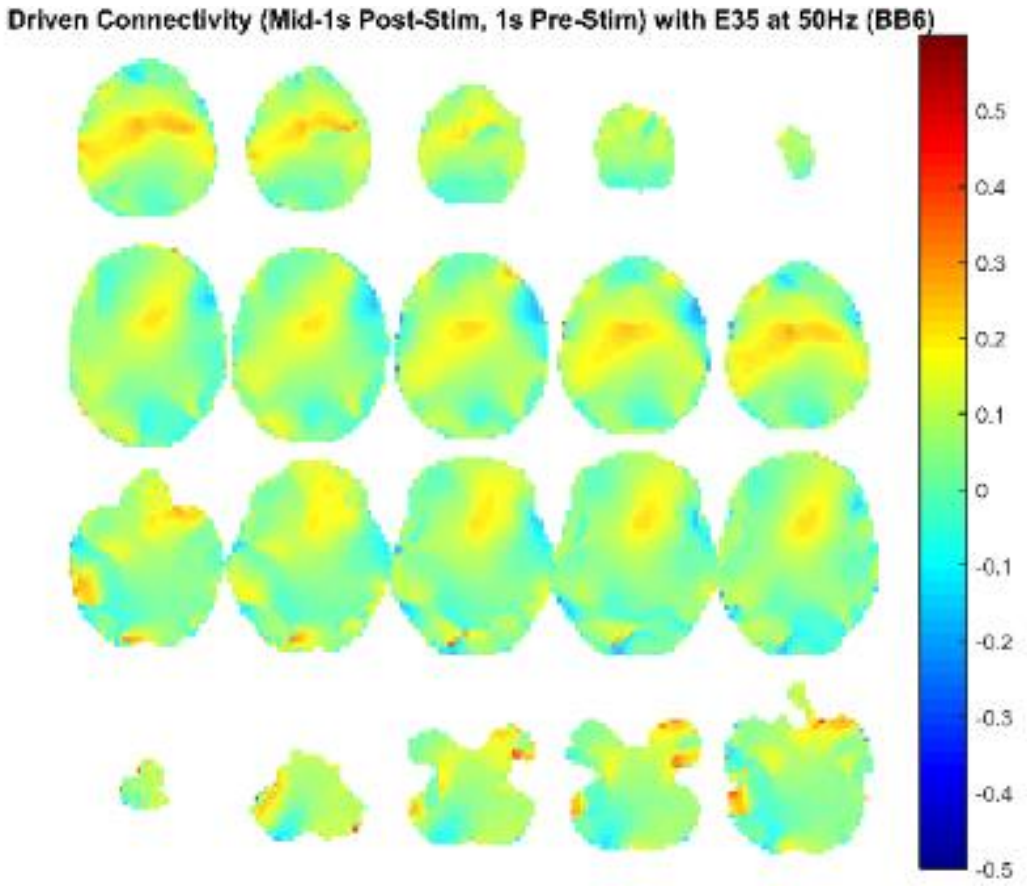

Figure 195. Source level connectivity with a dipole at E35 (left central) in 50 Hz during the middle one-second of 6 Hz binaural beat tone stimulation (total stimulation was 3 seconds), performed with DICS and a standardized BEM headmodel. Unit is the percent change in coherence from baseline (i.e., difference between coherence during stimulation and coherence during baseline divided by coherence during baseline). Darker reds indicate increases in coherence with E45 while darker blues indicate decreases in coherence.

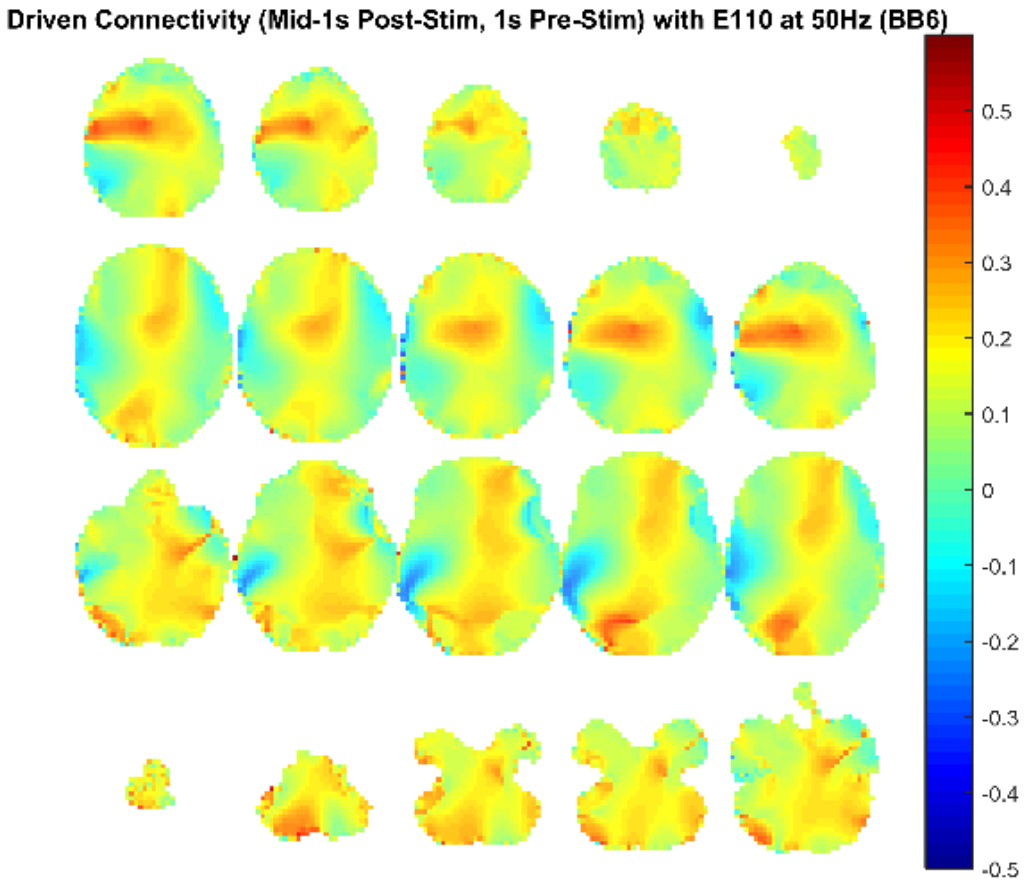

Figure 196. Source level connectivity with a dipole at E110 (right central) in 50 Hz during the middle one-second of 6 Hz binaural beat tone stimulation (total stimulation was 3 seconds), performed with DICS and a standardized BEM headmodel. Unit is the percent change in coherence from baseline (i.e., difference between coherence during stimulation and coherence during baseline divided by coherence during baseline). Darker reds indicate increases in coherence with E45 while darker blues indicate decreases in coherence.

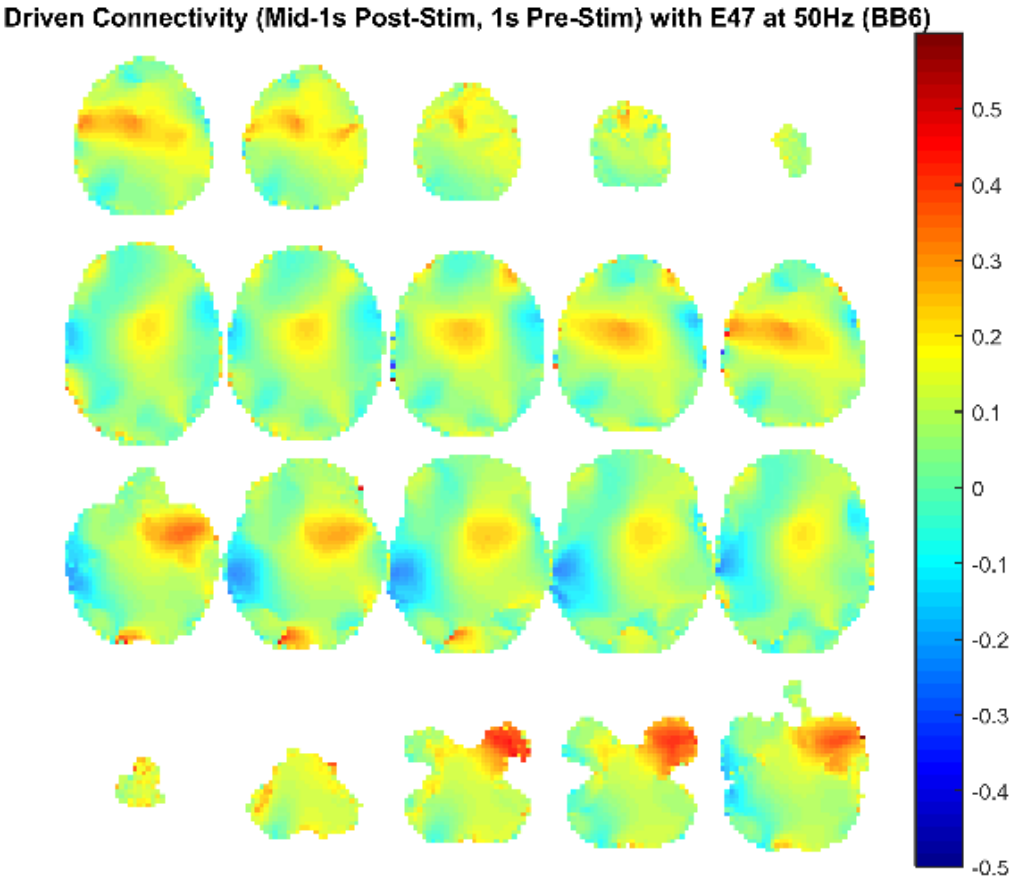

Figure 197. Source level connectivity with a dipole at E47 (left parietal) in 50 Hz during the middle one-second of 6 Hz binaural beat tone stimulation (total stimulation was 3 seconds), performed with DICS and a standardized BEM headmodel. Unit is the percent change in coherence from baseline (i.e., difference between coherence during stimulation and coherence during baseline divided by coherence during baseline). Darker reds indicate increases in coherence with E45 while darker blues indicate decreases in coherence.

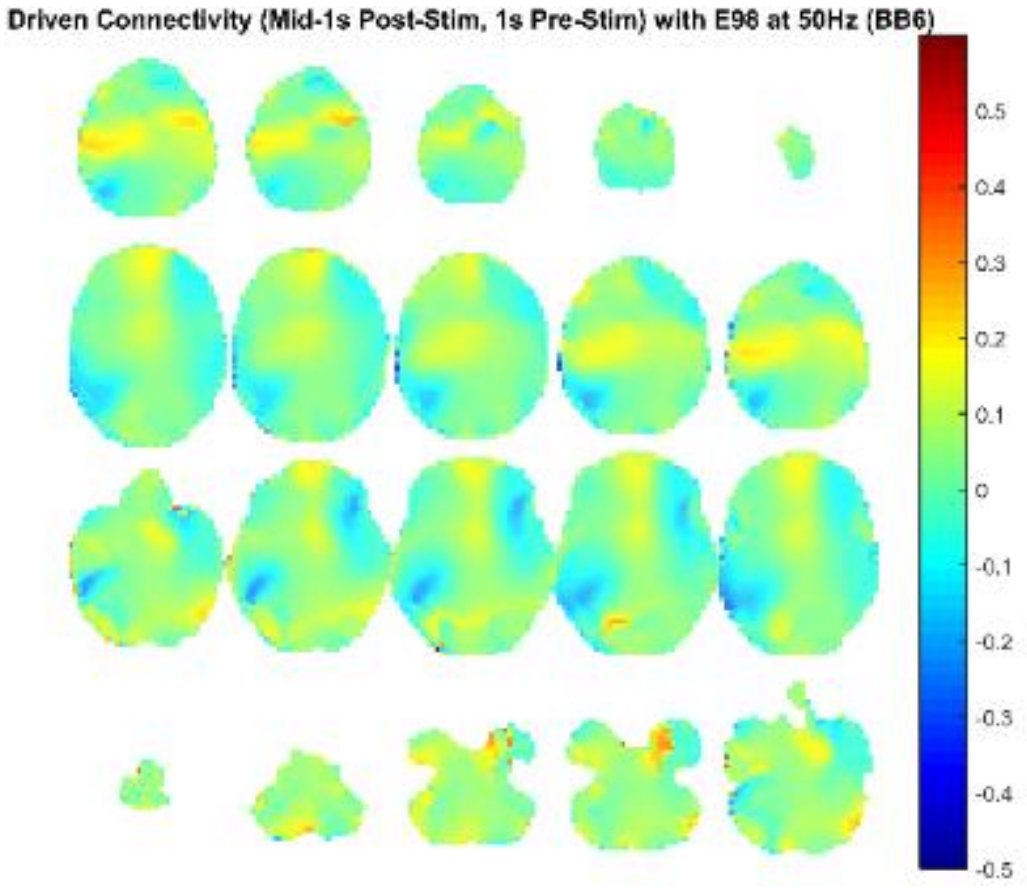

Figure 198. Source level connectivity with a dipole at E98 (right parietal) in 50 Hz during the middle one-second of 6 Hz binaural beat tone stimulation (total stimulation was 3 seconds), performed with DICS and a standardized BEM headmodel. Unit is the percent change in coherence from baseline (i.e., difference between coherence during stimulation and coherence during baseline divided by coherence during baseline). Darker reds indicate increases in coherence with E45 while darker blues indicate decreases in coherence.

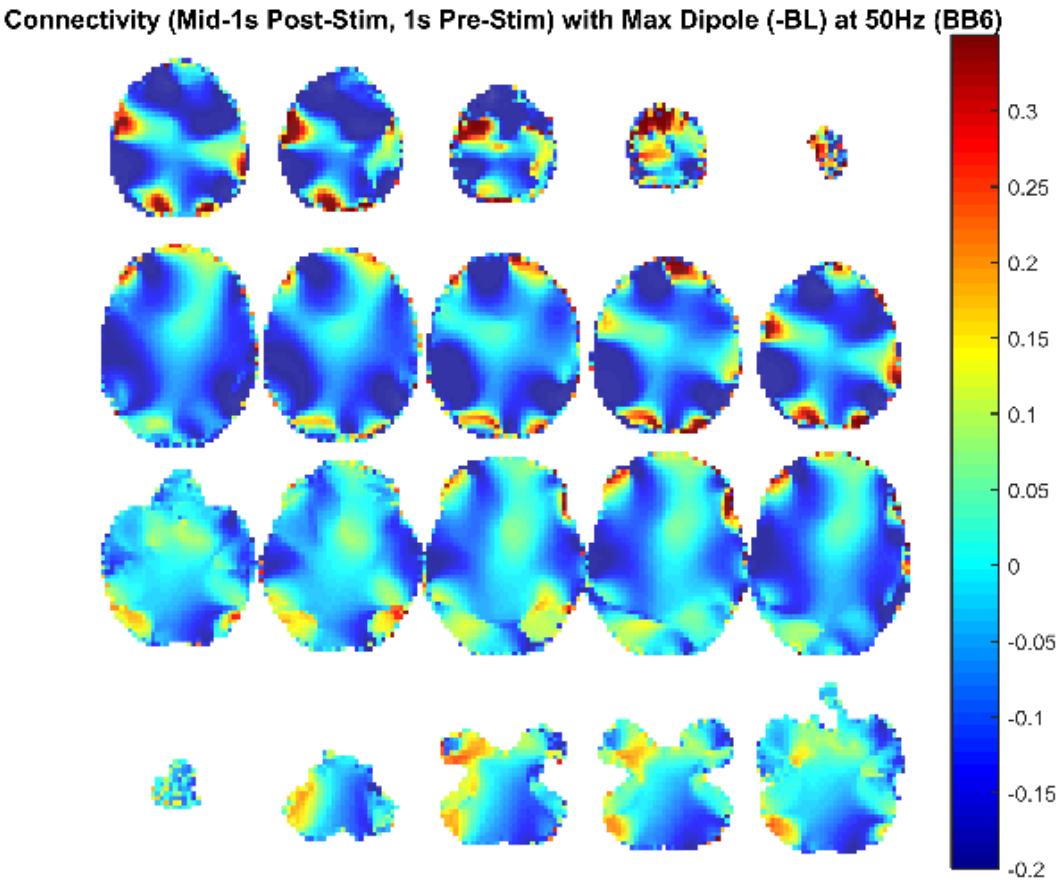

Figure 199. Source level connectivity with a dipole at dip2 (maximum power dipole for the middle one-second period corrected for the baseline one-second period) in 50 Hz during the middle one-second of 6 Hz binaural beat tone stimulation (total stimulation was 3 seconds), performed with DICS and a standardized BEM headmodel. Unit is the percent change in coherence from baseline (i.e., difference between coherence during stimulation and coherence during baseline divided by coherence during baseline). Darker reds indicate increases in coherence with E45 while darker blues indicate decreases in coherence.

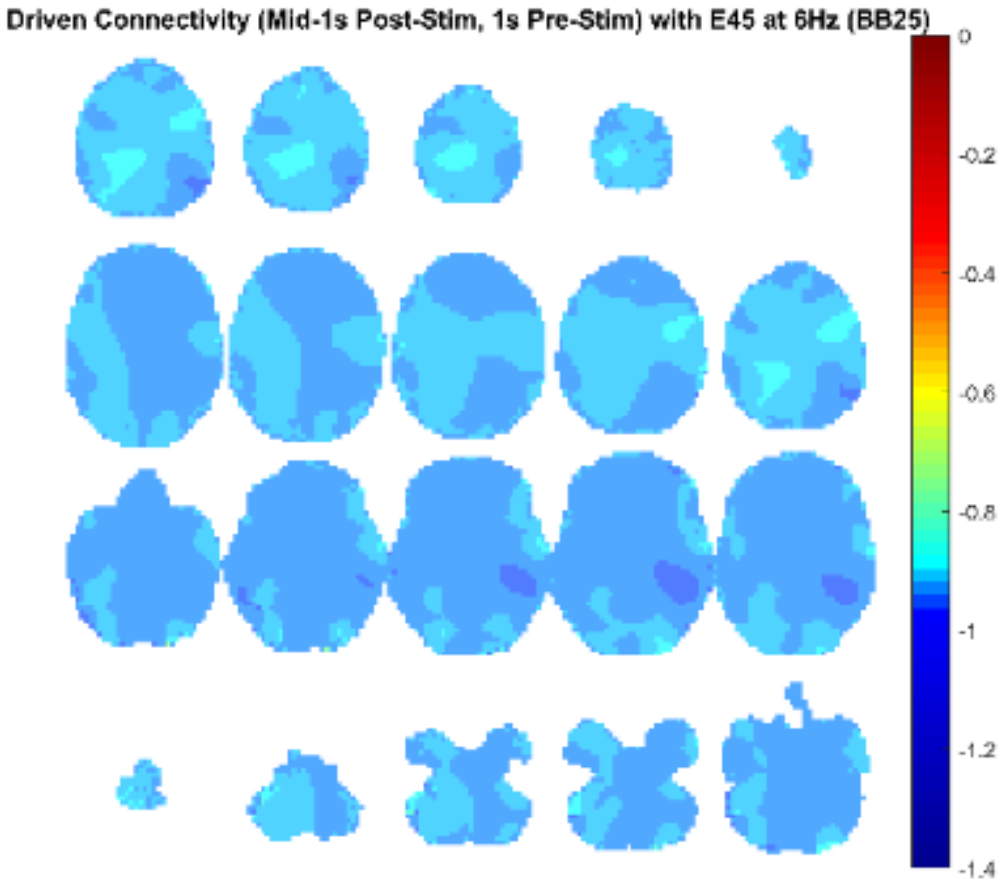

Figure 200. Source level connectivity with a dipole at E45 (left temporal, auditory cortex) in 6 Hz during the middle one-second of 25 Hz binaural beat tone stimulation (total stimulation was 3 seconds), performed with DICS and a standardized BEM headmodel. Unit is the percent change in coherence from baseline (i.e., difference between coherence during stimulation and coherence during baseline divided by coherence during baseline). Darker reds indicate increases in coherence with E45 while darker blues indicate decreases in coherence.

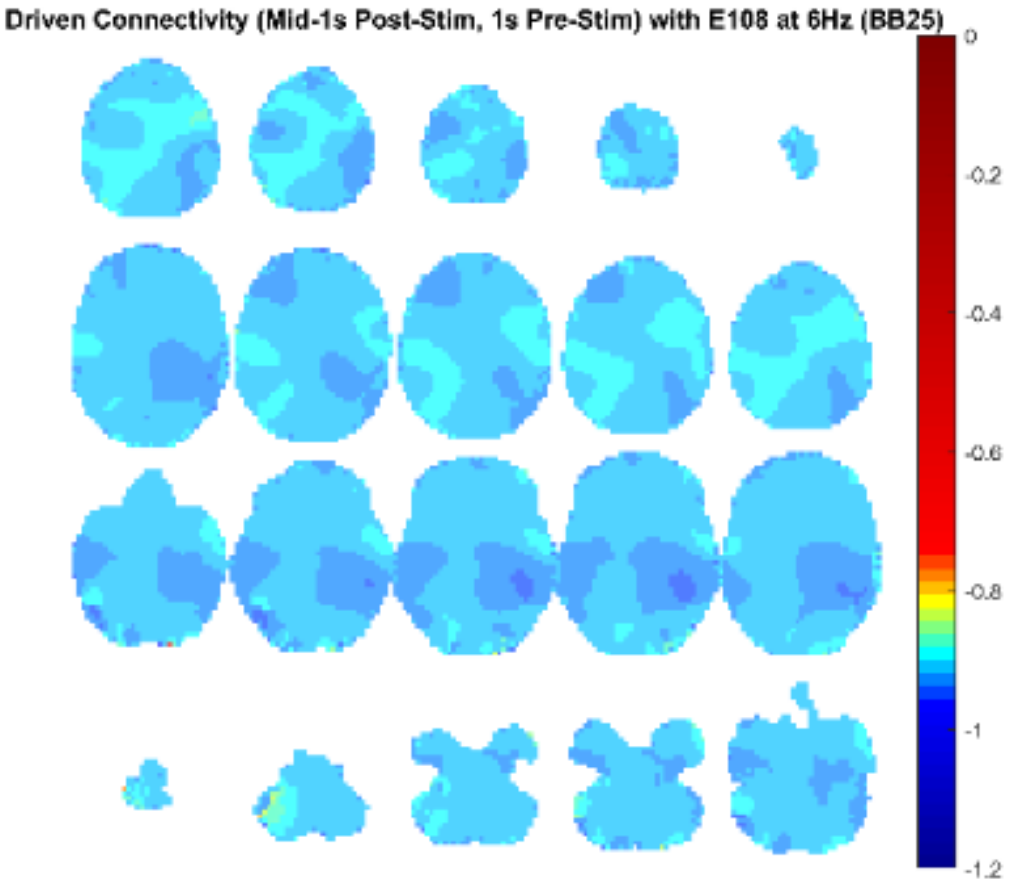

Figure 201. Source level connectivity with a dipole at E108 (right temporal, auditory cortex) in 6 Hz during the middle one-second of 25 Hz binaural beat tone stimulation (total stimulation was 3 seconds), performed with DICS and a standardized BEM headmodel. Unit is the percent change in coherence from baseline (i.e., difference between coherence during stimulation and coherence during baseline divided by coherence during baseline). Darker reds indicate increases in coherence with E45 while darker blues indicate decreases in coherence.

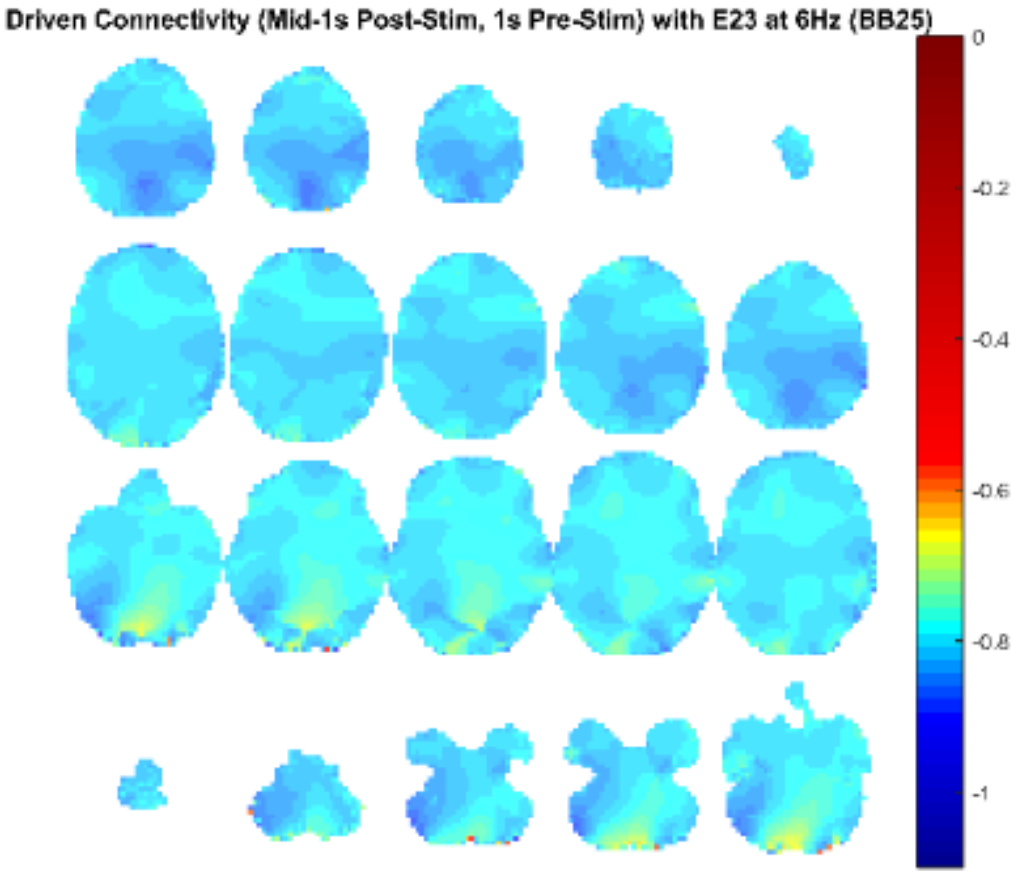

Figure 202. Source level connectivity with a dipole at E23 (left frontal) in 6 Hz during the middle one-second of 25 Hz binaural beat tone stimulation (total stimulation was 3 seconds), performed with DICS and a standardized BEM headmodel. Unit is the percent change in coherence from baseline (i.e., difference between coherence during stimulation and coherence during baseline divided by coherence during baseline). Darker reds indicate increases in coherence with E45 while darker blues indicate decreases in coherence.

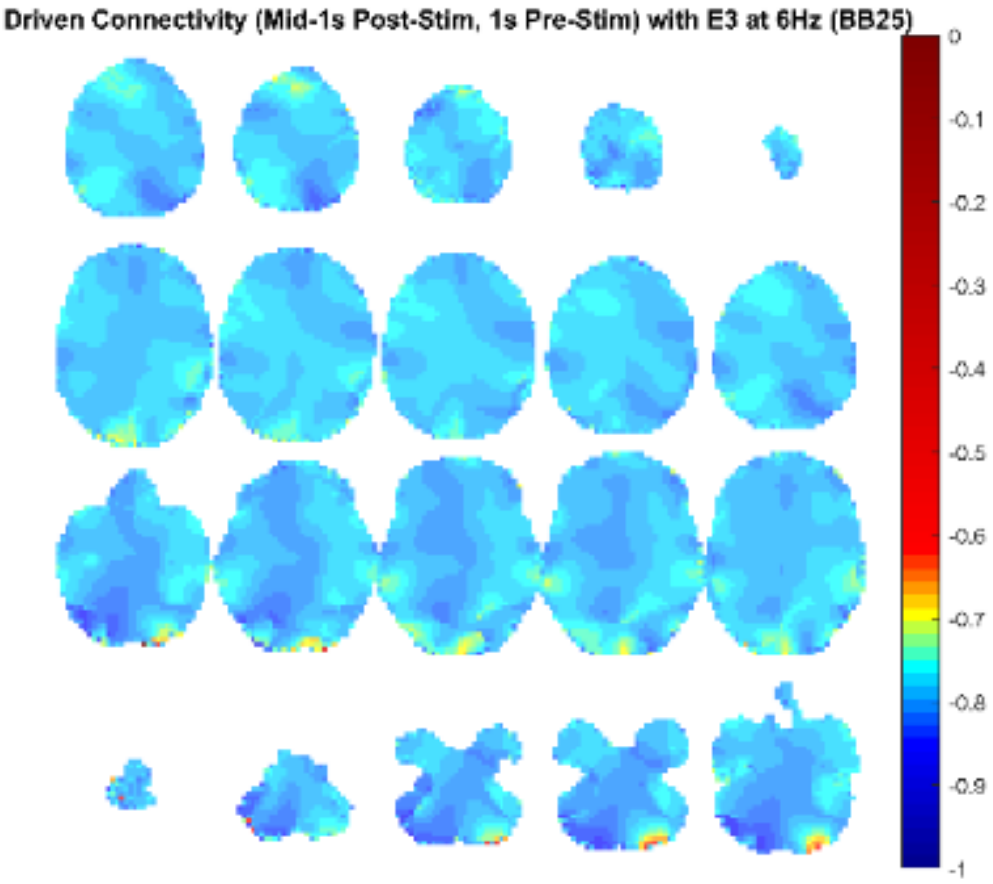

Figure 203. Source level connectivity with a dipole at E3 (right frontal) in 6 Hz during the middle one-second of 25 Hz binaural beat tone stimulation (total stimulation was 3 seconds), performed with DICS and a standardized BEM headmodel. Unit is the percent change in coherence from baseline (i.e., difference between coherence during stimulation and coherence during baseline divided by coherence during baseline). Darker reds indicate increases in coherence with E45 while darker blues indicate decreases in coherence.

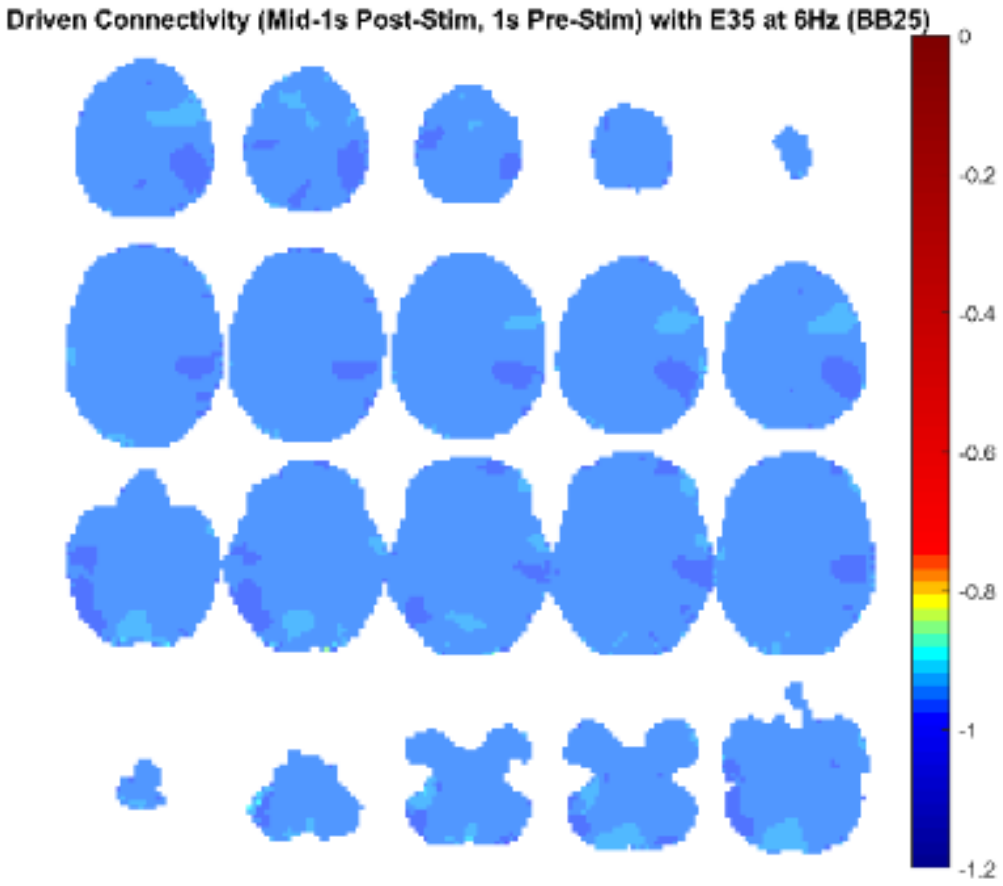

Figure 204. Source level connectivity with a dipole at E35 (left central) in 6 Hz during the middle one-second of 25 Hz binaural beat tone stimulation (total stimulation was 3 seconds), performed with DICS and a standardized BEM headmodel. Unit is the percent change in coherence from baseline (i.e., difference between coherence during stimulation and coherence during baseline divided by coherence during baseline). Darker reds indicate increases in coherence with E45 while darker blues indicate decreases in coherence.

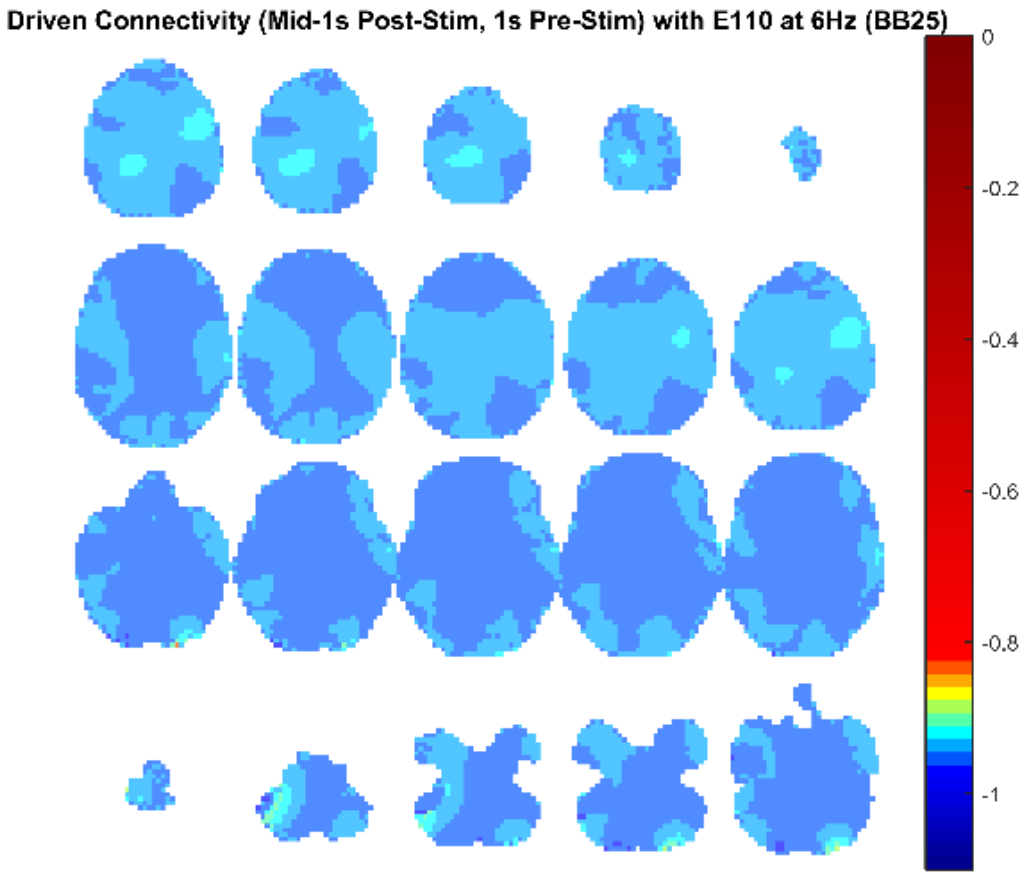

Figure 205. Source level connectivity with a dipole at E110 (right central) in 6 Hz during the middle one-second of 25 Hz binaural beat tone stimulation (total stimulation was 3 seconds), performed with DICS and a standardized BEM headmodel. Unit is the percent change in coherence from baseline (i.e., difference between coherence during stimulation and coherence during baseline divided by coherence during baseline). Darker reds indicate increases in coherence with E45 while darker blues indicate decreases in coherence.

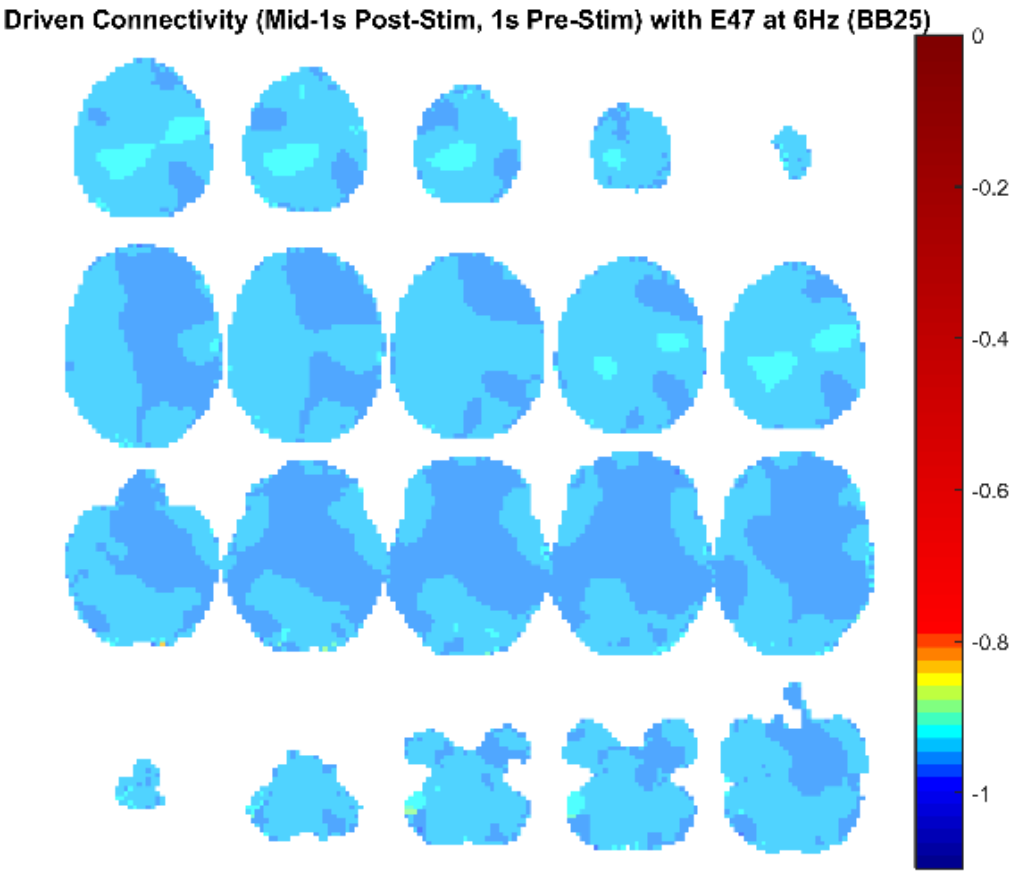

Figure 206. Source level connectivity with a dipole at E47 (left parietal) in 6 Hz during the middle one-second of 25 Hz binaural beat tone stimulation (total stimulation was 3 seconds), performed with DICS and a standardized BEM headmodel. Unit is the percent change in coherence from baseline (i.e., difference between coherence during stimulation and coherence during baseline divided by coherence during baseline). Darker reds indicate increases in coherence with E45 while darker blues indicate decreases in coherence.

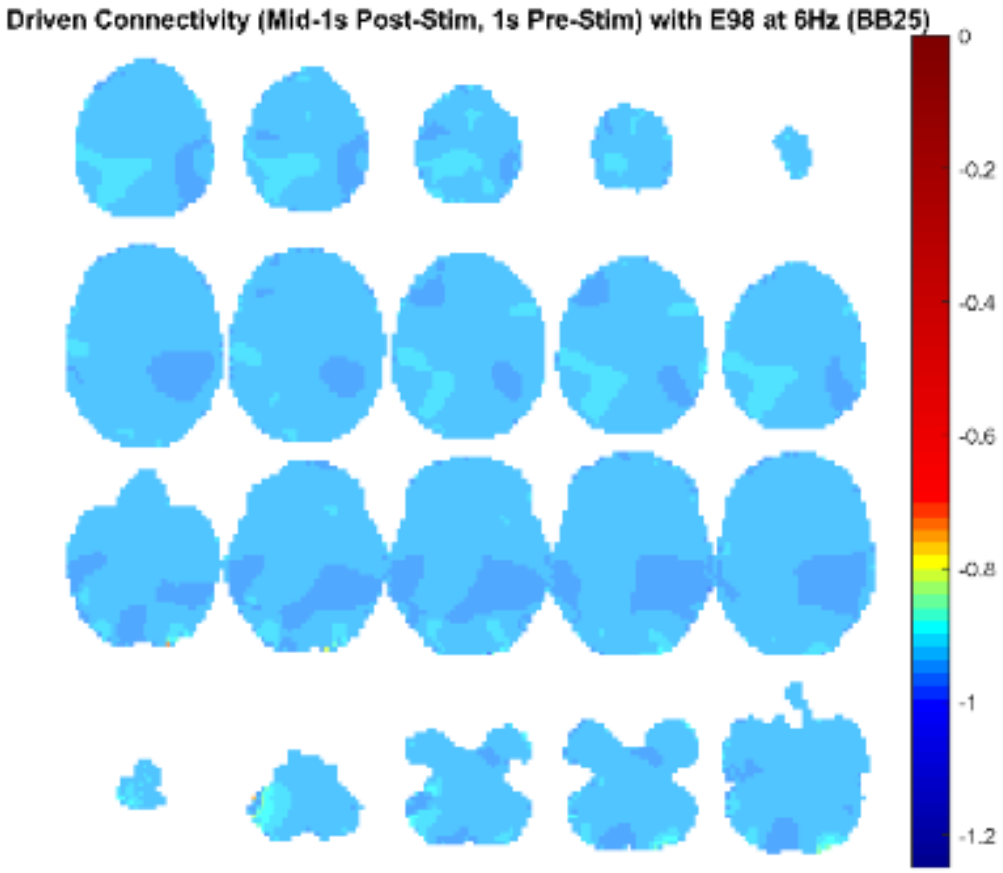

Figure 207. Source level connectivity with a dipole at E98 (right parietal) in 6 Hz during the middle one-second of 25 Hz binaural beat tone stimulation (total stimulation was 3 seconds), performed with DICS and a standardized BEM headmodel. Unit is the percent change in coherence from baseline (i.e., difference between coherence during stimulation and coherence during baseline divided by coherence during baseline). Darker reds indicate increases in coherence with E45 while darker blues indicate decreases in coherence.

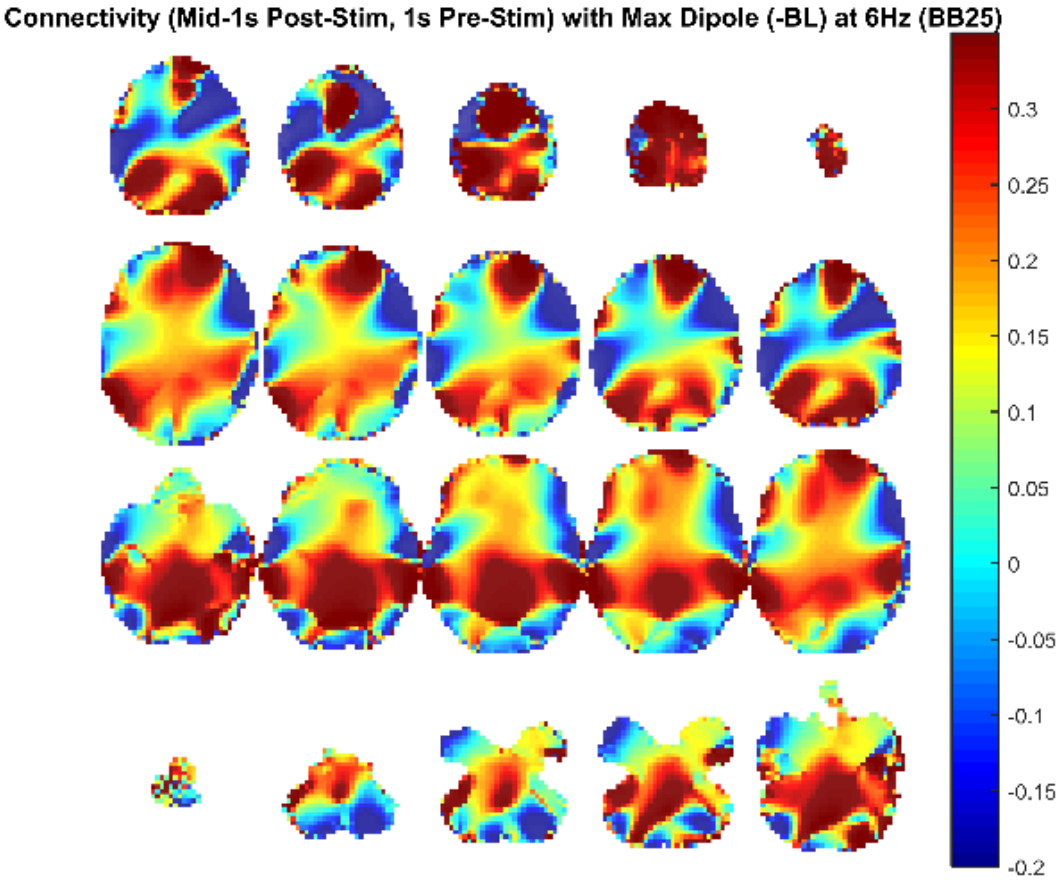

Figure 208. Source level connectivity with a dipole at dip2 (maximum power dipole for the middle one-second period corrected for the baseline one-second period) in 6 Hz during the middle one-second of 25 Hz binaural beat tone stimulation (total stimulation was 3 seconds), performed with DICS and a standardized BEM headmodel. Unit is the percent change in coherence from baseline (i.e., difference between coherence during stimulation and coherence during baseline divided by coherence during baseline). Darker reds indicate increases in coherence with E45 while darker blues indicate decreases in coherence.

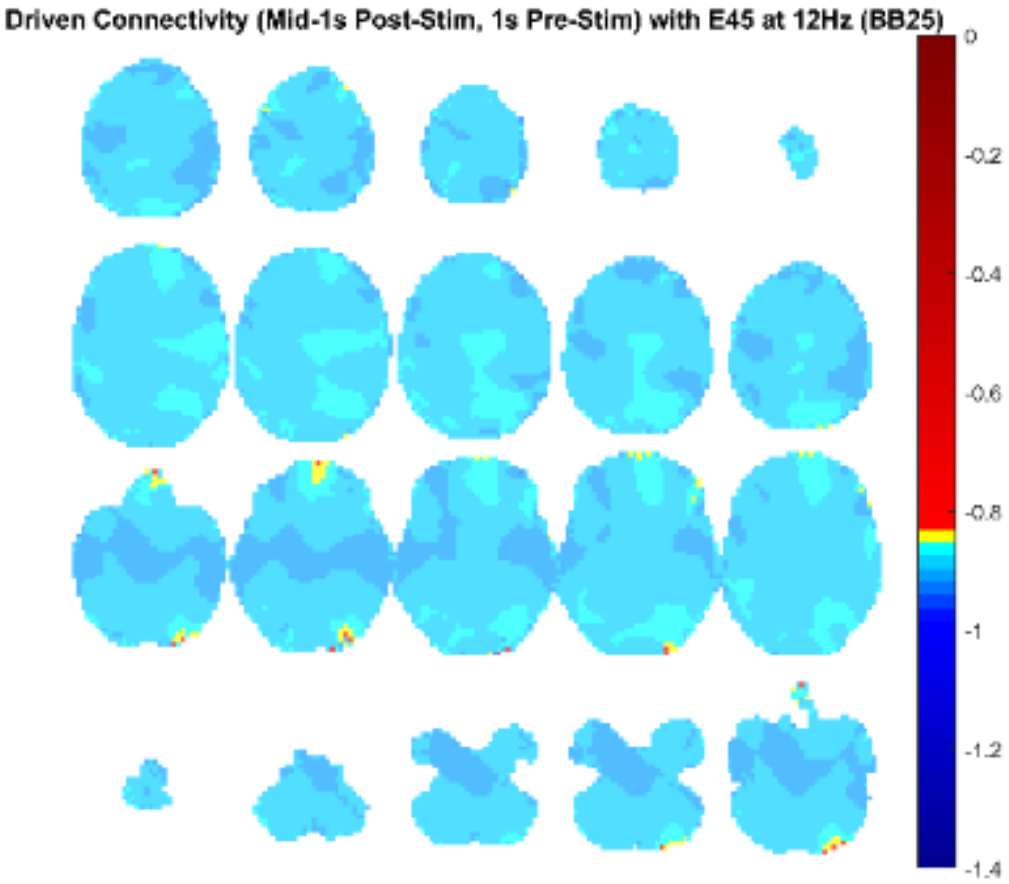

Figure 209. Source level connectivity with a dipole at E45 (left temporal, auditory cortex) in 12 Hz during the middle one-second of 25 Hz binaural beat tone stimulation (total stimulation was 3 seconds), performed with DICS and a standardized BEM headmodel. Unit is the percent change in coherence from baseline (i.e., difference between coherence during stimulation and coherence during baseline divided by coherence during baseline). Darker reds indicate increases in coherence with E45 while darker blues indicate decreases in coherence.

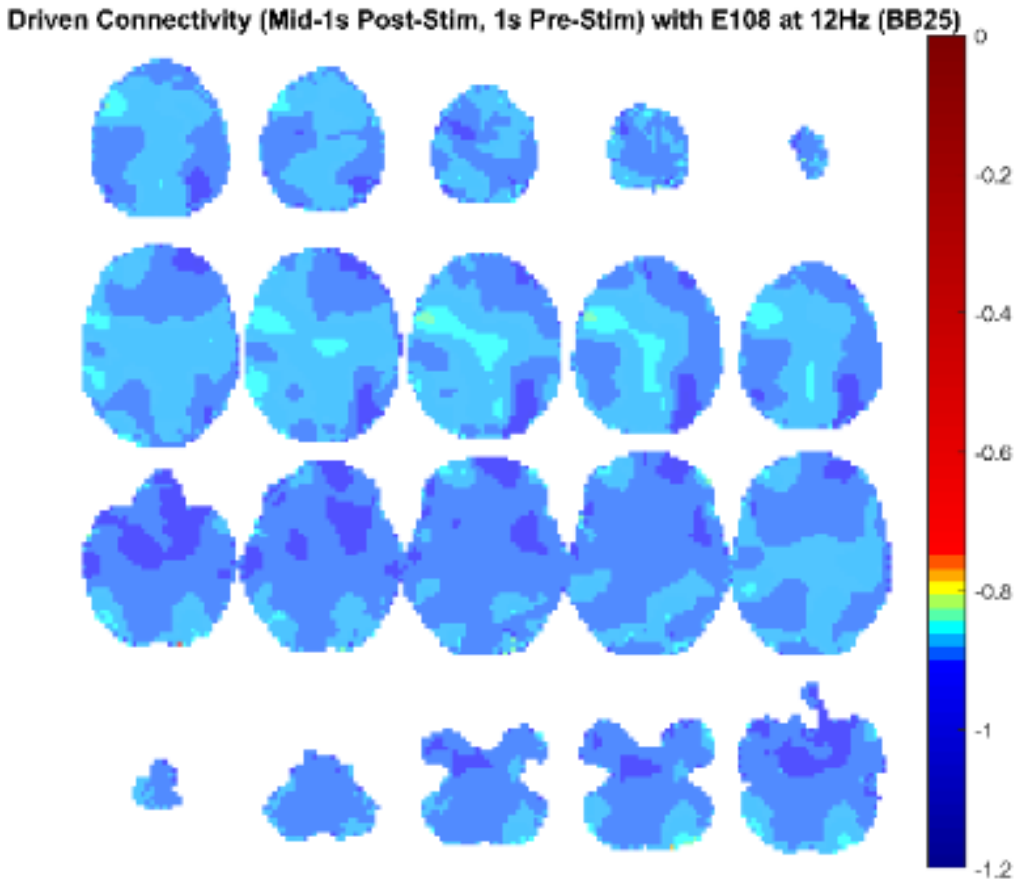

Figure 210. Source level connectivity with a dipole at E108 (right temporal, auditory cortex) in 12 Hz during the middle one-second of 25 Hz binaural beat tone stimulation (total stimulation was 3 seconds), performed with DICS and a standardized BEM headmodel. Unit is the percent change in coherence from baseline (i.e., difference between coherence during stimulation and coherence during baseline divided by coherence during baseline). Darker reds indicate increases in coherence with E45 while darker blues indicate decreases in coherence.

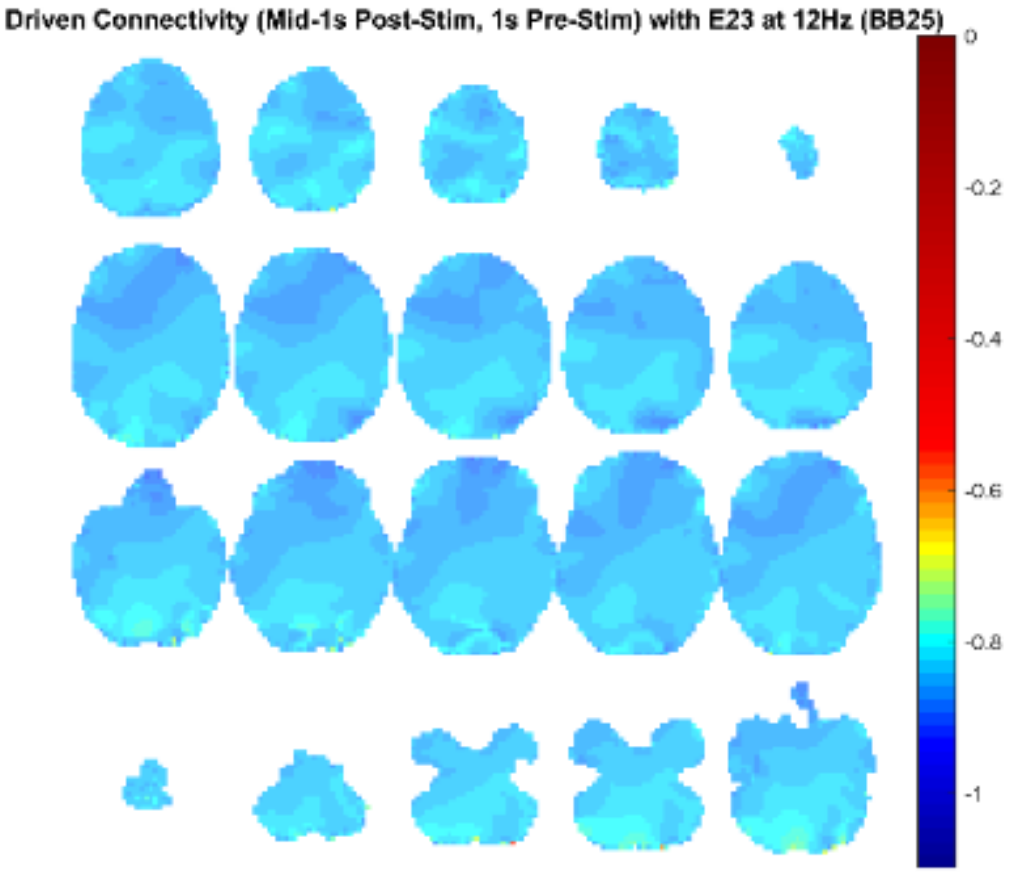

Figure 211. Source level connectivity with a dipole at E23 (left frontal) in 12 Hz during the middle one-second of 25 Hz binaural beat tone stimulation (total stimulation was 3 seconds), performed with DICS and a standardized BEM headmodel. Unit is the percent change in coherence from baseline (i.e., difference between coherence during stimulation and coherence during baseline divided by coherence during baseline). Darker reds indicate increases in coherence with E45 while darker blues indicate decreases in coherence.

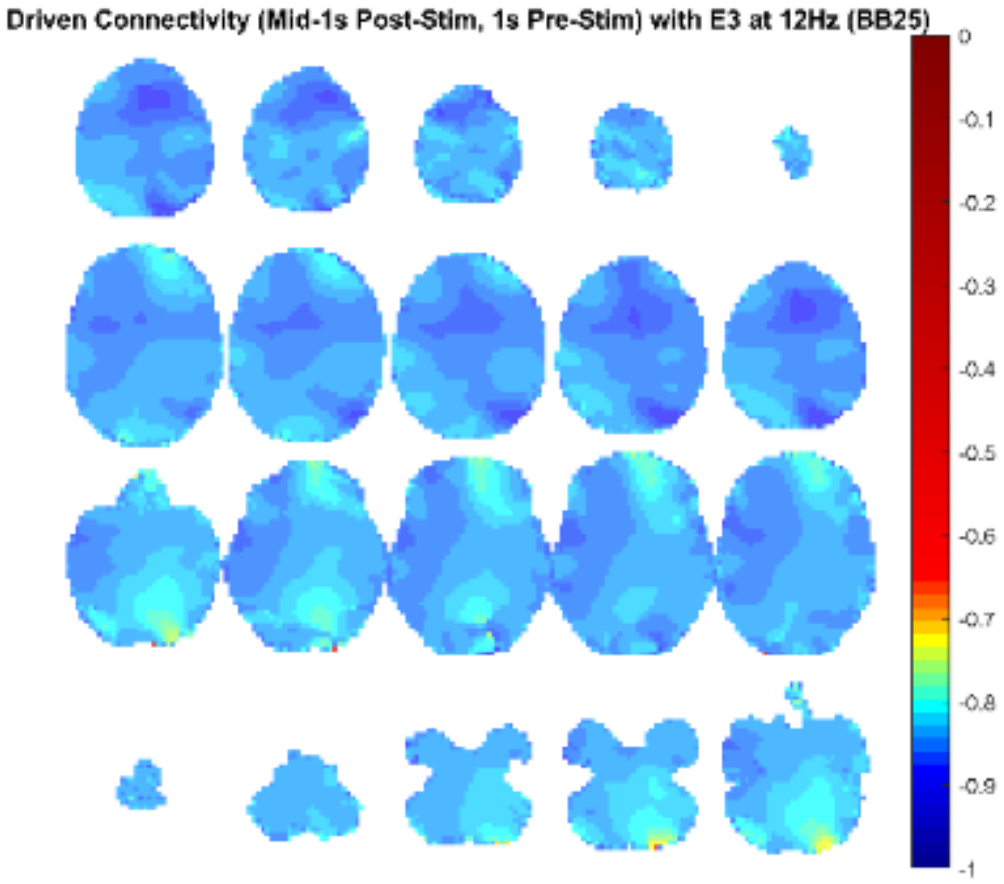

Figure 212. Source level connectivity with a dipole at E3 (right frontal) in 12 Hz during the middle one-second of 25 Hz binaural beat tone stimulation (total stimulation was 3 seconds), performed with DICS and a standardized BEM headmodel. Unit is the percent change in coherence from baseline (i.e., difference between coherence during stimulation and coherence during baseline divided by coherence during baseline). Darker reds indicate increases in coherence with E45 while darker blues indicate decreases in coherence.

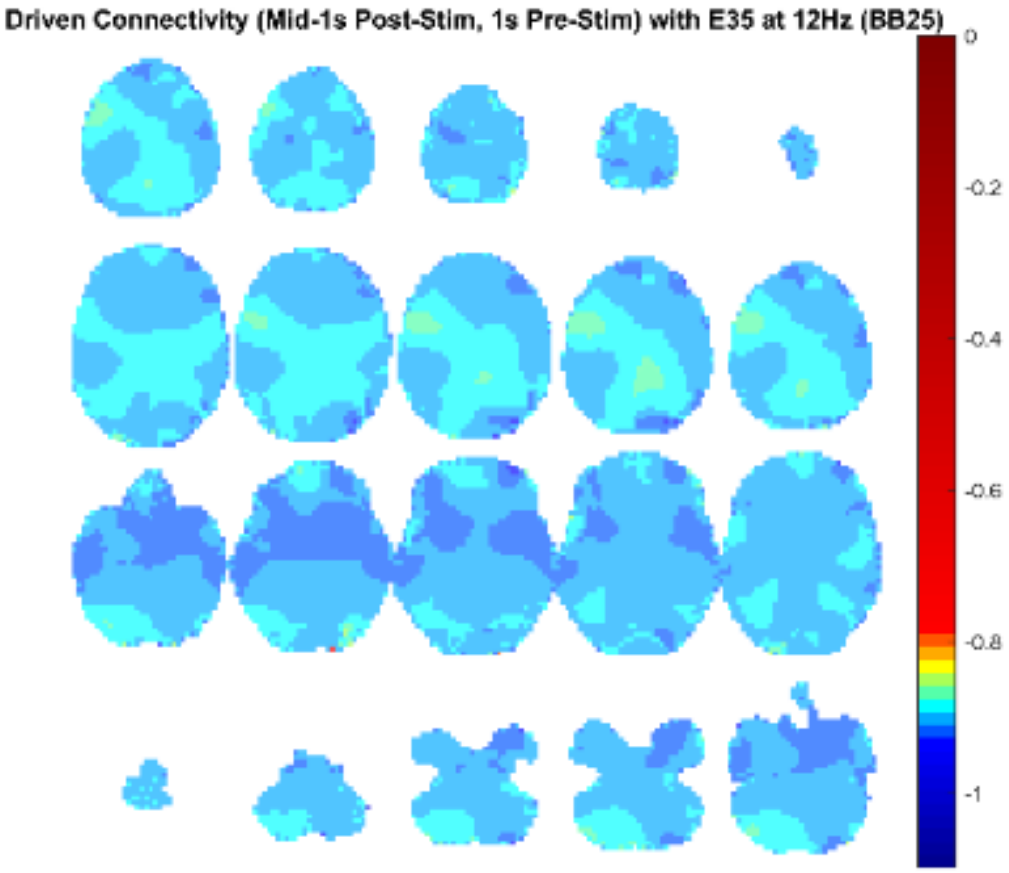

Figure 213. Source level connectivity with a dipole at E35 (left central) in 12 Hz during the middle one-second of 25 Hz binaural beat tone stimulation (total stimulation was 3 seconds), performed with DICS and a standardized BEM headmodel. Unit is the percent change in coherence from baseline (i.e., difference between coherence during stimulation and coherence during baseline divided by coherence during baseline). Darker reds indicate increases in coherence with E45 while darker blues indicate decreases in coherence.

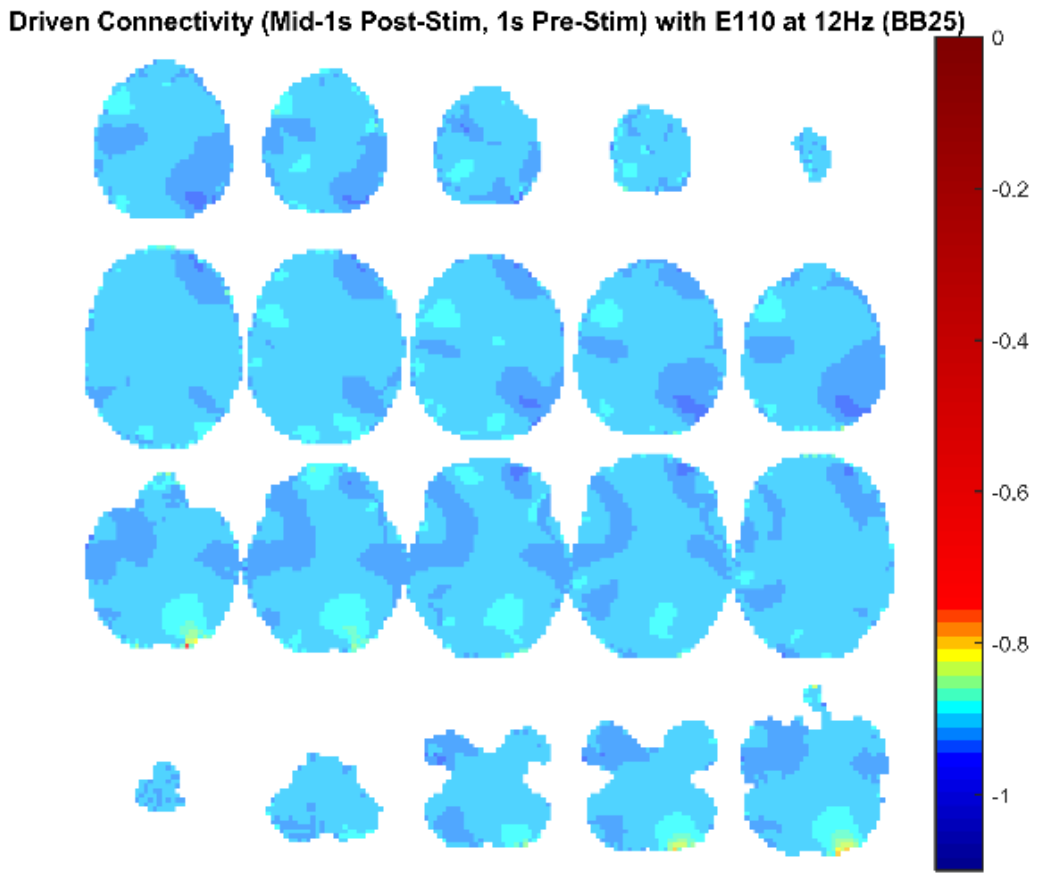

Figure 214. Source level connectivity with a dipole at E110 (right central) in 12 Hz during the middle one-second of 25 Hz binaural beat tone stimulation (total stimulation was 3 seconds), performed with DICS and a standardized BEM headmodel. Unit is the percent change in coherence from baseline (i.e., difference between coherence during stimulation and coherence during baseline divided by coherence during baseline). Darker reds indicate increases in coherence with E45 while darker blues indicate decreases in coherence.

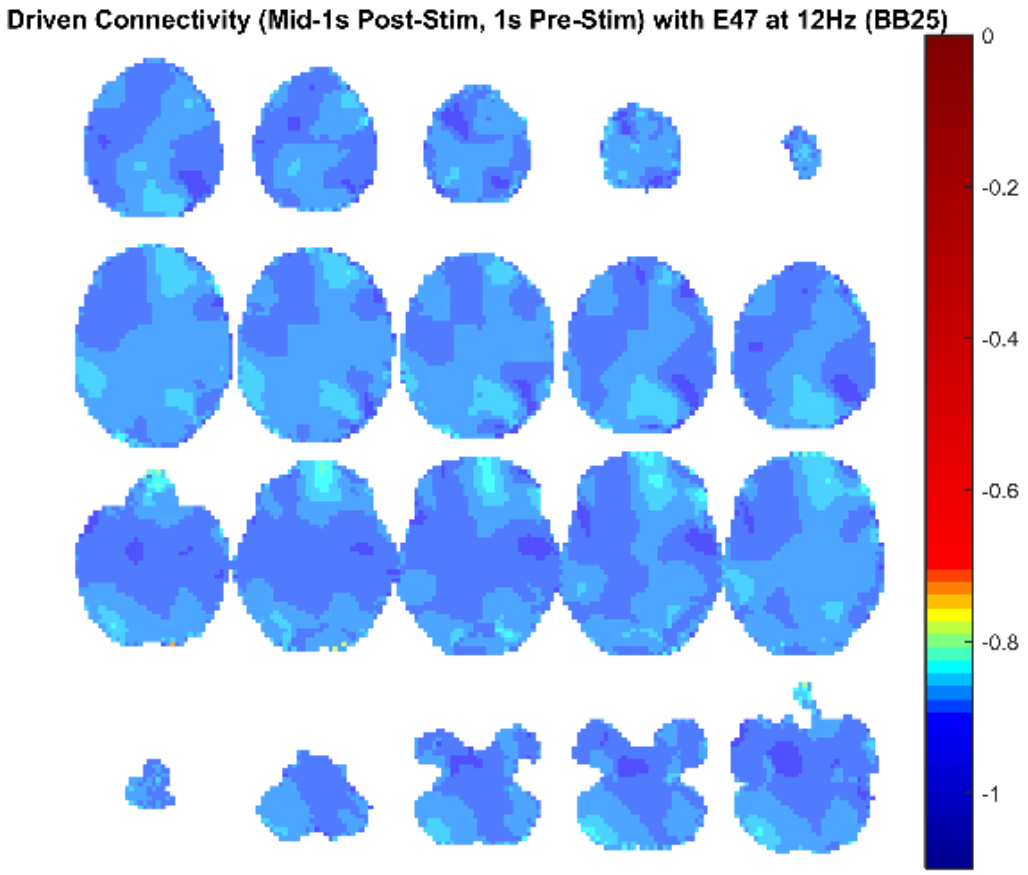

Figure 215. Source level connectivity with a dipole at E47 (left parietal) in 12 Hz during the middle one-second of 25 Hz binaural beat tone stimulation (total stimulation was 3 seconds), performed with DICS and a standardized BEM headmodel. Unit is the percent change in coherence from baseline (i.e., difference between coherence during stimulation and coherence during baseline divided by coherence during baseline). Darker reds indicate increases in coherence with E45 while darker blues indicate decreases in coherence.

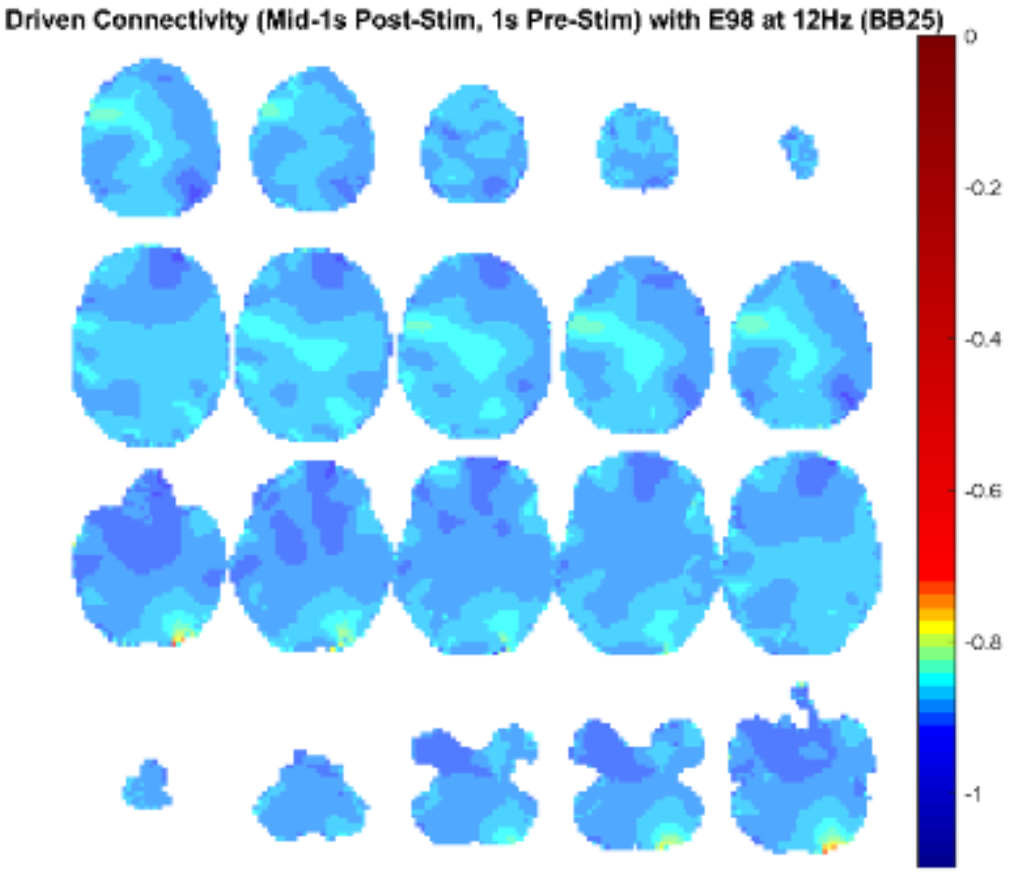

Figure 216. Source level connectivity with a dipole at E98 (right parietal) in 12 Hz during the middle one-second of 25 Hz binaural beat tone stimulation (total stimulation was 3 seconds), performed with DICS and a standardized BEM headmodel. Unit is the percent change in coherence from baseline (i.e., difference between coherence during stimulation and coherence during baseline divided by coherence during baseline). Darker reds indicate increases in coherence with E45 while darker blues indicate decreases in coherence.

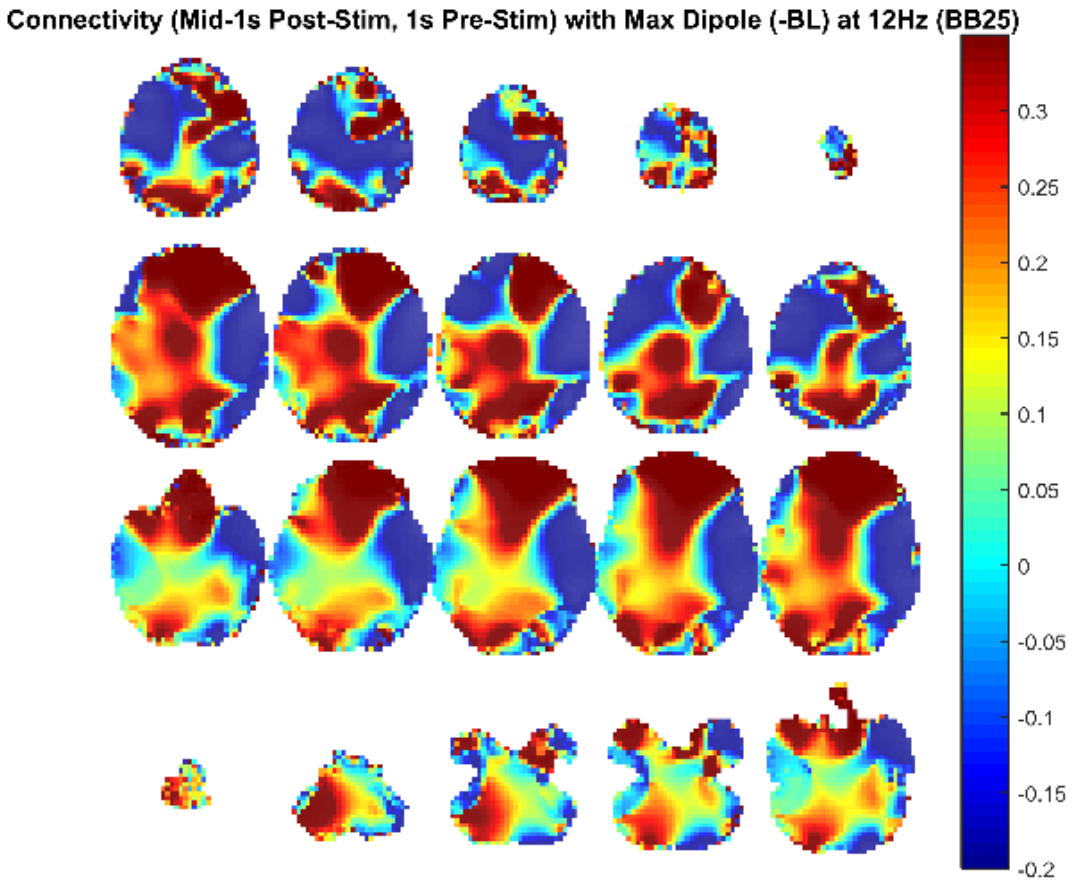

Figure 217. Source level connectivity with a dipole at dip2 (maximum power dipole for the middle one-second period corrected for the baseline one-second period) in 12 Hz during the middle one-second of 25 Hz binaural beat tone stimulation (total stimulation was 3 seconds), performed with DICS and a standardized BEM headmodel. Unit is the percent change in coherence from baseline (i.e., difference between coherence during stimulation and coherence during baseline divided by coherence during baseline). Darker reds indicate increases in coherence with E45 while darker blues indicate decreases in coherence.

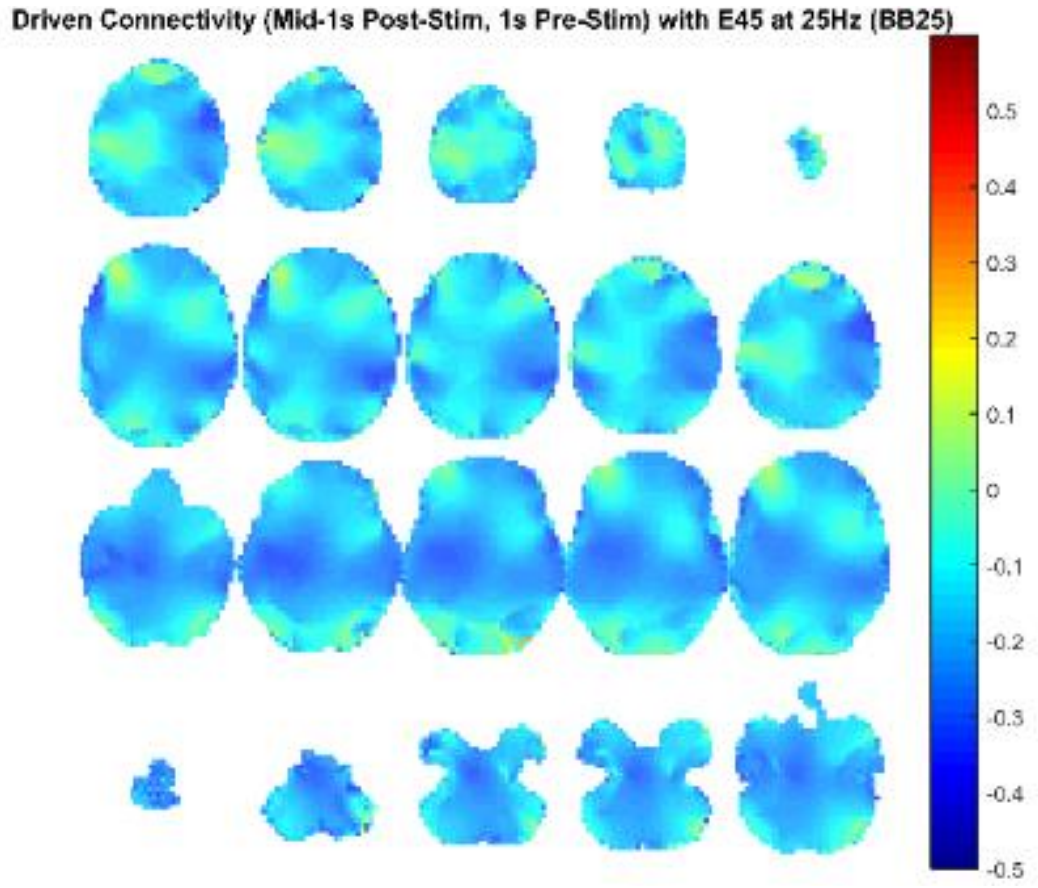

Figure 218. Source level connectivity with a dipole at E45 (left temporal, auditory cortex) in 25 Hz during the middle one-second of 25 Hz binaural beat tone stimulation (total stimulation was 3 seconds), performed with DICS and a standardized BEM headmodel. Unit is the percent change in coherence from baseline (i.e., difference between coherence during stimulation and coherence during baseline divided by coherence during baseline). Darker reds indicate increases in coherence with E45 while darker blues indicate decreases in coherence.

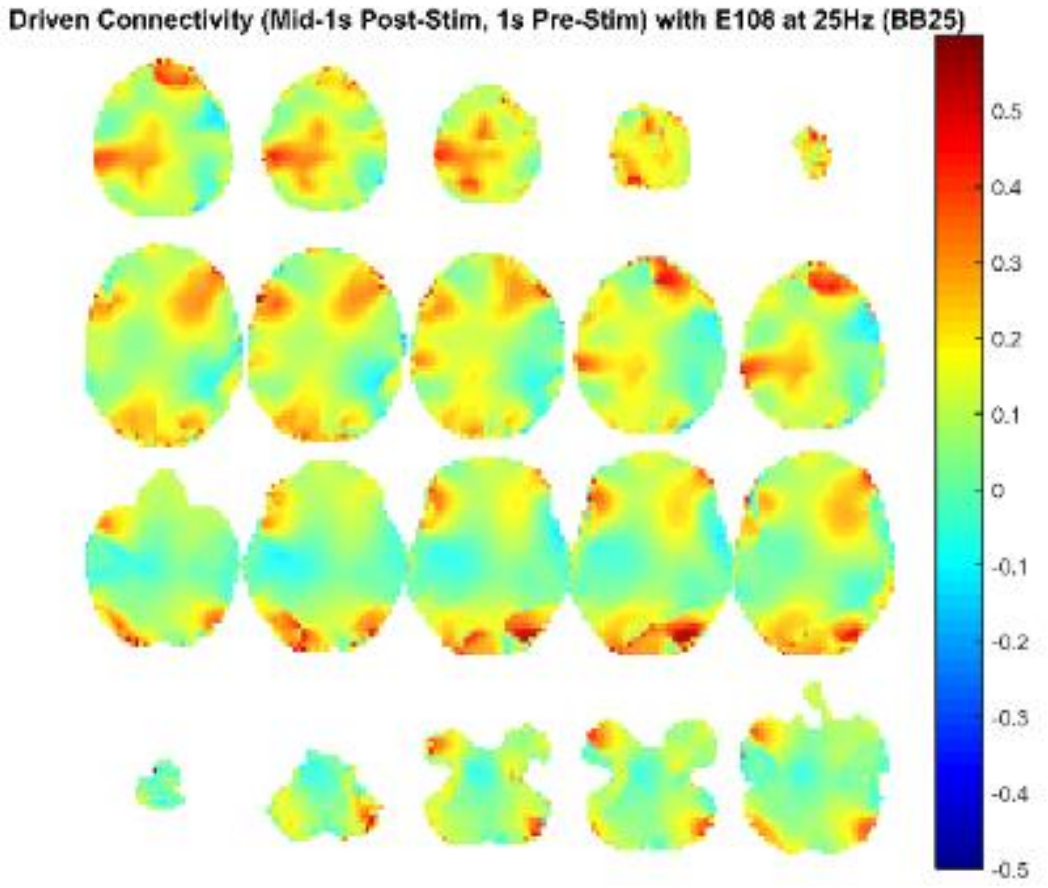

Figure 219. Source level connectivity with a dipole at E108 (right temporal, auditory cortex) in 25 Hz during the middle one-second of 25 Hz binaural beat tone stimulation (total stimulation was 3 seconds), performed with DICS and a standardized BEM headmodel. Unit is the percent change in coherence from baseline (i.e., difference between coherence during stimulation and coherence during baseline divided by coherence during baseline). Darker reds indicate increases in coherence with E45 while darker blues indicate decreases in coherence.

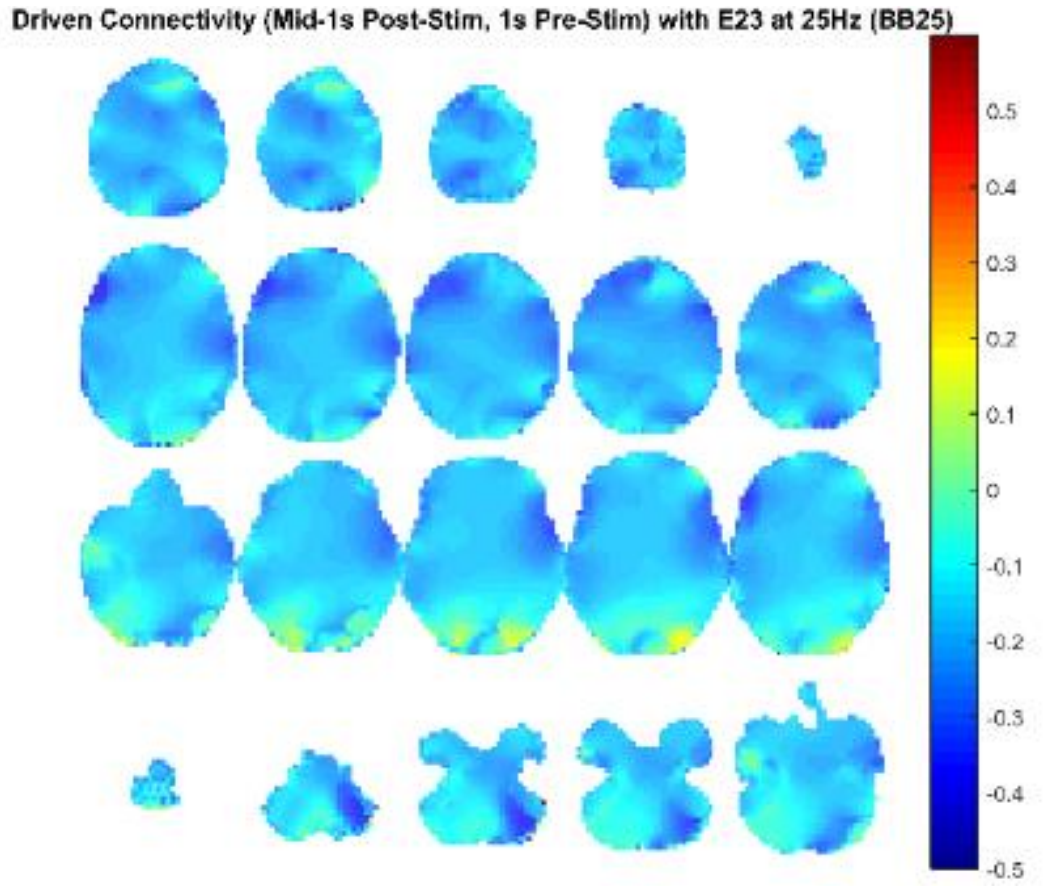

Figure 220. Source level connectivity with a dipole at E23 (left frontal) in 25 Hz during the middle one-second of 25 Hz binaural beat tone stimulation (total stimulation was 3 seconds), performed with DICS and a standardized BEM headmodel. Unit is the percent change in coherence from baseline (i.e., difference between coherence during stimulation and coherence during baseline divided by coherence during baseline). Darker reds indicate increases in coherence with E45 while darker blues indicate decreases in coherence.

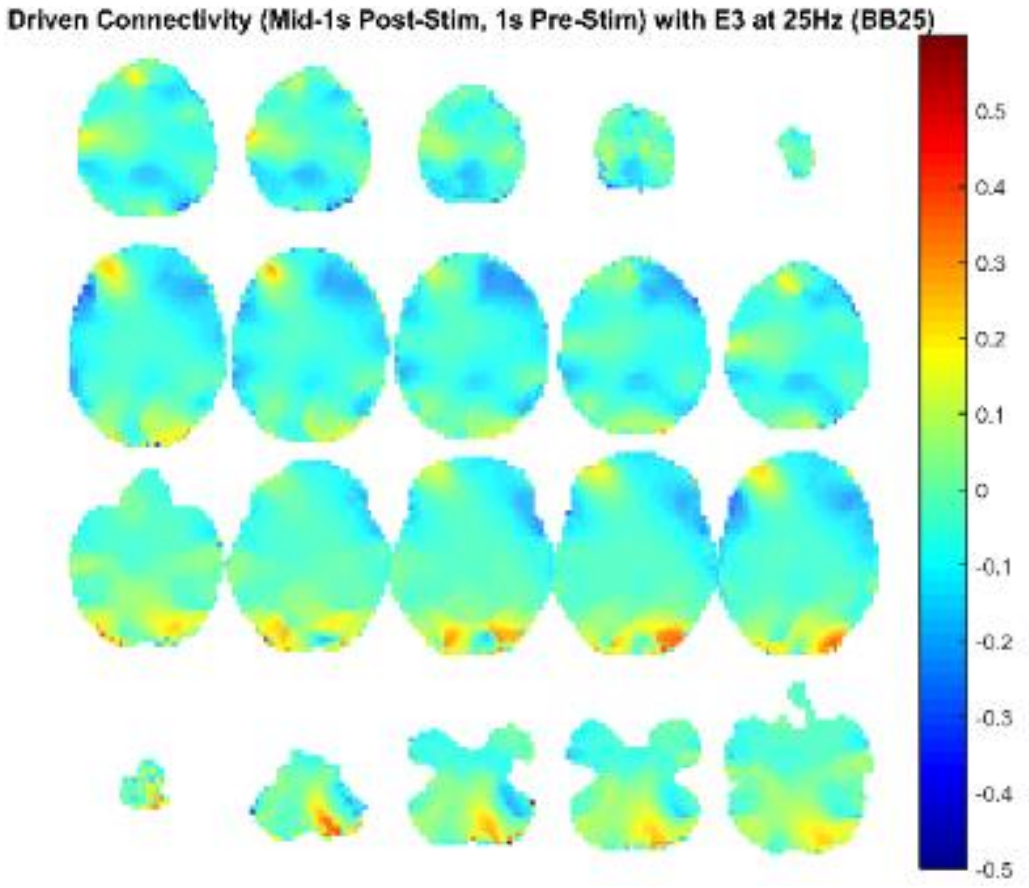

Figure 221. Source level connectivity with a dipole at E3 (right frontal) in 25 Hz during the middle one-second of 25 Hz binaural beat tone stimulation (total stimulation was 3 seconds), performed with DICS and a standardized BEM headmodel. Unit is the percent change in coherence from baseline (i.e., difference between coherence during stimulation and coherence during baseline divided by coherence during baseline). Darker reds indicate increases in coherence with E45 while darker blues indicate decreases in coherence.

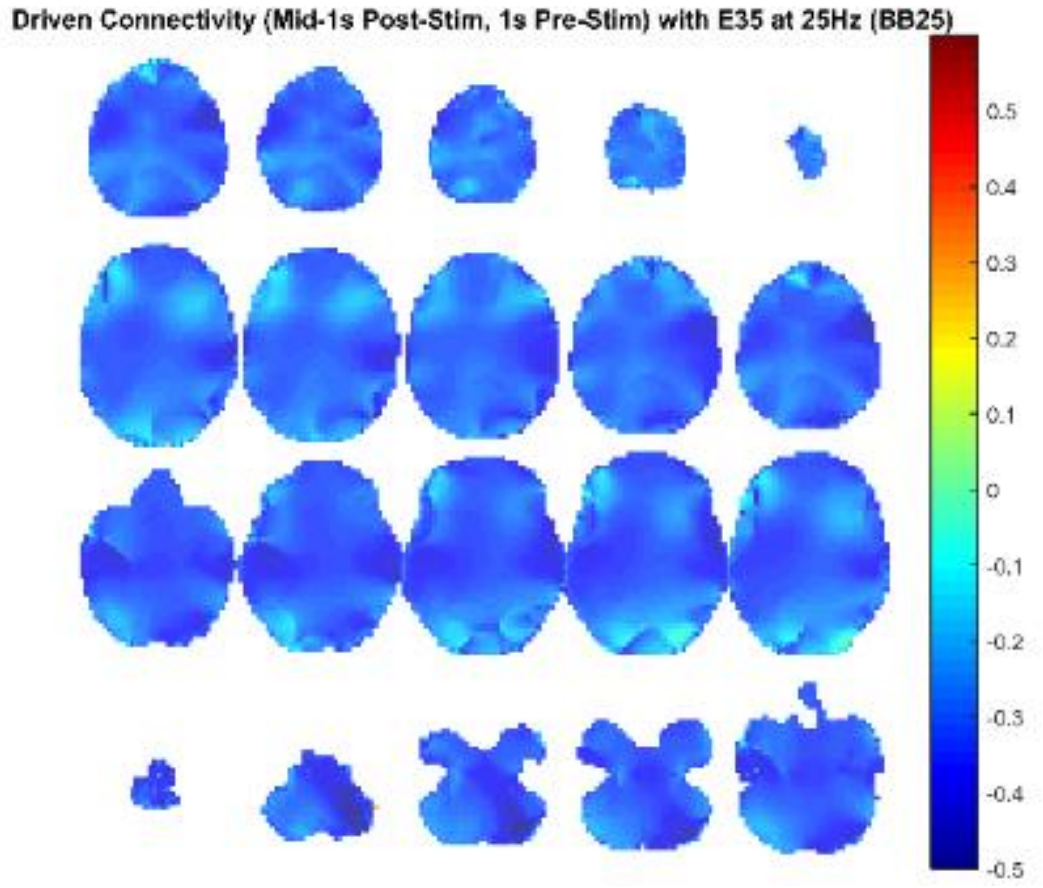

Figure 222. Source level connectivity with a dipole at E35 (left central) in 25 Hz during the middle one-second of 25 Hz binaural beat tone stimulation (total stimulation was 3 seconds), performed with DICS and a standardized BEM headmodel. Unit is the percent change in coherence from baseline (i.e., difference between coherence during stimulation and coherence during baseline divided by coherence during baseline). Darker reds indicate increases in coherence with E45 while darker blues indicate decreases in coherence.

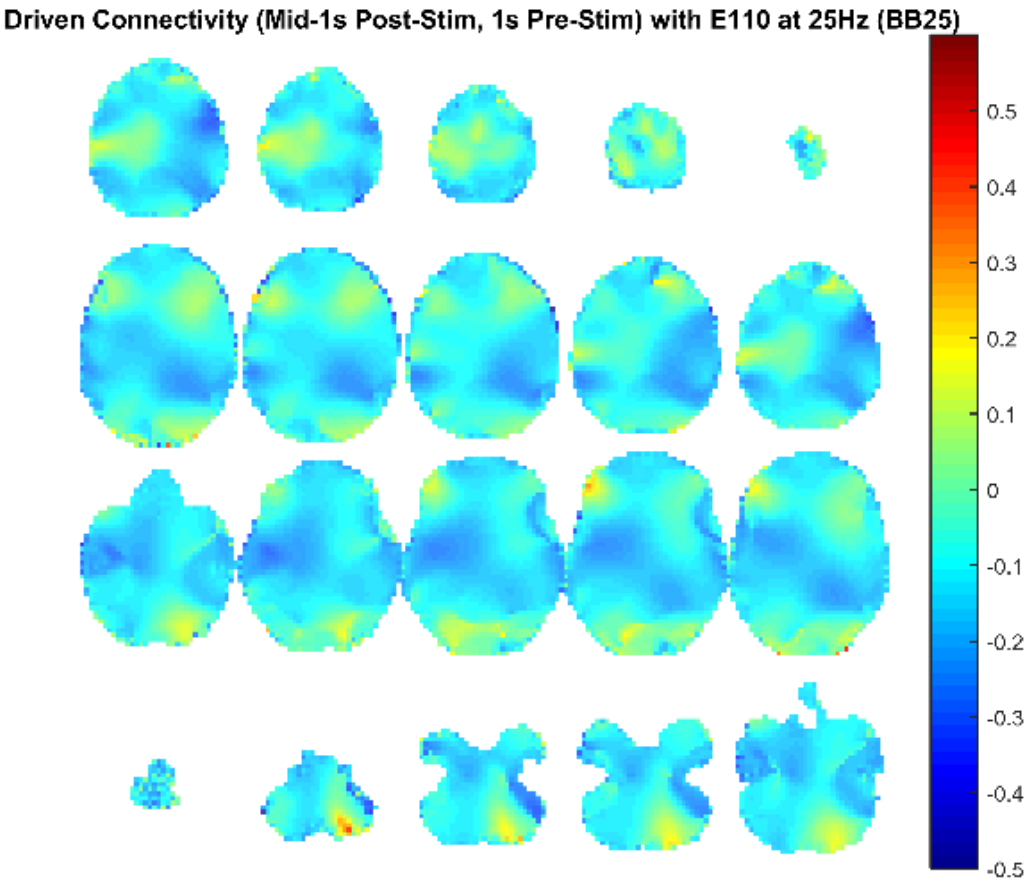

Figure 223. Source level connectivity with a dipole at E110 (right central) in 25 Hz during the middle one-second of 25 Hz binaural beat tone stimulation (total stimulation was 3 seconds), performed with DICS and a standardized BEM headmodel. Unit is the percent change in coherence from baseline (i.e., difference between coherence during stimulation and coherence during baseline divided by coherence during baseline). Darker reds indicate increases in coherence with E45 while darker blues indicate decreases in coherence.

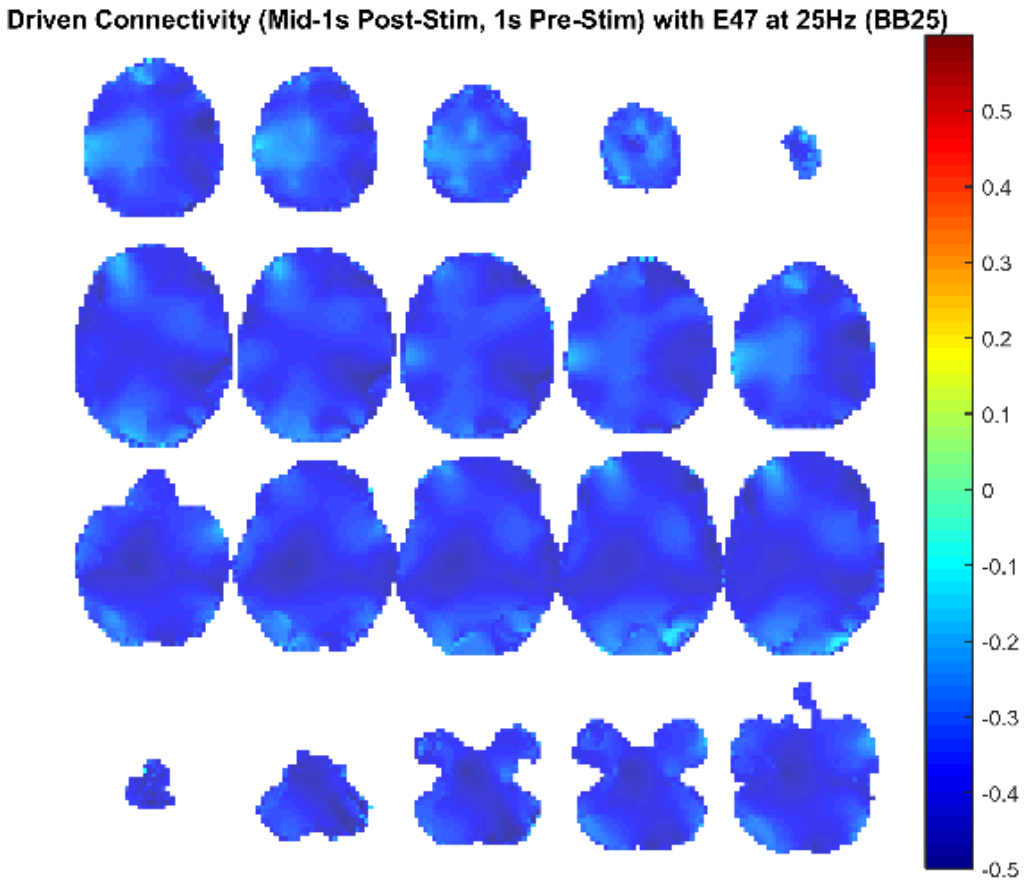

Figure 224. Source level connectivity with a dipole at E47 (left parietal) in 25 Hz during the middle one-second of 25 Hz binaural beat tone stimulation (total stimulation was 3 seconds), performed with DICS and a standardized BEM headmodel. Unit is the percent change in coherence from baseline (i.e., difference between coherence during stimulation and coherence during baseline divided by coherence during baseline). Darker reds indicate increases in coherence with E45 while darker blues indicate decreases in coherence.

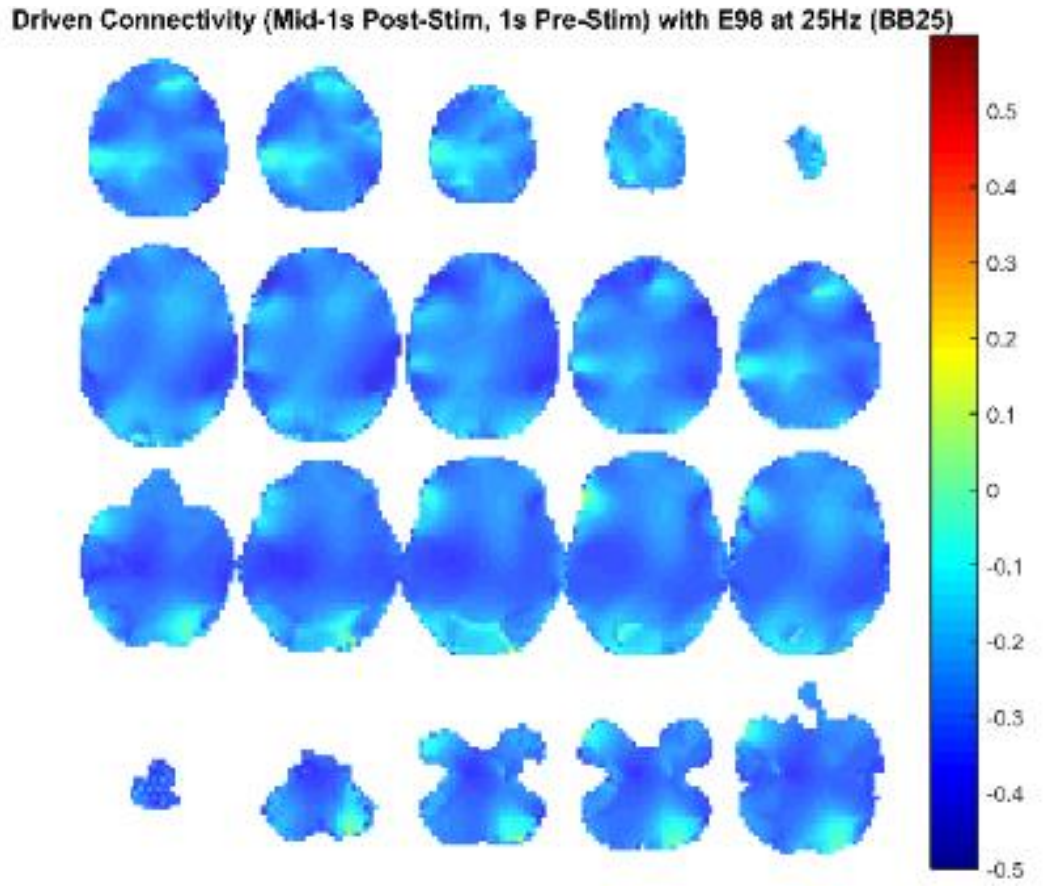

Figure 225. Source level connectivity with a dipole at E98 (right parietal) in 25 Hz during the middle one-second of 25 Hz binaural beat tone stimulation (total stimulation was 3 seconds), performed with DICS and a standardized BEM headmodel. Unit is the percent change in coherence from baseline (i.e., difference between coherence during stimulation and coherence during baseline divided by coherence during baseline). Darker reds indicate increases in coherence with E45 while darker blues indicate decreases in coherence.

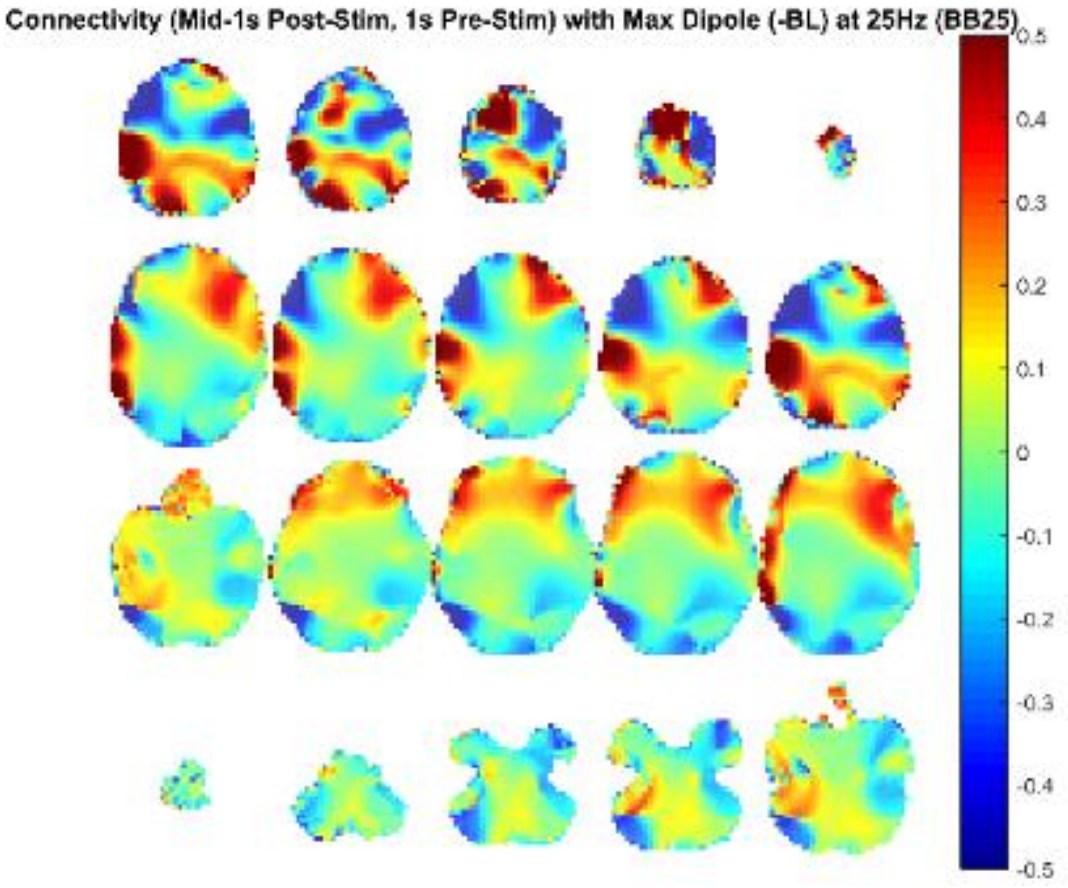

Figure 226. Source level connectivity with a dipole at dip2 (maximum power dipole for the middle one-second period corrected for the baseline one-second period) in 25 Hz during the middle one-second of 25 Hz binaural beat tone stimulation (total stimulation was 3 seconds), performed with DICS and a standardized BEM headmodel. Unit is the percent change in coherence from baseline (i.e., difference between coherence during stimulation and coherence during baseline divided by coherence during baseline). Darker reds indicate increases in coherence with E45 while darker blues indicate decreases in coherence.

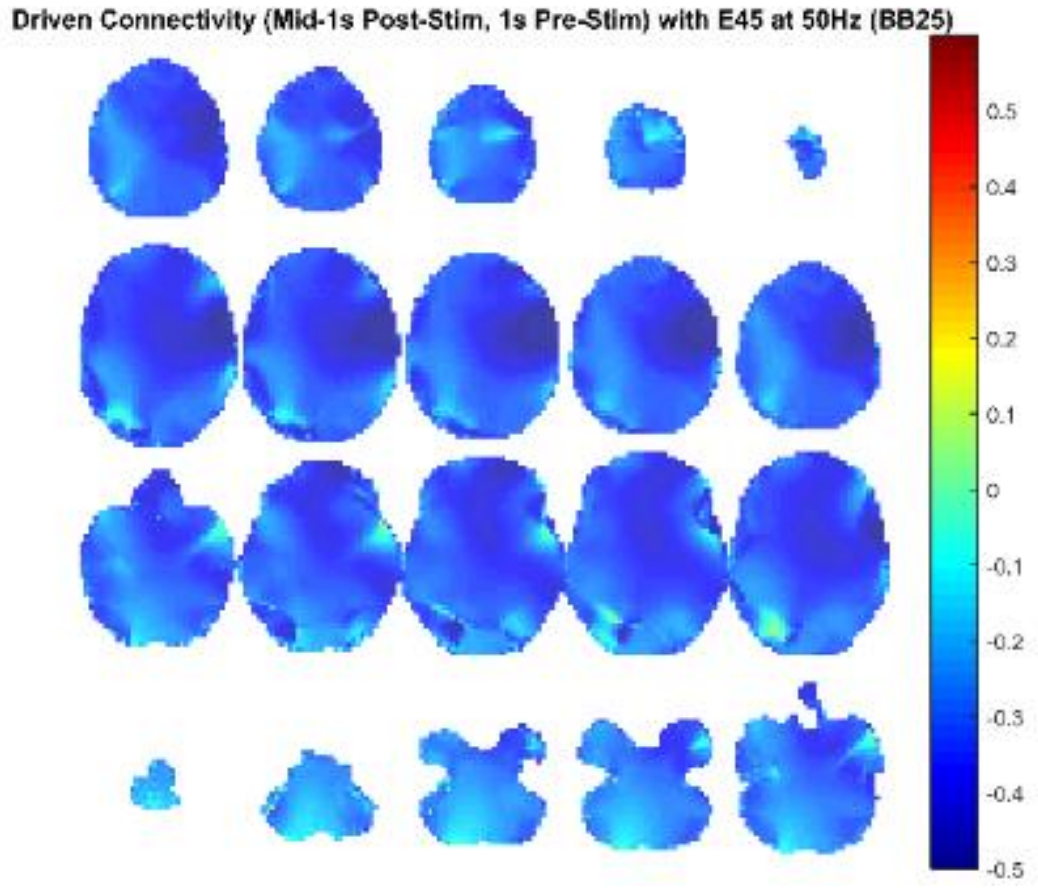

Figure 227. Source level connectivity with a dipole at E45 (left temporal, auditory cortex) in 50 Hz during the middle one-second of 25 Hz binaural beat tone stimulation (total stimulation was 3 seconds), performed with DICS and a standardized BEM headmodel. Unit is the percent change in coherence from baseline (i.e., difference between coherence during stimulation and coherence during baseline divided by coherence during baseline). Darker reds indicate increases in coherence with E45 while darker blues indicate decreases in coherence.

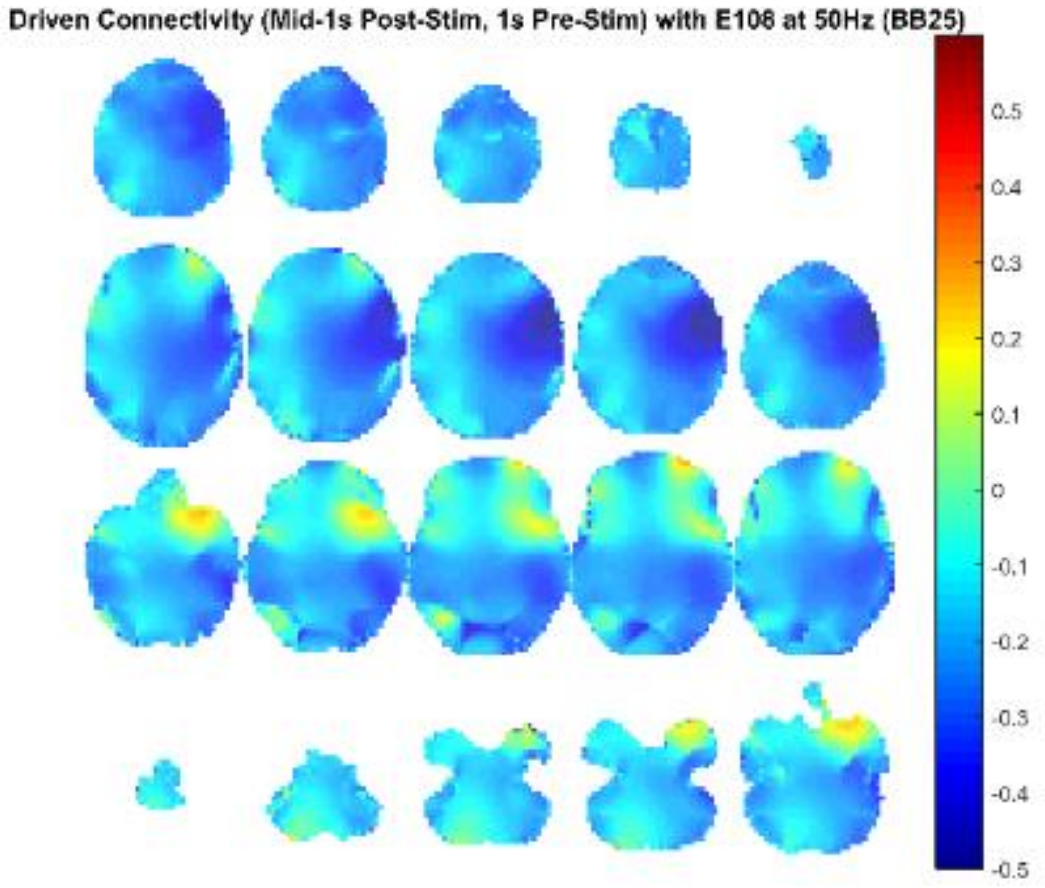

Figure 228. Source level connectivity with a dipole at E108 (right temporal, auditory cortex) in 50 Hz during the middle one-second of 25 Hz binaural beat tone stimulation (total stimulation was 3 seconds), performed with DICS and a standardized BEM headmodel. Unit is the percent change in coherence from baseline (i.e., difference between coherence during stimulation and coherence during baseline divided by coherence during baseline). Darker reds indicate increases in coherence with E45 while darker blues indicate decreases in coherence.

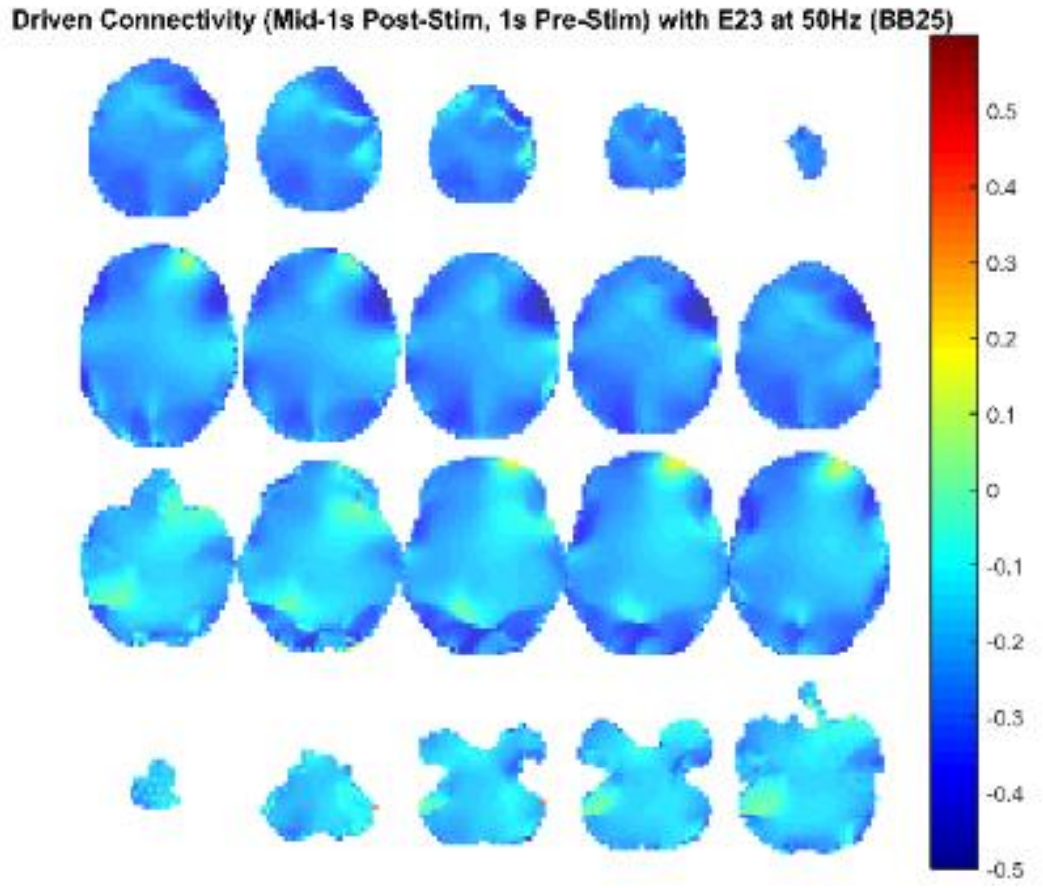

Figure 229. Source level connectivity with a dipole at E23 (left frontal) in 50 Hz during the middle one-second of 25 Hz binaural beat tone stimulation (total stimulation was 3 seconds), performed with DICS and a standardized BEM headmodel. Unit is the percent change in coherence from baseline (i.e., difference between coherence during stimulation and coherence during baseline divided by coherence during baseline). Darker reds indicate increases in coherence with E45 while darker blues indicate decreases in coherence.

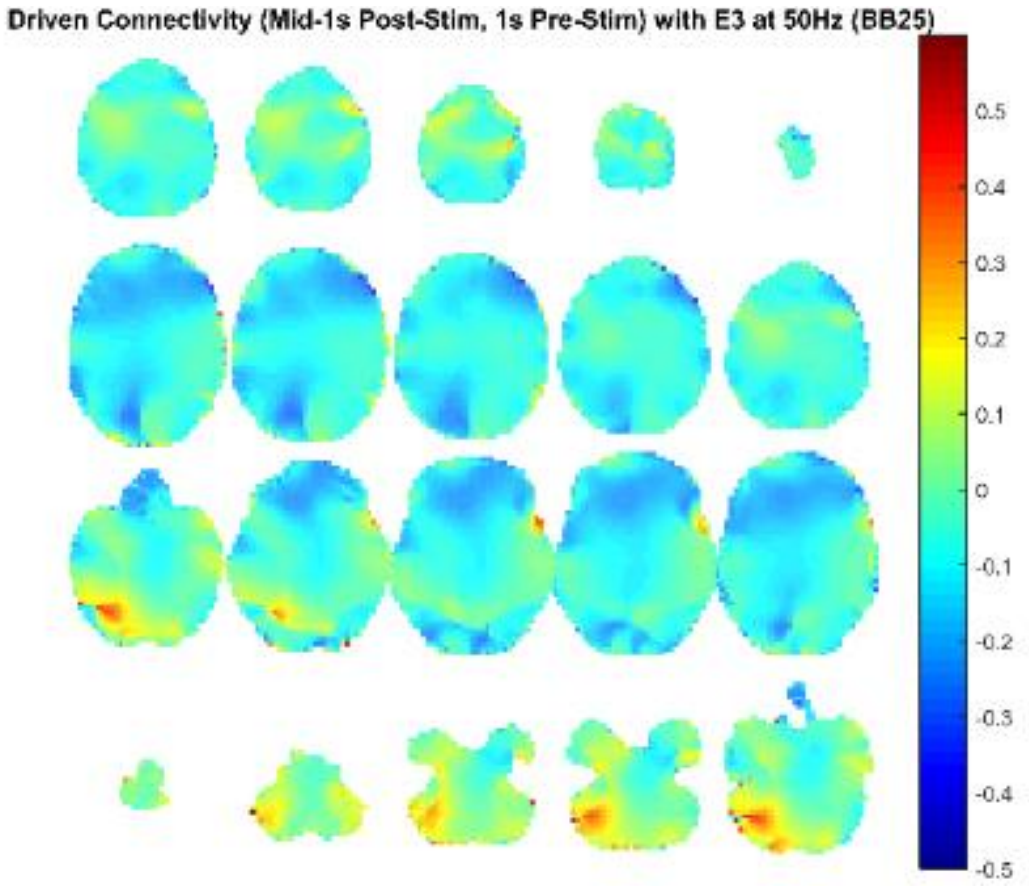

Figure 230. Source level connectivity with a dipole at E3 (right frontal) in 50 Hz during the middle one-second of 25 Hz binaural beat tone stimulation (total stimulation was 3 seconds), performed with DICS and a standardized BEM headmodel. Unit is the percent change in coherence from baseline (i.e., difference between coherence during stimulation and coherence during baseline divided by coherence during baseline). Darker reds indicate increases in coherence with E45 while darker blues indicate decreases in coherence.

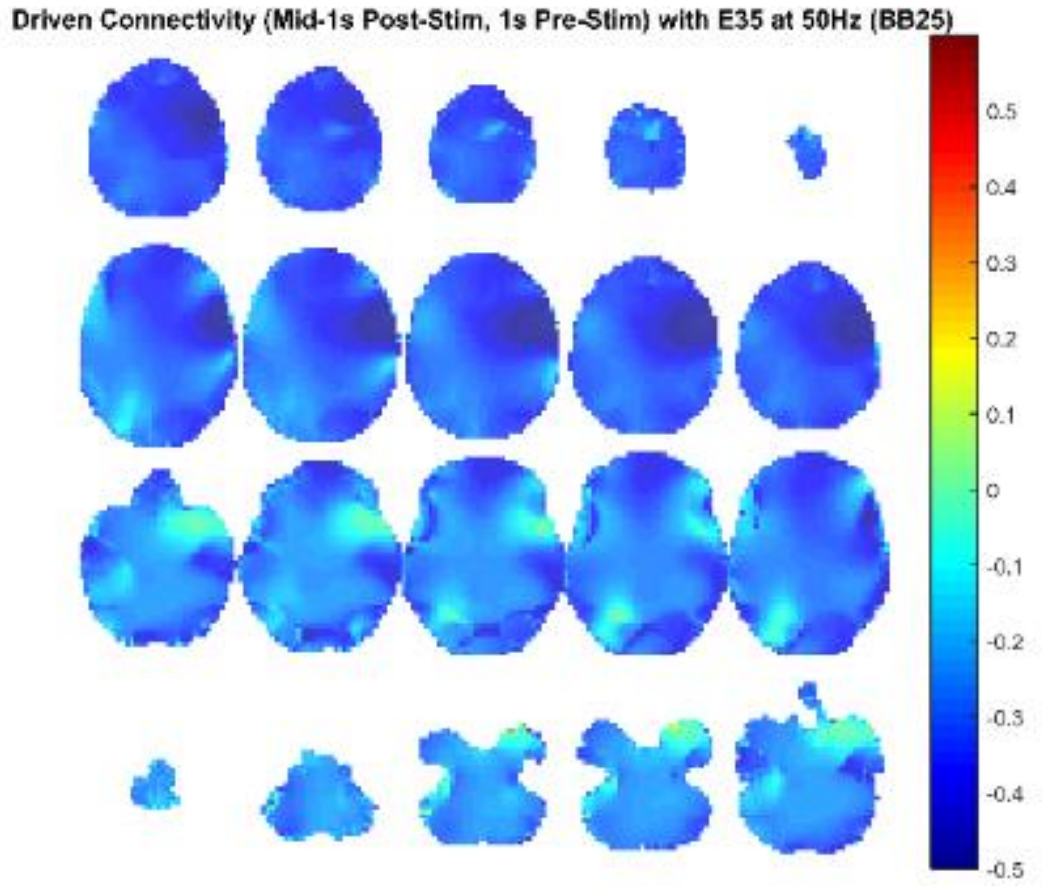

Figure 231. Source level connectivity with a dipole at E35 (left central) in 50 Hz during the middle one-second of 25 Hz binaural beat tone stimulation (total stimulation was 3 seconds), performed with DICS and a standardized BEM headmodel. Unit is the percent change in coherence from baseline (i.e., difference between coherence during stimulation and coherence during baseline divided by coherence during baseline). Darker reds indicate increases in coherence with E45 while darker blues indicate decreases in coherence.

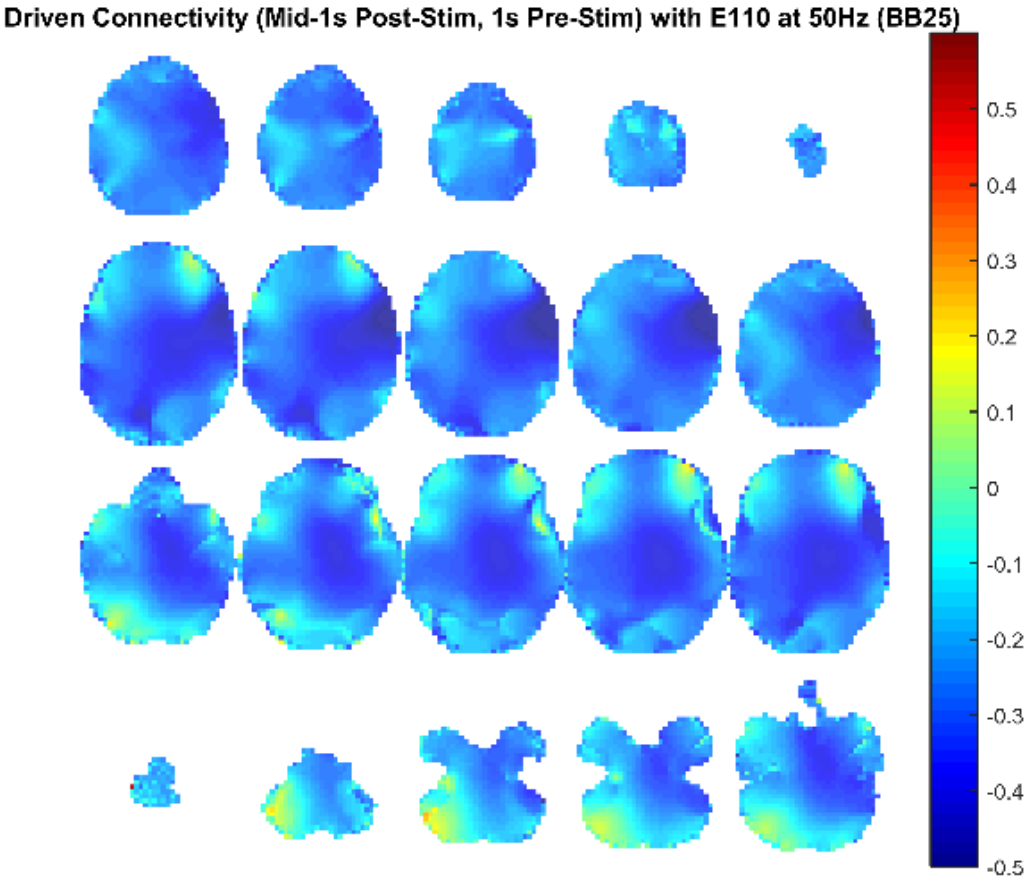

Figure 232. Source level connectivity with a dipole at E110 (right central) in 50 Hz during the middle one-second of 25 Hz binaural beat tone stimulation (total stimulation was 3 seconds), performed with DICS and a standardized BEM headmodel. Unit is the percent change in coherence from baseline (i.e., difference between coherence during stimulation and coherence during baseline divided by coherence during baseline). Darker reds indicate increases in coherence with E45 while darker blues indicate decreases in coherence.

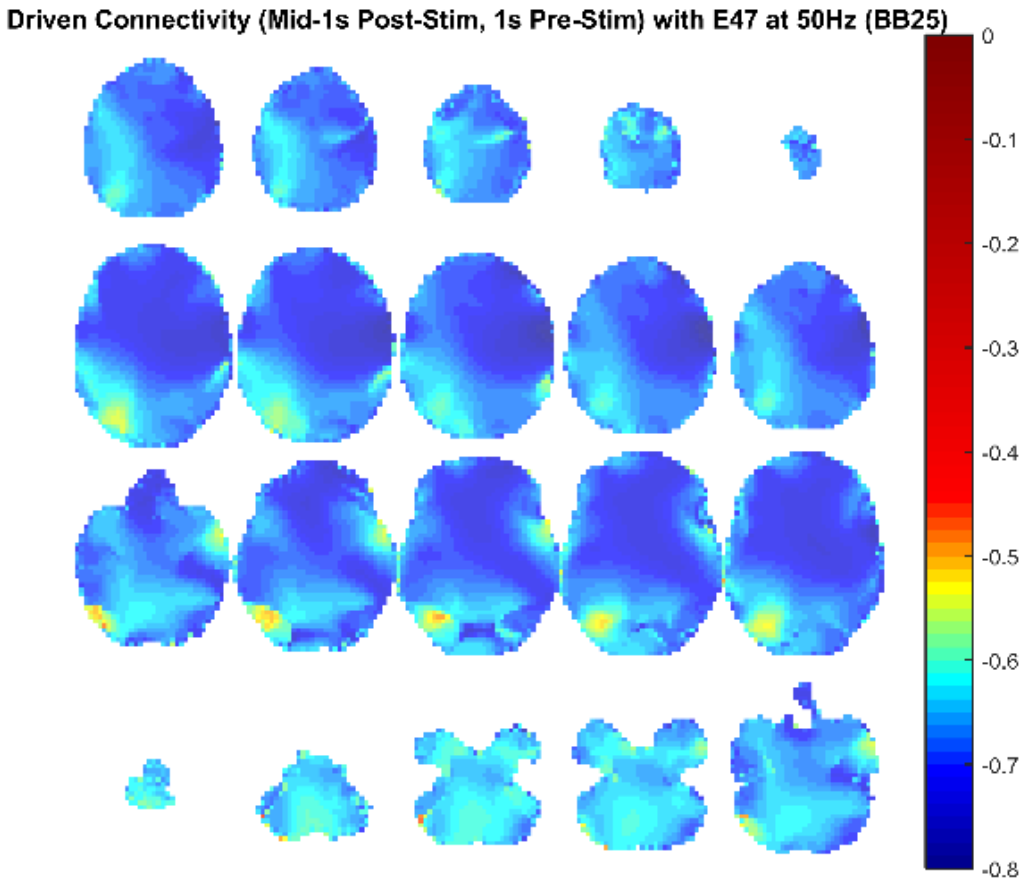

Figure 233. Source level connectivity with a dipole at E47 (left parietal) in 50 Hz during the middle one-second of 25 Hz binaural beat tone stimulation (total stimulation was 3 seconds), performed with DICS and a standardized BEM headmodel. Unit is the percent change in coherence from baseline (i.e., difference between coherence during stimulation and coherence during baseline divided by coherence during baseline). Darker reds indicate increases in coherence with E45 while darker blues indicate decreases in coherence.

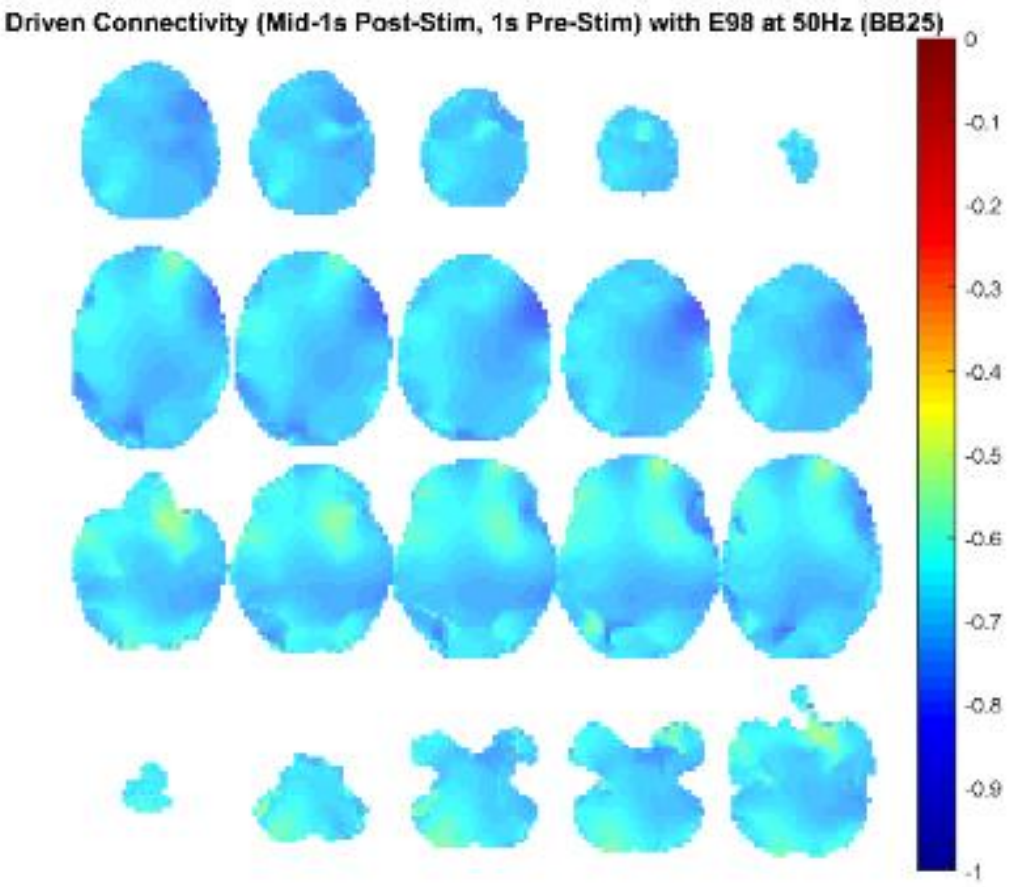

Figure 234. Source level connectivity with a dipole at E98 (right parietal) in 50 Hz during the middle one-second of 25 Hz binaural beat tone stimulation (total stimulation was 3 seconds), performed with DICS and a standardized BEM headmodel. Unit is the percent change in coherence from baseline (i.e., difference between coherence during stimulation and coherence during baseline divided by coherence during baseline). Darker reds indicate increases in coherence with E45 while darker blues indicate decreases in coherence.

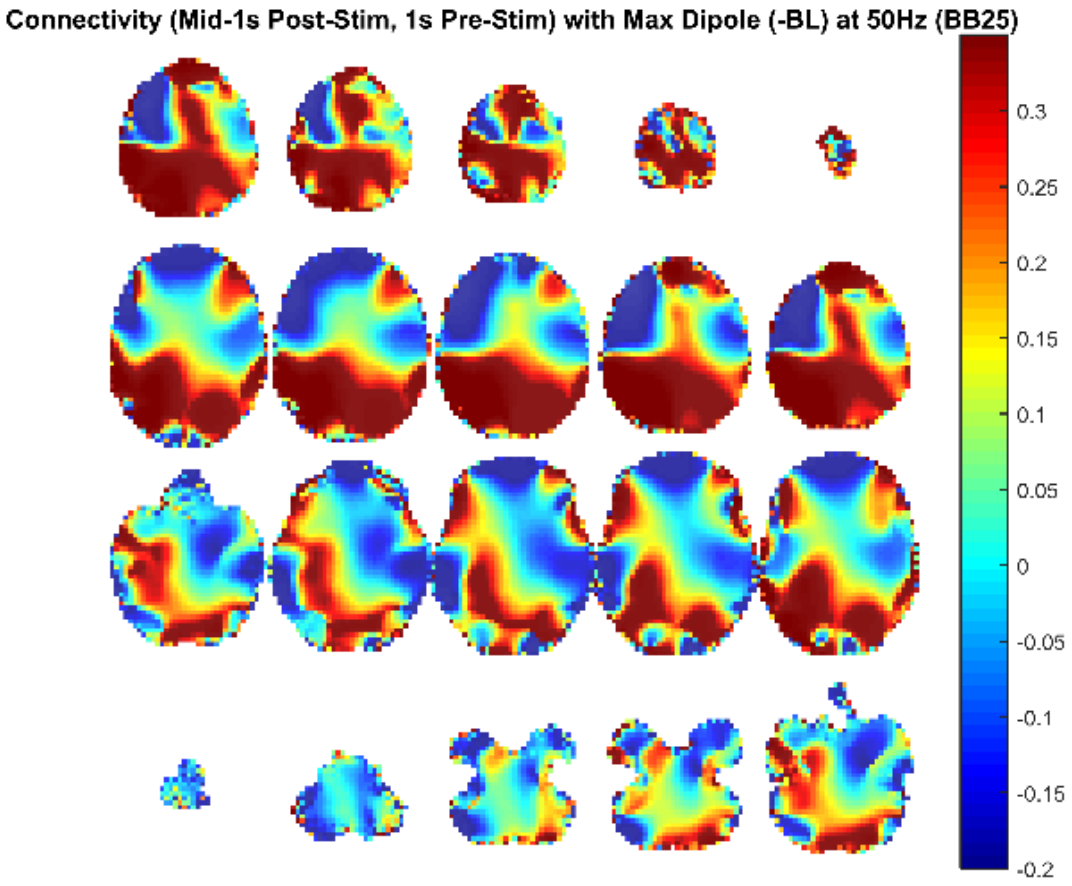

Figure 235. Source level connectivity with a dipole at dip2 (maximum power dipole for the middle one-second period corrected for the baseline one-second period) in 50 Hz during the middle one-second of 25 Hz binaural beat tone stimulation (total stimulation was 3 seconds), performed with DICS and a standardized BEM headmodel. Unit is the percent change in coherence from baseline (i.e., difference between coherence during stimulation and coherence during baseline divided by coherence during baseline). Darker reds indicate increases in coherence with E45 while darker blues indicate decreases in coherence.

Appendix: Amplitude Modulated Versus Binaural Beat Comparison

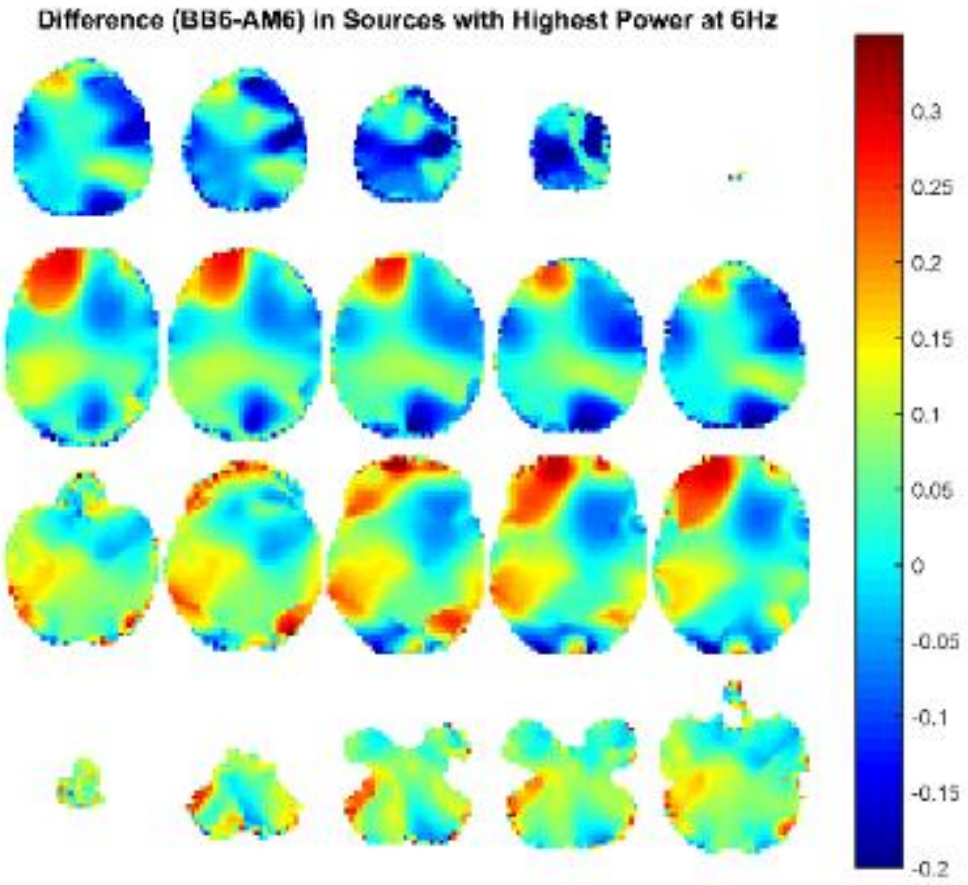

Figure 236. Source activity in power in 6 Hz during the middle one-second of 6 Hz binaural beat stimulation with 6 Hz amplitude modulated tone stimulation subtracted. Source analysis performed with DICS and a standardized BEM headmodel and was baseline corrected. Darker reds indicate higher power in 6 Hz at that location during binaural beat stimulation while darker blues indicate higher power in 6 Hz at that location during amplitude modulated stimulation.

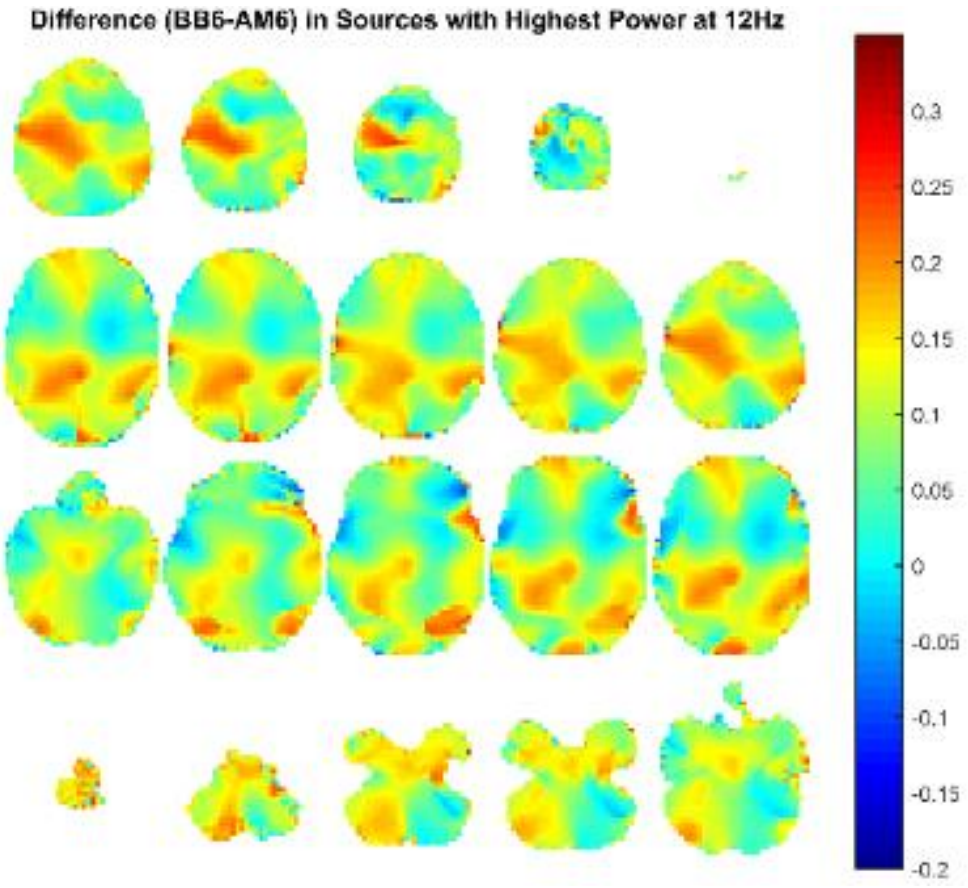

Figure 237. Source activity in power in 12 Hz during the middle one-second of 6 Hz binaural beat stimulation with 6 Hz amplitude modulated tone stimulation subtracted. Source analysis performed with DICS and a standardized BEM headmodel and was baseline corrected. Darker reds indicate higher power in 12 Hz at that location during binaural beat stimulation while darker blues indicate higher power in 12 Hz at that location during amplitude modulated stimulation.

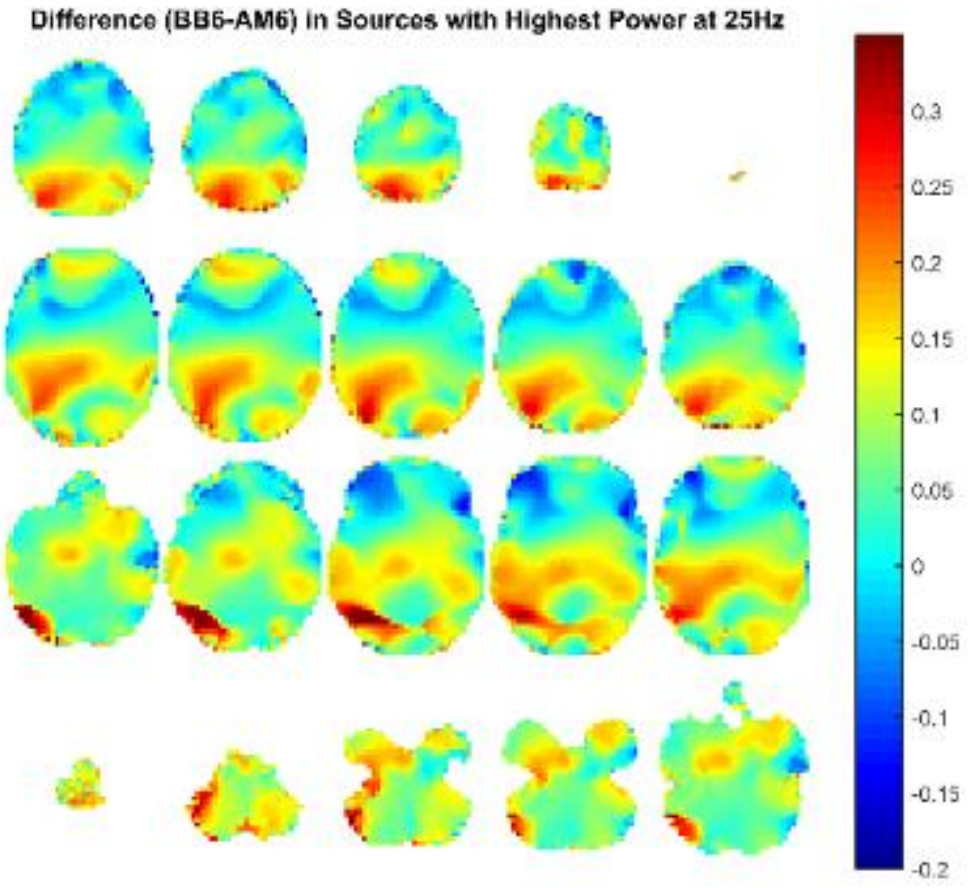

Figure 238. Source activity in power in 25 Hz during the middle one-second of 6 Hz binaural beat stimulation with 6 Hz amplitude modulated tone stimulation subtracted. Source analysis performed with DICS and a standardized BEM headmodel and was baseline corrected. Darker reds indicate higher power in 25 Hz at that location during binaural beat stimulation while darker blues indicate higher power in 25 Hz at that location during amplitude modulated stimulation.

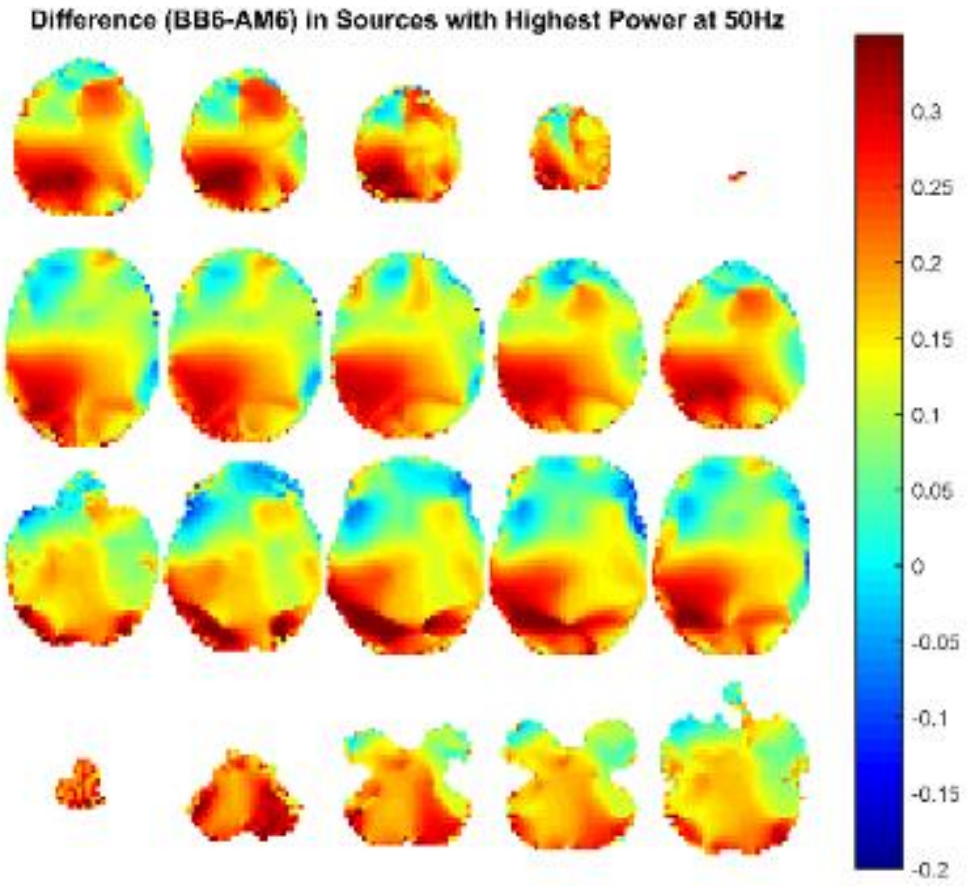

Figure 239. Source activity in power in 50 Hz during the middle one-second of 6 Hz binaural beat stimulation with 6 Hz amplitude modulated tone stimulation subtracted. Source analysis performed with DICS and a standardized BEM headmodel and was baseline corrected. Darker reds indicate higher power in 50 Hz at that location during binaural beat stimulation while darker blues indicate higher power in 50 Hz at that location during amplitude modulated stimulation.

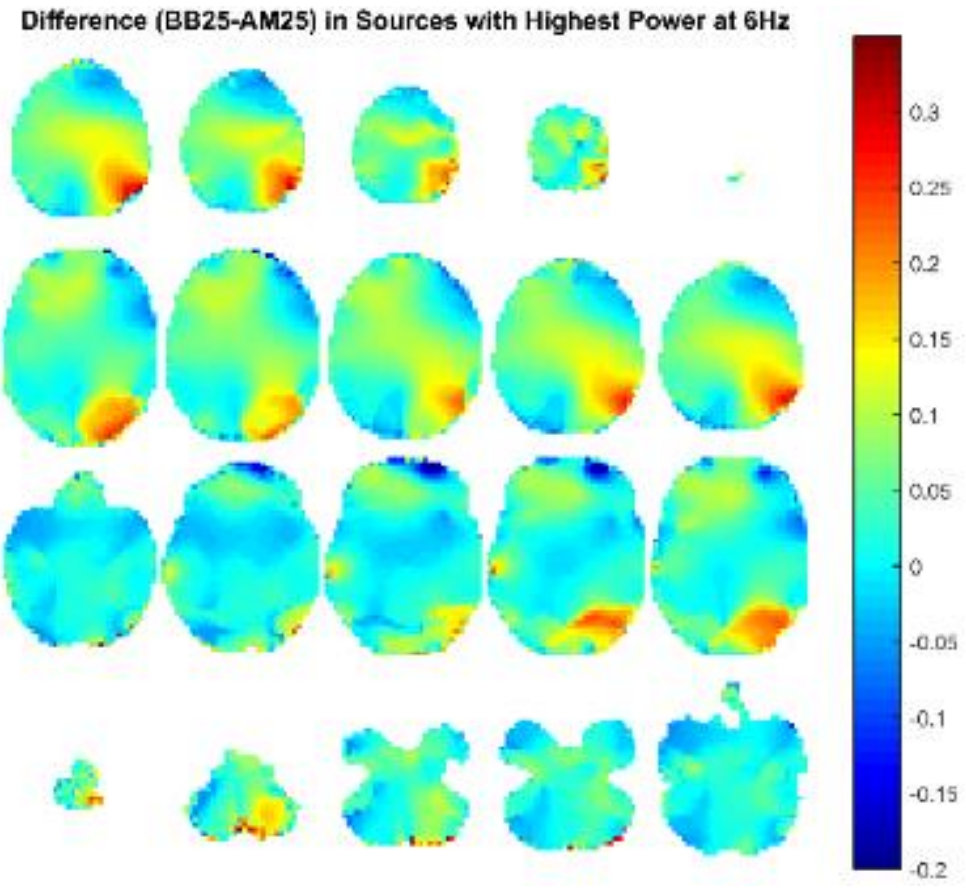

Figure 240. Source activity in power in 6 Hz during the middle one-second of 25 Hz binaural beat stimulation with 25 Hz amplitude modulated tone stimulation subtracted. Source analysis performed with DICS and a standardized BEM headmodel and was baseline corrected. Darker reds indicate higher power in 6 Hz at that location during binaural beat stimulation while darker blues indicate higher power in 6 Hz at that location during amplitude modulated stimulation.

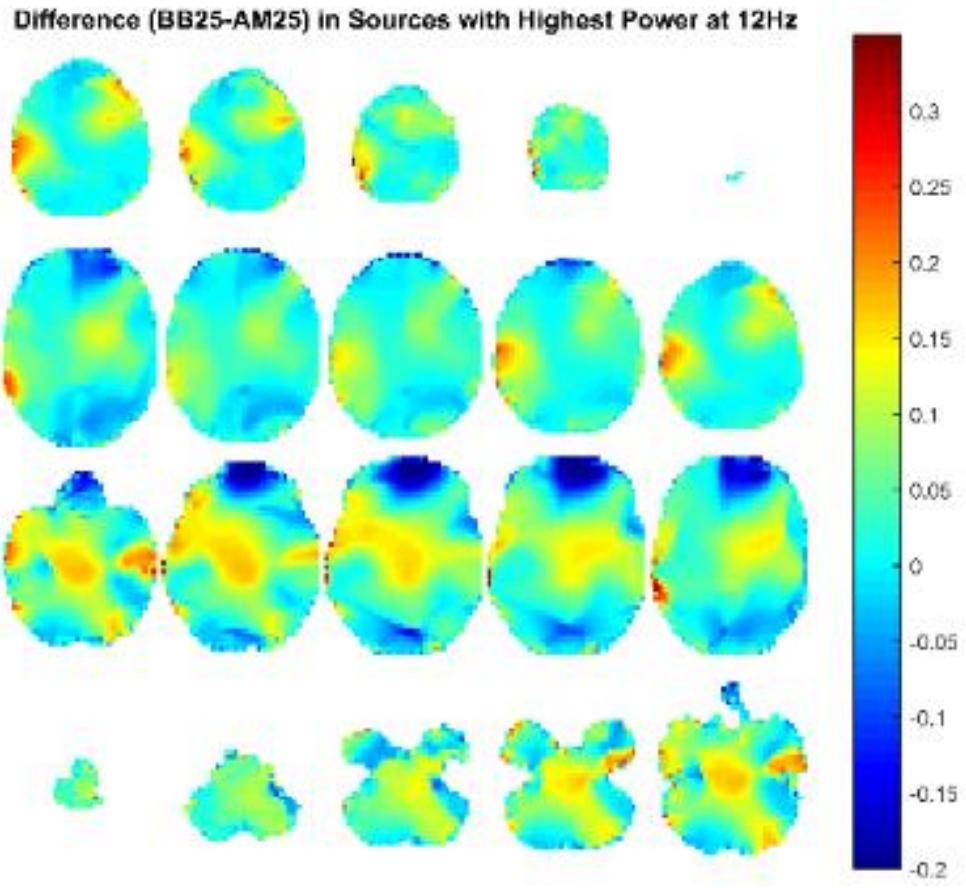

Figure 241. Source activity in power in 12 Hz during the middle one-second of 25 Hz binaural beat stimulation with 25 Hz amplitude modulated tone stimulation subtracted. Source analysis performed with DICS and a standardized BEM headmodel and was baseline corrected. Darker reds indicate higher power in 12 Hz at that location during binaural beat stimulation while darker blues indicate higher power in 12 Hz at that location during amplitude modulated stimulation.

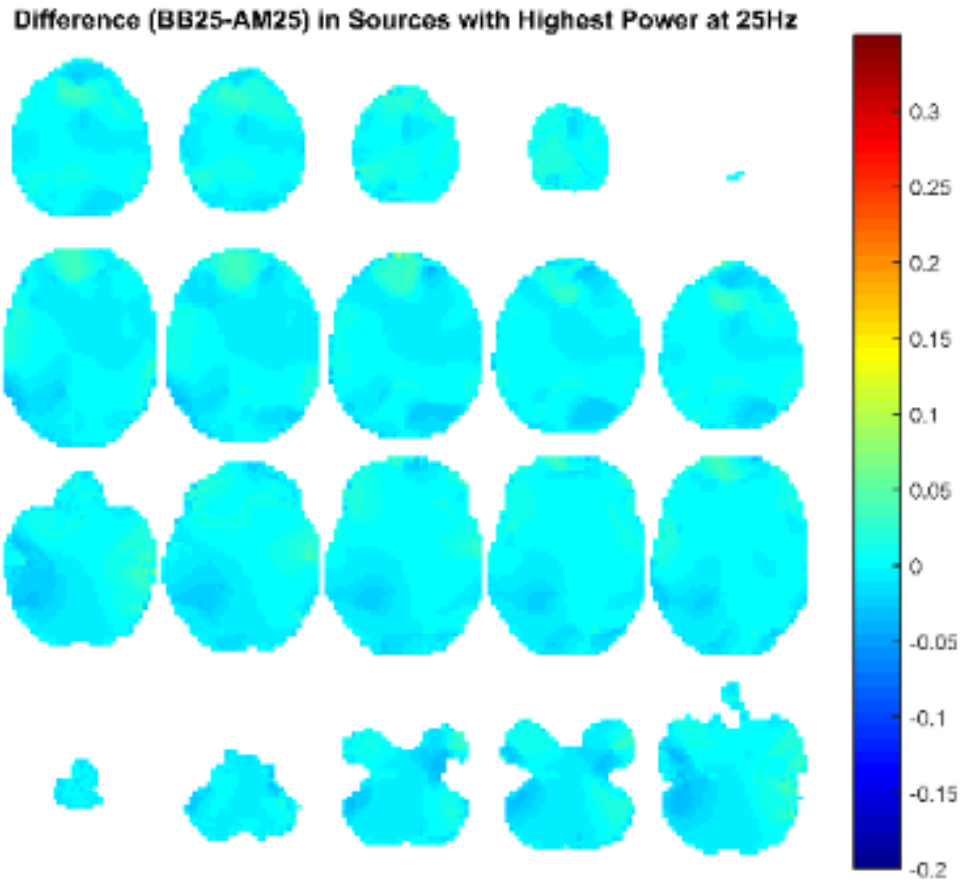

Figure 242. Source activity in power in 25 Hz during the middle one-second of 25 Hz binaural beat stimulation with 25 Hz amplitude modulated tone stimulation subtracted. Source analysis performed with DICS and a standardized BEM headmodel and was baseline corrected. Darker reds indicate higher power in 25 Hz at that location during binaural beat stimulation while darker blues indicate higher power in 25 Hz at that location during amplitude modulated stimulation.

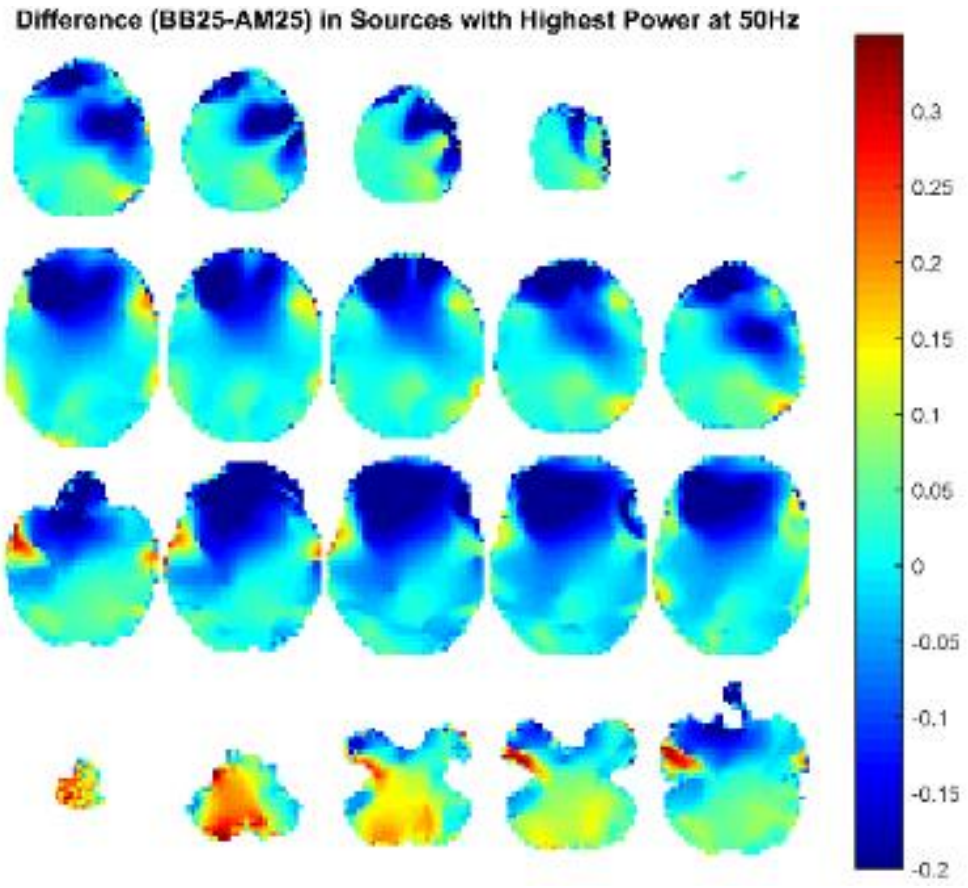

Figure 243. Source activity in power in 50 Hz during the middle one-second of 25 Hz binaural beat stimulation with 25 Hz amplitude modulated tone stimulation subtracted. Source analysis performed with DICS and a standardized BEM headmodel and was baseline corrected. Darker reds indicate higher power in 50 Hz at that location during binaural beat stimulation while darker blues indicate higher power in 50 Hz at that location during amplitude modulated stimulation.

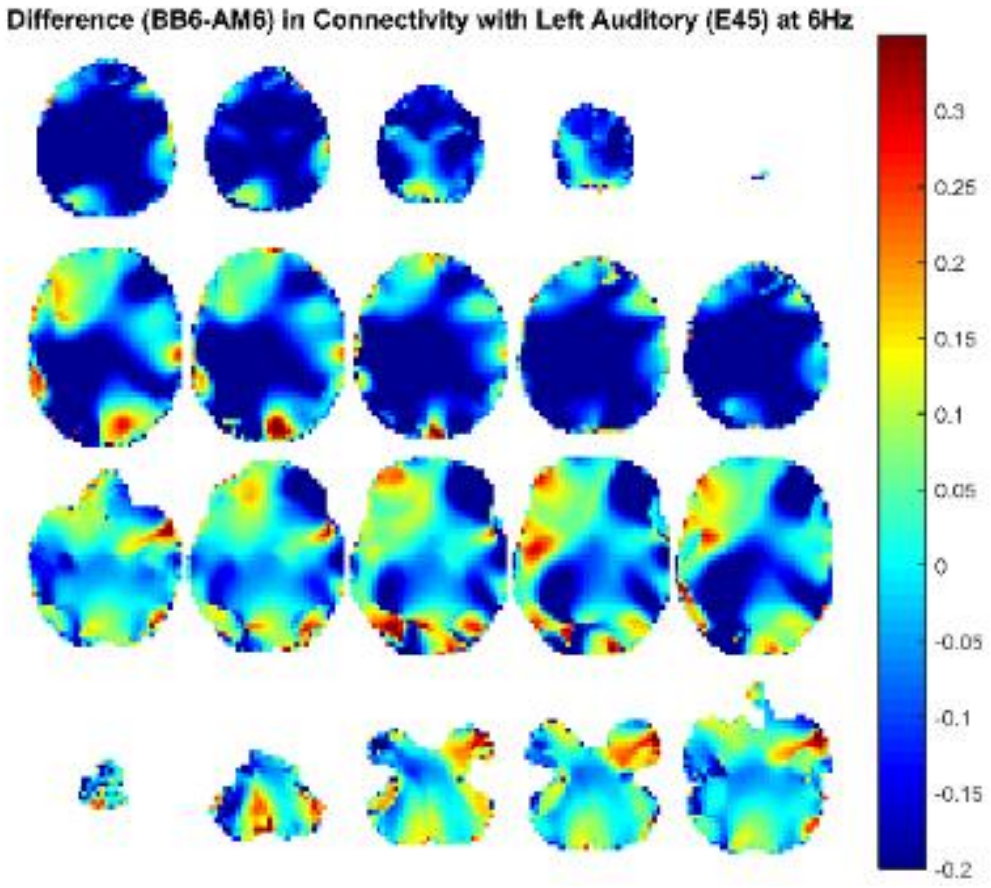

Figure 244. Binaural beat Source level connectivity with a dipole at E45 (left temporal, auditory cortex) in 6 Hz during the middle one-second of 6 Hz stimulation with 6 Hz amplitude modulated connectivity subtracted. Connectivity analysis performed with DICS and a standardized BEM headmodel and was baseline corrected. Darker reds indicate coherence with E45 is higher for BB while darker blues indicate coherence with E45 is higher for AM.

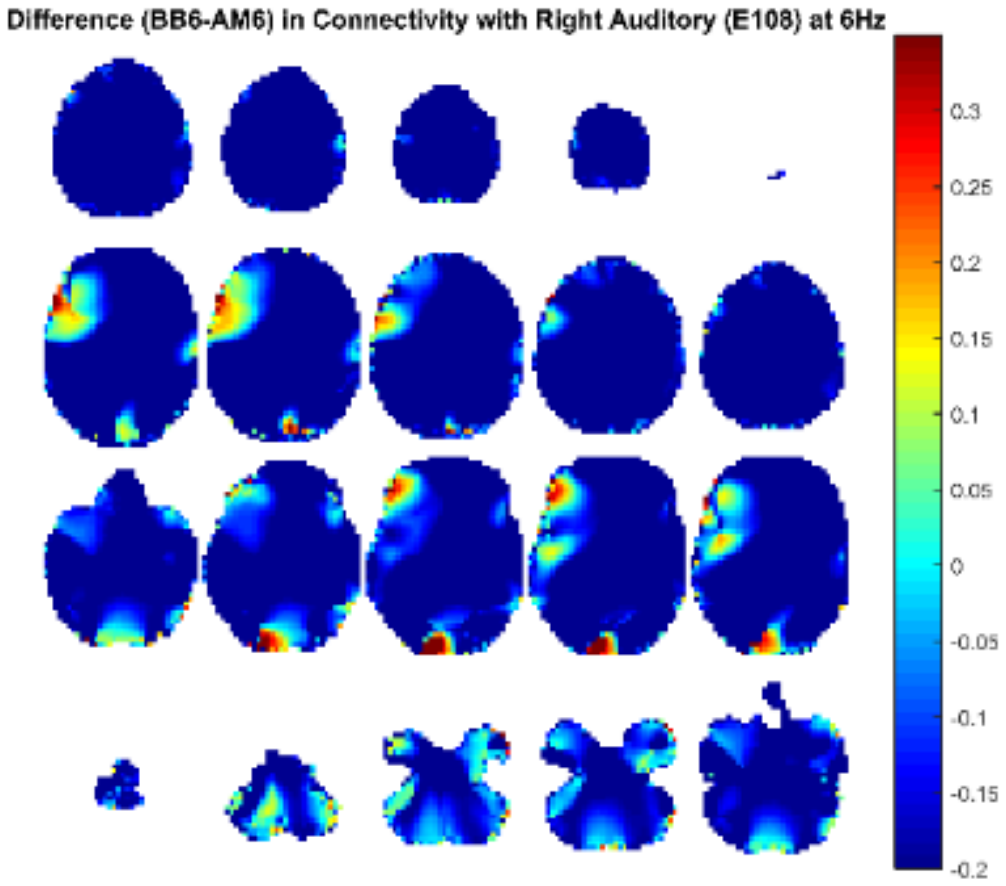

Figure 245. Binaural beat Source level connectivity with a dipole at E108 (right temporal, auditory cortex) in 6 Hz during the middle one-second of 6 Hz stimulation with 6 Hz amplitude modulated connectivity subtracted. Connectivity analysis performed with DICS and a standardized BEM headmodel and was baseline corrected. Darker reds indicate coherence with E45 is higher for BB while darker blues indicate coherence with E45 is higher for AM.

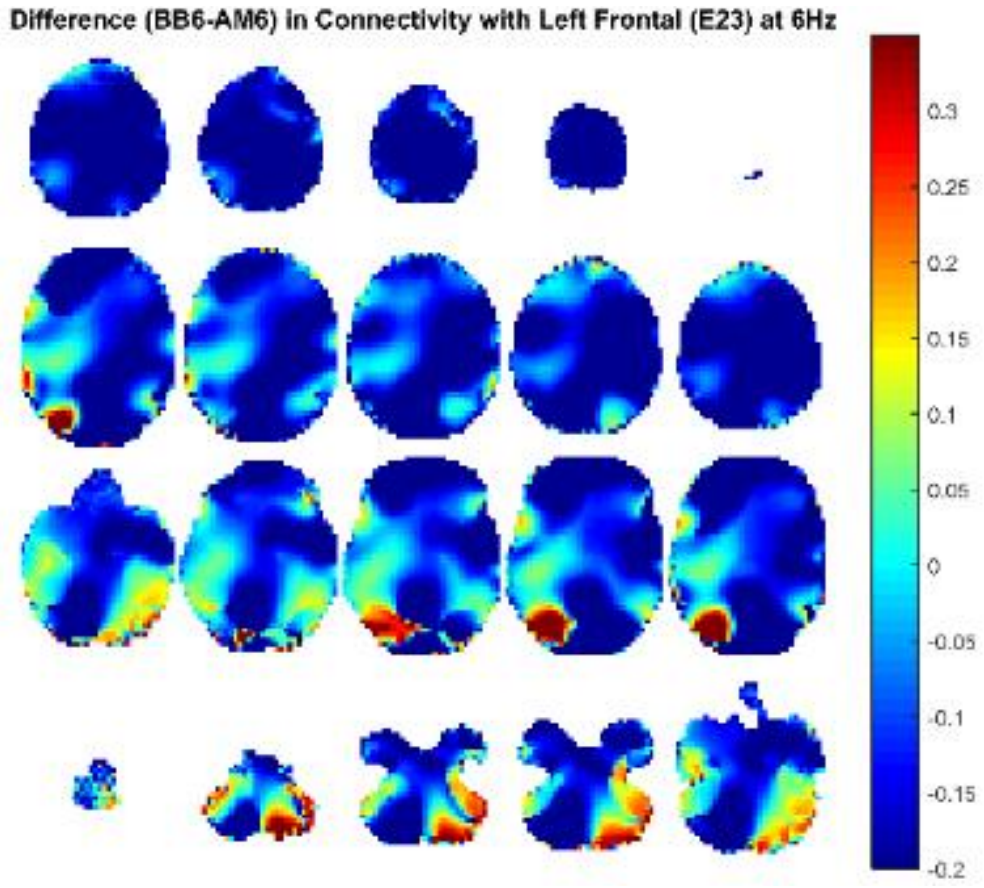

Figure 246. Binaural beat Source level connectivity with a dipole at E23 (left temporal, frontal cortex) in 6 Hz during the middle one-second of 6 Hz stimulation with 6 Hz amplitude modulated connectivity subtracted. Connectivity analysis performed with DICS and a standardized BEM headmodel and was baseline corrected. Darker reds indicate coherence with E45 is higher for BB while darker blues indicate coherence with E45 is higher for AM.

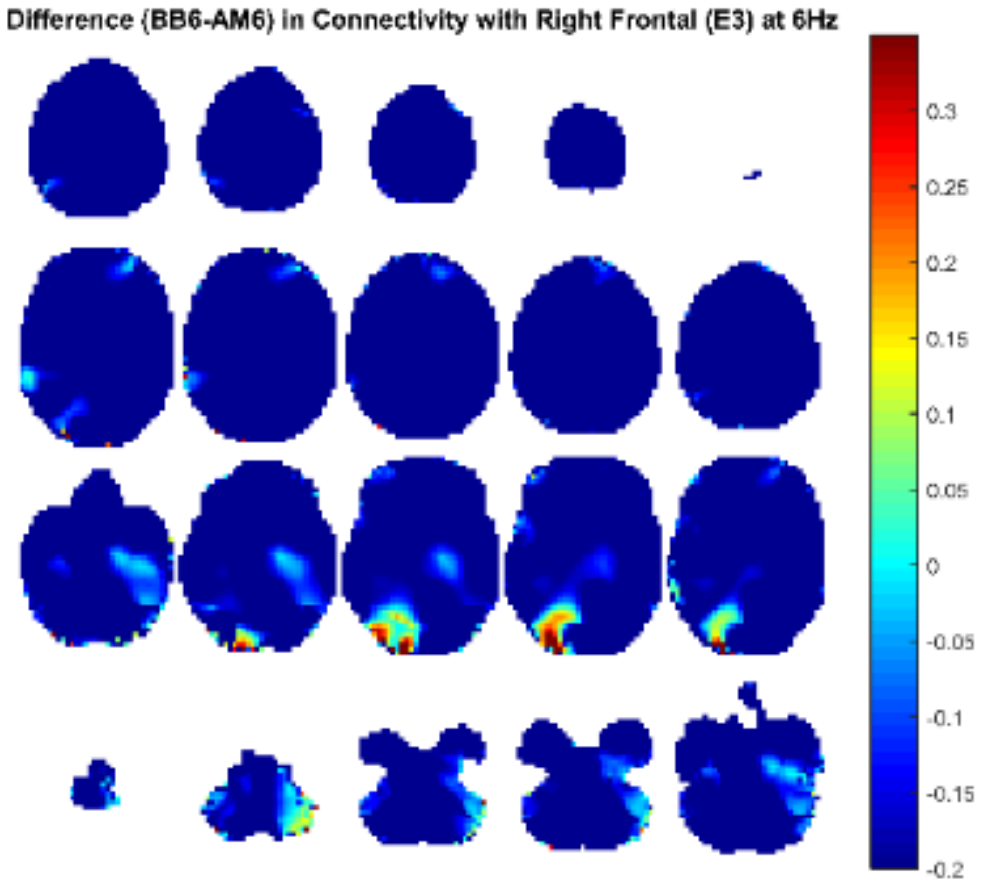

Figure 247. Binaural beat Source level connectivity with a dipole at E3 (right temporal, frontal cortex) in 6 Hz during the middle one-second of 6 Hz stimulation with 6 Hz amplitude modulated connectivity subtracted. Connectivity analysis performed with DICS and a standardized BEM headmodel and was baseline corrected. Darker reds indicate coherence with E45 is higher for BB while darker blues indicate coherence with E45 is higher for AM.

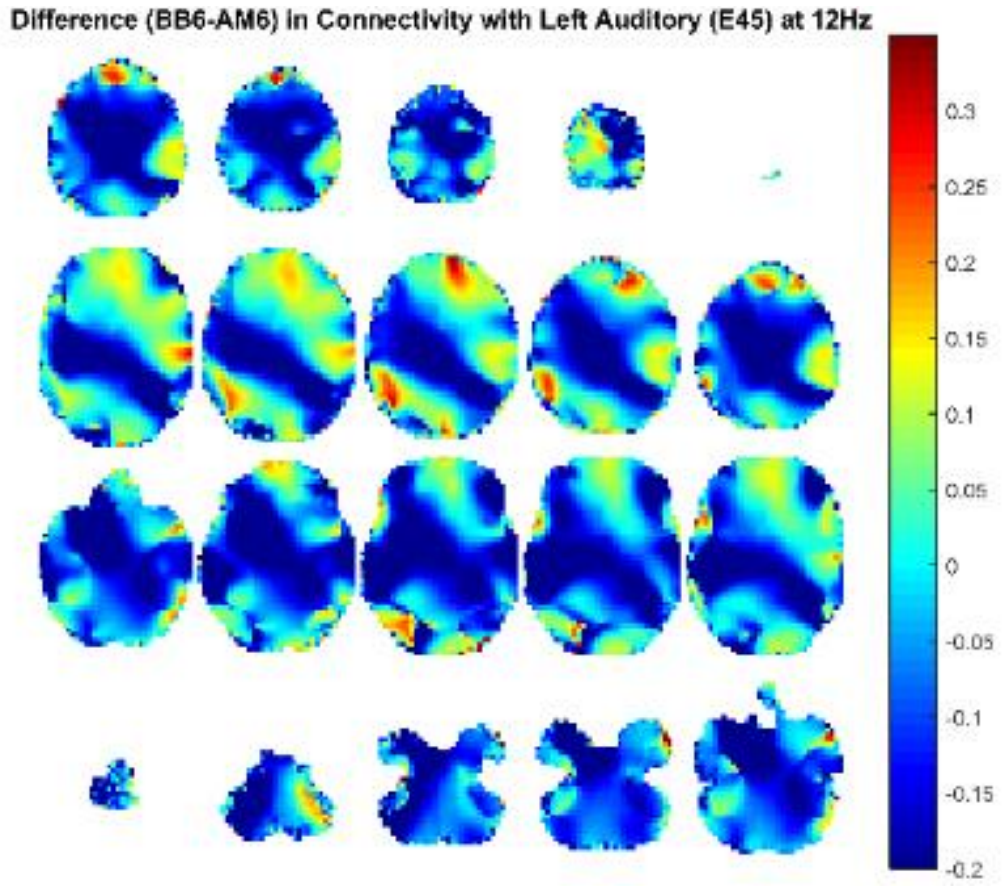

Figure 248. Binaural beat Source level connectivity with a dipole at E45 (left temporal, auditory cortex) in 12 Hz during the middle one-second of 6 Hz stimulation with 6 Hz amplitude modulated connectivity subtracted. Connectivity analysis performed with DICS and a standardized BEM headmodel and was baseline corrected. Darker reds indicate coherence with E45 is higher for BB while darker blues indicate coherence with E45 is higher for AM.

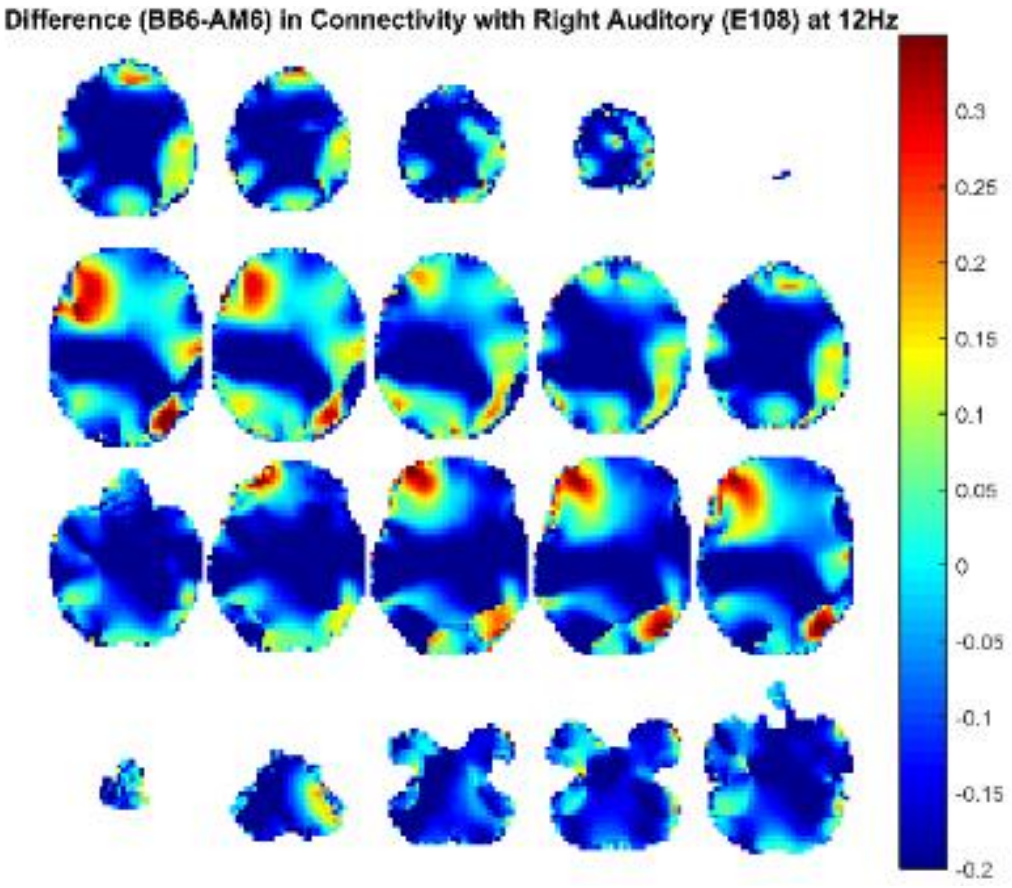

Figure 249. Binaural beat Source level connectivity with a dipole at E108 (right temporal, auditory cortex) in 12 Hz during the middle one-second of 6 Hz stimulation with 6 Hz amplitude modulated connectivity subtracted. Connectivity analysis performed with DICS and a standardized BEM headmodel and was baseline corrected. Darker reds indicate coherence with E45 is higher for BB while darker blues indicate coherence with E45 is higher for AM.

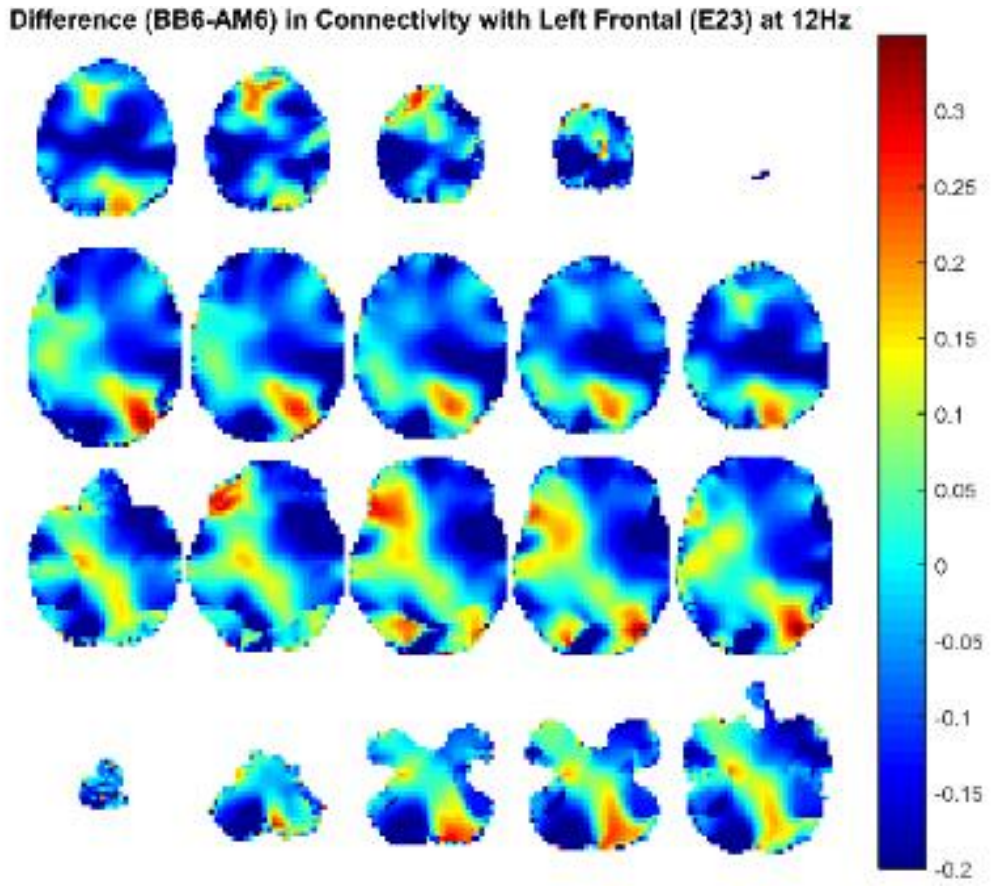

Figure 250. Binaural beat Source level connectivity with a dipole at E23 (left temporal, frontal cortex) in 12 Hz during the middle one-second of 6 Hz stimulation with 6 Hz amplitude modulated connectivity subtracted. Connectivity analysis performed with DICS and a standardized BEM headmodel and was baseline corrected. Darker reds indicate coherence with E45 is higher for BB while darker blues indicate coherence with E45 is higher for AM.

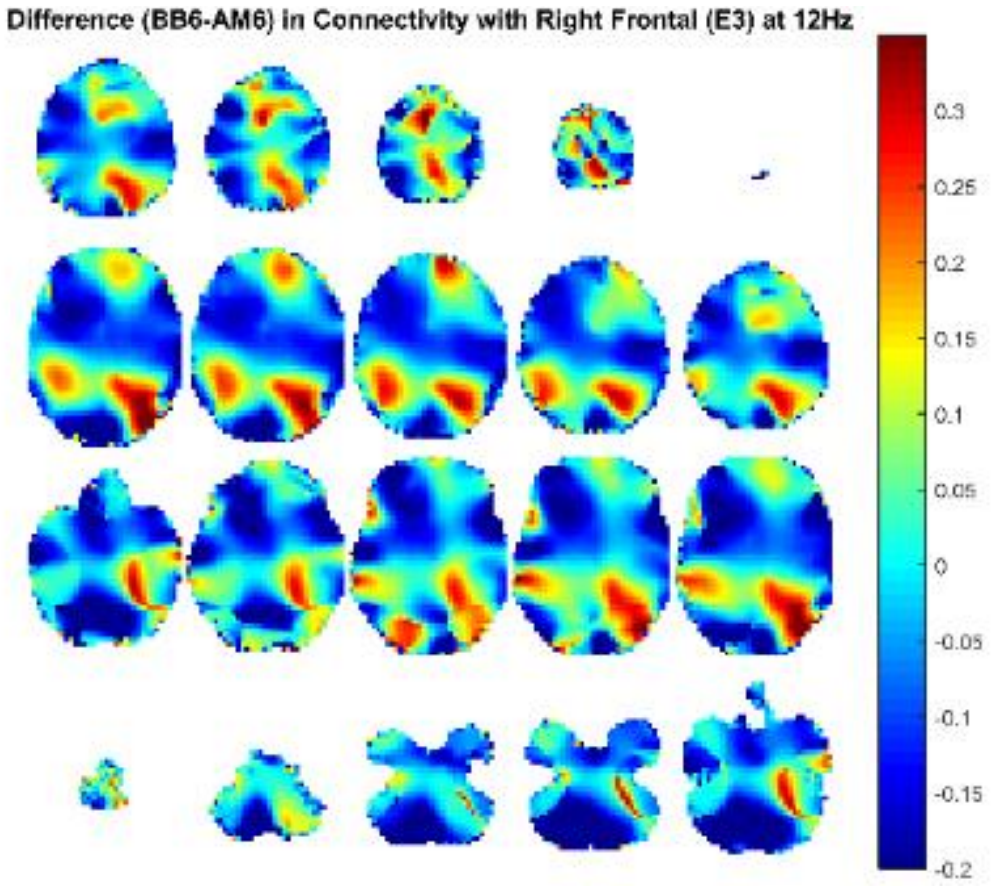

Figure 251. Binaural beat Source level connectivity with a dipole at E3 (right temporal, frontal cortex) in 12 Hz during the middle one-second of 6 Hz stimulation with 6 Hz amplitude modulated connectivity subtracted. Connectivity analysis performed with DICS and a standardized BEM headmodel and was baseline corrected. Darker reds indicate coherence with E45 is higher for BB while darker blues indicate coherence with E45 is higher for AM.

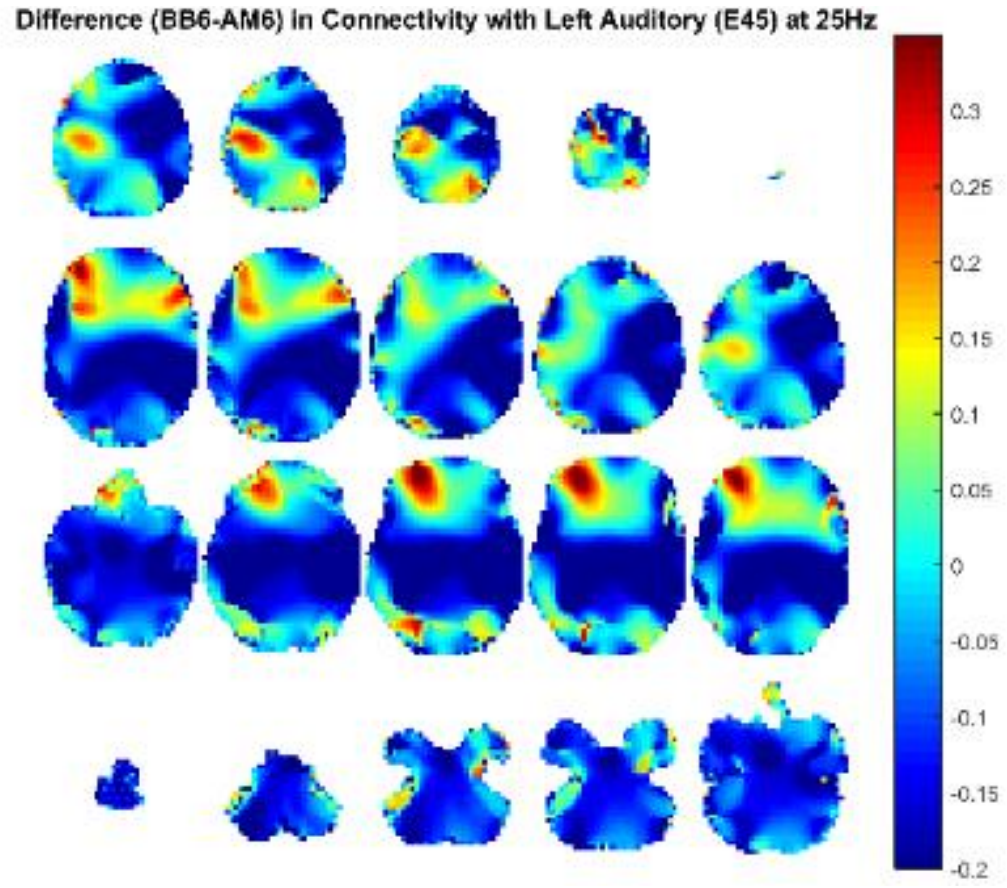

Figure 252. Binaural beat Source level connectivity with a dipole at E45 (left temporal, auditory cortex) in 25 Hz during the middle one-second of 6 Hz stimulation with 6 Hz amplitude modulated connectivity subtracted. Connectivity analysis performed with DICS and a standardized BEM headmodel and was baseline corrected. Darker reds indicate coherence with E45 is higher for BB while darker blues indicate coherence with E45 is higher for AM.

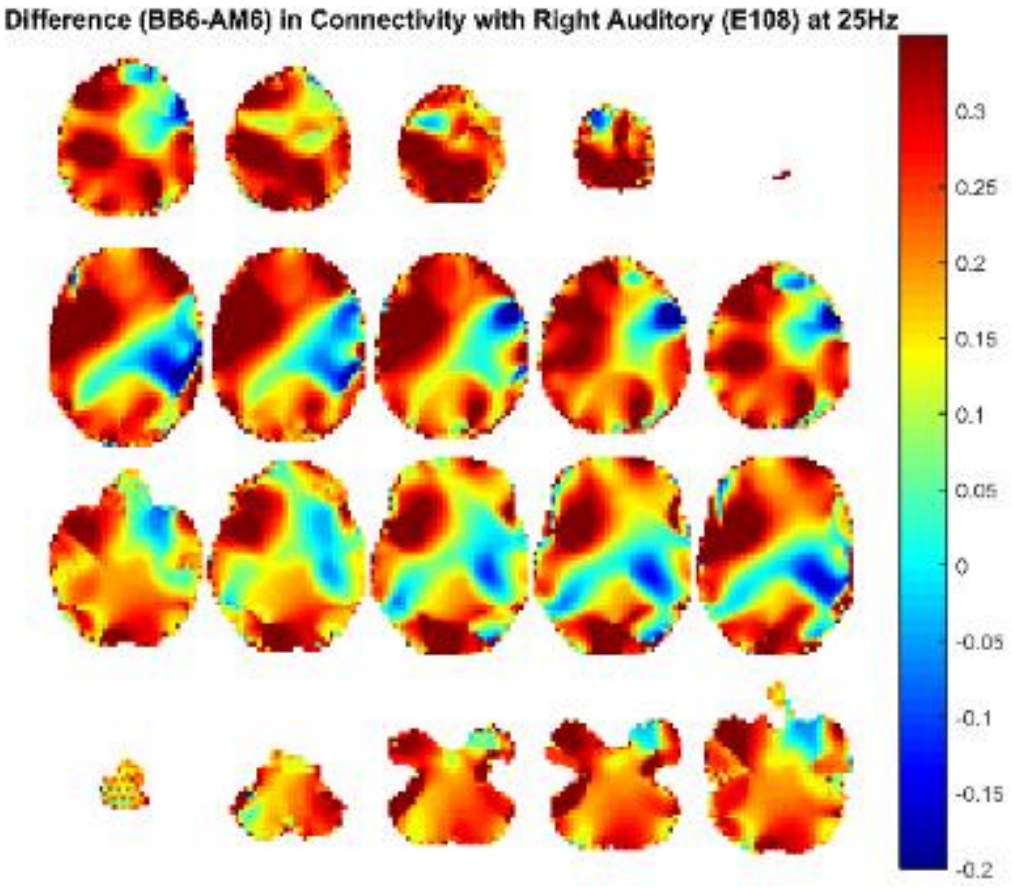

Figure 253. Binaural beat Source level connectivity with a dipole at E108 (right temporal, auditory cortex) in 25 Hz during the middle one-second of 6 Hz stimulation with 6 Hz amplitude modulated connectivity subtracted. Connectivity analysis performed with DICS and a standardized BEM headmodel and was baseline corrected. Darker reds indicate coherence with E45 is higher for BB while darker blues indicate coherence with E45 is higher for AM.

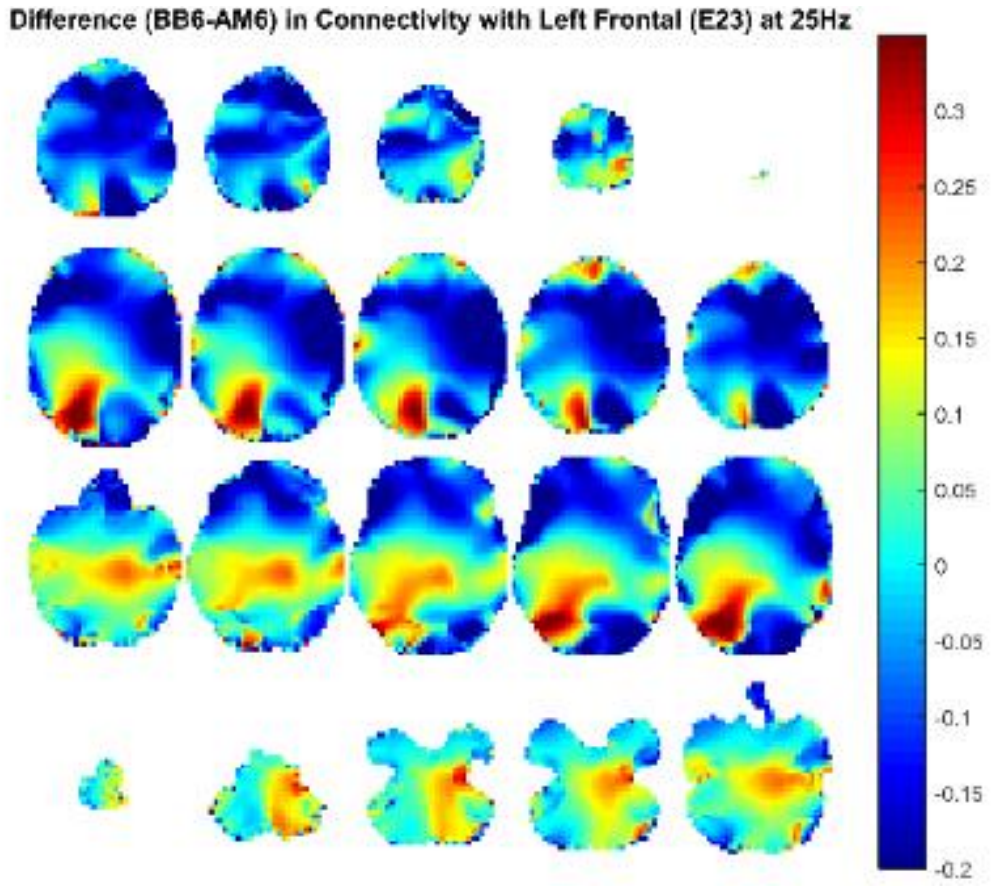

Figure 254. Binaural beat Source level connectivity with a dipole at E23 (left temporal, frontal cortex) in 25 Hz during the middle one-second of 6 Hz stimulation with 6 Hz amplitude modulated connectivity subtracted. Connectivity analysis performed with DICS and a standardized BEM headmodel and was baseline corrected. Darker reds indicate coherence with E45 is higher for BB while darker blues indicate coherence with E45 is higher for AM.

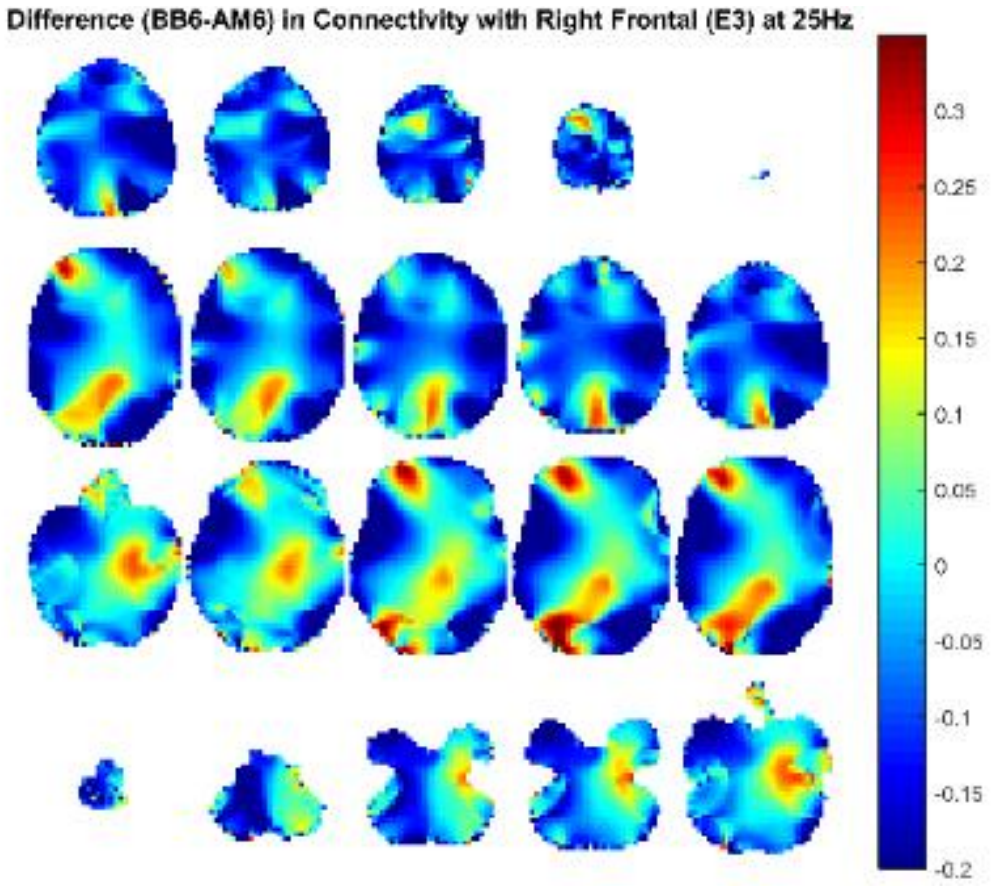

Figure 255. Binaural beat Source level connectivity with a dipole at E3 (right temporal, frontal cortex) in 25 Hz during the middle one-second of 6 Hz stimulation with 6 Hz amplitude modulated connectivity subtracted. Connectivity analysis performed with DICS and a standardized BEM headmodel and was baseline corrected. Darker reds indicate coherence with E45 is higher for BB while darker blues indicate coherence with E45 is higher for AM.

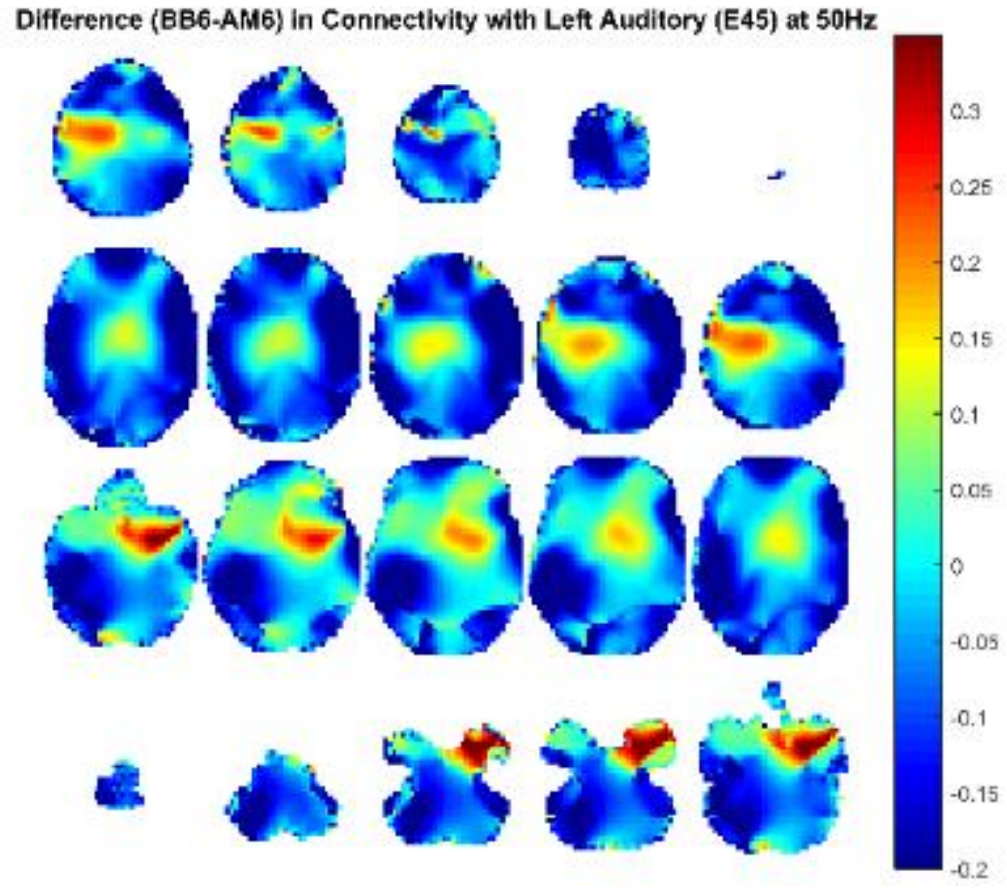

Figure 256. Binaural beat Source level connectivity with a dipole at E45 (left temporal, auditory cortex) in 50 Hz during the middle one-second of 6 Hz stimulation with 6 Hz amplitude modulated connectivity subtracted. Connectivity analysis performed with DICS and a standardized BEM headmodel and was baseline corrected. Darker reds indicate coherence with E45 is higher for BB while darker blues indicate coherence with E45 is higher for AM.

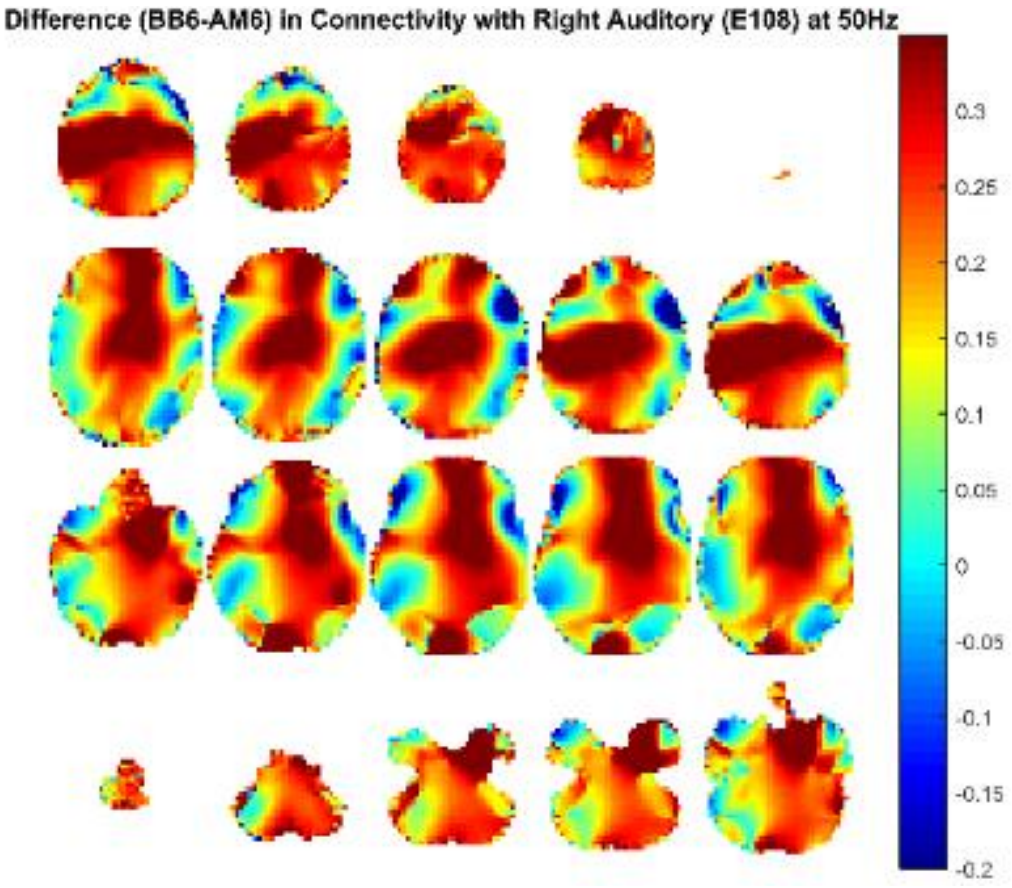

Figure 257. Binaural beat Source level connectivity with a dipole at E108 (right temporal, auditory cortex) in 50 Hz during the middle one-second of 6 Hz stimulation with 6 Hz amplitude modulated connectivity subtracted. Connectivity analysis performed with DICS and a standardized BEM headmodel and was baseline corrected. Darker reds indicate coherence with E45 is higher for BB while darker blues indicate coherence with E45 is higher for AM.

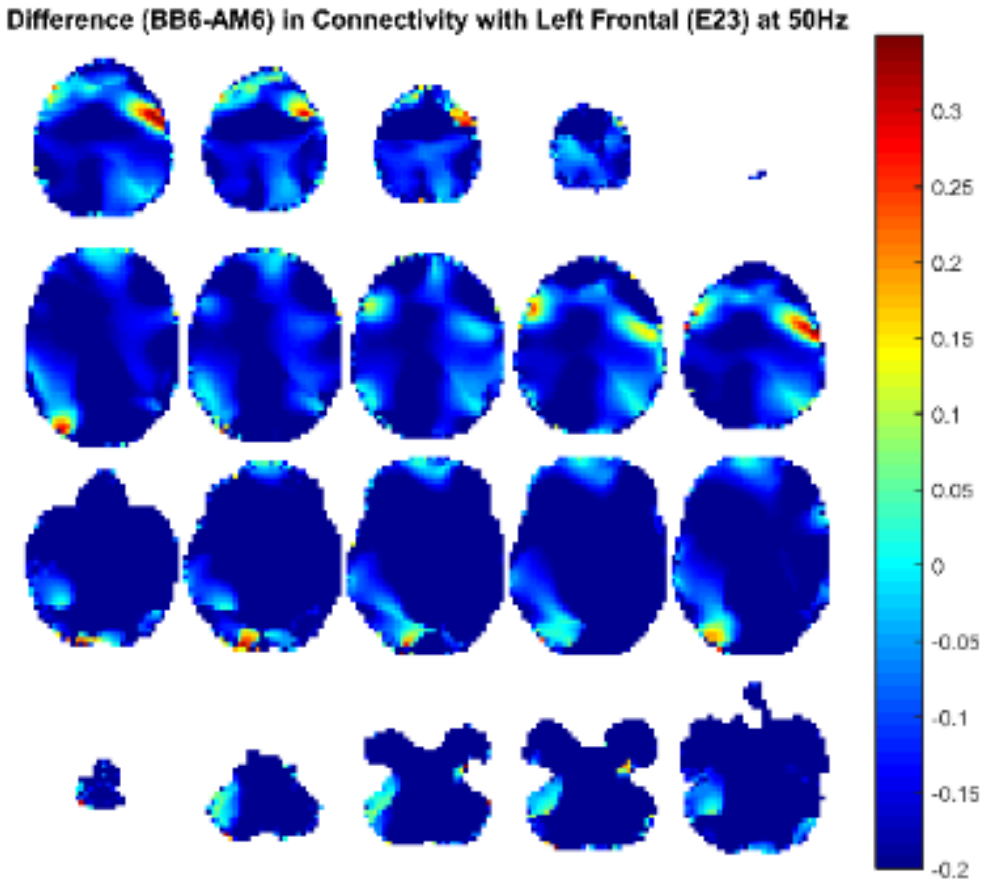

Figure 258. Binaural beat Source level connectivity with a dipole at E23 (left temporal, frontal cortex) in 50 Hz during the middle one-second of 6 Hz stimulation with 6 Hz amplitude modulated connectivity subtracted. Connectivity analysis performed with DICS and a standardized BEM headmodel and was baseline corrected. Darker reds indicate coherence with E45 is higher for BB while darker blues indicate coherence with E45 is higher for AM.

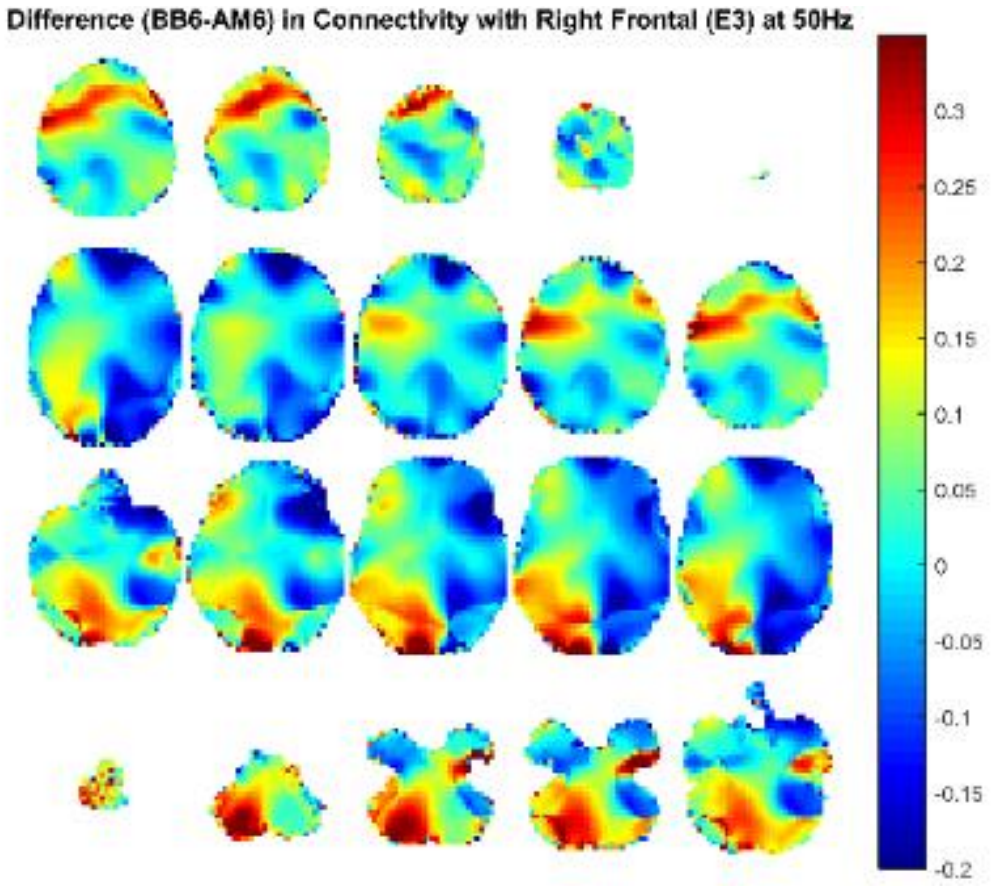

Figure 259. Binaural beat Source level connectivity with a dipole at E3 (right temporal, frontal cortex) in 50 Hz during the middle one-second of 6 Hz stimulation with 6 Hz amplitude modulated connectivity subtracted. Connectivity analysis performed with DICS and a standardized BEM headmodel and was baseline corrected. Darker reds indicate coherence with E45 is higher for BB while darker blues indicate coherence with E45 is higher for AM.

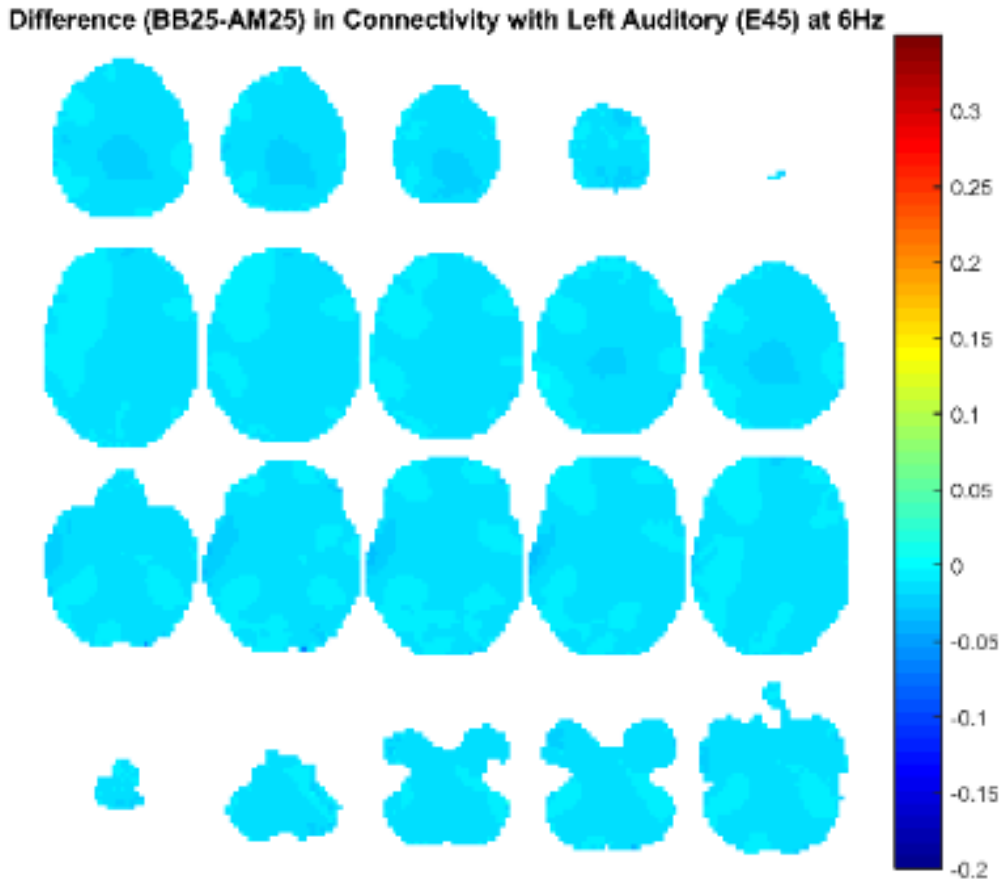

Figure 260. Binaural beat Source level connectivity with a dipole at E45 (left temporal, auditory cortex) in 6 Hz during the middle one-second of 25 Hz stimulation with 25 Hz amplitude modulated connectivity subtracted. Connectivity analysis performed with DICS and a standardized BEM headmodel and was baseline corrected. Darker reds indicate coherence with E45 is higher for BB while darker blues indicate coherence with E45 is higher for AM.

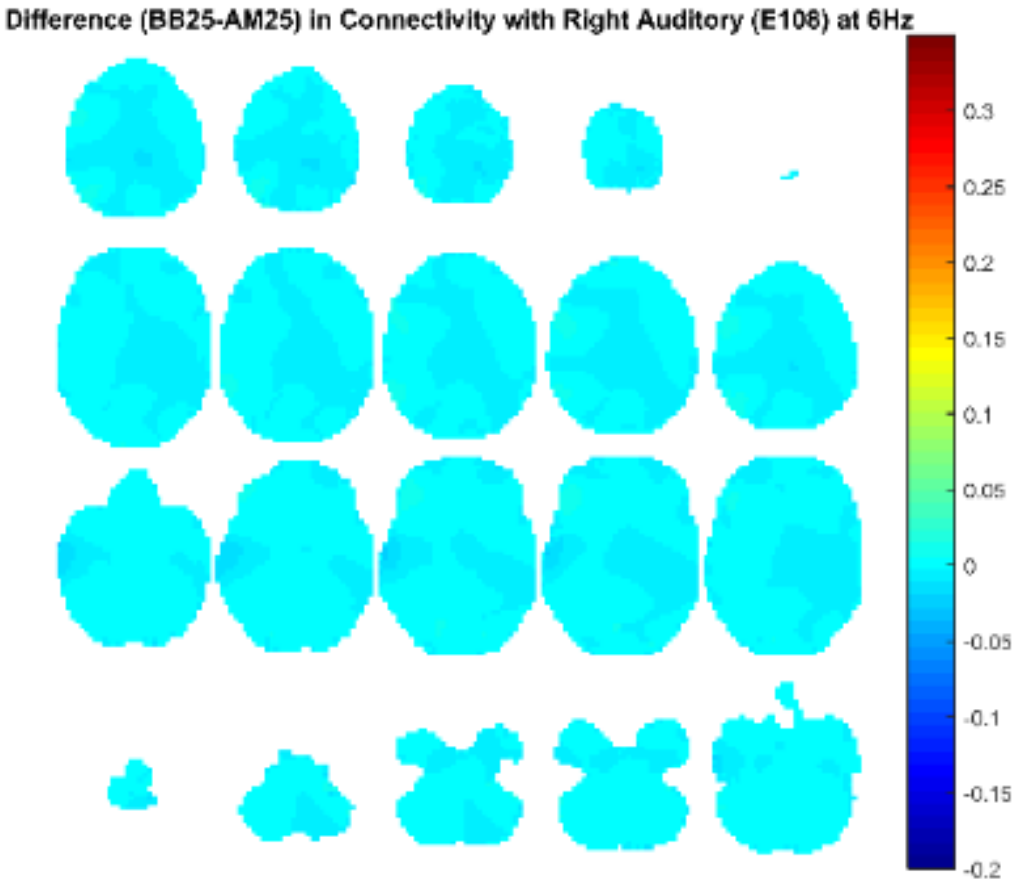

Figure 261. Binaural beat Source level connectivity with a dipole at E108 (right temporal, auditory cortex) in 6 Hz during the middle one-second of 25 Hz stimulation with 25 Hz amplitude modulated connectivity subtracted. Connectivity analysis performed with DICS and a standardized BEM headmodel and was baseline corrected. Darker reds indicate coherence with E45 is higher for BB while darker blues indicate coherence with E45 is higher for AM.

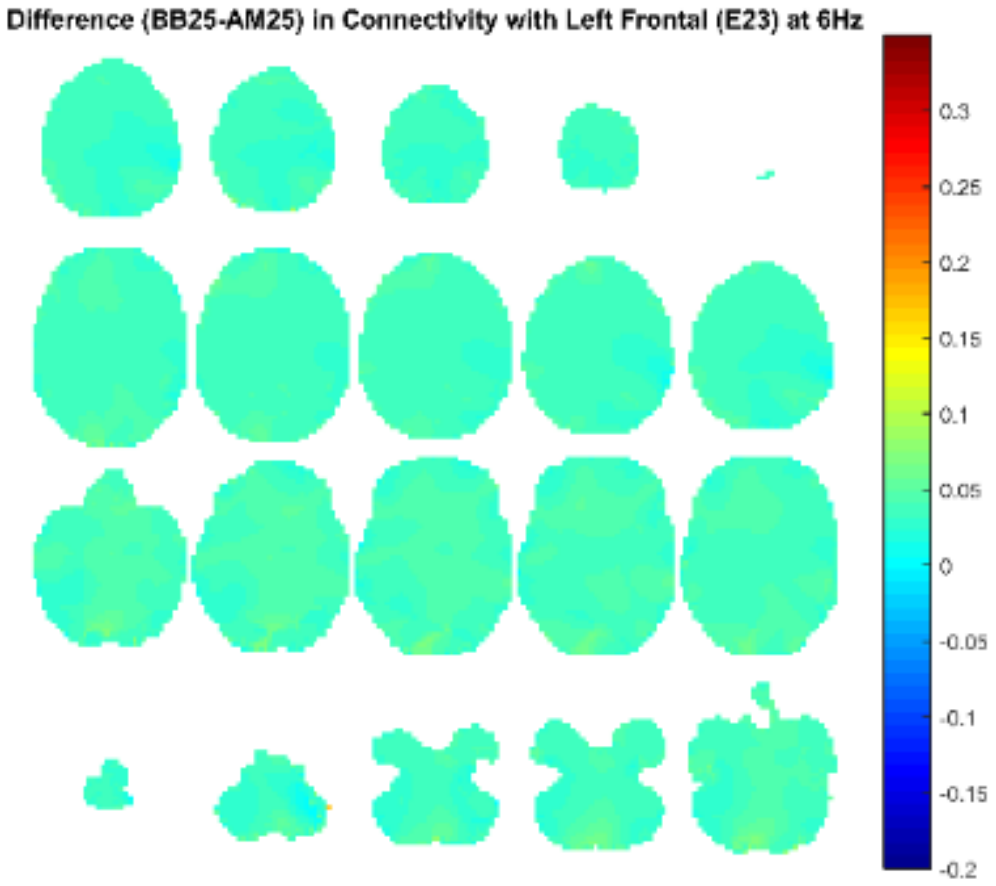

Figure 262. Binaural beat Source level connectivity with a dipole at E23 (left temporal, frontal cortex) in 6 Hz during the middle one-second of 25 Hz stimulation with 25 Hz amplitude modulated connectivity subtracted. Connectivity analysis performed with DICS and a standardized BEM headmodel and was baseline corrected. Darker reds indicate coherence with E45 is higher for BB while darker blues indicate coherence with E45 is higher for AM.

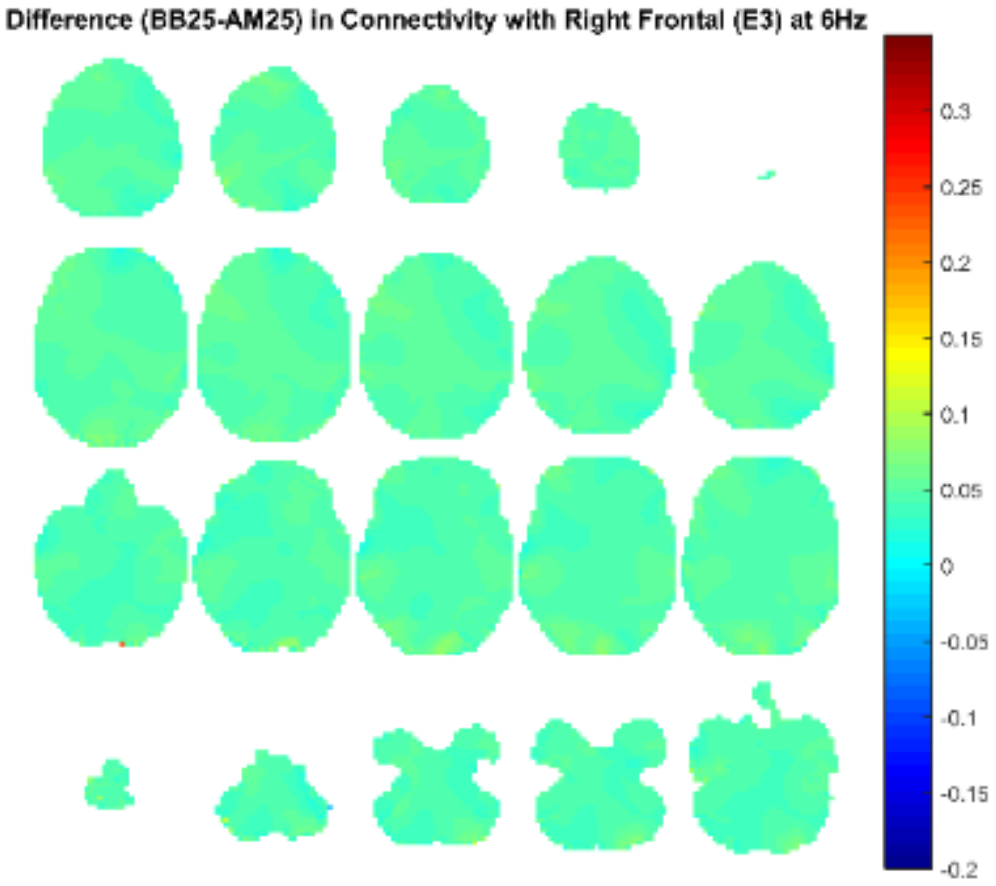

Figure 263. Binaural beat Source level connectivity with a dipole at E3 (right temporal, frontal cortex) in 6 Hz during the middle one-second of 25 Hz stimulation with 25 Hz amplitude modulated connectivity subtracted. Connectivity analysis performed with DICS and a standardized BEM headmodel and was baseline corrected. Darker reds indicate coherence with E45 is higher for BB while darker blues indicate coherence with E45 is higher for AM.

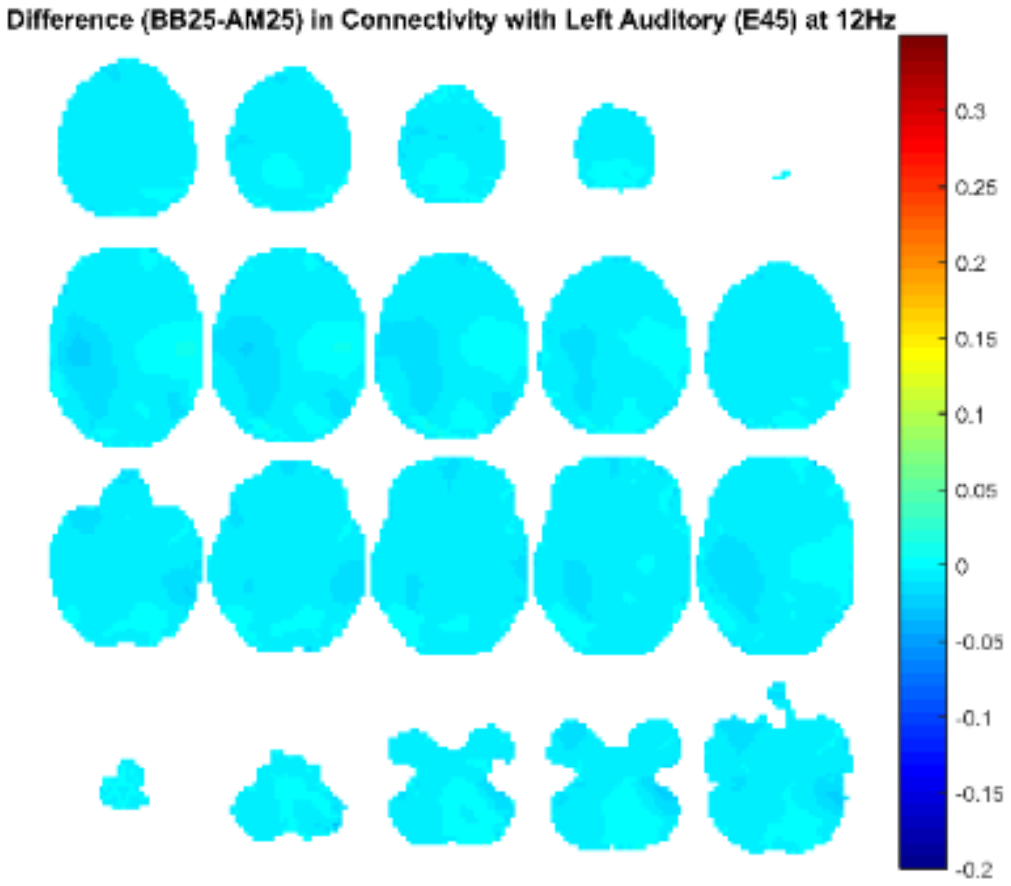

Figure 264. Binaural beat Source level connectivity with a dipole at E45 (left temporal, auditory cortex) in 12 Hz during the middle one-second of 25 Hz stimulation with 25 Hz amplitude modulated connectivity subtracted. Connectivity analysis performed with DICS and a standardized BEM headmodel and was baseline corrected. Darker reds indicate coherence with E45 is higher for BB while darker blues indicate coherence with E45 is higher for AM.

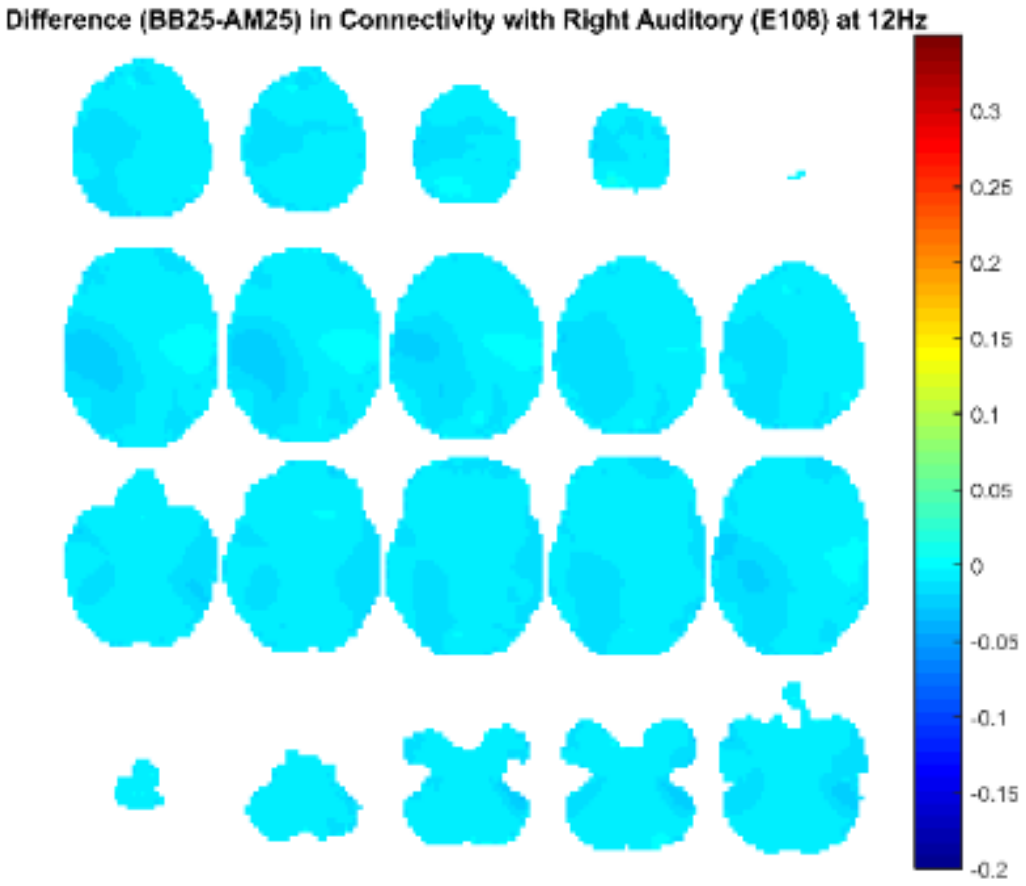

Figure 265. Binaural beat Source level connectivity with a dipole at E108 (right temporal, auditory cortex) in 12 Hz during the middle one-second of 25 Hz stimulation with 25 Hz amplitude modulated connectivity subtracted. Connectivity analysis performed with DICS and a standardized BEM headmodel and was baseline corrected. Darker reds indicate coherence with E45 is higher for BB while darker blues indicate coherence with E45 is higher for AM.

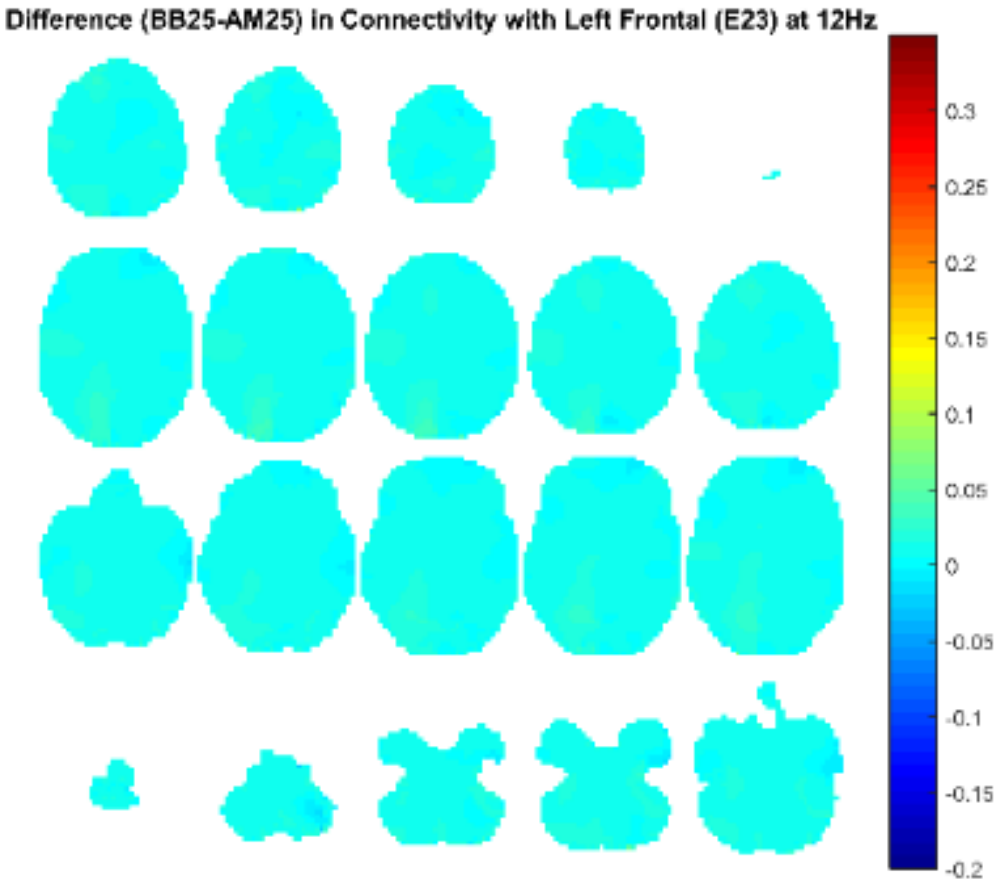

Figure 266. Binaural beat Source level connectivity with a dipole at E23 (left temporal, frontal cortex) in 12 Hz during the middle one-second of 25 Hz stimulation with 25 Hz amplitude modulated connectivity subtracted. Connectivity analysis performed with DICS and a standardized BEM headmodel and was baseline corrected. Darker reds indicate coherence with E45 is higher for BB while darker blues indicate coherence with E45 is higher for AM.

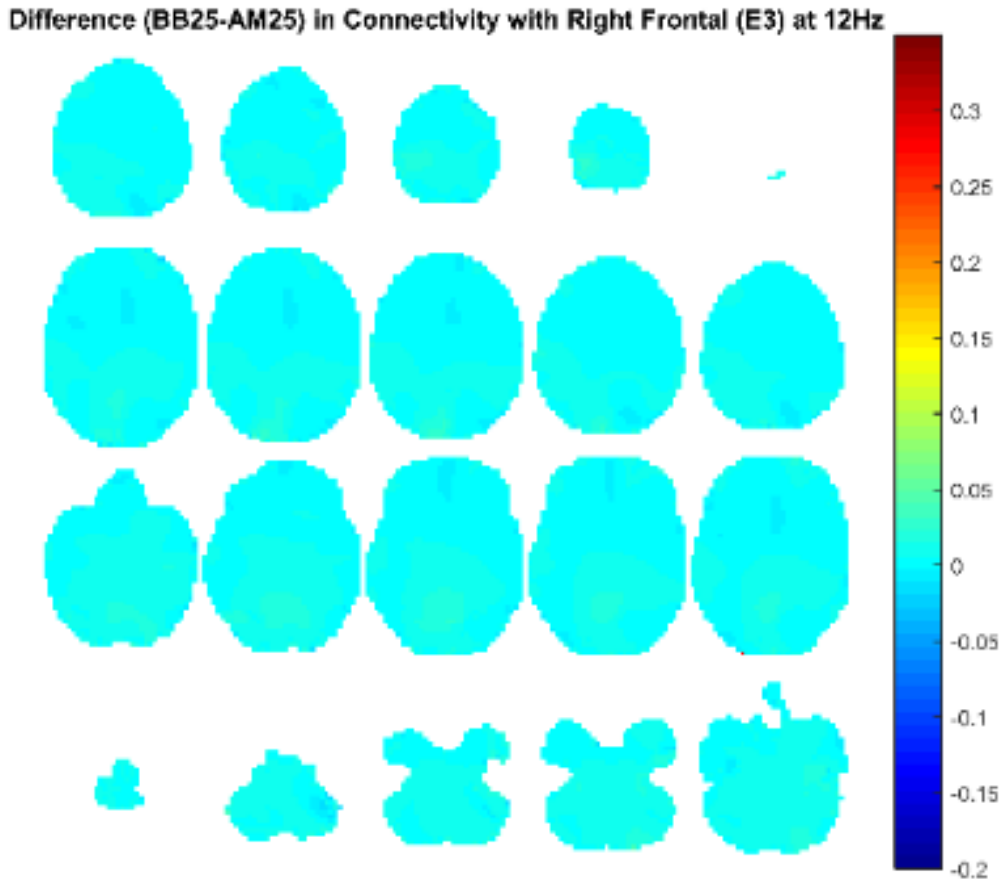

Figure 267. Binaural beat Source level connectivity with a dipole at E3 (right temporal, frontal cortex) in 12 Hz during the middle one-second of 25 Hz stimulation with 25 Hz amplitude modulated connectivity subtracted. Connectivity analysis performed with DICS and a standardized BEM headmodel and was baseline corrected. Darker reds indicate coherence with E45 is higher for BB while darker blues indicate coherence with E45 is higher for AM.

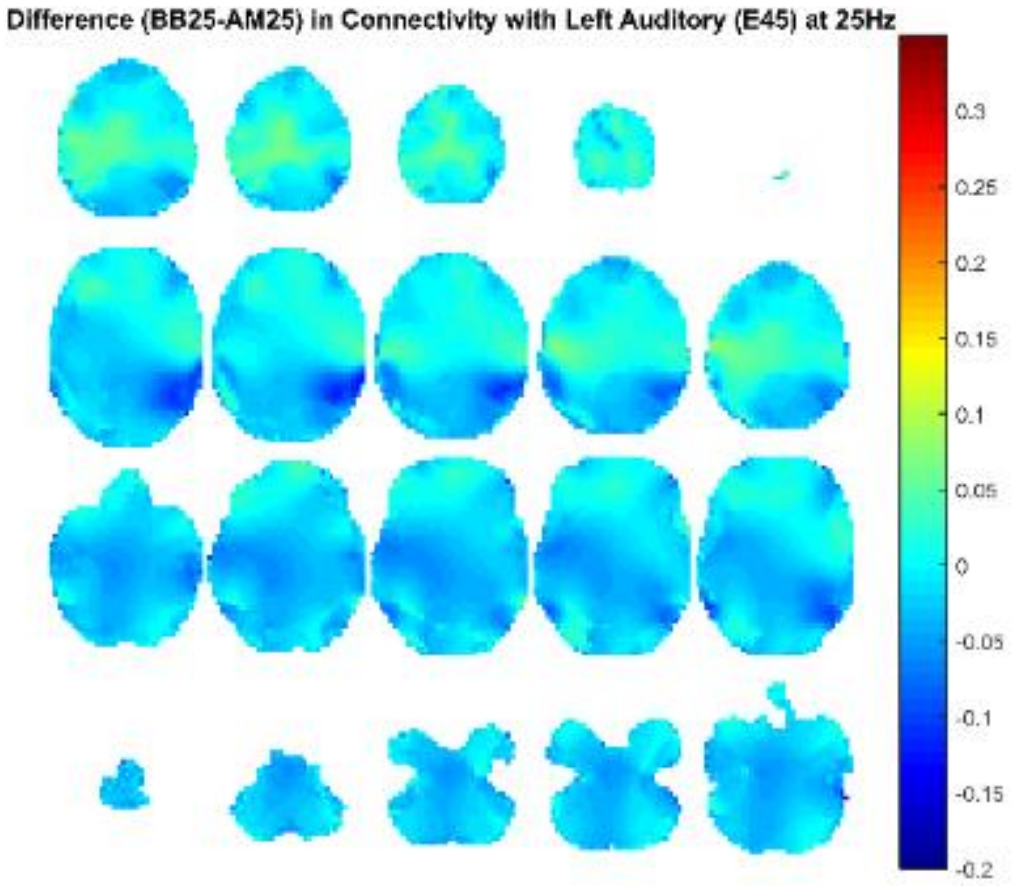

Figure 268. Binaural beat Source level connectivity with a dipole at E45 (left temporal, auditory cortex) in 25 Hz during the middle one-second of 25 Hz stimulation with 25 Hz amplitude modulated connectivity subtracted. Connectivity analysis performed with DICS and a standardized BEM headmodel and was baseline corrected. Darker reds indicate coherence with E45 is higher for BB while darker blues indicate coherence with E45 is higher for AM.

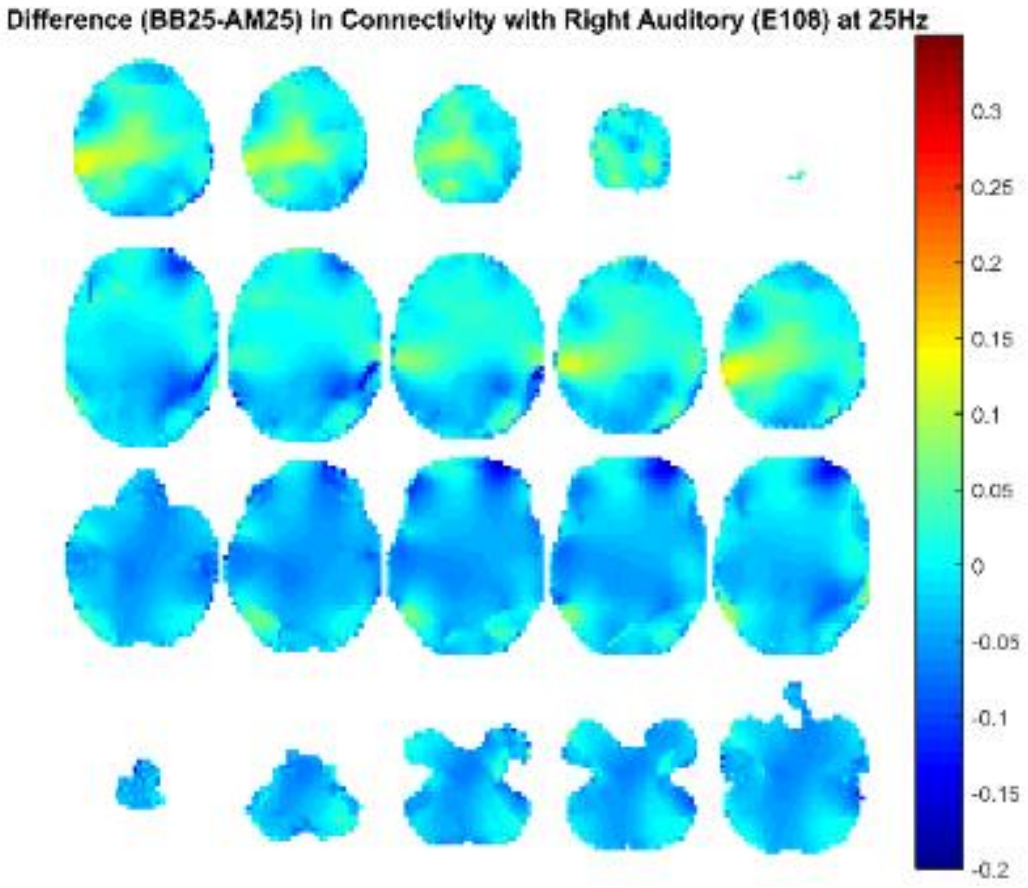

Figure 269. Binaural beat Source level connectivity with a dipole at E108 (right temporal, auditory cortex) in 25 Hz during the middle one-second of 25 Hz stimulation with 25 Hz amplitude modulated connectivity subtracted. Connectivity analysis performed with DICS and a standardized BEM headmodel and was baseline corrected. Darker reds indicate coherence with E45 is higher for BB while darker blues indicate coherence with E45 is higher for AM.

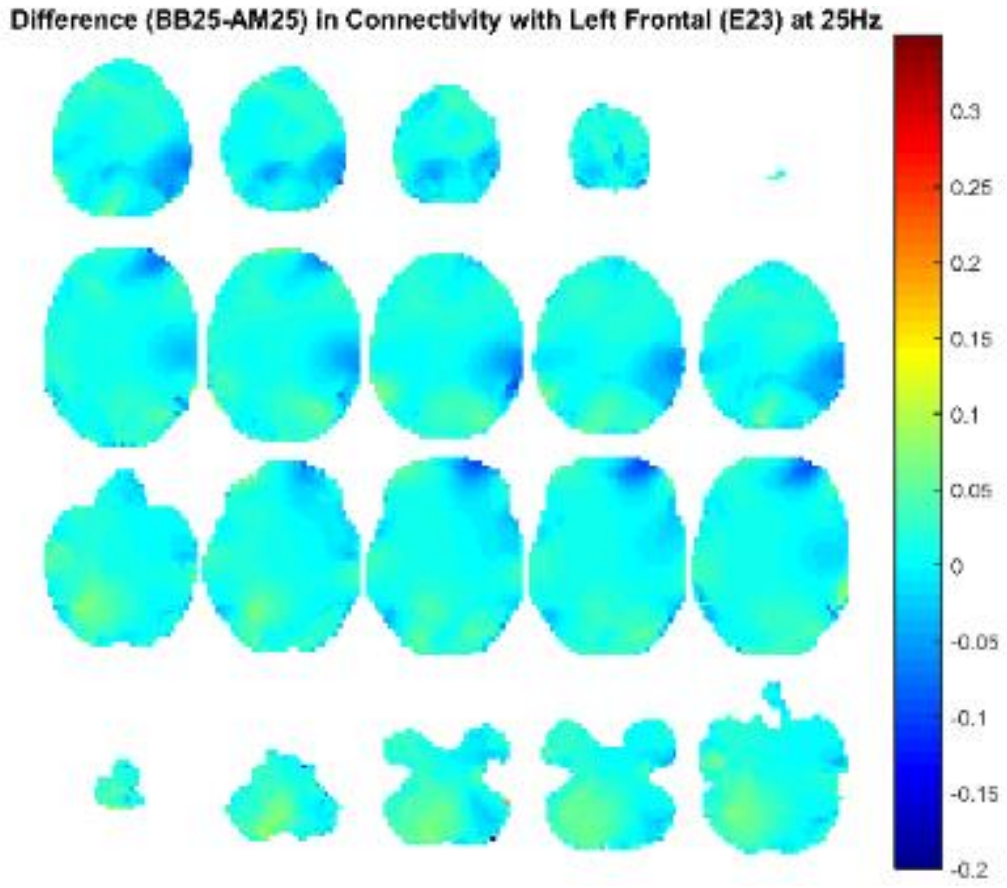

Figure 270. Binaural beat Source level connectivity with a dipole at E23 (left temporal, frontal cortex) in 25 Hz during the middle one-second of 25 Hz stimulation with 25 Hz amplitude modulated connectivity subtracted. Connectivity analysis performed with DICS and a standardized BEM headmodel and was baseline corrected. Darker reds indicate coherence with E45 is higher for BB while darker blues indicate coherence with E45 is higher for AM.

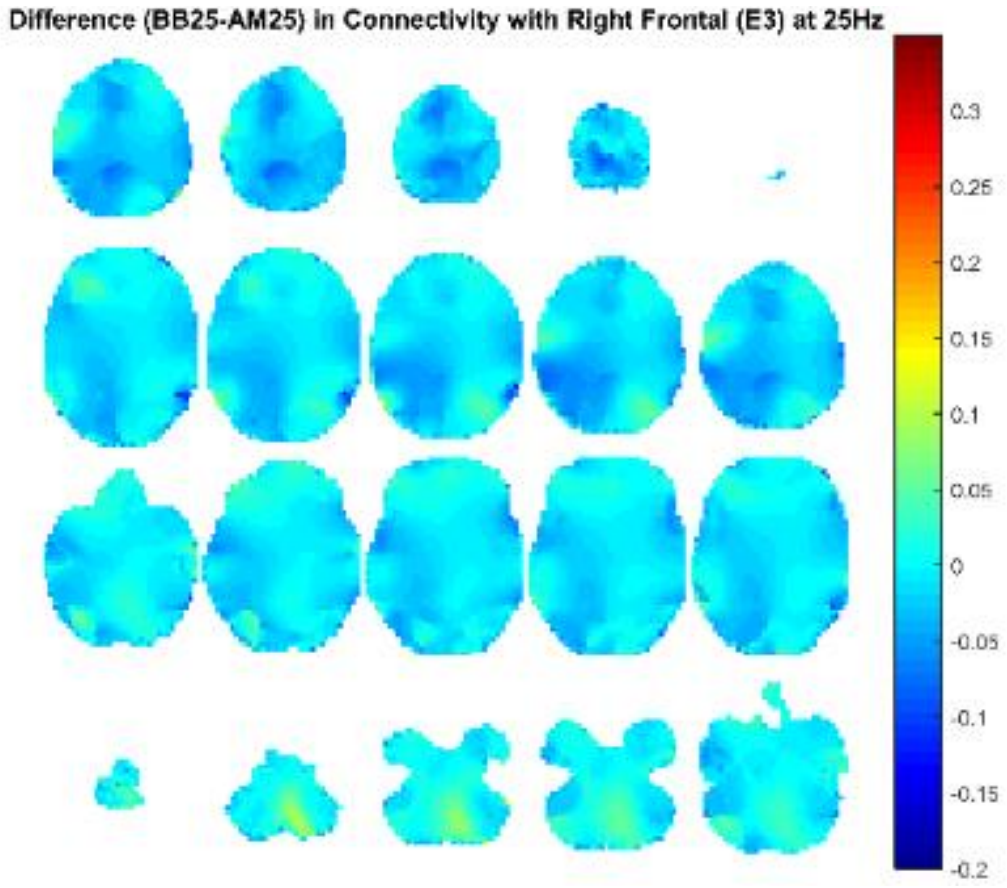

Figure 271. Binaural beat Source level connectivity with a dipole at E3 (right temporal, frontal cortex) in 25 Hz during the middle one-second of 25 Hz stimulation with 25 Hz amplitude modulated connectivity subtracted. Connectivity analysis performed with DICS and a standardized BEM headmodel and was baseline corrected. Darker reds indicate coherence with E45 is higher for BB while darker blues indicate coherence with E45 is higher for AM.

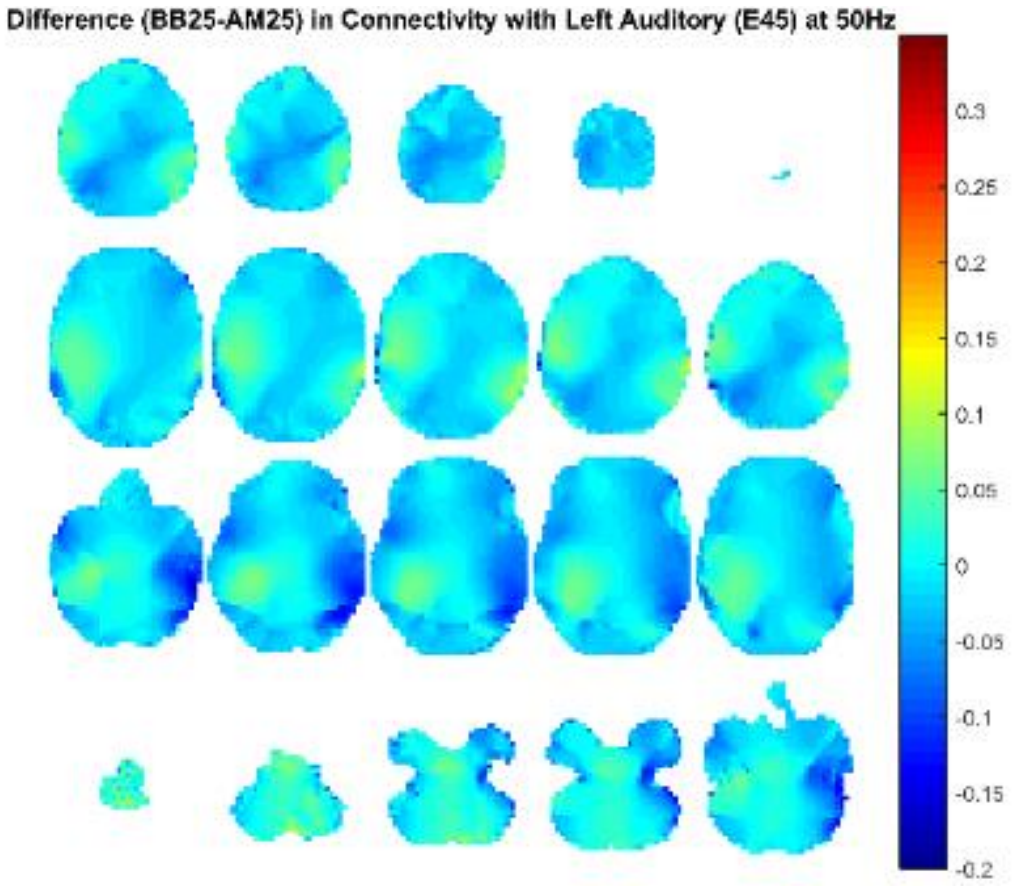

*Figure 272.*Binaural beat Source level connectivity with a dipole at E45 (left temporal, auditory cortex) in 50 Hz during the middle one-second of 25 Hz stimulation with 25 Hz amplitude modulated connectivity subtracted. Connectivity analysis performed with DICS and a standardized BEM headmodel and was baseline corrected. Darker reds indicate coherence with E45 is higher for BB while darker blues indicate coherence with E45 is higher for AM.

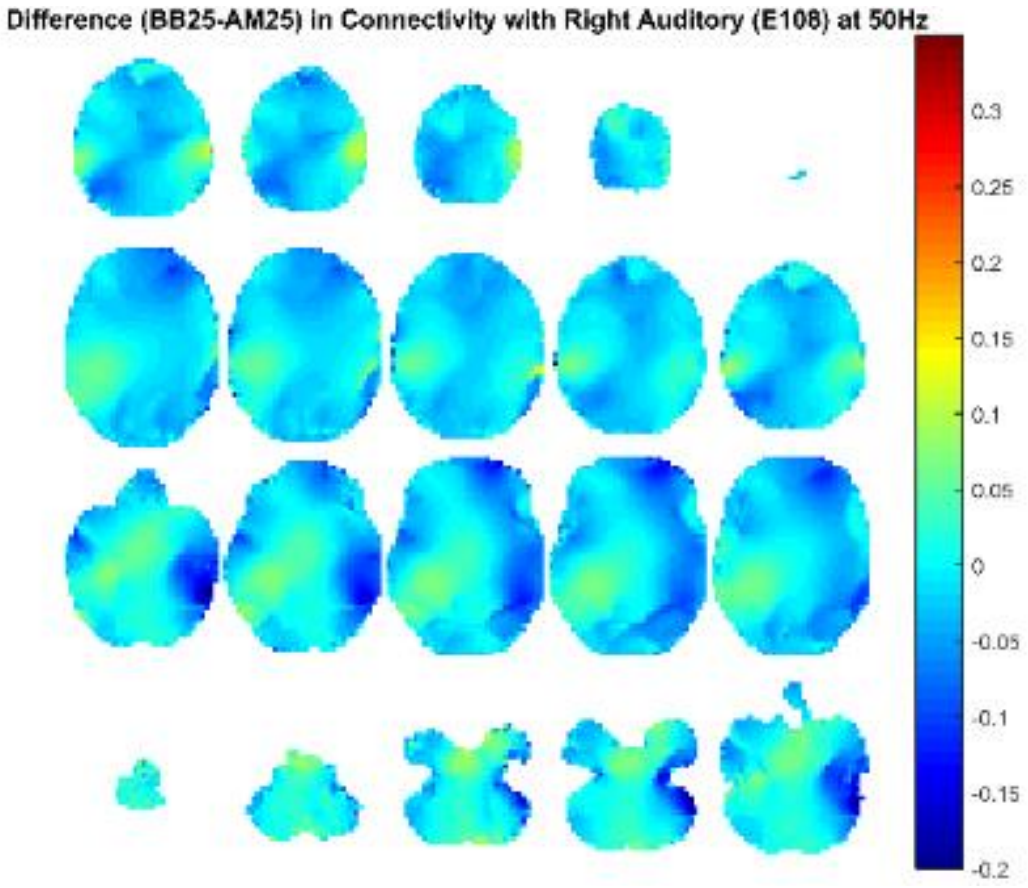

Figure 273. Binaural beat Source level connectivity with a dipole at E108 (right temporal, auditory cortex) in 50 Hz during the middle one-second of 25 Hz stimulation with 25 Hz amplitude modulated connectivity subtracted. Connectivity analysis performed with DICS and a standardized BEM headmodel and was baseline corrected. Darker reds indicate coherence with E45 is higher for BB while darker blues indicate coherence with E45 is higher for AM.

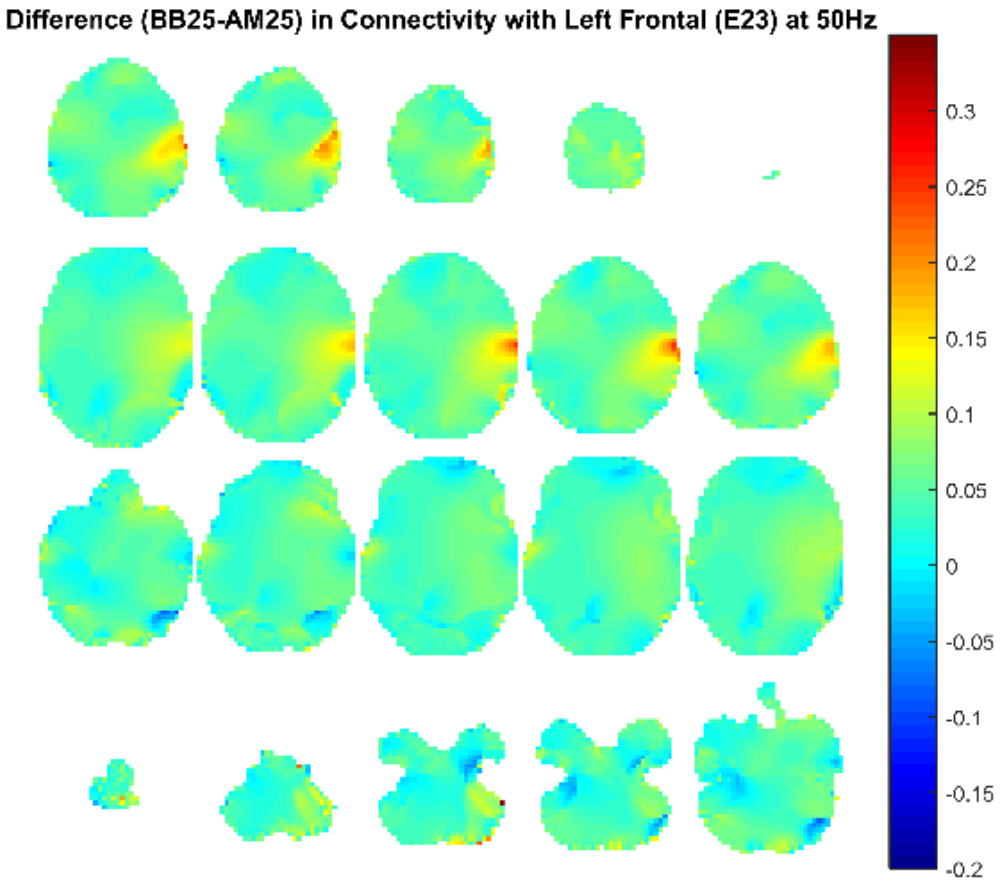

Figure 274. Binaural beat Source level connectivity with a dipole at E23 (left temporal, frontal cortex) in 50 Hz during the middle one-second of 25 Hz stimulation with 25 Hz amplitude modulated connectivity subtracted. Connectivity analysis performed with DICS and a standardized BEM headmodel and was baseline corrected. Darker reds indicate coherence with E45 is higher for BB while darker blues indicate coherence with E45 is higher for AM.

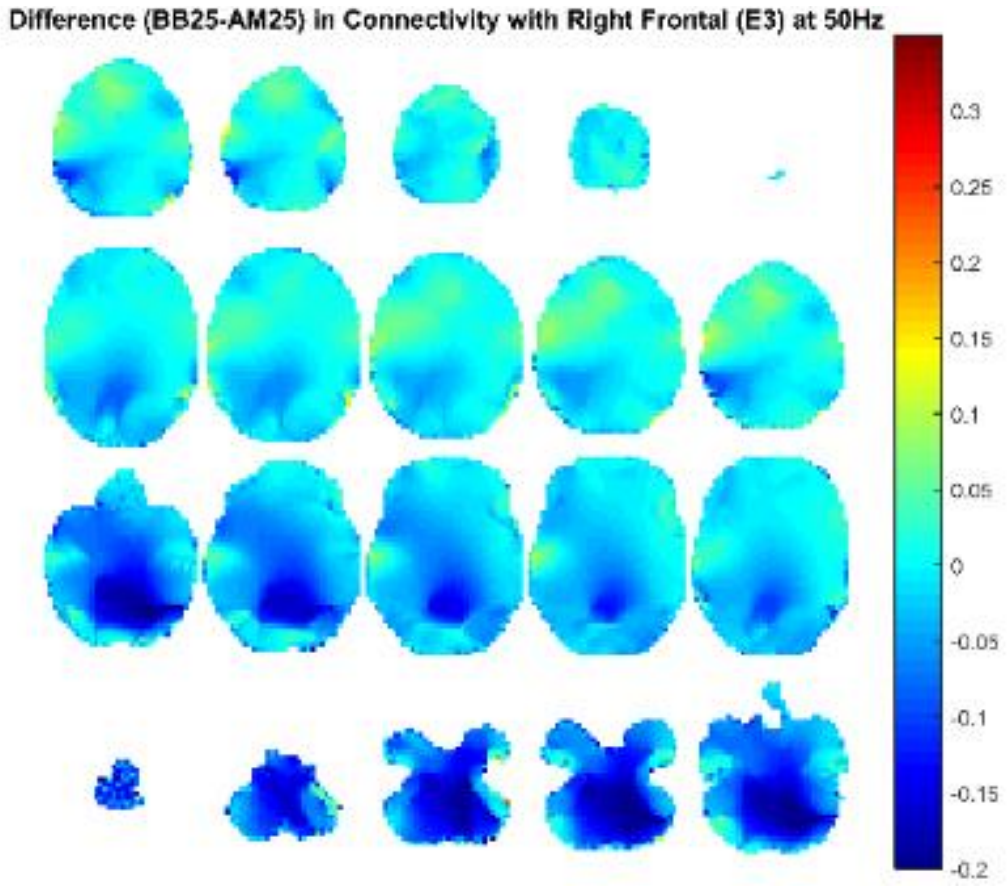

Figure 275. Binaural beat Source level connectivity with a dipole at E3 (right temporal, frontal cortex) in 50 Hz during the middle one-second of 25 Hz stimulation with 25 Hz amplitude modulated connectivity subtracted. Connectivity analysis performed with DICS and a standardized BEM headmodel and was baseline corrected. Darker reds indicate coherence with E45 is higher for BB while darker blues indicate coherence with E45 is higher for AM.